U.PORTO

**DOUTORAMENTO**

PROGRAMA DOUTORAL EM CIÊNCIAS BIOMÉDICAS

# Bladder cancer: tackling epigenetic players and immuno-oncology

Sandra Pinto Nunes

**D**

**2024**

U.PORTO

**Sandra Pinto Nunes.** Bladder cancer: tackling epigenetic players and immuno-oncology

**Bladder cancer: tackling epigenetic players and immune-oncology**

Sandra Isabel Pinto Nunes

**D.**ICBAS **2024**

SEDE ADMINISTRATIVA INSTITUTO DE **CIÊNCIAS BIOMÉDICAS ABEL SALAZAR**

Sandra Isabel Pinto Nunes

# Bladder Cancer: Tackling Epigenetic Players and Immuno-oncology

Tese de Candidatura ao grau de Doutor em Ciências Biomédicas;
Programa Doutoral da Universidade do Porto (Instituto de Ciências Biomédicas Abel Salazar)

Orientadora:
**Professora Doutora Carmen de Lurdes Fonseca Jerónimo**
Professora Catedrática Convidada
Departamento de Patologia e Imunologia Molecular
Instituto de Ciências Biomédicas Abel Salazar (ICBAS) - Universidade do Porto, Porto, Portugal
Coordenadora do Grupo de Epigenética e Biologia do Cancro e Diretora do Centro de Investigação
Instituto Português de Oncologia do Porto Francisco Gentil EPE (IPO Porto) / Porto Comprehensive Cancer Center Raquel Seruca (Porto.CCC), Porto, Portugal

Coorientador:
**Professor Doutor Jesús María Paramio González**
Coordenador da Divisão de Oncologia Molecular e Translacional
Centro de Investigaciones Energéticas, Medioambientales y Tecnológicas (CIEMAT), Madrid, Espanha
Coordenador do Grupo de Oncologia Celular e Molecular de Tumores Geniturinários
Instituto de Investigação Biomédica do Hospital Universitário “12 de Octubre”, Madrid, Espanha

Coorientador:
**Professor Doutor Rui Manuel Ferreira Henrique**
Professor Catedrático Convidado
Departamento de Patologia e Imunologia Molecular
Instituto de Ciências Biomédicas Abel Salazar (ICBAS) - Universidade do Porto
Assistente Graduado Sénior do Serviço de Anatomia Patológica & Investigador Sénior do Grupo de

Epigenética e Biologia do Cancro - Centro de Investigação
Instituto Português de Oncologia do Porto Francisco Gentil EPE (IPO Porto) / Porto Comprehensive Cancer Center Raquel Seruca (Porto.CCC), Porto, Portugal

Sandra Isabel Pinto Nunes

# Bladder Cancer: Tackling Epigenetic Players and Immuno-oncology

Thesis for the degree of Doctor in Biomedical Sciences; Doctoral Program of the University of Porto (School of Medicine and Biomedical Sciences)

Supervisor:
**Professor Doctor Carmen de Lurdes Fonseca Jerónimo**
Guest Full Professor
Department of Pathology and Molecular Immunology
ICBAS-School of Medicine and Biomedical Sciences, University of Porto, Porto, Portugal
Coordinator of Cancer Biology and Epigenetics Group and Director of the Research Center
Portuguese Oncology Institute of Porto Francisco Gentil EPE (IPO Porto) / Porto Comprehensive Cancer Center Raquel Seruca (Porto.CCC)

Co-supervisor:
**Professor Doctor Jesús María Paramio González**
Head of the Molecular and Translational Oncology Division
Centro de Investigaciones Energéticas, Medioambientales y Tecnológicas (CIEMAT), Madrid, Spain
Head of the Cell and Molecular Oncology Group
Institute of Biomedical Investigation University Hospital "12 de Octubre", Madrid, Spain

Co-supervisor:
**Professor Doctor Rui Manuel Ferreira Henrique**
Guest Full Professor
Department of Pathology and Molecular Immunology
ICBAS-School of Medicine and Biomedical Sciences, University of Porto, Porto, Portugal
Senior Consultant, Department of Pathology and Senior Researcher, Cancer Biology and Epigenetics Group - Research Center

Portuguese Oncology Institute of Porto Francisco Gentil EPE (IPO Porto) / Porto Comprehensive Cancer Center Raquel Seruca (Porto.CCC), Porto, Portugal

# Bladder cancer: Tackling Epigenetic players and Immuno-oncology

**Sandra Isabel Pinto Nunes**

**Copyright © 2024 by Sandra Isabel Pinto Nunes**

All rights reserved. No part of this book may be reproduced, stored in a database or retrieval system, or published, in any form or in any way, electronically, mechanically, by print, photo print, microfilm or any other means without prior written permission by the author, or when appropriate, of the publisher of the publications.

The candidate performed the experimental work with the support of a doctoral fellowship (**SFRH/BD/144241/2019**) supported by the “Fundação para a Ciência e a Tecnologia”.

**The research described in this Thesis was conducted at:**

Molecular and Translational Oncology Division, Centro de Investigaciones Energéticas, Medioambientales y Tecnológicas (CIEMAT), Madrid, Spain

Institute of Biomedical Investigation University Hospital “12 de Octubre”, Madrid, Spain

Cancer Biology and Epigenetics Group – Research Center, Portuguese Oncology Institute of Porto Francisco Gentil EPE (IPO Porto) / Porto Comprehensive Cancer Center Raquel Seruca (Porto.CCC), Porto, Portugal

## Declaração de honra

Declaro que a presente tese é de minha autoria e não foi utilizada previamente noutro curso ou unidade curricular, desta ou de outra instituição. As referências a outros autores (afirmações, ideias, pensamentos) respeitam escrupulosamente as regras da atribuição, e encontram-se devidamente indicadas no texto e nas referências bibliográficas, de acordo com as normas de referenciação. Tenho consciência de que a prática de plágio e auto-plágio constitui um ilícito académico.

Porto, 3 de janeiro de 2024

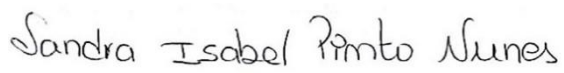

**Scientific Publications Articles in international peer-reviewed journals**

### *Review paper 1*

**Nunes SP**, Henrique R, Jerónimo C, Paramio JM. DNA Methylation as a Therapeutic Target for Bladder Cancer. Cells. 2020 Aug 7;9(8):1850.

### *Review paper 2*

Lodewijk I*, **Nunes SP***, Henrique R, Jerónimo C, Dueñas M, Paramio JM. Tackling tumor microenvironment through epigenetic tools to improve cancer immunotherapy. Clinical Epigenetics. 2021 Mar 24;13(1):63. * Co-first authors

### *Research paper 1*

**Nunes SP**, Morales L, Rubio C, Munera-Maravilla E, Lodewijk I, Suárez-Cabrera C, Martínez VG, Pérez-Escavy M, Pérez-Crespo M, Sánchez MA, Montesinos E, San José-Enériz E, Agirre X, Prósper F, Pineda-Lucena A, Henrique R, Dueñas M, Correia MP, Jerónimo C, Paramio JM. Modulation of tumor microenvironment by targeting histone acetylation in bladder cancer. Cell Death Discovery. 2024 Jan 10, 1.

### *Research paper 2*

**Nunes SP**, Munera-Maravilla E, Rubio C, Morales L, Lodewijk I, Suárez-Cabrera C, Martínez VG, Pérez-Escavy M, Pérez-Crespo M, Sánchez MA, San José-Enériz E, Agirre X, Prósper F, Pineda-Lucena A, Henrique R, Dueñas M, Correia MP, Jerónimo C, Paramio JM. Impact of G9a/DNMT inhibition in combination with immunotherapy behind an enhanced anti-tumoral response in bladder cancer upon rechallenge. *Manuscript in preparation*.

### *Research paper 3*

**Nunes SP**, Bao-Caamano A, Costa-Fraga N, Constâncio V, Leite-Silva P, Rubio C, Suárez-Cabrera C, Morales L, Henrique R, Dueñas M, Castellano D, Real FX, Díaz-Lagares A, Jerónimo C, Paramio JM. Uncovering DNA methylation patterns and their impact on immunotherapy in bladder cancer. *Manuscript in preparation*.

### *Awards to the scientific output of the thesis*

Best oral communication (850 €) awarded to the work “Modulation of tumor microenvironment by targeting histone acetylation in bladder cancer” attributed by the evaluation scientific committee of the 5$^{th}$ Meeting of Young Researchers in Oncology (5º

ENJIO) organized by Liga Portuguesa Contra o Cancro – Núcleo Regional do Norte – Porto, September 2023.

The present thesis has been submitted in fulfilment of the requirements for the doctoral degree in Biomedical Sciences at ICBAS-School of Medicine and Biomedical Sciences of the University of Porto. The PhD project of the candidate and the present Thesis have additionally adhered to the norms stipulated in the regulation by University of Porto for attribution of the European PhD Title.

# Acknowledgments

*Madrid me has conquistado*

En primer lugar, quiero expresar mi más profundo agradecimiento a Jesús. Gracias por aceptar a una estudiante portuguesa un tanto perdida al principio para hacer la Tesis. Gracias por hacerme mejor científica y por ser un verdadero mentor y director de tesis. Gracias por hacerme sentir que tengo una “casa científica” y que soy parte del grupo de vejiga. Esta Tesis te la debo a ti.

Ester, mi valenciana intensa. Con qué palabras te puedo agradecer? Gracias por ayudarme a integrarme en el grupo, por enseñarme tanto a nivel personal y profesional. Sabes que siempre voy a recordar con mucho cariño nuestras conversaciones de todo y nada en el animalario y cultivos.

Lucía, gracias por tu apoyo incondicional y por toda la ayuda con los 10,000 XTT y 5,000 frascos de cultivo. Además, gracias por todas nuestras conversaciones científicas y personales. No solo eres una compañera excepcional, sino también una amiga.

Carol, gracias por tu amistad y por todo tu apoyo y la invaluable ayuda durante la tesis y más allá de ella. Gracias por todos tus consejos. Nuestro amor por Stitch será siempre algo que nos una.

Iris, gracias por tu compañía y amistad, por confiar en mí y permitirme desahogarme sin límites sobre mis problemas y tristezas. Tu apoyo ha sido fundamental para mí, y quiero que sepas que siempre estaré aquí para ti, como tú lo has estado para mí.

Marta, gracias por todas las enriquecedoras discusiones científicas, las memorables barbacoas en tu casa y tu contagiosa alegría. Cristian, gracias por tu apoyo inestimable en el animalario y tus perspicaces comentarios científicos. Victor, gracias por tu imprescindible ayuda con la citometría y por las “semanas fatídicas”. Miri, gracias por tu ayuda en el animalario con tratamientos y por la gestión de mil ratones, además de tu continuo apoyo. Mereces, pequeña bola de energía inagotable que eres, gracias por ser una pieza fundamental durante las semanas fatídicas y por expandir alegría en el CIEMAT. Ignacio, agradezco tu ayuda en el animalario y por haberme introducido al 'burrito sabanero'. Ismael, gracias por todas esas conversaciones profundas sobre la vida. Álvaro y Miguel, gracias por vuestra ayuda durante la tesis.

Bladderianos, muchas gracias por toda vuestra ayuda, apoyo y momentos felices. Gracias por estar presentes cuando llegaban los correos en las “semanas fatídicas” y por ayudar sin dudar. Sin vosotros, no habría llegado hasta aquí.

A Vero, sabes que tú y yo somos una. Gracias por aceptar la invitación al primer helado de muchos en medio de una pandemia. Gracias por todas nuestras aventuras en Madrid y fuera, por tu apoyo y por ser mi amiga. Mi estancia en Madrid no habría sido la misma sin ti, y sabes lo importante que eres para mí.

La Jose, gracias por tus consejos y apoyo. Siempre voy a querer tus abrazos, así que prepárate para darme muchos más.

Jorge, gracias por hacerme compañía siempre que estabas aburrido o tenías hambre. Richi, mi compañero de tesis, gracias por todas las risas que compartimos en el laboratorio. Sabes que siempre seré tu secretaria. Raque, gracias por los helados y las conversaciones profundas sobre la vida. Sari, gracias por tus consejos y disposición para ayudar siempre. Raúl, gracias por las risas y feliz Navidad!

A Rebe y Oma, muchas gracias por toda la ayuda con citometría, por vuestra simpatía y disponibilidad. Pilar y Kiko, gracias por todo el trabajo con las histologías. Sole, Mamen, Sergio y Aurora, gracias por gestionar todos los pedidos, incluso cuando eran urgentes. Al equipo del animalario, gracias por mantener a nuestros ratones. A todos los demás miembros del grupo de Onco, Epi y Hemato, gracias por vuestra ayuda puntual y por los recuerdos que nunca olvidaré.

Gracias a todos los ciemateros que me han acogido como una de vosotros. Sin vosotros, no habría llegado al final de esta tesis.

Bego, gracias por tu amistad, por llevarnos a conocer Madrid y sus rincones, por todo tu apoyo y por nuestras conversaciones. Ana y Ohana, gracias por las 'salidas varias', por ser mis amigas y por todos los momentos inolvidables que hemos pasado. Que vengan muchos más! Bere, gracias por ser la mejor compañera de piso y por siempre poder hablar contigo en portugués.

*A minha casa*

Em primeiro lugar, quero agradecer à Professora Doutora Carmen Jerónimo, orientadora da minha Tese de doutoramento, por me acompanhar deste o início do Mestrado em Oncologia, por me permitir fazer parte do Grupo de Epigenética e Biologia do Cancro e por me incentivar e dar-me a oportunidade de fazer uma parte do meu doutoramento fora do país. Agradeço ao Professor Doutor Rui Henrique, co-orientador desta Tese, pelo apoio dado desde o início do meu percurso no IPO-Porto.

Obrigada, Margareta, por todas as discussões científicas, por todo o apoio que me deste enquanto estive em Madrid e por todas as "ajudas imunológicas".

Agradeço à Fundação para a Ciência e Tecnologia por me conceder o financiamento para realizar esta Tese e ao Professor Doutor Eduardo Rocha por me ter aceitado no doutoramento em Ciências Biomédicas do Instituto de Ciências Biomédicas Abel Salazar da Universidade do Porto.

Quero agradecer também ao Grupo de Epigenética e Biologia do Cancro pelos últimos sete anos da minha carreira científica. Em particular, obrigada ao "Jesus". Clauds, a minha "pre-tésica" favorita, obrigada por todos os momentos felizes e de mágoa também. És a melhor compincha que eu podia pedir, #teamepimmunebla. Dani e Macedo, obrigada pela vossa amizade e pelos momentos de companhia durante meses de pandemia fechadas em casa. Obrigada, Verita, por saber que tenho sempre alguém com quem posso desaguar as minhas frustrações da Tese e por ter sempre um conselho ou palavras encorajadoras desse lado. Teixas, obrigada pelas conversas "heart-to-heart" no nosso cantinho da sala e por todo o apoio que me deste nos momentos mais difíceis. Nunca me vou esquecer do teu carinho. Obrigada, Pipa, por partilharmos boleias, histórias de vida e aulas de Zumba e Kravmaga. Gonças, obrigada por sempre me fazeres rir com as coisas mais parvas. Louros e Nuno, obrigada por todos os momentos engraçados que nunca vou esquecer e por ter alguém com quem partilhar memes da F1. Vera, obrigada por todas as tuas ajudas e por sempre seres a voz da razão.

Ao restante GEBC, nomeadamente à Sara, Rui, Johnny e Carina, obrigada por todas as conversas fugazes (ou não), por toda a partilha de conhecimento e pela vossa ajuda ao longo do meu percurso. Obrigada, também aos membros antigos do GEBC. Lameirinhas, a minha parceira de aventuras. Obrigada por todas as aventuras por Espanha, por sempre estares presente, porque podemos não falar ou vermo-nos todos os dias, mas sabemos que podemos sempre contar uma com a outra. Kate, obrigada por me ajudares no meu início atribulado no GEBC. Se cheguei a este momento, também o devo a ti porque nunca desististe de mim e sempre me apoiaste.

Aos meus amigos desde a pré-história, Joana, Clara e Gabriel. Obrigada por estarem na minha vida, pelos áudios intermináveis de atualizações de vida, por estarmos sempre presentes nos momentos mais importantes das nossas vidas e pelas nossas aventuras, sempre difíceis de marcar, mas que sempre acontecem. Miguel, obrigada pelo teu apoio incondicional durante este período e por fazer com que eu nunca esquecesse de mim própria.

E, por fim, quero agradecer à minha família. Obrigada, Mãe, por sempre me apoiares nas minhas escolhas e por nunca questionares aquilo que me faz feliz, mesmo que isso signifique estar longe. Obrigada, Nini, por seres a irmã e a pessoa que és. Por todo o teu apoio, carinho e preocupação, quero que saibas que és muito importante para mim. Pai, obrigada por todas as conversas sobre a vida, que tanto me fazem pensar e aprender. Joca, obrigada pela companhia incondicional ao longo da escrita da tese. Por fim, aos meus queridos avós, obrigada por todo o vosso carinho, mesmo quando não percebem muito bem o que eu faço. Vou sempre guardar-vos no meu coração e em tudo o que faço.

Sem todos vocês, não teria chegado aqui. Obrigada.

**Em qualquer aventura,**
**O que importa é partir, não é chegar.**

*Miguel Torga, Viagem*

## Abstract

Bladder cancer (BC) ranks as the 10th most common cancer worldwide, representing the 9th cause of death in men by cancer. While non-muscle invasive bladder cancer (NMIBC) is associated with a better prognosis, these patients often recur or progress to a more advanced stage of the disease in the form of muscle-invasive bladder cancer (MIBC) or metastatic dissemination. The emergence of immune checkpoint inhibitors (ICI) such as anti-PD-1/PD-L1 as a treatment option has transformed the management of advanced BC. However, a significant subset of BC patients displays limited clinical benefit from immunotherapy. Epigenetics is the study of the mechanisms that regulate gene expression without altering the DNA sequence. Aberrant DNA methylation and histone modifications constitute key players contributing to BC development. Indeed, these alterations impact not just tumor cells but also the tumor microenvironment, including immune cells. Understanding the intricate BC molecular landscape can reveal novel therapeutic targets and predictive biomarkers to improve BC management. Thus, the main goal of this Thesis was to explore the interplay between epigenetic mechanisms and the immune landscape of advanced BC, aiming to enhance therapeutic approaches and identify predictive biomarkers.

The first work presented in this Thesis focuses on the therapeutic potential of a novel histone deacetylase (HDAC) inhibitor CM-1758, either alone or in combination with ICI in advanced BC. Results from the *in vitro* studies on BC cell lines and an immunocompetent mouse model of metastatic BC showcased the anti-tumoral effects of CM-1758 by inducing broad transcriptional changes, modulating PD-L1 expression and reprogramming the tumor microenvironment alone or in combination with anti-PD-L1. On the second work, mice previously treated with a combination of CM-272, a G9a/DNMT inhibitor, and anti-PD-L1 displayed an enhanced immune response against tumor cells in the rechallenge with tumor cells. The analysis of the tumor microenvironment revealed that tumors from mice previously treated with the combination displayed increased infiltration of CD8+ T cells and M1-like macrophages. On the other hand, the third paper focused on the differential DNA methylation patterns found between responders and non-responders to immunotherapy in BC, highlighting the potential of DNA methylation signatures as a biomarker for selecting BC patients for ICI.

Collectively, the three different works presented in this Thesis demonstrate the intricate interplay between epigenetic mechanisms and immune responses in BC. These studies reveal the promising effects of combining epigenetic modulators and ICI, pointing out the importance of the tumor microenvironment and epigenetic marks underlying bladder tumors' response to ICI.

## Resumo

O cancro da bexiga (CB) ocupa o 10º lugar entre os cancros mais frequentes a nível mundial, sendo a 9ª causa de morte por cancro nos homens. Embora o carcinoma da bexiga não-músculo invasivo esteja associado a um melhor prognóstico, estes pacientes frequentemente têm recorrência ou progridem para estadios mais avançados da doença, como o cancro da bexiga músculo invasivo ou disseminação metastática. O uso de inibidores de checkpoints imunológicos (ICI) como anti-PD-1/PD-L1 como opção de tratamento para pacientes com CB avançado levou a uma melhoria no prognóstico. No entanto, uma parte significativa destes pacientes não apresenta benefícios clínicos significativos. A epigenética é o estudo dos mecanismos que regulam a expressão génica sem alterar a sequência do DNA. As alterações na metilação do DNA e nas modificações das histonas constituem elementos-chave que contribuem para o desenvolvimento do CB. Estas alterações afetam não só as células tumorais, mas também o microambiente tumoral, incluindo as células imunes. Compreender a complexidade do CB pode levar à descoberta de novos alvos terapêuticos e biomarcadores preditivos de resposta à terapia para melhorar o tratamento do CB. Desta forma, o principal objetivo desta Tese foi explorar a interação entre a epigenética e o sistema imune no CB avançado, visando encontrar novas abordagens terapêuticas e identificar biomarcadores preditivos de resposta à imunoterapia.

O primeiro trabalho centrou-se no potencial terapêutico de um novo inibidor de histona desacetilases (HDAC), o CM-1758, sozinho ou em combinação com ICI no CB invasivo. Os resultados dos estudos *in vitro* em linhas celulares de CB e num modelo de murganho imunocompetente de CB avançado mostraram os efeitos antitumorais do CM-1758, induzindo alterações na expressão génica, modulando a expressão do PD-L1 e reprogramando o microambiente tumoral. No segundo trabalho, murganhos previamente tratados com uma combinação de CM-272, um inibidor de G9a/DNMT, e anti-PD-L1 mostraram uma resposta imune aumentada aquando de uma segunda injeção de células tumorais. A análise do microambiente tumoral revelou um aumento na infiltração de células T CD8+ e macrófagos do tipo M1 em tumores de murganhos previamente tratados com a combinação. Por outro lado, no terceiro trabalho, foram encontrados diferentes padrões de metilação do DNA entre respondedores e não-respondedores à imunoterapia no CB, destacando o potencial da metilação do DNA como biomarcador para a seleção de pacientes com CB para o tratamento com ICI.

Coletivamente, os três trabalhos originais apresentados nesta Tese demonstram a cooperação dos mecanismos epigenéticos e das respostas imunes no CB. Estes estudos revelaram efeitos promissores da combinação de moduladores epigenéticos

com a imunoterapia, destacando a importância do microambiente tumoral e das marcas epigenéticas na resposta dos tumores da bexiga à ICI.

## Table of Contents

Declaração de honra ..... vi
Acknowledgments ..... ix
Abstract ..... xiv
Resumo ..... xv
List of Figures ..... xix
List of Tables ..... xxii
List of Abbreviations ..... xxiv
**Chapter I: General Introduction ..... 1**
Cancer: a prevailing global health challenge ..... 2
Bladder cancer ..... 3
Molecular landscape of bladder cancer ..... 9
References ..... 14
**Review paper 1: DNA methylation as a therapeutic target for bladder cancer ..... 21**
Abstract ..... 22
Keywords ..... 22
1.Introduction ..... 23
2. DNA Methylation ..... 25
3. DNMT Inhibitors ..... 28
4. DNA Methylation as a Therapeutic Target in BC ..... 33
5. Conclusions ..... 49
References ..... 50
**Review paper 2: Tackling tumor microenvironment through epigenetic tools to improve cancer immunotherapy ..... 65**
Abstract ..... 66
Keywords ..... 66
Background ..... 67
Epigenetic regulatory mechanisms ..... 68
Epigenetic regulation of immune cell function in TME ..... 70
Inhibition of epigenetic modulators as therapeutic option to modify the immunosuppressive TME ..... 81
Immunotherapy – an overview ..... 83
Epi-drugs in cancer ..... 85
Bladder cancer ..... 95
Conclusions ..... 97
References ..... 98
Supplementary Information ..... 115
**Chapter II: Aims ..... 117**

**Chapter III: Improving bladder cancer treatment: epidrugs and immunotherapy.....119**

**Research paper 1: Modulation of tumor microenvironment by targeting histone acetylation in bladder cancer..... 120**

Abstract ..... 121

Keywords..... 121

Introduction..... 122

Materials and Methods..... 123

Results ..... 132

Discussion ..... 145

References ..... 148

Supplementary Information ..... 154

**Research paper 2: Impact of G9a/DNMT inhibition in combination with immunotherapy behind an enhanced anti-tumoral response in bladder cancer upon rechallenge ..... 170**

Abstract ..... 171

Keywords..... 171

Introduction..... 172

Material and Methods ..... 173

Results ..... 178

Discussion ..... 188

References ..... 148

Supplementary Information ..... 194

**Chapter IV: Epimarkers of response to immunotherapy.....198**

**Research paper 3: Uncovering DNA methylation patterns and their impact on immunotherapy in bladder cancer..... 199**

Abstract ..... 200

Keywords..... 200

Introduction..... 201

Material and Methods ..... 202

Results ..... 204

Discussion ..... 215

References ..... 218

Supplementary Information ..... 222

**Chapter V: Major findings and challenges.....235**

**Chapter VI: General discussion and conclusions.....240**

References ..... 246

**Appendix – Original PDF files of the published papers included in the Thesis…247**

# List of Figures

## Chapter I: General Introduction

**Figure 1.** The updated hallmarks of cancer.. ..... 2
**Figure 2.** Clinical and histopathological staging of bladder cancer based on tumor invasion of the bladder wall with respective layers. ..... 5
**Figure 3.** Summary of main characteristics of each class included in the consensus for molecular classification of muscle-invasive bladder cancer (MIBC) from 2016. ..... 12

*Review paper 1*

**Figure 1.** Main epigenetic mechanisms involved in gene expression regulation. ..... 24
**Figure 2.** DNA methylation in normal and cancer cells. ..... 27
**Figure 3.** Mechanisms of action of DNA methyltransferase (DNMT) inhibitors. ..... 30
**Figure 4.** Summary of the main effects of DNMT inhibitors observed in bladder cancer in vitro and in vivo models, as well as in clinical trials. ..... 49

*Review paper 2*

**Figure 1.** DNA methylation, histone modifications and chromatin remodeling as regulatory mechanisms of epigenetic gene regulation. ..... 70
**Figure 2.** Epigenetic regulation of immune cells in the tumor microenvironment. ..... 78
**Figure 3.** Modalities of immunotherapy in bladder cancer. ..... 97

## Chapter III: Improving bladder cancer treatment: epidrugs and immunotherapy

*Research paper 1*

**Figure 1.** Cytotoxic and cytostatic effects of CM-1758 in bladder cancer cell lines. .. 133
**Figure 2.** CM-1758 effects on the transcriptomic profile of 253J, J82, RT112 and TCCSUP cells. ..... 135
**Figure 3.** Histone acetylation and DNA methylation levels after treatment with CM-1758. PD-L1 epigenetic regulation by promoter acetylation. ..... 137
**Figure 4.** *In vivo* effects of CM-1758 alone and in combination with immune checkpoint inhibitors. ..... 139
**Figure 5.** Effects of CM-1758 and immune checkpoint inhibitors in tumor lymphoid cells, the non-immune compartment and cytokine profile. ..... 142
**Figure 6.** Myeloid repertoire changes after treatment with CM-1758 and PD-L1 blockade therapy. ..... 144
**Figure S1.** Representative gating strategy for tumor T (CD4+ and CD8+) and B cells. ..... 154
**Figure S2.** Representative gating strategy for tumor myeloid cells and tumor cells .. 155

**Figure S3.** Representative gating strategy for fibroblasts, lymphatic and blood endothelial cells. ..... 156
**Figure S4.** Representative gating strategy for tumor macrophages and respective status. ..... 157
**Figure S5.** (a) Principal component analysis (PCA) graph of 253J, J82, RT112 and TCCSUP together showing the aggrupation of the conditions control vs. treated for each cell line. (b-e) Individual heatmaps of (b) 253J, (c) J82, (d) RT112 and (e) TCCSUP of the dysregulated genes between untreated control *vs.* treated cells. ..... 158
**Figure S6.** Enrichment bubble plot of (a) 253J, (b) J82, (c) RT112 and (d) TCCSUP cells for the hallmark gene signatures of GSEA analysis (e) Regulon activity profile for transcription factors hierarchically clustered. ..... 159
**Figure S7.** (a) Quantification of H3ac, H3K9ac and H3K27ac levels by western blot respect to total H3. (b) Relative expression by RT-qPCR of HDAC1 through 11 and (c) Western blot analysis of HDAC1, HDAC3, HDAC5, DNMT1, DNMT3a and DNMT3b with respective β-actin levels for 253J and J82 cells after treatment with CM-1758. (d) DNMT1, DNMT3a and DNMT3b respect to TBP for 253J and J82 cells after treatment with CM-1758..... 160
**Figure S8.** (a) CGs associated with PD-L1 expression using the Shiny Methylation Analysis Resource Tool (SMART). (b) Relative methylation levels of cg02823866 and cg14305799 in PD-L1 promoter normalized for β-actin x 1000 for easier tabulation.. 161
**Figure S9.** (a-d) Individual tumor growth curves respect to the day of 4K5 cells injection of (a) control, (b) anti-PD-L1, (c) CM-1758 and (d) CM-1758+anti-PD-L1. (e) Immunohistochemistry quantification of BrdU positive cells in the different treatment groups presented as percentage of positive cells. (f1-4) Representative immunohistochemistry staining of BrdU in each treatment group included in the study (1 – control; 2 – anti-PD-L1; 3 – CM-1758 and 4 – CM-1758 + anti-PD-L1. (g) Immunohistochemistry quantification of CD8+ T positive cells in the different treatment groups presented as cells/mm$^2$. (h-k) Spearman correlation analysis of CD8+ T cells and percentage of necrosis in (h) control, (i) anti-PD-L1, (j) CM-1758 and (k) CM-1758+anti-PD-L1 with respective Spearman's rank correlation coefficient (r). ..... 162
**Figure S10**. (a) Percentage of cancer-associated fibroblasts (CAFs) positive for α-SMA present in the tumor microenvironment gated in CD140a+ cells. (b) Relative expression by RT-qPCR of PD-L1 in respect to TBP in tumors from the groups control, anti-PD-L1, CM-1758 and CM-1758+anti-PD-L1..... 163
*Research paper 2*
**Figure 1.** Effects of anti-PD-L1, CM-272 or in combination in the 1$^{st}$ challenge. combination of both. ..... 179

**Figure 2.** Second challenge of bladder cancer cells in mice previously challenged and treated with CM-272 and/or anti-PD-L1. setting. In the 2nd challenge, mice were injected. ..... 181
**Figure 3.** Characterization of immune cell infiltrates from the 1st challenge tumors (4K5) from non-responders (NR) and responders (R) in the 2nd challenge injected with 3K20 cells. ..... 183
**Figure 4.** Analysis of the immune infiltrate in 2nd challenge tumors in growth control, control and CM-272 + anti-PD-L1 mice injected with 3K20 cells. ..... 185
**Figure 5.** Transcriptomic changes induced in 4K5 cells after treatment with CM-272. ..... 187
**Figure S1.** (a) Schematic representation of the treatment scheme used for treatment with anti-PD-L1, CM-272 and combination of both. Anti-PD-L1 (avelumab) was injected once a week, whereas CM-272 was applied for 5 consecutive days, with 2 rest days represented in orange. Surgery was performed after 15 days of the start of the treatment course. (b) Normalized individual tumor growth curves for mice in control, anti-PD-L1, CM-272 and CM-272 + anti-PD-L1 groups. Day 0 corresponds to the first day of treatment. ..... 194
**Figure S2.** Percentage from total population of infiltrating (a) leucocytes, (b) T cells, (c) CD4+ T cells, (d) CD8+ T cells, (e) B cells, (f) myeloid cells, (g) phagocytic myeloid cells, (h) tumor cells, (i) PD-L1+ myeloid cells, (j) PD-L1+ phagocytic myeloid cells, (k) PD-L1+ tumor cells, (l) macrophages, (m) macrophages M1-like, (n) macrophages transition M1/M2, (o) macrophages M2-like and (p) phagocytic macrophages. ..... 195

**Chapter IV: Epimarkers of response to immunotherapy**

*Research paper 3*
**Figure 1.** Schematic representation of the experimental setting used in this study. .. 205
**Figure 2.** Differential methylation patterns between responders and non-responders to immune checkpoint inhibitors in TURBT samples. ..... 206
**Figure 3.** Comparative methylation profiling between non-responders and responders to immunotherapy. ..... 208
**Figure 4.** Differential methylation patterns between paired TURBT and cystectomy samples. ..... 210
**Figure 5.** Comparative methylation profiling between paired TURBT and cystectomy samples.. ..... 212

**Figure 6.** Comparison of the methylation patterns of previously identified differentially methylated CpG sites in cystectomy samples of non-responders and partial responders to immunotherapy. ..... 214
**Figure S1.** Principal component analysis of paired samples of (a) CpG sites, (B) promoters and (c) CpG islands. Non-responders represented as green circles and responders as orange triangles. (d) Supervised hierarchical clustering heatmap of the 4,502 significantly different CpG sites between non-responders and complete responders in TURBT.....222
**Figure S2.** Principal component analysis of paired TURBT and cystectomy samples of (a) CpG sites, (b) promoters and (c) CpG islands. Cystectomy represented as green circles and TURBT as orange triangles.....223
**Figure S3.** Supervised hierarchical clustering heatmap of the (a) 14 promoters and (b) 27 CpG islands significantly different CpG sites between cystectomy samples from non-responders and partial responders. Supervised hierarchical clustering heatmap of the (b) 14 promoters and (e) 27 CpG islands significantly different CpG sites between TURBT and cystectomy samples from non-responders. Supervised hierarchical clustering heatmap of the (b) 14 promoters and (e) 27 CpG islands significantly different CpG sites between TURBT and cystectomy samples from partial responders.....223

# List of Tables

### Chapter I: General Introduction

**Table 1.** Summary of European Association of Urology (EAU) guidelines for surveillance of non-muscle invasive bladder cancer (NMIBC) based on risk. ..... 6

*Review paper 1*

**Table 1.** Summary of pre-clinical studies targeting DNMTs in bladder cancer (BC). ... 36

**Table 2**. Summary of combination studies targeting DNMTs in BC. ..... 40

**Table 3.** Clinical trials in BC using DNMT inhibitors. ..... 45

*Review paper 2*

**Table 1.** Cell populations contributing to the development of a favorable tumor microenvironment. ..... 79

**Table 2.** Epi-drugs approved and in clinical trial for cancer treatment, with respective effects and drug category. ..... 88

**Table 3.** Major clinical trials comprising epi-drugs and immunotherapy for cancer treatment. ..... 92

**Table S1.** Main studies comprising epigenetic drugs and biomarkers associated with immunotherapy……115

### Chapter III: Improving bladder cancer treatment: epidrugs and immunotherapy

*Research paper 1*

**Table 1.** Antitumor efficacy of anti-PD-L1, CM-1758 and CM-1758+anti-PD-L1 in comparison with the control group. ..... 140

**Table S1.** Primers' sequences for RT-qPCR, PD-L1 CUT&RUN and PD-L1 methylation (qMSP). The h before the primer's name denotes human sequence and m mouse sequence. F – Forward; R – Reverse. ..... 163

**Table S2.** Primary and secondary antibodies used for western blot, immunofluorescence, immunohistochemistry..... 164

**Table S3.** Antibodies used for cell population characterization by flow cytometry. .... 166

**Table S4.** $IC_{50}$ values for each cell line with respective standard deviation (SD). ..... 167

**Table S5.** Mean concentration (pg/mL) with respective standard deviation and fold-change with respective standard error of the mean value of each cytokine in each treatment group. GM-CSF, IL-10 and IFN-α did not show any differences compared to the control group and were not represented in Figure 5i……..167

*Research paper 2*

**Table 1.** Number and percentage of responders to the 2nd challenge with 4K5 or 3K20 in control, anti-PD-L1, CM-272 and CM-272 + anti-PD-L1 groups. Responders comprise mice that were able eliminate or control tumor growth after the second injection of tumor cells. ..... 180

**Table S1.** Antibodies with respective fluorochrome used for cell population characterization by flow cytometry. ..... 196

**Table S2.** List of genes up- and downregulated obtained from Venn Diagram analysis common to 4K5 cells treated with $IC_{50}$ dose of CM-272 for 48 h and 3K20 without any treatment in comparison with 4K5 control cells. ..... 197

**Chapter IV: Epimarkers of response to immunotherapy**

*Research paper 3*

**Table 1.** Parameters describing sample type and response to immunotherapy in the sample set. ..... 204

**Table S1.** Genes associated with the CpG sites differently methylated (hyper- and hypomethylated) in responders compared to non-responders from the Enrichr analysis using Gene Ontology (GO) dataset biological processes and MSigDB Hallmark 2020 representing some of the most cancer and immune relevant gene signatures based on the 10,000 most differently methylated CpGs sites..... 224

**Table S2.** Genes associated with the CpG sites differently methylated (hyper- and hypomethylated) in cystectomy compared to TURBT samples from the Enrichr analysis using Gene Ontology (GO) dataset biological processes and MSigDB Hallmark 2020 representing some of the most cancer and immune relevant gene signatures based on the 10,000 most differently methylated CpGs sites..... 230

**Table S3.** Genes associated with the CpG sites differently methylated (hyper- and hypomethylated) in cystectomy samples comparing non-responders and partial responders from the Enrichr analysis using Gene Ontology (GO) dataset biological processes and MSigDB Hallmark 2020 representing some of the most cancer and immune relevant gene signatures based on the 3,309 differently methylated CpGs sites..... 234

## List of Abbreviations

5-aza - 5-azacytidine

5hmC - 5-hydroxymethylcytosine

**A**

ADCC - Antibody-dependent cell-mediated cytotoxicity

AID - Activation-induced cytidine deaminase

ALOX15 - Arachidonate 15-lipoxygenase

AML - Acute myeloid leukemia

APAF-1 - Apoptotic peptidase activating factor 1

APCs - Antigen presenting cells

APM - Antigen processing and presentation machinery

APOBEC1 - Apolipoprotein B mRNA editing enzyme catalytic subunit 1

Arg1 - Arginase 1

ATCC - American type culture collection

**B**

B7-H1 - B7 homologue 1

BBN - *N*-butyl-*N*-(4-hydroxybutyl)nitrosamine)

BC - Bladder cancer

BCG - Bacillus Calmette-Guérin

BTG2 - BTG anti-proliferation factor 2

**C**

CAFs - Cancer-associated fibroblasts

CAR - Chimeric antigen receptor

CASP-3 – Caspase 3

CCND1 - Cyclin D1

CD274 - Cluster of differentiation 274

CIS - Carcinoma in situ

CK5 - Cytokeratin 5

CMML - Chronic myelomonocytic leukemia

CpG - Cytosine–phosphatidyl–guanine

COL1A2 - collagen type I alpha 2 chain

CT - Computed tomography

CTLs - Cytotoxic T cells

CTLA-4 - Cytotoxic T-lymphocyte-associated protein 4

CTCs - Circulating tumor cells

CUT&RUN - Cleavage under targets & release using nuclease

**D**

DAC - Decitabine

DAPK-1 - Death associated protein kinase 1

DCs - Dendritic cells

DKO – Double knock-out

DM – Differently methylated

DNMTs - DNA methyltransferases

DPI - Data processing inequality

**E**

EAU – European Association of Urology

ECM - Extracellular matrix

EGCG - Epigallocatechin-3-gallate

EMA - Europe Medicines Agency

EZH2 - Enhancer of zeste homolog 2

**F**

FDA - Food and Drugs Administration

FdCyd - 5'-Fluoro-2'-deoxycytidine

FELASA - Federation of European Laboratory Animal Science Associations

FFPE - Formalin-fixed paraffin-embedded

FHL1 - Four and a half LIM domains 1

FoxO1 - Forkhead box O1

**G**

GSEA - Gene set enrichment analysis

GSK3β - Glycogen synthase kinase 3 beta

GSTM1 - Glutathione S-transferase mu 1

GSVA - Gene set variation analysis

**H**

HATs - Histone acetyltransferases

HDACs - Histone deacetylases

**I**

$IC_{50}$ - Half maximal inhibitory concentration

ICI - Immune checkpoint inhibitors

IDO1 - Indoleamine 2,3-dioxygenase 1

IFN – Interferon

IL - Interleukin

ISUP - International Society of Urological Pathology

**J**

JMJD3 - Jumonji domain-containing protein D3

**K**

KDMs - Lysine demethylases

KLF4 - Kruppel-like factor 4

KRT14 - Keratin 14

**M**

MBPs - Methyl-CpG-binding proteins

MDSCs - Myeloid-derived suppressor cells

MIBC – Muscle invasive bladder cancer

MLH1 - MutL homolog 1

MMAE - Monomethyl auristatin E

MRI - Magnetic resonance imaging

mRNA - Messenger RNA

MSH3 - MutS homolog 3

MSigDB - Molecular Signature Database

MTD - Maximum tolerated dose

MVAC - Methotrexate, vinblastine, doxorubicin, and cisplatin

MyCAFs - Myofibroblast-like CAFs

**N**

NACT - Neoadjuvant chemotherapy

NK - Natural killer

NMIBC - Non-muscle invasive bladder cancer

NOTCH1 - Notch receptor 1

NR - Non-responder

**O**

Opt-tSNE - Optimization of t-Distributed Stochastic Neighbor Embedding

ORR - Objective response rate

**P**

PARP - Poly(ADP-ribose) polymerase

PBMCs - Peripheral blood mononuclear cells

PCA - Principal component analysis

PD-1 - Programmed death 1

PD-L1 - Programmed death-ligand 1

PFS - Progression-free survival

PMSF - Phenylmethylsulfonyl fluoride

PPARγ - Peroxisome proliferator-activated receptor γ

PRMT1 - Protein arginine methyltransferase 1

PTMs - Posttranslational modifications

PUNLMP - Papillary urothelial neoplasm of low malignant potential

**Q**

QC - Quality control

QKO - Quadruple-knockout

qMSP – quantitative methylation-specific PCR

**R**

R - Responder

RARβ - Retinoic acid receptor beta

RASSF1A - Ras association domain family 1 isoform A

Rb - Retinoblastoma gene

RT-qPCR - Real-time quantitative PCR

**S**

SAM - S-adenosyl methionine

SATB1 - Special AT-rich sequence binding 1

SDS-PAGE - Sodium dodecyl sulfate polyacrylamide gel electrophoresis

SECAL - Spanish Society for the Laboratory Animal Science

SMYD3 - SET and MYND Domain 3

SOCS3 - suppressor of cytokine signaling 3

SOX2 - SRY-box transcription factor 2

STAT3 - Signal transducer and activator of transcription 3

**T**

TAAs - Tumor-associated antigens

TAMs - Tumor-associated macrophages

Tap73 - tumor protein P73

TBS - Tris-buffer saline

TCGA - The Cancer Genome Atlas

TEAEs - Treatment-emergent adverse events

TECs - Tumor endothelial cells

TET - Ten-eleven translocation

TFBS - Transcription factor-binding sites

Th – T helper

THU - Tetrahydrouridine

TILs - Tumor infiltrating lymphocytes

TIMP3 - Metalloproteinase inhibitor

TME - Tumor Microenvironment

TNF - Tumor necrosis factor

Tregs - Regulatory T cells

TSA - Trichostatin A

TSGs - Tumor suppressor genes

TSS - Transcription starting site

TUR - Transurethral resection

TURBT - Transurethral resection of the bladder tumor

**W**

WHO - World Health Organization

Wif-1 - Wnt inhibitory factor 1

# *CHAPTER I*

# GENERAL INTRODUCTION

## Cancer: a prevailing global health challenge

According to the World Health Organization (WHO), cancer comprises a diverse group of diseases that can originate from virtually any organ or tissue where abnormal cells proliferate uncontrollably, potentially invading neighboring areas and metastasizing to other organs (1). Consequently, each tumor is unique in its histopathological and biological characteristics, which represents the major challenge in cancer treatment. Globally, cancer represents the first or second leading cause of death before age 70 (2). In 2020, 19.3 million of new cancer cases and 10 million deaths related to cancer were reported. Breast cancer is the most diagnosed cancer worldwide, followed by lung and colorectal cancers. Lung cancer represents the major cause of death by cancer, with colorectal and liver cancers raking as second and third, respectively (3).

Tumorigenesis is a multistep process that drive the transformation of normal cells into a malignant state. For that, various features and pathways of normal cells must undergo alterations, commonly referred to as the hallmarks of cancer (4). In the first Hallmarks of Cancer proposed by Hanahan and Weinberg in 2000, only 6 hallmarks were considered, including evading apoptosis, self-sufficiency in growth signals, insensitivity to anti-growth signals, limitless replicative potential, sustained angiogenesis and tissue invasion & metastasis (4). Nevertheless, with the advances made on cancer research, several other hallmarks were added in the following years. These include deregulating cellular energetics, genome instability and mutation, avoiding immune destruction, tumor-promoting inflammation and, more recently, unlocking phenotypic plasticity, senescent cells, polymorphic microbiomes and nonmutational epigenetic reprogramming (5, 6). Cancer is a dynamic and evolving disease, shaped by the intricate process of overcoming the hallmarks of cancer.

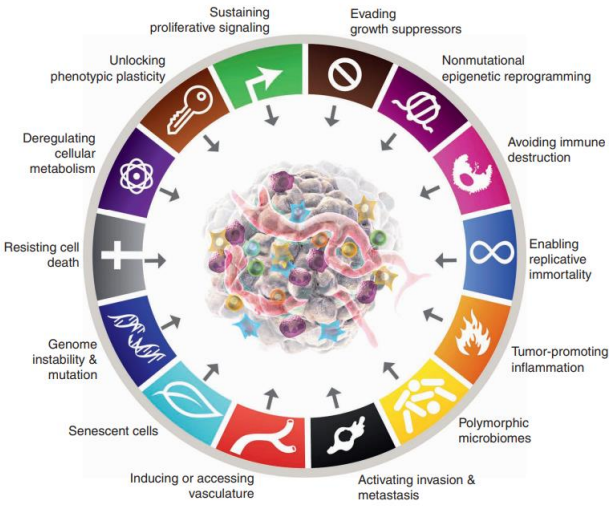


**Figure 1.** The updated hallmarks of cancer. Adapted from (6).

## Bladder cancer

### *Epidemiology and risk factors of bladder cancer*

The urinary bladder is an organ composed of singular layers of muscle that serves as a temporary storage vessel for urine—a liquid that harbors diverse waste compounds filtered by the kidneys (7). The urothelium is the innermost stratified epithelium of the bladder consisting of a basal layer (outer layer), an intermediate layer and an apical layer, where the luminal cells are located (topmost layer of the urothelium) (7). The urothelium is covered by the lamina propria, muscle layer and a surrounding layer of perivesical fat, forming the outermost layer of the urinary bladder (7).

Bladder cancer (BC) is the 10$^{th}$ most common cancer worldwide (3) with 573,000 new BC cases and 213,000 deaths related to BC in 2020 (8). BC is about four times more frequent in men (9.5 per 100,000 males) than in women (2.4 per 100,000 females) (9), making it the 6$^{th}$ more common in men and the 9$^{th}$ cause of death in men by cancer (3). The median age of BC patients is 70 years-old, however BC can appear at any age (10). Additionally, BC incidence varies worldwide, with Southern Europe, Western Europe and North America showing the highest rates (3). Nevertheless, Northern Africa and Southern Europe display the highest mortality rates by BC (3). The variations observed in BC incidence and mortality is likely due to factors such as tobacco, occupational exposures, and economic development, since industrialized countries display high incidence but lower mortality rates due to a higher availability of information related to BC detection, risk factors and treatments (11).

Tobacco smoking remains the main risk factor for BC, contributing to approximately half of all cases and associating with a 3x increase in the risk of developing BC in comparison with non-smokers (12). As it is known, tobacco contains carcinogens responsible for DNA damage, resulting in neoplastic transformation of normal bladder cells (13). Indeed, since the bladder is a reservoir of urine, carcinogens are in direct contact with the bladder wall, prompting the formation of cancer cells. Furthermore, tobacco smoking also has an impact on the treatment outcomes, associating with worst overall survival and an increase on metastatic dissemination (11, 14). Interestingly, e-cigarette smokers displayed a high concentration of carcinogenic compounds in urine associated with BC (15). Following tobacco smoking, occupational exposure to carcinogens lists as the second risk factor, responsible for 10% of all bladder tumors (12). Occupational exposure to dye, rubber, metal, petroleum, and hairdressers/barbers represents the main risk (12). Other risk factors include air pollution, genetic susceptibility such as Lynch syndrome (16), diet, gender differences, *i.e.*, females are more likely to be diagnosed with muscle invasive bladder cancer (MIBC) than males (11, 12, 17).

***Diagnosis, tumor staging and grading***

The main symptom associated with BC is the presence of hematuria in the urine. Other symptoms include frequent urination, dysuria, and high rate of urinary infections (18). Patients with suspected BC are proposed to do a cystoscopy (endoscopic evaluation of the bladder) and if a suspicious lesion is found, either a biopsy or transurethral resection of the bladder tumor (TURBT) is performed (19). If a BC diagnosis is confirmed, imaging is frequently the next step to complement the initial diagnosis evaluating the locoregional extension of the tumor and the presence of distant metastasis. These include ultrasound, computed tomography (CT) and magnetic resonance imaging (MRI) (18).

The staging of BC follows the TNM (tumor, node, and metastasis) classification (20). Bladder tumors origin from the urothelium layer and, with progression, invade through the lamina propria, muscle and fat layers (Figure 2). Then, tumors can invade adjacent organs including prostate, uterus, vagina, and abdomen and can also spread to distant organs such as liver, lungs, and bones (21). About 75% of BC are classified as non-muscle invasive bladder cancer (NMIBC), confined to the urothelium (Ta or Tis) or lamina propria (T1) (Figure 2). Ta denotes noninvasive papillary urothelial carcinomas, where histological grade is the most important factor for prognosis, being high grade and Tis urothelial carcinoma *in situ* (CIS) associated with poor prognosis (20, 22). On the other hand, 25% of BC cases are diagnosed as MIBC, invading the muscle layer (T2), the fat layer (T3) or other organs beyond the perivesical fat (T4) (Figure 2) (20). The N stage accounts for the invasion of the regional lymph nodes considering the number of nodes with metastasis (single lymph node – N1; multiple lymph nodes – N2) and the site of metastasis (metastasis in a common iliac lymph node – N3) (20). M stage is subdivided in M0 (no distant metastasis), M1a accounting for lymph node metastasis beyond common iliac and M1b in distant organs (20).

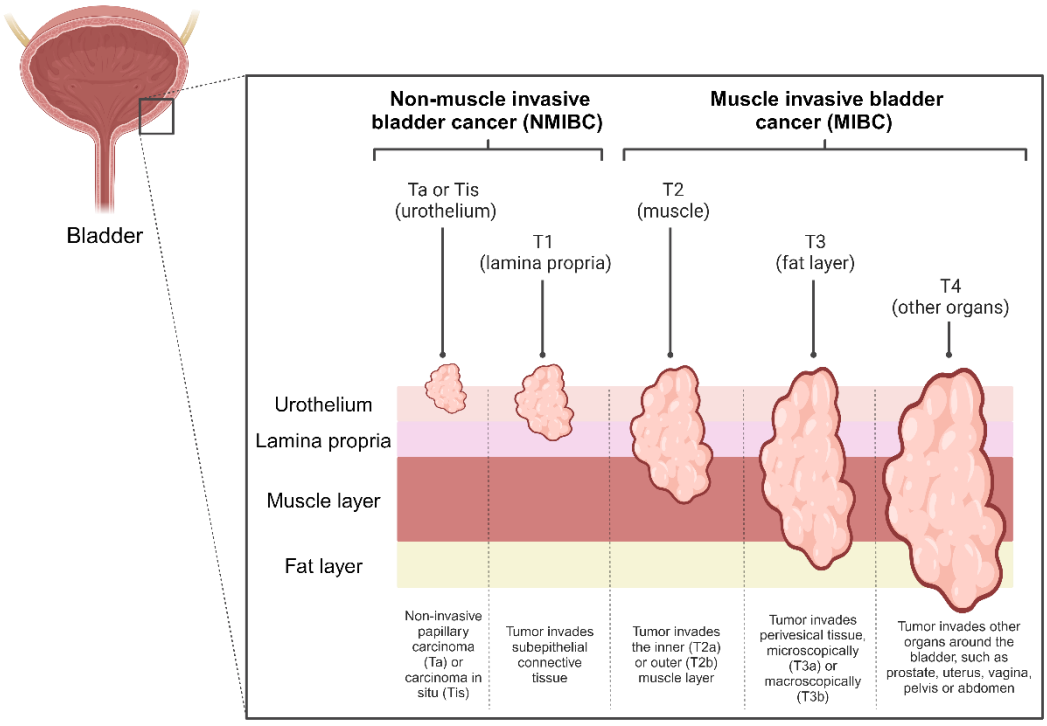


**Figure 2.** Clinical and histopathological staging of bladder cancer based on tumor invasion of the bladder wall with respective layers. Created with BioRender.com. Nunes SP, unpublished.

Histologically, approximately 75% of the BC are pure urothelial carcinomas, whereas the remaining 25% comprise other histological variants including squamous cell carcinoma accounting for 5% of all bladder tumors, glandular including adenocarcinoma, and neuroendocrine carcinoma (23). In this Thesis, the terms “bladder cancer (BC)” and “urothelial carcinoma” will be used as synonyms. Since bladder tumors are highly heterogenous in its morphology, several grading systems have been proposed based on tumors’ histological characteristics such as cell atypia, growth pattern and mitotic activity. The most frequent grading system used in clinical practice is the WHO/International Society of Urological Pathology (ISUP) grading system from 2016 and first proposed in 1973 (24). Tumors can be divided in three categories: papillary urothelial neoplasm of low malignant potential (PUNLMP), low grade and high grade (24). This classification is particularly important in NMIBC to define risk of recurrence/progression of the disease, having implications in treatment options and management (25).

Thus, surveillance of BC patients depends on the pathological evaluation of the tumors’ invasion and grade. Regarding NMIBC, patients can be classified according to risk stratification. All NMIBC should be submitted to cystoscopy and urine cytology at regular times depending on the risk category defined by the histopathological characteristics of the tumors (Table 1). In contrast, MIBC should be submitted to imaging

examination in regular intervals of time for monitoring of recurrence/progression or distant metastasis (26).

**Table 1.** Summary of European Association of Urology (EAU) guidelines for surveillance of non-muscle invasive bladder cancer (NMIBC) based on risk (26).

| Risk category | Definition | Surveillance |
|---|---|---|
| **Low risk** | Ta, G1 (PUNLMP, low-grade), <3 cm, no CIS | Cystoscopy at 3 and 12 months. Once a year for 5 years, discharge if disease-free at 5 years |
| **Intermediate risk** | All tumors not classified as low or high risk | 1st and 2nd years – cystoscopy and cytology every 3-12 months<br>3rd and 4th years – cystoscopy and cytology every 6-12 months<br>After 5th year – lifelong cystoscopy and cytology every 12 months<br>Upper tract imaging every 1-2 years |
| **High risk** | T1 tumors, G3 (high-grade) CIS, multiple and recurrent and large (>3 cm) ta G1/2 tumors | 1st and 2nd years – cystoscopy and cytology every 3 months<br>3rd and 4th years – cystoscopy and cytology every 6 months<br>After 5th year – cystoscopy and cytology every 6-12 months<br>Upper tract imaging every 1-2 years |

***Bladder cancer management***

The approach to treat BC depends on stage, histopathology, and grade of the disease when it is detected (19). Currently, TURBT is the first line of treatment for BC having a dual role as a diagnosis and treatment technique to ensure a complete tumor resection of endoscopically evident tumors and to contribute to the definition of a pathological diagnosis (27). Regarding the management of NMIBC, intravesical chemotherapy is recommended for low and intermediate-risk disease with mitomycin c, anthracyclines, and gemcitabine (19). Alternatively, Bacillus Calmette-Guerin (BCG) instillations are used as an adjuvant option after TURBT for high-risk NMIBC patients, *i.e.* with high probability of recurrence/progression (19). BCG one of the earliest forms of immunotherapy approved for cancer treatment, tracing back to the early 20th century and originally being developed as a vaccine for tuberculosis by Albert Calmette and Camille Guérin (28). In the 1970s, it was shown that BCG can induce both an immune response against BC and direct toxicity in cancer cells (29). Subsequent clinical trials showcased BCG's actions to reduce BC recurrence and progression, establishing it as a cornerstone in the management of superficial bladder tumors (30). Nevertheless, new approaches

have been proposed for BCG unresponsive patients, including combining intravesical BCG with pembrolizumab (31) and an intravesical drug delivery system releasing gemcitabine in the bladder over several days (TAR-200) (32).

MIBC management employs more aggressive treatments and requires a multidisciplinary approach (33). Radical cystectomy remains the standard treatment for localized MIBC and high-risk NMIBC with BCG failure (33). Neoadjuvant chemotherapy has been shown to increase overall survival, improving success rates of radical cystectomy (34), whereas adjuvant chemotherapy is administered in patients with pT3/4 disease and lymphatic dissemination (33). However, around 5-10% of BC patients are diagnosed with metastatic disease initially, and following treatment, roughly 50% of those with MIBC experience progression, involving spread to the lymph nodes, bones, lungs, liver, and peritoneum (33). In this case, chemotherapy remains the primary choice of treatment with cisplatin, gemcitabine or methotrexate, vinblastine, doxorubicin, and cisplatin (MVAC) chemotherapy regimen (19). In patients that are not eligible for first-line treatment with chemotherapy, immunotherapy with immune checkpoint inhibitors (ICI) is recommended (19). The pan-FGFR tyrosine kinase inhibitor (FGFR1-4) is recommended as an alternative to ICI in relapsed advanced or metastatic BC patients having genetic alterations in FGFR (19). Recently, the combination of enfortumab vedotin with pembrolizumab was approved by the Food and Drugs Administration (FDA) for locally advanced or metastatic ineligible for cisplatin (35). Enfortumab vedotin is an antibody-drug conjugate targeting nectin-4 chemically linked to monomethyl auristatin E (MMAE), an inhibitor of tubulin polymerization (36). Nevertheless, a significant percentage of BC patients do not present significant benefits from the current therapies' options, leading to a high recurrence and progression rate in these patients and requiring extended follow-up periods. Introducing novel therapeutic approaches that yield improved outcomes for BC patients would not just enhance overall survival rates but also mitigate the costs linked to BC treatments.

### *Immune checkpoint inhibitors in bladder cancer*

The history of immunotherapy dates back to the late 19$^{th}$ century when William Coley observed that bacterial infections led to tumor regression in some patients (37). The discovery of T and B cells (38), monoclonal antibodies in the 1970s (39), cytokines therapies (40) and the ICI in the 2000s transformed cancer treatment (41). Recently, the development of chimeric antigen receptor (CAR) T-cell therapy (42) and personalized vaccines (43) continue to shape the landscape of cancer immunotherapy, offering new

promising alternatives for targeted and durable responses against various cancers. Nevertheless, the focus of this Thesis will be on ICI.

The concepts of immune checkpoints and cancer immunoediting are closely related and the basis for immunotherapy with ICI in cancer (44). The hypothesis of cancer immunoediting implies 3 phases: elimination, equilibrium, and escape (45). At first, transformed neoplastic cells are recognized by the immune system – elimination phase. Nevertheless, when not all the transformed cells are eliminated, a selection of clones with low immunogenicity progressively more resistant to the immune system actions occurs – equilibrium phase. After that, an immunosuppressive microenvironment is created, impairing the host immune system, and leading to tumor growth – escape (45). One of the main mechanisms associated with the escape is the upregulation of immune checkpoints by the tumor, "turning off" the immune system against cancer cells (46). Immune checkpoints include the molecular pathways that are crucial regulators of the immune response to maintain immune balance by preventing excessive immune activation and controlling self-tolerance (47). In a tumor context, cancer cells upregulate these checkpoints in order to evade immune surveillance (47). Key checkpoint molecules include cytotoxic T-lymphocyte-associated protein 4 (CTLA-4) and programmed cell death protein 1 (PD-1) with its respective ligand programmed death-ligand 1 (PD-L1) (48). With the activation of these checkpoints, the function of immune cells and, in particular T cells, is impaired, allowing for tumor escape and growth (48). The understanding of these mechanisms led to the discovery of the immune checkpoint inhibitors which revolutionized the cancer treatment and culminated in the 2018 Nobel Prize in Physiology or Medicine to James P. Allison and Tasuku Honjo (49). Specifically, the authors found that the blockage of CTLA-4 and PD-1 augmented the immune response against cancer cells (41, 50, 51). Their collective efforts led the way for a paradigm shift in cancer treatment, offering better outcomes for patients across various malignancies.

PD-1 is a 55 kDa transmembrane protein expressed on immune cells including T cells, natural killer (NK), B lymphocytes, macrophages, dendritic cells, and monocytes (52). Transcription factors such as NFAT, NOTCH, FOXO1 and IRF9 can trigger PD-1 expression, as well promoter demethylation (53). PD-L1, also known as cluster of differentiation 274 (CD274) or B7 homologue 1 (B7-H1), is a 33kDa glycoprotein expressed by macrophages, dendritic cells and non-immune cells including epithelial, endothelial and tumor cells (54). In a physiological context, PD-1/PD-L1 expression is associated with chronic inflammation and in preventing further damage in peripheral tissues of inflammation sites (55). When a T cell recognizes an antigen, inflammatory cytokines are produced, which leads to an increase of both PD-1 and PD-L1 expression,

functioning as immune checkpoints and contributing to immune tolerance (56). In contrast, tumor cells use the PD-1/PD-L1 axis as a mechanism to escape anti-tumoral immune responses, protecting themselves from cytotoxic CD8+ T cells-mediated death (57). Additionally, the population of regulatory T cells is also increased as well as the myeloid-derived suppressor cells population (MDSCs), contributing to the immunosuppression of the tumor microenvironment (TME) (58).

The blockage of immune checkpoints PD-1 or PD-L1 counteracts immune suppression and restores the anti-tumoral immune response (47). Currently, ICI is approved for treatment in a wide range of cancers, including melanoma, lung cancer, renal cell carcinoma, head and neck cancer and BC (59). Urothelial carcinoma is described as an immunogenic or “hot” tumor with several types of tumor-immune cells reported as infiltrating the TME (47, 60). Furthermore, BC is associated with a high mutational load ranking as the one of the more mutagenic tumors (61) and bladder tumors display an expression of PD-L1 in tumor or immune cells ranging from 32% to 66% (62, 63). High PD-L1 expression associated with poor overall survival, higher tumor stage and presence of distant metastasis in BC (64), making urothelial carcinomas a potential target for ICI using PD-1/PD-L1 antibodies (47). Indeed, several ICI targeting PD-1/PD-L1 have been approved for treatment of BC. Firstly, atezolizumab, durvalumab and avelumab are anti-PD-L1 approved by FDA and European Medicines Agency (EMA) for treatment of locally advanced or metastatic urothelial carcinoma for patients PD-L1 positive that are not eligible for cisplatin-based chemotherapy (19, 47, 65). In line, pembrolizumab and nivolumab block PD-1 and are also approved by FDA and EMA for advanced and metastatic urothelial carcinoma (19, 47). Several ongoing clinical trials are currently assessing the effects of combining different ICIs (66), the combination of ICIs with other therapies (67) and ICIs in a neoadjuvant setting (68).

Despite the increase on overall survival observed in BC patients with the implementation of immunotherapy (69), a substantial percentage of patients (17-26%) show limit clinical benefit from ICI (70). Understanding the mechanisms behind the lack of response to ICI and finding reliable biomarkers that can correctly predict and better select patients that will benefit from ICI is pivotal.

## Molecular landscape of bladder cancer

### *Genomic alterations in bladder cancer*

The development of BC is associated with a wide array of genomic aberrations. The first genetic alteration associated with transformation of the normal urothelium is the

loss of heterozygosity of chromosome 9 (71). Then, two major molecular pathways have been described for the development of BC: the papillary and non-papillary pathways (72). Specifically, the papillary pathway is associated with low-grade NMIBC development and frequent recurrences, however low rates of progression. This pathway arises from the mutually exclusive activating mutations of *FGFR3* or *RAS*, activating the RTK/RAS/RAF/MAPK signaling pathway. *FGFR3* mutations are found in 80% of low-grade NMIBC, and 30% of high-grade NMIBC, being associated with a favorable prognosis (73, 74). On the same note, mutations on the PIK3K/AKT/mTOR pathway, namely on *PIK3CA*, are frequently found in BC and have an additive oncogenic effect with *FGFR3* or *RAS* mutations, leading to the formation of low-grade urothelial carcinoma (75). Remarkably, a significant percentage of the normal bladder tissue displayed the same *PIK3CA* mutations as the corresponding tumor, showing that *PIK3CA* mutations are important for the cancerization process (76). Furthermore, NMIBC patients with mutations in the *PIK3CA* gene displayed a reduced rate of recurrence, which associates with a decrease of EZH2 levels in non-muscle invasive tumors, a known indication of poor prognosis in BC (77). In contrast, the non-papillary pathway is associated with *TP53* and *RB1* mutations. These mutations lead to the formation of dysplasia or CIS from those mutations, resulting in high-grade urothelial carcinoma. Mutation on *TP53* and *RB1* are also thought to be responsible for the progression from recurrent low-grade urothelial carcinoma to high-grade and, ultimately, MIBC (73, 78).

Contrary to what is observed in NMIBC, muscle-invasive tumors rank high in the frequency of somatic mutations, only surpassed by lung cancer and melanoma (61). As expected, invasive bladder tumors have high frequency of mutated *TP53* and *RB1*, but also *PTEN* and *ERBB2* (73, 79). About 89% of the invasive tumors have mutations on chromatin-modifying genes such as *ARID1A*, *KDM6A*, *KMT2D*, and *EP300* (73). Interestingly, *KMT2D* and *KDM6A* were found to be frequently mutated in normal urothelium, in contrast with the low occurrence of *PIK3CA* and *FGFR3* mutations, demonstrating that epigenetic mechanisms play a pivotal a role in clonal expansion contributing to BC development (80).

### *Molecular subtypes of bladder cancer*

In order to improve risk stratification and provide possible personalized treatment approaches for BC patients, efforts were made to categorize bladder tumors into different molecular subtypes based on molecular alterations using whole exome sequencing and transcriptomic approaches. The UNC classification into luminal or basal of muscle-invasive bladder tumors is widely accepted (81). Luminal describes tumors that express

epithelial luminal markers (uroplakin 3, cytokeratin 20, GATA3 and FOXA1), whereas basal includes the tumors expressing basal markers including cytokeratin 5 and cytokeratin 14 (72). A study performed in Lund University identified 5 subtypes of urothelial carcinoma: urobasal A, genomically unstable, urobasal B, SCC-like, and infiltrated. Urobasal A tumors associated with good prognosis, whereas the urobasal B and genomically unstable group were characterized by high frequency of *FGFR3* and *TP53* mutations, respectively (82). Another classification was proposed on 2014 using data from The Cancer Genome Atlas (TCGA) from 131 urothelial carcinomas: Cluster I and Cluster II, both displaying a luminal phenotype, and Cluster III and Cluster IV with basal characteristics (73). Nevertheless, this molecular classification was updated in 2017 to include a wider characterization of MIBC. Muscle-invasive tumors were divided in 5 groups: luminal, luminal-infiltrated, luminal-papillary, positive for KRT20, GATA3 and FOXA1, basal-squamous (KRT5,6,14+, GATA3- and FOXA1-), and neuronal (83). Having all this data and more into account, a consensus molecular classification of MIBC was published in 2019 identifying 6 different molecular subtypes: luminal papillary (24%), luminal non-specified (8%), luminal unstable (15%), stroma-rich (15%), basal/squamous (35%), and neuroendocrine-like (3%). Basal/squamous and neuroendocrine-like displayed the worst overall survival (84). Molecular subtyping of BC allows for an in-depth assessment of the tumors' biology, potentially offering crucial direction in BC management as a complement to the pathological evaluation. Nevertheless, factors such as obtaining good quality samples, tumor plasticity (spontaneous or induced by treatments) and the intra-tumoral heterogeneity represent significant challenges to this day. The possible inclusion of novel high-throughput techniques such as single-cell data could help overcome some of these obstacles.

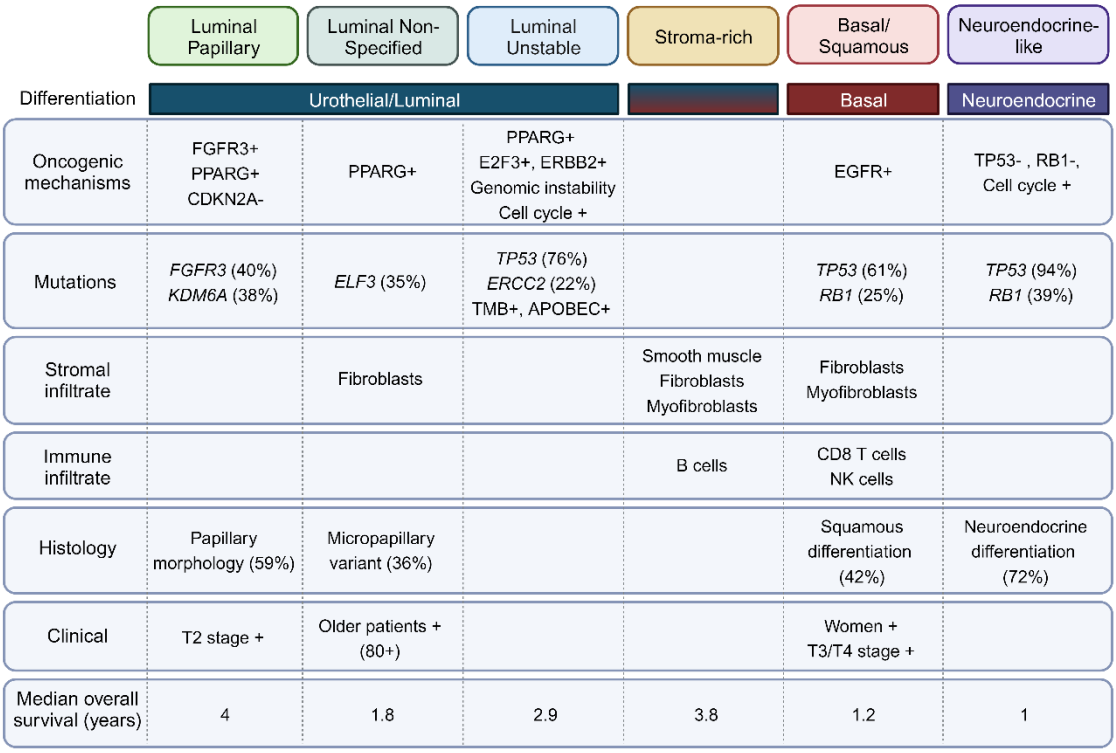


**Figure 3.** Summary of main characteristics of each class included in the consensus for molecular classification of muscle-invasive bladder cancer (MIBC) from 2016. Adapted from (84). Created with Biorender.com.

### *Epigenetic alterations*

Epigenetics is defined as the study of the mechanisms that change gene expression without altering the DNA sequence. Epigenetic marks are preserved during cell division and can be passed onto new generations (85). DNA methylation, histone post-translational modifications, histone variants and chromatin remodeling complexes constitute the main epigenetic mechanisms described (86). Other RNA-associated molecules such as microRNAs and non-coding RNAs, often categorized as epigenetic mechanisms or epitranscriptomics, will not be included in this Thesis. These processes play a pivotal role in regulating normal processes of the cell by regulating gene expression and maintaining cellular identity (87). Nonetheless, aberrant epigenetic marks contribute to cancer development, being recently added as a hallmark of cancer (6), as mentioned before. Particularly, alterations in epigenetic mechanisms drive the process of carcinogenesis in BC, affecting not only tumor cells, but also the immune and non-immune compartment (86). Thus, numerous studies have focused on the effects of epigenetic alterations in BC TME and how these can be used as therapeutic targets and biomarkers to detect or define response to therapy in BC. These topics will be the focus of the 2 review papers included in this Thesis. The first review extensively explores the

therapeutic potential of targeting DNA methylation in BC (**Review paper 1**). It offers a comprehensive summary of key findings derived from *in vitro*, *in vivo*, and clinical trial studies on this subject (**Review paper 1**). On the other hand, the second review paper explores the role of epigenetic mechanisms on the immune compartment of the TME, highlighting epigenetics in the context of immunotherapy and the use of epigenetic drugs on cancer treatment (**Review paper 2**).

**References**


1. (WHO) WHO. Overview of cancer 2023 [Available from: https://www.who.int/health-topics/cancer#tab=tab_1].
2. Bray F, Laversanne M, Weiderpass E, Soerjomataram I. The ever-increasing importance of cancer as a leading cause of premature death worldwide. Cancer. 2021;127(16):3029-30.
3. Sung H, Ferlay J, Siegel RL, Laversanne M, Soerjomataram I, Jemal A, et al. Global Cancer Statistics 2020: GLOBOCAN Estimates of Incidence and Mortality Worldwide for 36 Cancers in 185 Countries. CA Cancer J Clin. 2021;71(3):209-49.
4. Hanahan D, Weinberg RA. The hallmarks of cancer. Cell. 2000;100(1):57-70.
5. Hanahan D, Weinberg RA. Hallmarks of cancer: the next generation. Cell. 2011;144(5):646-74.
6. Hanahan D. Hallmarks of Cancer: New Dimensions. Cancer Discov. 2022;12(1):31-46.
7. Khandelwal P, Abraham SN, Apodaca G. Cell biology and physiology of the uroepithelium. Am J Physiol Renal Physiol. 2009;297(6):F1477-501.
8. Ferlay J, Colombet M, Soerjomataram I, Parkin DM, Piñeros M, Znaor A, et al. Cancer statistics for the year 2020: An overview. Int J Cancer. 2021.
9. Lobo N, Afferi L, Moschini M, Mostafid H, Porten S, Psutka SP, et al. Epidemiology, Screening, and Prevention of Bladder Cancer. Eur Urol Oncol. 2022;5(6):628-39.
10. Greiman AK, Rosoff JS, Prasad SM. Association of Human Development Index with global bladder, kidney, prostate and testis cancer incidence and mortality. BJU Int. 2017;120(6):799-807.
11. Lobo N, Afferi L, Moschini M, Mostafid H, Porten S, Psutka SP, et al. Epidemiology, Screening, and Prevention of Bladder Cancer. Eur Urol Oncol. 2022.
12. Jubber I, Ong S, Bukavina L, Black PC, Compérat E, Kamat AM, et al. Epidemiology of Bladder Cancer in 2023: A Systematic Review of Risk Factors. Eur Urol. 2023;84(2):176-90.
13. Stern MC, Lin J, Figueroa JD, Kelsey KT, Kiltie AE, Yuan JM, et al. Polymorphisms in DNA repair genes, smoking, and bladder cancer risk: findings from the international consortium of bladder cancer. Cancer Res. 2009;69(17):6857-64.
14. Cacciamani GE, Ghodoussipour S, Mari A, Gill KS, Desai M, Artibani W, et al. Association between Smoking Exposure, Neoadjuvant Chemotherapy Response and Survival Outcomes following Radical Cystectomy: Systematic Review and Meta-Analysis. J Urol. 2020;204(4):649-60.

15. Fuller TW, Acharya AP, Meyyappan T, Yu M, Bhaskar G, Little SR, et al. Comparison of Bladder Carcinogens in the Urine of E-cigarette Users Versus Non E-cigarette Using Controls. Sci Rep. 2018;8(1):507.
16. Skeldon SC, Semotiuk K, Aronson M, Holter S, Gallinger S, Pollett A, et al. Patients with Lynch syndrome mismatch repair gene mutations are at higher risk for not only upper tract urothelial cancer but also bladder cancer. European urology. 2013;63(2):379-85.
17. Viswambaram P, Hayne D. Gender discrepancies in bladder cancer: potential explanations. Expert Rev Anticancer Ther. 2020;20(10):841-9.
18. Gharbieh S, Omar K, Thurairajah R, Khan MS, Nair R. Diagnosis and Clinical Staging. In: Singh P, Nayak B, Panaiyadiyan S, editors. A Guide to Management of Urological Cancers. Singapore: Springer Nature Singapore; 2023. p. 113-24.
19. Powles T, Bellmunt J, Comperat E, De Santis M, Huddart R, Loriot Y, et al. Bladder cancer: ESMO Clinical Practice Guideline for diagnosis, treatment and follow-up☆. Annals of Oncology. 2022;33(3):244-58.
20. Amin MB, Edge SB, Greene FL, Byrd DR, Brookland RK, Washington MK, et al. AJCC Cancer Staging Manual: Springer International Publishing; 2018.
21. Sanli O, Dobruch J, Knowles MA, Burger M, Alemozaffar M, Nielsen ME, et al. Bladder cancer. Nature Reviews Disease Primers. 2017;3(1):17022.
22. Babjuk M, Burger M, Capoun O, Cohen D, Compérat EM, Escrig JLD, et al. European Association of Urology guidelines on non–muscle-invasive bladder cancer (Ta, T1, and carcinoma in situ). European urology. 2022;81(1):75-94.
23. Moschini M, D'Andrea D, Korn S, Irmak Y, Soria F, Compérat E, et al. Characteristics and clinical significance of histological variants of bladder cancer. Nat Rev Urol. 2017;14(11):651-68.
24. Humphrey PA, Moch H, Cubilla AL, Ulbright TM, Reuter VE. The 2016 WHO Classification of Tumours of the Urinary System and Male Genital Organs-Part B: Prostate and Bladder Tumours. Eur Urol. 2016;70(1):106-19.
25. Kurth K-H, Sylvester RJ. Prognostic factors in non–muscle-invasive bladder tumors: i. clinical prognostic factors: a review of the experience of the eortc genito-urinary group II. Biologic prognostic markers. European urology supplements. 2007;6(14):789-99.
26. Witjes JA, Bruins HM, Cathomas R, Compérat EM, Cowan NC, Gakis G, et al. European Association of Urology guidelines on muscle-invasive and metastatic bladder cancer: summary of the 2020 guidelines. European urology. 2021;79(1):82-104.

27. Regmi SK. Management of Non-Muscle Invasive Bladder Cancer. In: Singh P, Nayak B, Panaiyadiyan S, editors. A Guide to Management of Urological Cancers. Singapore: Springer Nature Singapore; 2023. p. 141-52.
28. Hawgood BJ. Albert Calmette (1863-1933) and Camille Guérin (1872-1961): the C and G of BCG vaccine. J Med Biogr. 2007;15(3):139-46.
29. Pettenati C, Ingersoll MA. Mechanisms of BCG immunotherapy and its outlook for bladder cancer. Nature reviews urology. 2018;15(10):615-25.
30. Sylvester RJ, van der MEIJDEN AP, Lamm DL. Intravesical bacillus Calmette-Guerin reduces the risk of progression in patients with superficial bladder cancer: a meta-analysis of the published results of randomized clinical trials. The Journal of urology. 2002;168(5):1964-70.
31. Kamat AM, Shore N, Hahn N, Alanee S, Nishiyama H, Shariat S, et al. KEYNOTE-676: Phase III study of BCG and pembrolizumab for persistent/recurrent high-risk NMIBC. Future Oncology. 2020;16(10):507-16.
32. Necchi A, Jacob J, Daneshmand S, Simone G, Xylinas E, Morris D, et al. LBA105 Results from SunRISe-1 in patients (Pts) with bacillus Calmette–Guérin (BCG)-unresponsive high-risk non–muscle-invasive bladder cancer (HR NMIBC) receiving TAR-200 monotherapy. Annals of Oncology. 2023;34:S1343-S4.
33. Hayes J, Chhaya S, Manning H, Ng K, Sharma A, Vasdev N. Management of MIBC. In: Singh P, Nayak B, Panaiyadiyan S, editors. A Guide to Management of Urological Cancers. Singapore: Springer Nature Singapore; 2023. p. 153-67.
34. Vale C. Neoadjuvant chemotherapy in invasive bladder cancer: a systematic review and meta-analysis. The Lancet. 2003;361(9373):1927-34.
35. Hoimes CJ, Flaig TW, Milowsky MI, Friedlander TW, Bilen MA, Gupta S, et al. Enfortumab Vedotin Plus Pembrolizumab in Previously Untreated Advanced Urothelial Cancer. J Clin Oncol. 2023;41(1):22-31.
36. Maas M, Stühler V, Walz S, Stenzl A, Bedke J. Enfortumab vedotin–next game-changer in urothelial cancer. Expert Opinion on Biological Therapy. 2021;21(7):801-9.
37. McCarthy EF. The toxins of William B. Coley and the treatment of bone and soft-tissue sarcomas. Iowa Orthop J. 2006;26:154-8.
38. Crotty S. A brief history of T cell help to B cells. Nat Rev Immunol. 2015;15(3):185-9.
39. Köhler G, Milstein C. Continuous cultures of fused cells secreting antibody of predefined specificity. Nature. 1975;256(5517):495-7.
40. Vilcek J, Feldmann M. Historical review: Cytokines as therapeutics and targets of therapeutics. Trends Pharmacol Sci. 2004;25(4):201-9.

41. Leach DR, Krummel MF, Allison JP. Enhancement of Antitumor Immunity by CTLA-4 Blockade. Science. 1996;271(5256):1734-6.
42. Albelda SM. CAR T cell therapy for patients with solid tumours: key lessons to learn and unlearn. Nat Rev Clin Oncol. 2023.
43. Katsikis PD, Ishii KJ, Schliehe C. Challenges in developing personalized neoantigen cancer vaccines. Nat Rev Immunol. 2023.
44. Gubin MM, Vesely MD. Cancer Immunoediting in the Era of Immuno-oncology. Clin Cancer Res. 2022;28(18):3917-28.
45. Dunn GP, Bruce AT, Ikeda H, Old LJ, Schreiber RD. Cancer immunoediting: from immunosurveillance to tumor escape. Nat Immunol. 2002;3(11):991-8.
46. Gubin MM, Vesely MD. Cancer Immunoediting in the Era of Immuno-oncology. Clinical Cancer Research. 2022;28(18):3917-28.
47. Siefker-Radtke A, Curti B. Immunotherapy in metastatic urothelial carcinoma: focus on immune checkpoint inhibition. Nat Rev Urol. 2018;15(2):112-24.
48. He X, Xu C. Immune checkpoint signaling and cancer immunotherapy. Cell Res. 2020;30(8):660-9.
49. Huang PW, Chang JW. Immune checkpoint inhibitors win the 2018 Nobel Prize. Biomed J. 2019;42(5):299-306.
50. Iwai Y, Ishida M, Tanaka Y, Okazaki T, Honjo T, Minato N. Involvement of PD-L1 on tumor cells in the escape from host immune system and tumor immunotherapy by PD-L1 blockade. Proc Natl Acad Sci U S A. 2002;99(19):12293-7.
51. Agata Y, Kawasaki A, Nishimura H, Ishida Y, Tsubata T, Yagita H, et al. Expression of the PD-1 antigen on the surface of stimulated mouse T and B lymphocytes. Int Immunol. 1996;8(5):765-72.
52. Ahmadzadeh M, Johnson LA, Heemskerk B, Wunderlich JR, Dudley ME, White DE, et al. Tumor antigen-specific CD8 T cells infiltrating the tumor express high levels of PD-1 and are functionally impaired. Blood. 2009;114(8):1537-44.
53. Salmaninejad A, Valilou SF, Shabgah AG, Aslani S, Alimardani M, Pasdar A, et al. PD-1/PD-L1 pathway: Basic biology and role in cancer immunotherapy. J Cell Physiol. 2019;234(10):16824-37.
54. Sharpe AH, Wherry EJ, Ahmed R, Freeman GJ. The function of programmed cell death 1 and its ligands in regulating autoimmunity and infection. Nat Immunol. 2007;8(3):239-45.
55. Fife BT, Bluestone JA. Control of peripheral T-cell tolerance and autoimmunity via the CTLA-4 and PD-1 pathways. Immunol Rev. 2008;224:166-82.

56. Alsaab HO, Sau S, Alzhrani R, Tatiparti K, Bhise K, Kashaw SK, et al. PD-1 and PD-L1 Checkpoint Signaling Inhibition for Cancer Immunotherapy: Mechanism, Combinations, and Clinical Outcome. Front Pharmacol. 2017;8:561.
57. Zou W, Chen L. Inhibitory B7-family molecules in the tumour microenvironment. Nat Rev Immunol. 2008;8(6):467-77.
58. Ohaegbulam KC, Assal A, Lazar-Molnar E, Yao Y, Zang X. Human cancer immunotherapy with antibodies to the PD-1 and PD-L1 pathway. Trends Mol Med. 2015;21(1):24-33.
59. Shiravand Y, Khodadadi F, Kashani SMA, Hosseini-Fard SR, Hosseini S, Sadeghirad H, et al. Immune Checkpoint Inhibitors in Cancer Therapy. Current Oncology. 2022;29(5):3044-60.
60. Viveiros N, Flores BC, Lobo J, Martins-Lima C, Cantante M, Lopes P, et al. Detailed bladder cancer immunoprofiling reveals new clues for immunotherapeutic strategies. Clin Transl Immunology. 2022;11(9):e1402.
61. Lawrence MS, Stojanov P, Polak P, Kryukov GV, Cibulskis K, Sivachenko A, et al. Mutational heterogeneity in cancer and the search for new cancer-associated genes. Nature. 2013;499(7457):214-8.
62. Massard C, Gordon MS, Sharma S, Rafii S, Wainberg ZA, Luke J, et al. Safety and Efficacy of Durvalumab (MEDI4736), an Anti-Programmed Cell Death Ligand-1 Immune Checkpoint Inhibitor, in Patients With Advanced Urothelial Bladder Cancer. J Clin Oncol. 2016;34(26):3119-25.
63. Sharma P, Callahan MK, Bono P, Kim J, Spiliopoulou P, Calvo E, et al. Nivolumab monotherapy in recurrent metastatic urothelial carcinoma (CheckMate 032): a multicentre, open-label, two-stage, multi-arm, phase 1/2 trial. Lancet Oncol. 2016;17(11):1590-8.
64. Zhu L, Sun J, Wang L, Li Z, Wang L, Li Z. Prognostic and Clinicopathological Significance of PD-L1 in Patients With Bladder Cancer: A Meta-Analysis. Front Pharmacol. 2019;10:962.
65. Balar AV, Galsky MD, Rosenberg JE, Powles T, Petrylak DP, Bellmunt J, et al. Atezolizumab as first-line treatment in cisplatin-ineligible patients with locally advanced and metastatic urothelial carcinoma: a single-arm, multicentre, phase 2 trial. Lancet. 2017;389(10064):67-76.
66. Sharma P, Siefker-Radtke A, de Braud F, Basso U, Calvo E, Bono P, et al. Nivolumab Alone and With Ipilimumab in Previously Treated Metastatic Urothelial Carcinoma: CheckMate 032 Nivolumab 1 mg/kg Plus Ipilimumab 3 mg/kg Expansion Cohort Results. J Clin Oncol. 2019;37(19):1608-16.

67. Peng M, Xiao D, Bu Y, Long J, Yang X, Lv S, et al. Novel Combination Therapies for the Treatment of Bladder Cancer. Front Oncol. 2020;10:539527.
68. Szabados B, Kockx M, Assaf ZJ, van Dam PJ, Rodriguez-Vida A, Duran I, et al. Final Results of Neoadjuvant Atezolizumab in Cisplatin-ineligible Patients with Muscle-invasive Urothelial Cancer of the Bladder. Eur Urol. 2022;82(2):212-22.
69. Rhea LP, Mendez-Marti S, Kim D, Aragon-Ching JB. Role of immunotherapy in bladder cancer. Cancer Treat Res Commun. 2021;26:100296.
70. Hussain SA, Birtle A, Crabb S, Huddart R, Small D, Summerhayes M, et al. From Clinical Trials to Real-life Clinical Practice: The Role of Immunotherapy with PD-1/PD-L1 Inhibitors in Advanced Urothelial Carcinoma. Eur Urol Oncol. 2018;1(6):486-500.
71. Miyao N, Tsai YC, Lerner SP, Olumi AF, Spruck III CH, Gonzalez-Zulueta M, et al. Role of chromosome 9 in human bladder cancer. Cancer research. 1993;53(17):4066-70.
72. Alifrangis C, McGovern U, Freeman A, Powles T, Linch M. Molecular and histopathology directed therapy for advanced bladder cancer. Nat Rev Urol. 2019;16(8):465-83.
73. Comprehensive molecular characterization of urothelial bladder carcinoma. Nature. 2014;507(7492):315-22.
74. Hedegaard J, Lamy P, Nordentoft I, Algaba F, Høyer S, Ulhøi BP, et al. Comprehensive transcriptional analysis of early-stage urothelial carcinoma. Cancer cell. 2016;30(1):27-42.
75. Platt FM, Hurst CD, Taylor CF, Gregory WM, Harnden P, Knowles MA. Spectrum of phosphatidylinositol 3-kinase pathway gene alterations in bladder cancer. Clin Cancer Res. 2009;15(19):6008-17.
76. Dueñas M, Martínez-Fernández M, García-Escudero R, Villacampa F, Marqués M, Saiz-Ladera C, et al. PIK3CA gene alterations in bladder cancer are frequent and associate with reduced recurrence in non-muscle invasive tumors. Mol Carcinog. 2015;54(7):566-76.
77. Segovia C, Martínez-Fernández M, Dueñas M, Rubio C, López-Calderón FF, Costa C, et al. Opposing roles of PIK3CA gene alterations to EZH2 signaling in non-muscle invasive bladder cancer. Oncotarget. 2017;8(6):10531-42.
78. Deshpande G, Menon S, Desai S. Pathology and Staging. In: Singh P, Nayak B, Panaiyadiyan S, editors. A Guide to Management of Urological Cancers. Singapore: Springer Nature Singapore; 2023. p. 125-40.
79. Knowles MA, Hurst CD. Molecular biology of bladder cancer: new insights into pathogenesis and clinical diversity. Nat Rev Cancer. 2015;15(1):25-41.

80. Li R, Du Y, Chen Z, Xu D, Lin T, Jin S, et al. Macroscopic somatic clonal expansion in morphologically normal human urothelium. Science. 2020;370(6512):82-9.
81. Damrauer JS, Hoadley KA, Chism DD, Fan C, Tiganelli CJ, Wobker SE, et al. Intrinsic subtypes of high-grade bladder cancer reflect the hallmarks of breast cancer biology. Proc Natl Acad Sci U S A. 2014;111(8):3110-5.
82. Sjödahl G, Lauss M, Lövgren K, Chebil G, Gudjonsson S, Veerla S, et al. A molecular taxonomy for urothelial carcinoma. Clin Cancer Res. 2012;18(12):3377-86.
83. Robertson AG, Kim J, Al-Ahmadie H, Bellmunt J, Guo G, Cherniack AD, et al. Comprehensive Molecular Characterization of Muscle-Invasive Bladder Cancer. Cell. 2017;171(3):540-56.e25.
84. Kamoun A, de Reyniès A, Allory Y, Sjödahl G, Robertson AG, Seiler R, et al. A Consensus Molecular Classification of Muscle-invasive Bladder Cancer. Eur Urol. 2020;77(4):420-33.
85. Feinberg AP, Tycko B. The history of cancer epigenetics. Nature Reviews Cancer. 2004;4(2):143-53.
86. Esteller M. Epigenetics in cancer. N Engl J Med. 2008;358(11):1148-59.
87. Eccleston A, DeWitt N, Gunter C, Marte B, Nath D. Epigenetics. Nature. 2007;447(7143):395-6.

## DNA Methylation as a Therapeutic Target for Bladder Cancer

*Review paper 1*

**Sandra P. Nunes**, Rui Henrique, Carmen Jerónimo, and Jesús M. Paramio

**DOI**: https://doi.org/10.3390/cells9081850

Published: 7 August 2020

**Cells**, 9(8):1850.

Author personal contribution:

Conceptual design, retrieval of records to review, interpretation of the gathered information and manuscript preparation.

**Abstract**

Bladder cancer (BC) is the tenth most frequent cancer worldwide and is associated with high mortality when diagnosed in its most aggressive form, which is not reverted by the current treatment options. Thus, the development of new therapeutic strategies, either alternative or complementary to the current ones, is of major importance. The disruption of normal epigenetic mechanisms, namely, DNA methylation, is a known early event in cancer development. Consequently, DNA methyltransferase (DNMT) inhibitors constitute a promising therapeutic target for the treatment of BC. Although these inhibitors, mainly nucleoside analogues such as 5-azacytidine (5-aza) and decitabine (DAC), cause re-expression of tumor suppressor genes, inhibition of tumor cell growth, and increased apoptosis in BC experimental models and clinical trials, they also show important drawbacks that prevent their use as a valuable option for the treatment of BC. However, their combination with chemotherapy and/or immune-checkpoint inhibitors could aid in their implementation in the clinical practice. Here, we provide a comprehensive review of the studies exploring the effects of DNA methylation inhibition using DNMTs inhibitors in BC, from in vitro and in vivo studies to clinical trials.

**Keywords**

Bladder cancer; DNA methylation; DNA methyltransferases; nucleoside analogues; therapy

## 1. Introduction

Bladder cancer (BC) is estimated to be the tenth most frequent cancer worldwide, being more common in men, in which it is the sixth most frequent cancer and the ninth cause of death due to cancer (1). At diagnosis, approximately 75% of patients display a non-muscle invasive BC (NMIBC), whereas 25% are diagnosed with muscle invasive BC (MIBC) (2). These differences have important implications regarding the treatment and clinical outcome (3). NMIBC comprises Ta, T1, and carcinoma in situ (CIS), which do not reach the bladder muscle layer and show relatively good outcomes (4), being treated by transurethral resection (TUR) (3). Depending on different clinicopathological features, such as number of implants, size, and patient's age, NMBICs are classified as high or low risk. High risk tumor management includes a regimen of local instillation, mainly of Bacillus Calmette Guérin (BCG), after TUR to prevent recurrences and progression. BCG instillations promote local acute inflammation responses and represent the first approved immunotherapy for human cancers (5). Recurrence is extremely frequent in NMIBC (up to 70%), and, in a proportion of cases, tumors progress to MIBC (stage T2 or higher) (4, 6). This represents a clinical problem demanding systematic follow-up of patients, frequently requiring cystoscopy, with a serious impact on the patient's quality of life and generating important costs to health systems (7). The management of MIBC often requires radical cystectomy and, depending on the clinicopathological characteristics of the neoplasm, platin-based chemotherapy schemes in neoadjuvant or adjuvant settings can be administered (3). MIBC recurrence and progression are also frequent, with survival at metastatic stage below 5% (6). In addition to this poor outcome, a percentage of MIBC patients cannot be treated using standard protocols due to comorbidities or other health problems, regularly related to old age at diagnosis. Currently, patients that are considered to be unfit for such protocols have few therapeutic options. The development of immune checkpoint blockade (ICI) with antibodies inhibiting programmed death 1 (PD-1), programmed death-ligand 1 (PD-L1), or cytotoxic T-lymphocyte antigen 4 (CTLA-4) allowed for a substantial improvement in patient survival with good and sustained responses (8). However, the percentage of patients showing clinical response is still rather limited (9). Hence, a full understanding of the biological mechanisms underlying the development of BC would not only provide novel biomarkers for early detection but also as candidate therapeutic targets, improving patient survival. To gain better knowledge of BC molecular features, different international initiatives and multiple groups generated large amounts of data including different genomic analyses (10, 11). Such studies revealed the existence of different molecular subtypes and

suggested the possibility for designing appropriate subtype-specific therapeutic approaches (12).

One of the most prevalent characteristics of BC is the presence of alterations in the cancer cell epigenetic machinery. The genetic and epigenetic landscapes allow for a cell to acquire an identity associated with a specific tissue, establishing proper organismal physiology (13), and their disruption represents the basis of multiple disorders (13). Epigenetics comprises the study of heritable alterations that modify gene expression patterns without changing their DNA sequence (13-15). DNA methylation, histone variants, chromatin remodeling, and histone post-translation modifications are the main epigenetic mechanisms with an impact on gene expression (Figure 1) (16). Although often considered to be independent, different mechanisms cooperate closely in regulating the epigenome (17). Because the deregulation of such epigenetic mechanisms is implicated in cancer development, in-depth characterization of the cancer epigenome boosted the understanding of tumor initiation and progression (14).

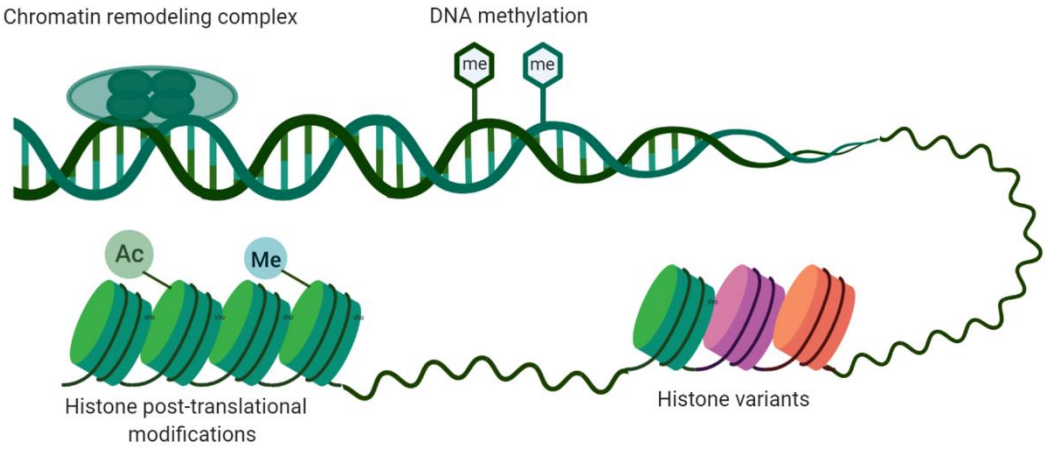


**Figure 1.** Main epigenetic mechanisms involved in gene expression regulation. DNA methylation consists of the addition of a methyl group in cytosine present in a cytosine–phosphate–guanine (CpG) dinucleotide. Histone post-translational modifications comprise alterations in histone tails such as methylation, acetylation, phosphorylation, and ubiquitination. Histone variants differ in few amino acids from canonical histones and regulate chromatin remodeling and histone post-translational modifications. Chromatin-remodeling complexes regulate the nucleosome structure by removing, relocating, and shifting histones.

Early in their development and progression, several epigenetic mechanisms are disrupted in BC (18). For example, mutations in *EP300* and *CREBBP*, two chromatin-remodeling genes, led to the inactivation of the complex's histone-acetyltransferase domain, resulting in changes in chromatin conformation. Furthermore, a gene expression signature allied with the loss of histone acetyltransferase activity was associated with

more aggressive bladder tumors (19). Interestingly, 89% of MIBC lesions display mutations in the histone-modifying genes (20). Specifically, a high mutation rate was found in *KMT2D* (also known as *MLL2*) gene and in *KDM6A* (also referred as *UTX*), which encode a histone H3 lysine 4 methyltransferase and a histone lysine demethylase, respectively (21-23). The most explored epigenetic mechanism is DNA methylation (18, 24). By comparing methylation patterns, Wolff et al. found global hypomethylation in NMIBC, whereas hypermethylation patters were more commonly found in invasive tumors, supporting the concept that DNA methylation has an important role in BC development and aggressiveness, constituting a putative target for anti-cancer therapy (24, 25).

The main goal of this review is to summarize the impact of aberrant DNA methylation in BC, focusing on therapeutic strategies that target this epigenetic alteration, based on the information provided by preclinical studies, both in vitro and in vivo, and clinical trials.

## 2. DNA Methylation

DNA methylation is the covalent addition of a methyl group at the 5-position carbon of cytosine in a cytosine–phosphatidyl–guanine (CpG) dinucleotide (17). Methylation occurs mainly at CpG islands—CpG-rich regions (at least 50% of cytosines and guanines) in the genome with a size larger than 200 bp (26, 27). Moreover, methylation can also be found in repetitive sequences such as retrotransposon elements and centromeres, in the X chromosome (leading to its inactivation) and genomic imprinting (28). Approximately 29,000 CpG islands can be found in the human genome, most commonly in the promoter regions, close to the transcription starting site (TSS) or first exons (27). Remarkably, 75% of cytosines in CpG dinucleotides dispersed throughout the genome are methylated, whereas cytosines of CpG islands located within gene promoters remain mostly hypomethylated (27, 29). Promoter DNA methylation is classically associated with transcription repression by inducing binding of transcriptional repressors or hampering binding of transcriptional factors (15, 17). In fact, a family of methyl-CpG-binding proteins (MBPs) intervenes in gene silencing by binding to methylated CpGs and recruiting histone modifier enzymes to establish histone post-translation modifications, which further sustain transcriptional repression (30). DNA methylation can also be found in CpG island shores, 2-kb areas upstream of a CpG island, displaying lower CpG dinucleotide density. CpG island shore methylation is also associated with transcriptional repression (31). On the other hand, methylation in the gene body was shown to stimulate transcription elongation and to have an impact on

splicing, with exons disclosing higher methylation levels than introns (28, 32). Furthermore, tissue-specific methylation seems to be more frequent in intragenic CpG islands (33). CpG islands in enhancers also influence gene regulation, *i.e.*, hypermethylation is associated with loss of enhancer marks resulting in gene silencing (34).

DNMTs catalyze the covalent bond between the methyl group donated by S-adenosyl methionine (SAM) and the unmethylated CpG dinucleotide at the fifth position of the cytosine by positioning the target base into the catalytic pocket of the enzyme using a base-flipping mechanism (35-37). Five DNA methyltransferases (DNMTs) are encoded by the human genome, including DNMT1, DNMT2, DNMT3a, DNMT3b, and DNMT3L (37-39). Specifically, DNMT3a and DNMT3b catalyze de novo DNA methylation, whereas DNMT1 preferentially maintains methylation patterns already existing by copying methylation patterns in the course of replication during embryonic development (37-39). DNMT2 and DNMT3L do not display DNMT catalytic activity, serving as post-transcriptional gene regulation and cofactors of other DNMTs, respectively. By contrast, ten-eleven translocation (TET) enzymes mediate active DNA demethylation through 5-hydroxymethylcytosine (5hmC) (40, 41), followed by deamination by activation-induced cytidine deaminase (AID), apolipoprotein B mRNA editing enzyme catalytic subunit 1 (APOBEC1) proteins, and base or nucleotide excision repair (17, 42, 43).

Overall, the cancer epigenome is characterized by global hypomethylation, which contributes to the overexpression of proto-oncogenes, an increased mutation rate, and the loss of imprinting (44). Indeed, a decrease from 80% to 40–60% in the methylation levels from normal to cancer cells was observed (44, 45). More specifically, genomic repetitive regions become unmethylated, stimulating early cancer events through chromosomal instability that result in increased mutation rates, chromosomal rearrangements, and centromere instability (Figure 2) (46, 47). Simultaneously, the promoter hypermethylation of tumor suppressor genes (TSG) is also a frequent event in cancer cells (48), thus contributing to processes such as invasion, metastasis, and angiogenesis (44). Typically, 5–10% of CpG islands at gene promoters are methylated in cancer (Figure 2) (44).

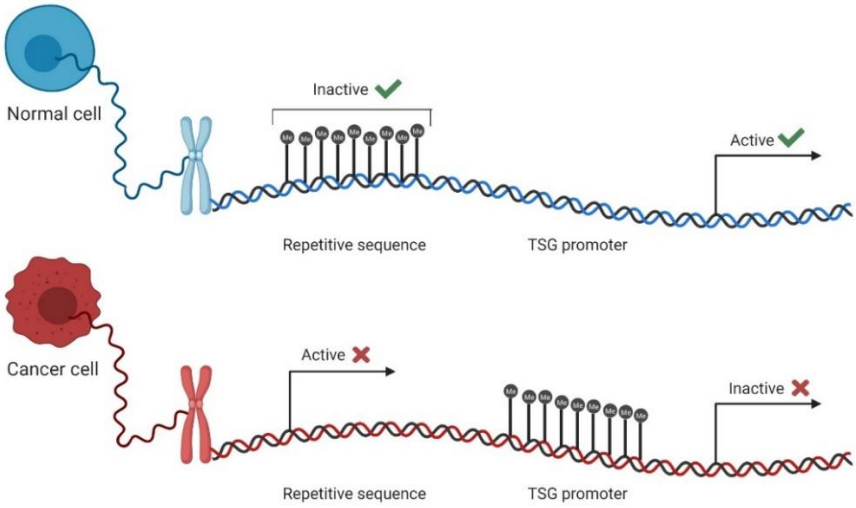


**Figure 2.** DNA methylation in normal and cancer cells. In normal cells, most repetitive sequences are methylated, whereas the promoters of tumor suppressor genes (TSG) stay unmethylated, remaining active and leading to gene expression (green check mark). Contrarily, in cancer cells, repetitive sequences become unmethylated and active, contributing to genomic instability, and TSG promoters become methylated, inactivating these genes and promoting cell aggressiveness and escape (red cross mark).

DNA methylation is a known contributor to BC development (49). Hence, aberrant DNA methylation was proposed as a promising biomarker for BC detection, prognosis, and therapeutic target (50, 51). For example, a panel comprising *HOXA9*, *PCDH17*, *POU4F2*, and *ONECUT2* methylation detected BC with 90.5% sensitivity and 73.2% specificity in urine samples from Chinese patients presenting hematuria, leading the authors to estimate that about 60% of cystoscopies could be avoided (52). Furthermore, a methylation panel composed of *GDF15*, *TMEFF2*, and *VIM* discriminated BC patients from healthy controls and prostate or renal cancer patients with a sensitivity of 94% and specificity of 90% in urine sediment samples (53), whereas the UroMark assay based on 150 CpG loci detected BC in voided urine samples with 98% sensitivity and 97% specificity (54). On the other hand, in an analysis of formalin-fixed paraffin-embedded primary BC tissue samples, methylation of SFRP5 was associated with recurrence and *CACNA1G* was associated with BC progression (55). Moreover, DNMTs were shown to be overexpressed in BC, representing an attractive target for anti-cancer therapies (56).

## 3. DNMT Inhibitors

As previously stated, DNA methylation is a reversible alteration that contributes to BC development and progression, and DNMTs are overexpressed in this tumor type (49, 56). Thus, DNMTs constitute attractive targets for cancer treatment, and several "epidrugs" are already approved for the treatment of specific conditions (57). Indeed, 5-azacytidine (or azacytidine (5-aza, Vidaza®)) and 5-aza-2J-deoxycytidine (or decitabine (DAC, Dacogen®)) are two DNMT inhibitors approved by the European Medicines Agency (EMA) and Food and Drug Administration (FDA) for the treatment of acute myeloid leukemia (AML), myelodysplastic syndrome, and chronic myelomonocytic leukemia (CMML) (30, 57, 58). DNMT inhibitors can be classified, depending on their mechanism of action, as nucleoside and non-nucleoside analogues (24).

### *3.1. Nucleoside Analogues*

Nucleoside analogues (or cytidine analogues) are a group of compounds that integrate into DNA instead of cytosine, resulting in the formation of a covalent bond with a DNMT in the carbon-6 position of the cytosine during the synthesis (S) phase of the cell cycle (57, 59) (Figure 3; Figure S1, Supplementary Materials). 5-Aza and DAC are the nucleoside analogues most commonly used as therapeutic agents in cancer (60), with DAC having 90% more demethylating power than 5-aza (61). Although their mode of action remains controversial, several mechanisms were proposed (59, 62-64). After the cellular uptake, mediated by nucleoside transporters, nucleoside analogues are activated through conversion to 5-aza-2'-deoxycytidine-5'-triphosphate, a substrate for the DNA replication machinery, to be incorporated in DNA, replacing cytosine (59). At that point, DNMTs recognize azacytosine–guanine dinucleotides and catalyze the methylation reaction by forming a covalent bond with the cytosine ring (65, 66). Since azacytosine has a nitrogen substituting the carbon at position 5, the covalent bond cannot be broken, resulting in DNMT inactivation (59). In addition to DNMT degradation, the complex formed between DNA and DNMT prompts DNA damage by causing double-strand breaks, leading to loss of methylation marks (59, 67). DAC and 5-aza seem to cause different effects in cancer cells. Although they both lead to a depletion of DNMT1 and a decrease in DNA methylation levels in non-small-cell lung cancer cells, 5-aza induces DNA damage, apoptosis, and cell arrest at phase sub-gap 1 (G1), whereas DAC increases the number of cells arrested in gap 2 (G2)/mitosis (M). As a consequence, their effects on gene expression are also different, with 5-aza decreasing the expression of genes related to cell cycle and metabolic processes, while DAC upregulates genes related to cell differentiation (63). Furthermore, response rates to DAC treatment in AML patients with p53 mutations were higher in comparison with patients with wild-type p53,

showing that mutations in p53 may play a role in epigenetically mediated cell death after DAC treatment (62, 68). Remarkably, phosphorylation of DNMT1 by protein kinase δ leads to its faster degradation after treatment with 5-aza or DAC, constituting another possible mechanism via which hypomethylation is achieved (64). However, 5-aza and DAC are characterized by poor bioavailability, since they are easily degraded by hydrolysis in aqueous acidic or basic environments and have a limited half-life (59, 69). Indeed, both compounds can be deaminated by cytidine deaminase and converted into 5-azauridine, which results in their inactivation (70). Furthermore, DAC is only incorporated into DNA, whereas 5-aza is incorporated into both DNA and RNA (70) and, since none of the compounds target specific DNMT isoforms, DAC and 5-aza cause significant side effects (70). Thus, several alternative nucleoside analogues were developed to overcome these limitations.

Zebularine is a cytidine analogue that lacks the amino group at position 4 of the pyrimidine ring. It displays high stability as it inhibits both DNMTs and cytidine deaminase, and it is stable in acidic and neutral pH, enabling oral administration (71). Moreover, zebularine has low cytotoxicity, which might translate into longer treatments with low doses to maintain a demethylated state (71), as well as an apparent specificity for cancer cells and not fibroblasts (72, 73). Zebularine leads to S-phase delay and cell death in mesothelioma cells (72), causes formation of replication-dependent double-strand DNA breaks (74), and enhances colon cancer cell immunogenicity (75). Nevertheless, high concentrations of zebularine are needed to achieve demethylation levels similar to those of DAC since it forms a reversible complex with DNMTs, with slow dissociation kinetics (76), hindering the transition to clinical practice (57, 71). 5'-Fluoro-2'-deoxycytidine (FdCyd) is a fluoropyrimidine nucleoside analogue with a mechanism of action similar to 5-aza and DAC (24). However, it is more stable and induces less toxicity compared to 5-aza and DAC (77). As these nucleoside analogues are rapidly metabolized, combining them with tetrahydrouridine (THU), a cytidine deaminase inhibitor, was proposed to overcome such limitation (78-81). Indeed, co-administration of FdCyd and THU induced plasma concentrations of FdCyd in patients similar to those established as needed for inhibiting DNA methylation in vitro (80).

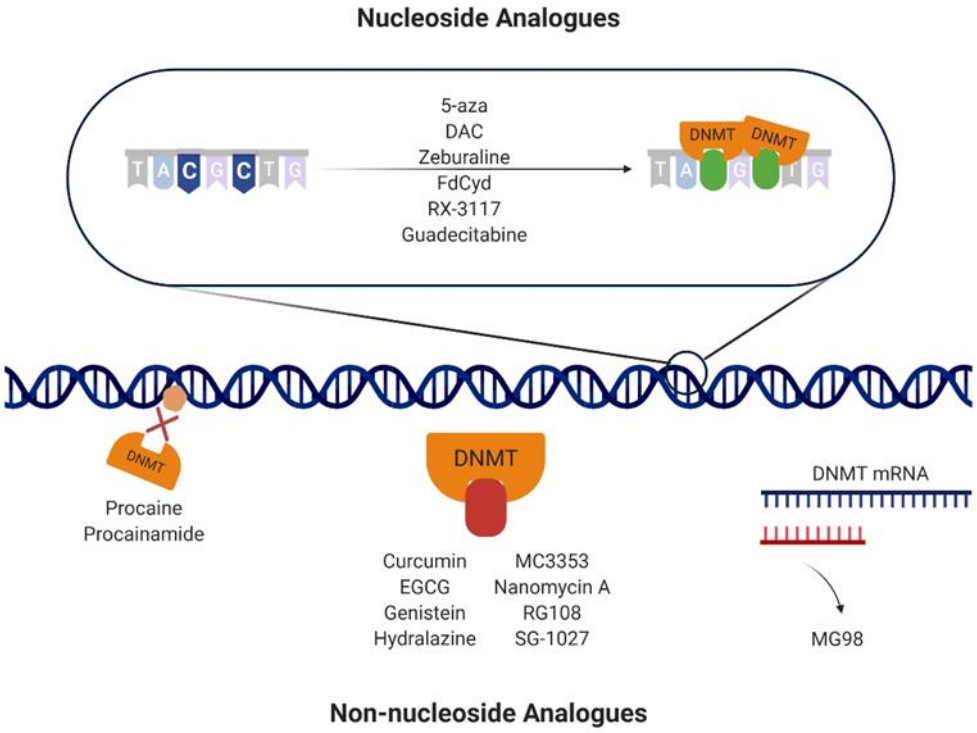


**Figure 3.** Mechanisms of action of DNA methyltransferase (DNMT) inhibitors. The nucleoside analogues 5-azacitydine (5-aza), decitabine (DAC), zebularine, 5J-fluoro-2J-deoxycytidine (FdCyd), RX-3117, and guadecitabine are integrated into DNA instead of cytosine. When DNMTs bind, a covalent bond is formed between the DNMT and the cytosine analogue. The non-nucleoside analogues have different mechanism of action to achieve inhibition of DNA methylation. Specifically, procaine and procainamide bind directly to the DNA, impeding DNMT binding. Curcumin, epigallocatechin-3-gallate (EGCG), genistein, hydralazine, MC3353, nanomycin A, RG108, and SG-1027 bind directly to the catalytic pockets of DNMTs, hampering their action. MG98 is an oligodeoxynucleotide that binds to the DNMT1 messenger RNA (mRNA) by base pair complementarity, impeding its translation.

SGI-110 or guadecitabine is a second-generation hypomethylating agent containing DAC coupled with a deoxyguanosine—a CpG dinucleotide analogue (70). It is not a substrate for cytidine deaminase, a fact that increases the compound's exposure time without being inactivated (82). Guadecitabine was tested in several clinical trials. Specifically, a combination of guadecitabine and irinotecan was shown to be safe and to possess clinical activity in metastatic colorectal cancer patients in a phase I dose escalation study (83). Likewise, guadecitabine was clinically active in intermediate- and high-risk myelodysplastic syndromes, namely, in patients who did not respond to the currently approved demethylating agents (84). More recently, an oral formulation of 5-aza, CC-486, was developed and tested in several clinical trials (85-88). Some advantages of the oral route include a more convenient and easier administration to monitor, a high exposure time to the drug, and the elimination of local reactions (88).

Although a combination treatment with CC-486 and pembrolizumab was not effective in improving progression-free survival (PFS) in non-small-cell lung cancer patients (86), CC-486 as a single treatment showed clinical activity in nasopharyngeal cancer in a phase I clinical trial (87). Furthermore, extending doses of CC-486 in low-risk myelodysplastic syndromes patients might provide an effective long-term treatment (88). RX-3117 (fluorocyclopentenylcytosine) is a novel cytidine analogue with a modified ribose molecule (89). To be incorporated into DNA or RNA, the RX-3117 molecule is firstly activated through transformation into a triphosphate form by uridine–cytidine kinase 2 (90). Although RX-3117 is not a substrate for cytidine deaminase (89), other enzymes such as NT5C3 may have a role in breaking an intermediate monophosphate form, resulting in RX-3117 inactivation (90). RX-3117's anti-tumor effects were evaluated in nine different xenograft mouse models and showed promise for the treatment of tumors that are sensitive and resistant to gemcitabine (91).

### *3.2. Non-Nucleoside Analogues*

Although nucleoside analogues are potent inhibitors of DNA methylation, they lack specificity, resulting in important side effects. To overcome this, non-nucleoside molecules were developed in the last few years. Non-nucleoside analogues comprise all DNMT inhibitors whose mechanism is independent of DNA incorporation (92), including DNA binders, oligonucleotides, natural compounds, SAM competitors, and repurposed drugs, *i.e.*, drugs that were designed for a specific target and treatment but were found to have a novel therapeutic effect (92, 93) (Figure 3; Figure S1, Supplementary Materials).

Procaine and procainamide, derivatives of 4-aminobenzoic acid, are FDA-approved drugs as anesthetic and anti-arrhythmic, respectively (94, 95). Both drugs were shown to cause global DNA hypomethylation in MCF7 cells inducing cell growth inhibition (94). Additionally, procaine reduces the activity of DNMT1 and DNMT3a without influencing their expressions (96). By directly binding to DNA, procaine and procainamide hamper DNMTs binding, leading to decreased global DNA methylation levels, although to a lesser extent when compared to DAC (94, 96). The antibiotic nanaomycin A also induces global hypomethylation and reactivates TSGs such as Ras association domain family 1 isoform A (RASSF1A) (97). Remarkably, nanaomycin A showed specificity for DNMT3b inhibition by interacting with key amino-acid residues of this enzyme (98). Hydralazine is an arterial vasodilator approved for the treatment of severe hypertension and heart failure (99). It causes re-expression of TSGs by reversing promoter hypermethylation, both in cancer cell lines and in primary tumors (100). Hydralazine inhibits DNA methylation, although weakly, by interacting with the DNMT active site (99). Furthermore,

hydralazine treatment caused a decrease in cell growth and invasiveness, increased apoptosis, cell-cycle arrest, and lowered DNMT messenger RNA (mRNA) and protein levels (101). On the other hand, the combined treatment with hydralazine and valproic acid also demonstrated anti-metastatic effects, both in vitro and in vivo (102), and it showed potential clinical benefit in patients with disease progression under chemotherapy (103) including advanced cervical cancer patients (104).

Oligodeoxynucleotides that bind a target mRNA by base pair complementarity also show promise as DNMTs inhibitors (105). In particular, MG98 is a second-generation 20-nucleotide antisense oligonucleotide that binds specifically to DNMT1 mRNA, causing a decrease in DNMT levels (105). In an initial phase I clinical trial, MG98 was not well tolerated in high doses, and its anticancer effects were not observed in patients with solid tumors (106). The lack of clinical activity was also observed in patients with high-risk myelodysplasia and acute myeloid leukemia (107). However, in another clinical trial in patients with advanced solid tumors using escalating doses, MG98 was well tolerated and showed early clinical benefit (108), similarly to a combination of MG98 and interferon (IFN) α-2β in the treatment of advanced renal cell carcinoma (109). RG108 is a synthetic molecule considered to be a SAM competitor that targets the binding pockets of DNMTs, establishing covalent bonds and leading to inhibition of their enzymatic activity (110). Treatment with RG108 caused inhibition of DNMTs and cell growth, and it increased apoptosis in endometrial and prostate cancer cell lines (111, 112). SGI-1027 is a quinolone-based molecule which directly binds to the cofactor-binding site of DNMT3a and to both the cofactor- and the substrate-binding sites of DNMT1 (113). Treatment of RKO cells with SGI-1027 resulted in demethylation and re-expression of TSGs including p16, mutL homolog 1 (MLH1), and metalloproteinase inhibitor 3 (TIMP3), with no significant toxicity (114). Another quinolone-based molecule, MC3353, caused cell arrest and decreased cell viability in a panel of different cancer cell lines. Furthermore, E-cadherin mRNA and protein levels increased while a reduction of matrix metalloproteinase levels was observed in PC-3 and HCT116 cells, hampering their epithelial-to-mesenchymal transition (115).

Several natural compounds were shown to have DNMT inhibitory activity (24). The natural polyphenol epigallocatechin-3-gallate (EGCG), found in green tea, was shown to inhibit DNMT activity by interacting with the enzyme catalytic pocket, reactivating the expression of several TSGs by reversing the hypermethylation status (116, 117). EGCG also decreased cell viability, migration and invasion of breast cancer cells, and SCUBE2 methylation by decreasing DNMT expression and activity (118). Genistein is an isoflavone present in soybeans which displays anti-cancer activity (24). In prostate tissue cancer samples, differences in methylation patterns and expressed genes were found

comparing patients with genistein supplementation prior to prostatectomy and those receiving placebo (119). After genistein treatment, DNA methylation levels decreased in several promoters of TSGs such as *ATM*, *APC*, *PTEN*, and *SERPINB5*, with a concomitant increase in the mRNA levels of those genes. Genistein interacts with the catalytic domain of DNMT1, competing with hemi-methylated DNA for the catalytic pocket (120). Furthermore, in colon cancer cells, genistein demethylated *WIF1* and decreased invasiveness and migration of cancer cells by reducing expression of matrix metalloproteinases 2 and 9 (121). Curcumin, a polyphenol compound with anti-inflammatory properties, also influences methylation status. In colorectal cancer cells, exposure to curcumin led to demethylation of specific CpG loci without inducing global methylation changes (122).

## 4. DNA Methylation as a Therapeutic Target in BC

### *4.1. Preclinical Studies*

A summary of the preclinical studies testing DNMT inhibitors in BC is depicted in Table 1. The effects of 5-aza were evaluated in cell lines in vitro and in a tumor xenograph model. 5-Aza was shown to inhibit cell proliferation and arrest cells at G0/G1, whereas volume and weight of tumor xenografts in mice were reduced. Interestingly, DNMT3a and DNMT3b expressions were also reduced after 5-aza treatment, causing the re-expression of hepaCAM, a TSG (56). DAC treatment also led to an increase in hepaCAM expression in T24 and BIU87 cells, associated with arrest at G0/G1 phase (123). In a canine model of invasive urothelial carcinoma, 5-aza disclosed anti-tumor effects, with 22.2% of the dogs demonstrating partial response and 50% depicting stable disease (124).

Non-toxic concentrations of DAC were used to treat four BC cell lines in order to evaluate the impact of hypomethylation in the BC cell transcriptome. Notch receptor 1 (NOTCH1) expression increased after treatment with DAC, in parallel with 50% demethylation of the promoter and enhancer regions. Interestingly, DAC-treated cells displayed morphological changes, *i.e.*, cell enlargement compared to the controls. To explore these effects, the active intracellular domain of NOTCH1, ICN1, was overexpressed in cell lines and a decrease in cell proliferation was observed. Moreover, there was an increase of interleukin (IL)-6, probably due to a rise in ICN1 expression and double-stranded RNA levels (125). ICN1 overexpression also led to a decrease in basal stem-like cells, as assessed by the decreased cytokeratin 5 (CK5) levels, contributing to a more differentiated cell state (125), which may prevent BC progression (126). DAC

was also shown to inhibit cell proliferation, migration, and invasiveness, inducing apoptosis in T24 cells while increasing the expression of the TSG Maspin (127). Another gene that appears to be regulated by methylation in BC is *BTG2*. After treating EJ cells with DAC, BTG anti-proliferation factor 2 (BTG2) expression increased mainly due to DNMT1 inhibition, and cell growth decreased. Furthermore, H3K9me2 levels decreased, whereas H3K4me3 increased, leading to an open chromatin state in the promoter and intronic region of *BTG2* (128). Apoptotic peptidase activating factor 1 (APAF-1) and death associated protein kinase 1 (DAPK-1) expressions also increased after DAC treatment in both RT4 and T24 cells, whereas zebularine caused an increased expression of those genes in cell line T24, which is p53 mutated (129). Remarkably, Cheng et al. showed that treatment of T24 cells with zebularine for 48 h was not enough to maintain a long-term hypomethylated state and sustained p16 expression, as the percentage of methylation at day 0 was 97% and decreased to 75% at day 3. Inversely, a continuous treatment for 40 days, renewing dosage every three days, repressed cell growth and sustained p16 expression, while DNMT1 recovery was null. However, sequential treatment with DAC and zebularine was the most effective in increasing and retaining p16 expression, maintaining promoter hypomethylation, and hampering re-methylation patterns observed before treatment (130). Therefore, to increase treatment efficacy with this type of drug, a prolonged treatment seems to be pivotal.

The epigenetic regulation of Wnt inhibitory factor 1 (Wif-1), an antagonist of the Wnt pathway, important for carcinogenesis, was explored in four BC cell lines. DAC treatment led to increased Wif-1 mRNA levels with a simultaneous decrease in promoter methylation levels. Furthermore, Wif-1 expression was primarily regulated by DNA methylation and not genetic alterations (131). DAC treatment in T24 cells induced the expression of several genes related to the IFN pathway, which could theoretically lead to inhibition of tumor cell growth (132). Interestingly, Velicescu et al. showed that de novo methylation does not occur in non-dividing BC cells. Treating T24 cells with DAC allows for cell arrest at G0/G1 and determines how much time is necessary for re-methylation to occur. Indeed, no re-methylation was found in CpG islands, whereas various degrees of methylation reappeared in CpG poor regions. Furthermore, DNMT1 and 3b3 protein levels were not detected, whereas DNMT3a mRNA levels were maintained after day 10 of the experiment. This result demonstrates that DNMT3a might catalyze a de novo methylation in CpG poor regions outside the S phase of the cell cycle (133). In another study, the carcinogen *N*-butyl-*N*-(4-hydroxybutyl)nitrosamine) (BBN) was used to induce bladder tumors in mice. These tumors showed downregulation of several genes including GSTM1, which seems to be regulated, in part, by DNA methylation, since treatment with DAC in 5637 cells increased GSTM1 expression (134). Kawakami et al. reported for the

first time that *MSH3* epigenetic regulation by means of DNA methylation might contribute to gene silencing, being implicated in BC carcinogenesis (135).

Recently, a study comprising a wide range of different cancer cell lines, containing BC, showed that DNMT inhibitors, including DAC and 5-aza, increase methylation levels throughout the cancer epigenome. Specifically, in BC cell lines, DAC treatment increased methylation levels of 616 common CpGs and decreased methylation levels of 590 different CpGs, demonstrating that the DNMT inhibitor mechanism of action is complex and requires further exploration (136).

After treatment with S110, global methylation levels decreased, concomitantly with increased p16 expression (137). The effects of S110 in vivo were also assessed in a tumor xenograft mouse model using EJ6 cells. Tumor-free animals tolerated S110 better than DAC, with less weight loss and mortality. S110 failed to cause reduction in tumor sizes, yet their growth rate was lower and p16 expression was induced (138). The development of DAC and 5-aza variants could potentially increase their half-life, improving bioavailability and therapeutic efficacy.

Procainamide and hydralazine inhibitory effects on DNA methylation were studied in T24 cells. Both compounds decreased the methylation levels of TSGs *p16* and *RARβ*, which associated with their re-expression, both at the transcript and at the protein levels. Interestingly, hydralazine treatment maintained p16 reactivation for longer than DAC (100). A novel strategy to inhibit DNMT1, using an essential enzyme for cancer cell viability (139) highly expressed in BC (140), was proposed using DNAzymes. A DNAzyme is a stable DNA molecule with catalytic activity that targets specific RNA molecules leading to their destruction (141, 142). The DNAzyme DT433, constructed and selected to target DNMT1, displayed effects that were similar to those of 5-aza. Additionally, DT433 led to an increase in p16 expression and inhibition of cell proliferation (142). Novel strategies applying repurposed drugs or DNAzymes to achieve DNMT inhibition constitute interesting alternatives to the demethylating drugs already approved. On the one hand, DNAzymes showed that increasing specificity toward the target may be achieved, whereas repurposed drugs, with negligible toxicity and known safety profiles, may be administered for longer periods and be considered as the next step for DNA methylation inhibition as anti-cancer therapy.

**Table 1.** Summary of pre-clinical studies targeting DNMTs in bladder cancer (BC).

| Drug | Model | Concentration | Treatment Scheme | Effects | Year | Reference |
|---|---|---|---|---|---|---|
| DAC | T24 | 1 μM | 1 day | ↑ Gene expression related to IFN pathway | 2002 | (132) |
| DAC | T24 | 3 μM | 1 day | No remethylation in CpG islands in the absence of cell division | 2002 | (133) |
| Hydralazine and procainamide | T24 | 10 μM | 5 days | ↓ *p16* and *RARβ* methylation levels<br>↑ p16 and RARβ expression | 2003 | (100) |
| DAC | TCC and UMUC | 5 μM | n.a. | ↑ MSH3 mRNA levels | 2004 | (135) |
| Zebularine | T24 | 100 μM | Every 3 days for 40 days | ↓ Global methylation levels<br>↑ p16 expression | 2004 | (130) |
| DAC | J82C, T24C, TCC, and UMUC | 5 μM | 3 days | ↑ Wif-1 mRNA expression levels | 2006 | (131) |
| DAC<br>Zebularine | RT4 and T24 | 2 μM<br>100 μM | 2 days<br>Every 3 days for 7 days | ↑ Cells doubling time<br>↑ APAF-1 and DAPK-1 expression | 2006 | (129) |
| S110 | T24 | 0.1–10 μM | Every 3 days for 6 days | ↓ Global methylation levels<br>↑ p16 expression | 2007 | (137) |
| DAC | BIU87 | 0.1–5 μM | 3 days | Re-expression of RASSF1A | 2009 | (143) |
| DAC | BOY | 1 μM | 4 days | ↑ COL1A2 expression | 2009 | (144) |
| DAC | BOY, T24, and UMUC | 10 μM | 7 days | ↑ FHL1 mRNA expression levels | 2010 | (145) |
| S110 | Mouse tumor xenograft | 10 mg/kg | Daily injection for 6 days | ↓ Tumor growth rate<br>↑ p16 expression | 2010 | (138) |
| 5-Aza | Dogs with naturally occurring invasive urothelial carcinoma | 0.1–0.3 mg/kg | Two doses schedules: Everyday days 1 to 5 or days 1 to 5 and 15 to 19 | 22.2% Tumor partial response<br>50% Stable disease<br>22.2% Progressive disease | 2012 | (124) |

| | | | | | | |
|---|---|---|---|---|---|---|
| | | | Each cycle 28 days | | | |
| DAC | BIU87 and T24 | 0.1–10 μM | 3 days | Cell arrest at G0/G1<br>↑ hepaCAM expression | 2013 | (123) |
| DAC | T24 | 0.25–2 μM | 2 days [1] | ↑ Maspin expression levels<br>↓ Cell proliferation, migration and invasion | 2013 | (127) |
| DAC | 5637 | 1–3 μM | 6 days | ↑ GSTM1 expression | 2014 | (134) |
| DAC | EJ | 1 μM | Every day for 3 days | ↓ Cell tumorigenesis and invasiveness<br>Cell arrest at G2/M<br>↑ BTG2 expression | 2014 | (128) |
| DNAzyme | T24 | n.a. | n.a. | ↓ Cell proliferation<br>↑ p16 expression | 2015 | (142) |
| 5-Aza | BIU87, EJ, and T24<br>Mouse tumor xenograft | 0.5–7 μM<br>n.a. | 1–4 days<br>Every 3 days for 18 days | ↓ Cell proliferation<br>↓ Tumor volume and weight | 2016 | (56) |
| DAC | T24 and J82 | 0.3 μM | 1 day | ↓ *RSPH9* methylation levels | 2016 | (146) |
| DAC | BLCAb001 (B01), BLCAb002 (B02), HT1376, and T24 | 0.1–1 μM | Every 2 days for 5 days | ↑ NOTCH1 expression<br>↓ CK5 positive cells<br>↑ IL-6 release | 2017 | (125) |
| DAC | T24 | 1 μM | 1 day | ↓ Methylation of 590 CpGs<br>↑ Methylation of 616 CpGs | 2019 | (136) |

[1] For migration and invasiveness assays. Abbreviations: 5-aza—5-azacytidine; APAF-1 - apoptotic peptidase activating factor 1; BTG2 - BTG anti-proliferation factor 2; CK5 – Cytokeratin 5; CpG - Cytosine–phosphatidyl–guanine; COL1A2 - collagen type I alpha 2 chain; DAC—decitabine; DAPK-1 - death associated protein kinase 1; FHL1 - four and a half LIM domains 1; GSTM1 - glutathione S-transferase mu 1; IFN – Interferon; IL-6 – Interleukin 6; MSH3 - mutS homolog 3; n.a.—not available; NOTCH1 - Notch receptor 1; RARβ - retinoic acid receptor beta; RASSF1A - Ras association domain family 1 isoform A; ↑—increase, ↓—decrease.

### *4.2. Combination Studies*

The anti-tumor effects of 5-aza, trichostatin A (TSA), and FK228 (the latter is a class I histone deacetylase (HDAC) inhibitor) were evaluated individually and in combination in a set of BC cell lines, as well as xenograft and orthotopic mouse models. The combination 5-aza and FK228 was shown to be toxic for 90% of the BC cells, inducing apoptosis and decreasing the G2/M cell population. The same combination in in vivo models led to a decrease in tumor size, mainly due to the effect of FK228 alone (147). Combination treatments using 5-aza and TSA also reduced the cell number and a shift in the expression of proteins that regulate the cell cycle in canine BC cell lines (148). More recently, combination of DAC and entinostat, another HDAC1 inhibitor, was tested in bladder cell lines, including two cisplatin-sensitive (J82 and RT112) and one cisplatin-resistant (J82CisR) cell lines, as well as one urothelial cell line isolate from normal tissue (HBLAK). The combination treatment did not revert cisplatin resistance of J82CisR, although treatment with both drugs promoted cell growth arrest. Additionally, increased apoptosis was observed, related to caspases 3 and 7, prompting cell arrest at G2/M transition. Forkhead box O1 (FoxO1) expression increased after the combination treatment, as well as BIM and p21, along with a decrease in survivin expression (149).

Several strategies using epigenetic drugs were devised to overcome chemoresistance and increase therapy success. Ramachandran et al. showed that pre-treatment with 5-aza followed by cisplatin or docetaxel exposure increased cytotoxicity in BC cells. Moreover, in UMUC3 cells that developed resistance to cisplatin or docetaxel in vitro, pre-treatment with 5-aza resulted in 44% and 55% of cytotoxicity in cisplatin- and docetaxel-resistant cells, respectively, in opposition to 2% with no pre-treatment (150). Pre-treatment with DAC also enhanced cytotoxicity of cisplatin and doxorubicin in BC cells. Furthermore, RASSF1A expression was observed concomitantly with activation of the Hippo pathway (151). Interestingly, UMUC14, RT4, 96-1, and 97-1 cell lines displayed low sensitivity to cisplatin, being associated with high *HOXA9* methylation levels. This was also verified in MIBC patients in which high *HOXA9* methylation levels were associated with resistance to chemotherapy. In line with other studies, DAC led to a 4–5-fold decrease in half maximal inhibitory concentration (IC50) for cisplatin, vinblastine, doxorubicin, and etoposide in BC cells (152). Wu et al. demonstrated for the first time that DAC treatment reduced the cancer stem-cell population in mice. Specifically, in a BNN-induced mouse model of BC, DAC alone or in combination with cisplatin or gemcitabine led to a decline in the keratin 14 (KRT14)+ cell population, which originates from the bladder urothelium (153). Consistently, the percentage of SRY-box transcription factor 2 (SOX2)+ cell population assumed to be responsible for the spread

of the tumor (154) was also lower. Curiously, the percentage of such cells increased in mice treated with chemotherapy only (155). These results were replicated in patient sample-derived xenografts, demonstrating that a combination treatment of DAC with chemotherapeutic agents might constitute a valuable option for BC therapy (155). Another study showed that a quadruple combination therapy comprising gemcitabine, cisplatin, DAC, and TSA increased apoptosis via cyclin D1 (CCND1) downregulation, DNA fragmentation, and caspase 3 expression in T24 cells. On the other hand, a cell proliferation reduction and lower BCL2L1 mRNA levels were observed after treatment (156).

A novel dual inhibitor, CM-272, targeting G9a, a histone methyltransferase that catalyzes H3K9me2, and DNMTs demonstrated activity against a wide range of cancer cells (157). Specifically, treatment of hematologic malignancies cell lines with concentrations in the nanomolar range led to a global decrease in H3K9me2 and 5-methylcytosine levels, a reduction in cell proliferation, induction of cell-cycle arrest and apoptosis, and a decrease in TSG promoter methylation. Interestingly, CM-272 also induced an IFN-γ type I response and immunogenic cell death. In an in vivo mouse model, CM-272 was safe to administer, with an increased overall survival of the treated mice (157). Furthermore, CM-272 was also active against hepatocellular carcinoma cell lines (158). Recently, the effects of CM-272 were evaluated in in vitro and in vivo models of BC. CM-272 in combination with cisplatin led to inhibition of cell proliferation, which was also verified in a BC xenograft mouse model, leading to a decreased tumor growth, whereas apoptosis and autophagy were increased (159). These effects were also observed in a quadruple-knockout transgenic mouse model of advanced BC. Remarkably, BC cells treated with CM-272 showed upregulation of genes linked to the immune response, including IFN-α and γ, and tumor necrosis factor (TNF)-α, probably through induction of an endogenous retrovirus response (159). Taking into account these results, the combination of CM-272 with anti-PD-L1 in the quadruple-knockout mouse model was explored. A sustained response to the combination treatment was observed, with the number of animals developing tumors or metastases being lower in the combination group when compared with the group treated with anti-PD-L1 monotherapy (159). Remarkably, CM-272 treatment led to an immune reactivation of tumor cells, turning “cold” tumors into “hot” ones (159). A brief overview of the main studies exploring the combination therapies in BC experimental models can be found in Table 2.

**Table 2**. Summary of combination studies targeting DNMTs in BC.

| Drug | Model | Concentration | Treatment Scheme | Effects | Year | Reference |
|---|---|---|---|---|---|---|
| 5-Aza and FK228 | 253J, T24, TCCSUP, UMUC3, and WH | 5-aza 1–25 μM<br>FK228 0.25-5 ng/mL | 3 days | ↑ Apoptosis<br>↓ G2/M cell population | 2007 | (147) |
| DAC and cisplatin | 253J, RT112, T24, and TCCSUP | DAC 0.1–8 μM<br>Cisplatin 0.25–2 μg/mL | 3 days | ↑ Cell arrest at G2/M<br>↓ Proliferative ability<br>↑ Apoptosis<br>↑ Susceptibility to cisplatin | 2008 | (160) |
| 5-Aza, cisplatin, and docetaxel | T24, TCCSUP, and UMUC3 | 5-Aza 0.6 μM<br>Cisplatin 1 μM<br>Docetaxel 5 nM | 5-Aza for 72 h followed by cisplatin or docetaxel for 72 h | ↑ Cell toxicity with combined treatment | 2011 | (150) |
| 5-Aza and TSA | K9TCC, K9TCC-PU-Nk, and K9TCC-PU-Sh | 5-Aza 1–50 μM<br>TSA 0.5 μM | 2 days | ↑ p16 expression<br>↓ Cell number<br>↓ Cyclin D1, p21, pRb, survivin, and PARP expression | 2013 | (148) |
| DAC, TSA, cisplatin, and gemcitabine | T24 | Gemcitabine 2.5 μM<br>Cisplatin 1.25 μM<br>DAC 10 μM<br>TSA 300 nM | Gemcitabine and cisplatin for 48 h followed by DAC for 48 h and TSA for 6 h | ↑ Apoptosis<br>↓ Cell proliferation<br>↑ DNA fragmentation<br>↑ CASP-3 mRNA levels<br>↑ GSK3β mRNA levels<br>↑ Canonical Wnt pathway<br>↓ BCL2L1 mRNA levels | 2014 | (156) |
| DAC, cisplatin, doxorubicin, etoposide, and vinblastine | 96-1, 97-1, RT4, and SW1710 | DAC 100 nM<br>Cisplatin 0.3–3000 μM<br>Etoposide, vinblastine, and doxorubicin 0.1–1000 μM | DAC for 120 h followed by chemotherapeutic drugs for 48 h | ↓ $IC_{50}$ of chemotherapeutic drugs with combined treatment | 2016 | (152) |

| | | | | | | |
|---|---|---|---|---|---|---|
| DAC, cisplatin, and doxorubicin | HT1376 and T24 | DAC 1 and 5 μM<br>Cisplatin and doxorubicin 1–10 μg/mL | DAC for 72 h followed by cisplatin or doxorubicin for 72 h | ↑ Cell toxicity<br>↑ RASSF1A expression<br>Hippo pathway activation | 2018 | (151) |
| DAC, cisplatin, and gemcitabine | 5637 and SCaBER | DAC 100 nM<br>Cisplatin 100–150 ng/mL<br>Gemcitabine 2–150 ng/mL | Daily for 72 h | ↑ Apoptosis<br>↓ Ratio of CD44v6+ and ALDH+ cells<br>↑ SOCS3 expression | 2019 | (155) |
| | BNN-induced mouse model | Cisplatin 2.5 mg/kg<br>Gemcitabine 120 mg/kg<br>DAC 0.05–0.2 mg/kg | Cisplatin weekly for 3 weeks<br>Gemcitabine weekly for 3 weeks<br>DAC once daily for 5 consecutive days and 3 times per week | ↓ Number of invasive tumors<br>↓ Cancer cells proliferation<br>↑ Apoptosis<br>↓ KRT14+ expressing cells<br>↓ SOX2+ expression cells<br>↓ STAT3 phosphorylation | | |
| | Patient sample-derived xenografts | | | | | |
| DAC and cisplatin | CR-T24 and T24 | DAC 2 μM<br>Cisplatin 1 μg/mL | DAC for 48 h followed by cisplatin for 24 h | ↓ Colonies formation<br>↑ Tap73 expression<br>↑ Cisplatin response | 2019 | (161) |
| CM-272 and anti-PD-L1 | Quadruple-knockout transgenic mouse model of metastatic BC. Cre-dependent inactivation of *Pten*, *Trp53*, and *Rb1* specifically | CM-272 5 mg $kg^{-1}$<br>Anti-PD-L1 200 μg per injection | Treatment of mice started at the time of tumor detection. CM-272 intraperitoneally 5 days per week. Anti-PD-L1 once a week for a total of 3 injections. | Extensive immune infiltrations comprising CD3+, CD8+, and NK cells<br>Low number of animals showing tumor or metastasis evidence. | 2019 | (159) |

| | | | | | | |
|---|---|---|---|---|---|---|
| | in urothelial cells (AdK5Cre) of Rbl1-deficient mice | | | Prolonged anti-tumor effect without any treatment | | |
| DAC and entinostat | J82, J82CisR, HBLAK, and RT112 | DAC 0.1 and 1 μM<br>Entinostat $IC_{50}$ according to cell line | DAC for 48 h followed by entinostat for 48 h | Growth inhibition<br>↑ Apoptosis<br>↑ Cell arrest in G2/M transition<br>↑ FoxO1 expression<br>↑ BIM and p21 expression<br>↓ Survivin expression | 2020 | (149) |

Abbreviations: 5-aza—5-azacytidine; CASP-3 – caspase 3; DAC—decitabine; FoxO1 - forkhead box O1; GSK3β - glycogen synthase kinase 3 beta; KRT14 – keratin 14; PARP - poly(ADP-ribose) polymerase; RASSF1A - Ras association domain family 1 isoform A; SOCS3 - suppressor of cytokine signaling 3; SOX2 - SRY-box transcription factor 2; STAT3 - signal transducer and activator of transcription 3; Tap73 - tumor protein P73; TSA—trichostatin A. ↑—increase, ↓—decrease.

### *4.3. Clinical Studies*

A non-randomized multicenter phase II study evaluated the effects of FdCyd in THU (80, 162). The safety, maximum tolerated dose (MTD), pharmacokinetics, and pharmacodynamics of this combination were determined in a previous phase I clinical trial (FyCyd 100 mg/m2/day and THU 350 mg/m2/day) (81). Patients with metastatic or unresectable breast cancer (n = 29), head and neck cancer (n = 21), non-small-cell lung cancer (n = 25), and urothelial cell carcinoma (n = 18) which endured progression after at least one line of standard therapy were included in this study. The combination was well tolerated, and urothelial carcinoma patients showed some clinical responses, with an objective response rate (ORR) of 5.6%, a PFS of 3.6 months, and a four-month PFS probability of 42%. Furthermore, increased p16 expression was observed in cytokeratin-positive circulating tumor cells (CTCs) of some patients, although it did not associate with clinical response (Table 3) (162).

The pharmacokinetics, toxicity, and clinical relevance of combining 5-aza and sodium phenylbutyrate, a first-generation HDAC inhibitor, was assessed in 34 patients with refractory solid tumors with no curative options, including two BC patients. Twenty-seven patients were eligible to proceed with treatment in three different regiments. The treatment was well tolerated with the most common toxicity effects including neutropenia, anemia, nausea, vomiting, transaminase elevation, and edema. The results of the study were mostly disappointing, with only one leiomyosarcoma patient displaying stable disease for 4.5 months and the rest disclosing disease progression. Although inhibition of DNMT activity was observed in two patients, this drug combination failed to show clinical benefit (Table 3) (163).

In a phase Ib clinical trial, the effects of CC-486 to potentiate carboplatin or paclitaxel protein-bound particles (ABI-007) in 169 patients with relapsed or refractory solid tumors including BC were evaluated. Two arms were defined: arm A comprising treatment with CC-486 and carboplatin and arm B including combination treatment of CC-486 and ABI-007 (164). Preliminary results showed that CC-486 (200 and 300 mg) was well tolerated, with treatment-emergent adverse events (TEAEs) including anemia and neutropenia in about 50% of the patients in arm A and nausea/vomiting and peripheral neuropathy in patients of arm B. Five patients in arm A showed stable disease whereas three patients displayed partial response, with both combinations disclosing clinical value. Interestingly, peripheral blood mononuclear cells (PBMCs) were found to be hypomethylated. A recommended phase II dose (RP2D) study will comprise an expansion of cohorts and the combinations of 300 mg of CC-486 with carboplatin and 200 mg of CC-486 with ABI-007 (165).

Other clinical trials are at this date assessing the clinical benefit of combining immune checkpoint inhibitors with epigenetic drugs. In a recently completed study, the combination of pembrolizumab, epacadostat [indoleamine 2,3-dioxygenase 1 (IDO1)-selective inhibitor], and 5-aza was assessed in a phase I and II trial enrolling 70 patients, including urothelial cancer patients (166). Furthermore, in a currently recruiting phase II clinical trial, the biological and clinical efficacy of atezolizumab (which targets PD-L1) in combination with guadecitabine will be evaluated in 53 patients with checkpoint inhibitor-refractory or -resistant urothelial carcinoma (Table 3) (167).

**Table 3.** Clinical trials in BC using DNMT inhibitors.

| Drug | Phase (ID) | Status | Enrollment | Schedule | Results | Period | Reference |
|---|---|---|---|---|---|---|---|
| 5-Aza and sodium phenylbutyrate | I (NCT00005639) | Completed | Patients with diagnosis of a refractory solid tumor malignancy with no curative options including BC (*n* = 34) | Regimen A: Low-dose of 5-aza with intermittent phenylbutyrate 400 mg/m$^2$/day over 24 h on days 6 and 13. Regiment B: 5-aza 75 mg/m$^2$/day for 7 days, followed by two different doses of phenylbutyrate starting on day 8 and continuing for 7 days. Each cycle lasts 35 days for A and B. Regiment C: 2 different daily doses of 5-AC for 21 days and phenylbutyrate 400 mg/m$^2$/day over 24 h once per week. Each cycle lasts 42 days. | Three doses were well tolerated. Common toxicities included bone marrow suppression-related neutropenia and anemia. One patient showed stable disease; the remaining did not show any clinical response. | 2000–2005 | (163) |
| DAC | I (NCT00030615) | Completed | Advanced metastatic solid tumor patients after other standard therapies fail including BC (*n* = 24) | DAC intravenous (IV) over 30 min on days 1–5 weekly for 4 weeks. Course repeated every 6 weeks in the absence of disease progression or unacceptable toxicity. | Not available | 2001–2008 | (168) |
| FdCyd and THU | II (NCT00978250) | Completed | Metastatic or unresectable solid tumors including urothelial transitional cell carcinoma (*n* = 18), whose | FdCyd (100 mg/m$^2$/day) by 3 h intravenous infusion and THU (350 mg/m$^2$/day) 20% as a bolus, with the remaining co-administered with FdCyd over 3-h infusion on days 1–5 and 8–12 of each 28-day cycle. | Co-administration with THU was shown to increase the area under the curve of FdCyd more than 4-fold. Combination was well tolerated. | 2009–2019 | (162, 169) |

| | | | | | | | |
|---|---|---|---|---|---|---|---|
| | | | disease progressed after at least one line of standard therapy. | | ORR of 5.6%, PFS of 3.6 months, and 42% of 4-month PFS probability for urothelial cancer patients. | | |
| CC-486, carboplatin, and paclitaxel protein-bound particles (ABI-007) | I (NCT01478685) | Completed | Patients with relapsed or refractory solid tumors including urinary bladder neoplasms (*n* = 169) | Arm A: CC-486 (doses between 100–300 mg) was administered orally daily either 14 or 21 days. Carboplatin was given by intravenous (IV) infusion once every 21 days<br>Arm B: CC-486 (doses between 100–300 mg) was administered orally daily for either 14 or 21 days<br>ABI-007 was administered by intravenous (IV) infusion on two of every three weeks<br>Arm C: CC-486 (doses between 100–300 mg) was administered orally daily for either 14 or 21 days. | CC-486 dosed 14/21 days was tolerated as a priming agent with carboplatin and ABI-007. Both combinations show evidence of clinical activity. | 2011–2015 | (164, 165) |
| RX-3317 | I (NCT02030067) | Completed | Patients with advanced or metastatic solid tumors including advanced BC (*n* = 124) | A cycle was 4 weeks, with up to 8 cycles. RX-3117 dosing was given 3 times each week for 3 weeks followed by 1 week off treatment. All subjects were followed for at least 30 days after the last dose of RX-3117. | Not available | 2013–2019 | (170) |
| CC-486 | I (NCT02223052) | Completed | Subjects with hematologic or solid tumor malignancies | Arm 1: Two 150-mg tablets of CC-486 on day 1 and 1 × 300 mg CC-486 on day 2 Arm 2: 1 × 300 mg tablet of CC-486 on day 1 and 2 × 150 mg CC-486 on day 2. | Not available | 2014–2018 | (171) |

| | | | | | | | |
|---|---|---|---|---|---|---|---|
| | | | including BC patients (*n* = 89) | | | | |
| SGI-110, gemcitabine, and cisplatin | Ib/IIa (2015-004062-29) | Recruiting | Urothelial BC patients with stages T2-4aN0M0 (*n* = 20) | Arm 1: SGI-110 days 1–5 at the determined dose, gemcitabine 1000 mg/m$^2$ days 8 + 15, cisplatin 70 mg/m$^2$ day 8. 3–4 cycles of 21 days each. Arm 2: Gemcitabine 1000 mg/m$^2$ days 8 + 15, cisplatin 70 mg/m$^2$ day 8 3–4 cycles of 21 days each for both arms. 3–4 cycles of 21 days each. | Not available | 2015–present | (172) |
| 75 approved agents | II (NCT02788201) | Completed | Patients with a diagnosis of metastatic, progressive urothelial carcinoma of the bladder, urethra, ureter, or renal pelvis (*n* = 8) | COXEN algorithm was used to determine the best therapy from among 75 FDA-approved agents (single agent or combination). Patients had regular visits for blood, urine, and tumor scans. | Not available | 2017–2019 | (173) |
| Azacitidine, pembrolizumab, and epacadostat | I (NCT02959437) | Completed | Subjects with advanced or metastatic solid tumors including BC patients (*n* = 70) | Five doses of azacitidine were administered by subcutaneous injection or intravenously (IV) over days 1 to 7 in cycles 1 through 6. Pembrolizumab was administered in a 30-min IV infusion every 3 weeks on day 1 of each 21-day cycle. Epacadostat tablets were administered orally twice daily. | Not available | 2017–2020 | (166) |
| Atezolizumab and guadecitabine | II (NCT03179943) | Suspended | Recurrent/advanced urothelial carcinoma | Atezolizumab is administered intravenously on day 1 and day 22 of a 6-week cycle for a period of 8 cycles. | Not available | 2017–estimated end 2022 | (167) |

| | | | | | | | |
|---|---|---|---|---|---|---|---|
| | | | (stage IV) patients who previously progressed on checkpoint inhibitor therapy with anti- PD-1 or PD-L1 therapy (*n* = 53) | Guadecitabine is administered subcutaneously on days 1 through 5 of the 6-week cycle for a period of 4 cycles. | | | |

Abbreviations: 5-aza—5-azacytidine; DAC—decitabine

## 5. Conclusions

DNA methylation machinery is a promising target for BC treatment. Among the anti-tumor effects caused by DNMT inhibitors, the most frequently reported are reactivation of TSGs and inhibition of tumor cell growth (Figure 4). However, DNMT inhibitors still present several drawbacks that preclude their use for BC treatment, including the reversal of the inhibitory effects after drug withdrawal, short half-life, and significant toxicity. To overcome these, combination therapies comprising DNMT inhibitors, chemotherapeutic agents, and, more recently, immune checkpoint inhibitors might constitute a valid option for BC patients, as demonstrated by the currently ongoing clinical trials. Furthermore, the discovery of novel biomarkers to select patients more likely to respond to those therapies and the evaluation of the long-term effect of this class of compounds are required for the transition into clinical practice.

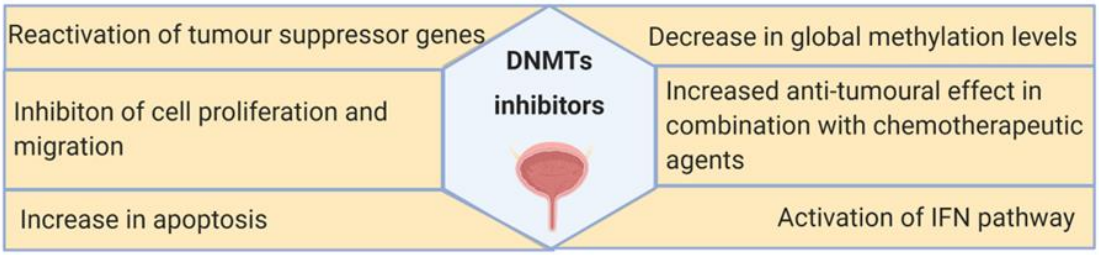


**Figure 4.** Summary of the main effects of DNMT inhibitors observed in bladder cancer in vitro and in vivo models, as well as in clinical trials.

In conclusion, modulation of the epigenetic landscape of BC tumors constitutes an encouraging alternative to the currently available therapeutic strategies for BC patients, requiring further exploitation in a clinical trial setting, aiming at a future implementation in clinical practice.

## References


1. Bray F, Ferlay J, Soerjomataram I, Siegel RL, Torre LA, Jemal A. Global cancer statistics 2018: GLOBOCAN estimates of incidence and mortality worldwide for 36 cancers in 185 countries. CA: a cancer journal for clinicians. 2018;68(6):394-424.
2. Kamat AM, Hahn NM, Efstathiou JA, Lerner SP, Malmström PU, Choi W, et al. Bladder cancer. Lancet. 2016;388(10061):2796-810.
3. Bellmunt J, Orsola A, Leow J, Wiegel T, De Santis M, Horwich A. Bladder cancer: ESMO Practice Guidelines for diagnosis, treatment and follow-up. Annals of oncology. 2014;25:iii40-iii8.
4. Amin MB, Edge S, Greene F, Byrd DR, Brookland RK, Washington MK, et al. AJCC Cancer Staging Manual Eighth edition ed: Springer International Publishing: American Joint Commission on Cancer; 2017.
5. Redelman-Sidi G, Glickman MS, Bochner BH. The mechanism of action of BCG therapy for bladder cancer--a current perspective. Nat Rev Urol. 2014;11(3):153-62.
6. Cancer Stat Facts: Bladder Cancer: National Cancer Institute; 2017 [cited 01 April 2020 01 April 2020]. Available from: https://seer.cancer.gov/statfacts/html/urinb.html.
7. Mariotto AB, Yabroff KR, Shao Y, Feuer EJ, Brown ML. Projections of the cost of cancer care in the United States: 2010-2020. Journal of the National Cancer Institute. 2011;103(2):117-28.
8. Lobo J, Jerónimo C, Henrique R. Targeting the Immune system and Epigenetic Landscape of Urological Tumors. Int J Mol Sci. 2020;21(3).
9. Hussain SA, Birtle A, Crabb S, Huddart R, Small D, Summerhayes M, et al. From Clinical Trials to Real-life Clinical Practice: The Role of Immunotherapy with PD-1/PD-L1 Inhibitors in Advanced Urothelial Carcinoma. Eur Urol Oncol. 2018;1(6):486-500.
10. Tan TZ, Rouanne M, Tan KT, Huang RY, Thiery JP. Molecular Subtypes of Urothelial Bladder Cancer: Results from a Meta-cohort Analysis of 2411 Tumors. Eur Urol. 2019;75(3):423-32.
11. Choi W, Ochoa A, McConkey DJ, Aine M, Höglund M, Kim WY, et al. Genetic Alterations in the Molecular Subtypes of Bladder Cancer: Illustration in the Cancer Genome Atlas Dataset. Eur Urol. 2017;72(3):354-65.
12. Robertson AG, Kim J, Al-Ahmadie H, Bellmunt J, Guo G, Cherniack AD, et al. Comprehensive Molecular Characterization of Muscle-Invasive Bladder Cancer. Cell. 2017;171(3):540-56.e25.
13. Kelly AD, Issa JJ. The promise of epigenetic therapy: reprogramming the cancer epigenome. Current opinion in genetics & development. 2017;42:68-77.

14. Baylin SB, Jones PA. A decade of exploring the cancer epigenome - biological and translational implications. Nat Rev Cancer. 2011;11(10):726-34.
15. Bennett RL, Licht JD. Targeting Epigenetics in Cancer. Annual review of pharmacology and toxicology. 2018;58:187-207.
16. Voyias P, Patel A, Arasaradnam R. Epigenetic Biomarkers of Disease. Medical Epigenetics: Elsevier; 2016. p. 159-76.
17. Inbar-Feigenberg M, Choufani S, Butcher DT, Roifman M, Weksberg R. Basic concepts of epigenetics. Fertility and sterility. 2013;99(3):607-15.
18. Porten SP. Epigenetic Alterations in Bladder Cancer. Current urology reports. 2018;19(12):102.
19. Duex JE, Swain KE, Dancik GM, Paucek RD, Owens C, Churchill MEA, et al. Functional Impact of Chromatin Remodeling Gene Mutations and Predictive Signature for Therapeutic Response in Bladder Cancer. Molecular cancer research : MCR. 2018;16(1):69-77.
20. Comprehensive molecular characterization of urothelial bladder carcinoma. Nature. 2014;507(7492):315-22.
21. Hurst CD, Alder O, Platt FM, Droop A, Stead LF, Burns JE, et al. Genomic Subtypes of Non-invasive Bladder Cancer with Distinct Metabolic Profile and Female Gender Bias in KDM6A Mutation Frequency. Cancer Cell. 2017;32(5):701-15.e7.
22. Ler LD, Ghosh S, Chai X, Thike AA, Heng HL, Siew EY, et al. Loss of tumor suppressor KDM6A amplifies PRC2-regulated transcriptional repression in bladder cancer and can be targeted through inhibition of EZH2. Sci Transl Med. 2017;9(378).
23. Ding B, Yan L, Zhang Y, Wang Z, Zhang Y, Xia D, et al. Analysis of the role of mutations in the KMT2D histone lysine methyltransferase in bladder cancer. FEBS open bio. 2019;9(4):693-706.
24. Marques-Magalhães Â, Graça I, Henrique R, Jerónimo C. Targeting DNA Methyltranferases in Urological Tumors. Front Pharmacol. 2018;9:366.
25. Wolff EM, Chihara Y, Pan F, Weisenberger DJ, Siegmund KD, Sugano K, et al. Unique DNA methylation patterns distinguish noninvasive and invasive urothelial cancers and establish an epigenetic field defect in premalignant tissue. Cancer Res. 2010;70(20):8169-78.
26. Wu H, Caffo B, Jaffee HA, Irizarry RA, Feinberg AP. Redefining CpG islands using hidden Markov models. Biostatistics (Oxford, England). 2010;11(3):499-514.
27. Ferreira HJ, Esteller M. CpG Islands in Cancer: Heads, Tails, and Sides. Methods Mol Biol. 2018;1766:49-80.
28. Rodríguez-Paredes M, Esteller M. Cancer epigenetics reaches mainstream oncology. Nat Med. 2011;17(3):330-9.

29. Kanwal R, Gupta S. Epigenetic modifications in cancer. Clinical genetics. 2012;81(4):303-11.
30. Pasculli B, Barbano R, Parrella P. Epigenetics of breast cancer: Biology and clinical implication in the era of precision medicine. Semin Cancer Biol. 2018;51:22-35.
31. Lao VV, Grady WM. Epigenetics and colorectal cancer. Nature reviews Gastroenterology & hepatology. 2011;8(12):686-700.
32. Maunakea AK, Chepelev I, Cui K, Zhao K. Intragenic DNA methylation modulates alternative splicing by recruiting MeCP2 to promote exon recognition. Cell Res. 2013;23(11):1256-69.
33. Maunakea AK, Nagarajan RP, Bilenky M, Ballinger TJ, D'Souza C, Fouse SD, et al. Conserved role of intragenic DNA methylation in regulating alternative promoters. Nature. 2010;466(7303):253-7.
34. Bae MG, Kim JY, Choi JK. Frequent hypermethylation of orphan CpG islands with enhancer activity in cancer. BMC medical genomics. 2016;9 Suppl 1(Suppl 1):38.
35. Baubec T, Colombo DF, Wirbelauer C, Schmidt J, Burger L, Krebs AR, et al. Genomic profiling of DNA methyltransferases reveals a role for DNMT3B in genic methylation. Nature. 2015;520(7546):243-7.
36. Timinskas A, Butkus V, Janulaitis A. Sequence motifs characteristic for DNA [cytosine-N4] and DNA [adenine-N6] methyltransferases. Classification of all DNA methyltransferases. Gene. 1995;157(1-2):3-11.
37. Lyko F. The DNA methyltransferase family: a versatile toolkit for epigenetic regulation. Nat Rev Genet. 2018;19(2):81-92.
38. Gruenbaum Y, Cedar H, Razin A. Substrate and sequence specificity of a eukaryotic DNA methylase. Nature. 1982;295(5850):620-2.
39. Bestor TH, Ingram VM. Two DNA methyltransferases from murine erythroleukemia cells: purification, sequence specificity, and mode of interaction with DNA. Proc Natl Acad Sci U S A. 1983;80(18):5559-63.
40. Tahiliani M, Koh KP, Shen Y, Pastor WA, Bandukwala H, Brudno Y, et al. Conversion of 5-methylcytosine to 5-hydroxymethylcytosine in mammalian DNA by MLL partner TET1. Science. 2009;324(5929):930-5.
41. Kohli RM, Zhang Y. TET enzymes, TDG and the dynamics of DNA demethylation. Nature. 2013;502(7472):472-9.
42. Cedar H, Bergman Y. Programming of DNA methylation patterns. Annual review of biochemistry. 2012;81:97-117.
43. Bhutani N, Burns DM, Blau HM. DNA demethylation dynamics. Cell. 2011;146(6):866-72.

44. Baylin SB, Jones PA. Epigenetic Determinants of Cancer. Cold Spring Harb Perspect Biol. 2016;8(9).
45. Hansen KD, Timp W, Bravo HC, Sabunciyan S, Langmead B, McDonald OG, et al. Increased methylation variation in epigenetic domains across cancer types. Nature genetics. 2011;43(8):768-75.
46. Ross JP, Rand KN, Molloy PL. Hypomethylation of repeated DNA sequences in cancer. Epigenomics. 2010;2(2):245-69.
47. Rodriguez J, Frigola J, Vendrell E, Risques RA, Fraga MF, Morales C, et al. Chromosomal instability correlates with genome-wide DNA demethylation in human primary colorectal cancers. Cancer Res. 2006;66(17):8462-9468.
48. Saif I, Kasmi Y, Allali K, Ennaji MM. Prediction of DNA methylation in the promoter of gene suppressor tumor. Gene. 2018;651:166-73.
49. Kandimalla R, van Tilborg AA, Zwarthoff EC. DNA methylation-based biomarkers in bladder cancer. Nat Rev Urol. 2013;10(6):327-35.
50. Larsen LK, Lind GE, Guldberg P, Dahl C. DNA-Methylation-Based Detection of Urological Cancer in Urine: Overview of Biomarkers and Considerations on Biomarker Design, Source of DNA, and Detection Technologies. Int J Mol Sci. 2019;20(11).
51. Padrão NA, Monteiro-Reis S, Torres-Ferreira J, Antunes L, Leça L, Montezuma D, et al. MicroRNA promoter methylation: a new tool for accurate detection of urothelial carcinoma. British journal of cancer. 2017;116(5):634-9.
52. Wu Y, Jiang G, Zhang N, Liu S, Lin X, Perschon C, et al. HOXA9, PCDH17, POU4F2, and ONECUT2 as a Urinary Biomarker Combination for the Detection of Bladder Cancer in Chinese Patients with Hematuria. European urology focus. 2020;6(2):284-91.
53. Costa VL, Henrique R, Danielsen SA, Duarte-Pereira S, Eknaes M, Skotheim RI, et al. Three epigenetic biomarkers, GDF15, TMEFF2, and VIM, accurately predict bladder cancer from DNA-based analyses of urine samples. Clin Cancer Res. 2010;16(23):5842-51.
54. Feber A, Dhami P, Dong L, de Winter P, Tan WS, Martínez-Fernández M, et al. UroMark-a urinary biomarker assay for the detection of bladder cancer. Clin Epigenetics. 2017;9:8.
55. García-Baquero R, Puerta P, Beltran M, Alvarez-Mújica M, Alvarez-Ossorio JL, Sánchez-Carbayo M. Methylation of tumor suppressor genes in a novel panel predicts clinical outcome in paraffin-embedded bladder tumors. Tumour biology : the journal of the International Society for Oncodevelopmental Biology and Medicine. 2014;35(6):5777-86.

56. Wang X, Chen E, Yang X, Wang Y, Quan Z, Wu X, et al. 5-azacytidine inhibits the proliferation of bladder cancer cells via reversal of the aberrant hypermethylation of the hepaCAM gene. Oncol Rep. 2016;35(3):1375-84.
57. Erdmann A, Halby L, Fahy J, Arimondo PB. Targeting DNA methylation with small molecules: what's next? J Med Chem. 2015;58(6):2569-83.
58. Bohl SR, Bullinger L, Rücker FG. Epigenetic therapy: azacytidine and decitabine in acute myeloid leukemia. Expert review of hematology. 2018;11(5):361-71.
59. Stresemann C, Lyko F. Modes of action of the DNA methyltransferase inhibitors azacytidine and decitabine. Int J Cancer. 2008;123(1):8-13.
60. Egger G, Liang G, Aparicio A, Jones PA. Epigenetics in human disease and prospects for epigenetic therapy. Nature. 2004;429(6990):457-63.
61. Jones PA, Taylor SM. Cellular differentiation, cytidine analogs and DNA methylation. Cell. 1980;20(1):85-93.
62. Levine AJ. The p53 protein plays a central role in the mechanism of action of epigentic drugs that alter the methylation of cytosine residues in DNA. Oncotarget. 2017;8(5):7228-30.
63. Nguyen AN, Hollenbach PW, Richard N, Luna-Moran A, Brady H, Heise C, et al. Azacitidine and decitabine have different mechanisms of action in non-small cell lung cancer cell lines. Lung Cancer (Auckland, NZ). 2010;1:119-40.
64. Datta J, Ghoshal K, Motiwala T, Jacob ST. Novel Insights into the Molecular Mechanism of Action of DNA Hypomethylating Agents: Role of Protein Kinase C δ in Decitabine-Induced Degradation of DNA Methyltransferase 1. Genes & cancer. 2012;3(1):71-81.
65. Santi DV, Norment A, Garrett CE. Covalent bond formation between a DNA-cytosine methyltransferase and DNA containing 5-azacytosine. Proc Natl Acad Sci U S A. 1984;81(22):6993-7.
66. Chen L, MacMillan AM, Chang W, Ezaz-Nikpay K, Lane WS, Verdine GL. Direct identification of the active-site nucleophile in a DNA (cytosine-5)-methyltransferase. Biochemistry. 1991;30(46):11018-25.
67. Mortusewicz O, Schermelleh L, Walter J, Cardoso MC, Leonhardt H. Recruitment of DNA methyltransferase I to DNA repair sites. Proc Natl Acad Sci U S A. 2005;102(25):8905-9.
68. Welch JS, Petti AA, Miller CA, Fronick CC, O'Laughlin M, Fulton RS, et al. TP53 and Decitabine in Acute Myeloid Leukemia and Myelodysplastic Syndromes. N Engl J Med. 2016;375(21):2023-36.

69. Gros C, Fahy J, Halby L, Dufau I, Erdmann A, Gregoire JM, et al. DNA methylation inhibitors in cancer: recent and future approaches. Biochimie. 2012;94(11):2280-96.
70. Ganesan A, Arimondo PB, Rots MG, Jeronimo C, Berdasco M. The timeline of epigenetic drug discovery: from reality to dreams. Clin Epigenetics. 2019;11(1):174.
71. Yoo CB, Cheng JC, Jones PA. Zebularine: a new drug for epigenetic therapy. Biochemical Society transactions. 2004;32(Pt 6):910-2.
72. Takemura Y, Satoh M, Hatanaka K, Kubota S. Zebularine exerts its antiproliferative activity through S phase delay and cell death in human malignant mesothelioma cells. Bioscience, biotechnology, and biochemistry. 2018;82(7):1159-64.
73. Chen X, Xu R, He D, Zhang Y, Chen H, Zhu Y, et al. CD8(+) T effector and immune checkpoint signatures predict prognosis and responsiveness to immunotherapy in bladder cancer. Oncogene. 2021;40(43):6223-34.
74. Orta ML, Pastor N, Burgos-Morón E, Domínguez I, Calderón-Montaño JM, Huertas Castaño C, et al. Zebularine induces replication-dependent double-strand breaks which are preferentially repaired by homologous recombination. DNA repair. 2017;57:116-24.
75. Liu H, Xue ZT, Sjögren HO, Salford LG, Widegren B. Low dose Zebularine treatment enhances immunogenicity of tumor cells. Cancer letters. 2007;257(1):107-15.
76. Champion C, Guianvarc'h D, Sénamaud-Beaufort C, Jurkowska RZ, Jeltsch A, Ponger L, et al. Mechanistic insights on the inhibition of c5 DNA methyltransferases by zebularine. PloS one. 2010;5(8):e12388.
77. Gowher H, Jeltsch A. Mechanism of inhibition of DNA methyltransferases by cytidine analogs in cancer therapy. Cancer biology & therapy. 2004;3(11):1062-8.
78. Beumer JH, Eiseman JL, Parise RA, Joseph E, Holleran JL, Covey JM, et al. Pharmacokinetics, metabolism, and oral bioavailability of the DNA methyltransferase inhibitor 5-fluoro-2'-deoxycytidine in mice. Clin Cancer Res. 2006;12(24):7483-91.
79. Neil GL, Moxley TE, Kuentzel SL, Manak RC, Hanka LJ. Enhancement by tetrahydrouridine (NSC-112907) of the oral activity of 5-azacytidine (NSC-102816) in L1210 leukemic mice. Cancer chemotherapy reports. 1975;59(3):459-65.
80. Beumer JH, Parise RA, Newman EM, Doroshow JH, Synold TW, Lenz HJ, et al. Concentrations of the DNA methyltransferase inhibitor 5-fluoro-2'-deoxycytidine (FdCyd) and its cytotoxic metabolites in plasma of patients treated with FdCyd and tetrahydrouridine (THU). Cancer chemotherapy and pharmacology. 2008;62(2):363-8.
81. Newman EM, Morgan RJ, Kummar S, Beumer JH, Blanchard MS, Ruel C, et al. A phase I, pharmacokinetic, and pharmacodynamic evaluation of the DNA

methyltransferase inhibitor 5-fluoro-2'-deoxycytidine, administered with tetrahydrouridine. Cancer chemotherapy and pharmacology. 2015;75(3):537-46.
82. Kantarjian HM, Roboz GJ, Kropf PL, Yee KWL, O'Connell CL, Tibes R, et al. Guadecitabine (SGI-110) in treatment-naive patients with acute myeloid leukaemia: phase 2 results from a multicentre, randomised, phase 1/2 trial. Lancet Oncol. 2017;18(10):1317-26.
83. Lee V, Wang J, Zahurak M, Gootjes E, Verheul HM, Parkinson R, et al. A Phase I Trial of a Guadecitabine (SGI-110) and Irinotecan in Metastatic Colorectal Cancer Patients Previously Exposed to Irinotecan. Clin Cancer Res. 2018;24(24):6160-7.
84. Garcia-Manero G, Roboz G, Walsh K, Kantarjian H, Ritchie E, Kropf P, et al. Guadecitabine (SGI-110) in patients with intermediate or high-risk myelodysplastic syndromes: phase 2 results from a multicentre, open-label, randomised, phase 1/2 trial. The Lancet Haematology. 2019;6(6):e317-e27.
85. Laille E, Savona MR, Scott BL, Boyd TE, Dong Q, Skikne B. Pharmacokinetics of different formulations of oral azacitidine (CC-486) and the effect of food and modified gastric pH on pharmacokinetics in subjects with hematologic malignancies. Journal of clinical pharmacology. 2014;54(6):630-9.
86. Levy BP, Giaccone G, Besse B, Felip E, Garassino MC, Domine Gomez M, et al. Randomised phase 2 study of pembrolizumab plus CC-486 versus pembrolizumab plus placebo in patients with previously treated advanced non-small cell lung cancer. European journal of cancer (Oxford, England : 1990). 2019;108:120-8.
87. Von Hoff DD, Rasco DW, Heath EI, Munster PN, Schellens JHM, Isambert N, et al. Phase I Study of CC-486 Alone and in Combination with Carboplatin or nab-Paclitaxel in Patients with Relapsed or Refractory Solid Tumors. Clin Cancer Res. 2018;24(17):4072-80.
88. Garcia-Manero G, Gore SD, Kambhampati S, Scott B, Tefferi A, Cogle CR, et al. Efficacy and safety of extended dosing schedules of CC-486 (oral azacitidine) in patients with lower-risk myelodysplastic syndromes. Leukemia. 2016;30(4):889-96.
89. Peters GJ, Smid K, Vecchi L, Kathmann I, Sarkisjan D, Honeywell RJ, et al. Metabolism, mechanism of action and sensitivity profile of fluorocyclopentenylcytosine (RX-3117; TV-1360). Investigational new drugs. 2013;31(6):1444-57.
90. Balboni B, El Hassouni B, Honeywell RJ, Sarkisjan D, Giovannetti E, Poore J, et al. RX-3117 (fluorocyclopentenyl cytosine): a novel specific antimetabolite for selective cancer treatment. Expert opinion on investigational drugs. 2019;28(4):311-22.
91. Yang MY, Lee YB, Ahn CH, Kaye J, Fine T, Kashi R, et al. A novel cytidine analog, RX-3117, shows potent efficacy in xenograft models, even in tumors that are resistant to gemcitabine. Anticancer Res. 2014;34(12):6951-9.

92. Castillo-Aguilera O, Depreux P, Halby L, Arimondo PB, Goossens L. DNA Methylation Targeting: The DNMT/HMT Crosstalk Challenge. Biomolecules. 2017;7(1).
93. Pushpakom S, Iorio F, Eyers PA, Escott KJ, Hopper S, Wells A, et al. Drug repurposing: progress, challenges and recommendations. Nature Reviews Drug Discovery. 2019;18(1):41-58.
94. Villar-Garea A, Fraga MF, Espada J, Esteller M. Procaine is a DNA-demethylating agent with growth-inhibitory effects in human cancer cells. Cancer Res. 2003;63(16):4984-9.
95. Moreira-Silva F, Camilo V, Gaspar V, Mano JF, Henrique R, Jerónimo C. Repurposing Old Drugs into New Epigenetic Inhibitors: Promising Candidates for Cancer Treatment? Pharmaceutics. 2020;12(5).
96. Li YC, Wang Y, Li DD, Zhang Y, Zhao TC, Li CF. Procaine is a specific DNA methylation inhibitor with anti-tumor effect for human gastric cancer. Journal of cellular biochemistry. 2018;119(2):2440-9.
97. Kuck D, Caulfield T, Lyko F, Medina-Franco JL. Nanaomycin A selectively inhibits DNMT3B and reactivates silenced tumor suppressor genes in human cancer cells. Molecular cancer therapeutics. 2010;9(11):3015-23.
98. Caulfield T, Medina-Franco JL. Molecular dynamics simulations of human DNA methyltransferase 3B with selective inhibitor nanaomycin A. Journal of structural biology. 2011;176(2):185-91.
99. Dueñas-Gonzalez A, Coronel J, Cetina L, González-Fierro A, Chavez-Blanco A, Taja-Chayeb L. Hydralazine-valproate: a repositioned drug combination for the epigenetic therapy of cancer. Expert opinion on drug metabolism & toxicology. 2014;10(10):1433-44.
100. Segura-Pacheco B, Trejo-Becerril C, Perez-Cardenas E, Taja-Chayeb L, Mariscal I, Chavez A, et al. Reactivation of tumor suppressor genes by the cardiovascular drugs hydralazine and procainamide and their potential use in cancer therapy. Clin Cancer Res. 2003;9(5):1596-603.
101. Graça I, Sousa EJ, Costa-Pinheiro P, Vieira FQ, Torres-Ferreira J, Martins MG, et al. Anti-neoplastic properties of hydralazine in prostate cancer. Oncotarget. 2014;5(15):5950-64.
102. Pérez-Cárdenas E, Taja-Chayeb L, Trejo-Becerril C, Chanona-Vilchis J, Chávez-Blanco A, Domínguez-Gómez G, et al. Antimetastatic effect of epigenetic drugs, hydralazine and valproic acid, in Ras-transformed NIH 3T3 cells. OncoTargets and therapy. 2018;11:8823-33.
103. Candelaria M, Gallardo-Rincón D, Arce C, Cetina L, Aguilar-Ponce JL, Arrieta O, et al. A phase II study of epigenetic therapy with hydralazine and magnesium valproate

to overcome chemotherapy resistance in refractory solid tumors. Ann Oncol. 2007;18(9):1529-38.

104. Coronel J, Cetina L, Pacheco I, Trejo-Becerril C, González-Fierro A, de la Cruz-Hernandez E, et al. A double-blind, placebo-controlled, randomized phase III trial of chemotherapy plus epigenetic therapy with hydralazine valproate for advanced cervical cancer. Preliminary results. Medical oncology (Northwood, London, England). 2011;28 Suppl 1:S540-6.

105. Amato RJ. Inhibition of DNA methylation by antisense oligonucleotide MG98 as cancer therapy. Clinical genitourinary cancer. 2007;5(7):422-6.

106. Davis AJ, Gelmon KA, Siu LL, Moore MJ, Britten CD, Mistry N, et al. Phase I and pharmacologic study of the human DNA methyltransferase antisense oligodeoxynucleotide MG98 given as a 21-day continuous infusion every 4 weeks. Investigational new drugs. 2003;21(1):85-97.

107. Klisovic RB, Stock W, Cataland S, Klisovic MI, Liu S, Blum W, et al. A phase I biological study of MG98, an oligodeoxynucleotide antisense to DNA methyltransferase 1, in patients with high-risk myelodysplasia and acute myeloid leukemia. Clin Cancer Res. 2008;14(8):2444-9.

108. Plummer R, Vidal L, Griffin M, Lesley M, de Bono J, Coulthard S, et al. Phase I study of MG98, an oligonucleotide antisense inhibitor of human DNA methyltransferase 1, given as a 7-day infusion in patients with advanced solid tumors. Clin Cancer Res. 2009;15(9):3177-83.

109. Amato RJ, Stephenson J, Hotte S, Nemunaitis J, Bélanger K, Reid G, et al. MG98, a second-generation DNMT1 inhibitor, in the treatment of advanced renal cell carcinoma. Cancer investigation. 2012;30(5):415-21.

110. Rondelet G, Fleury L, Faux C, Masson V, Dubois J, Arimondo PB, et al. Inhibition studies of DNA methyltransferases by maleimide derivatives of RG108 as non-nucleoside inhibitors. Future medicinal chemistry. 2017;9(13):1465-81.

111. Yang L, Hou J, Cui XH, Suo LN, Lv YW. RG108 induces the apoptosis of endometrial cancer Ishikawa cell lines by inhibiting the expression of DNMT3B and demethylation of HMLH1. European review for medical and pharmacological sciences. 2017;21(22):5056-64.

112. Graça I, Sousa EJ, Baptista T, Almeida M, Ramalho-Carvalho J, Palmeira C, et al. Anti-tumoral effect of the non-nucleoside DNMT inhibitor RG108 in human prostate cancer cells. Current pharmaceutical design. 2014;20(11):1803-11.

113. Yoo J, Choi S, Medina-Franco JL. Molecular modeling studies of the novel inhibitors of DNA methyltransferases SGI-1027 and CBC12: implications for the mechanism of inhibition of DNMTs. PloS one. 2013;8(4):e62152.

114. Datta J, Ghoshal K, Denny WA, Gamage SA, Brooke DG, Phiasivongsa P, et al. A new class of quinoline-based DNA hypomethylating agents reactivates tumor suppressor genes by blocking DNA methyltransferase 1 activity and inducing its degradation. Cancer Res. 2009;69(10):4277-85.
115. Zwergel C, Schnekenburger M, Sarno F, Battistelli C, Manara MC, Stazi G, et al. Identification of a novel quinoline-based DNA demethylating compound highly potent in cancer cells. Clin Epigenetics. 2019;11(1):68.
116. Fang MZ, Wang Y, Ai N, Hou Z, Sun Y, Lu H, et al. Tea polyphenol (-)-epigallocatechin-3-gallate inhibits DNA methyltransferase and reactivates methylation-silenced genes in cancer cell lines. Cancer Res. 2003;63(22):7563-70.
117. Nandakumar V, Vaid M, Katiyar SK. (-)-Epigallocatechin-3-gallate reactivates silenced tumor suppressor genes, Cip1/p21 and p16INK4a, by reducing DNA methylation and increasing histones acetylation in human skin cancer cells. Carcinogenesis. 2011;32(4):537-44.
118. Sheng J, Shi W, Guo H, Long W, Wang Y, Qi J, et al. The Inhibitory Effect of (-)-Epigallocatechin-3-Gallate on Breast Cancer Progression via Reducing SCUBE2 Methylation and DNMT Activity. Molecules (Basel, Switzerland). 2019;24(16).
119. Bilir B, Sharma NV, Lee J, Hammarstrom B, Svindland A, Kucuk O, et al. Effects of genistein supplementation on genome-wide DNA methylation and gene expression in patients with localized prostate cancer. Int J Oncol. 2017;51(1):223-34.
120. Xie Q, Bai Q, Zou LY, Zhang QY, Zhou Y, Chang H, et al. Genistein inhibits DNA methylation and increases expression of tumor suppressor genes in human breast cancer cells. Genes, chromosomes & cancer. 2014;53(5):422-31.
121. Zhu J, Ren J, Tang L. Genistein inhibits invasion and migration of colon cancer cells by recovering WIF1 expression. Molecular medicine reports. 2018;17(5):7265-73.
122. Link A, Balaguer F, Shen Y, Lozano JJ, Leung HC, Boland CR, et al. Curcumin modulates DNA methylation in colorectal cancer cells. PloS one. 2013;8(2):e57709.
123. Tao J, Liu Q, Wu X, Xu X, Zhang Y, Wang Q, et al. Identification of hypermethylation in hepatocyte cell adhesion molecule gene promoter region in bladder carcinoma. International journal of medical sciences. 2013;10(13):1860-7.
124. Hahn NM, Bonney PL, Dhawan D, Jones DR, Balch C, Guo Z, et al. Subcutaneous 5-azacitidine treatment of naturally occurring canine urothelial carcinoma: a novel epigenetic approach to human urothelial carcinoma drug development. J Urol. 2012;187(1):302-9.
125. Ramakrishnan S, Hu Q, Krishnan N, Wang D, Smit E, Granger V, et al. Decitabine, a DNA-demethylating agent, promotes differentiation via NOTCH1 signaling

and alters immune-related pathways in muscle-invasive bladder cancer. Cell Death Dis. 2017;8(12):3217.

126. Maraver A, Fernandez-Marcos PJ, Cash TP, Mendez-Pertuz M, Dueñas M, Maietta P, et al. NOTCH pathway inactivation promotes bladder cancer progression. J Clin Invest. 2015;125(2):824-30.

127. Zhang H, Qi F, Cao Y, Zu X, Chen M, Li Z, et al. 5-Aza-2'-deoxycytidine enhances maspin expression and inhibits proliferation, migration, and invasion of the bladder cancer T24 cell line. Cancer biotherapy & radiopharmaceuticals. 2013;28(4):343-50.

128. Devanand P, Kim SI, Choi YW, Sheen SS, Yim H, Ryu MS, et al. Inhibition of bladder cancer invasion by Sp1-mediated BTG2 expression via inhibition of DNA methyltransferase 1. Febs j. 2014;281(24):5581-601.

129. Christoph F, Kempkensteffen C, Weikert S, Köllermann J, Krause H, Miller K, et al. Methylation of tumour suppressor genes APAF-1 and DAPK-1 and in vitro effects of demethylating agents in bladder and kidney cancer. British journal of cancer. 2006;95(12):1701-7.

130. Cheng JC, Weisenberger DJ, Gonzales FA, Liang G, Xu GL, Hu YG, et al. Continuous zebularine treatment effectively sustains demethylation in human bladder cancer cells. Molecular and cellular biology. 2004;24(3):1270-8.

131. Urakami S, Shiina H, Enokida H, Kawakami T, Tokizane T, Ogishima T, et al. Epigenetic inactivation of Wnt inhibitory factor-1 plays an important role in bladder cancer through aberrant canonical Wnt/beta-catenin signaling pathway. Clin Cancer Res. 2006;12(2):383-91.

132. Liang G, Gonzales FA, Jones PA, Orntoft TF, Thykjaer T. Analysis of gene induction in human fibroblasts and bladder cancer cells exposed to the methylation inhibitor 5-aza-2'-deoxycytidine. Cancer Res. 2002;62(4):961-6.

133. Velicescu M, Weisenberger DJ, Gonzales FA, Tsai YC, Nguyen CT, Jones PA. Cell division is required for de novo methylation of CpG islands in bladder cancer cells. Cancer Res. 2002;62(8):2378-84.

134. Chuang JJ, Dai YC, Lin YL, Chen YY, Lin WH, Chan HL, et al. Downregulation of glutathione S-transferase M1 protein in N-butyl-N-(4-hydroxybutyl)nitrosamine-induced mouse bladder carcinogenesis. Toxicology and applied pharmacology. 2014;279(3):322-30.

135. Kawakami T, Shiina H, Igawa M, Deguchi M, Nakajima K, Ogishima T, et al. Inactivation of the hMSH3 mismatch repair gene in bladder cancer. Biochemical and biophysical research communications. 2004;325(3):934-42.

136. Giri AK, Aittokallio T. DNMT Inhibitors Increase Methylation in the Cancer Genome. Front Pharmacol. 2019;10:385.

137. Yoo CB, Jeong S, Egger G, Liang G, Phiasivongsa P, Tang C, et al. Delivery of 5-aza-2'-deoxycytidine to cells using oligodeoxynucleotides. Cancer Res. 2007;67(13):6400-8.
138. Chuang JC, Warner SL, Vollmer D, Vankayalapati H, Redkar S, Bearss DJ, et al. S110, a 5-Aza-2′-deoxycytidine–containing dinucleotide, is an effective DNA methylation inhibitor in vivo and can reduce tumor growth. Molecular cancer therapeutics. 2010;9(5):1443-50.
139. Chen T, Hevi S, Gay F, Tsujimoto N, He T, Zhang B, et al. Complete inactivation of DNMT1 leads to mitotic catastrophe in human cancer cells. Nature genetics. 2007;39(3):391-6.
140. Wu CT, Wu CF, Lu CH, Lin CC, Chen WC, Lin PY, et al. Expression and function role of DNA methyltransferase 1 in human bladder cancer. Cancer. 2011;117(22):5221-33.
141. Santoro SW, Joyce GF. A general purpose RNA-cleaving DNA enzyme. Proc Natl Acad Sci U S A. 1997;94(9):4262-6.
142. Wang X, Zhang L, Ding N, Yang X, Zhang J, He J, et al. Identification and characterization of DNAzymes targeting DNA methyltransferase I for suppressing bladder cancer proliferation. Biochemical and biophysical research communications. 2015;461(2):329-33.
143. Liu X, Dai X, Wu B. Study of 5-Aza-CdR on transcription regulation of RASSF1A gene in the BIU87 cell line. Urologia internationalis. 2009;82(1):108-12.
144. Mori K, Enokida H, Kagara I, Kawakami K, Chiyomaru T, Tatarano S, et al. CpG hypermethylation of collagen type I alpha 2 contributes to proliferation and migration activity of human bladder cancer. Int J Oncol. 2009;34(6):1593-602.
145. Matsumoto M, Kawakami K, Enokida H, Toki K, Matsuda R, Chiyomaru T, et al. CpG hypermethylation of human four-and-a-half LIM domains 1 contributes to migration and invasion activity of human bladder cancer. International journal of molecular medicine. 2010;26(2):241-7.
146. Yoon HY, Kim YJ, Kim JS, Kim YW, Kang HW, Kim WT, et al. RSPH9 methylation pattern as a prognostic indicator in patients with non-muscle invasive bladder cancer. Oncol Rep. 2016;35(2):1195-203.
147. Karam JA, Fan J, Stanfield J, Richer E, Benaim EA, Frenkel E, et al. The use of histone deacetylase inhibitor FK228 and DNA hypomethylation agent 5-azacytidine in human bladder cancer therapy. Int J Cancer. 2007;120(8):1795-802.
148. Dhawan D, Ramos-Vara JA, Hahn NM, Waddell J, Olbricht GR, Zheng R, et al. DNMT1: an emerging target in the treatment of invasive urinary bladder cancer. Urol Oncol. 2013;31(8):1761-9.

149. Wang C, Hamacher A, Petzsch P, Köhrer K, Niegisch G, Hoffmann MJ, et al. Combination of Decitabine and Entinostat Synergistically Inhibits Urothelial Bladder Cancer Cells via Activation of FoxO1. Cancers (Basel). 2020;12(2).
150. Ramachandran K, Gordian E, Singal R. 5-azacytidine reverses drug resistance in bladder cancer cells. Anticancer Res. 2011;31(11):3757-66.
151. Khandelwal M, Anand V, Appunni S, Seth A, Singh P, Mathur S, et al. Decitabine augments cytotoxicity of cisplatin and doxorubicin to bladder cancer cells by activating hippo pathway through RASSF1A. Molecular and cellular biochemistry. 2018;446(1-2):105-14.
152. Xylinas E, Hassler MR, Zhuang D, Krzywinski M, Erdem Z, Robinson BD, et al. An Epigenomic Approach to Improving Response to Neoadjuvant Cisplatin Chemotherapy in Bladder Cancer. Biomolecules. 2016;6(3).
153. Papafotiou G, Paraskevopoulou V, Vasilaki E, Kanaki Z, Paschalidis N, Klinakis A. KRT14 marks a subpopulation of bladder basal cells with pivotal role in regeneration and tumorigenesis. Nat Commun. 2016;7:11914.
154. Zhu F, Qian W, Zhang H, Liang Y, Wu M, Zhang Y, et al. SOX2 Is a Marker for Stem-like Tumor Cells in Bladder Cancer. Stem cell reports. 2017;9(2):429-37.
155. Wu M, Sheng L, Cheng M, Zhang H, Jiang Y, Lin S, et al. Low doses of decitabine improve the chemotherapy efficacy against basal-like bladder cancer by targeting cancer stem cells. Oncogene. 2019;38(27):5425-39.
156. Varol N, Konac E, Onen IH, Gurocak S, Alp E, Yilmaz A, et al. The epigenetically regulated effects of Wnt antagonists on the expression of genes in the apoptosis pathway in human bladder cancer cell line (T24). DNA and cell biology. 2014;33(7):408-17.
157. San José-Enériz E, Agirre X, Rabal O, Vilas-Zornoza A, Sanchez-Arias JA, Miranda E, et al. Discovery of first-in-class reversible dual small molecule inhibitors against G9a and DNMTs in hematological malignancies. Nat Commun. 2017;8:15424.
158. Bárcena-Varela M, Caruso S, Llerena S, Álvarez-Sola G, Uriarte I, Latasa MU, et al. Dual Targeting of Histone Methyltransferase G9a and DNA-Methyltransferase 1 for the Treatment of Experimental Hepatocellular Carcinoma. Hepatology. 2019;69(2):587-603.
159. Segovia C, San José-Enériz E, Munera-Maravilla E, Martínez-Fernández M, Garate L, Miranda E, et al. Inhibition of a G9a/DNMT network triggers immune-mediated bladder cancer regression. Nat Med. 2019;25(7):1073-81.
160. Shang D, Liu Y, Matsui Y, Ito N, Nishiyama H, Kamoto T, et al. Demethylating agent 5-aza-2'-deoxycytidine enhances susceptibility of bladder transitional cell carcinoma to Cisplatin. Urology. 2008;71(6):1220-5.

161. Bunch B, Krishnan N, Greenspan RD, Ramakrishnan S, Attwood K, Yan L, et al. TAp73 expression and P1 promoter methylation, a potential marker for chemoresponsiveness to cisplatin therapy and survival in muscle-invasive bladder cancer (MIBC). Cell cycle (Georgetown, Tex). 2019;18(17):2055-66.
162. Coyne GO, Wang L, Zlott J, Juwara L, Covey JM, Beumer JH, et al. Intravenous 5-fluoro-2'-deoxycytidine administered with tetrahydrouridine increases the proportion of p16-expressing circulating tumor cells in patients with advanced solid tumors. Cancer chemotherapy and pharmacology. 2020.
163. Lin J, Gilbert J, Rudek MA, Zwiebel JA, Gore S, Jiemjit A, et al. A phase I dose-finding study of 5-azacytidine in combination with sodium phenylbutyrate in patients with refractory solid tumors. Clin Cancer Res. 2009;15(19):6241-9.
164. A Phase 1 Study of CC-486 as a Single Agent and in Combination With Carboplatin or ABI-007 in Subjects With Relapsed or Refractory Solid Tumors 2019 [Available from: https://clinicaltrials.gov/ct2/show/results/NCT01478685.
165. LoRusso P, Rasco D, Bendell J, Sachdev J, Ramanathan R, Weiss G, et al. Abstract A120: A Phase Ib study of CC-486 (Oral Azacitidine) as a priming agent for carboplatin or NAB-paclitaxel in subjects with relapsed and refractory solid tumors. Molecular cancer therapeutics. 2013;12(11 Supplement):A120-A.
166. Azacitidine Combined With Pembrolizumab and Epacadostat in Subjects With Advanced Solid Tumors (ECHO-206) 2020 [Available from: https://clinicaltrials.gov/ct2/show/results/NCT02959437.
167. Atezolizumab + Guadecitabine in Patients With Checkpoint Inhibitor Refractory or Resistant Urothelial Carcinoma 2020 [Available from: https://clinicaltrials.gov/ct2/show/results/NCT03179943.
168. Decitabine in Treating Patients With Advanced Solid Tumors: ClinicalTrials.gov; 2013 [Available from: https://clinicaltrials.gov/ct2/show/study/NCT00030615.
169. A Multi-Histology Phase II Study of 5-Fluoro-2'-Deoxycytidine With Tetrahydrouridine (FdCyd + THU) 2019 [Available from: https://clinicaltrials.gov/ct2/show/results/NCT00978250.
170. Dose-Finding and Safety Study for Oral Single-Agent to Treat Advanced Malignancies 2020 [Available from: https://clinicaltrials.gov/ct2/show/results/NCT02030067.
171. Bioequivalence & Food Effect Study in Patients With Solid Tumor or Hematologic Malignancies 2020 [Available from: https://clinicaltrials.gov/ct2/show/study/NCT02223052.
172. Crabb S, Danson SJ, Catto JWF, McDowell C, Lowder JN, Caddy J, et al. SPIRE - combining SGI-110 with cisplatin and gemcitabine chemotherapy for solid malignancies

including bladder cancer: study protocol for a phase Ib/randomised IIa open label clinical trial. Trials. 2018;19(1):216.
173. Genomic Based Assignment of Therapy in Advanced Urothelial Carcinoma 2020 [Available from: https://clinicaltrials.gov/ct2/show/study/NCT02788201.

## Tackling tumor microenvironment through epigenetic tools to improve cancer immunotherapy

*Review paper 2*

Iris Lodewijk*, **Sandra P. Nunes***, Rui Henrique, Carmen Jerónimo, Marta Dueñas and Jesús M. Paramio

*Co-first authors

**DOI**: https://doi.org/10.1186/s13148-021-01046-0

Published: 24 March 2021

**Clinical Epigenetics**, 13, 63.

Author personal contribution:

Conceptual design, retrieval of records to review, interpretation of the gathered information and manuscript preparation.

**Abstract**

Background: Epigenetic alterations are known contributors to cancer development and aggressiveness. Additional to alterations in cancer cells, aberrant epigenetic marks are present in cells of the tumor microenvironment, including lymphocytes and tumor-associated macrophages, which are often overlooked but known to be a contributing factor to a favorable environment for tumor growth. Therefore, the main aim of this review is to give an overview of the epigenetic alterations affecting immune cells in the tumor microenvironment to provoke an immunosuppressive function and contribute to cancer development. Moreover, immunotherapy is briefly discussed in the context of epigenetics, describing both its combination with epigenetic drugs and the need for epigenetic biomarkers to predict response to immune checkpoint blockage.

Main body: Combining both topics, epigenetic machinery plays a central role in generating an immunosuppressive environment for cancer growth, which creates a barrier for immunotherapy to be successful. Furthermore, epigenetic-directed compounds may not only affect cancer cells but also immune cells in the tumor microenvironment, which could be beneficial for the clinical response to immunotherapy.

Conclusion: Thus, modulating epigenetics in combination with immunotherapy might be a promising therapeutic option to improve the success of this therapy. Further studies are necessary to (1) understand in-depth the impact of the epigenetic machinery in the tumor microenvironment; (2) how the epigenetic machinery can be modulated according to tumor type to increase response to immunotherapy and (3) find reliable biomarkers for a better selection of patients eligible to immunotherapy.

**Keywords**

Epigenetics; Immunotherapy; Tumor microenvironment; Therapy; Bladder cancer

## Background

The epigenome is defined by heritable alterations in gene expression, either activation or suppression, without altering the DNA nucleotide sequence. The mechanisms responsible for these changes can be broadly divided into altered gene accessibility for the transcriptional machinery, disrupted chromatin organization or modulation of gene expression at the posttranscriptional level through altered mRNA translation mainly by non-coding RNAs, including miRNAs. Fundamental mechanisms for epigenetic regulation include DNA methylation, histone modifications, chromatin remodeling and non-coding RNA interference (1). Nevertheless, these modifications of the RNA sequence and their associated regulatory factors represent functionally relevant changes to the transcriptome without altering the RNA ribonucleotide sequence, recently encompassed by the term 'epitranscriptomics' (2). Since epitranscriptomics is recognized as a different area of study that goes beyond the scope of this review, we will only focus on DNA methylation, histone modifications and chromatin remodeling as epigenetic regulatory mechanisms. Those mechanisms are briefly discussed below.

Epigenome functions are essential for normal gene expression and their modifications affect primary cellular processes like proliferation, differentiation, and apoptosis. Even though its effect on human carcinogenesis is not entirely acknowledged, epigenetic dysfunction is a rising hallmark of malignancy. As epigenetic modifications are essential in the regulation of normal gene expression, epigenetic deregulation results in aberrant gene expression patterns which have been found to favor tumorigenesis, among others (1).

Whereas the role of epigenetic modifications in cancer research has been mainly focused on cancer cells, rising evidence indicates their contribution to the development of a favorable tumor microenvironment (TME), including their effect on surrounding cell phenotypes like fibroblasts, immune cells, endothelial and inflammatory cells, blood and lymphatic vascular networks, and the extracellular matrix (Table 1) (3). Nevertheless, due to the extreme complexity of the variety of cells and their potential epigenetic modifications affecting tumorigenesis, this review will be focused on the epigenetic regulation of different immune cell types in the TME and their involvement in the generation of a cancer prone TME.

We further discuss the inhibition of epigenetic modulators as therapeutic option to modify the immunosuppressive TME and we provide an overview on immunotherapy and the potential of epigenetic biomarkers of response to this therapy. Finally, the application and success of immunotherapy as well as the inhibition of epigenetic

processes involved in immune activation will be briefly discussed in the context of bladder cancer (BC).

## Epigenetic regulatory mechanisms

### *DNA methylation*

DNA methylation represents a process by which methyl groups are transferred onto the 5' position of a cytosine molecule without altering the DNA sequence. Methylation commonly occurs on the cytosine of CpG sites, meaning that the cytosine molecule precedes a guanine. DNA regions with a higher density of these CpG sites (so-called CpG islands) have been found throughout the genome, mostly coinciding with gene regulatory regions. This way, methylation of CpG islands plays an important role in the regulation of normal gene expression (Figure 1) (4,5).

DNA methyltransferases (DNMTs) are the enzymes responsible for the control of DNA methylation patterns through maintenance DNA methylation and *de novo* DNA methylation. In general, DNMT1 is the enzyme responsible for maintenance of inherited DNA methylation, whereas DNMT3a and DNMT3b provide *de novo* DNA methylation. Nevertheless, DNMT3a and DNMT3b methyltransferases have been described to perform maintenance methylation as well, and DNMT1 has also been found to carry out *de novo* DNA methylation (5).

Alterations in DNA methylation status have been described in various diseases, including cancer. For example, gene silencing of tumor suppressor genes (TSGs) is the result of the hypermethylation of CpG islands in the promoter regions of those genes. TSGs are mainly involved in biological pathways like cell cycle control, DNA repair and apoptosis, and its silencing has been frequently found in tumorigenesis (6).

### *Histone modifications*

Chromatin structure changes as a result of dynamic processes involving posttranslational modifications (PTMs) at the histone N-terminal tails. Various PTMs can be distinguished, including histone acetylation, methylation and phosphorylation as well as less known ubiquitylation, deamination and sumoylation, which affect chromatin packaging and availability to the gene transcription machinery (Figure 1) (7). Currently known histone PTMs have been extensively reviewed. Here, we briefly mention the three most common histone PTM activities.

Histone acetylation consists of the reversible addition of acetyl groups to the histone tail by histone acetyltransferases (HATs), which weakens the DNA-histone bonds and allows binding of transcription factors. Contrarily, histone deacetylases

(HDACs) remove those acetyl groups, allowing for compact wrapping of the DNA around histones, disabling the access of other enzymes. Regarding histone methylation, the transfer of methyl groups is a reversible process regulated by histone methyltransferases and demethylases. The attachment of a methyl group to the histone tail may differentially affect gene expression depending on the specific residue modified. Likewise, the interaction between the DNA and histone tails is regulated by histone (de)phosphorylation processes (8).

*Chromatin remodeling*

Changes in nucleosome position have also been found responsible for rearrangement of chromatin structure, a process known as chromatin remodeling. Nucleosomes, consisting of a histone core (H2A, H2B, H3, and H4) wrapped by an approximately 150 bp DNA sequence, can be affected in several ways, including nucleosome sliding, nucleosome ejection and histone eviction. Nucleosome sliding represents the movement of the histone octamer across the DNA sequence, whereas nucleosome ejection implies the complete segregation of the histone core from the DNA. Histone eviction includes the disintegration of the core histone octamer trough removal or replacement of H2A-H2B dimers (Figure 1) (9).

Since nucleosome sliding and ejection as well as removal of the H2A-H2B dimers result in DNA exposition and nucleosome destabilization, these processes play an important role in the regulation of gene accessibility to the transcriptional machinery.

*Histone variants*

Histone variants add further complexity to epigenetic regulation of the genome. They represent a unique protein sequence compared to core histones and can be identified by a combination of variant-specific proteins and chromatin remodeling complexes which control their localization within the genome. Various histone variants are characterized for H2A (such as macroH2A, H2A.B, H2A.J, H2A.X and H2A.Z.1/2), H2B (including TSH2B) and H3 (like H3.1 till H3.8, H3.X, H3.Y and CENP-A), whereas no variants have been described for H4. Additionally, histone variants are subjected to post-translational modifications which elaborates the epigenetic control of gene expression (Figure 1) (10,11).

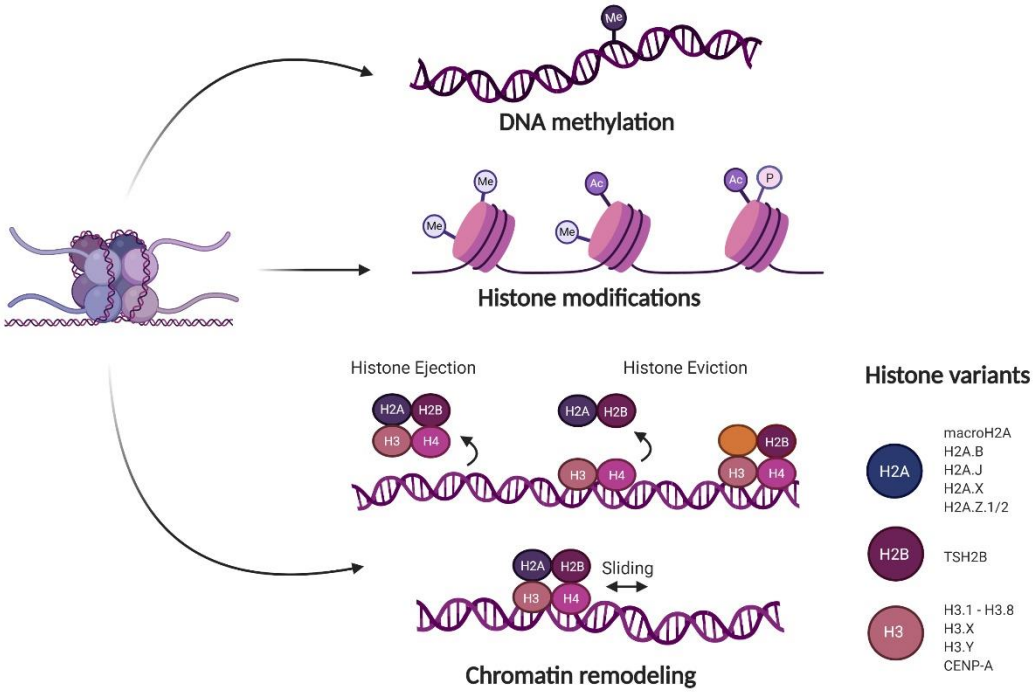


**Figure 1.** DNA methylation, histone modifications and chromatin remodeling as regulatory mechanisms of epigenetic gene regulation. DNA methylation represents a process by which methyl groups are transferred onto the 5' position of a cytosine molecule, commonly in the context of CpG sites, without altering the DNA sequence. Histone modifications include posttranslational modifications at the histone N-terminal tails, such as acetylation, methylation and phosphorylation, causing chromatin structure alterations. Changes in nucleosome position are also responsible for rearrangement of chromatin structure, a process known as chromatin remodeling. Nucleosomes can be affected in several ways, including nucleosome sliding, nucleosome ejection and histone eviction. Histone variants add further complexity to epigenetic regulation of the genome. Various histone variants are characterized for H2A, H2B and H3. All these mechanisms are highly interrelated and play an important role in the regulation of gene accessibility to the transcriptional machinery.

## Epigenetic regulation of immune cell function in TME

A favorable TME is characterized by immune tolerance. Cancer cells employ a variety of epigenetic regulated-immune escape mechanisms, including downregulation of tumor-associated antigens (TAAs), loss of antigen processing and presentation machinery (APM) as well as expression of a tumor-promoting balance in co-stimulatory and co-inhibitory molecules (also known as immune checkpoint receptors). Whereas these processes have been extensively studied and reviewed, epigenetic alterations affecting immune cell function in the TME represent a growing area of investigation. The epigenetic-induced immunosuppressive function of dendritic cells (DCs), myeloid-derived suppressor cells (MDSCs), tumor-associated macrophages (TAMs), tumor

infiltrating lymphocytes (TILs), regulatory T cells (Tregs) and natural killer cells (NK cells) in the TME will be discussed below.

*Dendritic Cells*

DCs represent important antigen presenting cells (APCs) that mediate antigen-specific anti-tumor immune responses mainly through the activation of T cells. Whereas these cells are normally able to capture TAAs expressed on cancer cells through accurate MHC expression and cross-present them to cytotoxic T cells (CTLs) by the expression of co-stimulatory molecules, resulting in tumor elimination, tumor-infiltrating DCs show an immune-tolerant phenotype favoring tumor growth (12). Next to low MHC expression and repression of various co-stimulatory molecules in tumor-infiltrating DCs, epigenetic alterations affecting DC polarization and activity are suggested to impair an effective anti-tumor immune response.

For example, dynamic changes in the levels of chromatin regulator special AT-rich sequence binding 1 (SATB1) are essential for the generation of inflammatory DCs and their anti-tumorigenic activity. SATB1 recruits chromatin remodeling complexes to anchored DNA regions, consisting of a characteristic 'ATC-sequence context' (well-mixed A's, T's and C's but not G's on a single strand), thereby controlling gene transcription over long-distance DNA sequences through the regulation of nucleosomal positioning and histone modification (13). Additionally, the recruitment of HATs and HDACs directly to gene promoter regions has been reported (14). A continuous increased expression of SATB1 has been described to convert inflammatory anti-tumor DCs into pro-tumor DCs by enhanced secretion of pro-tumorigenic cytokine IL-6 and immunosuppressive factor Galectin-1, activating immune-evasive pathways in these cells (15). Accordingly, SATB1 has been found to be overexpressed in a wide range of tumors, including breast, lung, pancreas, colorectal, liver, bladder, prostate and ovarian cancer, and has been associated with tumor progression and poor prognosis (16). Additionally, next to its role in the direct activation of *IL-6* transcription, Kruppel-like factor 4 (KLF4) modulates IL-6 production at the posttranslational level through histone acetylation. Decreased expression of KLF4 has been described in many tumors, including esophageal, lung, gastric, intestinal, colon and prostate cancer, leading to altered production of cytokine IL-6 in DCs (Figure 2; Table 1) (17,18).

Taken together, increasing our knowledge on tumor-induced epigenetic modifications affecting DC polarization and activity might help modifying the TME to become more "receptive" to the development of an effective anti-tumor response.

*Myeloid-Derived Suppressor Cells*

MDSCs represent immature myeloid cells and are mainly characterized by their immunosuppressive function providing tumor immune evasion (19). These cells are known to have a major impact on cancer progression as the TME has been found to support this cell population, promoting MDSC persistence, proliferation and function. Indeed, the presence of MDSCs has been associated with poor prognosis and reduced patients' survival in many cancer types, including head and neck, breast, lung, kidney and prostate (19,20). Several studies have suggested the role of epigenetic mechanisms in MDSC accumulation and functions.

For example, an elevated expression of signal transducer and activator of transcription 3 (STAT3) has been defined in several tumor types including lung, pancreas and renal cancer (21–24). Overexpression of STAT3 can be the result of promoter silencing of DNMT3a and DNMT3b through hypermethylation, followed by promotor hypomethylation of the *STAT3* gene. Besides, Villagra et al. proposed HDAC11 as a transcriptional repressor of IL-10 (a STAT3-activating cytokine) through interaction with the IL-10 promotor at the chromatin level and indicated that elevated levels of STAT3 in APCs might be associated with the absence of HDAC11 (25). More recently, HDAC11 has been described as an essential regulator of IL-10 levels in myeloid cells and its role in the MDSC expansion was demonstrated (26). Moreover, Cheng et al. showed that HDAC6 has a regulatory function in STAT3 activation in the MDSC population. Surprisingly, HDAC6 seems to act as a transcriptional activator of *IL-10* expression (27). Next to their possible individual implications, HDAC6 and HDAC11 have been reported to interact and be recruited together towards the *IL-10* promoter site where they control *IL-10* transcription and subsequent STAT3 expression (27). Increased STAT3 expression leads to augmented expression of immunosuppressive factors S100A8 and Arginase 1 (Arg1) in MDSCs. Additionally, the induction of these proteins, together with the STAT3-mediated induction of S100A9 expression, has been shown to provide expansion, accumulation and recruitment of immunosuppressive MDSCs in TME (Figure 2; Table 1) (22,28).

As abovementioned, this MDSC population represents immature myeloid cells which fail to differentiate into macrophages and DCs. Several studies already described the accumulation of immature myeloid cells as a result of retinoblastoma gene (*Rb*) transcriptional silencing (29,30). Concordantly, Young et al. proposed that HDAC2 might be the epigenetic regulator provoking Rb transcriptional silencing in this cell population through its direct interaction with the *Rb1* gene promotor (31).

Taken together, the MDSC population represents a major barrier for immunotherapy. Accordingly, further research is needed to increase our knowledge on MDSCs in the TME and be able to improve the ability to revert their immunosuppressive function.

*Tumor-Associated Macrophages*

TAMs represent the main component of the immune infiltrates in TME of solid tumors and have frequently been associated with worse prognosis (32). By continuously sensing their surrounding environment, this cell population has refined regulatory epigenetic mechanisms to manage their polarization state. Depending on their polarization into classically-activated (M1) or alternatively-activated (M2) macrophages, they inhibit or promote tumor growth respectively. Epigenetic modifications have been widely shown to be involved in macrophage differentiation, activation and survival (33).

Yang et al. indicated a significant role for DNMT3b in macrophage polarization. They showed that DNMT3b knockdown induces elevated expression of M2 macrophage markers, such as Arg1, as well as increased Arg1 function. In concordance with these results, Arg1 activity has been reported to define immunosuppressive subsets of TAMs. Additionally, DNMT3 knockdown resulted in significantly decreased expression of inflammatory genes, such as *TNFα* and *IL-1β*, emphasizing the importance of DNMT3b in the regulation of both macrophage differentiation and inflammation (34,35). Moreover, DNMT3b has been reported to methylate the peroxisome proliferator-activated receptor γ (PPARγ) promotor region.

Protein arginine methyltransferase 1 (PRMT1) has been reported as a positive regulator of PPARγ-dependent M2 polarization through methylation of the arginine located at residue 3 on the tail of histone 4 (H4R3me2a). Furthermore, Ishii et al. demonstrated that expression of M2 macrophage markers seems to be epigenetically controlled by convertible changes in H3K4 and H3K27 methylation (36). Accordingly, H3K4 methyltransferase SET and MYND Domain 3 (SMYD3) has been shown to play a role in M2 differentiation. Kittan et al. showed that the increased expression of SMYD3 is associated with the methylation and activation of the M2 marker arachidonate 15-lipoxygenase (ALOX15) (37). The only histone demethylase recognized as a crucial regulator of M2 polarization is Jumonji domain-containing protein D3 (JMJD3), a H3K27 demethylase. IL-4-induced STAT6 activation leads to STAT6-mediated increased expression of JMJD3, provoking H3K27me2/3 demethylation and subsequent transcriptional activation of several M2 marker genes, including *Arg1* (36,38). IL-4

increased expression has been found in various tumor types, including breast, lung, pancreatic, colon, bladder and ovarian carcinomas (39).

Whereas the role of HATs in macrophage polarization remains unclear, the function of HDACs as epigenetic modifiers in the regulation of M2 differentiation and phenotypic control has been explored by various studies. Mullican et al. indicated that HDAC3 activity leads to suppressed IL-4 activity through deacetylation of histone tails at regulatory sequences. Together with the finding that HDAC3 knockdown resulted in decreased inflammatory gene expression, HDAC3 has been proposed to negatively regulate M2 polarization (40,41). HDAC9 has also been described as a negative regulator of M2 phenotype as HDAC9 deficiency results in PPARγ promotor acetylation and increased PPARγ expression levels, promoting M2 polarization and downregulating M1 phenotype inflammatory genes (42). Contrarily, HDAC4 positively regulates the M2 phenotype through IL-4-activated HDAC4-induced STAT6 signaling and Arg1 expression (43). Another HDAC, SIRT2, positively controls M2 polarization through its function in the expression of M2 macrophage markers, such as Arg1, and downregulation of M1 polarization by NFkB acetylation, provoking decreased NFkB signaling and suppression of IL-1β expression (Figure 2; Table 1) (44).

Accordingly, targeting these epigenetic enzymes responsible for polarization of TAMs into M2 macrophages would prevent their tumor supporting function. Nevertheless, it should be considered that these regulators disclose secondary functions and that histone modifying enzymes also affect proteins other than histones.

*Tumor Infiltrating Lymphocytes*

TILs represent the major component of the adaptive immune system in the TME and can be classified into two main categories: 1) CD4-expressing T cells (CD4+ T cells), which can differentiate into the Thelper1 (Th1) or Thelper2 (Th2) phenotype, and 2) CD8-expressing T cells (CD8+ T cells), which are able to eliminate tumor cells after differentiation into cytotoxic effector T lymphocytes.

Whereas the important role of CD8+ CTLs in anti-tumor immune response has been known for many years, the potential importance of CD4+ Th cells in the generation and maintenance of anti-tumor activity has only recently been reported (45). Even though further research is needed to find out whether and, if so, how epigenetic mechanisms affect CD4+ cells in an immunosuppressive TME, DNA demethylation has been reported to play an important role in differentiation of CD4+ T cells towards Th1/Th2 lymphocytes (46).

Additionally, epigenetic modulation has been found to control rapid activation and differentiation of naïve CD8+ into CTLs upon antigen stimulation. For example, Peng et al. associated DNMT1-mediated DNA methylation and enhancer of zeste homolog 2 (EZH2)-mediated H3K27 trimethylation with impaired T-cell infiltration in the TME through downregulation of CXCL9 and CXCL10 chemokine expression (47). Furthermore, Yang et al. reported that whole-genome methylation profiling showed a distinct methylome pattern for tumor-reactive CD8+ T cells compared to the naïve subtype. Moreover, specific DNA methylation patterns have been discovered in exhausted CD8+ T cells. *PDCD1* and *CTLA4* expression in exhausted CD8+ T cells has been found to be epigenetically controlled by DNA demethylation, and the *LAG3* gene has been found methylated in naïve cells but demethylated during the activation of naïve CD8+ T cells (48). Ghoneim et al. found that high programmed death 1 (PD-1) expressing tumor-infiltrating CD8+ T cells in prostate cancer display exhaustion-associated DNA methylation patterns (49). Stephen et al. further showed that chromatin organizer Satb1 recruits the nucleosome remodeling deacetylase complex to regulatory regions of the *Pdcd1* gene, reducing PD-1 expression levels upon T-cell activation. Nevertheless, Satb1 is known to be downregulated by Smad proteins under the influence of TGF-β, an immunosuppressive cytokine found to play a relevant role in cancer, resulting in elevated PD-1 levels. Accordingly, Satb1 prevents premature T-cell exhaustion by controlling PD-1 expression, a pathway that is altered in cancer, causing reduced anti-tumor activity (50,51). Another mechanism underlying tumor-specific T-cell dysfunction in tumor progression is represented by chromatin state dynamics. Philip et al. reported that naïve T cells differentiate into a dysfunctional but reprogrammable chromatin state upon tumor antigen recognition in premalignant lesions, which converts into a fixed non-reprogrammable dysfunctional state during tumor progression. The presence of surface markers CD101 and CD38 has been associated with reduced reprogrammability of high PD-1 expressing tumor-infiltrating CD8+ T cells, a finding with important clinical relevance as these markers can be used to discriminate reprogrammable from non-reprogrammable PD-1 high T cells within the heterogeneous TIL populations (52). This mechanism might explain why certain patients do not respond to therapies based on immune-checkpoint blockade as well as it provides new insights in possible strategies to revert non-reprogrammable PD-1 high T cells into tumor-reactive CD8+ T cells (Figure 2; Table 1).

Taken together, impaired CD8+ T cell functions seem to play a major role in the generation of an immunosuppressive TME. Importantly, the prevention of T-cell exhaustion might represent a potential strategy to reverse a TIL-mediated immunosuppressive TME.

*Regulatory T cells*

Tregs represent a functionally different T cell population which is essential for the maintenance of homeostasis and immune tolerance. Accordingly, mature Tregs provide a tumor-supportive microenvironment (53). Various studies have reported a key role for Foxp3 in the development of these cells as well as their function, and epigenetic regulation of Tregs through Foxp3 has been emphasized by recent studies (54,55).

Moreover, epigenetic modifications controlling Treg development and function have been found to play an important role in the establishment of an immunosuppressive TME. Ohkura et al. reported that Treg maturation involves the generation of genome-wide CpG DNA hypomethylation pattern, needed for Treg specific gene expression and immunosuppressive activity (56). Besides, Foxp3 seems to exert an EZH2-mediated repressive role upon CD28-mediated Treg activation as target genes show elevated H2K27me3 levels. As CD28 not only provides a key role in the stimulation of Tregs, but also in effector T-cell (CD4+/CD8+) activation, this suppressive role of Foxp3 might be essential to preserve the Treg-specific gene expression profile upon T cell stimulation through downregulation of genes involved in the effector T-cell activation (57). Indeed, Wang et al. showed that inhibition of EZH2 resulted in Treg-mediated pro-inflammatory activities in the TME, supporting the generation of an effector T-cell-mediated anti-tumor immune response (Figure 2; Table 1) (58).

Taken together, targeting the maturation of functional Tregs might be a potential strategy to convert an immunosuppressive TME into a microenvironment able to provide anti-tumor activity.

*Natural Killer cells*

The NK cell population forms part of the innate immune system and is able to control tumor growth by their ability to recognize and eliminate tumor cells. Epigenetic modification has been reported to play an key role in the NK cell maturation, differentiation and activation (59). Regulation of the effector function of this cell population mainly depends on the balance between inhibiting and activating receptors present on NK cell surface, the activation status of which seems to be epigenetically modulated, as well. Accordingly, rising evidence indicates the involvement of epigenetic processes in impairing NK-cell mediated anti-tumor immune response.

An impaired NK-cell mediated anti-tumor immune response is highly associated with NK-cell exhaustion because of diminished expression of activating receptors and increased expression of inhibitory receptors, amongst others. Specific activating NK-cell receptors include NKG2D, NKp30, NKp44, NKp46 and DNAM-1/CD226, whereas

inhibitory receptors are represented by PD-1, TIM-3, TIGIT and CD94-NKG2A. Fernandez-Sanchez et al. reported the involvement of DNA methylation and histone acetylation in the regulation of NKG2D levels, with *NKG2D* gene demethylation and H3K9 acetylation providing *NKG2D* expression (60). Nevertheless, whether reduced expression of this receptor is due to *NKG2D* hypermethylation remains unknown. Additionally, Ogbomo et al. proposed that the regulation of NKp30 and NKp46 expression levels is controlled by histone acetylation (61). Using an HDAC inhibitor (HDACi), they showed that the suppression of NK-cell activity is caused by decreased expression of NKp30 and NKp46, but is independent of activating NKG2D, NKp44 and DNAM-1 expression levels as well as inhibitory *NKG2A* expression. Finally, Yin et al. revealed that enhanced levels of the activating NKG2D receptor are associated with elevated NK cell expansion and cytotoxicity against the tumor. Inhibition of EZH2 activity has been associated with decreased H3K27me3 levels, providing increased expression of the NKG2D receptor (Figure 2; Table 1) (62,63).

Although epigenetic modifications affecting NK cell development and function are widely examined, further studies are needed to increase our knowledge on the epigenetic regulation of NK cells and the potential of epigenetic enzymes/markers as therapeutic targets.

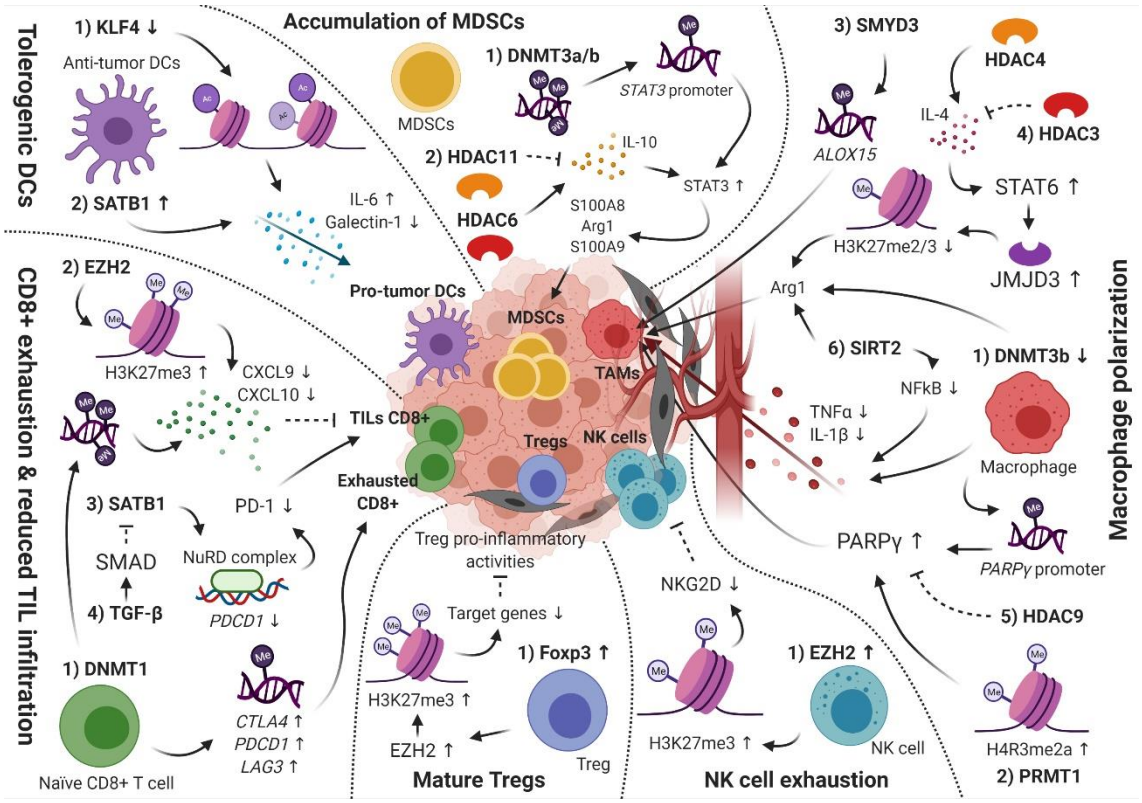


**Figure 2.** Epigenetic regulation of immune cells in the tumor microenvironment. Decreased KLF4 and increased SATB1 expression affect IL-6 (upregulation) and Galectin (downregulation) expression, remodeling anti-tumor DCs into pro-tumor DCs. MDSCs expansion, accumulation and recruitment is favored by STAT3-induced expression of immunosuppressive factors S100A8, Arg1 and S100A9. In this cell population, STAT3 expression is controlled by DNMTT3a/b, HDAC6 and HDAC11. Macrophages can convert into TAMs under the influence of multiple epigenetic factors, including DNMT3b, PRMT1, HDAC3/4, HDAC9 and SIRT2, favoring acquisition of the M2 phenotype through various pathways, such as increased PARPγ and Arg1 expression as well as downregulation of inflammatory factors TNFα and IL-1β. SMYD3 activates M2 marker ALOX15. Impaired NK-cell anti-tumor cytotoxicity can be the result of increased EZH2 expression, which downregulates activating NK-cell receptor NKG2D through enhanced H3K27me3 levels. The same way, EZH2 also regulates inhibition of regulatory T-cell pro-inflammatory activities. Naïve CD8+ T-cells differentiate into TILs or exhausted CD8+ cells dependent on epigenetic profile. Whereas specific DNA methylation patterns of CTLA4, PDCD1 and LAG3 are identified in exhausted CD8+ T-cells, DNMT1 and EZH2 inhibit CD8+ TILs infiltration trough downregulation of CXCL9 and CXCL10 chemokines. TGF-β and SATB1 affect TILs infiltration by controlling PD-1 expression. DCs, dendritic cells; MDSCs, myeloid-derived suppressor cells; TAMs, tumor-associated macrophages; NK, natural killer; Tregs, regulatory T-cells; TILs, tumor infiltrating lymphocytes.

**Table 1.** Cell populations contributing to the development of a favorable tumor microenvironment.

| TME components | Reported in various tumor types, including: | Characteristics controlled by epigenetic regulation | Contribution to favorable TME | Reference |
|---|---|---|---|---|
| Pro-tumor DCs | Bladder, Breast, Colon, Colorectal, Esophageal, Gastric, Glioma, Intestinal, Liver, Lung, Lymphomas, Osteosarcoma, Ovarian, Pancreas, Prostate | - Enhanced production of pro-tumorigenic cytokine IL-6<br>- Augmented secretion of immunosuppressive Galectin-1 | Tumor-infiltrating DCs show an immune-tolerant phenotype favoring tumor growth | (12,15,69–76,16–18,64–68) |
| Immunosuppressive MDSCs | Bladder, Breast, Colorectal, Head and Neck, Liver, Lung, Pancreas, Prostate, Renal | - Expression of immunosuppressive factors S100A8, S100A9 and Arg1 | MDSCs promote immune suppression favoring tumor growth and metastasis | (19,20,80,21–24,75,77–79) |
| TAMs | Bladder, Breast, Colon, Cervical, Gastric, Glioma, Lung, Lymphoma, Melanoma, Nueroblastoma, Ovarian, Pancreas, Prostate | - Increased expression of Arg1<br>- Activation of ALOX15<br>- Enhanced expression of PPARγ<br>- Decreased NFkB signaling and suppression of IL-1β expression | Immunosuppressive subsets of TAMs promote tumor growth | (39,75,89,90,81–88) |
| TILs | Bladder, Brain, Breast, Colorectal, Gastric, Genitourinary, Glioblastoma, Glioma, Head and Neck, Liver, Lung, Melanoma, Meningioma, Ovarian, Pancreatic, Prostate, Renal | <u>Impaired TILs CD8+ infiltration:</u><br>- Downregulation of CXCL9 and CXCL10 chemokine expression<br>- Elevated levels of PD-1<br><u>Exhausted CD8+ T cells:</u><br>- Enhanced expression of *CTLA4, PDCD1* and *LAG3* | Impaired CD8+ T cell functions as well as T-cell exhaustion seem to play a major role in the generation of an immunosuppressive TME | (91–94) |
| Mature Tregs | Bladder, Breast, Colorectal, Glioblastoma, Lung, Lymphoma, Melanoma, Ovarian, Pancreas | - Downregulation of genes involved in effector T-cell activation | Mature Tregs provide a tumor-supportive microenvironment | (53,75,95–97) |
| NK cells | Breast, Colorectal, Gastric, Melanoma, Multiple myeloma, Pancreas, Renal | - Decreased expression of activating NKG2D NK-cell receptor | Impaired NK-cell mediated anti-tumor immune response | (98–101) |

| | | |
|---|---|---|
| Fibroblasts | Fibroblasts in the TME differentiate into cancer-associated fibroblasts (CAFs), representing one of the main components in the tumor stroma. The majority of the studies show pro-tumoral functions for CAFs, which include immune suppression, extracellular remodeling and angiogenesis. | (102–104) |
| Endothelial cells | Angiogenesis refers to the de novo formation of blood vessels, a process essential for tumor growth. This blood vasculature consists of tumor endothelial cells (TECs), which line the insides of the blood vessels. Different characteristics between TECs and normal endothelium have been described. | (105,106) |
| Blood and lymphatic vascular networks | Blood and lymphatic vascular networks play a key role in supporting tumor growth and progression. They support oxygen supply and adequate nourishment to the tumor and provide a gateway for metastasizing tumor cells. | (107) |
| Extracellular matrix | The tumor extracellular matrix (ECM) differs greatly from the ECM in normal tissue, not only in amount of deposition but also in organization and composition. The tumor ECM is generally stiffer, a characteristic that has been associated with an increase in nuclear localization of transcription factors able to drive epithelial-mesenchymal-transition and, consequently, tumor metastasis. | (108) |

**Inhibition of epigenetic modulators as therapeutic option to modify the immunosuppressive TME**

A favorable TME, created by tumor cells affecting different immune cell populations, forms a major barrier for cancer therapy. Nevertheless, the study into epigenetic mechanisms underlying the generation of this immunosuppressive TME currently represents subject of utmost interest. As previously stated, a variety of epigenetic modifications affects the phenotypes of diverse immune cell populations in the TME to become immunosuppressive. Accordingly, modifying the TME to become more “receptive” to the development of an effective anti-tumor response could be achieved by molecular re-wiring using pharmacologic modulators of epigenetic enzymes. In this regard, when considering the use of compounds targeting the epigenetic machinery, it is worth considering that these compounds not only affect tumor cells, but also TME cells. Accordingly, a proper selection of inhibitors could become a two-edge sword to tackle tumors.

For example, SATB1 represents an attractive therapeutic target as it modifies different immune cell populations under tumor’s influence, including DCs and CTLs. The statins fluvastatin and simvastatin have been found to suppress SATB1 expression, probably acting at the posttranslational level (109,110). Additionally, *in vivo* silencing of *Satb1* expression in tumor-associated DCs was found to diminish immunosuppression in the TME, boost T-cell mediated anti-tumor activity and delay tumor progression (15). In the context of immunotherapy, Satb1 has been described as a possible TAA that can be recognized by CD8+ T cells. Accordingly, Wang et al. proposed that Satb1-derived epitope might be used as immune target for cancer vaccine generation (111).

Furthermore, the importance of HDAC activation and IL-6 signaling in controlling the immunosuppressive function of MDSCs as well as its recruitment to the TME has been reported by Nair et al. (20). Various studies demonstrated the potential of entinostat, a class I HDACi, as therapeutic compound to modulate the immunosuppressive TME through inhibition of MDSC activity. Besides, the application of entinostat not only resulted in decreased MDSC function, but also augmented the effect of checkpoint inhibitor treatment (112–115). Kim et al. reported that entinostat reduces the MDSC population and the combination of entinostat with PD-1 and cytotoxic T-lymphocyte-associated protein 4 (CTLA-4) antibodies resulted in an elimination of approximately 80% of the tumor, whereas the use of immune checkpoint inhibitors against PD-1 and CTLA-4 alone did not provide an anti-tumor immune response (113). The potential role of HDACi in priming the TME for enhanced response to immunotherapy has been further emphasized by Briere et al., who obtained similar

results using a class I/IV HDACi (mocetinostat) in combination with anti-programmed death-ligand 1 (PD-L1) antibody (114). Additionally, Orillion et al. observed reduced macrophage population in the TME after entinostat treatment (112). Other potential therapeutic targets to suppress MDSCs function would be HDAC2, HDAC6 and HDAC11. Nevertheless, further studies are needed to investigate the therapeutic potential of their corresponding inhibitors (31,115,116).

Regarding the polarization of TAMs into M2 macrophages, targeting the enzymes responsible for the acquisition of M2 phenotype would attenuate their tumor-promoting function. Accordingly, Tikhanovich et al. reported the therapeutic potential of AMI-1, a PRMT1 inhibitor, inhibiting M2 processes (117). Additionally, GSK-J4 might diminish the immunosuppressive, tumor-supporting function of M2 macrophages through KDM6B (a lysine-specific demethylase that demethylates H3K27me2 or H3K27me3) inhibition. Nevertheless, in concordance with the essential role of KDM6B in both M1 and M2 polarization, GSK-J4 has also been found to inhibit the expression of TNF and other M1 inflammatory cytokines (118,119). Noteworthy is the effect of histone modifying enzymes on proteins other than histones and the importance of non-histone protein modifications in macrophage-polarizing process. Moreover, macrophage polarization is a complex dynamic process in which most epigenetic enzymes are neither involved exclusively in the polarization towards M1 or M2 phenotype nor do they all have opposing roles in M1 versus M2 phenotype acquisition (120). Accordingly, the discovery of therapeutic epigenetic targets in this cell population is very challenging.

Another attractive therapeutic target is EZH2, responsible for the immunosuppressive phenotype of several immune cell populations in the TME, including TILs, Tregs and NK cells. This epigenetic regulator has already been extensively studied for its potential as therapeutic target to convert the immunosuppressive TME into an immune-promoting microenvironment. Various studies described an enhanced effector-T cell infiltration and cytotoxic activation in the TME upon EZH2 inhibition as well as functional alterations of the Treg population resulting in Treg-mediated pro-inflammatory activities (47,58,121,122). Additionally, targeting EZH2 has been reported as an attractive strategy to combine with immunotherapy, as it might overcome resistance to immune checkpoint therapies, including CTLA-4, PD-1 and PD-L1 (47,121–123). Among the EZH2-inhibiting compounds, small molecule inhibitors of EZH2, GSK-126, PF-06821497, MAK683, CPI-0209, CPI-1205 and DS-3201 have entered into clinical trials, although none of these has been approved for cancer treatment, yet (122). Tazemetostat, a selective inhibitor of EZH2, has been approved by the FDA in 2020.

Another relevant aspect is the profound interaction between the different immune cell populations in immune response regulation. Therefore, it is important to take into

account that epigenetic reprogramming of a certain immunosuppressive immune cell population might positively co-opt other immune cell populations to provoke an effective anti-tumor immune response. One example is the Treg-mediated pro-inflammatory function upon EZH2 inhibition causing increased effector-T cell infiltration and activity. Furthermore, MDSCs play a central role in the immunosuppressive, tumor-promoting TME and have been found to interact with many of the other immune cell populations. Accordingly, epigenetic targeting of this cell type might be sufficient to modify the TME to become more “receptive” to the development of an effective anti-tumor response.

**Immunotherapy – an overview**

The immune system plays a critical role in cancer development and progression by both eliminating cancer cells and determining tumor immunogenicity (124). Thus, cancer immunoediting helps to understand how tumors escape the immune system by dividing the process in three distinct phases: “elimination”, “equilibrium” and “escape”. At first, when cancer cells are present, the immune system can recognize these and eliminate them. However, when not all cancer cells are eradicated in this process and an equilibrium is reached, the adaptive immune system impedes tumor’s growth associated with a dormancy state and high genomic instability. T cells, IL-12 and interferon (IFN)-γ are needed to maintain tumor dormancy (125,126). Subsequently, cancer cells escape from the immune system by expressing suppressive effects and losing target antigen expression. At this stage, tumor immune escape occurs, since the adaptive immune system fails to recognize cancer cells, which became resistant to immune effector mechanisms and induced an immunosuppressive state (127).

Immune responses are regulated by an interplay of costimulatory and inhibitory signals that balance the immune response and self-tolerance (128). Immune checkpoint inhibitors are essential as negative signals to stop immune response and impede autoimmunity (129). PD-1 is expressed in T lymphocytes and prevents the activation of these cells by binding to its ligands PD-L1 and PD-L2 (130). Additionally, cytotoxic T lymphocyte-associated antigen 4 (CTLA-4) leads to suppression of T-cells activation by competing with the costimulatory signal CD28 for binding to B7-1 and B7-2, attenuating the activation signals of CD28 (131,132). Interestingly, PD-L1 is overexpressed in cancer cells, facilitating cancer cells to escape immune surveillance by T cells (133).

Checkpoint inhibitor immunotherapies consist of monoclonal antibodies that target CTLA-4 or the programmed cell death protein 1 pathway (PD-L1, PD-1) (133). When the antibodies bind to PD-L1/PD-1 or CTLA-4, the inhibitory effect is canceled and an immunological response against cancer cells starts by activation of tumor-reactive T

cells (134). Of note, several clinical trials have demonstrated increased efficacy of combining anti PD-L1/PD1 and anti-CTLA4, although with increased risk of adverse reactions. The use of immune checkpoint inhibitors as cancer therapy was firstly approved for treatment of metastatic melanoma. Since then, several antibodies have been approved for treatment of non-small cell lung cancer, head and neck squamous cell carcinoma, hepatocellular carcinoma and BC (134).

A significant subset of cancer patients does not respond or respond poorly to immune checkpoint blockage treatments (135). This can be a consequence of primary resistance that occurs prior to treatment, associated with a reduction of antigen expression and changes in metabolic pathways or through acquired resistance during the course of the treatment (136). The one and foremost biomarker used for prediction of response to PD-L1/PD-1 blockade is PD-L1 expression (137). It seems to be a biomarker of aggressive disease and it might also be considered a prognostic biomarker. However, the evaluation of PD-L1 as a single biomarker across clinical trials was shown to be heterogeneous (138). Several reasons can be appointed for the presence of this heterogeneity: (1) clinical trials used different PD-L1 immunohistochemistry scoring assays (137); (2) the scoring compartment differs for each specific therapy, namely pembrolizumab and nivolumab use PD-L1 tumor cell expression whereas atezolizumab use PD-L1 immune cell expression; (3) intratumoral heterogeneity and (4) the sample available may not represent the full intratumoral heterogeneity (139). All these data indicate that PD-L1 expression as a single biomarker is probably not adequate to accurately predict immunotherapy response and more reliable biomarkers could help to better predict and improve patient selection for these therapies (139).

Other approaches have been used to try to predict immunotherapy response including tumor mutational burden, tumor mismatch-repair deficiency, grade of TILs (140–142), among others, depending on tumor type. For example, the TCGA-based molecular subtypes in BC have been associated with response to immune checkpoint blockage. Specifically, the neuronal subtype seems to display a better response to immunotherapy (143). However, the criteria to define BC subtypes has to be uniformed before it may be considered a possible biomarker for immunotherapy (144). Moreover, tumor mutational burden has been proposed to predict response to immunotherapy (145). With a high rate of mutations, novel antigens emerge regularly so it could potentiate the use of immunotherapy. Nonetheless, some patients with low mutational burden endure response to immunotherapy, which demonstrates that criteria to define the tumor mutational burden have to be clarified (145). Interestingly, pembrolizumab was approved for patients with microsatellite instability and mismatch repair deficient malignancies showing progression after failure of other approved treatments (142).

Finally, immune expression profiling has the potential to correctly identify “hot” or “cold” tumors by assessing levels of chemokines, cytokines and cell surface proteins reflecting the inflammatory status (146). Also, it can take into account the several cell types present in the TME, which can be useful in defining immunotherapy response (147). Examples include IFN-γ, CXCL9 and CXLC10 whose expression correlates with response to immunotherapy (146)(148).

Epigenetic mechanisms are known to regulate several aspects related to immune regulation and actions (149). 5-azacytidine (5-aza), a demethylating agent, was shown to upregulate innate and adaptative immune-related genes, specifically to immune invasion, such as PD-L1 at both transcript and protein levels without altering CD80 and CD86. Furthermore, genes related to antigen presentation including HLA class I, B2M, CD58, TAP1, PMSB9 and PSMB8 were upregulated after 5-aza treatment (150). Treatment of leukemia cells with decitabine (DAC) translated into upregulation of PD-L1, PD-L2, PD-1 and CTLA-4 in these cells (151). This topic is thoroughly discussed in a recently published review (152). A DNA methylation-based profile - EPIMMUNE signature - of stage IV non-small cell lung cancer patients treated with anti-PD-1 therapies associated with improved progression-free and overall survival. EPIMMUNE-negative tumors disclosed a TME enriched in TAMs, cancer-associated fibroblasts and neutrophils. Moreover, unmethylated *FOXP1* associated with better progression-free and overall survival (153). Promoter methylation of *RAD51B* seems to associate with PD-L1 expression in lung cancer patients, with high levels of *RAD51B* methylation associating with lower risk of disease progression. Remarkably, combining *RAD51B* methylation and PD-L1 improved sensitivity to predict response to anti-PD-1 blockade and associated with a lower risk of death (154).

Although several studies showed that modulating epigenetic marks can improve therapeutic response to immune checkpoint inhibitors, the search for biomarkers is ongoing and needs further exploitation.

**Epi-drugs in cancer**

Epigenetic mechanisms including DNA methylation and histone post-translational modifications represent an alluring target for cancer therapy since they are reversible alterations important for tumor cells’ development (155,156). Therefore, a class of compounds that came to be known as “epi-drugs” were developed targeting these alterations (Table 2) (157). Currently, DNMT and HDAC inhibitors are the most used epi-drugs for cancer treatment in both clinic and clinical trials, namely in combination with chemo- and immunotherapy (Table 2).

DNMT inhibitors are classified in two main groups: nucleoside and non-nucleoside analogues (Table 2) (158). 5aza was the first compound developed and approved for clinical usage for DNMT inhibition. Indeed, 5-aza and decitabine (5-aza-2′-deoxycytidine) are already approved for treatment of hematological malignancies including acute myeloid leukemia (AML), myelodysplastic syndrome, and chronic myelomonocytic leukemia (CMML) by European Medicines Agency (EMA) and Food and Drug Administration (FDA) (Table 3) (157,159,160). Nucleoside analogues include analogues of cytosine that are integrated in DNA and lead to the formation of a covalent bond with the DNMT, which results in its degradation and DNA methylation inhibition (157,161). Both are nucleoside analogues characterized by replacing cytosine during DNA replication, which translates in the formation of a covalent bond when DNMTs exert their function, resulting in DNMTs' inhibition and further degradation (161)(162,163). Despite both showing to have anti-tumoral effects, namely by inducing apoptosis, cell and re-expression of tumor suppressor genes (164)(165), 5-aza and DAC display low bioavailability and a limited half-life, which hinders their wide implementation in clinical practice (161,166). More stable compounds with the same effect and mechanism of action have been described in the past years including zebularine, 5′-fluoro-2′-deoxycytidine (FdCyd), guadecitabine and RX-3117. For example, FdCyd, a fluoropyrimidine analogue, is less toxic and more stable when compared to 5-aza and DAC (77). Furthermore, FdCyd showed to stop cell arrest at G2/M in HCT116 cells though the DNA damage response pathway (167). RX-3117 (fluorocyclopentenylcytosine) is a recent cytidine analogue with a modified ribose molecule being activated specifically by uridine-cytidine kinase 2 (UCK2), leading do DNA damage and lowe DNA methylation levels though DNMT1 inhibition (168). Another compound that shows great stability, including being possible to administer orally, is zebularine (169), which showed to have a specific effect on cancer cells and not fibroblasts (170,171) However, since it showed great toxicity in primates, it was not continued for clinical trials (Table 3) (172)(173). Guadecitabine is a CpG dinucleotide analogue hypomethylating agent (174) with proven anti-tumoral activity, such as in combination with cisplatin in platinum-refractory germ cell tumors (175).

Another heterogenous group of compounds with DNMT inhibition activity is the non-nucleoside analogs, which inhibit DNMTs independently from DNA incorporation (Table 2) (176), These include natural compounds, DNA binders, SAM competitors and repurposed drugs (176,177). Regarding natural compounds, molecules such as genistein, the natural polyphenol epigallocatechin-3-gallate (EGCG) and curcumin that displays anti-inflammatory and antioxidant properties showed to inhibit DNA methylation, translating in anti-tumoral activity (178,179)(158)(180). 3-halo-3-nitroflavanones, a novel

class of DNMT inhibitors described recently, showed anti-tumoral activity associated with higher stability and low cytotoxicity than the most used DNMT inhibitors (181). Interestingly, a compound from this family MLo1302 caused a decrease in cell viability, namely in cisplatin resistant cell lines, pluripotency markers and an activation of apoptosis and cell cycle arrest in germ cell tumors cell lines (182). RG108 is a SAM competitor that binds to the catalytic pockets of DNMTs, forming covalent bonds and inhibiting the enzyme action (183). Treatment with RG108 caused radiosensitivity of esophageal cancer cells, enhancing apoptosis and G2/M phase arrest by radiation (184). SGI-1027, a quinolone-based molecule which binds to both DNMT3a and DNMT1 (185), combined with AH057 (JAK inhibitor) increased cervical cancer cells apoptotic cell death and cell-cycle arrest (186). Furthermore, MG98 is a second-generation 20-nucleotide antisense oligonucleotide that binds specifically to DNMT1 mRNA, decreasing DNMT1 levels (187).

Selected repurposed drugs, designed for a specific treatment that were found to have other therapeutic targets, also showed effect against DNMTs (176,177). For example, procaine and procainamide, approved as anesthetic and anti-arrhythmic drugs respectively, bind to the catalytic center of DNMTs, which translated in a decrease in DNA methylation levels (188,189). The arterial vasodilator hydralazine also leads to the loss of promoter hypermethylation of TSGs in cancer cell lines and primary tumors (190)(191). In this line, the antibiotic nanaomycin A also causes the same effects, being selective for DNMT3b (192).

HDAC inhibitors can be classified according to chemical group as hydroxamic acids, short-chain and aromatic fatty acids, benzamides, and cyclic peptides (Table 2). The hydroxamic acids and cycle peptides constitute the most potent inhibitors, with $IC_{50}$ in the low micro- or nanomolar range, while short-chain fatty acids require doses in the millimolar range (193).

**Table 2.** Epi-drugs approved and in clinical trial for cancer treatment, with respective effects and drug category.

| Drug | Approved | Clinical Trial | Effects |
|---|---|---|---|
| Azacitidine<br>Vidaza® | High risk Myelodysplastic syndromes<br>Chronic Myelomonocytic Leukemia<br>Acute Myeloid Leukemia | Pancreatic, colorectal, prostate, esophageal, breast, non-small cell lung cancer, thyroid, ovarian, nasopharyngeal and bladder cancer, hematological malignancies sarcoma, melanoma, germ cell tumors and renal cell carcinomas. | Nucleoside DNMT inhibitor |
| Decitabine<br>Dacogen® | High risk Myelodysplastic syndromes<br>Chronic Myelomonocytic Leukemia<br>Acute Myeloid Leukemia | Ovary, head and neck, colorectal, breast, esophageal, non-small cell lung, prostate, thyroid cancers, B cell lymphoma, glioma and medulloblastoma | Nucleoside DNMT inhibitor |
| 5′-fluoro-2′-deoxycytidine (FdCyd) | - | Head and neck, lung, urinary bladder, breast cancer and acute myeloid leukemia | Nucleoside DNMT inhibitor |
| Guadecitabine | - | Kidney, lung, ovarian, prostate, colorectal, gallbladder, pancreatic, urothelial cancer, extrahepatic bile duct adenocarcinoma, biliary type, testicular germ cell tumors, chondrosarcoma, melanoma, acute myeloid leukemia and myelodysplastic syndrome. | Nucleoside DNMT inhibitor |
| RX-3117 (Fluorocyclopentenylcytosine) | - | Pancreatic and bladder cancer | Nucleoside DNMT inhibitor |
| Genistein | - | Breast, prostate, colorectal, lung, pancreatic, bladder, kidney, endometrial cancer and melanoma | Isoflavone non-nucleoside DNMT inhibitor |
| Curcumin | - | Prostate, colorectal, breast, lung, head and neck and cervical cancer | Natural phenol non-nucleoside DNMT inhibitor |
| Hydralazine | - | Ovarian, cervical, lung and breast cancer | Repurposed drug non-nucleoside DNMT inhibitor |
| Belinostat<br>Beleodaq® | Peripheral T-cell Lymphoma | Lung, breast, ovary, hematological malignancies, bladder, liver cancer and chondrosarcoma | Hydroxamic acid pan-HDAC inhibitor |

| | | | |
|---|---|---|---|
| Givinostat | - | Chronic Myeloproliferative Neoplasms<br>Polycythemia Vera | Hydroxamic acid pan-HDAC inhibitor |
| Panobinostat<br>Farydak® | Multiple Myeloma | Breast, lung, pancreatic, prostate, colorectal, head and neck, esophageal, neuroendocrine, renal, thyroid, brain cancer, hematologic neoplasms and melanoma | Hydroxamic acid pan-HDAC inhibitor |
| Trichostatin A | - | Hematological malignancies | Hydroxamic acid pan-HDAC inhibitor |
| Vorinostat<br>Zolinza® | Cutaneous T cell Lymphoma | Breast, ovarian, pancreatic, lung, colorectal, gastric, liver, prostate, renal, bladder brain cancer, melanoma and hematological malignancies | Hydroxamic acid pan-HDAC inhibitor |
| Entinostat | - | Breast, colorectal, ovarian, neuroendocrine, lung, prostate, renal, pancreatic, endometrial cancer, hematological malignancies and cholangiocarcinoma | Benzamide class I HDAC inhibitor |
| Romidepsin<br>Istodax® | Cutaneous T-cell lymphoma | Lung, breast, pancreatic, colorectal, thyroid, bladder, ovarian cancer, glioma and hematological malignancies | Benzamide class I HDAC inhibitor |
| Valproic acid | - | Cervical, brain, lung. breast, pancreatic, prostate, bladder, thyroid, head and neck cancer and hematological malignancies | Short-chain and aromatic fatty acids panHDAC inhibitor |

| | | | |
|---|---|---|---|
| Abexinostat | - | Breast cancer, renal cell carcinoma, sarcoma, melanoma and hematologic malignancies | Hydroxamic acid pan-HDAC inhibitor |
| Tazemetostat Tazverik® | Advanced epithelioid sarcoma Follicular lymphoma | Prostate, ovarian, endometrial, head and neck cancer, melanoma, hematological malignancies, urothelial carcinoma and malignant mesothelioma | EZH2 inhibitor |
| Domatinostat | - | Melanoma and Merkel cell carcinoma | Benzamide class I HDAC inhibitor |

Hydroxamic acids include belinostat (approved for peripheral T-cell lymphoma), givinostat, panobinostat, trichostatin A and vorinostat, all pan-HDAC inhibitors. Vorinostat or suberanilohydroxamic acid (SAHA) was the first HDAC inhibitor to be approved for the treatment of advanced cutaneous T-cell lymphoma and it shows several anti-tumor effects in several hematological and solid tumors *in vitro* and *in vivo* (Table 3)(194). It inhibits class I and II HDACs by binding to the catalytic domain of the enzymes (195). Similar to vorinostat, trichostatin A (TSA), also a class I and II inhibitor, acts as a noncompetitive inhibitor of HDAC by mimicking the lysin substrate as a chelating agent to the zinc atom in the active site (195). Interestingly, it showed to reverse chemoresistance in lung cancer cell lines with high expression of IGFBP2, with IGFBP2 being a biomarker of chemoresistance poor outcome in lung cancer patients (196). Panobinostat is approved for patients with recurrent multiple myeloma who have received at least two prior treatment regiments (Table 3) (193). Indeed, the progression-free survival of patients treated with panobinostat was 10.6 months in comparison with 5.8 months in the control arm (197). Belinostat also inhibits HDACs by binding to the zinc finger in the enzymes' active catalytic site and, recently, showed to be active in testicular germ cell tumor cell lines resistant to cisplatin, with $IC_{50}$ in the low nanomolar range for all cell lines (198).

Entinostat belongs to the benzamide group of HDAC inhibitors and inhibits class I HDACs (193). Remarkably, entinostat boosted the effects of PD-1 inhibition in *in vivo* models of lung and renal cancers by impairing the immunosuppressive function of polymorphonuclear and monocytic-myeloid derived suppressor cell populations (112). Another inhibitor of class I HDACs is romidepsin (FK228) belonging to the cyclic peptide family (193). Romidepsin has been approved by the FDA for the treatment of advanced cutaneous T-cell lymphoma and peripheral T-cell lymphoma (Table 3) (199). The triple combination of romidepsin, gemcitabine and cisplatin acted synergically and induced death by creating reactive oxygen-species in triple-negative breast cancer cell lines (200).

The short-chain and aromatic fatty acids sodium butyrate and valproic acid also were shown to be pan-HDACs inhibitors (193). Sodium butyrate is a short chain fatty acid produced by fermentation by anaerobic bacterial fermentation that inhibits growth, induces apoptosis, migration and EMT of colorectal cancer cells (201). Valproic acid, used for the treatment of epilepsy and bipolar disorder, in combination with cisplatin and cetuximab, showed antiproliferative and pro-apoptotic effects in 3D-self-assembled spheroid models of ad and neck squamous cell carcinoma cells (202).

**Table 3.** Major clinical trials comprising epi-drugs and immunotherapy for cancer treatment.

| Clinical trial | Phase | State | Cancer | Combination | Dates |
|---|---|---|---|---|---|
| **NCT01928576** | II | Recruiting | Non-Small Cell Lung Cancer | Nivolumab<br>Entinostat<br>Azacitidine | 2013-estimated end 2022 |
| **NCT02260440** | II | Completed | Metastatic Colorectal Cancer | Pembrolizumab<br>Azacitidine | 2015-2017 |
| **NCT02546986** | II | Active, not recruiting | Non-Small-Cell Lung Carcinoma | CC-486<br>Pembrolizumab | 2015-estimated end 2021 |
| **NCT02453620** | I | Active, not recruiting | Breast Cancer | Ipilimumab<br>Nivolumab<br>Entinostat | 2015-estimated end 2021 |
| **NCT02961101** | I/II | Recruiting | Non-Hodgkin lymphoma, Hodgkin lymphoma, gastrointestinal cancers, hepatocellular carcinoma, breast cancer, ovarian cancer, lung cancer, renal-cell cancer, pancreatic cancer and bile duct cancer | Anti-PD-1 antibody<br>Decitabine<br>Chemotherapy | 2016-2020 |
| **NCT02890069** | I | Recruiting | Colorectal Cancer<br>Non-small Cell Lung Adenocarcinoma<br>Triple Negative Breast Cancer<br>Renal Cell Carcinoma | PDR001 (Anti-PD-1 antibody)<br>Everolimus<br>Panobinostat | 2016-estimated end 2021 |
| **NCT02619253** | I/Ib | Active, not recruiting | Renal Cell Carcinoma<br>Urinary Bladder Neoplasms | Pembrolizumab<br>Vorinostat | 2016-estimated end 2022 |
| **NCT02512172** | I | Active, not recruiting | Colorectal Cancer | CC-486 (Oral 5-Aza)<br>Romidepsin<br>MK–3475 (Anti-PD-1 antibody) | 2016-estimated end 2022 |
| **NCT02811497** | II | Active, not recruiting | Microsatellite Stable Colorectal Carcinoma<br>Platinum Resistant Epithelial Ovarian Cancer Type II<br>Estrogen Receptor Positive and HER2 Negative Breast Cancer | Durvalumab<br>Azacitidine | 2016-estimated end 2022 |
| **NCT02957968** | II | Recruiting | Breast Cancer | Decitabine<br>Pembrolizumab | 2016-estimated end 2023 |

| | | | | | |
|---|---|---|---|---|---|
| | | | | Doxorubicin<br>Cyclophosphamide<br>Paclitaxel<br>Carboplatin | |
| **NCT02638090** | I/II | Recruiting | Lung Cancer | Vorinostat<br>Pembrolizumab | 2016-estimated end 2023 |
| **NCT02959437** | I/II | Completed | Advanced or Metastatic Solid Tumors | Azacitidine<br>Pembrolizumab<br>Epacadostat<br>INCB057643 (BET inhibitor)<br>INCB059872 (LSD1 inhibitor) | 2017-2020 |
| **NCT03308396** | Ib/II | Active, not recruiting | Advanced Kidney Cancer<br>Kidney Cancer<br>Clear Cell Renal Cell Carcinoma | Durvalumab<br>Guadecitabine | 2017-estimated end 2021 |
| **NCT03206047** | I/II | Active, not recruiting | Platinum-Resistant Fallopian Tube Carcinoma<br>Platinum-Resistant Ovarian Carcinoma<br>Platinum-Resistant Primary Peritoneal Carcinoma<br>Recurrent Fallopian Tube Carcinoma<br>Recurrent Ovarian Carcinoma<br>Recurrent Primary Peritoneal Carcinoma | Atezolizumab<br>Guadecitabine | 2017-estimated end 2021 |
| **NCT03264404** | II | Recruiting | Pancreas Cancer | Pembrolizumab<br>Azacitidine | 2017-estimated end 2021 |
| **NCT03179943** | II | Active, not recruiting | Urothelial Carcinoma | Atezolizumab<br>Guadecitabine | 2017-estimated end 2022 |
| **NCT03019003** | I/II | Recruiting | Head and Neck Cancer | Durvalumab<br>Oral Decitabine | 2017-estimated end 2024 |
| **NCT02816021** | II | Recruiting | Melanoma and other Malignant Neoplasms of Skin<br>Metastatic Melanoma | Pembrolizumab<br>Azacitidine | 2017-estimated end 2026 |

| | | | | | |
|---|---|---|---|---|---|
| **NCT03590054** | I | Recruiting | Melanoma<br>Metastatic Head and Neck Squamous Cell Carcinoma<br>Urothelial Carcinoma<br>Non-Small Cell Lung Carcinoma | Pembrolizumab<br>Abexinostat | 2018-estimated end 2022 |
| **NCT03426891** | I | Recruiting | Glioblastoma<br>Brain Tumor | Pembrolizumab<br>Vorinostat<br>Temozolomide | 2018-estimated end 2022 |
| **NCT03233724** | I/II | Recruiting | Non-Small Cell Lung Cancer<br>Esophageal Carcinoma<br>Malignant Pleural Mesotheliomas | Pembrolizumab<br>Decitabine<br>Tetrahydrouridine (THU) | 2018-estimated end 2026 |
| **NCT03854474** | I/II | Recruiting | Locally and Metastatic Urothelial Carcinoma | Pembrolizumab<br>Tazemetostat | 2019-estimated end 2021 |
| **NCT03812796** | II | Recruiting | Gastrointestinal cancer | Domatinostat<br>Avelumab | 2019-estimated end 2021 |
| **NCT03765229** | II | Recruiting | Melanoma | Pembrolizumab<br>Entinostat | 2019-estimated end 2023 |
| **NCT03978624** | II | Recruiting | Bladder Cancer | Pembrolizumab<br>Entinostat | 2020-estimated end 2022 |
| **NCT04357873** | II | Recruiting | Squamous Cell Lung Cancer<br>Vulvar Cancer<br>Penile Cancer<br>Cervix Cancer<br>Head and Neck Squamous Cell Carcinoma<br>Anal Cancer | Pembrolizumab<br>Vorinostat | 2020-estimated end 2024 |
| **NCT04624113** | I/II | Not yet recruiting | Head and Neck Squamous Cell Carcinoma | Pembrolizumab<br>Tazemetostat | 2021-estimated end 2024 |
| **NCT04190056** | II | Not yet recruiting | Breast Cancer | Pembrolizumab<br>Tamoxifen<br>Vorinostat | 2021-estimated end 2029 |

**Bladder cancer**

BC is estimated to be the tenth most frequent cancer worldwide and the ninth cause of death by cancer (203). About 70% of the patients are diagnosed as a non-muscle invasive BC (NMIBC), while 30% are diagnosed with muscle invasive BC (MIBC) (204). NMIBC is mostly comprised of urothelial papillary neoplasms with varying propensity for recurrence and progression, which may be predicted based on grading (205). According to the 2016 WHO classification, the spectrum of papillary neoplasms includes urothelial papilloma, papillary urothelial neoplasm of low malignant potential, low-grade and high-grade papillary urothelial carcinoma, in ascending order of biological and clinical aggressiveness (206). On the other hand, urothelial carcinoma *in situ* (CIS) represents a high-grade form of non-papillary NMIBC, with substantial risk of progression to invasive disease (206). Although NMIBC mostly contributes to the overall BC 5-year survival rate of 77.1%, 80% of high-grade papillary carcinomas and CIS recur and 20-50% progress to MIBC (207). In addition to grade, evaluation of disease stage [by means of clinical examination, cystoscopy, radiographic evaluation and/or pathological examination using tissue collected by transurethral resection of the bladder tumor (TURBT) is mandatory to define the best therapeutic strategy (208,209). For NMIBC, treatment mostly consists of TURBT eventually complemented with mitomycin or Bacillus Calmette-Guérin (BCG) instillation, whereas radical cystectomy with lymphadenectomy remains the gold standard for MIBC, complemented with neo-adjuvant or adjuvant cisplatin-based chemotherapy, which is also the main option for metastatic BC (209). Recently, immunotherapies targeting PD-1/PD-L1 immune checkpoint were approved for BC patients that are refractory or ineligible to cisplatin-based chemotherapy (210). Although chemotherapy and immunotherapy have improved the outcome of locally advanced and metastatic disease, 5-year survival remains poor (36% and 5%, respectively) (207).

BCG, which is a weakened strain of *Mycobacterium bovis*, was the first form of immunotherapy approved for cancer treatment and, specifically, for BC. Currently, it is administrated by intravesical instillation after TURBT in NMIBC patients with high risk of recurrence (211). Although the mechanism is not fully known, BCG leads to localized innate and adaptative immune responses, including CD4 and CD8 lymphocytes, NK cells, macrophages, granulocytes and DCs (212). About 55-75% of the high-risk patients suffering from papillary tumors to CIS respond to this therapy. However, 25 to 45% of these eventually relapse and progress to invasive disease. Hypermethylation of *CDKN2B* as well as of *MUS81a* and *MSH6* involved in DNA repair and *THBS1*, important for cell adhesion, have been associated with response to BCG therapy (210,213).

Likewise, low methylation levels of *PMF1* have been associated with disease recurrence, poor outcome and lack of response to BCG in BC patients (Figure 3) (214).

The immune landscape of BC is composed by different immune populations, including CD8+ T lymphocytes and Th1 CD4+ T lymphocytes. Interestingly, tumor-infiltrating CD4+ lymphocytes were found to be hypomethylated in four lineage loci compared to CD4+ lymphocytes in lymph nodes and blood. Patients with complete response to neoadjuvant chemotherapy (NACT) showed hypomethylation in CD4+ T cells, namely in IFN- γ. Furthermore, shifts in methylation patterns of Th1 CD4+ T cells after NACT shows a relocation of cells from blood to the tumor (Figure 3) (215). Tissue-resident memory T cells showed low PRF1 DNA methylation levels concomitantly with increased perforin expression (216). The analysis of DNA methylation in neutrophils and lymphocytes predicted the outcome of BC patients, *i.e.*, high levels of DNA methylation-derived neutrophil-to-lymphocyte ratio associated with poor outcome (217).

Demethylating agents lead to reactivation of TSGs, inhibition of cancer cells' proliferation and migration, increased apoptosis and activation of IFN pathway in BC (218). Ramakrishnan et al. showed that low concentrations of DAC lead to the activation of NOTCH1, which may prevent epithelial-mesenchymal transition of tumor cells, thus impairing cancer cell dissemination (219,220). Moreover, increased IL-6 levels were observed in DAC-treated cells, and reduction of cytokeratin 5 expression associated with cell differentiation and impaired BC progression (221). Another epigenetic inhibitor for G9a, CM-272, in combination with cisplatin caused an increase in expression of genes associated with immune response, such as TNF-α, IFN-α and IFN-γ, which correlated with an endogenous retrovirus response. Furthermore, an extensive infiltration of CD8+ T cells and NK cells was observed in tumors and metastases in an *in vivo* immunocompetent model of MIBC. This was also observed with CM-272 in combination with an anti-PD-L1 antibody, with immune infiltration by CD3+, CD8+ and NK cells, and the absence of CD4+ and CD163+ cells (222).

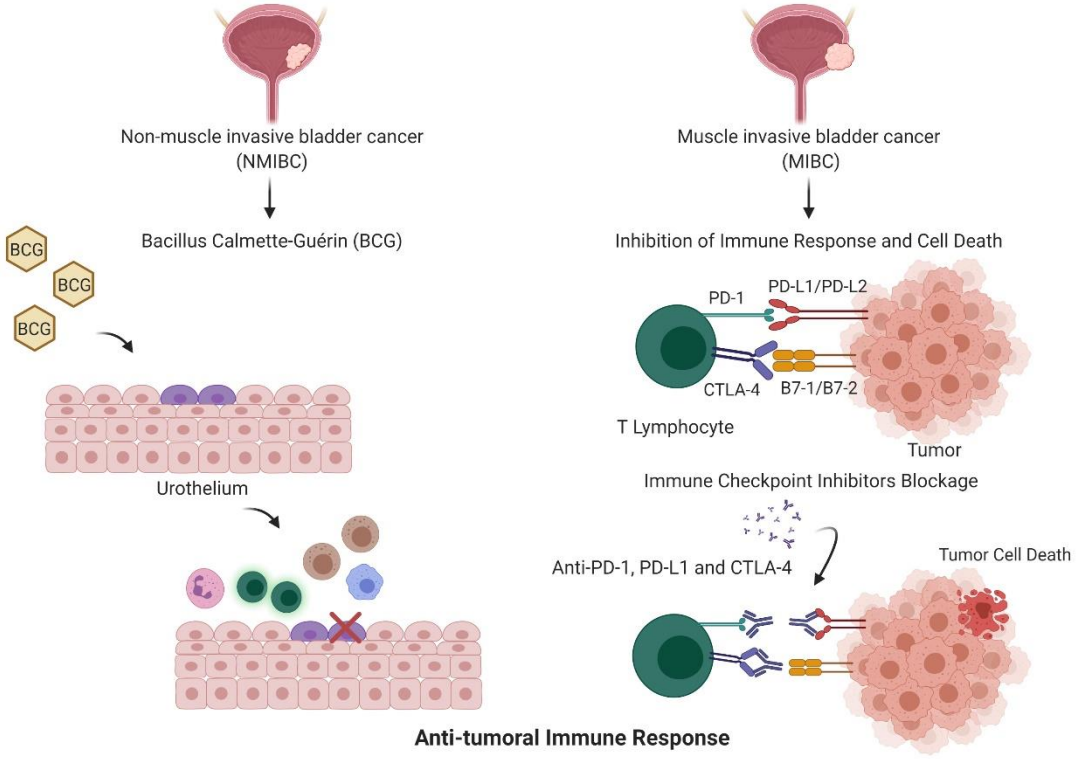


**Figure 4.** Modalities of immunotherapy in bladder cancer. BCG is a weakened strain of *Mycobacterium bovis* and was the first of immunotherapy approved for BC. NMIBC patients with high risk of recurrence are subjected to BCG therapy. The administration of BCG leads to a stimulation of both adaptative and innate immune response by recruiting lymphocytes, macrophages, NK cells and neutrophils, leading to the elimination of the remaining tumor cells. On the other hand, BC patients with MIBC are candidates for immune checkpoint blockage. Tumor cells express repression signals that lead to the inhibition of the immune response, namely by expressing PD-L1/PD-L2 and B7-1/B7-2, that will bind to PD-1 and CTLA-4 present in T lymphocytes, respectively. Nevertheless, with the administration of antibodies against PD-1, PD-L1 or CTL4-A, this process is reverted, leading to the activation of T cells and the start of an immune response against tumor cells, leading ultimately to their death.

## Conclusions

Epigenetic alterations in cells of the TME play a major role in creating an immunosuppressive environment ideal for tumor development, which translates in a lack of effectiveness of immune checkpoint blockage therapies. The inhibition of epigenetic modulators might be an interesting therapeutic option to modify the immunosuppressive TME and their potential in combination with immunotherapy has already been discussed. Additionally, refining patient selection for immunotherapy by exploring new biomarkers with higher sensitivity and specificity might improve the success rate of this therapy. Combining these findings, exploring aberrant epigenetic marks in both cancer cells and in cells of the TME might provide potential biomarkers for this purpose.

Thus, further studies are needed to increase our knowledge on the epigenetic mechanisms underlying the acquisition of immunosuppressive immune cell phenotypes and how this affect immunotherapy response. Additionally, a promising strategy to

generate an immune-promoting TME might be the combination of epigenetic modulator targeting and immunotherapy.

**References**


1. Baylin SB, Jones PA. Epigenetic determinants of cancer. Cold Spring Harb Perspect Biol. 2016;8(9).
2. Song H, Liu D, Dong S, et al. Epitranscriptomics and epiproteomics in cancer drug resistance: therapeutic implications. Signal Transduct Target Ther. 2020;5(1).
3. Rinaldi G, Rossi M, Fendt SM. Metabolic interactions in cancer: cellular metabolism at the interface between the microenvironment, the cancer cell phenotype and the epigenetic landscape. Wiley Interdiscip Rev Syst Biol Med. 2018;10(1).
4. Lyko F. The DNA methyltransferase family: A versatile toolkit for epigenetic regulation. Nat Rev Genet. 2018;19(2):81-92.
5. Chen Z, Chen Z, Chen Z, et al. Role of Mammalian DNA Methyltransferases in Development. Annu Rev Biochem. 2020;89:135-158.
6. Esteller M. Epigenetic gene silencing in cancer: The DNA hypermethylome. Hum Mol Genet. 2007;16(R1):50-59.
7. Rothbart SB, Strahl BD. Interpreting the language of histone and DNA modifications. Biochim Biophys Acta - Gene Regul Mech. 2014;1839(8):627-643.
8. Zhao Z, Shilatifard A. Epigenetic modifications of histones in cancer. Genome Biol. 2019;20(1):1-16.
9. Cairns BR. Chromatin remodeling: Insights and intrigue from single-molecule studies. Nat Struct Mol Biol. 2007;14(11):989-996.
10. Martire S, Banaszynski LA. The roles of histone variants in fine-tuning chromatin organization and function. Nat Rev Mol Cell Biol. 2020;21(9):522-541.
11. Kurumizaka H, Kujirai T, Takizawa Y. Contributions of Histone Variants in Nucleosome Structure and Function. J Mol Biol. Published online October 14, 2020.
12. Tran Janco JM, Lamichhane P, Karyampudi L, Knutson KL. Tumor-Infiltrating Dendritic Cells in Cancer Pathogenesis. J Immunol. 2015;194(7):2985-2991.
13. Yasui D, Miyano M, Cai S, Varga-Weisz P, Kohwi-Shigematsu T. SATB1 targets chromatin remodelling to regulate genes over long distances. Nature. 2002;419(6907):641-645.
14. Pavan Kumar P, Purbey PK, Sinha CK, et al. Phosphorylation of SATB1, a Global Gene Regulator, Acts as a Molecular Switch Regulating Its Transcriptional Activity

In Vivo. Mol Cell. 2006;22(2):231-243.

15. Tesone AJ, Rutkowski MR, Brencicova E, et al. Satb1 Overexpression Drives Tumor-Promoting Activities in Cancer-Associated Dendritic Cells. Cell Rep. 2016;14(7):1774-1786.
16. Glatzel-Plucí Nska N, Piotrowska A, Dzi¸ Egiel P, Podhorska-Okołów M. The Role of SATB1 in Tumour Progression and Metastasis. Int J Mol Sci. 2019;(20):4156.
17. Ding B, Liu P, Liu W, Sun P, Wang CL. Emerging roles of krüppel-like factor 4 in cancer and cancer stem cells. Asian Pacific J Cancer Prev. 2015;16(9):3629-3633.
18. Rosenzweig JM, Glenn JD, Calabresi PA, Whartenby KA. KLF4 modulates expression of IL-6 in dendritic cells via both promoter activation and epigenetic modification. J Biol Chem. 2013;288(33):23868-23874.
19. Gabrilovich DI, Bronte V, Chen SH, et al. The terminology issue for myeloid-derived suppressor cells [1]. Cancer Res. 2007;67(1):425.
20. Sasidharan Nair V, Saleh R, Toor SM, et al. Transcriptomic profiling disclosed the role of DNA methylation and histone modifications in tumor-infiltrating myeloid-derived suppressor cell subsets in colorectal cancer. Clin Epigenetics. 2020;12(1):13.
21. Wu L, Du H, Li Y, Qu P, Yan C. Signal transducer and activator of transcription 3 (Stat3C) promotes myeloid-derived suppressor cell expansion and immune suppression during lung tumorigenesis. Am J Pathol. 2011;179(4):2131-2141.
22. Trikha P, Carson WE. Signaling pathways involved in MDSC regulation. Biochim Biophys Acta - Rev Cancer. 2014;1846(1):55-65.
23. Mace TA, Bloomston M, Lesinski GB. Pancreatic cancer-associated stellate cells: A viable target for reducing immunosuppression in the tumor microenvironment. Oncoimmunology. 2013;2(7).
24. Xin H, Zhang C, Herrmann A, Du Y, Figlin R, Yu H. Sunitinib inhibition of Stat3 induces renal cell carcinoma tumor cell apoptosis and reduces immunosuppressive cells. Cancer Res. 2009;69(6):2506-2513.
25. Villagra A, Cheng F, Wang HW, et al. The histone deacetylase HDAC11 regulates the expression of interleukin 10 and immune tolerance. Nat Immunol. 2009;10(1):92-100.
26. Sahakian E, Powers JJ, Chen J, et al. Histone deacetylase 11: A novel epigenetic regulator of myeloid derived suppressor cell expansion and function. Mol Immunol. 2015;63(2):579-585.
27. Cheng F, Lienlaf M, Perez-Villarroel P, et al. Divergent roles of histone deacetylase 6 (HDAC6) and histone deacetylase 11 (HDAC11) on the

transcriptional regulation of IL10 in antigen presenting cells. Mol Immunol. 2014;60(1):44-53.

28. Sido JM, Yang X, Nagarkatti PS, Nagarkatti M. Δ 9 -Tetrahydrocannabinol-mediated epigenetic modifications elicit myeloid-derived suppressor cell activation via STAT3/S100A8 . J Leukoc Biol. 2015;97(4):677-688.
29. Viatour P, Somervaille TC, Venkatasubrahmanyam S, et al. Hematopoietic Stem Cell Quiescence Is Maintained by Compound Contributions of the Retinoblastoma Gene Family. Cell Stem Cell. 2008;3(4):416-428.
30. Walkley CR, Shea JM, Sims NA, Purton LE, Orkin SH. Rb Regulates Interactions between Hematopoietic Stem Cells and Their Bone Marrow Microenvironment. Cell. 2007;129(6):1081-1095.
31. Youn JI, Kumar V, Collazo M, et al. Epigenetic silencing of retinoblastoma gene regulates pathologic differentiation of myeloid cells in cancer. Nat Immunol. 2013;14(3):211-220.
32. Ojalvo LS, Whittaker CA, Condeelis JS, Pollard JW. Gene Expression Analysis of Macrophages That Facilitate Tumor Invasion Supports a Role for Wnt-Signaling in Mediating Their Activity in Primary Mammary Tumors. J Immunol. 2010;184(2):702-712.
33. Rubio C, Munera-Maravilla E, Lodewijk I, et al. Macrophage polarization as a novel weapon in conditioning tumor microenvironment for bladder cancer: can we turn demons into gods? Clin Transl Oncol. 2019;21(4):391-403.
34. Yang X, Wang X, Liu D, Yu L, Xue B, Shi H. Epigenetic Regulation of Macrophage Polarization by DNA Methyltransferase 3b. Mol Endocrinol. 2014;28(4):565-574.
35. Arlauckas SP, Garren SB, Garris CS, et al. Arg1 expression defines immunosuppressive subsets of tumor-associated macrophages. Theranostics. 2018;8(21):5842-5854.
36. Ishii M, Wen H, Corsa CAS, et al. Epigenetic regulation of the alternatively activated macrophage phenotype. Blood. 2009;114(15):3244-3254.
37. Kittan NA, Allen RM, Dhaliwal A, et al. Cytokine Induced Phenotypic and Epigenetic Signatures Are Key to Establishing Specific Macrophage Phenotypes. Zissel G, ed. PLoS One. 2013;8(10):e78045.
38. Satoh T, Takeuchi O, Vandenbon A, et al. The Jmjd3-Irf4 axis regulates M2 macrophage polarization and host responses against helminth infection. Nat Immunol. 2010;11(10):936-944.
39. Setrerrahmane S, Xu H. Tumor-related interleukins: Old validated targets for new anti-cancer drug development. Mol Cancer. 2017;16(1):1-17.
40. Chen X, Barozzi I, Termanini A, et al. Requirement for the histone deacetylase

Hdac3 for the inflammatory gene expression program in macrophages. Proc Natl Acad Sci U S A. 2012;109(42):E2865-E2874.

41. Mullican SE, Gaddis CA, Alenghat T, et al. Histone deacetylase 3 is an epigenomic brake in macrophage alternative activation. Genes Dev. 2011;25(23):2480-2488.
42. Cao Q, Rong S, Repa JJ, Clair RS, Parks JS, Mishra N. Histone deacetylase 9 represses cholesterol efflux and alternatively activated macrophages in atherosclerosis development. Arterioscler Thromb Vasc Biol. 2014;34(9):1871-1879.
43. Yang Q, Wei J, Zhong L, et al. Cross Talk between Histone Deacetylase 4 and STAT6 in the Transcriptional Regulation of Arginase 1 during Mouse Dendritic Cell Differentiation. Mol Cell Biol. 2015;35(1):63-75.
44. Lo Sasso G, Joe Menzies K, Mottis A, et al. SIRT2 Deficiency Modulates Macrophage Polarization and Susceptibility to Experimental Colitis. PLoS One. 2014;9(7).
45. Tay RE, Richardson EK, Toh HC. Revisiting the role of CD4+ T cells in cancer immunotherapy—new insights into old paradigms. Cancer Gene Ther. Published online May 27, 2020.
46. Janson PCJ, Marits P, Thörn M, Ohlsson R, Winqvist O. CpG Methylation of the IFNG Gene as a Mechanism to Induce Immunosupression in Tumor-Infiltrating Lymphocytes . J Immunol. 2008;181(4):2878-2886.
47. Peng D, Kryczek I, Nagarsheth N, et al. Epigenetic silencing of TH1-type chemokines shapes tumour immunity and immunotherapy. Nature. 2015;527(7577):249-253.
48. Yang R, Cheng S, Luo N, et al. Distinct epigenetic features of tumor-reactive CD8+ T cells in colorectal cancer patients revealed by genome-wide DNA methylation analysis. Genome Biol. 2019;21(1):2.
49. Ghoneim HE, Fan Y, Moustaki A, et al. De Novo Epigenetic Programs Inhibit PD-1 Blockade-Mediated T Cell Rejuvenation. Cell. 2017;170(1):142-157.e19.
50. Massagué J. TGFβ in Cancer. Cell. 2008;134(2):215-230.
51. Stephen TL, Payne KK, Chaurio RA, et al. SATB1 Expression Governs Epigenetic Repression of PD-1 in Tumor-Reactive T Cells. Immunity. 2017;46(1):51-64.
52. Philip M, Fairchild L, Sun L, et al. Chromatin states define tumour-specific T cell dysfunction and reprogramming. Nature. 2017;545(7655):452-456.
53. Li C, Jiang P, Wei S, Xu X, Wang J. Regulatory T cells in tumor microenvironment: New mechanisms, potential therapeutic strategies and future prospects. Mol Cancer. 2020;19(1):116.

54. Waight JD, Takai S, Marelli B, et al. Cutting Edge: Epigenetic Regulation of Foxp3 Defines a Stable Population of CD4 + Regulatory T Cells in Tumors from Mice and Humans . J Immunol. 2015;194(3):878-882.
55. Ohkura N, Kitagawa Y, Sakaguchi S. Development and Maintenance of Regulatory T cells. Immunity. 2013;38(3):414-423.
56. Ohkura N, Hamaguchi M, Morikawa H, et al. T Cell Receptor Stimulation-Induced Epigenetic Changes and Foxp3 Expression Are Independent and Complementary Events Required for Treg Cell Development. Immunity. 2012;37(5):785-799.
57. DuPage M, Chopra G, Quiros J, et al. The chromatin-modifying enzyme Ezh2 is critical for the maintenance of regulatory T cell identity after activation. Immunity. 2015;42(2):227-238.
58. Wang D, Quiros J, Mahuron K, et al. Targeting EZH2 Reprograms Intratumoral Regulatory T Cells to Enhance Cancer Immunity. Cell Rep. 2018;23(11):3262-3274.
59. Schenk A, Bloch W, Zimmer P. Natural killer cells—An epigenetic perspective of development and regulation. Int J Mol Sci. 2016;17(3).
60. Fernández-Sánchez A, Raneros AB, Palao RC, et al. DNA demethylation and histone H3K9 acetylation determine the active transcription of the NKG2D gene in human CD8+ T and NK cells. Epigenetics. 2013;8(1):66-78.
61. Ogbomo H, Michaelis M, Kreuter J, Doerr HW, Cinatl J. Histone deacetylase inhibitors suppress natural killer cell cytolytic activity. FEBS Lett. 2007;581(7):1317-1322.
62. Yin J, Leavenworth JW, Li Y, et al. Ezh2 regulates differentiation and function of natural killer cells through histone methyltransferase activity. Proc Natl Acad Sci U S A. 2015;112(52):15988-15993.
63. Sauvageau M, Sauvageau G. Polycomb group proteins: Multi-faceted regulators of somatic stem cells and cancer. Cell Stem Cell. 2010;7(3):299-313.
64. Mao L, Yang C, Wang J, et al. SATB1 is overexpressed in metastatic prostate cancer and promotes prostate cancer cell growth and invasion. J Transl Med. 2013;11(1):111.
65. Guo L, Zheng J, Yu T, Liu Y, Duo L. Elevated expression of SATB1 is involved in pancreatic tumorigenesis and is associated with poor patient survival. Mol Med Rep. 2017;16(6):8842-8848.
66. Nodin B, Hedner C, Uhlén M, Jirström K. Expression of the global regulator SATB1 is an independent factor of poor prognosis in high grade epithelial ovarian cancer. J Ovarian Res. 2012;5(1).
67. Zhang H, Qu S, Li S, et al. Silencing SATB1 inhibits proliferation of human

osteosarcoma U2OS cells. Mol Cell Biochem. 2013;378(1-2):39-45.
68. Selinger CI, Cooper WA, Al-Sohaily S, et al. Loss of special at-rich binding protein 1 expression is a marker of poor survival in lung cancer. J Thorac Oncol. 2011;6(7):1179-1189.
69. Tu W, Luo M, Wang Z, et al. Upregulation of SATB1 promotes tumor growth and metastasis in liver cancer. Liver Int. 2012;32(7):1064-1078.
70. Chu SH, Ma Y Bin, Feng DF, et al. Upregulation of SATB1 is associated with the development and progression of glioma. J Transl Med. 2012;10(1):149.
71. Yuan CL, Li L, Zhou X, Liz H, Han L. Expression of SATB1 and HER2 in gastric cancer and its clinical significance. Eur Rev Med Pharmacol Sci. 2016;20(11):2256-2264.
72. Nodin B, Johannesson H, Wangefjord S, et al. Molecular correlates and prognostic significance of SATB1 expression in colorectal cancer. Diagn Pathol. 2012;7(1).
73. Fromberg A, Rabe M, Aigner A. Multiple effects of the Special AT-rich Binding Protein 1 (SATB1) in colon carcinoma. Int J Cancer. 2014;135(11):2537-2546.
74. Palucka K, Coussens LM, O'Shaughnessy J. Dendritic cells, inflammation, and breast cancer. Cancer J (United States). 2013;19(6):511-516.
75. Crispen PL, Kusmartsev S. Mechanisms of immune evasion in bladder cancer. Cancer Immunol Immunother. 2020;69:3-14.
76. Han B, Luan L, Xu Z, Wu B. Expression and biological roles of SATB1 in human bladder cancer. Tumor Biol. 2013;34(5):2943-2949.
77. Gabrilovich DI, Nagaraj S. Myeloid-derived suppressor cells as regulators of the immune system. Nat Rev Immunol. 2009;9(3):162-174.
78. Sanaei M, Salimzadeh L, Bagheri N. Crosstalk between myeloid-derived suppressor cells and the immune system in prostate cancer. J Leukoc Biol. 2020;107(1):43-56.
79. Medina-Echeverz J, Eggert T, Han M, Greten TF. Hepatic myeloid-derived suppressor cells in cancer.
80. Ma J, Xu H, Wang S. Immunosuppressive role of myeloid-derived suppressor cells and therapeutic targeting in lung cancer. J Immunol Res. 2018;2018.
81. Lissbrant IF, Stattin P, Wikstrom P, Damber JE, Egevad L, Bergh A. Tumor associated macrophages in human prostate cancer: relation to clinicopathological variables and survival. Int J Oncol. 2000;17(3):445-451.
82. Mielgo A, Schmid MC. Impact of tumour associated macrophages in pancreatic cancer. BMB Rep. 2013;46(3):131-138.
83. Yin M, Shen J, Yu S, et al. Tumor-associated macrophages (Tams): A critical

activator in ovarian cancer metastasis. Onco Targets Ther. 2019;12:8687-8699.
84. Malfitano AM, Pisanti S, Napolitano F, Di Somma S, Martinelli R, Portella G. Tumor-associated macrophage status in cancer treatment. Cancers (Basel). 2020;12(7).
85. Sumitomo R, Hirai T, Fujita M, Murakami H, Otake Y, Huang C. M2 tumor-associated macrophages promote tumor progression in non-small-cell lung cancer. Exp Ther Med. 2019;18(6).
86. Vidyarthi A, Agnihotri T, Khan N, et al. Predominance of M2 macrophages in gliomas leads to the suppression of local and systemic immunity. Cancer Immunol Immunother. 2019;68(12):1995-2004.
87. Gambardella V, Castillo J, Tarazona N, et al. The role of tumor-associated macrophages in gastric cancer development and their potential as a therapeutic target. Cancer Treat Rev. 2020;86:102015.
88. Liu Y, Li L, Li Y, Zhao X. Research Progress on Tumor-Associated Macrophages and Inflammation in Cervical Cancer. Biomed Res Int. 2020;2020.
89. Zhong X, Chen B, Yang Z. The Role of Tumor-Associated Macrophages in Colorectal Carcinoma Progression. Cell Physiol Biochem. 2018;45(1):356-365.
90. Choi J, Gyamfi J, Jang H, Koo JS. The role of tumor-associated macrophage in breast cancer biology. Histol Histopathol. 2018;33(2):133-145.
91. Hendry S, Salgado R, Gevaert T, et al. Assessing Tumor-Infiltrating Lymphocytes in Solid Tumors: A Practical Review for Pathologists and Proposal for a Standardized Method from the International Immuno-Oncology Biomarkers Working Group: Part 2: TILs in Melanoma, Gastrointestinal Tract Carcinomas, Non-Small Cell Lung Carcinoma and Mesothelioma, Endometrial and Ovarian Carcinomas, Squamous Cell Carcinoma of the Head and Neck, Genitourinary Carcinomas, and Primary Brain Tumors. Adv Anat Pathol. 2017;24(6):311-335.
92. Hendry S, Salgado R, Gevaert T, et al. Assessing Tumor-infiltrating Lymphocytes in Solid Tumors: A Practical Review for Pathologists and Proposal for a Standardized Method from the International Immunooncology Biomarkers Working Group: Part 1: Assessing the Host Immune Response, TILs in Invasive Breast Carcinoma and Ductal Carcinoma in Situ, Metastatic Tumor Deposits and Areas for Further Research. Adv Anat Pathol. 2017;24(5):235-251.
93. Woroniecka K, Chongsathidkiet P, Rhodin K, et al. T-cell exhaustion signatures vary with tumor type and are severe in glioblastoma. Clin Cancer Res. 2018;24(17):4175-4186.
94. Baitsch L, Baumgaertner P, Devêvre E, et al. Exhaustion of tumor-specific CD8+ T cells in metastases from melanoma patients. J Clin Invest. 2011;121(6):2350-

2360.
95. Halim L, Romano M, McGregor R, et al. An Atlas of Human Regulatory T Helper-like Cells Reveals Features of Th2-like Tregs that Support a Tumorigenic Environment. Cell Rep. 2017;20(3):757-770.
96. Tao H, Mimura Y, Aoe K, et al. Prognostic potential of FOXP3 expression in non-small cell lung cancer cells combined with tumor-infiltrating regulatory T cells. Lung Cancer. 2012;75(1):95-101.
97. Sayour EJ, McLendon P, McLendon R, et al. Increased proportion of FoxP3+ regulatory T cells in tumor infiltrating lymphocytes is associated with tumor recurrence and reduced survival in patients with glioblastoma. Cancer Immunol Immunother. 2015;64(4):419-427.
98. Judge SJ, Murphy WJ, Canter RJ. Characterizing the Dysfunctional NK Cell: Assessing the Clinical Relevance of Exhaustion, Anergy, and Senescence. Front Cell Infect Microbiol. 2020;10:49.
99. Peng YP, Zhu Y, Zhang JJ, et al. Comprehensive analysis of the percentage of surface receptors and cytotoxic granules positive natural killer cells in patients with pancreatic cancer, gastric cancer, and colorectal cancer. J Transl Med. 2013;11(1):262.
100. Bi J, Tian Z. NK cell exhaustion. Front Immunol. 2017;8(JUN):760.
101. Mamessier E, Sylvain A, Thibult ML, et al. Human breast cancer cells enhance self tolerance by promoting evasion from NK cell antitumor immunity. J Clin Invest. 2011;121(9):3609-3622.
102. Kalluri R. The biology and function of fibroblasts in cancer. Nat Rev Cancer. 2016;16(9):582-598.
103. Tao L, Huang G, Song H, Chen Y, Chen L. Cancer associated fibroblasts: An essential role in the tumor microenvironment (review). Oncol Lett. 2017;14(3):2611-2620.
104. Ziani L, Chouaib S, Thiery J. Alteration of the antitumor immune response by cancer-associated fibroblasts. Front Immunol. 2018;9(MAR):1.
105. Hashizume H, Baluk P, Morikawa S, et al. Openings between defective endothelial cells explain tumor vessel leakiness. Am J Pathol. 2000;156(4):1363-1380.
106. Hida K, Hida Y, Amin DN, et al. Tumor-associated endothelial cells with cytogenetic abnormalities. Cancer Res. 2004;64(22):8249-8255.
107. Farnsworth RH, Lackmann M, Achen MG, Stacker SA. Vascular remodeling in cancer. Oncogene. 2014;33(27):3496-3505.
108. Henke E, Nandigama R, Ergün S. Extracellular Matrix in the Tumor

Microenvironment and Its Impact on Cancer Therapy. Front Mol Biosci. 2020;6:160.

109. Gao XY, Xue XH, Ma YN, Zhang SQ. Effect of baicalein on the expression of SATB1 in human breast cancer cells. Exp Ther Med. 2015;9(5):1665-1669.
110. Lakshminarayana Reddy CN, Vyjayanti VN, Notani D, Galande S, Kotamraju S. Down-regulation of the global regulator SATB1 by statins in COLO205 colon cancer cells. Mol Med Rep. 2010;3(5):857-861.
111. Wang M, Yin B, Matsueda S, et al. Identification of Special AT-Rich Sequence Binding Protein 1 as a Novel Tumor Antigen Recognized by CD8+ T Cells: Implication for Cancer Immunotherapy. Appel S, ed. PLoS One. 2013;8(2):e56730.
112. Orillion A, Hashimoto A, Damayanti N, et al. Entinostat neutralizes myeloid-derived suppressor cells and enhances the antitumor effect of PD-1 inhibition in murine models of lung and renal cell carcinoma. Clin Cancer Res. 2017;23(17):5187-5201.
113. Kim K, Skora AD, Li Z, et al. Eradication of metastatic mouse cancers resistant to immune checkpoint blockade by suppression of myeloid-derived cells. Proc Natl Acad Sci U S A. 2014;111(32):11774-11779.
114. Briere D, Sudhakar N, Woods DM, et al. The class I/IV HDAC inhibitor mocetinostat increases tumor antigen presentation, decreases immune suppressive cell types and augments checkpoint inhibitor therapy. Cancer Immunol Immunother. 2018;67(3):381-392.
115. Hashimoto A, Fukumoto T, Zhang R, Gabrilovich D. Selective targeting of different populations of myeloid-derived suppressor cells by histone deacetylase inhibitors. Cancer Immunol Immunother. 2020;69(9):1929-1936.
116. Liu SS, Wu F, Jin YM, Chang WQ, Xu TM. HDAC11: a rising star in epigenetics. Biomed Pharmacother. 2020;131(May):110607.
117. Tikhanovich I, Zhao J, Olson J, et al. Protein arginine methyltransferase 1 modulates innate immune responses through regulation of peroxisome proliferator-activated receptor γ-dependent macrophage differentiation. J Biol Chem. 2017;292(17):6882-6894.
118. Yildirim-Buharalioğlu G, Bond M, Sala-Newby GB, Hindmarch CCT, Newby AC. Regulation of epigenetic modifiers, including KDM6B, by interferon-γ and interleukin-4 in human macrophages. Front Immunol. 2017;8(FEB):1.
119. Kruidenier L, Chung CW, Cheng Z, et al. A selective jumonji H3K27 demethylase inhibitor modulates the proinflammatory macrophage response. Nature. 2012;488(7411):404-408.

120. de Groot AE, Pienta KJ. Epigenetic control of macrophage polarization: Implications for targeting tumor-associated macrophages. Oncotarget. 2018;9(29):20908-20927.
121. Goswami S, Apostolou I, Zhang J, et al. Modulation of EZH2 expression in T cells improves efficacy of anti-CTLA-4 therapy. J Clin Invest. 2018;128(9):3813-3818.
122. Qiu J, Sharma S, Rollins RA, Paul TA. The complex role of EZH2 in the tumor microenvironment: Opportunities and challenges for immunotherapy combinations. Future Med Chem. 2020;12(15):1415-1430.
123. Zingg D, Arenas-Ramirez N, Sahin D, et al. The Histone Methyltransferase Ezh2 Controls Mechanisms of Adaptive Resistance to Tumor Immunotherapy. Cell Rep. 2017;20(4):854-867.
124. Schreiber RD, Old LJ, Smyth MJ. Cancer immunoediting: Integrating immunity's roles in cancer suppression and promotion. Science (80- ). 2011;331(6024):1565-1570.
125. Aqbi HF, Wallace M, Sappal S, Payne KK, Manjili MH. IFN-γ orchestrates tumor elimination, tumor dormancy, tumor escape, and progression. J Leukoc Biol. 2018;103(6):1219-1223.
126. Jahanban-Esfahlan R, Seidi K, Manjili MH, Jahanban-Esfahlan A, Javaheri T, Zare P. Tumor Cell Dormancy: Threat or Opportunity in the Fight against Cancer. Cancers (Basel). 2019;11(8).
127. O'Donnell JS, Teng MWL, Smyth MJ. Cancer immunoediting and resistance to T cell-based immunotherapy. Nat Rev Clin Oncol. 2019;16(3):151-167.
128. Chen L, Flies DB. Molecular mechanisms of T cell co-stimulation and co-inhibition. Nat Rev Immunol. 2013;13(4):227-242.
129. Pardoll DM. The blockade of immune checkpoints in cancer immunotherapy. Nat Rev Cancer. 2012;12(4):252-264.
130. Okazaki T, Honjo T. PD-1 and PD-1 ligands: From discovery to clinical application. Int Immunol. 2007;19(7):813-824.
131. Wei SC, Levine JH, Cogdill AP, et al. Distinct Cellular Mechanisms Underlie Anti-CTLA-4 and Anti-PD-1 Checkpoint Blockade. Cell. 2017;170(6):1120-1133.e17.
132. Van Der Merwe PA, Bodian DL, Daenke S, Linsley P, Davis SJ. CD80 (B7-1) binds both CD28 and CTLA-4 with a low affinity and very fast kinetics. J Exp Med. 1997;185(3):393-403.
133. Ohaegbulam KC, Assal A, Lazar-Molnar E, Yao Y, Zang X. Human cancer immunotherapy with antibodies to the PD-1 and PD-L1 pathway. Trends Mol Med. 2015;21(1):24-33.
134. Lee HT, Lee SH, Heo YS. Molecular interactions of antibody drugs targeting PD-

1, PD-L1, and CTLA-4 in immuno-oncology. Molecules. 2019;24(6).

135. Borcoman E, Nandikolla A, Long G, Goel S, Le Tourneau C. Patterns of Response and Progression to Immunotherapy. Am Soc Clin Oncol Educ B. 2018;38(38):169-178.
136. Rieth J, Subramanian S. Mechanisms of intrinsic tumor resistance to immunotherapy. Int J Mol Sci. 2018;19(5).
137. Patel SP, Kurzrock R. PD-L1 expression as a predictive biomarker in cancer immunotherapy. Mol Cancer Ther. 2015;14(4):847-856.
138. Haragan A, Field JK, Davies MPA, Escriu C, Gruver A, Gosney JR. Heterogeneity of PD-L1 expression in non-small cell lung cancer: Implications for specimen sampling in predicting treatment response. Lung Cancer. 2019;134:79-84.
139. Aggen DH, Drake CG. Biomarkers for immunotherapy in bladder cancer: A moving target. J Immunother Cancer. 2017;5(1).
140. Lee N, Zakka LR, Mihm MC, Schatton T. Tumour-infiltrating lymphocytes in melanoma prognosis and cancer immunotherapy. Pathology. 2016;48(2):177-187.
141. Fumet JD, Truntzer C, Yarchoan M, Ghiringhelli F. Tumour mutational burden as a biomarker for immunotherapy: Current data and emerging concepts. Eur J Cancer. 2020;131:40-50.
142. Zhao P, Li L, Jiang X, Li Q. Mismatch repair deficiency/microsatellite instability-high as a predictor for anti-PD-1/PD-L1 immunotherapy efficacy. J Hematol Oncol. 2019;12(1).
143. Kim J, Kwiatkowski D, McConkey DJ, et al. The Cancer Genome Atlas Expression Subtypes Stratify Response to Checkpoint Inhibition in Advanced Urothelial Cancer and Identify a Subset of Patients with High Survival Probability. Eur Urol. 2019;75(6):961-964.
144. Kamoun A, de Reyniès A, Allory Y, et al. A Consensus Molecular Classification of Muscle-invasive Bladder Cancer[Formula presented]. Eur Urol. 2020;77(4):420-433.
145. Goodman AM, Kato S, Bazhenova L, et al. Tumor mutational burden as an independent predictor of response to immunotherapy in diverse cancers. Mol Cancer Ther. 2017;16(11):2598-2608.
146. Qin Y, Bollin K, De MacEdo MP, et al. Immune profiling of uveal melanoma identifies a potential signature associated with response to immunotherapy. J Immunother Cancer. 2020;8(2).
147. Wargo JA, Reddy SM, Reuben A, Sharma P. Monitoring immune responses in the tumor microenvironment. Curr Opin Immunol. 2016;41:23-31.

148. House IG, Savas P, Lai J, et al. Macrophage-derived CXCL9 and CXCL10 are required for antitumor immune responses following immune checkpoint blockade. Clin Cancer Res. 2020;26(2):487-504.
149. Ali MA, Matboli M, Tarek M, et al. Epigenetic regulation of immune checkpoints: Another target for cancer immunotherapy? Immunotherapy. 2017;9(1):99-108.
150. Wrangle J, Wang W, Koch A, et al. Alterations of immune response of non-small cell lung cancer with Azacytidine. Oncotarget. 2013;4(11):2067-2079.
151. Yang H, Bueso-Ramos C, Dinardo C, et al. Expression of PD-L1, PD-L2, PD-1 and CTLA4 in myelodysplastic syndromes is enhanced by treatment with hypomethylating agents. Leukemia. 2014;28(6):1280-1288.
152. Chen X, Pan X, Zhang W, et al. Epigenetic strategies synergize with PD-L1/PD-1 targeted cancer immunotherapies to enhance antitumor responses. Acta Pharm Sin B. 2020;10(5):723-733.
153. Duruisseaux M, Martínez-Cardús A, Calleja-Cervantes ME, et al. Epigenetic prediction of response to anti-PD-1 treatment in non-small-cell lung cancer: a multicentre, retrospective analysis. Lancet Respir Med. 2018;6(10):771-781.
154. Guerreiro IM, Barros-Silva D, Lopes P, et al. RAD51Bme Levels as a Potential Predictive Biomarker for PD-1 Blockade Response in Non-Small Cell Lung Cancer. J Clin Med. 2020;9(4):1000.
155. Kandimalla R, van Tilborg AA, Zwarthoff EC. DNA methylation-based biomarkers in bladder cancer. Nat Rev Urol. 2013;10(6):327-335.
156. Wang X, Chen E, Yang X, et al. 5-azacytidine inhibits the proliferation of bladder cancer cells via reversal of the aberrant hypermethylation of the hepaCAM gene. Oncol Rep. 2016;35(3):1375-1384.
157. Erdmann A, Halby L, Fahy J, Arimondo PB. Targeting DNA methylation with small molecules: what's next? J Med Chem. 2015;58(6):2569-2583.
158. Marques-Magalhães Â, Graça I, Henrique R, Jerónimo C. Targeting DNA Methyltranferases in Urological Tumors. Front Pharmacol. 2018;9:366.
159. Pasculli B, Barbano R, Parrella P. Epigenetics of breast cancer: Biology and clinical implication in the era of precision medicine. Semin Cancer Biol. 2018;51:22-35.
160. Bohl SR, Bullinger L, Rücker FG. Epigenetic therapy: azacytidine and decitabine in acute myeloid leukemia. Expert Rev Hematol. 2018;11(5):361-371.
161. Stresemann C, Lyko F. Modes of action of the DNA methyltransferase inhibitors azacytidine and decitabine. Int J Cancer. 2008;123(1):8-13.
162. Santi D V, Norment A, Garrett CE. Covalent bond formation between a DNA-cytosine methyltransferase and DNA containing 5-azacytosine. Proc Natl Acad

Sci U S A. 1984;81(22):6993-6997.
163. Chen L, MacMillan AM, Chang W, Ezaz-Nikpay K, Lane WS, Verdine GL. Direct identification of the active-site nucleophile in a DNA (cytosine-5)-methyltransferase. Biochemistry. 1991;30(46):11018-11025.
164. Liu X, Dai X, Wu B. Study of 5-Aza-CdR on transcription regulation of RASSF1A gene in the BIU87 cell line. Urol Int. 2009;82(1):108-112.
165. Nguyen AN, Hollenbach PW, Richard N, et al. Azacitidine and decitabine have different mechanisms of action in non-small cell lung cancer cell lines. Lung Cancer. 2010;1:119-140.
166. Gros C, Fahy J, Halby L, et al. DNA methylation inhibitors in cancer: recent and future approaches. Biochimie. 2012;94(11):2280-2296.
167. Zhao Q, Fan J, Hong W, Li L, Wu M. Inhibition of cancer cell proliferation by 5-fluoro-2'-deoxycytidine, a DNA methylation inhibitor, through activation of DNA damage response pathway. Springerplus. 2012;1(1):65.
168. Balboni B, El Hassouni B, Honeywell RJ, et al. RX-3117 (fluorocyclopentenyl cytosine): a novel specific antimetabolite for selective cancer treatment. Expert Opin Investig Drugs. 2019;28(4):311-322.
169. Yoo CB, Cheng JC, Jones PA. Zebularine: a new drug for epigenetic therapy. Biochem Soc Trans. 2004;32(Pt 6):910-912.
170. Takemura Y, Satoh M, Hatanaka K, Kubota S. Zebularine exerts its antiproliferative activity through S phase delay and cell death in human malignant mesothelioma cells. Biosci Biotechnol Biochem. 2018;82(7):1159-1164.
171. Cheng JC, Yoo CB, Weisenberger DJ, et al. Preferential response of cancer cells to zebularine. Cancer Cell. 2004;6(2):151-158.
172. Raynal NJM, Issa JPJ. DNA methyltransferase inhibitors. In: *Drug Discovery in Cancer Epigenetics*. Elsevier; 2015:169-190.
173. Johnson WD, Harder JB, Naylor J, et al. A pharmacokinetic/pharmacodynamic approach to evaluating the safety of zebularine in non-human primates. Cancer Res. 2006;66(8 Supplement).
174. Ganesan A, Arimondo PB, Rots MG, Jeronimo C, Berdasco M. The timeline of epigenetic drug discovery: from reality to dreams. Clin Epigenetics. 2019;11(1):174.
175. Albany C, Fazal Z, Singh R, et al. A phase 1 study of combined guadecitabine and cisplatin in platinum refractory germ cell cancer. Cancer Med. 2021;10(1):156-163.
176. Castillo-Aguilera O, Depreux P, Halby L, Arimondo PB, Goossens L. DNA Methylation Targeting: The DNMT/HMT Crosstalk Challenge. Biomolecules.

2017;7(1).
177. Pushpakom S, Iorio F, Eyers PA, et al. Drug repurposing: progress, challenges and recommendations. Nat Rev Drug Discov. 2019;18(1):41-58.
178. Fang MZ, Wang Y, Ai N, et al. Tea polyphenol (-)-epigallocatechin-3-gallate inhibits DNA methyltransferase and reactivates methylation-silenced genes in cancer cell lines. Cancer Res. 2003;63(22):7563-7570.
179. Nandakumar V, Vaid M, Katiyar SK. (-)-Epigallocatechin-3-gallate reactivates silenced tumor suppressor genes, Cip1/p21 and p16INK4a, by reducing DNA methylation and increasing histones acetylation in human skin cancer cells. Carcinogenesis. 2011;32(4):537-544.
180. Link A, Balaguer F, Shen Y, et al. Curcumin modulates DNA methylation in colorectal cancer cells. PLoS One. 2013;8(2):e57709.
181. Pechalrieu D, Dauzonne D, Arimondo PB, Lopez M. Synthesis of novel 3-halo-3-nitroflavanones and their activities as DNA methyltransferase inhibitors in cancer cells. Eur J Med Chem. 2020;186.
182. Lobo J, Cardoso AR, Miranda-Gonçalves V, et al. Targeting germ cell tumors with the newly synthesized flavanone-derived compound mlo1302 efficiently reduces tumor cell viability and induces apoptosis and cell cycle arrest. Pharmaceutics. 2021;13(1):1-18.
183. Rondelet G, Fleury L, Faux C, et al. Inhibition studies of DNA methyltransferases by maleimide derivatives of RG108 as non-nucleoside inhibitors. Futur Med Chem. 2017;9(13):1465-1481.
184. Ou Y, Zhang Q, Tang Y, et al. DNA methylation enzyme inhibitor RG108 suppresses the radioresistance of esophageal cancer. Oncol Rep. 2018;39(3):993-1002.
185. Yoo J, Choi S, Medina-Franco JL. Molecular modeling studies of the novel inhibitors of DNA methyltransferases SGI-1027 and CBC12: implications for the mechanism of inhibition of DNMTs. PLoS One. 2013;8(4):e62152.
186. She S, Zhao Y, Kang B, et al. Combined inhibition of JAK1/2 and DNMT1 by newly identified small-molecule compounds synergistically suppresses the survival and proliferation of cervical cancer cells. Cell Death Dis. 2020;11(9).
187. Amato RJ. Inhibition of DNA methylation by antisense oligonucleotide MG98 as cancer therapy. Clin Genitourin Cancer. 2007;5(7):422-426.
188. Villar-Garea A, Fraga MF, Espada J, Esteller M. Procaine is a DNA-demethylating agent with growth-inhibitory effects in human cancer cells. Cancer Res. 2003;63(16):4984-4989.
189. Li YC, Wang Y, Li DD, Zhang Y, Zhao TC, Li CF. Procaine is a specific DNA

methylation inhibitor with anti-tumor effect for human gastric cancer. J Cell Biochem. 2018;119(2):2440-2449.

190. Dueñas-Gonzalez A, Coronel J, Cetina L, González-Fierro A, Chavez-Blanco A, Taja-Chayeb L. Hydralazine-valproate: a repositioned drug combination for the epigenetic therapy of cancer. Expert Opin Drug Metab Toxicol. 2014;10(10):1433-1444.
191. Segura-Pacheco B, Trejo-Becerril C, Perez-Cardenas E, et al. Reactivation of tumor suppressor genes by the cardiovascular drugs hydralazine and procainamide and their potential use in cancer therapy. Clin Cancer Res. 2003;9(5):1596-1603.
192. Kuck D, Caulfield T, Lyko F, Medina-Franco JL. Nanaomycin A selectively inhibits DNMT3B and reactivates silenced tumor suppressor genes in human cancer cells. Mol Cancer Ther. 2010;9(11):3015-3023.
193. Giannopoulou AF, Velentzas AD, Konstantakou EG, et al. Revisiting histone deacetylases in human tumorigenesis: The paradigm of urothelial bladder cancer. Int J Mol Sci. 2019;20(6).
194. Siegel D, Hussein M, Belani C, et al. Vorinostat in solid and hematologic malignancies. J Hematol Oncol. 2009;2.
195. Finnin MS, Donigian JR, Cohen A, et al. Structures of a histone deacetylase homologue bound to the TSA and SAHA inhibitors. Nature. 1999;401(6749):188-193.
196. Tang D, Yao R, Zhao D, et al. Trichostatin A reverses the chemoresistance of lung cancer with high IGFBP2 expression through enhancing autophagy. Sci Rep. 2018;8(1).
197. Yee AJ, Raje NS. Panobinostat and Multiple Myeloma in 2018. Oncologist. 2018;23(5):516-517.
198. Lobo J, Guimarães-Teixeira C, Barros-Silva D, et al. Efficacy of HDAC Inhibitors Belinostat and Panobinostat against Cisplatin-Sensitive and Cisplatin-Resistant Testicular Germ Cell Tumors. Cancers (Basel). 2020;12(10):2903.
199. Vandermolen KM, McCulloch W, Pearce CJ, Oberlies NH. Romidepsin (Istodax, NSC 630176, FR901228, FK228, depsipeptide): A natural product recently approved for cutaneous T-cell lymphoma. J Antibiot (Tokyo). 2011;64(8):525-531.
200. Pattarawat P, Wallace S, Pfisterer B, Odoi A, Wang HCR. Formulation of a triple combination gemcitabine plus romidepsin + cisplatin regimen to efficaciously and safely control triple-negative breast cancer tumor development. Cancer Chemother Pharmacol. 2020;85(1):141-152.
201. Wang W, Fang D, Zhang H, et al. Sodium butyrate selectively kills cancer cells

and inhibits migration in colorectal cancer by targeting thioredoxin-1. Onco Targets Ther. 2020;13:4691-4704.

202. Iannelli F, Zotti AI, Roca MS, et al. Valproic Acid Synergizes With Cisplatin and Cetuximab in vitro and in vivo in Head and Neck Cancer by Targeting the Mechanisms of Resistance. Front Cell Dev Biol. 2020;8.
203. Bray F, Ferlay J, Soerjomataram I, Siegel RL, Torre LA, Jemal A. Global cancer statistics 2018: GLOBOCAN estimates of incidence and mortality worldwide for 36 cancers in 185 countries. CA Cancer J Clin. 2018;68(6):394-424.
204. Kamat AM, Hahn NM, Efstathiou JA, et al. Bladder cancer. Lancet. 2016;388(10061):2796-2810.
205. Chen Z, Ding W, Xu K, et al. The 1973 WHO Classification is more suitable than the 2004 WHO Classification for predicting prognosis in non-muscle-invasive bladder cancer. PLoS One. 2012;7(10):e47199.
206. Humphrey PA, Moch H, Cubilla AL, Ulbright TM, Reuter VE. The 2016 WHO classification of tumours of the urinary system and male genital organs—part B: prostate and bladder tumours. Eur Urol. 2016;70(1):106-119.
207. Woldu SL, Şanli Ö, Lotan Y. Tackling non-muscle invasive bladder cancer in the clinic. Expert Rev Anticancer Ther. 2017;17(5):467-480.
208. Amin MB, Edge S, Greene F, et al. *AJCC Cancer Staging Manual* . Eighth edi. Springer International Publishing: American Joint Commission on Cancer; 2017.
209. Bellmunt J, Orsola A, Leow JJ, Wiegel T, De Santis M, Horwich A. Bladder cancer: ESMO Practice Guidelines for diagnosis, treatment and follow-up. Ann Oncol. 2014;25 Suppl 3:iii40-8.
210. Lobo J, Jerónimo C, Henrique R. Targeting the immune system and epigenetic landscape of urological tumors. Int J Mol Sci. 2020;21(3).
211. Herr HW, Morales A. History of Bacillus Calmette-Guerin and Bladder Cancer: An Immunotherapy Success Story. J Urol. 2008;179(1):53-56.
212. Zhang C, Berndt-Paetz M, Neuhaus J. Identification of key biomarkers in bladder cancer: Evidence from a bioinformatics analysis. Diagnostics. 2020;10(2).
213. Agundez M, Grau L, Palou J, Algaba F, Villavicencio H, Sanchez-Carbayo M. Evaluation of the methylation status of tumour suppressor genes for predicting bacillus Calmette-Guérin response in patients with T1G3 high-risk bladder tumours. Eur Urol. 2011;60(1):131-140.
214. Alvarez-Múgica M, Fernández-Gómez JM, Cebrian V, Fresno F, Escaf S, Sánchez-Carbayo M. Polyamine-modulated factor-1 methylation predicts bacillus Calmette-Guérin response in patients with high-grade non-muscle-invasive bladder carcinoma. Eur Urol. 2013;63(2):364-370.

215. Ahlén Bergman E, Hartana CA, Johansson M, et al. Increased CD4 + T cell lineage commitment determined by CpG methylation correlates with better prognosis in urinary bladder cancer patients. Clin Epigenetics. 2018;10(1).
216. Hartana CA, Ahlén Bergman E, Broomé A, et al. Tissue-resident memory T cells are epigenetically cytotoxic with signs of exhaustion in human urinary bladder cancer. Clin Exp Immunol. 2018;194(1):39-53.
217. Koestler DC, Usset J, Christensen BC, et al. DNA methylation-derived neutrophil-tolymphocyte ratio: An epigenetic tool to explore cancer inflammation and outcomes. Cancer Epidemiol Biomarkers Prev. 2017;26(3):328-338.
218. Nunes SP, Henrique R, Jerónimo C, Paramio JM. DNA Methylation as a Therapeutic Target for Bladder Cancer. Cells. 2020;9(8).
219. Maraver A, Fernandez-Marcos PJ, Cash TP, et al. NOTCH pathway inactivation promotes bladder cancer progression. J Clin Invest. 2015;125(2):824-830.
220. Rampias T, Vgenopoulou P, Avgeris M, et al. A new tumor suppressor role for the Notch pathway in bladder cancer. Nat Med. 2014;20(10):1199-1205.
221. Ramakrishnan S, Hu Q, Krishnan N, et al. Decitabine, a DNA-demethylating agent, promotes differentiation via NOTCH1 signaling and alters immune-related pathways in muscle-invasive bladder cancer. Cell Death Dis. 2017;8(12).
222. Segovia C, San José-Enériz E, Munera-Maravilla E, et al. Inhibition of a G9a/DNMT network triggers immune-mediated bladder cancer regression. Nat Med. 2019;25(7):1073-1081.

## Supplementary Information

**Table S1.** Main studies comprising epigenetic drugs and biomarkers associated with immunotherapy.

| Study | Major findings | Reference |
|---|---|---|
| Wrangle et al. (2013) | AZA upregulates genes and pathways related to both innate and adaptive immunity and genes related to immune evasion in a several non-small cell lung cancer lines. | (1) |
| Yang et al. (2014) | In a cohort of patients treated with epigenetic therapy, PD-L1, PD-L2, PD-1 and CTLA4 expression was upregulated. Exposure to decitabine resulted in partial demethylation of PD-1 in leukemia cell lines and human samples | (2) |
| Kim et al. (2014) | Entinostat reduces the MDSC population and the combination of entinostat with PD-1 and CTLA-4 antibodies resulted in an elimination of approximately 80% of the tumor, whereas the use of immune checkpoint inhibitors against PD-1 and CTLA-4 alone did not provide an anti-tumor immune response. | (3) |
| Zingg et al. (2017) | Targeting Ezh2 in melanoma cells reverts loss of immunogenicity and antigen presentation, and synergizes with anti-CTLA-4 and IL-2 immunotherapies | (4) |
| Orillion et al. (2017) | Entinostat increases the antitumor effect of PD-1 targeting by functional inhibition of immunosuppressive MDSCs, which helps the TME to become more receptive to the development of an effective anti-tumor response | (5) |
| Briere et al. (2018) | The class I/IV HDAC inhibitor mocetinostat increases tumor antigen presentation, decreases immune suppressive cell types and augments checkpoint inhibitor therapy with PD-L1 antibody. | (6) |
| Goswami et al. (2018) | Targeting EZH2 expression in T cells (CPI-1205) can improve anti-tumor immune responses provided by immune checkpoint inhibitor CTLA-4 (Ipilimumab). | (7) |
| Duruisseaux et al. (2018) | The methylation status of FOXP1 could be associated with validated predictive biomarkers such as PD-L1 staining and mutational load to better select patients who will experience clinical benefit with PD-1 blockade. | (8) |
| Segovia et al. (2019) | The antitumor effect was significantly improved when CM-272 was combined with anti-programmed cell death ligand 1. These effects were associated with an endogenous antitumor immune response and immunogenic cell death with the conversion of a cold immune tumor into a hot one. | (9) |
| Guerreiro et al. (2020) | RAD51Bme levels might be combined with validated predictive biomarker PD-L1 immunostaining to select patients who will most likely experience clinical benefit from PD-1 blockade | (10) |
| Lai et al. (2021) | Zebularine promoted infiltration of CD8 T cells and natural killer (NK) cells into tumor, decreasing tumor growth. Furthermore, zebularine sensitized the cGAS-STING pathway to promote anti-tumor immunity. | (11) |

**References**


1. Wrangle J, Wang W, Koch A, et al. Alterations of immune response of non-small cell lung cancer with Azacytidine. Oncotarget. 2013;4(11):2067-2079.
2. Yang H, Bueso-Ramos C, Dinardo C, et al. Expression of PD-L1, PD-L2, PD-1 and CTLA4 in myelodysplastic syndromes is enhanced by treatment with hypomethylating agents. Leukemia. 2014;28(6):1280-1288.
3. Kim K, Skora AD, Li Z, et al. Eradication of metastatic mouse cancers resistant to immune checkpoint blockade by suppression of myeloid-derived cells. Proc Natl Acad Sci U S A. 2014;111(32):11774-11779.
4. Zingg D, Arenas-Ramirez N, Sahin D, et al. The Histone Methyltransferase Ezh2 Controls Mechanisms of Adaptive Resistance to Tumor Immunotherapy. Cell Rep. 2017;20(4):854-867.
5. Orillion A, Hashimoto A, Damayanti N, et al. Entinostat neutralizes myeloid-derived suppressor cells and enhances the antitumor effect of PD-1 inhibition in murine models of lung and renal cell carcinoma. Clin Cancer Res. 2017;23(17):5187-5201.
6. Briere D, Sudhakar N, Woods DM, et al. The class I/IV HDAC inhibitor mocetinostat increases tumor antigen presentation, decreases immune suppressive cell types and augments checkpoint inhibitor therapy. Cancer Immunol Immunother. 2018;67(3):381-392.
7. Goswami S, Apostolou I, Zhang J, et al. Modulation of EZH2 expression in T cells improves efficacy of anti-CTLA-4 therapy. J Clin Invest. 2018;128(9):3813-3818.
8. Duruisseaux M, Martínez-Cardús A, Calleja-Cervantes ME, et al. Epigenetic prediction of response to anti-PD-1 treatment in non-small-cell lung cancer: a multicentre, retrospective analysis. Lancet Respir Med. 2018;6(10):771-781.
9. Segovia C, San José-Enériz E, Munera-Maravilla E, et al. Inhibition of a G9a/DNMT network triggers immune-mediated bladder cancer regression. Nat Med. 2019;25(7):1073-1081.
10. Guerreiro IM, Barros-Silva D, Lopes P, et al. RAD51Bme Levels as a Potential Predictive Biomarker for PD-1 Blockade Response in Non-Small Cell Lung Cancer. J Clin Med. 2020;9(4):1000.
11. Lai J, Fu Y, Tian S, et al. Zebularine elevates STING expression and enhances cGAMP cancer immunotherapy in mice. Mol Ther. 2021;0(0).

# *CHAPTER II*

# AIMS

Aberrant epigenetic alterations contribute to BC development, influencing the immune landscape of bladder tumors. These alterations constitute attractive therapeutic targets for BC management and potential predictive markers for immunotherapy response in BC. Given the rather limited knowledge of the interplay between epigenetic and immune mechanisms in advanced BC, this Thesis sought to investigate a combination treatment approach using ICI and selected epigenetic inhibitors in advanced BC using both *in vitro* and *in vivo* mouse models. Moreover, we aimed to uncover specific epigenetic signatures that could act as predictive markers for immunotherapy response in patient samples.

The specific goals of this Thesis are:

1. Establish a combination therapy with anti-PD-L1 antibody and a selected epigenetic inhibitor for HDACs, CM-1758, in an advanced BC mouse model.
2. Explore the effects of CM-1758 on the tumor immune landscape of BC.
3. Uncover the mechanisms that drive the prolonged anti-tumor effects observed when CM-272 is combined with anti-PD-L1 in an advanced BC mouse model.
4. Evaluate the potential of DNA methylation to identify the BC patients that would most likely benefit from ICI-based therapies.

The Results section of this Thesis is divided in two different chapters tackling these goals – **Chapter III** and **Chapter IV**, each one containing research papers related to the theme of the chapter. Each research paper is presented with classic structure of an original scientific paper, consisting of an introduction, material and methods, results, discussion, and conclusions. Specifically, **Chapter III** entitled “Improving bladder cancer treatment: Epidrugs and immunotherapy” includes both **Research paper 1** and **Research paper 2**. In this chapter, the combination between epidrugs and ICI are explored as therapeutic options for BC. Additionally, the TME is characterized to understand the impact of epigenetics on the TME and, particularly, on the tumors’ immune landscape. **Research paper 1** focuses on Goals 1 and 2, exploring the effects of CM-1758, an HDACs inhibitor, in combination with ICI in *in vitro* and *in vivo* models of BC. Furthermore, **Research paper 2** tackles Goal 3, where the mechanisms behind an enhanced immune response after treatment combining CM-272, a G9a and DNMT1 inhibitor, with ICI are investigated. **Chapter IV** is entitled “Epimarkers of response to immunotherapy” and contains **Research paper 3**. The major goal of this work was to understand the potential of DNA methylation as a predictive biomarker of response to ICI in BC, using tumors from BC patients treated to immunotherapy (Goal 4).

*CHAPTER III*

# IMPROVING BLADDER CANCER TREATMENT: EPIDRUGS AND IMMUNOTHERAPY

## Modulation of tumor microenvironment by targeting histone acetylation in bladder cancer

*Research paper 1*

**Sandra P. Nunes**, Lucia Morales, Carolina Rubio, Ester Munera-Maravilla, Iris Lodewijk, Cristian Suárez-Cabrera, Victor G. Martínez, Mercedes Pérez-Escavy, Miriam Pérez-Crespo, Miguel Alonso Sánchez, Esther Montesinos, Edurne San José-Enériz, Xabier Agirre, Felipe Prósper, Antonio Pineda-Lucena, Rui Henrique, Marta Dueñas, Margareta P. Correia, Carmen Jerónimo and Jesús M. Paramio

**DOI:** https://doi.org/10.1038/s41420-023-01786-3

Published: 4 of January 2024

**Cell Death Discovery**, 10, 1.

Author personal contribution:

Technical execution of the work, analysis and interpretation of the results, and manuscript preparation.

**Abstract**

Alterations in the epigenetic machinery in both tumor and immune cells contribute to bladder cancer (BC) development, constituting a promising target as an alternative therapeutic option. Here, we have explored the effects of a novel histone deacetylase (HDAC) inhibitor CM-1758, alone or in combination with immune checkpoint inhibitors (ICI) in BC. We determined the antitumor effects of CM-1758 in various BC cell lines together with the induction of broad transcriptional changes, with focus on the epigenetic regulation of PD-L1. Using an immunocompetent syngeneic mouse model of metastatic BC, we studied the effects of CM-1758 alone or in combination with anti-PD-L1 not only on tumor cells, but also in the tumor microenvironment.

*In vitro*, we found that CM-1758 has cytotoxic and cytostatic effects either by inducing apoptosis or cell cycle arrest in BC cells at low micromolar levels. PD-L1 is epigenetically regulated by histone acetylation marks and is induced after treatment with CM-1758. We also observed that treatment with CM-1758 led to an important delay in tumor growth and a higher CD8+ T cell tumor infiltration. Moreover, anti-PD-L1 alone or in combination with CM-1758 reprogramed macrophage differentiation towards a M1-like polarization state and increased of pro-inflammatory cytokines systemically, yielding potential further antitumor effects. Our results suggest the possibility of combining HDAC inhibitors with immunotherapies for the management of advanced metastatic BC.

**Keywords**

Bladder cancer, epigenetics, tumor microenvironment, histone acetylation, immunotherapy, immune checkpoint inhibitors, PD-L1.

## Introduction

Bladder cancer (BC) is the tenth most common cancer diagnosed worldwide, listing as the sixth most incident cancer in men (1). About 75% of the patients are diagnosed with non-muscle invasive BC (NMIBC), whereas the remaining 25% display muscle invasive BC (MIBC) (2). Although NMIBC patients are associated with a good outcome, up to 70% of patients recur, with a significant percentage progressing to MIBC (3). The treatment of MIBC comprises radical cystectomy and platin-based chemotherapy in a neoadjuvant or adjuvant setting (4). Nevertheless, MIBC patients considered to be unfit for chemotherapy or surgery, presenting comorbidities or metastatic disease have few therapeutic options available. The implementation of immune checkpoint inhibitors (ICI), such as anti-programmed death-ligand 1 (PD-L1), as an option for patients positive for PD-L1 expression led to an increase of overall survival (5). However, the percentage of patients with significant clinical response ranges between 17 and 26%, which is quite limited (6). Thus, understanding the mechanisms behind BC development can unravel new therapeutic targets and strategies, with the main goal of improving patients' survival.

Epigenetic landscape reprograming is one of the main mechanisms contributing to BC progression and is considered an emergent hallmark of cancer (7). Histone acetylation is of the most prominent mechanisms involved in gene expression regulation favoring tumorigenesis (8). Accordingly, histone acetylation is involved in transcriptional activation, through addition of acetyl groups in lysine residues of histone tails by histone acetyltransferases (HATs). Histone deacetylases (HDACs), by removing acetylation marks, lead to transcriptional repression by turning DNA into a closed-chromatin state (9).

Since epigenetic marks represent an enticing target for cancer therapeutics, a group of drugs has been developed throughout the years targeting several epigenetic enzymes, called epigenetic modulating drugs or epidrugs (10). The most well-known HDAC inhibitors (HDACi) comprise hydroxamic acids, including belinostat, vorinostat and panobinostat, all pan-HDACi FDA-approved for several haematological cancers (11). HDACi also display antitumoral effects in BC cells (12, 13).

Most studies comprising epidrugs focus on the effects on cancer cells, yet the tumor microenvironment cells can also be affected since they are also epigenetically regulated. HDACi have been previously shown to modulate tumor microenvironment and improve response to ICI in BC and other cancer types (14-16). Specifically, the combination of entinostat, a selective HDAC1/3 inhibitor, and anti-PD-1 therapy led to complete responses in an immunocompetent mouse model of BC (16). Having into

account the pre-clinical evidence, several clinical trials are being carried out to evaluate the efficacy of the combination of epidrugs and ICI in various solid tumors including BC (17). Nevertheless, HDACi were shown to have low bioavailability, limited half-life and dose-limiting toxicity, hampering their use in clinical practice for cancer treatment (18). Thus, the search for new epidrugs with more specific epigenetic targets at low therapeutic doses would fast-track their usage in clinical practice.

Here, we describe the antitumor efficacy of CM-1758, a novel HDAC inhibitor, in BC *in vitro* and *in vivo* models. First, the cytotoxic/cytostatic effects of CM-1758 were evaluated in several BC cell lines. Then, the effects on immune-related pathways were also studied, namely by assessing PD-L1 expression and its epigenetic regulation. Since CM-1758 up-regulated PD-L1, we postulated that combining CM-1758 and PD-L1 blockage could be a promising strategy for BC treatment. For that, an immunocompetent syngeneic mouse model of aggressive BC was used to assess CM-1758 effects *in vivo* alone or in combination with anti-PD-L1. The effects of CM-1758 were evaluated not only in tumor cells, but also in the tumor microenvironment comprising immune and non-immune cells and cytokine profile. CM-1758 displayed significant antitumor effects *in vitro* and *in vivo* concomitantly with tumor microenvironment remodeling.

## Materials and Methods

### *Cell culture*

American type culture collection (ATCC) human BC cell lines 253J, 5637, J82, RT112 and TCCSUP, including several tumor stages and BC subtypes (19) acquired in 2008, were selected for the purpose of this study. Cells lines were authenticated by short tandem repeat analysis (Unidad de Genómica, CIMA Lab Diagnostics) and routinely checked for the presence of mycoplasma using Venor®GeM One Step (Minerva Biolabs, Berlin, Germany). Additionally, a previously established mouse bladder tumor cell line 4K5 (*Pten* $^{-/-}$; *Trp53* $^{-/-}$; Adeno-Krt5-Cre) expressing GFP was also included in the study. 253J, J82, RT112 and 4K5 cells were maintained in DMEM GlutaMAX™ medium (Thermo Fisher Scientific, Waltham, Massachusetts, USA), whereas TCCSUP cells were grown in EMEM medium (Lonza, Basel, Switzerland) and 5637 cells were maintained in RPMI 1640 medium (Thermo Fisher Scientific), all supplemented with 10% fetal bovine serum (FBS) and 1% of Antibiotic Antimycotic solution (Thermo Fisher Scientific), at 5% CO2 and 37°C in a humidifying chamber.

*Cell treatment with CM-1758 and $IC_{50}$ calculation*

CM-1758 (HDACs inhibitor) was stored in DMSO (Sigma Aldrich, Burlington, Massachusetts, USA) at the concentration of 100 mM at -20°C. The chemical structure was described previously [Compound 13e (18)]. The half maximal inhibitory concentration ($IC_{50}$) of CM-1758 was calculated for all cell lines. Cells were plated in 96-well plates at different densities according to cell line and, after 24 h, cells were treated with concentrations of CM-1758 ranging from 0.01 to 10 µM in complete medium, and left in culture for 48 h. Two controls were added per plate, including one with complete medium and another containing 0.01% of DMSO. Cell Proliferation Kit II XTT (Roche, Basel, Switzerland) was then used according to the manufacturer's instructions. Absorbance was measured at 490 nm using a Genios Pro microplate reader (Tecan, Männedorf, Switzerland). At least four experimental replicates were used for $IC_{50}$ calculation.

*Cell cycle analysis*

All cell lines were seeded in 6-well plates and treated with CM-1758 for 48 h with the $IC_{50}$ concentration calculated for each cell line, or with DMSO control. After that, cells were trypsinized (Trypsin-EDTA Solution, Sigma-Aldrich), collected and counted. Cells from control and treated conditions were collected for cell cycle analysis. Next, cells were washed with PBS and fixed with ethanol 70% for 1.5 h at 4°C. Cells were treated with RNAse and incubated at 37°C for 20 min with shaking. Finally, propidium iodide (Sigma Aldrich) at 50 µL/mL was added and incubated for 15 min in the dark. Cell cycle was analyzed in a LSR Fortessa cell analyzer (Becton Dickinson (BD) Biosciences, Franklin Lakes, New Jersey USA). Results were analyzed using FlowJo™ v10.8.1 (BD Biosciences). Five experimental replicates were used for data analysis.

*PD-L1 expression and Apoptosis assay by flow cytometry*

Cells were seeded in 6-well plates and treated with CM-1758 at $IC_{50}$ concentration for 48 h, or DMSO as a control, for evaluation of PD-L1 expression and apoptosis. Cells were trypsinized, collected and washed with PBS. Then, cells were incubated with 1 µL of human or mouse FcR blocking reagent (Miltenyi Biotec, Bergisch Gladbach, Germany) for 10 min at room temperature (RT). Samples were stained with human anti-PD-L1 (clone MIH3; Biolegend, San Diego, California, USA) or mouse anti-PD-L1 antibody (clone MIH5; BD Biosciences) for 30 min at 4ºC in the dark. After washing, cells were incubated with a mix of Annexin Binding Buffer 1x (BD Biosciences), DAPI (Roche) and 2 µL of PE Annexin V (Ref 556421, BD Biosciences) for mouse, and FITC Annexin V (Ref 556419, BD Biosciences) for human cell lines, for 15 min in the dark at RT. Cells

were acquired in a BD LSR Fortessa cell analyzer, and data analysis was performed using FlowJo™ v10.8.1 (BD Biosciences). For apoptosis, live cells were identified as AnnexinV-DAPI-, early apoptotic as AnnexinV+DAPI-, late apoptotic as AnnexinV+DAPI+ and necrotic by Annexin-DAPI+. PD-L1 expression was analyzed only in live cells (DAPI-). Single stained and fluorescence minus one (FMO) controls were included.

*RNA extraction and RNA-sequencing sample preparation*

Total RNA was extracted using the miRNAeasy Mini kit (Qiagen, Hilden, Germany), according to the manufacturer's instructions. RNA concentration was measured on a Qubit 4 Fluorometer (Thermo Fisher Scientific), using a Qubit RNA broad range assay kit (Thermo Fisher Scientific) and stored at -80ºC. RNA integrity number (RIN) was measured using the Qubit RNA IQ assay kit (Thermo Fisher Scientific) and samples with values higher than 8 were considered for RNA sequencing (RNAseq) analysis. One µg of total RNA was sent for RNAseq analysis by Macrogen RNA-seq services (Seoul, South Korea) using the Truseq stranded total RNA Library with Ribo-Zero Gold (Illumina, San Diego, California, USA) and the NovaSeq 6000 (Illumina) of two independent biological replicates for each condition (control and treated with CM-1758) of 253J, J82, RT112 and TCCSUP.

*Real-time quantitative PCR (RT-qPCR)*

One µg of RNA was used to synthetize cDNA using the High Capacity cDNA Reverse Transcription kit (Applied Biosystems™, Waltham, Massachusetts, USA) according to the manufacturer's recommendations. Four µL of diluted 20x cDNA, 5 µL of GoTaq PCR Master Mix (Promega, Madison, Wisconsin, USA) and primers (Supplementary Table S1) at 0.5 µM were used per well. The RT-qPCR reactions were run in a QuantStudio™ 6 Flex Real-Time PCR (Thermo Fisher Scientific), along with the melting curves. *TBP* for mouse and human was used as housekeeping gene to normalize the results, and the relative expression for each transcript was calculated using the $2^{-\Delta\Delta Ct}$, as previously described (20). Primers sequences can be found in Supplementary Table S1.

*CUT&RUN*

Cleavage under targets & release using nuclease (CUT&RUN) was performed using the CUT&RUN assay kit (Cell Signaling Technology, Danvers, Massachusetts, USA), according to the manufacturer's instructions. Briefly, 100 000 of J82 cells treated with the $IC_{50}$ dose of CM-1758, or DMSO 0.01% as control, were collected, washed, and

incubated with 10 µL of concavalin A beads. Then, bead-bound cells were incubated with the primary antibodies for H3K9ac (dilution 1:50, #9649, Cell Signaling Technology), H3K27ac (dilution 1:100, #8173, Cell Signaling Technology), H3K4me3 for positive control (dilution 1:50, #9751, Cell Signaling Technology), or Rabbit IgG Isotype Control (dilution 1:50, #66362, Cell Signaling Technology), overnight at 4ºC with rotation. After a wash, the cell-bead mixture was incubated with pAG-MNase at 4ºC for 1 h. Next, after washing with wash buffer, calcium chloride was added, and samples were incubated at 4ºC. After 30 min, stop buffer was added and DNA was purified using the QIAquick PCR Purification kit (Qiagen). For input samples preparation, cells were incubated with DNA extraction buffer (plus proteinase K and RNAse A) for 1 h at 55ºC. Then, for cell lysis, cells were sonicated, and DNA was purified. Two µL of purified DNA, 5 µL of GoTaq PCR Master Mix (Promega) and 2 µM primers for four different regions of PD-L1 promoter were used for the qPCR analysis (Supplementary Table S1; Figure 3g) in a QuantStudio™ 6 Flex Real-Time PCR (Thermo Fisher Scientific). Intronic regions were not considered for qPCR analysis. Relative fold-change was calculated with $2^{-\Delta\Delta Ct}$ using *RPL30* as a reference gene.

*Immunofluorescence*

J82 and 4K5 cells treated with the respective $IC_{50}$ doses of CM-1758 or DMSO 0.01% as a control for 48 h were fixed in 4% paraformaldehyde for 15 min at 4ºC. Then, cells were washed with PBS and permeabilized with 0.1% Triton X-100 in PBS for 10 min at RT. After another wash with PBS, fixed cells were blocked with 10% horse serum for 1 h at RT, followed by the incubation with a primary antibody against 5-methylcytosine with the 10% horse serum overnight at 4ºC (Supplementary Table S2). Next, after a wash with PBS, cells were incubated with the respective secondary antibody conjugated with fluorochromes in 10% horse serum at RT for 1 h (Supplementary Table S2). Finally, mounting medium (Mowiol, Thermo Fisher Scientific) with DAPI at 1 µL/mL, for staining nuclei, was used for mounting the slides. Images were acquired with an Olympus IX51 microscope.

*Protein and histone extraction*

Total protein and histones were extracted from cells treated with the $IC_{50}$ dose of CM-1758, or DMSO-treated cells. Cells were scrapped, collected and total protein was extracted from cell pellets by adding 1:1 of lysis buffer (Hepes 40 mM, Triton X-100 2%, NaCl 200 mM, MgCl2 40 mM, EGTA 20 mM, β- glycerophosphate 80 mM and distilled water) and a mix of proteinase and phosphatase inhibitors, and phenylmethylsulfonyl

fluoride (PMSF) at a final dilution of 200x, followed by a centrifugation at 16 100 g for 10 min at 4°C. The supernatant was collected and stored at -80°C until further use.

For histone extraction, 500 µL of hypotonic buffer (Tris-HCL pH=8.0 10 mM, KCl 1 mM, $MgCl_2$ 1.5 mM, dithiothreitol 1 mM and distilled water), proteinase and phosphatase inhibitors, and PMSF, were added to each cell pellet and incubated for 30 min at 4°C with rotation. Then, after a 10 min centrifugation at 4°C at 10 400 g, the supernatant was discarded and 400 µL of $H_2SO_4$ at 0.2 M was added to the nucleus pellet and incubated overnight at 4°C with rotation. The samples were centrifugated at 4°C for 10 min at 10 400 g and the supernatant was transferred to another tube. Next, 132 µL of trichloroacetic acid was added and incubated for 30 min on ice. After another centrifugation, the supernatant was disregarded, and the histone pellet was washed with cold acetone. Lastly, after drying, the histone pellet was eluted in water and stored at -80°C until further use. Histones and total protein samples were quantified by Qubit™ Protein Assay Kit (ThermoFisher Scientific), according to the manufacturer's recommendations, using a Qubit 4 Fluorometer (ThermoFisher Scientific).

*Western blot*

Twenty µg or 3 µg of total protein or histones, respectively, were separated in Mini-protean TGX Stain-Free gels 4-15% (Bio-Rad, Hercules, California, USA) by sodium dodecyl sulfate polyacrylamide gel electrophoresis (SDS-PAGE). Then, were transferred by using a Trans-Blot Turbo transfer system (Bio-Rad) into an immunoblot nitrocellulose membrane in a transfer buffer containing ethanol, distilled water, and Trans-Blot® TurboTM 5x Tranfer Buffer (Bio-Rad). After that, membranes were blocked with 5% milk in tris-buffer saline (TBS)/0.1% Tween (TBS-T) for 1 h at RT. Then, membranes were incubated with primary antibodies overnight at 4°C (Supplementary Table S2). Next, membranes were washed with TBS-T and incubated with a secondary antibody coupled with horseradish peroxidase (Supplementary Table S2) for 1 h at RT. Blots were visualized by chemiluminescence (Clarity WB ECL substrate, Bio-Rad) using a ChemiDoc XRS+ (Bio-Rad). Western blots were quantified using band densitometry analysis with ImageJ software (version 1.6.1., National Institute of Health). All antibodies and dilutions used are described in Supplementary Table S2.

*Animal care and maintenance*

All the animal experiments were conducted according to the European and Spanish regulations in the field: European convention ETS 123, regarding the use and protection of vertebrate mammals used in experimentation and other scientific purposes, and Directive 2010/63/UE, Spanish Law 6/2013 and Real Decreto (R.D.) 53/2013

regarding the protection and use of animals in scientific research. Procedures involving genetically modified organisms were conducted according to the proper European and Spanish Regulations: Directive 2009/41/CE, Spanish Law 9/2003, and R.D. 178/2004. The protocols were approved by "Consejería de Medio Ambiente y Ordenación del Territorio y Sostenibilidad" (protocol number PROEX 150.8/21) and all procedures were approved by CIEMAT Animal Experimentation Ethics Committee according to external and internal biosafety and bio-ethics guidelines.

Mice were housed at the CIEMAT laboratory Animal Facility (registration number ES280790000183) and routinely screened for pathogens, following the Spanish Society for the Laboratory Animal Science (SECAL) and the Federation of European Laboratory Animal Science Associations (FELASA, Tamworth, UK) recommendations. Mice were provided with food (TEKLAD Global Diet 2918) and acidified and filtered (0.2 µm) water *ad libitum*. Mice were maintained in cages type IIL, in a maximum of 5 mice per cage. Room lighting was controlled with light/dark cycles for 12/12 h, with temperature and humidity being regulated at 21±2ºC and 55±10%, respectively.

*Syngeneic graft mouse model*

Immunocompetent double knock-out mice (DKO; $Pten^{F/F}$, $Trp53^{F/F}$) were developed by our group through a conventional crossing of mice from different collaborators (Netherlands Cancer Institute, Mass. Institute of Technology, Stanford University), resulting in a mixed FVB/129S background. A syngeneic graft mouse model was generated by injecting subcutaneously cells (4K5 cell line) previously established from an aggressive mouse bladder tumor ($Pten^{-/-}$; $Trp53^{-/-}$), generated with adenoviruses expressing Cre recombinase under the control of the regulatory elements of keratin 5 (Adeno-Krt5-Cre) (21). Three million 4K5 cells were resuspended in 100 µL of DMEM and injected subcutaneously in the right flank of 3–4-month-old male and female DKO mice. Tumor growth was monitored 3 times per week using a digital caliper and tumor volume was calculated using the formula $4\pi/3 \times (\text{length}/2) \times (\text{width}/2)^2$. After tumors reached volumes between 80-90 $mm^3$, mice were randomly assigned to four groups: control (n=8), anti-PD-L1 (n=9), CM-1758 (n=9) and CM-1758+anti-PD-L1 (n=9). CM-1758 (10 mg/kg; 5 times a week) and anti-PD-L1 (avelumab; 200 µg/mouse; once a week) were injected intraperitoneally. In the combination group, a phased dosing schedule was administered (Figure 4a). Tumor sizes were normalized by subtracting the volume calculated on the treatment initiation day. After two weeks of treatment, mice were sacrificed and tumors and whole blood were collected at the time of euthanasia. For RNA extraction, tumors were embedded in RNAlater™ Stabilization solution (Thermo Fisher Scientific) at 4ºC for 24 h, and then stored at -80ºC until further use. For flow

cytometry, tumor tissue was embedded in DMEM and kept at 4ºC overnight to be processed and analyzed in the following day. Regarding histological analysis, tumors were fixed in 3.7-4% buffered formalin overnight at the time of the harvesting. Then, samples were embedded in paraffin and sections of 3-5 µm were stained for hematoxylin and eosin. Blood was collected in Microvette® CB 300 blood collection system with lithium heparin (Kent Scientific, Torrington, Connecticut, USA). Tubes were centrifuged at 1 000 g for 10 min at 4ºC, plasma was collected and stored at -80ºC until further use.

*Cell population analysis by flow cytometry*

For cell population analysis, tumors were minced in small pieces and incubated with an enzymatic cocktail containing collagenase P (200 µg/mL; Roche), dispase II (800 µg/mL; Roche) and DNase I (100 µg/mL; Roche) in DMEM at 37ºC, with vortex and mixing every 20 min 3-4 times. Disaggregated tissue was filtered using a 40 µm cell strainer and centrifuged at 16 100 g for 7 min. Cells were resuspended in FACS buffer (0.05% sodium azide, 0.5% bovine serum albumin and PBS) and stained with the viability dye Zombie Aqua (Biolegend), for 20 min in the dark at RT. After washing, cells were incubated with mouse FcR blocking reagent (Milteny Biotec) for 10 min in the dark at RT. Then, the antibodies described in Supplementary Table S3 were added and incubated for 30 min at 4ºC. After washing, cells were fixed with 150 µL of BD Cytofix/Cytoperm™ (BD Biosciences) and acquired in the next day in a BD LSR Fortessa flow cytometer. FlowJo™ 10.8.1 software (BD Biosciences) and OMIQ (Dotmatics, Boston, Massachusetts, USA) were used for data analysis.

*Cytokine analysis*

Cytokine levels were analyzed using the LEGENDplex™ mouse anti-virus response panel (Biolegend) according to the manufacturer's recommendations and using a filter 96-well plate. Briefly, 25 µL of plasma was added to each well along with assay buffer and beads. The mixture was incubated for 2 h with shaking, and next wells were washed and incubated with the detection antibodies for 1 h with shaking at RT. Subsequently, SA-PE was added and incubated for 30 min at RT with shaking. Finally, samples were analyzed in CytoFLEX and CytExpert (Beckman Coulter, USA). Data was presented as fold-change in anti-PD-L1, CM-1758 and CM-1758+anti-PD-L1 groups relative to the mean value of each cytokine for control mice.

*Immunohistochemistry*

Sections of formalin-fixed paraffin-embedded (FFPE) tumors were deparaffinized and incubated with hydrogen peroxide (0.3%) in methanol for 10 min. Then, antigen

retrieval was performed using sodium citrate buffer (citric acid monohydrate 1.8 mM, trisodium citrate dihydrate 8.2 mM, pH=6.0) and a pressure cooker (Dako Agilent Tecnologies, Santa Clara, California, USA). Subsequently, tumor sections were blocked with 10% horse serum for 1 h at RT and incubated with the primary antibody overnight at 4ºC (Supplementary Table S2). In the next day, slides were incubated with the appropriate secondary antibody for 1 h at RT. Next, the slides were incubated with the biotin-avidin-peroxidase system Vectastain Elite ABC HRP kit (Vector Labs, Newark, California, USA) for 30 min at RT, and staining was revealed with a DAB substrate kit (Vector Labs). Slides were counterstained with hematoxylin and mounted with DPX mounting media. All slides were scanned in a Pannoramic MIDI II (3DHISTECH, Budapest, Hungary) at ×20 magnification.

*Bioinformatic analyzes*

For flow cytometry analysis, single and live cells were selected using the gating strategy demonstrated in Supplementary Figures S1-4. Optimization of t-Distributed Stochastic Neighbor Embedding (opt-tSNE) was performed using OMIQ (Dotmatics) for lymphocyte and macrophage populations. Subsampling with 3000 events for each sample and 3000 interactions were used for opt-tSNE.

Regarding RNA-sequencing data, differential analyzes were performed using the DESeq2 software package (version 1.38.2) in R software (22, 23). Normalized gene expression data were transformed into log2 scale, and the value range was adjusted for each gene. Hierarchical clustering was performed using Multi-Experiment Viewer (Mev 4.9.0). Supervised hierarchical clustering was applied using Pearson correlation and average linkage. Heatmaps were represented using SRplot (http://www.bioinformatics.com.cn/srplot). Gene set enrichment analysis (GSEA) was performed using GSEA version 4.3.2 and Molecular Signature Database (MSigDB) (24). The h.all.v7.5.symbols.gmt (Hallmarks) gene set database was used as the gene set collection analysis. GSEA was performed using 1000 permutations and the maximum and minimum sizes for gene sets were 500 and 15, respectively. Data was represented by enrichment bubble plots, using SRplot. Venn diagrams were plotted using jvenn (https://xcmsonline.scripps.edu/lib/jvenn/example.html). Genes with a log2(foldchange) >2 for up regulated genes and <-2 down regulated genes and a p-value adjust <0.01 were selected for venn diagram and Enrichr analysis (https://maayanlab.cloud/Enrichr/). Gene set variation analysis (GSVA) was performed using GSVA package in R software (v1.42.0) and a hallmark gene set. Data was represented by a heatmap using SRplot. We reconstructed transcriptional regulatory networks (regulons) using the R package RTN78. We investigated 1612 transcription factors (TFs) compiled from (25). Potential

associations between a regulator and all possible target genes were inferred from the expression matrix by Mutual Information and Spearman's correlation, and permutation analysis was used to remove associations with a BH-adjusted *p*-value > 0.05. Unstable associations were eliminated by bootstrap analysis (1000 resamplings, consensus bootstrap > 95%) and the weakest association in triangles of two regulators and common target genes were removed by data processing inequality (DPI) filtering (tolerance = 0.01). Regulon activity scores for all samples were calculated by two-tailed gene set enrichment analysis (25-27). Principal component analysis (PCA) was performed using the "prcomp" command in R and the normalized matrix obtained from DeSEq2. The PCA was plotted using the PCA 3D Visualiser tool (https://prismtc.co.uk/resources/free-tools/pca-3d-visualiser).

QuPath software was used for the analysis of the necrosis areas and BrdU immunohistochemistry (28). Briefly, the protocol for nucleus detection was optimized according to staining-intrinsic characteristics. Both BrdU and CD8 showed a clear staining and the positive cell detection tool was used to detect the positive cells using a threshold manually refined for each tumor. BrDU positive cells are displayed as a percentage of positive cells, whereas CD8+ T cells are presented as cells per $mm^2$ (cells/$mm^2$). The necrosis areas were defined manually by a trained pathologist and the area value was determined using the annotation tool. The percentage of necrosis was calculated for each tumor by dividing the value of the necrosis area by the total value of tumor area and multiplying by 100.

*Statistical analysis*

The *in vitro* studies were conducted in a minimum of 3 independent experiments. $IC_{50}$ analyzes were performed using GraphPad Prim 8.0 software (GraphPad Software, USA). Graphics are represented by mean ± SEM. Normal distribution was evaluated using the Shapiro-Wilk test ($p>0.05$). Data showing normal distribution were analyzed using parametric two-tailed t-test with Levene's test for equality of variances ($p<0.05$, variances considered not equal; $p>0.05$, variances considered equal). Non-parametric Mann-Whitney U test was used to compare data not having a normal distribution. Immunohistochemistry results were analyzed by Fisher's exact test. Two-tailed p-values calculation were performed using a computer assisted program (SPSS Version 28.0, USA). Graphics were assembled with GraphPad 8 Prism (GraphPad Software, USA). P-values were considered statistically significant when inferior to 0.05. Significance is depicted as follows: *$p < 0.05$, **$p < 0.01$, ***$p < 0.001$, ****$p < 0.0001$ and ns > 0.05 (non-significant).

## Results

*CM-1758 displayed cytotoxic/cytostatic effects in bladder cancer cells*

The effects of the CM-1758 inhibitor were evaluated in a wide array of BC cell lines. CM-1758 demonstrated effects on the low micromolar range, with $IC_{50}$ ranging between 0.33 and 4.8 μM (Figure 1a; Supplementary Table S4). Remarkably, CM-1758 also affected the cell cycle, with a decrease in the percentage of S-phase cells observed for 253J, 5637, J82 and TCCSUP cell lines after treatment (Figure 1b). J82 cells also displayed higher percentage of G2/M phase in the treated cells, which was more evident for RT112 cells (Figure 1b). The mouse 4K5 cell line disclosed cell arrest at the S-phase (Figure 1b). Interestingly, 253J and RT112 cells displayed a reduced percentage of G0/G1 phase upon treatment (Figure 1b).

A decrease in the percentage of live cells in 253J, RT112, TCCSUP and 4K5 treated cells was observed, in parallel with an increase in the percentage of cells in late apoptosis (Figure 1c and d), with a more pronounced effect in 253J and RT112 cell lines (Figure 1c and d). 253J, RT112, TCCSUP and 4K5 cells showed a higher percentage of early apoptosis, while only 253J displayed higher levels of necrotic cells, with no apparent differences for the other cell lines (Figure 1c and d). Altogether, these data demonstrate that CM-1758 has both cytotoxic and cytostatic effects in BC cell lines, either by inducing cell cycle arrest and/or apoptosis at low $IC_{50}$ micromolar concentration.

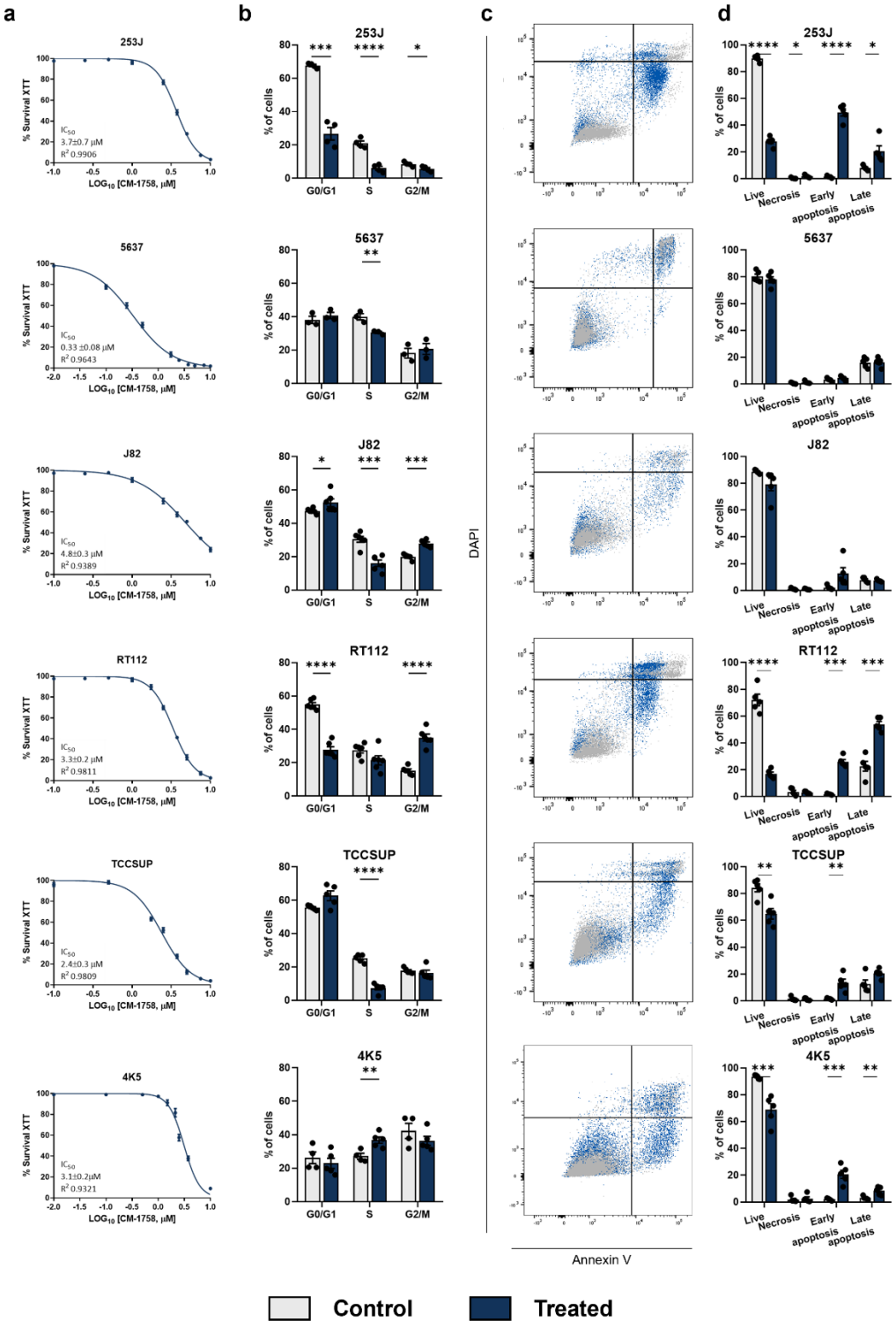


**Figure 1.** Cytotoxic and cytostatic effects of CM-1758 in bladder cancer cell lines. (a) Survival curves with the $IC_{50}$ value for the BC cell lines 253J, 5637, J82, RT112, TCCSUP and 4K5 (percentage of survival with calculated with XTT vs log10 of CM-1758 concentrations) with respective standard deviation and R2. (b) Cell cycle profiles containing G0/G1, S and G2/M phases for 253J, 5637, J82, RT112, TCCSUP and 4K5 after treatment with CM-1758. (c) Representative gating of live (DAPI negative, annexin V negative), necrotic (DAPI positive, annexin V negative), early apoptotic (DAPI negative, annexin V positive) and late apoptotic cells (DAPI positive, annexin V positive) cells. (d) Percentage of live, necrotic, early and late apoptotic

cells for all cell lines after treatment with CM-1758. Non-treated cells are represented in grey and CM-1758 treated cells are shown in blue. Treatment with CM-1758 was given for 48 h with $IC_{50}$ dose calculated for each cell line for cell cycle and annexin V analyzes. Data shown are the mean of ≥3 experiments ± SEM. P-values are represented as ns – not significant, *<0.05, **<0.01, ***<0.001 and ****<0.0001.

*CM-1758 induced changes in the transcriptomic profile of bladder cancer cells*

Hereafter, we evaluated the transcriptomic profile of BC cells by RNA-seq after treatment with the $IC_{50}$ doses of CM-1758. Treatment with CM-1758 drove marked changes in the transcriptomic profile of BC cells (Figure 2a). Remarkably, there was limited overlap in the genes upregulated (Figure 2b1) or downregulated (Figure 2b2) considering all cell lines, although all cell lines showed homogeneous clustering in PCA analysis when comparing control *versus* treated (Supplementary Figure S5). GSEA (Supplementary Figure S6a-d) and GSVA analysis (Figure 2c) revealed that the treatment decreased the expression of multiple genes involved in cell proliferation, such as E2F and MYC targets and epithelial mesenchymal transition. Moreover, in some cell lines there was an effect on various immunological pathways such as IL-2/STAT5, IFN-α, IFN-γ and TNF-α signaling via NF-κB (Figure 2c). However, these effects on immunological pathways were cell line dependent. Having into account the genes upregulated by CM-1758, further analyzes of the transcription factors and histone using the Enrichr webtool revealed a prominent role of IRF1 and IRF8 as well as acetylation of various histone H2B residues, more noticeable in TCCSUP cells (Figure 2d). Also, analyzes of transcriptional regulatory networks (regulons) showed that some key elements in BC such as *FOXM1* were downregulated, while others such as *STAT3*, were predominantly upregulated (Figure 2e, Supplementary Figure 6e). We also observed that many regulons modulating chromatin remodeling were also affected by treatment, including epigenetic machinery related not only to acetylation, but also histone and DNA methylation including lysine demethylases (KDMs) and DNA methyltransferases (DNMTs) (Figure 2f). Overall, CM-1758 led to profound changes in the transcriptomic profile of BC cells, affecting pathways related to tumor cell aggressiveness and epigenetic machinery.

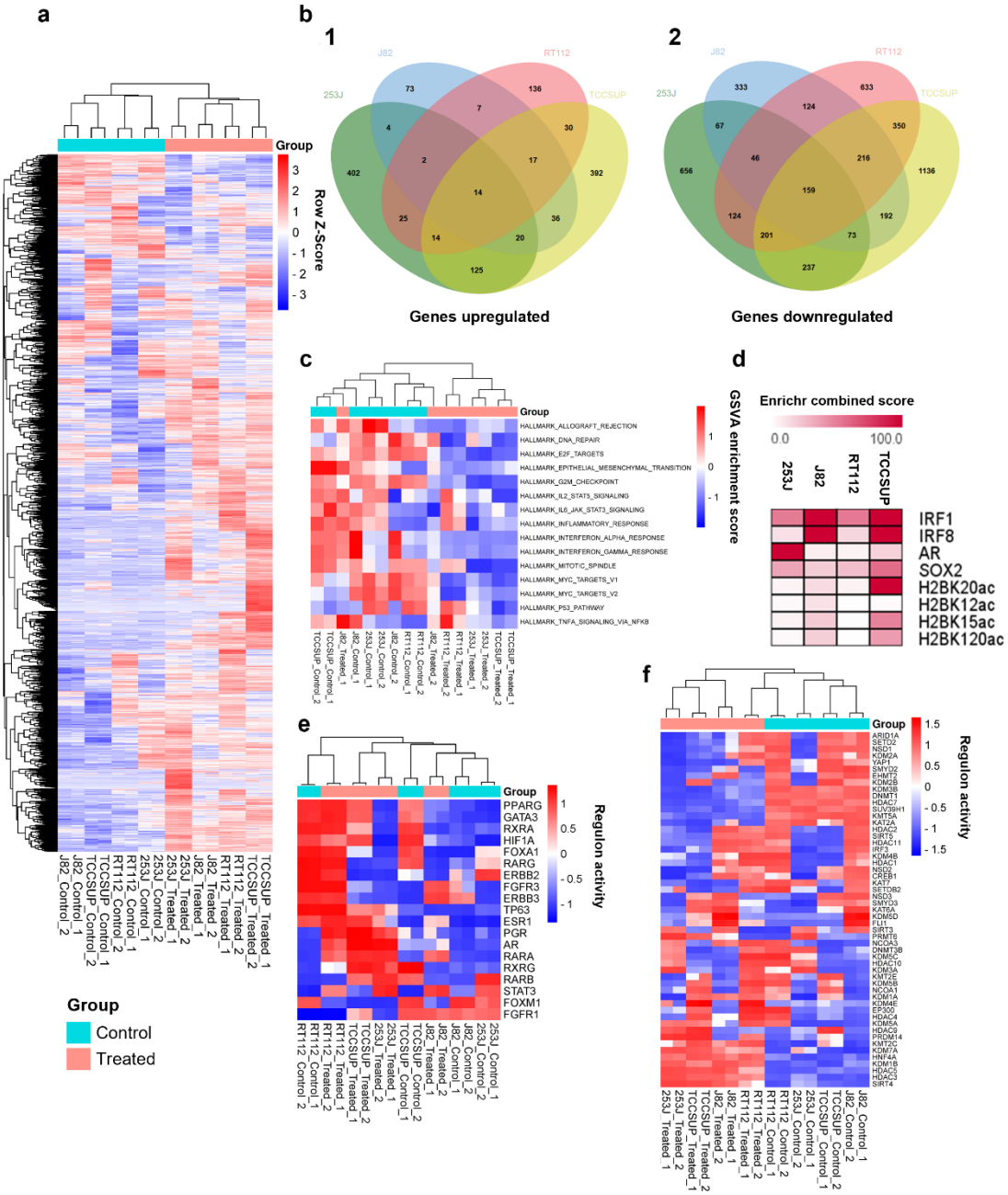


**Figure 2.** CM-1758 effects on the transcriptomic profile of 253J, J82, RT112 and TCCSUP cells. (a) Heatmap of the dysregulated genes between untreated control vs. treated cells with $IC_{50}$ dose of CM-1758. Genes and groups (control and treated) are hierarchically clustered. (b) Venn diagrams of genes (1) up and (2) downregulated in treated cells vs. control cells. (c) Heatmap of GSVA analysis showing the main signaling pathways from hallmarks in cancer enriched in control and treated cells. Control and treated groups are hierarchically clustered. (d) Enrichr analysis of the upregulated genes in all cell lines when compared to the respective untreated control cells. (e) Regulon activity profiles for potential regulators associated with BC. Control and treated groups are hierarchically clustered. (f) Regulon activity profiles for potential regulators associated with chromatin remodeling. Control and treated groups are hierarchically clustered. Control denotes untreated cells, whereas treated refers to CM-1758 treated cells. Treatment with CM-1758 was given for 48 h with $IC_{50}$ dose calculated for each cell line. Two independent experiments were included for each cell line and condition.

*CM-1758 treatment regulated PD-L1 expression by induction of histone acetylation*

Next, we studied the effects of CM-1758 on histone acetylation in BC cell lines. We observed increased H3, H3K9 and H3K27 acetylation levels by western blot (Figure 3a and Supplementary Figure S7a) in all the analyzed cell lines after treatment with CM-1758. Of note, expression of HDACs was altered in BC cells either by transcript or protein levels (Supplementary Figure S7b and d). Since DNA methylation and histone modifications are two epigenetic mechanisms intertwined in the regulation of gene expression, we also explored the global levels of 5-methylcytosine in J82 and 4K5 BC cells. Immunofluorescence analyzes demonstrated that total 5-methylcytosine levels were decreased in J82 and 4K5 BC cells after CM-1758 treatment (Figure 3b and c), which was paralleled by decreased DNMTs' levels (Supplementary Figure S7c and d). The lower levels of DNA methylation could be a direct consequence of the higher levels of acetylation observed after treatment with CM-1758. These results show that CM-1758 treatment affects histone acetylation, but also other epigenetic mechanisms such as DNA methylation indirectly.

Some epidrugs were shown by others to have synergistic effects with immunotherapies, since drug treatments can induce immune checkpoints' expression, conferring higher sensitivity to ICI (15, 16). Furthermore, transcriptomic data showed that CM-1758 has effects on immune pathways in cancer cells (Figure 2). Thus, we investigated whether the global changes in acetylation and DNA methylation levels induced by CM-1758 treatment could have an impact on PD-L1 expression in BC cell lines, as previously reported for other solid tumors (29, 30). Remarkably, we observed that PD-L1 levels increase in cells after CM-1758 treatment at both mRNA (Figure 3d) and membrane protein (Figure 3e-f) levels. Afterwards, we hypothesized whether this increased expression was attributable to epigenetic regulation of PD-L1. CUT&RUN experiments showed that H3K9ac and H3K27ac marks were increased at the PD-L1 promoter in 4 different regions, from 100 to 1200 bp upstream of initiation transcription site, after CM-1758 treatment (Figure 3g and h). On the other hand, DNA methylation levels in these regions, assessed by quantitative methylation-specific PCR (qMSP), were not affected by treatment showing low levels of DNA methylation on the analyzed CGs (Supplementary Figure S8a and b). These results indicated that CM-1758 increased PD-L1 levels through its effect on HDACs and, consequently, PD-L1 promoter acetylation marks.

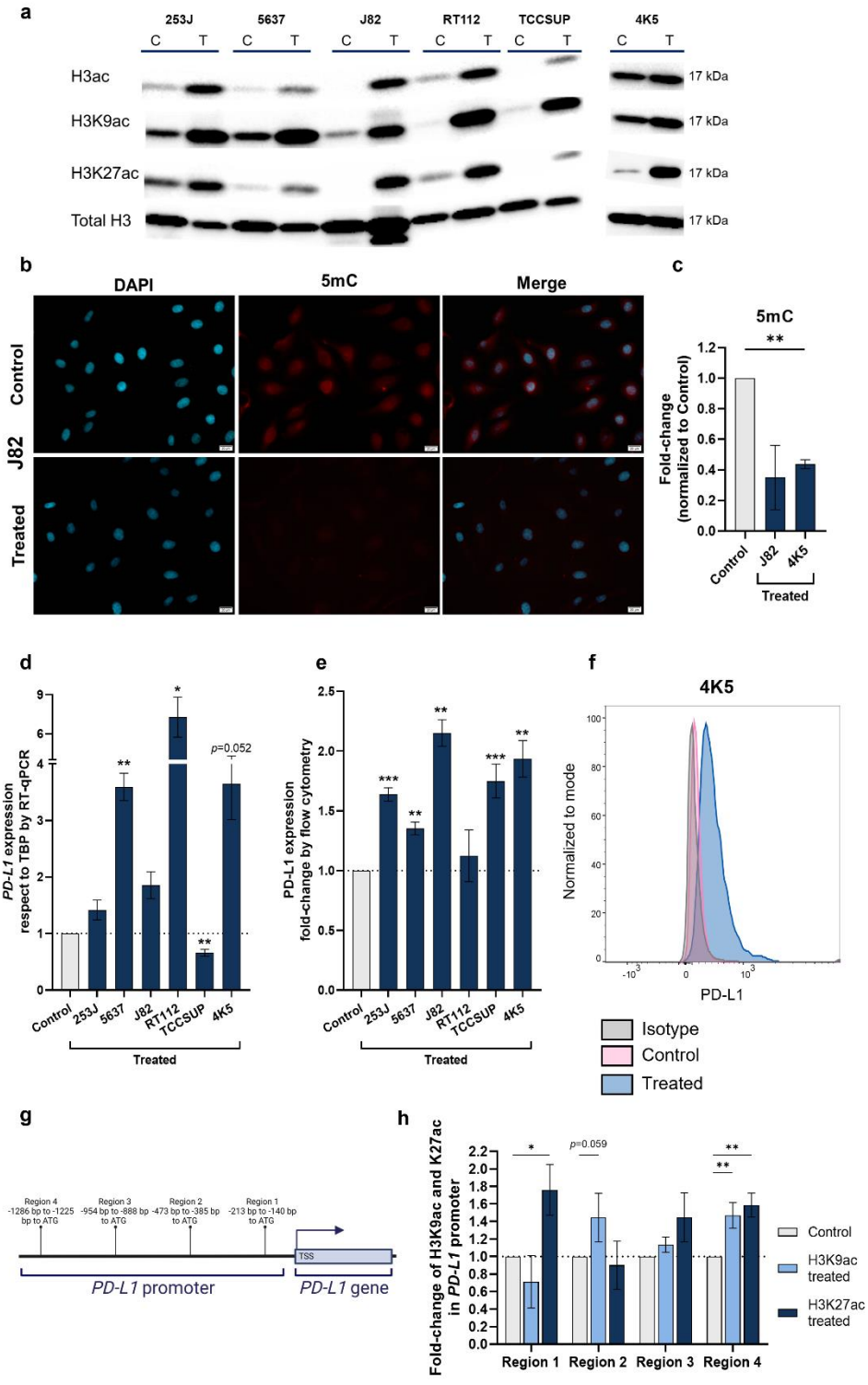


**Figure 3.** Histone acetylation and DNA methylation levels after treatment with CM-1758. PD-L1 epigenetic regulation by promoter acetylation. (a) Western blot analysis of total acetylation of H3 (H3ac), acetylation of lysine 9 of histone 3 (H3K9ac) and acetylation of lysine 27 of histone 3 (H3K27ac) respect to total histone 3 (H3) levels for all cell lines after treatment with CM-1758. C – Control, T - Treated. (b) Representative immunofluorescence for 5-methylcytosine of J82 cells after treatment with CM-1758 (in red). Cell nuclei were identified by DAPI staining (in blue). Scale

bar 20 µm. (c) Quantification of 5-methylcytosine levels by immunofluorescence after treatment with CM-1758 represented by fold-change respective to the untreated control cells in J82 and 4K5 cells. (d) Relative expression by RT-qPCR of PD-L1 respect to TBP for all BC lines after treatment with CM-1758. (e) PD-L1 expression evaluated by flow cytometry represented by fold-change respective to non-treated control cells and (f) Single parameter histogram of mean intensity fluorescence (MFI) of PD-L1 levels with CM-1758 treatment in 4K5 cells (g) Schematic representation of the PD-L1 promoter regions evaluated by CUT&RUN (h) Presence of H3K9 and H3K27 acetylation in four different regions [region 1 -213 to -140 bp, region 2 -473 to -385 bp, region 3 -954 to -888 bp and region 4 -1286 to -1225 bp before the transcription start site (TSS)] of PD-L1 promoter after treatment with CM-1758 evaluated by CUT&RUN. Values are represented as fold-change relative to the untreated control cells. Cells were treated with CM-1758 for 48 h with the $IC_{50}$ dose calculated for each cell line. Data shown are the mean of ≥3 experiments ± SEM. P-values are represented as ns – not significant, *<0.05, **<0.01 and ***<0.001.

*CM-1758 and anti-PD-L1 as a therapeutic strategy in a bladder cancer immunocompetent mouse model*

The data obtained concerning increased PD-L1 expression together with gene expression changes as a consequence of CM-1758 treatment *in vitro* prompted us to study *in vivo* the effects of CM-1758 combined with anti-PD-L1 using a double knock-out (*Pten*$^{F/F}$, *Trp53*$^{F/F}$; DKO) immunocompetent BC mouse model. For that, GFP-expressing 4K5 cells (derived from a BC tumor developed in a DKO mouse injected with adenoviruses expressing Cre-recombinase under the control of keratin 5 promoter) were subcutaneously injected in the flank of syngeneic mice and treated with CM-1758 and/or PD-L1 blockade (Figure 4a). Even with only two weeks of treatment period, an anti-tumoral effect of CM-1758 was observed, which was slightly increased by the combination with anti-PD-L1 (Table 1, Figure 4b-c and g1-4; Supplementary Figure S9a-d). Both Ki67 and BrdU immunohistochemistry analyses demonstrated a significant decrease in tumor cell proliferation levels in CM-1758 treatment group (Figure 4e and g5-8; Supplementary Figure S9e and S9f1-4). Furthermore, tumors treated with CM-1758 or with CM-1758+anti-PD-L1 displayed frequent hypocellular and necrotic areas (Figure 4g1-4), while more prominent immune infiltrates were found in the tumors treated with the combination, confirmed by the immunostaining analysis for CD8+ T cells (Supplementary Figure 9g). The assessment of necrotic areas revealed that CM-1758, either alone or in combination with anti-PD-L1, resulted in a higher percentage of necrotic regions within the examined tumors (Figure 4d). Interestingly, the combination-treated tumors displayed a clear tendency revealing a higher infiltration of CD8+ T cells in necrotic areas compared to control, anti-PD-L1, and CM-1758-treated tumors (Figure 4f and g9-12). However, it did not reach statistical significance, and there was no observed correlation between these variables (Figure 4f; Supplementary Figure 9h-k).

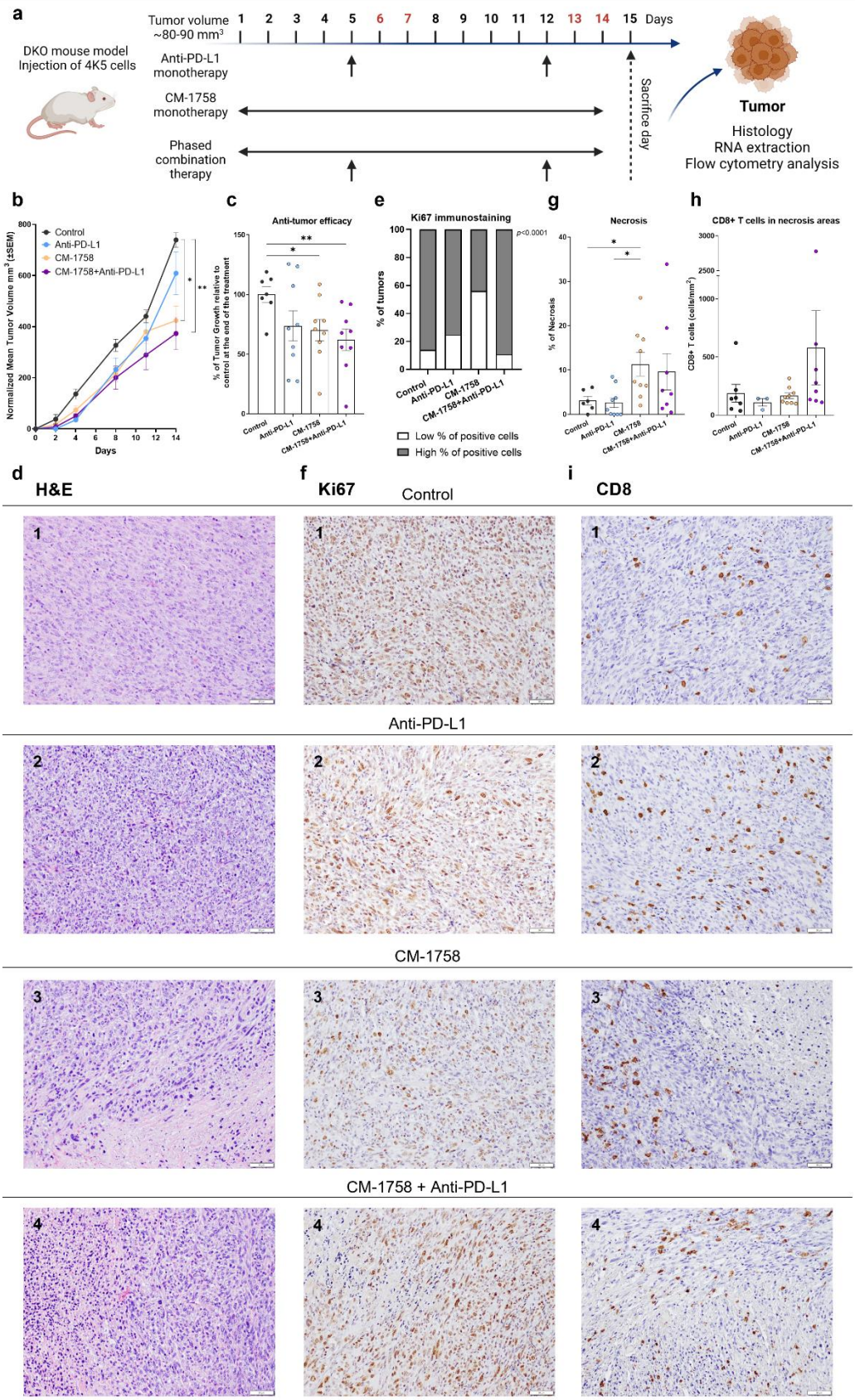


**Figure 4.** *In vivo* effects of CM-1758 alone and in combination with immune checkpoint inhibitors. (a) Schematic representation of the protocols used for treatment with CM-1758 and anti-PD-L1 alone or in combination. CM-1758 was applied for two weeks, five days a week with two rest days represented in red. Anti-PD-L1 was injected once a week for two weeks. Mice in all groups were

sacrificed at day 15. Tumors were collected for histology, flow cytometry analysis and RA extraction. Created with BioRender.com (b) Normalized tumor growth curves for the first day of treatment in control, anti-PD-L1, CM-1758 and CM-1758+anti-PD-L1 groups. (c) Anti-tumor efficacy of anti-PD-L1, CM-1758 and CM-1758+anti-PD-L1. (d) Percentage of necrosis present in tumors from each treatment group at the end of treatment of control, anti-PD-L1, CM-1758 or combination. (e) Graphical representation of percentage of Ki67 expression for each group. Cut-off was defined as <80% as low and >80% as high percentage of positive cells. (f) Number of CD8+ T cells (cells/mm2) infiltrating in necrosis areas in control, anti-PD-L1, CM-1758 and CM-1758+anti-PD-L1 groups. Only tumors displaying necrosis areas were evaluated. (g1-4) Representative H&E staining of the tumors from each group (control, anti-PD-L1, CM-1758 and CM-1758+anti-PD-L1); (g5-8) Representative immunohistochemistry staining of Ki67 (g9-12) Representative immunohistochemistry staining of CD8. Scale bar 50 µM. Graphs show individual values as the mean ± SEM for ≥8 mice included in each group. P-values are represented as ns – not significant, *<0.05, **<0.01 and ***<0.001.

**Table 1.** Antitumor efficacy of anti-PD-L1, CM-1758 and CM-1758+anti-PD-L1 in comparison with the control group. Percentage calculated as [T (tumor) / C (control)] x 100 of growth inhibition by anti-PD-L1, CM-1758 or the combination. Values represented as mean ± SD and p-values <0.05 were considered statistically significant.

| Treatment group | Mean % T/C (±SD) | *p* value | | |
|---|---|---|---|---|
| | | vs. Control | vs. Anti-PD-L1 | vs. CM-1758 |
| Anti-PD-L1 | 74±38 | 0.112 | - | - |
| CM-1758 | 70±27 | 0.023 | 0.822 | - |
| CM-1758+Anti-PD-L1 | 62±27 | 0.006 | 0.463 | 0.532 |

*CM-1758 treatment increased CD8+ cytotoxic T cells presence in the tumor microenvironment and promoted pro-inflammatory cytokine release*

Treatment with CM-1758, alone or in combination with anti-PD-L1, led to changes in tumor lymphoid repertoire. We did not find any differences in CD3+ T cells percentage respect to the CD45+ leucocytes population (Figure 5a). However, when we looked for the type of lymphocytes present in the tumor, we did observe a reduction in CD4+ T cells, alongside with an increase in CD8+ T cells in tumors treated with CM-1758 or upon combination treatment (Figure 5b, c and e), whereas no significant differences were observed for the B cell percentage (Figure 5d and e). Thus, CM-1758 led to increased CD8+ cytotoxic T cells presence independently of immunotherapy, whereas CD4+ T cells detection was decreased.

The non-immune compartment of the tumor microenvironment also underwent changes upon ICI and CM-1758 treatments (Figure 5f-h). The percentage of blood and lymphatic endothelial cells in the tumor significantly decreased after treatment with CM-1758+anti-PD-L1 in comparison with the control and anti-PD-L1 groups (Figure 5f and g). On the other hand, the percentage of lymphatic endothelial cells was increased in the CM-1758 treated group in comparison with control, anti-PD-L1 and combination groups

(Figure 5g). The percentage of fibroblasts was increased in both anti-PD-L1 and CM-1758 groups (Figure 5h). Almost all fibroblasts found in the tumor microenvironment were positive for α-SMA, a cancer-associated fibroblasts (CAFs) marker (Supplementary Figure S10a; mean percentage of cells positive for α-SMA higher than 97%).

Next, we explored whether the treatment with CM-1758 might led to the release of pro-inflammatory cytokines systemically. Thus, multiple cytokines were measured in plasma upon different treatments using a cytometric bead-based assay (mean concentrations of each cytokine per treatment group are displayed in Supplementary Table S5). Anti-PD-L1 treatment led to an increase in IFN-γ, which was further boosted by the combination with CM-1758 (Figure 5i). Moreover, increased TNF-α and IL-12 levels were observed in both anti-PD-L1 and CM-1758 treatment groups. The combination treatment increased CCL5 levels mainly by action of the anti-PD-L1 therapy and with no changes in CCL5 levels on the CM-1758 group, suggesting that CCL5 is regulated by ICI (Figure 5i). The same seems to happen with CXCL10, which levels were significantly increased in the anti-PD-L1 treatment group, with the same tendency observed for the combination (Figure 5i). These results highlight the importance of epigenetic mechanisms and ICI in cytokines' expression regulation, which remains a poorly explored topic in BC.

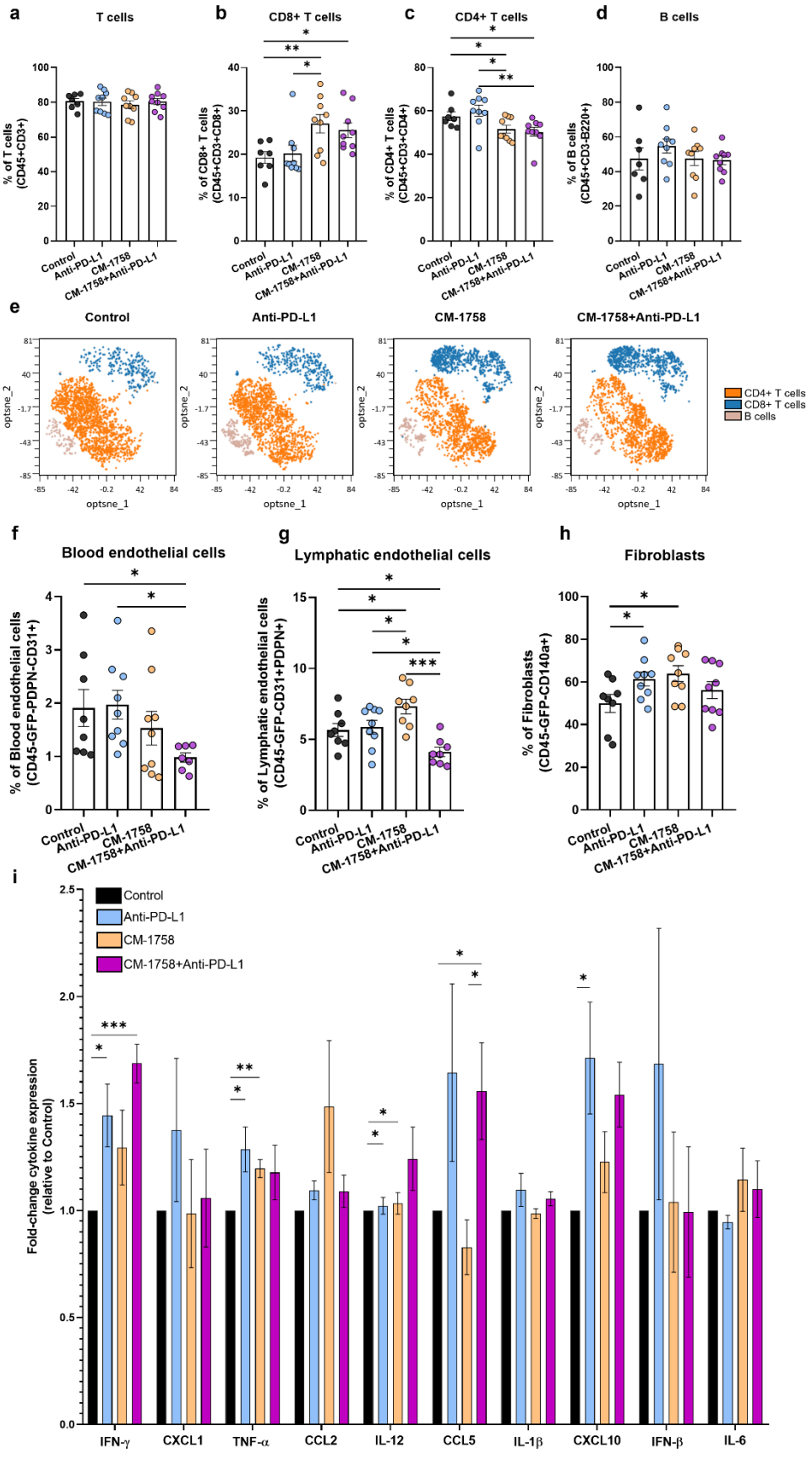


**Figure 5.** Effects of CM-1758 and immune checkpoint inhibitors in tumor lymphoid cells, the non-immune compartment and cytokine profile. Percentage of (a) T cells gated in CD45+ cells, (b)

CD8+ T cells gated in CD3+ cells, (c) CD4+ T cells gated in CD3+ cells and (d) B cells gated in CD45+ cells present in the tumors. (e) Representative opt-tSNE analysis of CD8+ T, CD4+ T and B cells repertoire according to treatment groups. Percentage of (f) blood endothelial cells gated in CD45-GFP- cells, (g) lymphatic endothelial cells gated in CD45-GFP- cells (h) fibroblasts gated in CD45-GFP- cells present in the tumor microenvironment. (i) Fold-change of cytokine profile (IFN-γ, CXCL1, TNF-α, CCL2, IL-12, CCL5, IL-1β, CXCL10, IFN-β and IL-6) analyzed in plasma of control, anti-PD-L1, CM-1758 and CM-1758+anti-PD-L1 treated mice. Graphs show individual values as the mean ± SEM for ≥8 mice included in each group. P-values are represented as ns – not significant, *<0.05, **<0.01 and ***<0.001.

*Anti-PD-L1 alone or in combination with CM-1758 reprogramed macrophages towards a M1-like polarization*

We also investigated whether anti-PD-L1 and/or CM-1758 treatments could induce myeloid compartment remodeling. Although no differences were apparent in the percentage of myeloid cell present in the tumor (Figure 6a), a lower percentage of phagocytic myeloid cells, identified by their positivity for GFP arising from the phagocytosis of GFP-expressing tumor cells, was found for anti-PD-L1 treated groups alone or in combination with CM-1758 (Figure 6b). Furthermore, a significant decrease in the percentage of tumor cells was found for the treatment groups, including CM-1758 alone or in combination as compared with non-treated control mice (Figure 6c).

Anti-PD-L1 treatment alone or in combination with CM-1758 led to significantly lower detectable PD-L1 levels in myeloid cells, both in all myeloid cells and phagocytic myeloid cells (Figure 6d-f). No significant changes were found in tumor cells' PD-L1 levels, showing that the anti-PD-L1 treatment mainly affected the myeloid cell population (Figure 6g). Additionally, no changes at PD-L1 transcriptional levels were observed in the tumor bulk, indicating that the decreased cell surface PD-L1 detection might be due to anti-PD-L1 antibody still bound to the cells or to PD-L1 loss at the cell membrane by internalization processes (Supplementary Figure S10b). On the other hand, CM-1758 alone seemed to slightly increase PD-L1 levels in tumor cells as observed in the *in vitro* conditions, although without statistical significance (Figure 6g).

Compared with untreated samples, single treatment with anti-PD-L1 or CM-1758 led to a partial decrease in total macrophages (Figure 6h). Interestingly, anti-PD-L1 (alone or in combination) treatment increased the presence of M1-like macrophages, while decreasing M2-like macrophages (Figure 6i-l). Contrarily, CM-1758 alone did not seem to have a major impact in macrophages polarization (Figure 6i-l). These findings suggest that the shift of macrophages toward an M1-like pro-inflammatory polarization is dependent on ICI treatment, with no observed syngeneic effect in combination with CM-1758.

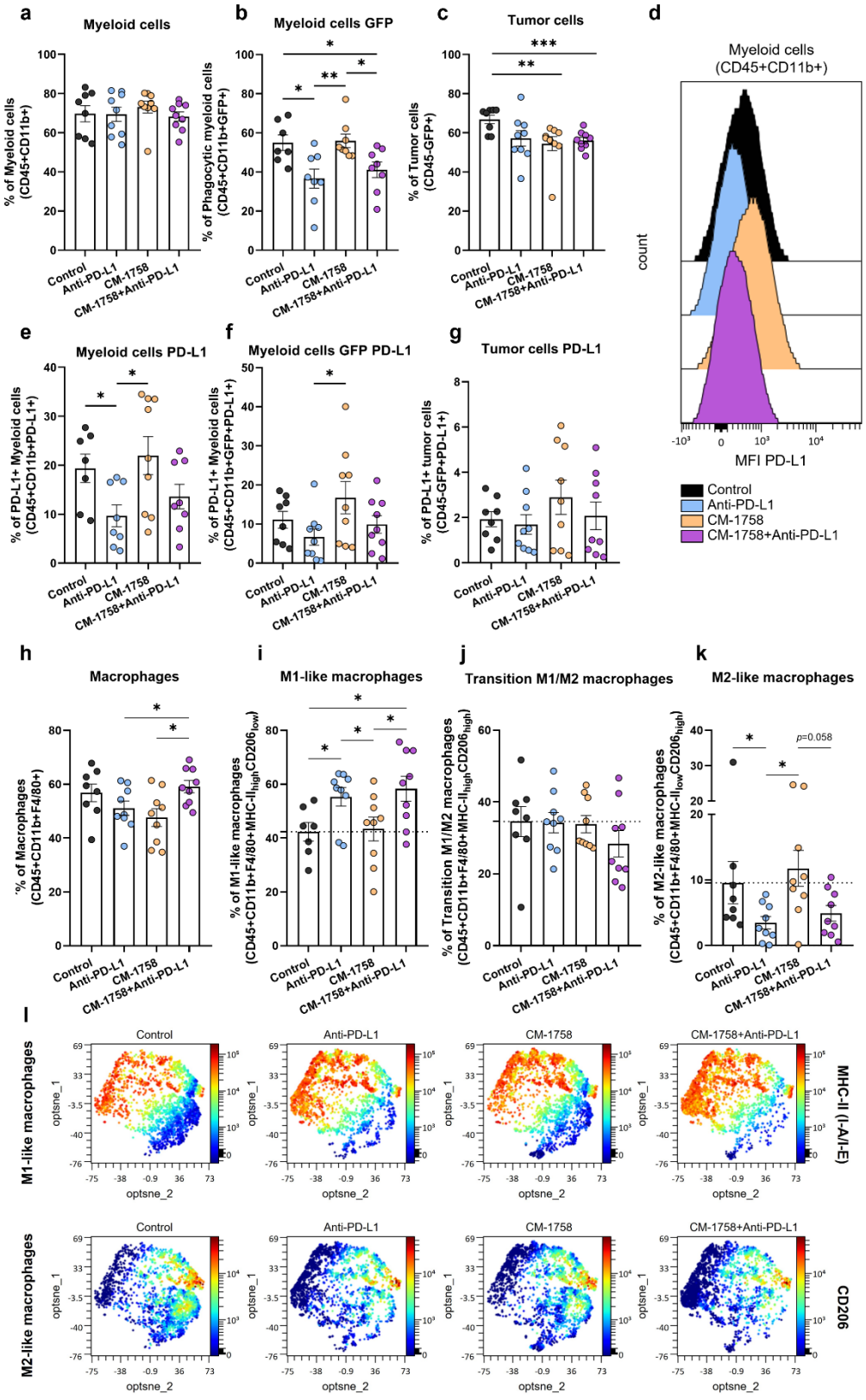


**Figure 6.** Myeloid repertoire changes after treatment with CM-1758 and PD-L1 blockade therapy. Percentage of (a) myeloid cells gated in CD45+ cells, (b) phagocytic myeloid cells gated in CD45+ cells and (c) tumor cells gated in live cells. (d) Single parameter histograms of mean intensity fluorescence (MFI) of PD-L1 expression in the four treatment groups. Percentage of PD-L1

positive of (e) myeloid cells gated in CD45+CD11b+ cells, (f) phagocytic myeloid cells gated in CD45+CD11b+GFP+ cells, and (g) tumor cells gated in GFP+ cells. Percentage of (h) macrophages gated in CD45+CD11b+ cells, (i) M1-like macrophages gated in CD45+CD11b+F4/80+ cells, (j) transition M1/M2 macrophages gated in CD45+CD1b+F4/80+ cells and (k) M2-like macrophages gated in CD45+CD11b+F4/80+ cells. (l) Opt-tSNE analyzes of tumor-present M1-like and M2-like macrophages for MHC-II (I-A/I-E) and CD206 markers. Graphs show individual values as the mean ± SEM for ≥8 mice included in each group. P-values are represented as ns – not significant, *<0.05, **<0.01 and ***<0.001.

## Discussion

BC represents a major public health concern due to its high incidence and prevalence, with current treatment options falling short to avoid disease recurrence and progression (1). Although implementation of immunotherapy in advanced BC improved patients' overall survival, a significant percentage of BC patients does not respond or become unresponsive within the course of ICI treatment (31). Thus, new treatment strategies, such as epidrugs, alone or in combination with immunotherapy, are currently being explored (17). Several HDACi are FDA-approved for treatment of hematologic malignancies, and are under clinical trials for BC patients, with a confirmed improvement of overall survival (32). Furthermore, several *in vivo* and *in vitro* studies showed the synergistic effect of commercial HDACi and immunotherapy (14, 15). Herein, we present encouraging data showing the anti-cancer effects of CM-1758, a novel inhibitor of HDACs, both in *in vitro* and *in vivo* models of advanced BC.

CM-1758 effects leading to cell cytotoxicity and cytostasis by either apoptosis or cell cycle arrest is in line with previous reports on HDACi such as vorinostat (SAHA) or entinostat (12, 13, 33-36). Additionally, CM-1758 had inhibitory effects on HDACs and further transcriptomic analyzes revealed that not only the epigenetic machinery associated with acetylation was altered, but also the machinery responsible for the regulation of methylation of both histones and DNA. It is known that histone acetylation and DNA methylation are epigenetic mechanisms closely related in regulating gene expression, *i.e.*, elevated histone acetylation can trigger DNA demethylation, promoting gene expression (37).

PD-L1 blocking antibodies are among the most frequently used ICI in BC (38) and, importantly, PD-L1 expression was shown to be regulated by epigenetic mechanisms (39, 40). In line with previous studies using HDACi, we found increased PD-L1 expression levels upon CM-1758 treatment in several BC cell lines, consequence of higher acetylation levels in the PD-L1 promoter (40). Histone acetylation increases gene expression since it neutralizes lysine residues positive charge, decreasing the interaction of histone proteins with DNA, making it more accessible for transcription factors (9, 41). Conversely, although PD-L1 expression has been reported to be regulated by DNA

methylation (39), no apparent effect was seen in PD-L1 promoter DNA methylation levels with CM-1758 treatment.

Since CM-1758 led to increased PD-L1 expression, the *in vivo* effects of a combinatory therapy of CM-1758 with anti-PD-L1 antibody were investigated. A subcutaneous syngeneic mouse model was used to evaluate the efficacy of CM-1758, with the main advantage of having a fully immunocompetent system and enabling easy following of tumor growth. Treatment with CM-1758 alone has significant anti-tumor effects, with better results than anti-PD-L1 blockade alone and a slightly synergistic effect when combined with ICI. Because a significant proportion of BC patients do not respond to ICI due to low PD-L1 expression levels or reduced immune cell infiltration (immune deserted and excluded tumors), our results suggest that CM-1758 may be a promising alternative approach to ICI.

It is acknowledged that epigenetics plays a major expression regulatory role not only in tumor cells, but also in tumor microenvironment cells including immune and non-immune compartment (17). In our hands, both CM-1758 and anti-PD-L1 induced changes in both immune and non-immune cells. Importantly, CM-1758 incremented CD8+ cytotoxic T cells infiltration, which is a rather favorable prognostic factor in BC (42). Also, we found an increase in CD8+ T cell infiltration within the necrotic regions of tumors following the combined administration of CM-1758 and anti-PD-L1. Necrotic areas often exhibit immune suppression, either through the recruitment of M2 macrophages or due to the absence of active T cells (43), characteristics commonly associated with high-risk pathological features in upper tract urothelial carcinoma (44). Our findings indicate that the combination treatment effectively counteracts the immune-suppressive effects associated with tumor necrosis, signifying a potential synergistic effect between CM-1758 and anti-PD-L1. In contrast, the decrease of CD4+ T cells after treatment may be associated with a reduction in regulatory T cells ($T_{reg}$), as previously observed after *in vivo* entinostat treatment in a different BC model (16). CM-1758 showed the ability to regulate the lymphoid repertoire, further supporting that epigenetic factors modulate BC tumors' immune infiltrate features, specifically of T cells (45). Henceforth, epidrugs to target tumor immune cells constitutes a strategy that should be exploited in conjunction with other immunotherapies in BC.

Myeloid cells are also key players for the effectiveness of immunotherapy (46). A lower percentage of phagocytic myeloid cells was observed in the anti-PD-L1 treated groups, alone or in combination with CM-1758. Additionally, in our experimental conditions, phagocytic myeloid cells seemed to be the main population affected by anti-PD-L1 antibody treatment. This might be consequence of antibody-dependent cell-mediated cytotoxicity (ADCC) against the phagocytic myeloid cells. Indeed, avelumab

was previously shown to mediate ADCC in tumor cells, which is in line with our findings (47). Importantly, anti-PD-L1 alone or in combination with CM-1758 impacted macrophage status, shifting from an M2 anti-inflammatory to an M1 pro-inflammatory profile and sustaining a “hot tumor” paradigm, as already reported by other studies for ICI (15, 48). Although epigenetic regulation has been previously implicated in macrophage polarization (15), in our hands CM-1758 did not alter macrophage differentiation. Moreover, despite observing a trend within the CM-1758 group, we did not find a significant change in the PD-L1 expression in tumor cells *in vivo*, which could be attributed to the fact that PD-L1 expression increase may be transient. Understanding when the PD-L1 levels detected are the highest by induction of CM-1758 could provide insights into alternative treatment regimens that may potentiate the synergy between CM-1758 and ICI. The non-immune compartment has a crucial role in tumor maintenance, either through angiogenesis, by providing nutrients and oxygen, or by supporting tumor cell growth (49). CM-1758 altered the non-immune cell compartment by reducing the percentage of blood endothelial cells, which may decrease the tumor access to nutrients and diminishing metastasis development via blood vessels. Nonetheless, the percentage of lymphatic endothelial cells was increased in the CM-1758 treated group. The role of lymphatic endothelial cells remains under discussion since it increases the amount of tumor antigens in circulation, augmenting the probability of immune system activation (50), although it has been also implicated in tumor cell dissemination. Further studies are needed to explore the role and the impact of epigenetic regulation in lymphatic endothelial cells. Interestingly, we found that virtually all fibroblasts were positive for α-SMA, being classified as myofibroblast-like CAFs (myCAFs) (51). MyCAFs play a crucial role in the tumor microenvironment by contributing to the deposition and organization of extracellular matrix components, including collagen and fibronectin, which provide structural support to the growing tumor mass in mouse subcutaneous tumor models (52). In this line, the increase in the percentage of myCAFs in the treatment groups could be associated with a remodeling in the tumor's extracellular matrix by treatments’ actions. However, comprehensive studies focusing on the effects of HDACi on CAFs in the context of BC in mouse orthotopic models are required to be better elucidate the contribution of these cells within the BC tumor microenvironment.

The cytokine profile was evaluated in plasma, indicating a systemic immune activation status of mice upon therapy by increasing pro-inflammatory cytokines in circulation. IFN-γ and TNF-α are mainly produced by CD4+ T helper type 1 (Th1) cells, CD8+ cytotoxic T cells and NK cells, stimulating M1 macrophages’ antitumor effects and promoting the cytotoxic activity of CD8+ T cells and NK cells (53, 54). Thus, the increase

in cytokines levels is in accordance with increased CD8+ T cells and M1-macrophages depicted by the tumor microenvironment analysis. In our study, both CCL5 and CXCL10 levels seemed to be regulated by ICI. CCL5 is often seen as a “double-edge sword” in cancer, since it has been associated both with promoting antitumor immunity, as well as being implicated in tumor growth and migration (55). In BC cell lines, conditioned media from TAMs increased invasiveness concomitantly with augmented CCL5 levels (56), although in BC patients high CCL5 expression in tumors associated with better prognosis (57). In contrast, CXCL10 was shown to increase infiltration of CD8+ T cells, increasing migration and activation of immune cells in the tumor microenvironment (58, 59). No relevant alterations in cytokines’ levels were exclusive to the combination treatment, suggesting that cytokines were independently regulated by ICI and/or CM-1758. Additional studies are required to unravel the exact role of cytokine epigenetic regulatory mechanisms in response to ICI and epidrugs in MIBC.

To conclude, our study describes a novel epigenetic inhibitor targeting HDACs, disclosing antitumor properties in BC both *in vitro* and *in vivo* models. Although CM-1758 was shown to have only a slight synergistic effect when combined with ICI, this epidrug may constitute an alternative to current ICI treatment schemes prescribed for BC patients. Besides having a direct impact in tumor growth, CM-1758 also leads to immune system activation. Undoubtedly, epigenetic mechanisms have an important role in regulating the tumor microenvironment and constitute an attractive target to modulate the immune system, with the final goal of tumor elimination and improving BC patients’ quality of life. Further investment in novel epidrugs, with extended bioavailability, reduced off-target effects and amenable to be tested in clinical trials as monotherapy, or in combination with chemotherapy and/or ICI, is mandatory to allow for development of new and more effective strategies for BC management.

**References**

1. Sung H, Ferlay J, Siegel RL, Laversanne M, Soerjomataram I, Jemal A, et al. Global Cancer Statistics 2020: GLOBOCAN Estimates of Incidence and Mortality Worldwide for 36 Cancers in 185 Countries. CA Cancer J Clin. 2021;71(3):209-49.

2. Cumberbatch MGK, Jubber I, Black PC, Esperto F, Figueroa JD, Kamat AM, et al. Epidemiology of Bladder Cancer: A Systematic Review and Contemporary Update of Risk Factors in 2018. Eur Urol. 2018;74(6):784-95.

3. Amin MB, Edge SB, Greene FL, Byrd DR, Brookland RK, Washington MK, et al. AJCC Cancer Staging Manual: Springer International Publishing; 2018.

4. Powles T, Bellmunt J, Comperat E, De Santis M, Huddart R, Loriot Y, et al. Bladder cancer: ESMO Clinical Practice Guideline for diagnosis, treatment and follow-up. Ann Oncol. 2022;33(3):244-58.
5. Rhea LP, Mendez-Marti S, Kim D, Aragon-Ching JB. Role of immunotherapy in bladder cancer. Cancer Treat Res Commun. 2021;26:100296.
6. Hussain SA, Birtle A, Crabb S, Huddart R, Small D, Summerhayes M, et al. From Clinical Trials to Real-life Clinical Practice: The Role of Immunotherapy with PD-1/PD-L1 Inhibitors in Advanced Urothelial Carcinoma. Eur Urol Oncol. 2018;1(6):486-500.
7. Hanahan D. Hallmarks of Cancer: New Dimensions. Cancer Discov. 2022;12(1):31-46.
8. Baylin SB, Jones PA. Epigenetic Determinants of Cancer. Cold Spring Harb Perspect Biol. 2016;8(9).
9. Audia JE, Campbell RM. Histone Modifications and Cancer. Cold Spring Harb Perspect Biol. 2016;8(4):a019521.
10. Miranda Furtado CL, Dos Santos Luciano MC, Silva Santos RD, Furtado GP, Moraes MO, Pessoa C. Epidrugs: targeting epigenetic marks in cancer treatment. Epigenetics. 2019;14(12):1164-76.
11. Ramaiah MJ, Tangutur AD, Manyam RR. Epigenetic modulation and understanding of HDAC inhibitors in cancer therapy. Life Sci. 2021;277:119504.
12. Rubio C, Avendaño-Ortiz J, Ruiz-Palomares R, Karaivanova V, Alberquilla O, Sánchez-Domínguez R, et al. Toward Tumor Fight and Tumor Microenvironment Remodeling: PBA Induces Cell Cycle Arrest and Reduces Tumor Hybrid Cells' Pluripotency in Bladder Cancer. Cancers (Basel). 2022;14(2).
13. Wang SC, Wang ST, Liu HT, Wang XY, Wu SC, Chen LC, et al. Trichostatin A induces bladder cancer cell death via intrinsic apoptosis at the early phase and Sp1-survivin downregulation at the late phase of treatment. Oncol Rep. 2017;38(3):1587-96.
14. Burke B, Eden C, Perez C, Belshoff A, Hart S, Plaza-Rojas L, et al. Inhibition of Histone Deacetylase (HDAC) Enhances Checkpoint Blockade Efficacy by Rendering Bladder Cancer Cells Visible for T Cell-Mediated Destruction. Front Oncol. 2020;10:699.
15. Li X, Su X, Liu R, Pan Y, Fang J, Cao L, et al. HDAC inhibition potentiates anti-tumor activity of macrophages and enhances anti-PD-L1-mediated tumor suppression. Oncogene. 2021;40(10):1836-50.
16. Truong AS, Zhou M, Krishnan B, Utsumi T, Manocha U, Stewart KG, et al. Entinostat induces antitumor immune responses through immune editing of tumor neoantigens. J Clin Invest. 2021;131(16).

17. Lodewijk I, Nunes SP, Henrique R, Jerónimo C, Dueñas M, Paramio JM. Tackling tumor microenvironment through epigenetic tools to improve cancer immunotherapy. Clin Epigenetics. 2021;13(1):63.
18. Rabal O, San José-Enériz E, Agirre X, Sánchez-Arias JA, de Miguel I, Ordoñez R, et al. Design and Synthesis of Novel Epigenetic Inhibitors Targeting Histone Deacetylases, DNA Methyltransferase 1, and Lysine Methyltransferase G9a with In Vivo Efficacy in Multiple Myeloma. J Med Chem. 2021;64(6):3392-426.
19. Earl J, Rico D, Carrillo-de-Santa-Pau E, Rodríguez-Santiago B, Méndez-Pertuz M, Auer H, et al. The UBC-40 Urothelial Bladder Cancer cell line index: a genomic resource for functional studies. BMC Genomics. 2015;16(1):403.
20. Livak KJ, Schmittgen TD. Analysis of relative gene expression data using real-time quantitative PCR and the 2(-Delta Delta C(T)) Method. Methods. 2001;25(4):402-8.
21. Ramírez A, Bravo A, Jorcano JL, Vidal M. Sequences 5' of the bovine keratin 5 gene direct tissue- and cell-type-specific expression of a lacZ gene in the adult and during development. Differentiation. 1994;58(1):53-64.
22. Team RC. R: A language and environment for statistical computing. R Foundation for Statistical Computing

2022.
23. Love MI, Huber W, Anders S. Moderated estimation of fold change and dispersion for RNA-seq data with DESeq2. Genome Biol. 2014;15(12):550.
24. Subramanian A, Tamayo P, Mootha VK, Mukherjee S, Ebert BL, Gillette MA, et al. Gene set enrichment analysis: a knowledge-based approach for interpreting genome-wide expression profiles. Proc Natl Acad Sci U S A. 2005;102(43):15545-50.
25. Lambert SA, Jolma A, Campitelli LF, Das PK, Yin Y, Albu M, et al. The Human Transcription Factors. Cell. 2018;172(4):650-65.
26. Robertson AG, Kim J, Al-Ahmadie H, Bellmunt J, Guo G, Cherniack AD, et al. Comprehensive Molecular Characterization of Muscle-Invasive Bladder Cancer. Cell. 2017;171(3):540-56.e25.
27. Lindskrog SV, Prip F, Lamy P, Taber A, Groeneveld CS, Birkenkamp-Demtröder K, et al. An integrated multi-omics analysis identifies prognostic molecular subtypes of non-muscle-invasive bladder cancer. Nat Commun. 2021;12(1):2301.
28. Bankhead P, Loughrey MB, Fernández JA, Dombrowski Y, McArt DG, Dunne PD, et al. QuPath: Open source software for digital pathology image analysis. Sci Rep. 2017;7(1):16878.

29. Huang KC, Chiang SF, Chen WT, Chen TW, Hu CH, Yang PC, et al. Decitabine Augments Chemotherapy-Induced PD-L1 Upregulation for PD-L1 Blockade in Colorectal Cancer. Cancers (Basel). 2020;12(2).
30. Woods DM, Sodré AL, Villagra A, Sarnaik A, Sotomayor EM, Weber J. HDAC Inhibition Upregulates PD-1 Ligands in Melanoma and Augments Immunotherapy with PD-1 Blockade. Cancer Immunol Res. 2015;3(12):1375-85.
31. Zang J, Ye K, Fei Y, Zhang R, Chen H, Zhuang G. Immunotherapy in the Treatment of Urothelial Bladder Cancer: Insights From Single-Cell Analysis. Front Oncol. 2021;11:696716.
32. Singh M, Kumar V, Sehrawat N, Yadav M, Chaudhary M, Upadhyay SK, et al. Current paradigms in epigenetic anticancer therapeutics and future challenges. Semin Cancer Biol. 2022;83:422-40.
33. Hoffmann MJ, Meneceur S, Hommel K, Schulz WA, Niegisch G. Downregulation of Cell Cycle and Checkpoint Genes by Class I HDAC Inhibitors Limits Synergism with G2/M Checkpoint Inhibitor MK-1775 in Bladder Cancer Cells. Genes (Basel). 2021;12(2).
34. Wang C, Hamacher A, Petzsch P, Köhrer K, Niegisch G, Hoffmann MJ, et al. Combination of Decitabine and Entinostat Synergistically Inhibits Urothelial Bladder Cancer Cells via Activation of FoxO1. Cancers (Basel). 2020;12(2).
35. Li QQ, Hao JJ, Zhang Z, Hsu I, Liu Y, Tao Z, et al. Histone deacetylase inhibitor-induced cell death in bladder cancer is associated with chromatin modification and modifying protein expression: A proteomic approach. Int J Oncol. 2016;48(6):2591-607.
36. Kaletsch A, Pinkerneil M, Hoffmann MJ, Jaguva Vasudevan AA, Wang C, Hansen FK, et al. Effects of novel HDAC inhibitors on urothelial carcinoma cells. Clin Epigenetics. 2018;10(1):100.
37. Moore LD, Le T, Fan G. DNA methylation and its basic function. Neuropsychopharmacology. 2013;38(1):23-38.
38. Witjes JA, Bruins HM, Cathomas R, Compérat EM, Cowan NC, Gakis G, et al. European Association of Urology Guidelines on Muscle-invasive and Metastatic Bladder Cancer: Summary of the 2020 Guidelines. Eur Urol. 2021;79(1):82-104.
39. Segovia C, San José-Enériz E, Munera-Maravilla E, Martínez-Fernández M, Garate L, Miranda E, et al. Inhibition of a G9a/DNMT network triggers immune-mediated bladder cancer regression. Nat Med. 2019;25(7):1073-81.
40. Shen Y, Liu L, Wang M, Xu B, Lyu R, Shi YG, et al. TET2 Inhibits PD-L1 Gene Expression in Breast Cancer Cells through Histone Deacetylation. Cancers (Basel). 2021;13(9).
41. Bannister AJ, Kouzarides T. Regulation of chromatin by histone modifications. Cell research. 2011;21(3):381-95.

42. Chen X, Xu R, He D, Zhang Y, Chen H, Zhu Y, et al. CD8(+) T effector and immune checkpoint signatures predict prognosis and responsiveness to immunotherapy in bladder cancer. Oncogene. 2021;40(43):6223-34.
43. Sprooten J, De Wijngaert P, Vanmeerbeerk I, Martin S, Vangheluwe P, Schlenner S, et al. Necroptosis in Immuno-Oncology and Cancer Immunotherapy. Cells. 2020;9(8).
44. Seitz C, Gupta A, Shariat SF, Matsumoto K, Kassouf W, Walton TJ, et al. Association of tumor necrosis with pathological features and clinical outcome in 754 patients undergoing radical nephroureterectomy for upper tract urothelial carcinoma: an international validation study. J Urol. 2010;184(5):1895-900.
45. Chow A, Perica K, Klebanoff CA, Wolchok JD. Clinical implications of T cell exhaustion for cancer immunotherapy. Nat Rev Clin Oncol. 2022;19(12):775-90.
46. Niu Y, Chen J, Qiao Y. Epigenetic Modifications in Tumor-Associated Macrophages: A New Perspective for an Old Foe. Front Immunol. 2022;13:836223.
47. Boyerinas B, Jochems C, Fantini M, Heery CR, Gulley JL, Tsang KY, et al. Antibody-Dependent Cellular Cytotoxicity Activity of a Novel Anti-PD-L1 Antibody Avelumab (MSB0010718C) on Human Tumor Cells. Cancer Immunol Res. 2015;3(10):1148-57.
48. Gubin MM, Esaulova E, Ward JP, Malkova ON, Runci D, Wong P, et al. High-Dimensional Analysis Delineates Myeloid and Lymphoid Compartment Remodeling during Successful Immune-Checkpoint Cancer Therapy. Cell. 2018;175(4):1014-30.e19.
49. Martinez VG, Munera-Maravilla E, Bernardini A, Rubio C, Suarez-Cabrera C, Segovia C, et al. Epigenetics of Bladder Cancer: Where Biomarkers and Therapeutic Targets Meet. Front Genet. 2019;10:1125.
50. He M, He Q, Cai X, Chen Z, Lao S, Deng H, et al. Role of lymphatic endothelial cells in the tumor microenvironment-a narrative review of recent advances. Transl Lung Cancer Res. 2021;10(5):2252-77.
51. Yang D, Liu J, Qian H, Zhuang Q. Cancer-associated fibroblasts: from basic science to anticancer therapy. Exp Mol Med. 2023;55(7):1322-32.
52. Martins-Lima C, Chianese U, Benedetti R, Altucci L, Jerónimo C, Correia MP. Tumor microenvironment and epithelial-mesenchymal transition in bladder cancer: Cytokines in the game? Front Mol Biosci. 2022;9:1070383.
53. Ivashkiv LB. IFNγ: signalling, epigenetics and roles in immunity, metabolism, disease and cancer immunotherapy. Nat Rev Immunol. 2018;18(9):545-58.
54. Quaranta V, Schmid MC. Macrophage-Mediated Subversion of Anti-Tumour Immunity. Cells. 2019;8(7).
55. Aldinucci D, Borghese C, Casagrande N. The CCL5/CCR5 Axis in Cancer Progression. Cancers (Basel). 2020;12(7).

56. Huang CP, Liu LX, Shyr CR. Tumor-associated Macrophages Facilitate Bladder Cancer Progression by Increasing Cell Growth, Migration, Invasion and Cytokine Expression. Anticancer Res. 2020;40(5):2715-24.
57. Li Y, Chen X, Li D, Yang Z, Bai Y, Hu S, et al. Identification of prognostic and therapeutic value of CC chemokines in Urothelial bladder cancer: evidence from comprehensive bioinformatic analysis. BMC Urol. 2021;21(1):173.
58. Fridman WH, Pagès F, Sautès-Fridman C, Galon J. The immune contexture in human tumours: impact on clinical outcome. Nat Rev Cancer. 2012;12(4):298-306.
59. Tham SM, Ng KH, Pook SH, Esuvaranathan K, Mahendran R. Tumor and microenvironment modification during progression of murine orthotopic bladder cancer. Clin Dev Immunol. 2011;2011:865684.

## Supplementary Information

## Supplementary Figures

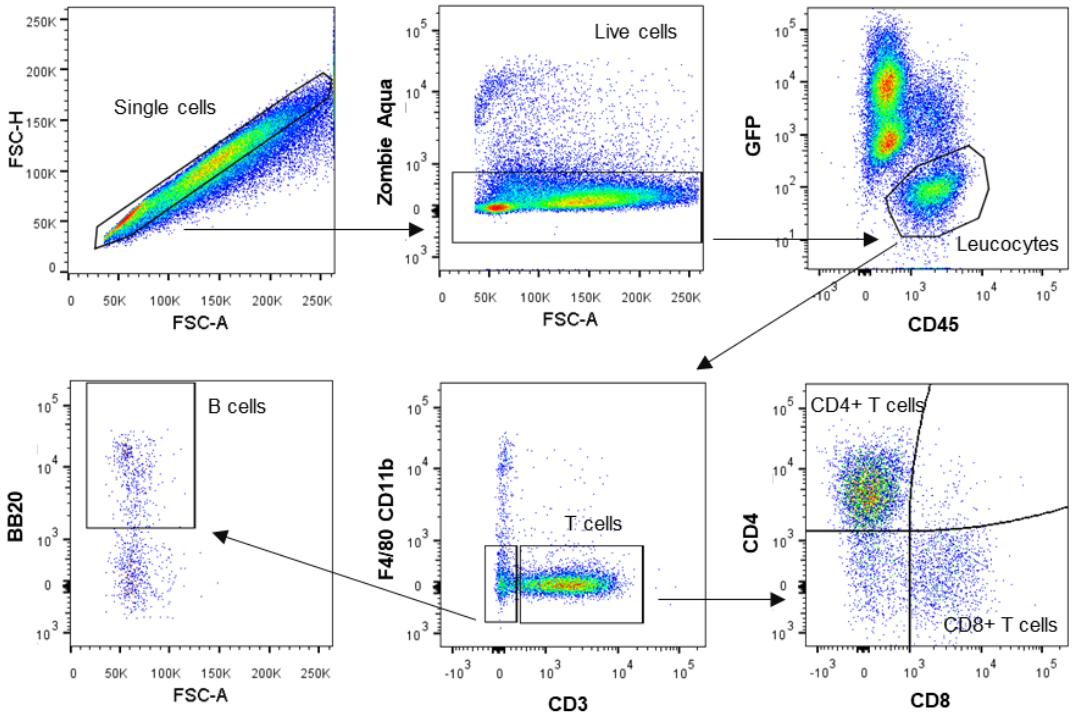


**Figure S1.** Representative gating strategy for tumor T (CD4+ and CD8+) and B cells gated as single cells, live cells, GFP negative CD45 positive, F4/80 CD11b negative CD3 positive, CD4 and CD8 positive for T cells and F4/80 CD11b negative CD3 negative.

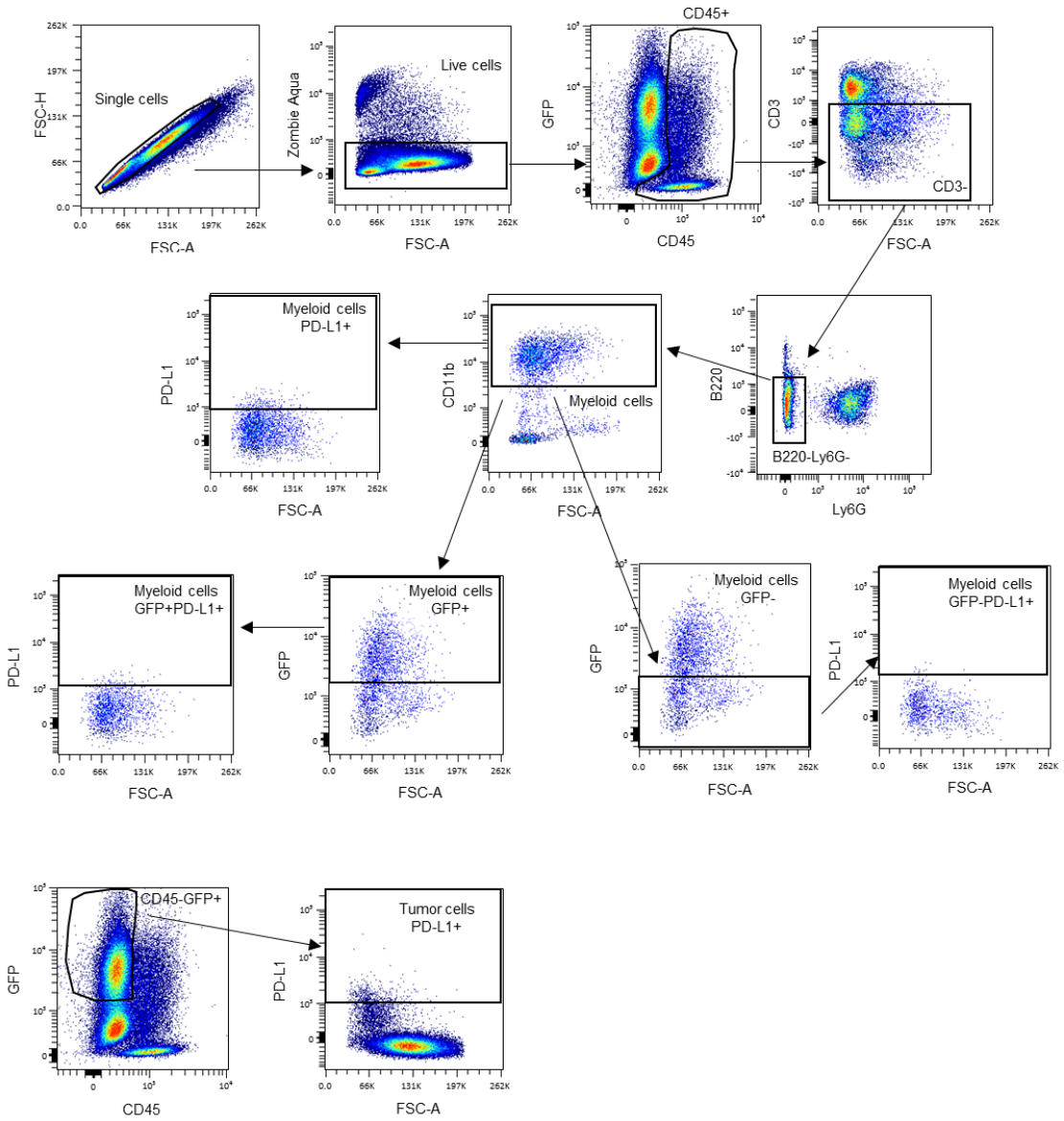


**Figure S2.** Representative gating strategy for tumor myeloid cells gated as single cells, live cells, CD45 positive, CD3, B220 and Ly6G negative, CD11b positive, GFP positive or negative. Tumor cells were gated using single cells, live cells, CD45 negative, GFP positive. PD-L1 levels were evaluated in both myeloid and tumor cells.

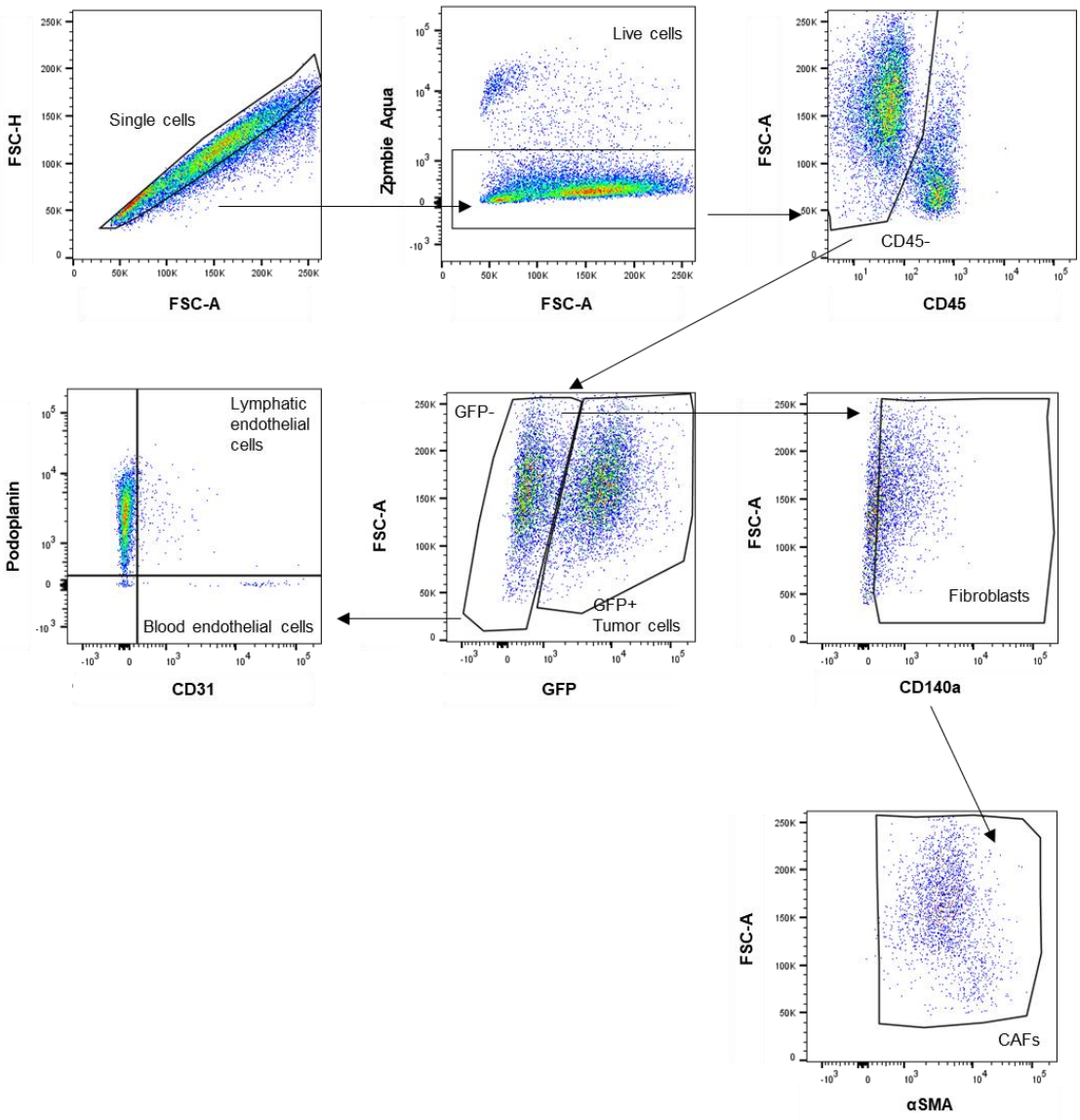


**Figure S3.** Representative gating strategy for fibroblasts, lymphatic and blood endothelial cells as single cells, live cells, CD45 negative, GFP negative, CD31 positive for blood endothelial cells, CD31 positive podoplanin positive for lymphatic endothelial cells. Fibroblasts were gated as GFP negative, CD140a positive. Cancer-associated fibroblasts (CAFs) were defined as GFP negative, CD140a positive and αSMA positive.

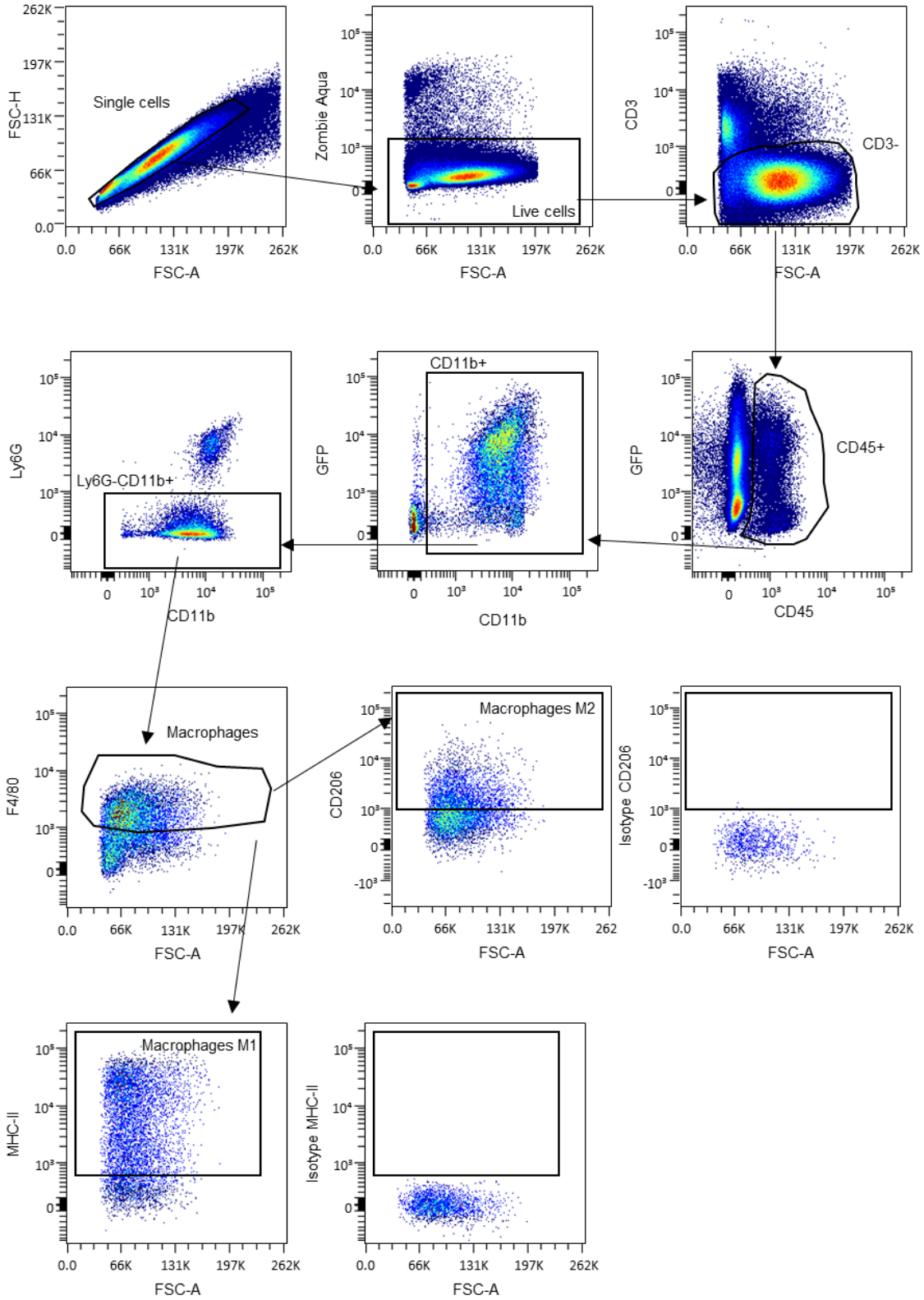


**Figure S4.** Representative gating strategy for tumor macrophages and respective status gated as single cells, live cells, CD3 negative, CD45 positive, CD11b positive, Ly6G negative, F4/80 positive, CD206 positive for M2-like macrophages, MHC-II positive for M1-like macrophages with respective isotype control.

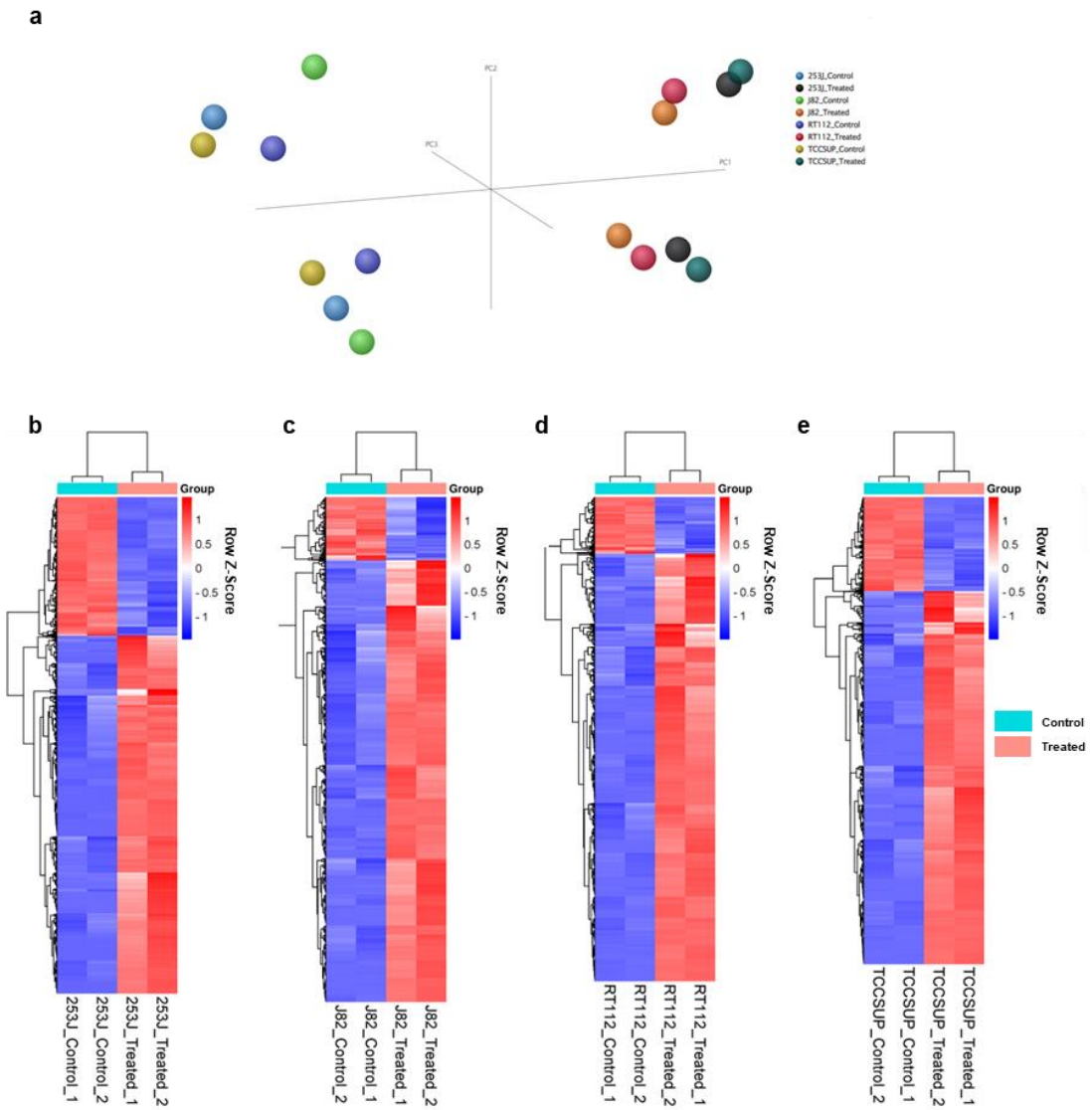


**Figure S5.** (a) Principal component analysis (PCA) graph of 253J, J82, RT112 and TCCSUP together showing the aggrupation of the conditions control vs. treated for each cell line. (b-e) Individual heatmaps of (b) 253J, (c) J82, (d) RT112 and (e) TCCSUP of the dysregulated genes between untreated control vs. treated cells. Genes and groups (control and treated) are hierarchically clustered. Control denotes untreated cells, whereas treated refers to CM-1758 treated cells. Treatment with CM-1758 was given for 48 h with $IC_{50}$ dose calculated for each cell line. Two independent experiments were included for each cell line and condition.

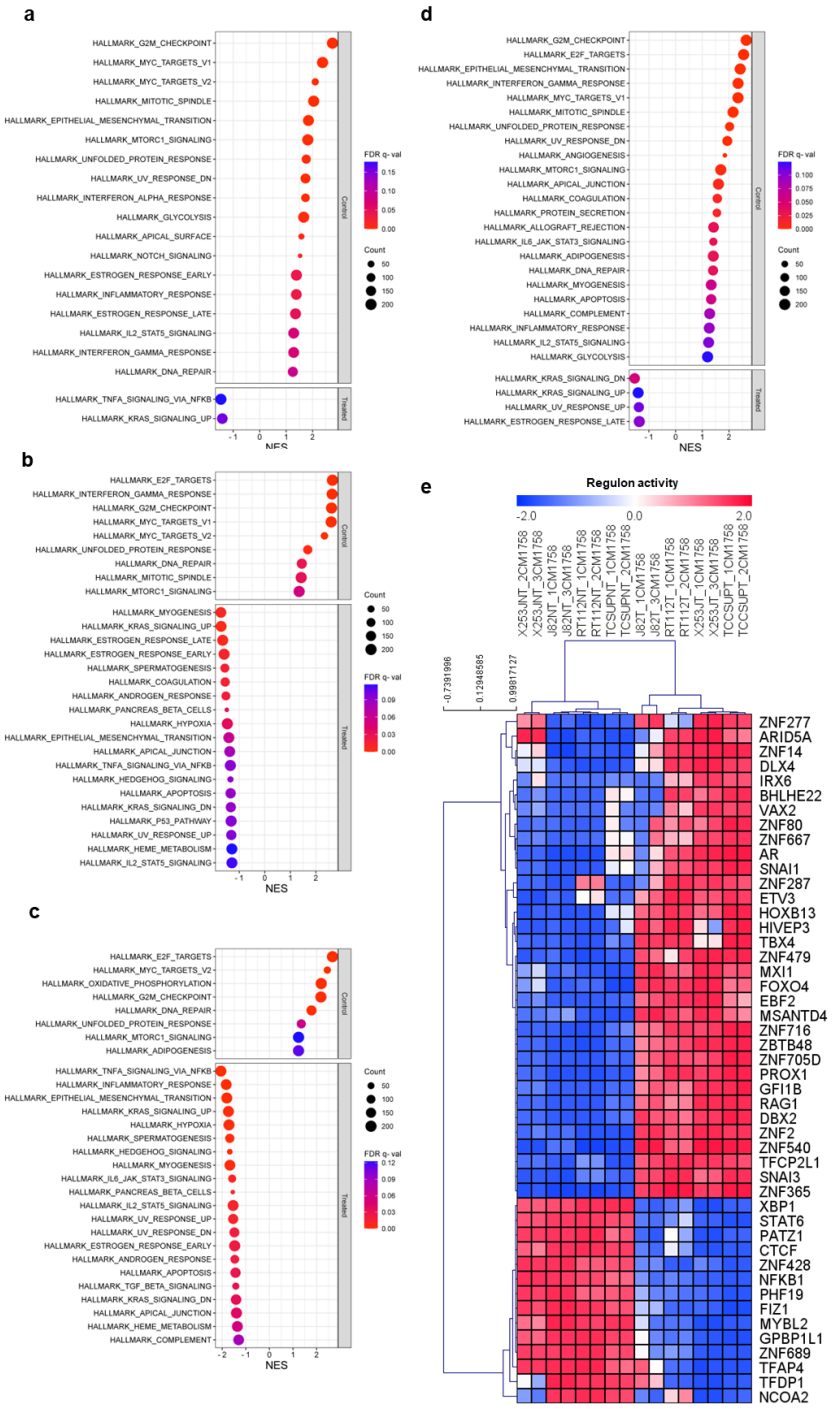


**Figure S6.** Enrichment bubble plot of (a) 253J, (b) J82, (c) RT112 and (d) TCCSUP cells for the hallmark gene signatures of GSEA analysis comparing untreated control cells vs. treated cells with $IC_{50}$ dose of CM-1758 for 48 h. NES – Normalized enrichment score; FDR q-value – False discovery rate q-value; (e) Regulon activity profile for transcription factors hierarchically clustered. Control denotes untreated cells, whereas treated refers to CM-1758 treated cells. Cells were treated the $IC_{50}$ dose of CM-1758 for 48 h.

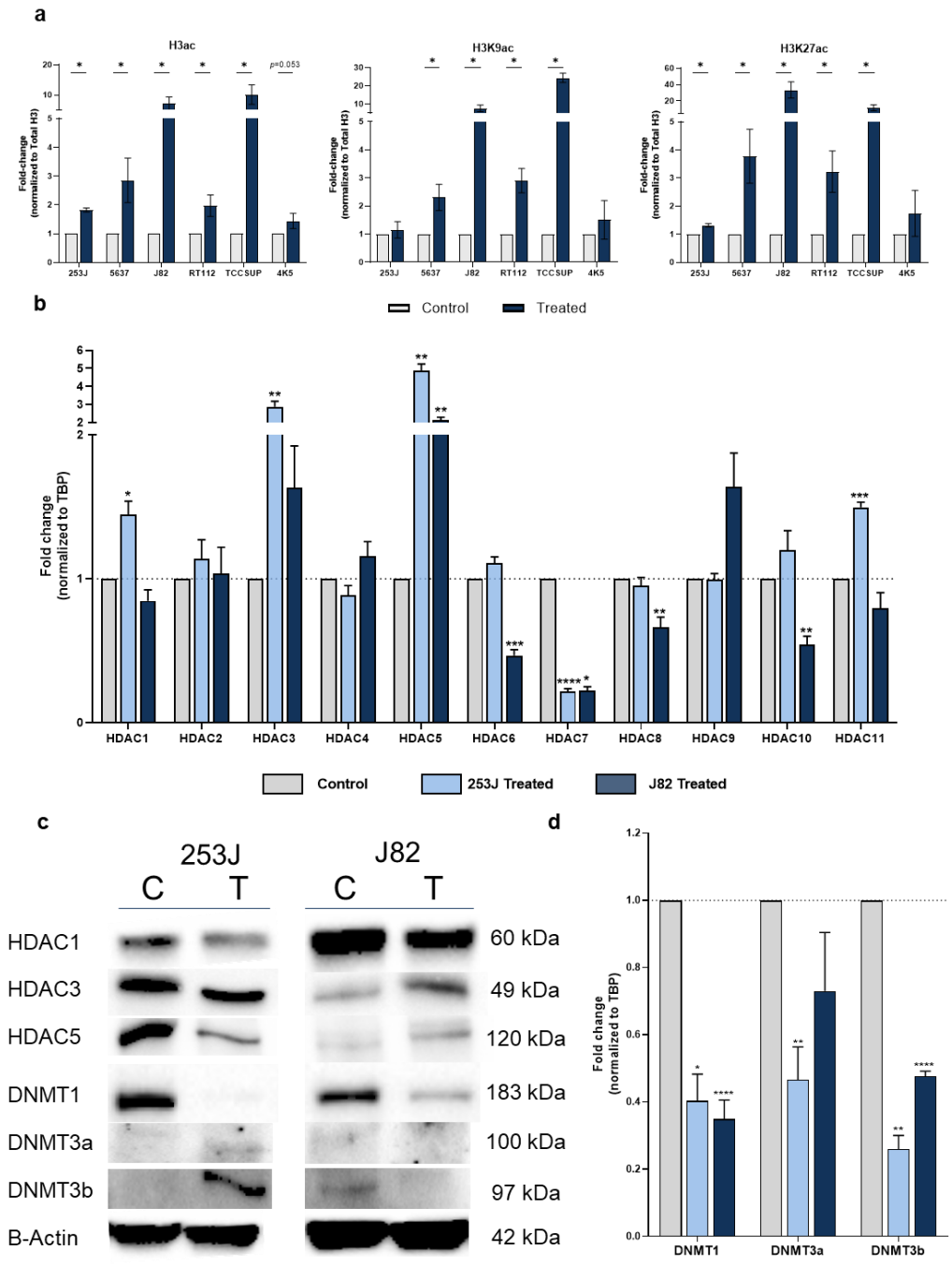


**Figure S7.** (a) Quantification of H3ac, H3K9ac and H3K27ac levels by western blot respect to total H3. Values represented as fold-change respective to control non-treated cells. (b) Relative expression by RT-qPCR of HDAC1 through 11 and (c) Western blot analysis of HDAC1, HDAC3, HDAC5, DNMT1, DNMT3a and DNMT3b with respective β-actin levels for 253J and J82 cells after treatment with CM-1758. (d) DNMT1, DNMT3a and DNMT3b respect to TBP for 253J and J82 cells after treatment with CM-1758. Cells were treated with CM-1758 for 48 h with the $IC_{50}$ dose calculated for each cell line. Data shown are the mean of ≥3 experiments ± SEM. P-values are represented as ns – not significant, *<0.05, **<0.01 and ***<0.001.

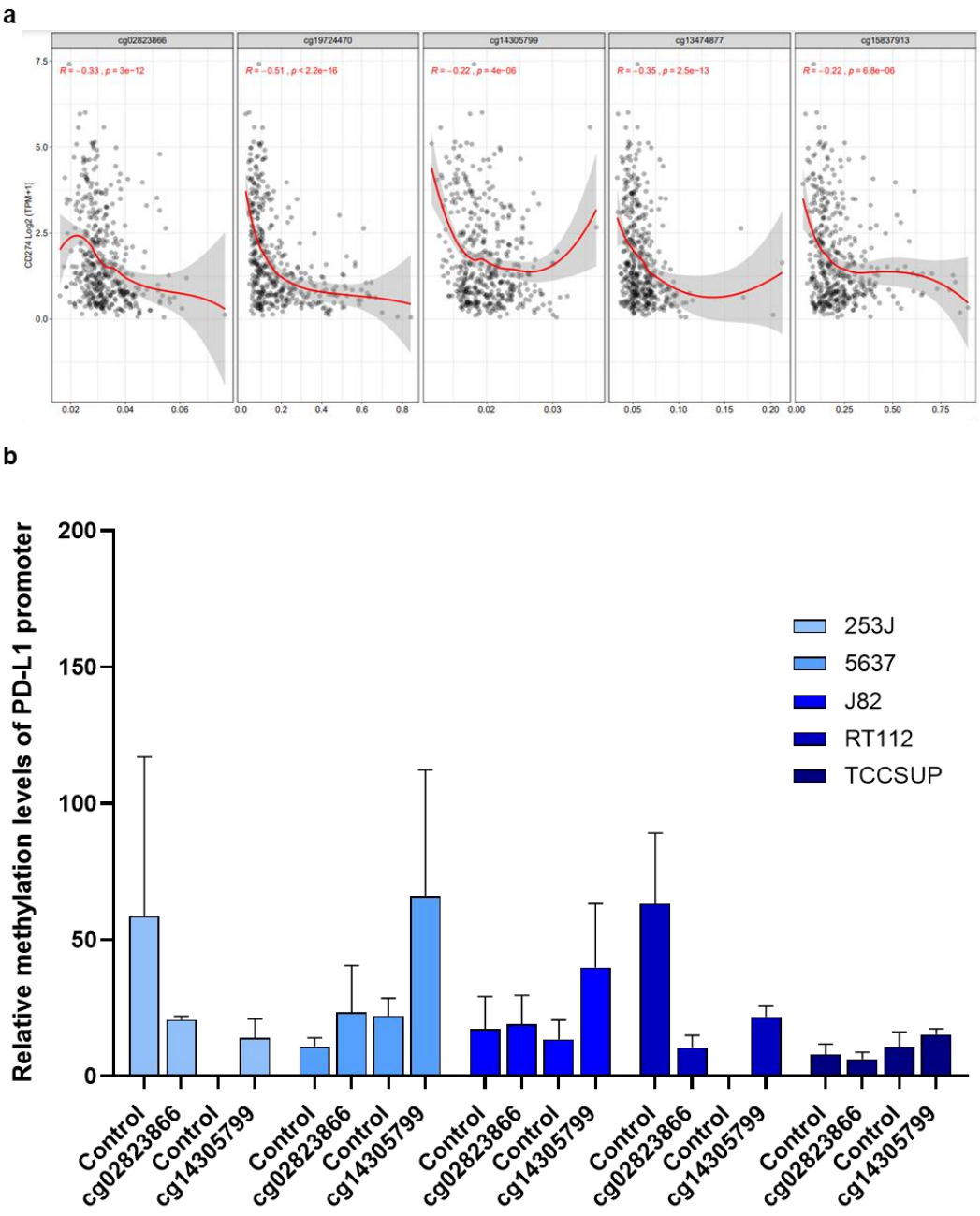


**Figure S8.** (a) CGs associated with PD-L1 expression using the Shiny Methylation Analysis Resource Tool (SMART). Two CGs cg02823866 and cg14305799 were selected for qMSP since they were localized inside a PD-L1 promoter CpG island and it was possible to design primers to specifically amplify these CGs regions of the promoter (b) Relative methylation levels of cg02823866 and cg14305799 in PD-L1 promoter normalized for β-actin x 1000 for easier tabulation. Data shown are the mean of ≥3 experiments ± SEM.

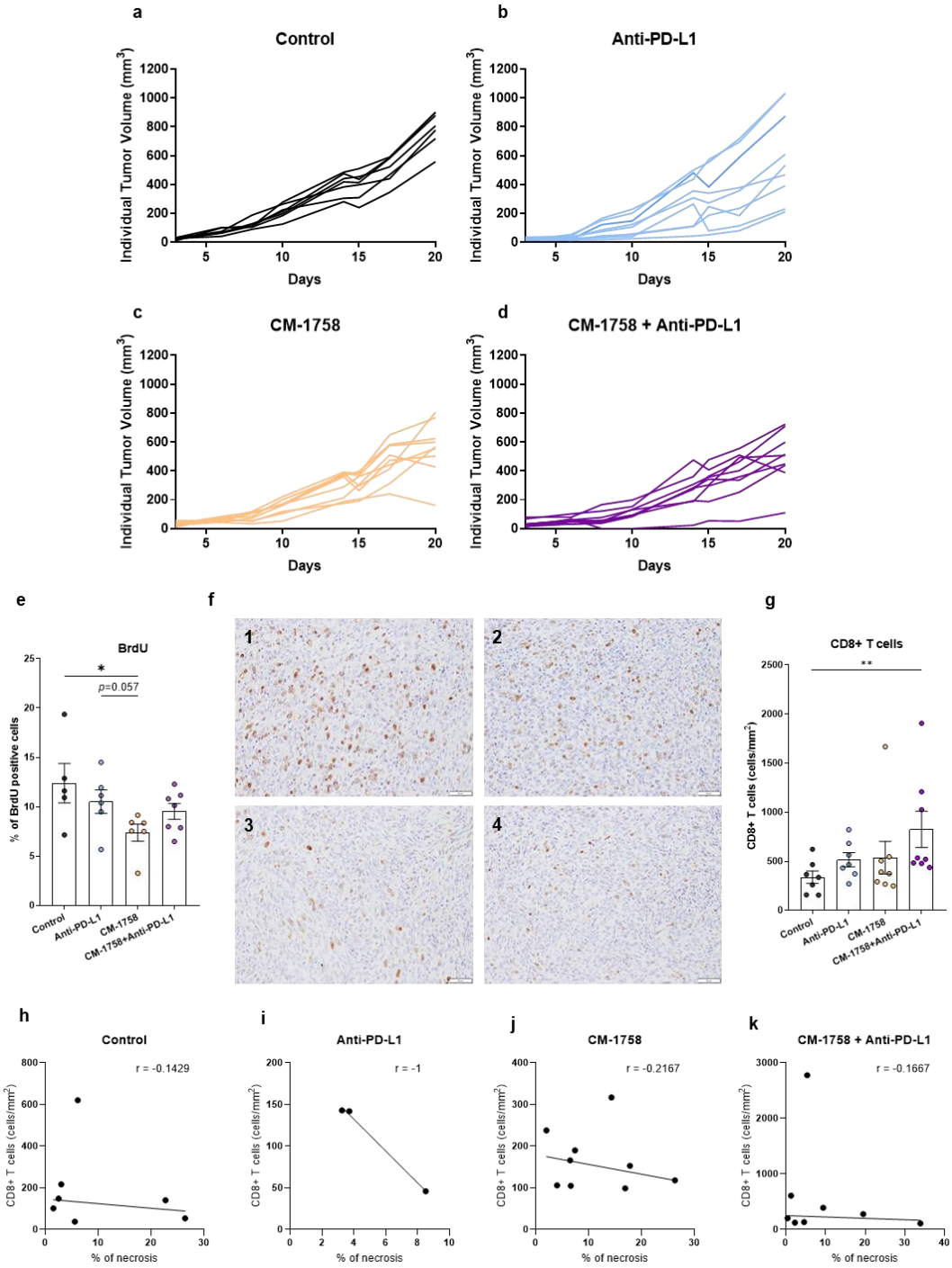


**Figure S9.** (a-d) Individual tumor growth curves respect to the day of 4K5 cells injection of (a) control, (b) anti-PD-L1, (c) CM-1758 and (d) CM-1758+anti-PD-L1. (e) Immunohistochemistry quantification of BrdU positive cells in the different treatment groups presented as percentage of positive cells. (f1-4) Representative immunohistochemistry staining of BrdU in each treatment group included in the study (1 – control; 2 – anti-PD-L1; 3 – CM-1758 and 4 – CM-1758 + anti-PD-L1. (g) Immunohistochemistry quantification of CD8+ T positive cells in the different treatment groups presented as cells/mm$^2$. (h-k) Spearman correlation analysis of CD8+ T cells and percentage of necrosis in (h) control, (i) anti-PD-L1, (j) CM-1758 and (k) CM-1758+anti-PD-L1 with respective Spearman's rank correlation coefficient (r). Graphs show individual values as the mean ± SEM. P-values are represented as ns – not significant, *<0.05 and **<0.01.

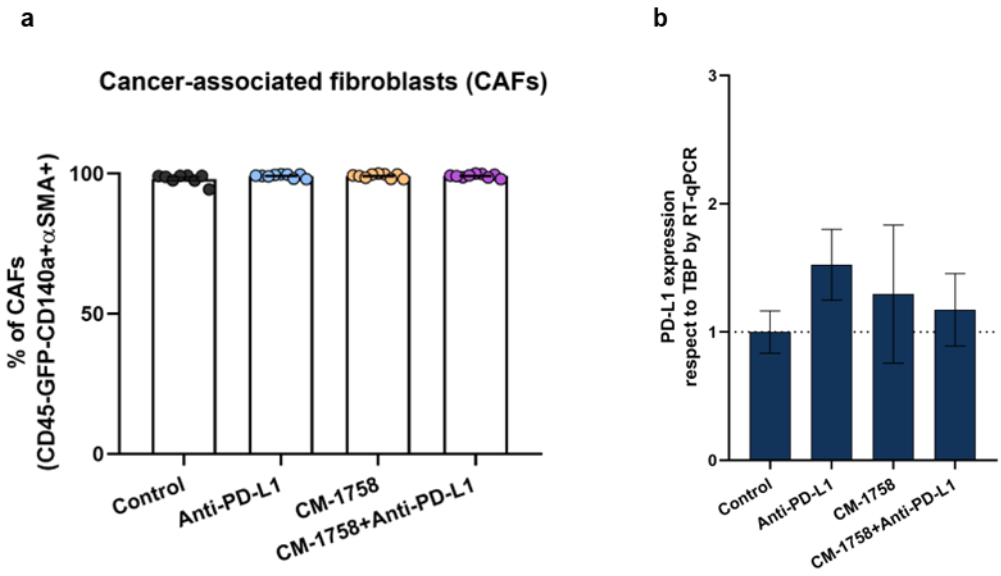


**Figure S10**. (a) Percentage of cancer-associated fibroblasts (CAFs) positive for α-SMA present in the tumor microenvironment gated in CD140a+ cells. (b) Relative expression by RT-qPCR of PD-L1 in respect to TBP in tumors from the groups control, anti-PD-L1, CM-1758 and CM-1758+anti-PD-L1. Graphs show individual values as the mean ± SEM. P-values are represented as ns – not significant.

## Supplementary Tables

**Table S1.** Primers' sequences for RT-qPCR, PD-L1 CUT&RUN and PD-L1 methylation (qMSP). The h before the primer's name denotes human sequence and m mouse sequence. F – Forward; R – Reverse.

| Gene | Primer sequence (5'-3') | | PCR product size |
|---|---|---|---|
| RT-qPCR | | | |
| *hPD-L1* | F | GGCATCCAAGATACAAACTCAA | 76 bp |
| | R | CAGAAGTTCCAATGCTGGATTA | |
| *hHDAC1* | F | CGAATCCGCATGACTCATAA | 93 bp |
| | R | CATCTCCTCAGCATTGGCTT | |
| *hHDAC2* | F | ATGGCGTACAGTCAAGGAGG | 102 bp |
| | R | ATGAGGCTTCATGGGATGAC | |
| *hHDAC3* | F | GCAAGGCTTCACCAAGAGTC | 92 bp |
| | R | CTGTGTAACGCGAGCAGAAC | |
| *hHDAC4* | F | CGTGGAAATTTTGAGCCATT | 98 bp |
| | R | CTGGTCTCGGCCAGAAAGT | |
| *hHDAC5* | F | GGGAACCATCCTTGGAAATC | 97 bp |
| | R | GAACTGGGCATGGCTCTTG | |
| *hHDAC6* | F | CCGGAGGGTCCTTATCGTAG | 100 bp |
| | R | GCGGTGGATGGAGAAATAGA | |
| *hHDAC7* | F | CTCTCTGTGGGCATCCTGG | 87 bp |
| | R | GGTTCCAGAGCCTTAGAGATTC | |
| *hHDAC8* | F | ATACTTGACCGGGGTCATCC | 101 bp |
| | R | GCGTGATTTCCAGCACATAA | |
| *hHDAC9* | F | GCAGAGGAAGAGCTTCAGGG | 79 bp |

| | | | |
|---|---|---|---|
| | R | TGTCGCTCCTAGTGCTGTTG | |
| *hHDAC10* | F | TGAACATCAGGGGCAAGGAG | 92 bp |
| | R | GATGCAGCTCAGGAAACCAC | |
| *hHDAC11* | F | GCACACGAGGCGCTATCTTA | 94 bp |
| | R | AAGGAAGTTGGGGAGGAAGA | |
| *hDNMT1* | F | CAAACCCCTTTCCAAACCTC | 86 bp |
| | R | TAATCCTGGGGCTAGGTGAA | |
| *hDNMT3a* | F | CCTGAAGCCTCAAGAGCAGT | 94 bp |
| | R | TGGTCTCCTTCTGTTCTTTGC | |
| *hDNMT3b* | F | AAGCGACAGGCTATGTCTGG | 90 bp |
| | R | CAGTGCCACCAGTTTGTCTG | |
| *hTBP* | F | AGTGAAGAACAGTCCAGACTG | 194 bp |
| | R | CCAGGAAATAACTCTGGCTCAT | |
| *mPD-L1* | F | GTTGTTCCTCATTGTAGTGTCCA | 77 bp |
| | R | CACATTTCTCCACATCTAGCATTC | |
| *mTBP* | F | GGGAGAATCATGGACCAGAA | 90 bp |
| | R | GATGGGAATTCCAGGAGTCA | |
| qMSP | | | |
| *hPD-L1* cg02823866 | F | AAAGTTTTCGTCGATTTTATCG | 116 bp |
| | R | ACTCAACGTTACGCCAAACC | |
| *hPD-L1* cg14305799 | F | CGTTTCGCGCGGTTTTAG | 150 bp |
| | R | ACCCTCCGTCCTAAAATACCCAA | |
| *hACTB* | F | TGGTGATGGAGGAGGTTTAGTAAG | 132 bp |
| | R | ACCAATAAAACCTACTCCTCCCTTAA | |
| CUT&RUN | | | |
| *hPD-L1* Region 1 | F | ACTGAAAGCTTCCGCCGATT | 74 bp |
| | R | CCCAAGGCAGCAAATCCAGT | |
| *hPD-L1* Region 2 | F | GGGGGACGCCTTTCTGATAA | 89 bp |
| | R | AAGCCAACATCTGAACGCAC | |
| *hPD-L1* Region 3 | F | CTTTGGCGGATCACTTGAGG | 67 bp |
| | R | TATCCCGCGCTGAACTTCTA | |
| *hPD-L1* Region 4 | F | GCTGGGCCCAAACCCTATT | 62 bp |
| | R | TTTGGCAGGAGCATGGAGTT | |

**Table S2.** Primary and secondary antibodies used for western blot, immunofluorescence, immunohistochemistry.

| Western Blot | | | |
|---|---|---|---|
| Primary antibody | Dilution | Secondary antibody | Company |
| H3ac (polyclonal) | 1:1000 | Anti-rabbit | Millipore 06-599 |
| H3K9ac (C5B11) | 1:1000 | Anti-rabbit | Cell Signaling #9649 |
| H3K27ac (polyclonal) | 1:1000 | Anti-rabbit | Cell Signaling #4353 |
| Total H3 (96C10) | 1:10 000 | Anti-mouse | Cell Signaling |

| | | | | |
|---|---|---|---|---|
| | | | #3638 | |
| HDAC1 (5C11) | 1:1000 | Anti-mouse | Sigma SAB1400121 | |
| HDAC3 (Y415) | 1:750 | Anti-rabbit | Abcam 32369 | |
| HDAC5 (B-11) | 1:500 | Anti-mouse | Santa Cruz sc-133106 | |
| DNMT1 (60B12201) | 1:500 | Anti-mouse | Abcam 176145 | |
| DNMT3a (D23G1) | 1:250 | Anti-rabbit | Cell Signaling #3598 | |
| DNMT3b (polyclonal) | 1:500 | Anti-rabbit | Abcam 2851 | |
| β-actin (polyclonal) | 1:10 000 | Anti-mouse | Abcam 8227 | |
| Immunofluorescence | | | | |
| Primary antibody | Dilution | Secondary antibody | Company | |
| 5-methylcytosine (33D3) | 1:100 | Anti-mouse | Sigma MABE146 | |
| Immunohistochemistry | | | | |
| Primary antibody | Dilution | Secondary antibody | Company | |
| BrdU (BMC9318) | 1:10 | Anti-mouse | Roche 11170376001 | |
| CD8 (EPR21769) | 1:400 | Anti-rabbit | Abcam ab217344 | |
| Ki67 (polyclonal) | 1:250 | Anti-rabbit | Abcam ab15580 | |
| Secondary antibodies | | | | |
| Antibody | Conjugate | Technique | Dilution | Company |
| IgG mouse (polyclonal) | Peroxidase | Western blot | 1:10 000 | Jackson 715-035-151 |
| IgG rabbit (polyclonal) | Peroxidase | Western blot | 1:10 000 | Amersham NA 934 |
| IgG mouse (polyclonal) | Alexa Fluor 594 | Immunofluorescence | 1:1000 | Invitrogen A11005 |
| IgG mouse (polyclonal) | Biotin | Immunohistochemistry | 1:1000 | Jackson 715-065-151 |
| IgG rabbit (polyclonal) | Biotin | Immunohistochemistry | 1:1000 | Jackson 711-065-152 |

**Table S3.** Antibodies used for cell population characterization by flow cytometry.

| Epitope | Fluorochrome | Company | Reference |
|---|---|---|---|
| CD45 (30-F11) | PerCP | Biolegend | 103130 |
| CD3 (145-2C11) | PE | BD | 553064 |
| CD3 (17A2) | APC-Cy7 | Biolegend | 100222 |
| CD8a (53-6.7) | APC-Cy7 | Biolegend | 100714 |
| CD4 (RM4-5) | BV711 | Biolegend | 100550 |
| CD45R/B220 (RA3-6B2) | PEFire700 | Biolegend | 103280 |
| F4/80 (BM8) | APC | Biolegend | 123116 |
| F4/80 (BM8) | BV605 | Biolegend | 123149 |
| CD11b (M1/70) | A647 | Biolegend | 101218 |
| CD11b (M1/70) | PE | BD | 553311 |
| Ly6G (1A8) | BV421 | BD | 562737 |
| I-A/I-E MHC-II (M5/114.15.2) | PECy7 | eBioscience | 25-5321-82 |
| I-A/I-E MHC-II (M5/114.15.2) | BV711 | Biolegend | 107643 |
| PD-L1/CD274 (MIH5) | BV711 | BD | 563369 |
| CD31 (390) | PECy7 | Biolegend | 102418 |
| PDPN (PMab-1) | A647 | Biolegend | 156204 |
| CD140a (APA5) | BV605 | Biolegend | 135916 |
| CD206 (C068C2) | A647 | Biolegend | 141712 |
| α-SMA (1A4) | Cy3 | Sigma-Aldrich | C6198 |
| Rat IgG2a, λ Isotype Control (B39-4) | BV711 | BD | 563394 |
| Rat IgG2b, κ Isotype Control (RTK4530) | BV711 | Biolegend | 400653 |
| Rat IgG2a, κ Isotype Control (RTK2758) | A647 | Biolegend | 400526 |

**Table S4.** $IC_{50}$ values for each cell line with respective standard deviation (SD).

| Cell Line | $IC_{50}$±SD/μM |
|---|---|
| 253J | 3.7±0.7 |
| 5637 | 0.33±0.08 |
| J82 | 4.8±0.3 |
| RT112 | 3.3±0.2 |
| TCCSUP | 2.4±0.3 |
| 4K5 | 3.1±0.2 |

**Table S5.** Mean concentration (pg/mL) with respective standard deviation and fold-change with respective standard error of the mean value of each cytokine in each treatment group. GM-CSF, IL-10 and IFN-α did not show any differences compared to the control group and were not represented in Figure 5i.

| | Treatment groups | Control | Anti-PD-L1 | CM-1758 | CM-1758 +Anti-PD-L1 |
|---|---|---|---|---|---|
| IFN-γ | Concentration (pg/mL) | 9.1±0.8 | 13±3 | 12±4 | 15±2 |
| | Fold-change | 1 | 1.4±0.1 | 1.3±0.2 | 1.69±0.08 |
| CXCL1 | Concentration (pg/mL) | 87±44 | 120±65 | 86±54 | 92±45 |
| | Fold-change | 1 | 1.4±0.3 | 1.0±0.3 | 1.0±0.2 |
| TNF-α | Concentration (pg/mL) | 22±3 | 28±5 | 26±2 | 26±7 |
| | Fold-change | 1 | 1.3±0.1 | 1.20±0.04 | 1.2±0.1 |
| CCL2 | Concentration (pg/mL) | 130±11 | 143±13 | 194±90 | 142±20 |
| | Fold-change | 1 | 1.09±0.04 | 1.5±0.3 | 1.09±0.07 |
| IL-12 | Concentration (pg/mL) | 11.1±0.5 | 11±1 | 12±1 | 14±4 |
| | Fold-change | 1 | 1.02±0.04 | 1.03±0.05 | 1.2±0.1 |
| CCL5 | Concentration (pg/mL) | 43±17 | 71±36 | 36±14 | 68±24 |
| | Fold-change | 1 | 1.6±0.4 | 0.8±0.1 | 1.6±0.2 |
| IL-1β | Concentration (pg/mL) | 44±3 | 48±8 | 43±2 | 46±4 |
| | Fold-change | 1 | 1.09±0.07 | 0.99±0.02 | 1.05±0.03 |
| CXCL10 | Concentration (pg/mL) | 1392±484 | 2384±814 | 1706±487 | 2146±517 |
| | Fold-change | 1 | 1.7±0.2 | 1.2±0.1 | 1.5±0.1 |
| GM-CSF | Concentration (pg/mL) | 47±0 | 47±0 | 51±4 | 49±4 |
| | Fold-change | 1 | 1±0 | 1.07±0.03 | 1.04±0.03 |
| IL-10 | Concentration (pg/mL) | 249±0 | 254±12 | 250±3 | 256±17 |
| | Fold-change | 1 | 1.02±0.02 | 1.004±0.004 | 1.03±0.03 |
| IFN-β | Concentration (pg/mL) | 3±1 | 4±3 | 3±2 | 2±2 |

| | | | | | |
|---|---|---|---|---|---|
| | Fold-change | 1 | 1.7±0.6 | 1.0±0.3 | 1.0±0.3 |
| IFN-α | Concentration (pg/mL) | 19.9±0.3 | 20±1 | 20.0±0.5 | 20±1 |
| | Fold-change | 1 | 1.02±0.02 | 1.007±0.009 | 1.03±0.02 |
| IL-6 | Concentration (pg/mL) | 25±4 | 24±2 | 29±7 | 28±8 |
| | Fold-change | 1 | 0.95±0.03 | 1.1±0.1 | 1.1±0.1 |

**Supplementary Methods**

*DNA extraction and sodium-bisulfite modification*

For DNA extraction, cell pellets were digested with lysis buffer (Tris-HCl 100 mM pH 8.5, EDTA 5 mM, SDS 0.2%, NaCl 200 mM and proteinase K 500 µg/mL) for 2 h at 55ºC with shaking. Then, isopropanol was added and the DNA pellet was washed two times with ethanol 70% and resuspended in TE buffer (Tris-HCl 10 mM pH 8, EDTA 1 mM). DNA concentration was measured on a Qubit 4 Fluorometer (Thermo Fisher Scientific, USA) using the Qubit DNA broad range assay kit (Thermo Fisher Scientific, USA). Fifty ng of DNA were bisulfite-modified using EZ DNA Methylation-Gold™ Kit (Zymo Research, USA), according to the manufacturer's recommendations. The bisulfite-converted DNA was eluted in 40 µL of sterile distilled water and stored at −80 °C until further use.

*Quantitative methylation-specific PCR (qMSP)*

*PD-L1* promoter methylation levels were evaluated by qMSP using sodium-bisulfite modified DNA. Two CGs of interest in *PD-L1* promoter associated with PD-L1 expression were selected (cg02823866 and cg14305799) using the Shiny Methylation Analysis Resource Tool (SMART). *ACTB* was used as a housekeeping gene and specific primer sequences can be found in Table S1. One µL of modified DNA, 5 µL Xpert Fast SYBR (GRiSP, Portugal) and 0.3 µL of each primer pair were used in the qMSP reaction. Each sample was run in triplicate in 384-well plates in a QuantStudio 12K Flex Real-Time PCR (Thermo Fisher Scientific, USA). A standard curve using the methylated positive control (5x dilution factor) for PCR efficiency evaluation was included, along with a negative non-methylated control. Relative methylation levels were calculated as the ratio between the mean methylation levels of each primers pair and the respective value for *ACTB* for each sample.

## Impact of G9a/DNMT inhibition in combination with immunoth erapy behind an enhanced anti-tumoral response in bladder cancer upon rechallenge

*Research paper 2*

**Sandra P. Nunes**, Ester Munera-Maravilla, Carolina Rubio, Lucia Morales, Iris Lodewijk, Cristian Suárez-Cabrera, Victor G. Martínez, Mercedes Pérez-Escavy, Miriam Pérez-Crespo, Miguel Alonso Sánchez, Edurne San José-Enériz, Xabi Agirre, Felipe Prosper, Antonio Pineda-Lucena, Rui Henrique, Marta Dueñas, Margareta P. Correia, Carmen Jerónimo and Jesús M. Paramio

**Manuscript in preparation**

Author personal contribution:

Technical execution of the work, analysis and interpretation of the results, and manuscript preparation.

**Abstract**

Introduction**:** Epigenetic modifications are pivotal in driving the development and progression of bladder cancer (BC), influencing the tumor microenvironment. A G9a/DNMT inhibitor, CM-272, was shown to have anti-tumor effects in combination with immune checkpoint blockade in a BC mouse model, with no significant tumor reappearance one month after completing the combination treatment. Hence, the aim of this study was to further uncover the mechanisms underlying the sustained anti-tumoral effects observed with CM-272 in combination with anti-PD-L1.

Materials and Methods: Using an immunocompetent syngeneic mouse model of metastatic BC (*Pten*$^{F/F}$; *Trp53*$^{F/F}$, DKO), 4K5 cells, previously established from a mouse bladder tumor (*Pten*$^{-/-}$; *Trp53*$^{-/-}$), were injected subcutaneously and treatment with CM-272, anti-PD-L1 or combination was applied (1$^{st}$ challenge). Next, tumors were surgically removed, and, after recovery, mice were rechallenged with either 4K5 or a distinct syngeneic mouse BC cell line originating from the same DKO strain (3K20) (2$^{nd}$ challenge). All tumors were harvested for histological and flow cytometry analyses. Additionally, 4K5 cells were treated *in vitro* with CM-272 and the transcriptomic profile was evaluated.

Results: Upon rechallenge, mice inoculated with the same cell line as in the 1$^{st}$ tumor challenge did not display tumor growth in control nor treated groups, indicating the generation of immunity against these cells. In contrast, the growth of 3K20 tumor cells was prevented preferentially in animals previously treated with anti-PD-L1, CM-272 or combination, indicating an enhanced immune response upon treatment. In the rechallenged mice, we observed that tumors collected from mice previously treated with CM-272 and anti-PD-L1 exhibited higher infiltration of CD8+ T cells and M1-like macrophages than control mice. Distinct transcriptomic profiles were evident between 4K5 control, 4K5 treated with CM-272 and 3K20 cells, revealing an enrichment of immune-related pathways in 4K5 treated cells.

Conclusions: The increased tumor elimination upon rechallenge in CM-272 and anti-PD-L1 pre-treated mice underscores an enhanced immune response against distinct BC cell lines post-treatment. Next, we explored the immune memory compartment, unraveling key immune mechanisms behind these findings.

**Keywords**

Bladder cancer, G9a/DNMT inhibitor, epigenetics, immunotherapy, tumor microenvironment, rechallenge.

## Introduction

Bladder cancer (BC) represents a major global health issue, raking as the 10th most frequent cancer worldwide (1). Although most of BC patients present non-muscle invasive bladder cancer (NMIBC) at the time of diagnosis, a significant percentage of NMIBC patients recur or progress to a more aggressive stage of the disease after treatment (2). Additionally, about 25% present an advanced stage of the disease at diagnosis, either muscle invasive (MIBC) or metastatic, being the latter associated with 7% of survival at 5 years (3). The therapeutic options for advanced BC remain few and invasive, consisting of cystectomy in association or not with chemotherapy and immunotherapy (4). Although the implementation of immunotherapy with immune checkpoint inhibitors (ICI) as an option for patients that are refractory or ineligible for chemotherapy treatments improved the prognosis, the success rate remains low (5). Gaining insight into the mechanisms underlying the response to ICI and exploring new therapeutic venues could open doors to novel strategies for these patients.

Alterations in epigenetic marks including histone modifications and DNA methylation play a pivotal role in cancer development by regulating genes expression (6). G9a (EHMT2), a histone methyltransferase that establishes and maintains the H3K9 dimethylation (H3K9me2) mark, is closely associated both with normal and pathological processes, including cancer (7). In fact, G9a is overexpressed in advanced-stage and recurrent or progressive bladder tumors, being associated with poor prognosis (8). Furthermore, G9a-mediated H3K9 dimethylation has been linked to cancer drug resistance, reducing the effectiveness of chemotherapy and targeted therapies (9). On the other hand, DNA methyltransferases (DNMTs) are responsible for establishing and maintaining DNA methylation patterns, contributing for cancer development (10). Though targeting DNMTs has emerged as a promising therapeutic approach for cancer treatment, the clinical application of DNMT inhibitors poses significant challenges due to the associated side effects. Moreover, their anti-tumoral effects on solid tumors is still a subject of extensive study (11).

Recently, CM-272, a new dual G9a/DNMT1 inhibitor, was described as a potent therapeutic agent against cancer (12). CM-272 impairs the activity of these enzymes by binding to their catalytic center, leading to a reduction of DNA methylation and H3K9me2 levels (12). Indeed, CM-272 was shown to have anti-tumoral effects in hematological malignancies (12), prostate cancer (13), hepatocellular carcinomas (14) and BC (8). Specifically, CM-272 led to an inhibition of cell proliferation, cell cycle arrest and induction of apoptosis and autophagy in BC cell lines, also increasing the expression of interferon alpha and gamma, and PD-L1 (8). In a quadruple-knockout (QKO) transgenic mouse

model of metastatic BC, treatment with CM-272 and anti-PD-L1 led to an increase in tumor immune infiltration and promoted a sustained anti-tumoral response in time. Indeed, mice treated with CM-272 and anti-PD-L1 combination that were maintained without treatment for 28 days did not display significant tumor regrowth or metastases (8).

Thus, our main goal is to uncover the mechanisms underlying the sustained anti-tumoral effects observed with CM-272 in combination with anti-PD-L1 in BC. Firstly, an immunocompetent syngeneic mouse model of metastatic BC was injected with 4K5 cells and treated with anti-PD-L1, CM-272 or the combination of both (1$^{st}$ challenge). The remaining tumors were removed surgically, and the same mice were rechallenged either with the same cell line 4K5 or a different syngeneic mouse BC cell line 3K20 (2$^{nd}$ challenge). Interestingly, upon rechallenge, mice previously treated with anti-PD-L1, CM-272, or the combination of both, showed increased elimination of tumors, compared with mice that did not receive any treatment during 1$^{st}$ challenge. Furthermore, 2$^{nd}$ challenge tumors from combination-treated displayed higher tumor immune infiltration.

## Material and Methods

### *Cell culture*

Two mouse primary bladder tumor cell lines, 4K5 *(Pten$^{-/-}$*; *Trp53$^{-/-}$*; Adeno-Krt5-Cre) and 3K20 (*Pten$^{-/-}$*; *Trp53$^{-/-}$*; Adeno-Krt20-Cre) expressing GFP were included in the study previously established by our group were used (Munera-Maravilla et al., manuscript in preparation). Briefly, double knock-out mice (DKO; *Pten$^{F/F}$*; *Trp53$^{F/F}$*) were inoculated in the bladder with adenoviruses expressing Cre recombinase under the control of the regulatory elements of keratin 5 (Adeno-Krt5-Cre) or keratin 20 (Adeno-Krt20-Cre). After inoculation, the Cre recombinase was expressed in K5 (basal cells) or K20 (intermediate and suprabasal cells) and floxed genes were deleted, leading to tumor development. Tumors were collected and primary cell cultures were established. (Munera-Maravilla et al., manuscript in preparation). 4K5 and 3K20 cells were maintained in DMEM GlutaMAX™ medium (Thermo Fisher Scientific, Waltham, Massachusetts, USA), which was supplemented with 10% fetal bovine serum (FBS) and 1% Antibiotic-Antimycotic solution (Thermo Fisher Scientific). Cells were kept in a humidified chamber at 37°C with 5% $CO_2$. Cell lines were regularly screened for mycoplasma contamination using the Venor®GeM One Step kit (Minerva Biolabs, Berlin, Germany).

*CM-272 half-maximal inhibitory concentration ($IC_{50}$) calculation*

CM-272 (G9a/DNMT inhibitor) was stored in DMSO (Sigma Aldrich, Burlington, Massachusetts, USA) at the concentration of 100 mM at -20°C. The chemical structure was described before (12). The half maximal inhibitory concentration ($IC_{50}$) of CM-272 was calculated for 4K5. Cells were seeded in 96-well plates and treated with concentrations of CM-272 ranging from 0.01 to 10 µM in complete medium after 24 h. Two controls were added per plate, including one with complete medium and another containing 0.01% of DMSO. After 48 h treatment, Cell Proliferation Kit II XTT (Roche, Basel, Switzerland) was used according to the manufacturer's instructions. Absorbance was measured in a Genios Pro microplate reader (Tecan, Männedorf, Switzerland) at 490 nm.

*RNA isolation and RNA-sequencing (RNAseq) sample preparation*

Total RNA was extracted using the miRNAeasy Mini kit (Qiagen, Hilden, Germany), following the manufacturer's protocol. RNA concentration was determined using a Qubit 4 Fluorometer (Thermo Fisher Scientific), with the Qubit RNA broad range assay kit (Thermo Fisher Scientific) and stored at -80ºC. RNA integrity number (RIN) was measured using the Qubit RNA IQ assay kit (Thermo Fisher Scientific) and samples with values higher than 8 were considered suitable for RNA sequencing (RNAseq) analysis. One µg of total RNA was used for library preparation by TruSeq Stranded Total RNA Library with Ribo-Zero Gold kit from Illumina (San Diego, California, USA). RNAseq was performed on the Illumina NovaSeq 6000 platform from Macrogen RNA-seq services (Seoul, South Korea) for 4K5 control, 4K5 treated with $IC_{50}$ dose of CM-272 and 3K20 without any treatment. Three independent biological replicates were sequenced for each condition.

*Animal care and maintenance*

All the animal experiments were conducted according to the European and Spanish regulations in the field. Specifically, European convention ETS 123, regarding the use and protection of vertebrate mammals used in experimentation and other scientific purposes, and Directive 2010/63/UE, Spanish Law 6/2013 and Real Decreto (R.D.) 53/2013 which pertain to the protection and utilization of animals in scientific research. Procedures involving genetically modified organisms were conducted according to the proper European and Spanish Regulations: Directive 2009/41/CE, Spanish Law 9/2003, and R.D. 178/2004. Our protocols received approval from the "Consejería de Medio Ambiente y Ordenación del Territorio y Sostenibilidad" (protocol number PROEX 150.8/21), and all activities followed the ethical standards set forth by

the CIEMAT Animal Experimentation Ethics Committee, following both external and internal biosafety and bio-ethics guidelines.

Mice were housed at the CIEMAT laboratory Animal Facility (registration number ES280790000183) and underwent routine pathogen screening, adhering to recommendations provided by the Spanish Society for the Laboratory Animal Science (SECAL) and the Federation of European Laboratory Animal Science Associations (FELASA, Tamworth, UK). These mice had access to food (TEKLAD Global Diet 2918) and ad libitum access to acidified and filtered (0.2 µm) water. Mice were maintained in cages type IIL, in a maximum of 5 mice per cage. Room conditions included controlled lighting cycles of 12 hours light and 12 hours dark, with temperature and humidity settings maintained at 21±2ºC and 55±10%, respectively.

*Syngeneic graft mouse model and 1$^{st}$ challenge*

We developed immunocompetent double knock-out mice (DKO; *Pten*$^{F/F}$, *Trp53*$^{F/F}$) through a conventional crossing of mice from different collaborators (Netherlands Cancer Institute, Mass. Institute of Technology, Stanford University), resulting in a mixed FVB/129S background. A syngeneic graft mouse model was generated by injecting subcutaneously 3 million of 4K5 cells expressing GFP (resuspended in 100 µL of DMEM) in the right flank of 3–4-month-old male and female DKO mice (1$^{st}$ challenge). Tumor growth was measured 3 times per week using a digital caliper and tumor volume was calculated using the formula $4\pi/3$ x (length/2) x (width/2)$^2$. Upon reaching volumes within the range of 80-90 mm$^3$, mice were randomly divided into four groups: control (n=15), anti-PD-L1 (n=9), CM-272 (n=9), and CM-272+anti-PD-L1 (n=13). CM-272 (5 mg/kg; administered five times a week) and anti-PD-L1 (avelumab; 200 µg/mouse; administered once a week) were delivered via intraperitoneal injection. The combination group followed a phased dosing regimen (see Supplementary Figure 1a). Tumor size data were normalized by subtracting the volume at the beginning of treatment. Percentage of antitumor efficacy was calculated as [T (tumor) / C (control)] x 100 of growth inhibition by anti-PD-L1, CM-272 or the combination.

Following two weeks of treatment, mice underwent surgical tumor removal under inhaled anesthesia (isoflurane; 3% induction, 1.5% maintenance) with $O_2$ (0.8-1 L/min) flow. Mice were prepped through shaving and disinfection with povidone-iodine and 70% ethanol. Post-surgery, enrofloxacin (0.2 mg/animal/day; Baytril) was administered via drinking water for three days as a broad-spectrum antibiotic, and analgesia was provided for 3-4 days through tramadol (0.5-1 mg/animal/day; Tradol) also in the drinking water. For flow cytometry, tumor tissue was embedded in DMEM and held at 4ºC overnight before processing and analysis on the subsequent day. As for histological examination,

tumors were fixed in 3.7-4% buffered formalin overnight at the time of harvest, followed by paraffin embedding. Sections measuring 3-5 µm were stained with hematoxylin and eosin for analysis.

*2nd challenge*

Two months after the surgery, mice from all groups (controls: 4K5 n=7 and 3K20 n=8, and treatments: anti-PD-L1 - 4K5 n=5 and 3K20 n=4, CM-272 - 4K5 n=4 and 3K20 n=5, and CM-272+anti-PD-L1 - 4K5 n=6 and 3K20 n=7; Figures 2a and 3a) were rechallenged with either 4K5 (the same cell line as the 1st challenge) or a distinct syngeneic mouse BC cell line originating from the same DKO strain - 3K20, also expressing GFP (2nd challenge) (Figure 3a). Additionally, mice never challenged with any tumor cells, with the same age as the mice previously included in the study – growth controls – were also included (n=5 for 4K5 and n=5 for 3K20). Three million 4K5 or 3K20 cells were resuspended in 100 µL of DMEM and injected subcutaneously in the left flank of the mice. Tumor growth was monitored 3 times per week using a digital caliper and tumor volume was calculated using the formula previously described. Mice displaying tumor growth two weeks after cell injection were sacrificed, whereas mice not showing or with only residual tumor growth were maintained for 3 months and then sacrificed. All tumors were harvested for flow cytometry analyses and histological analysis as described before.

*Flow cytometry for cell populations analysis*

For the analysis of cellular populations, tumors were minced into small fragments and subjected to enzymatic digestion using a cocktail containing collagenase P (200 µg/mL; Roche), dispase II (800 µg/mL; Roche), and DNase I (100 µg/mL; Roche) in DMEM. The enzymatic digestion process was carried out at 37ºC, with vortexing and mixing every 20 minutes, repeated 3-4 times. Following digestion, the disaggregated tissue was filtered through a 40 µm cell strainer and subsequently centrifuged at 16,100 g for 7 minutes. The harvested cells were resuspended in FACS buffer (0.05% sodium azide, 0.5% bovine serum albumin, PBS). Subsequently, the cells were stained with the viability dye Zombie Aqua (Biolegend) in the dark at room temperature (RT) for 20 minutes. Following staining, the cells were washed and then incubated with a mouse FcR blocking reagent (Milteny Biotec) for 10 minutes in the dark at RT. Next, the antibodies detailed in Supplementary Table S1, were incubated for 30 minutes at 4ºC. Following another round of washing, the cells were fixed using 150 µL of BD Cytofix/Cytoperm™ (BD Biosciences). The fixed cells were then acquired using a BD LSR Fortessa flow cytometer on the following day. Data analysis was performed using

FlowJoTM 10.8.1 software (BD Biosciences) and OMIQ (Dotmatics, Boston, Massachusetts, USA). Gating strategy was performed as described before in Research paper 1.

*Bioinformatic analyses*

Differential analyses of the RNAseq data were conducted utilizing the DESeq2 software package (version 1.38.2) within the R software (15, 16). We conducted Gene Set Enrichment Analysis (GSEA) version 4.3.2 and referenced Molecular Signature Database (MSigDB) for comparing 4K5 control and treated with CM-272 conditions (17). Specifically, we used the gene set collection analysis based on the mh.all.v2023.1.Mm.symbols.gmt dataset (Hallmarks). GSEA was performed using 1000 permutations and the maximum and minimum sizes for gene sets were 500 and 15, respectively. Enrichment bubble plots from SRplot were used to represent GSEA data (http://www.bioinformatics.com.cn/srplot).

Genes exhibiting a log2(fold change) greater than 2 for upregulated genes and less than -2 for downregulated genes, along with a p-value adjustment less than 0.01, were selected for subsequent Venn diagram. Venn diagrams were generated using SRplot. Principal component analysis (PCA) was performed using the "prcomp" command within the R software, employing the normalized matrix obtained through DESeq2. The resulting PCA plot was plotted using the Cubemaker tool (https://tools.altiusinstitute.org/cubemaker/). Hierarchical clustering was performed using Multi-Experiment Viewer (Mev 4.9.0). Normalized gene expression data were transformed into log2 scale, and the value range was adjusted for each gene. Supervised hierarchical clustering was applied using Pearson correlation and average linkage. Heatmaps were represented using SRplot.

*Statistical analysis*

Normal distribution was assessed using the Shapiro-Wilk test ($p>0.05$). Data displaying normal distribution were analyzed using parametric two-tailed t-test with Levene's test for equality of variances ($p<0.05$, variances considered not equal; $p>0.05$, variances considered equal) whereas non-parametric Mann-Whitney U test was used to compare data not having a normal distribution. Two-tailed p-values calculation were performed using a computer assisted program (SPSS Version 28.0, USA) and graphics were assembled using GraphPad Prim 8.0 software (GraphPad Software, USA). Graphics are represented by mean ± SEM. P-values were considered statistically significant when inferior to 0.05. Significance is depicted as follows: $*p < 0.05$, $**p < 0.01$,

***$p < 0.001$, ****$p < 0.0001$ and ns > 0.05 (non-significant). $IC_{50}$ analysis was performed using GraphPad Prim 8.0 software.

## Results

*CM-272 alone or in combination with anti-PD-L1 displayed anti-tumoral effects during the 1st challenge*

The experimental outline of this study is represented in Figure 1a. Firstly, syngeneic mice were injected subcutaneously in the right flank with 4K5 cells and treated with anti-PD-L1, CM-272 or a combination of both (Supplementary Figure 1a). CM-272 alone and in combination with anti-PD-L1 significantly decreased tumor growth, as seen by the individual growth curves displayed in Figure 1b1-4 and the mean of tumor size for each group shown in Supplementary Figure 1b. Histological analysis showed that those tumors treated with CM-272 immunotherapy or combined displayed prominent necrosis areas (Figure 1c1-4). Moreover, both CM-272 and CM-272+anti-PD-L1 significantly delayed tumor growth, as shown by the percentage of antitumor efficacy (69.7% and 71.2%, respectively) (Figure 1d). No major differences were found regarding the lymphocyte infiltrates among the several treatment groups, except for a decrease in B and CD8+ T lymphocytes in the CM-272-treated mice (Supplementary Figure 2a-h). On the other hand, the levels of PD-L1 detected differed among groups, with the mice treated with anti-PD-L1 alone or in combination with CM-272 were lower in myeloid cells including phagocytic myeloid cells, with no major impact on tumor cells (Supplementary Figure 2 i-k). A higher percentage of macrophages M1-like and phagocytic macrophages was found in the combination group as compared with control and CM-272 treated mice (Supplementary Figure 2l-p).

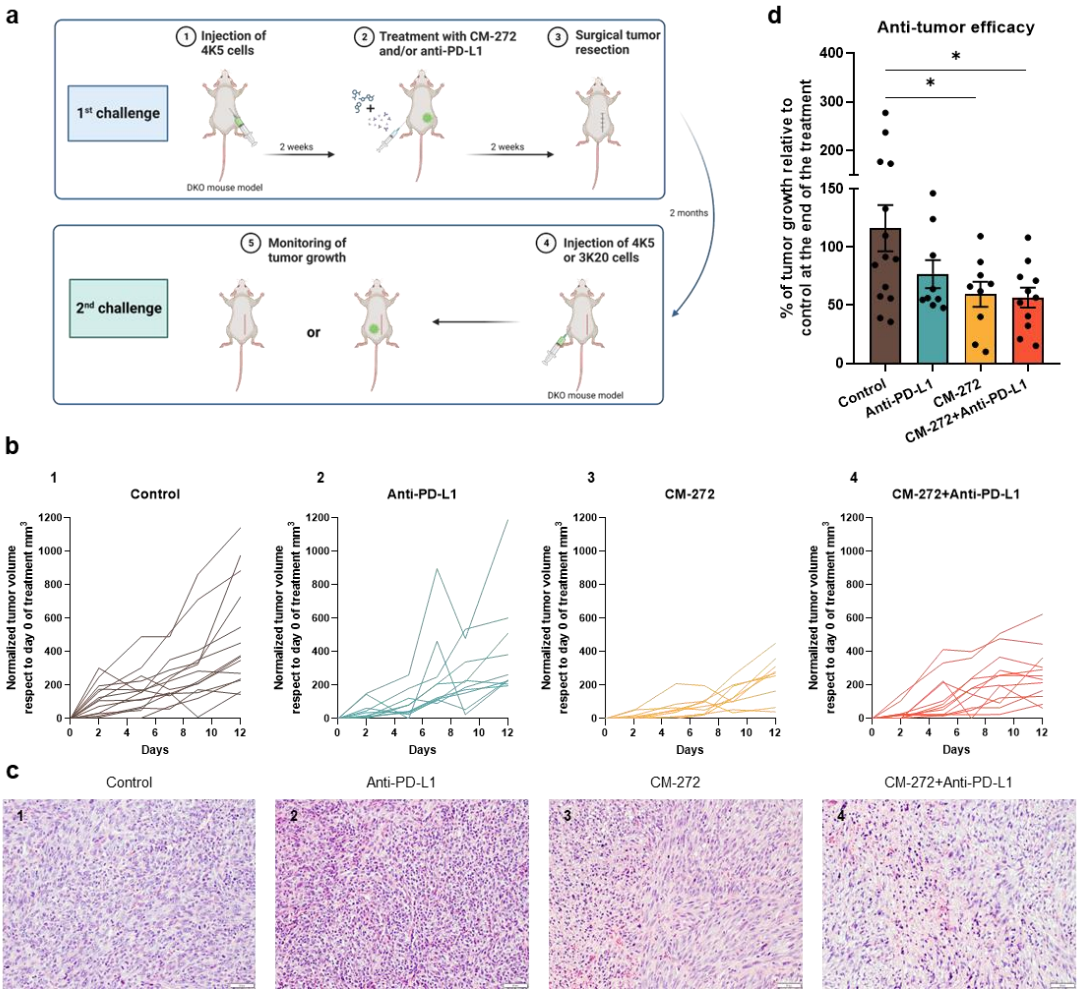


**Figure 1.** Effects of anti-PD-L1, CM-272 or in combination in the 1st challenge. (a) Schematic representation of the experimental protocol for this study. Double knockout mice (*PTEN*$^{F/F}$; *Trp53*$^{F/F}$) were injected subcutaneously with 4K5 cells (1st challenge) and, after tumor formation, mice were treated with anti-PD-L1, CM-272 or combination for 2 weeks. Then, mice were subjected to surgical tumor resection and, after recovery, were again injected with 4K5 cells or another syngeneic mouse bladder cancer cell line 3K20 (2nd challenge). Finally, tumor growth was monitored until mice reaching the experimental endpoint (either sacrifice 2 weeks after cell injection if they presented tumor growth or 3 months after if residual or absence of tumor growth was observed). (b) Normalized individual tumor growth curves after injection with 4K5 cells of (1) control, (2) anti-PD-L1, (3) CM-272 and (4) CM-272 + anti-PD-L1. Day 0 represents the first day of treatment. (c) Representative H&E staining of tumors for (1) control, (2) anti-PD-L1, (3) CM-272 and (4) CM-272 + anti-PD-L1 groups. (d) Anti-tumor efficacy of anti-PD-L1, CM-272 and combination of both. Graph shows individual values as the mean ± SEM for ≥9 mice included in each group. P-values are represented as ns – not significant and *<0.05.

*Treatment with anti-PD-L1 and/or CM-272 during 1st tumor challenge improves tumor control upon a 2nd challenge*

After the 1st challenge and treatment with anti-PD-L1 and CM-272, mice were subjected to surgical tumor resection and, after recovery, the same mice were rechallenged (2nd challenge) with the same cell line as in the 1st challenge, 4K5, or a distinct syngeneic mouse BC cell line originating from the same DKO strain, 3K20 (Figure 1a and 2a). Additionally, age-matched mice that were not previously challenged with BC cells were injected for the first time with 4K5 or 3K20 cells to monitor the expected tumor growth in our experimental conditions, denominated as growth controls (Figure 2a).

Mice rechallenged with the same cell line as the 1st challenge, 4K5, did not display any tumor growth in all groups, indicating the generation of immunity against 4K5 cells (Figure 2b). On the other hand, a heterogenous behavior was observed for mice injected with 3K20 (Figure 2c-d). The growth of 3K20 cells was controlled preferentially in animals previously treated with anti-PD-L1, CM-272 or combination, displaying a higher percentage of mice that eliminate or maintain tumor growth to residual levels (responders) than in control group (Table 1).

**Table 1.** Number and percentage of responders to the 2nd challenge with 4K5 or 3K20 in control, anti-PD-L1, CM-272 and CM-272 + anti-PD-L1 groups. Responders comprise mice that were able eliminate or control tumor growth after the second injection of tumor cells.

| Groups | 2nd challenge | |
|---|---|---|
| | **4K5**<br>n responders/n total<br>(% responders) | **3K20**<br>n responders/n total<br>(% responders) |
| Control | 6/6<br>(100%) | 4/8<br>(50%) |
| Anti-PD-L1 | 5/5<br>(100%) | 3/4<br>(75%) |
| CM-272 | 4/4<br>(100%) | 4/5<br>(80%) |
| CM-272 + Anti-PD-L1 | 6/6<br>(100%) | 4/7<br>(57%) |

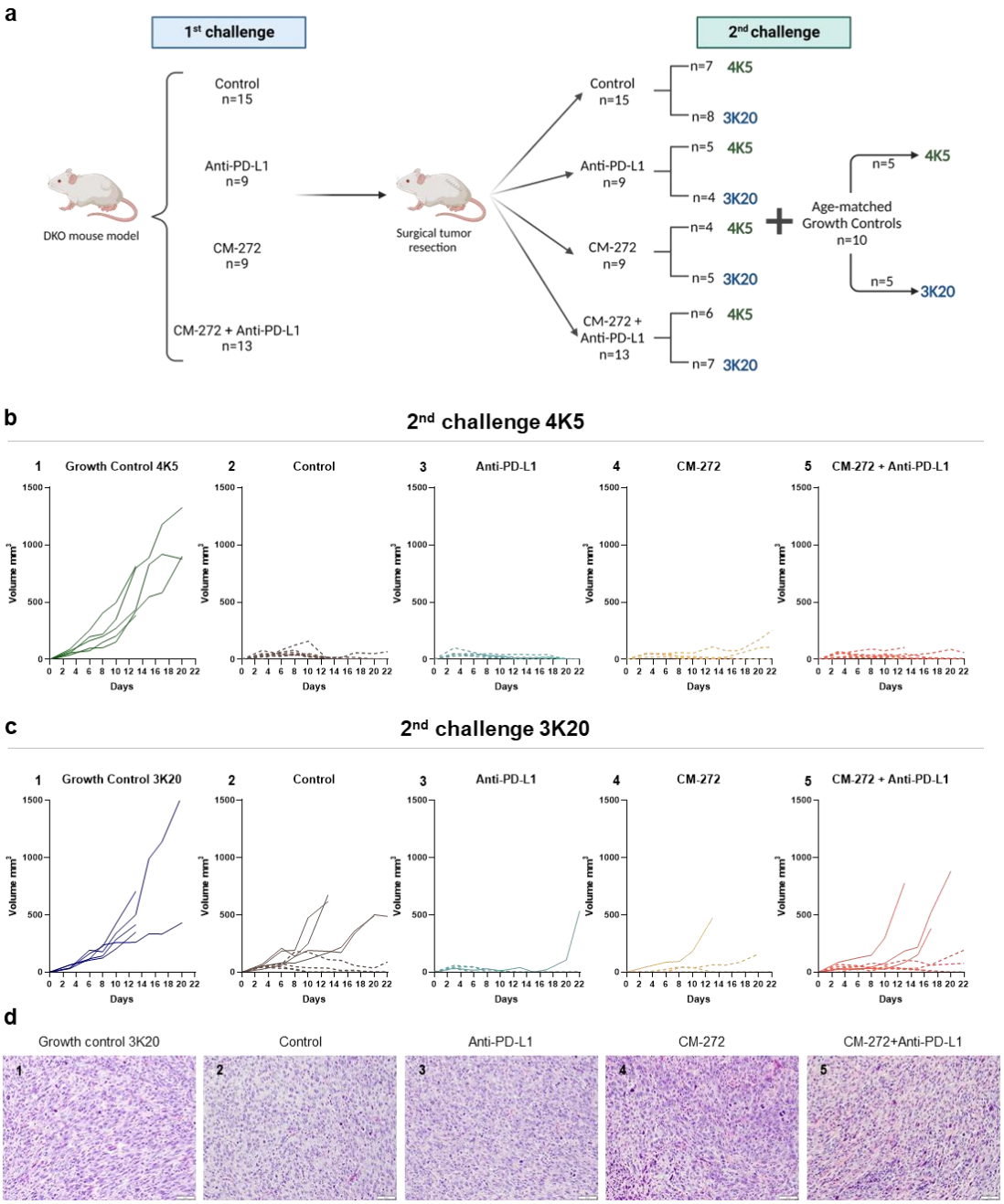


**Figure 2.** Second challenge of bladder cancer cells in mice firstly challenged and treated with CM-272 and/or anti-PD-L1. (a) Schematic representation of number of mice included in each phase of the experimental setting. In the 2nd challenge, mice were injected with either 4K5 or 3K20 cells. Age-matched mice that were never injected with tumor cells before (growth controls) were also include in the study. (b) Individual tumor growth curves after injection with 4K5 cells of (1) growth control, (2) control, (3) anti-PD-L1, (4) CM-272 and (5) CM-272 + anti-PD-L1. (c) Individual tumor growth curves after injection with 3K20 cells of (1) growth control, (2) control, (3) anti-PD-L1, (4) CM-272 and (5) CM-272 + anti-PD-L1. Day 0 represents the day of tumor cells' injection. (d) Representative H&E staining of 3K20 tumors from non-responders (1) growth control, (2) control, (3) anti-PD-L1, (4) CM-272 and (5) CM-272 + anti-PD-L1 groups.

*Responders from CM-272 + anti-PD-L1 combination treatment group displayed higher infiltration of immune cells in 1st challenge tumors*

Next, we aimed to assess whether tumors arising from the 1st challenge exhibited different percentages of tumor immune cells, depending on whether mice were responders and non-responders in the 2nd challenge. Only mice injected with the 3K20 cells in the 2nd challenge were studied, since animals injected with the 4K5 were all responders. A mouse was considered responder (R) when the 2nd tumor was eliminated, or tumor growth was maintained to residual levels. In contrast, a non-responder (NR) mouse, displayed relevant tumor growth in the 2nd challenge, similar to the growth controls.

Overall, responder mice from all groups presented higher levels of total leucocytes and T cells in the 1st tumor, indicating that the mice that became responders upon the 2nd challenge against 3K20 cells presented higher levels of intra-tumoral T cells in the first tumor (4K5) (Figure 3a-b). A higher percentage of CD4+ T cells was found in responder control tumors, whereas the presence of CD8+ T and B cells was higher in the combination CM-272 + anti-PD-L1 treated responder tumors (Figure 3d-e). Tumors from responder mice treated with the combination also showed a tendency towards a higher percentage of myeloid cells, specifically phagocytic myeloid cells, and macrophages (Figure 3f, g and l). Interestingly, a higher proportion of M1-like pro-inflammatory macrophages was found in combination-treated responder tumors, concomitantly with a lower percentage of M2-like anti-inflammatory macrophages (Figure 3m-o). Furthermore, responder tumors displayed higher levels of detected PD-L1 in myeloid, phagocytic myeloid and tumor cells in control mice (Figure 3i-k). Considering that only one tumor was classified as non-responder in the anti-PD-L1 and CM-272 groups, no statistical analysis was performed (Figure 3). Thus, while a general increase in tumor immune cell infiltration was observed in all responders compared to non-responders, those treated with the combination CM-272 + anti-PD-L1 displayed tumors with higher levels of CD8+ T cells, phagocytic myeloid cells, and M1-like macrophages, key immune cell players associated with effective anti-tumoral immune responses.

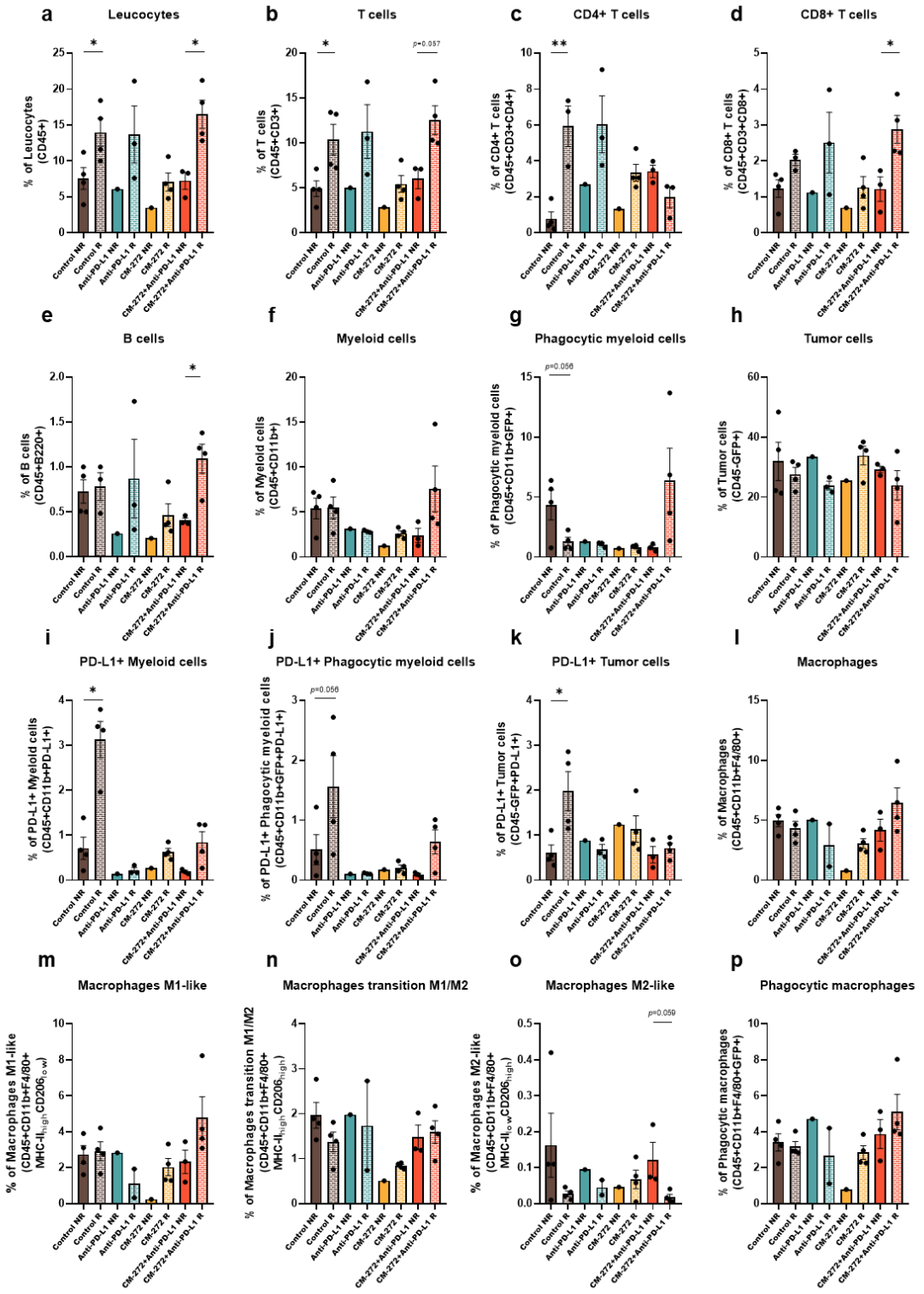


**Figure 3.** Characterization of immune cell infiltrates from the 1st challenge tumors (4K5) from non-responders (NR) and responders (R) in the 2nd challenge injected with 3K20 cells. NR denote mice displaying relevant tumor growth similar to growth controls, whereas R include mice that eliminated or maintained tumor growth in residual levels. Percentage from total population of infiltrating (a) leucocytes, (b) T cells, (c) CD4+ T cells, (d) CD8+ T cells, (e) B cells, (f) myeloid cells, (g) phagocytic myeloid cells, (h) tumor cells, (i) PD-L1+ myeloid cells, (j) PD-L1+ phagocytic myeloid cells, (k) PD-L1+ tumor cells, (l) macrophages, (m) macrophages M1-like, (n) macrophages transition M1/M2, (o) macrophages M2-like and (p) phagocytic macrophages.

Graphs display individual values as mean ± SEM for ≥3 mice included per group, except for anti-PD-L1 NR and CM-272 NR, where only one tumor was included. 4K5 mice were not included in this analysis, since NR were not found upon the 2nd challenge. P-values are represented as ns – not significant, *<0.05, **<0.01 and ***<0.001.

*Combination treatment with CM-272 and anti-PD-L1 during the 1st challenge leads to increased anti-tumoral immune infiltration in a distinct 2nd challenge tumor*

In the next step, we characterized the immune infiltrated from the tumors obtained upon the 2nd challenge. Our analysis was centered exclusively on growth controls, the control group, and CM-272 + anti-PD-L1-treated tumors from mice injected with 3K20 cells, as we had a single tumor sample each from the anti-PD-L1 and CM-272 treatment groups. Within the control group, 4 tumors collected from non-responder mice were included, while the combination group comprised 3 non-responder and 1 responder tumor (Figure 4).

Both control and combination-treated mice displayed higher tumor infiltration of total leucocytes, total T cells and CD4+ T cells in comparison with growth controls (Figure 4a-d). The same was observed for CD8+ T cell infiltration, however with a higher increase for the combination-treated group, in comparison with control and growth controls (Figure 4e). The percentage of phagocytic myeloid cells and macrophages was significantly higher in the combination group (Figure 4g and p). Furthermore, higher levels of detected PD-L1 were found in tumors from mice previously treated with CM-272 + anti-PD-L1 in myeloid, phagocytic myeloid and tumor cells (Figure 4i-k). The CM-272+anti-PD-L1 mice also displayed lower percentage of M2-like macrophages and higher presence of M1-like macrophages (Figure 4l-o). Thus, previous treatment with CM-272 in combination with anti-PD-L1 led to enhanced tumor immune cell infiltration upon 2nd challenge with a distinct BC cell line.

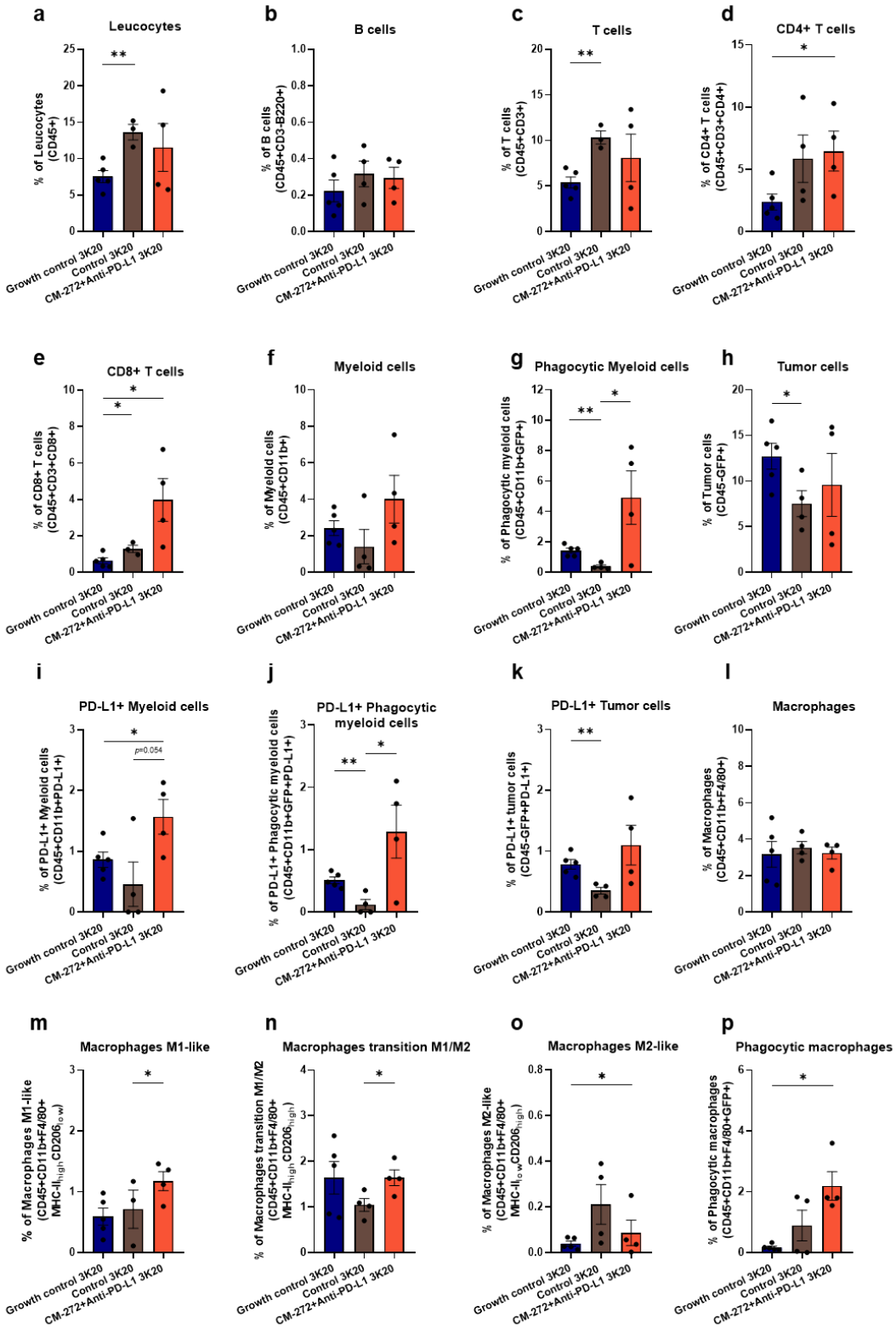


**Figure 4.** Analysis of the immune infiltrate in 2nd challenge tumors in growth control, control and CM-272 + anti-PD-L1 mice injected with 3K20 cells. Percentage from total population of infiltrating (a) leucocytes, (b) B cells, (c) T cells, (d) CD4+ T cells, (e) CD8+ T cells, (f) myeloid cells, (g) phagocytic myeloid cells, (h) tumor cells, (i) PD-L1+ myeloid cells, (j) PD-L1+ phagocytic myeloid cells, (k) PD-L1+ tumor cells, (l) macrophages, (m) macrophages M1-like, (n) macrophages transition M1/M2, (o) macrophages M2-like and (p) phagocytic macrophages. Graphs display

individual values as mean ± SEM for ≥3 mice included per group. Anti-PD-L1 and CM-272 mice were not included in this analysis, since only one tumor was collected in the 2nd challenge. Furthermore, this analysis was not performed for 4K5-injected mice because no 2nd challenge tumors were available. P-values are represented as ns – not significant, *<0.05, **<0.01 and ***<0.001.

*Distinct transcriptomic patterns between 4K5 and 3K20 cells*

Finally, we evaluated the changes induced by CM-272 treatment in the transcriptomic profile of 4K5 cells and how it compared with 3K20 cells. Firstly, CM-272 displayed a significant inhibitory effect on cell growth, reducing it by 50% at a low micromolar concentration (Figure 5a). Interestingly, CM-272 led to an enrichment of immune pathways, including interferon gamma and alpha responses, allograft rejection and inflammatory responses, as well as pathways associated with anti-tumoral effects such as DNA repair and apoptosis in CM-272-treated 4K5 cells, compared with non-treated 4K5 cells (Figure 5b).

Next, we compared the expression profile of 4K5 control, 4K5 treated with CM-272 and a different syngeneic mouse BC cell line originating from the same DKO strain, 3K20. The PCA analysis showed that the 4K5 control, 4K5 treated and 3K20 cells differ from each other by grouping separately (Figure 5c). Additionally, only a limited overlap of up- and downregulated genes were observed between 4K5 treated and 3K20 cells when compared with 4K5 control cells, with 0.4% and 9.1% in the up- and downregulated genes, respectively (Figure 5d; Supplementary Table S2). This difference was further confirmed by the supervised clustering observed in the heatmap (Figure 5e). Thus, CM-272 plays a direct role in modulating immune-related pathways within BC cells by upregulating the expression of these pathways. Additionally, the treatment with CM-272 induced distinct changes in the transcriptomic profile of 4K5 cells, which differs from the 3K20 cells profile. In future experiments, we aim to perform a comparative analysis of the neoantigen profiles between 4K5 and 3K20 cells, studying the influence of CM-272 on potential alterations within the neoantigen expression.

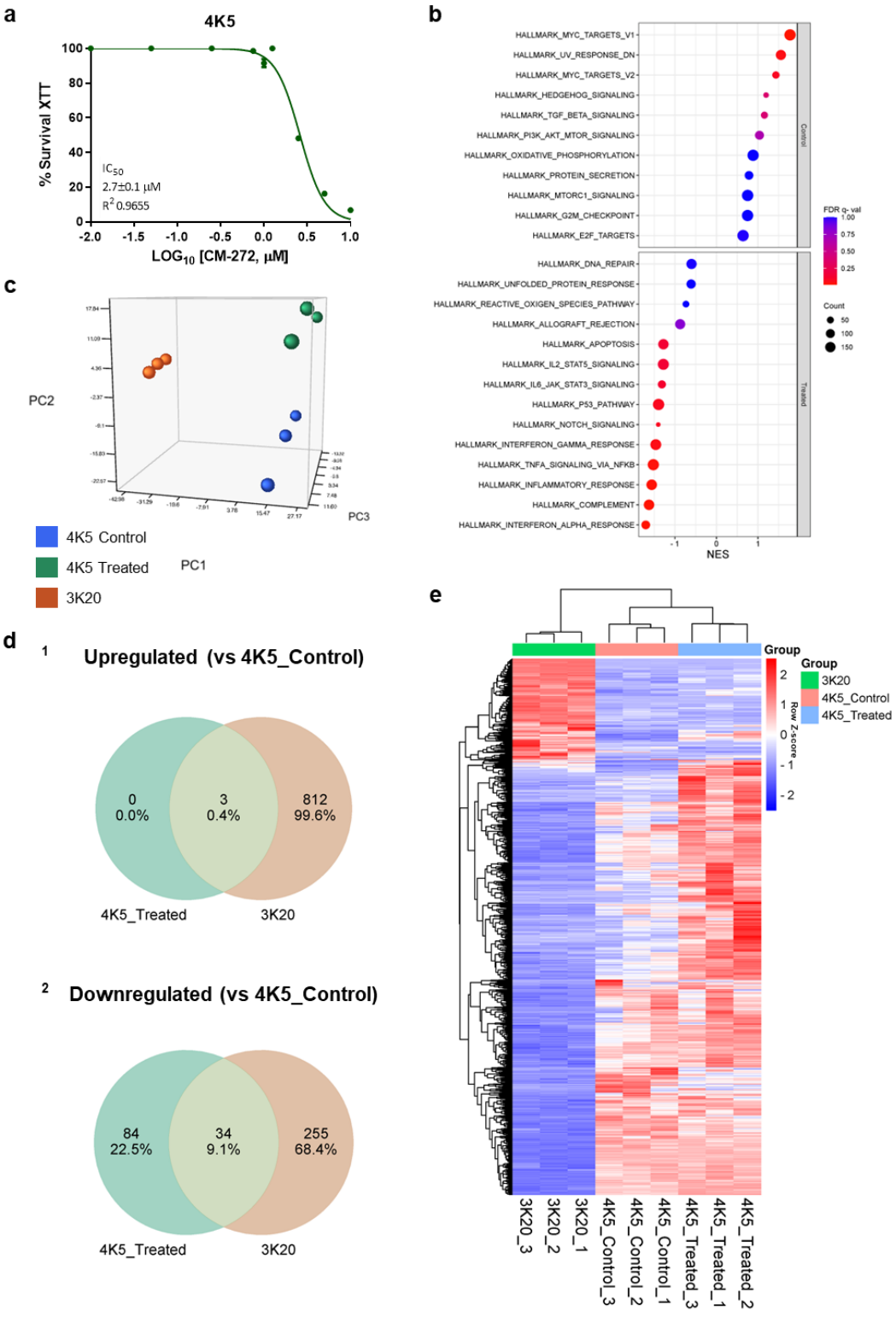


**Figure 5.** Transcriptomic changes induced in 4K5 cells after treatment with CM-272. (a) Survival curve of 4K5 cells after treatment with CM-272 with respective $IC_{50}$ value. (b) Enrichment bubble plot of 4K5 cells for the Hallmark gene signatures of gene set enrichment analysis (GSEA) analysis comparing control and treated 4K5 cells. (c) Principal component analysis (PCA) graph of 4K5 control, 4K5 treated with CM-272 and 3K20 cells. (d) Venn diagrams of genes (1) upregulated and (2) downregulated in 4K5 treated and 3K20 cells in comparison with 4K5 control cells. (e) Heatmap displaying hierarchical clustering of the dysregulated genes between 4K5 control, 4K5 treated and 3K20 cells. 4K5 cells were treated with the $IC_{50}$ dose of CM-272 for 48 h.

## Discussion

BC constitutes a major global health concern, given the significant number of patients initially diagnosed with a less aggressive form of the disease that ultimately recur or progress to more aggressive stages (2). Current treatment options for advanced BC are limited and invasive, and although immunotherapy with ICI has shown promise, its success rate remains low (18). Epigenetic targets such as G9a (EHMT2) or DNMTs have been emerging as promising strategies for BC treatment (11, 12). This study focuses on the novel dual inhibitor CM-272, targeting both G9a and DNMT1, with a specific emphasis on elucidating the mechanisms that underlie the sustained anti-tumoral effects of CM-272 when used in combination with anti-PD-L1 in the context of BC. Previous findings showed that the combination of CM-272 and anti-PD-L1 promoted a sustained anti-tumoral response after the treatment ended (8). Nonetheless, the understanding of these mechanisms may provide new insights on a new therapeutic strategy for BC patients with prolonged anti-tumoral effects.

Firstly, we selected a DKO immunocompetent mouse model of advanced BC and injected subcutaneously 4K5 cells (1$^{st}$ challenge). Although a significant reduction on tumor growth after treatment with CM-272 and CM-272+anti-PD-L1 in this mouse model was observed, synergy between CM-272 and anti-PD-L1 was not apparent, contrarily to a previous report, probably due to the different nature of the mouse model used in this study (8). Indeed, the DKO model presented lower immunogenicity than QKO model, exhibiting reduced activation of interferon gamma and alpha pathways (Munera-Maravilla et al., manuscript under preparation). Moreover, since we wanted to study the impact of treatments on the tumor microenvironment, mice were submitted to a treatment regimen of only two weeks with CM-272 concomitantly two injections of anti-PD-L1, in contrast to the four-week treatment duration in the prior study conducted (8).

After tumor resection and recovery, mice were inoculated with either the same cell line as in the 1$^{st}$ challenge or another syngeneic BC cell line (2$^{nd}$ challenge). As expected, all mice were able to eliminate 4K5 cells, indicating the generation of immune memory. Interestingly, even when a different cell line was injected on the 2$^{nd}$ challenge (3K20), more than 50% of the mice were able to eliminate those tumors, being mostly eliminated in mice previously treated anti-PD-L1 and/or CM-272. The possible presence of common antigens within these cell lines might explain the anti-tumor response observed in the 2$^{nd}$ challenge.

By analyzing the tumor microenvironment from the 1$^{st}$ challenge tumors, we found that tumors from mice that eliminated the 3K20 tumor in the 2$^{nd}$ challenge, displayed a higher percentage of immune cell infiltrates. This effect was particularly

pronounced among responders in the CM-272+anti-PD-L1 treatment group, which included an increased presence of CD8+ T cells and M1-like macrophages, recognized as favorable prognostic factors in BC (19, 20). Curiously, detected PD-L1 levels were the highest in the responders from control mice in myeloid and tumor cells, with no relevant differences for the remaining treated tumors. Since the immune response in these mice seems to be more effective, this can constitute a mechanism of immune evasion by overexpressing PD-L1 to escape immunological cell death (21).

Tumors collected from the 2$^{nd}$ challenge in mice previously exposed to 4K5 displayed a notable increase in immune cell infiltration. Although we did not observe a significant difference in the percentage of responders mice between the control and CM-272+anti-PD-L1-treated groups in terms of tumor growth, tumors from mice previously treated with the combination demonstrated a higher presence of infiltrating CD8+ T cells and phagocytic cells. Interestingly, detected PD-L1 levels are also higher in the tumors from mice treated with the combination, possibly being attributable to the immune escape mechanism mentioned before (21). In this scenario, prior treatment with the combination of CM-272 and anti-PD-L1 appears to be an important to boost the immune response during the rechallenge. Nevertheless, it is imperative to investigate the single-arm treatments to discern whether this effect comes from the combination treatment or if one of the individual treatments, CM-272 or anti-PD-L1.

In the last part of this study, we focused on the transcriptomic profiles of 4K5 and 3K20 cells. CM-272 inhibited 4K5 cell growth at a low micromolar concentration, although slightly higher than what was previously reported for human cancer cells (8, 13, 14). Upon treatment, 4K5 cells transcriptional profile was enriched in immune-related pathways such as interferon alpha and gamma response, which is in line with a previous report from our group (8), reinforcing that CM-272 has a prominent role in regulating immune-related genes in BC cells. Give that a significant proportion of the control mice also eliminated the 3K20 cells in the 2$^{nd}$ challenge, we compared the transcriptomic profiles of 4K5 and 3K20 cells to possibly find similarities/differences that could explain the results obtained *in vivo*. In terms of gene expression, 4K5 and 3K20 cells are distinct and that CM-272 induces further changes in 4K5, which differ from both 4K5 and 3K20 control cells. Our next aim is to compare the neoantigens expression of these two cell types and understand how the treatment with CM-272 alters the profile of these antigens. Neoantigens, also known as tumor-specific antigens, are proteins or peptides that are not present in normal, healthy cells but are expressed by cancer cells (22). Neoantigens can serve as targets for the immune system, as they are perceived as foreign or abnormal, and can potentially trigger an immune response against the cancer cells and generate immune memory cells (23). Immunological memory is primarily maintained by

specialized immune cells, such as memory T cells (24, 25). Memory cells are primed to respond rapidly and effectively if cancer cells related antigens are recognized, enabling effective and targeted immune response (26). Therapies such as ICI were reported to contribute to the formation of immune memory against cancer cells (27-29). Interestingly, this effect of generating immune memory seems to be potentiated when ICI are combined with epigenetic drugs, namely histone deacetylases (HDACs) inhibitors (30, 31). In fact, mice treated with anti-PD-L1 combined with a HDAC8 inhibitor exhibited protection against tumor rechallenge due to the activation of memory T cells (31). Entinostat, an inhibitor targeting HDAC1 and HDAC3, increased immune editing of tumor antigens, thus, expanding neoantigen-specific T cells. Moreover, after entinostat combined with anti-PD-1 treatment, mice rechallenged with tumor cells exhibited sustained immunologic memory in the context of BC (30). Thus, our hypothesis is that CM-272 potentiates a sustained and prolonged immune response *in vivo* by increasing the amount of neoantigens expressed by tumor cells, which could translate into a more diverse repertoire of immune memory cells, able to activate and eliminate different BC cells upon rechallenge.

In summary, our data offers insights into the complex interplay between epigenetic targeting, immune response, and the potential of combined therapeutic schemes in treating advanced BC. These findings have the potential to influence the development of novel treatment strategies that can offer prolonged anti-tumoral effects and improved outcomes for BC patients. However, further research and validation are needed to fully understand the mechanisms at play to eventually translate these findings into the clinical practice.

**References**


1. Sung H, Ferlay J, Siegel RL, Laversanne M, Soerjomataram I, Jemal A, et al. Global Cancer Statistics 2020: GLOBOCAN Estimates of Incidence and Mortality Worldwide for 36 Cancers in 185 Countries. CA Cancer J Clin. 2021;71(3):209-49.
2. Wallerand H, Bernhard JC, Culine S, Ballanger P, Robert G, Reiter RE, et al. Targeted therapies in non-muscle-invasive bladder cancer according to the signaling pathways. Urol Oncol. 2011;29(1):4-11.
3. Ripoll J, Ramos M, Montaño J, Pons J, Ameijide A, Franch P. Cancer-specific survival by stage of bladder cancer and factors collected by Mallorca Cancer Registry associated to survival. BMC Cancer. 2021;21(1):676.
4. Powles T, Bellmunt J, Comperat E, De Santis M, Huddart R, Loriot Y, et al. Bladder cancer: ESMO Clinical Practice Guideline for diagnosis, treatment and follow-up. Ann Oncol. 2022;33(3):244-58.
5. Hussain SA, Birtle A, Crabb S, Huddart R, Small D, Summerhayes M, et al. From Clinical Trials to Real-life Clinical Practice: The Role of Immunotherapy with PD-1/PD-L1 Inhibitors in Advanced Urothelial Carcinoma. Eur Urol Oncol. 2018;1(6):486-500.
6. Baylin SB, Jones PA. Epigenetic Determinants of Cancer. Cold Spring Harb Perspect Biol. 2016;8(9).
7. Jan S, Dar MI, Wani R, Sandey J, Mushtaq I, Lateef S, et al. Targeting EHMT2/ G9a for cancer therapy: Progress and perspective. Eur J Pharmacol. 2021;893:173827.
8. Segovia C, San José-Enériz E, Munera-Maravilla E, Martínez-Fernández M, Garate L, Miranda E, et al. Inhibition of a G9a/DNMT network triggers immune-mediated bladder cancer regression. Nat Med. 2019;25(7):1073-81.
9. Wang L, Dong X, Ren Y, Luo J, Liu P, Su D, et al. Targeting EHMT2 reverses EGFR-TKI resistance in NSCLC by epigenetically regulating the PTEN/AKT signaling pathway. Cell Death Dis. 2018;9(2):129.
10. Moore LD, Le T, Fan G. DNA methylation and its basic function. Neuropsychopharmacology. 2013;38(1):23-38.
11. Nunes SP, Henrique R, Jerónimo C, Paramio JM. DNA Methylation as a Therapeutic Target for Bladder Cancer. Cells. 2020;9(8).
12. San José-Enériz E, Agirre X, Rabal O, Vilas-Zornoza A, Sanchez-Arias JA, Miranda E, et al. Discovery of first-in-class reversible dual small molecule inhibitors against G9a and DNMTs in hematological malignancies. Nat Commun. 2017;8:15424.
13. Moreira-Silva F, Outeiro-Pinho G, Lobo J, Guimarães R, Gaspar VM, Mano JF, et al. G9a inhibition by CM-272: Developing a novel anti-tumoral strategy for castration-resistant prostate cancer using 2D and 3D in vitro models. Biomed Pharmacother. 2022;150:113031.

14. Bárcena-Varela M, Caruso S, Llerena S, Álvarez-Sola G, Uriarte I, Latasa MU, et al. Dual Targeting of Histone Methyltransferase G9a and DNA-Methyltransferase 1 for the Treatment of Experimental Hepatocellular Carcinoma. Hepatology. 2019;69(2):587-603.
15. Team RC. R: A language and environment for statistical computing. R Foundation for Statistical Computing 2022.
16. Love MI, Huber W, Anders S. Moderated estimation of fold change and dispersion for RNA-seq data with DESeq2. Genome Biol. 2014;15(12):550.
17. Subramanian A, Tamayo P, Mootha VK, Mukherjee S, Ebert BL, Gillette MA, et al. Gene set enrichment analysis: a knowledge-based approach for interpreting genome-wide expression profiles. Proc Natl Acad Sci U S A. 2005;102(43):15545-50.
18. Maiorano BA, De Giorgi U, Ciardiello D, Schinzari G, Cisternino A, Tortora G, et al. Immune-Checkpoint Inhibitors in Advanced Bladder Cancer: Seize the Day. Biomedicines. 2022;10(2).
19. Viveiros N, Flores BC, Lobo J, Martins-Lima C, Cantante M, Lopes P, et al. Detailed bladder cancer immunoprofiling reveals new clues for immunotherapeutic strategies. Clin Transl Immunology. 2022;11(9):e1402.
20. Zeng D, Ye Z, Wu J, Zhou R, Fan X, Wang G, et al. Macrophage correlates with immunophenotype and predicts anti-PD-L1 response of urothelial cancer. Theranostics. 2020;10(15):7002-14.
21. Liu J, Chen Z, Li Y, Zhao W, Wu J, Zhang Z. PD-1/PD-L1 Checkpoint Inhibitors in Tumor Immunotherapy. Front Pharmacol. 2021;12:731798.
22. Blass E, Ott PA. Advances in the development of personalized neoantigen-based therapeutic cancer vaccines. Nat Rev Clin Oncol. 2021;18(4):215-29.
23. Xie N, Shen G, Gao W, Huang Z, Huang C, Fu L. Neoantigens: promising targets for cancer therapy. Signal Transduct Target Ther. 2023;8(1):9.
24. Chen DS, Mellman I. Elements of cancer immunity and the cancer-immune set point. Nature. 2017;541(7637):321-30.
25. Byrne A, Savas P, Sant S, Li R, Virassamy B, Luen SJ, et al. Tissue-resident memory T cells in breast cancer control and immunotherapy responses. Nat Rev Clin Oncol. 2020;17(6):341-8.
26. Amsen D, van Gisbergen K, Hombrink P, van Lier RAW. Tissue-resident memory T cells at the center of immunity to solid tumors. Nat Immunol. 2018;19(6):538-46.
27. Leach DR, Krummel MF, Allison JP. Enhancement of antitumor immunity by CTLA-4 blockade. Science. 1996;271(5256):1734-6.

28. Waldman AD, Fritz JM, Lenardo MJ. A guide to cancer immunotherapy: from T cell basic science to clinical practice. Nat Rev Immunol. 2020;20(11):651-68.
29. Fritz JM, Lenardo MJ. Development of immune checkpoint therapy for cancer. J Exp Med. 2019;216(6):1244-54.
30. Truong AS, Zhou M, Krishnan B, Utsumi T, Manocha U, Stewart KG, et al. Entinostat induces antitumor immune responses through immune editing of tumor neoantigens. J Clin Invest. 2021;131(16).
31. Yang W, Feng Y, Zhou J, Cheung OK, Cao J, Wang J, et al. A selective HDAC8 inhibitor potentiates antitumor immunity and efficacy of immune checkpoint blockade in hepatocellular carcinoma. Sci Transl Med. 2021;13(588).

## Supplementary Information

## Supplementary Figures

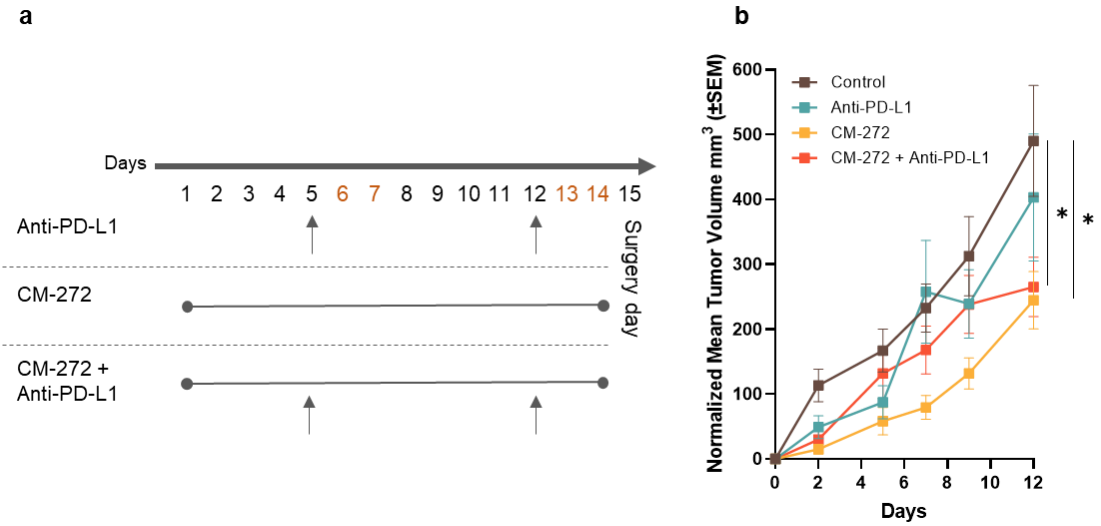


**Figure S1.** (a) Representation of the treatment scheme used for treatment with anti-PD-L1, CM-272 and combination of both. Anti-PD-L1 (avelumab) was injected once a week, whereas CM-272 was applied for 5 consecutive days, with 2 rest days represented in orange. Surgery was performed after 15 days of the start of the treatment course. (b) Normalized individual tumor growth curves for mice in control, anti-PD-L1, CM-272 and CM-272 + anti-PD-L1 groups. Day 0 corresponds to the first day of treatment.

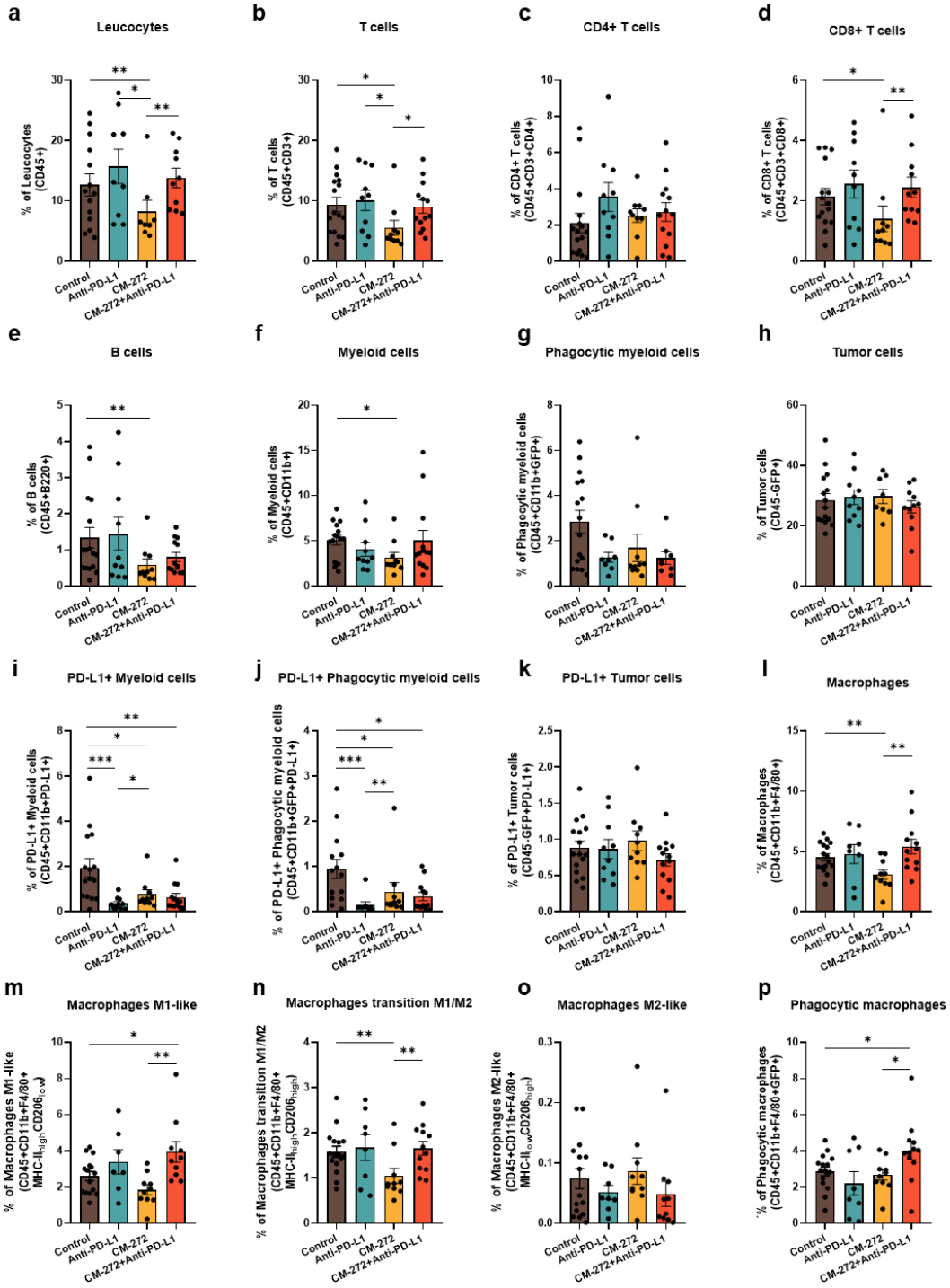


**Figure S2.** Percentage from total population of infiltrating (a) leucocytes, (b) T cells, (c) CD4+ T cells, (d) CD8+ T cells, (e) B cells, (f) myeloid cells, (g) phagocytic myeloid cells, (h) tumor cells, (i) PD-L1+ myeloid cells, (j) PD-L1+ phagocytic myeloid cells, (k) PD-L1+ tumor cells, (l) macrophages, (m) macrophages M1-like, (n) macrophages transition M1/M2, (o) macrophages M2-like and (p) phagocytic macrophages. Graphs display individual values as mean ± SEM for ≥9 mice included per group. P-values are represented as ns – not significant, *<0.05, **<0.01 and ***<0.001.

## Supplementary Tables

**Table S1.** Antibodies with respective fluorochrome used for cell population characterization by flow cytometry.

| Epitope | Fluorochrome | Company | Reference |
|---|---|---|---|
| CD45 (30-F11) | PerCP | Biolegend | 103130 |
| CD3 (145-2C11) | PE | BD | 553064 |
| CD3 (17A2) | APC-Cy7 | Biolegend | 100222 |
| CD8a (53-6.7) | APC-Cy7 | Biolegend | 100714 |
| CD4 (RM4-5) | BV711 | Biolegend | 100550 |
| CD45R/B220 (RA3-6B2) | PEFire700 | Biolegend | 103280 |
| F4/80 (BM8) | APC | Biolegend | 123116 |
| F4/80 (BM8) | BV605 | Biolegend | 123149 |
| CD11b (M1/70) | A647 | Biolegend | 101218 |
| CD11b (M1/70) | PE | BD | 553311 |
| Ly6G (1A8) | BV421 | BD | 562737 |
| I-A/I-E MHC-II (M5/114.15.2) | PECy7 | eBioscience | 25-5321-82 |
| I-A/I-E MHC-II (M5/114.15.2) | BV711 | Biolegend | 107643 |
| PD-L1/CD274 (MIH5) | BV711 | BD | 563369 |
| CD206 (C068C2) | A647 | Biolegend | 141712 |
| Rat IgG2a, λ Isotype Control (B39-4) | BV711 | BD | 563394 |
| Rat IgG2b, κ Isotype Control (RTK4530) | BV711 | Biolegend | 400653 |
| Rat IgG2a, κ Isotype Control (RTK2758) | A647 | Biolegend | 400526 |

**Table S2.** List of up- and downregulated genes common to 4K5 cells treated with $IC_{50}$ dose of CM-272 for 48 h and 3K20 without any treatment in comparison with 4K5 control cells obtained by Venn Diagram analysis.

| Genes DOWN | Genes UP |
|---|---|
| 4K5_Treated\|3K20 | 4K5_Treated\|3K20 |
| Fbxl13 | Npr3 |
| Gm40723 | Rgs5 |
| Slc15a3 | Clca3a2 |
| A530046M15Rik | |
| Ccl8 | |
| Col22a1 | |
| Hmgcll1 | |
| Gcnt3 | |
| Psca | |
| 5430425K12Rik | |
| Ly6f | |
| Pecam1 | |
| Gm29152 | |
| Dnm3 | |
| Htra3 | |
| Gm41934 | |
| Aldh1l1 | |
| Acsbg1 | |
| Syn1 | |
| Gm41215 | |
| Stmn2 | |
| Otogl | |
| Slc7a8 | |
| Glp1r | |
| Uox | |
| Slc6a12 | |
| P2ry10b | |
| Pde8b | |
| Foxq1 | |
| Onecut2 | |
| Mucl3 | |
| Ppm1e | |
| Afp | |
| Gpr149 | |

*CHAPTER IV*

# EPIMARKERS OF RESPONSE TO IMMUNOTHERAPY

## Uncovering DNA methylation patterns and their impact on immunotherapy in bladder cancer

*Research paper 3*

**Sandra P. Nunes**, Aida Bao-Caamano, Nicolás Costa-Fraga, Vera Constâncio, Pedro Leite-Silva, Carolina Rubio, Cristian Suárez-Cabrera, Lucia Morales, Rui Henrique, Marta Dueñas, Daniel Castellano, Francisco X. Real, Angel Díaz-Lagares, Carmen Jerónimo, and Jesús M. Paramio

**Manuscript in preparation**

Author personal contribution:

Technical execution of the work, analysis and interpretation of the results and manuscript preparation.

**Abstract**

Introduction: In recent years, the emergence of immunotherapy has changed the landscape of bladder cancer (BC) treatment. However, a significant subset of BC patients remains unresponsive to immune checkpoint blockade therapies, also because current biomarkers, such as tumor mutation burden and PD-L1 expression, fail in correctly identifying patients that would benefit from this therapy. A deeper understanding of the molecular mechanisms underlying BC has revealed DNA methylation as a pivotal player in BC tumorigenesis and as a potential disease biomarker. Here, we present an EPIC array-based study for the identification of differential DNA methylation signatures associated with responses to immune checkpoint inhibitors in BC.

Materials and Methods: A total of 54 samples corresponding to 36 BC patients submitted to neoadjuvant immune checkpoint inhibitors from different clinical trials were included. Specifically, 36 transurethral resection of bladder tumor (TURBT) (treatment naïve) and paired 18 samples from cystectomies (after immunotherapy) were used for the Infinium Methylation EPIC array (EPIC array) analysis. DNA was extracted from FFPE tumors, bisulfite-converted and hybridized using the EPIC array. Differential analyses using the RnBeads package from R and the Enrichr tool were performed.

Results: The methylation status of CpG sites, islands, and promoters of responders to immunotherapy was largely different from non-responders, as shown by the hierarchical clustering analysis. Enrichr analysis revealed that the most differential methylated CpG sites in responders associated immune responses and, specifically, antigen presentation. Moreover, paired samples from TURBT and cystectomies revealed distinct methylation patterns, disclosing that immune checkpoint inhibitors influence tumors' methylation profile.

Conclusions: Epigenomic profiling of bladder tumors has unveiled distinct DNA methylation signatures among responders and non-responders to immunotherapy, as well as between TURBT and cystectomy samples. Our data show the potential of DNA methylation to provide useful biomarkers for identifying BC patients that can benefit from checkpoint inhibitors' immunotherapy.

**Keywords**

Bladder cancer; immunotherapy; DNA methylation; Immune checkpoint inhibitors; EPIC array

## Introduction

According to GLOBOCAN, bladder cancer (BC) is the 10th most frequent cancer worldwide, ranking as the 6th more incident in males, and representing the 9th cause of death (1). About 25% of BC patients are diagnosed with muscle-invasive BC (MIBC) (2), associated with an overall survival of 30% for locally advanced BC and 6% for metastatic disease, respectively (3). While cystectomy and/or chemotherapy remain the gold standard for the treatment of advanced BC, the approval of immunotherapy featuring immune checkpoint inhibitors (ICI) improved the prognosis of these patients (4). Those include pembrolizumab and nivolumab blocking programmed death 1 (PD-1) and atezolizumab, durvalumab and avelumab, binding to programmed death-ligand 1 (PD-L1) (5). Currently, immunotherapy with ICI is recommended for locally advanced BC patients that are not eligible for chemotherapy and that are positive for PD-L1 expression (4). Nevertheless, 17 to 26% of patients do not exhibit significant clinical benefit from ICI (6) while several clinical trials showed that positive PD-L1 expression does not always associate with response (7).

One of the major challenges in the immunotherapy field remains the correct selection of patients that will indeed benefit from ICI (8). Although treatment guidelines recommend PD-L1 expression as a biomarker for patient selection, it lacks accuracy in identifying patients that will likely benefit from ICI. Indeed, around 20% of patients PD-L1 negative were reported to benefit from PD-1/PD-L1 blockage (9). Furthermore, the absence of standardization in evaluating PD-L1 expression poses a challenge. This includes the lack of a universally established optimal cut-off for defining PD-L1 positivity, as well as ambiguity regarding which tumor microenvironment population (tumor or stromal cell populations) should be evaluated (8). Thus, PD-L1 expression as a single biomarker does not accurately predict ICI response. Other biomarkers have been proposed including tumor mutational burden, tumor mismatch-repair deficiency, distribution of tumor-infiltrating lymphocytes or pro-inflammatory signature based on interferon gamma (IFN-γ) (8, 10-12). Nonetheless, none of these approaches are currently employed in clinical practice, as they are still awaiting validation and a definitive demonstration of efficacy in accurately identifying patients suitable for ICI.

DNA methylation deregulation is one of the pivotal epigenetic mechanisms implicated in bladder carcinogenesis (13). DNA methylation consists of an addition of a methyl group to the fifth position of a cytosine in a CpG dinucleotide (14). CpG islands are genomic regions rich in CpG sites, often found in promoter regions near the transcription starting site (TSS) or first exons (15). DNA methylation can also be found in CpG shores and shelfs, locating near CpG islands with a lower CpG sites density (15).

While methylation in CpG islands, shores, and shelfs is associated with transcription repression, gene body methylation may facilitate transcriptional elongation and increment gene expression (14). Tumors are characterized by global hypomethylation in genomic repetitive regions, contributing to chromosomal instability and mutations (16). On the contrary, CpG islands of tumor suppressor genes are frequently hypermethylated, promoting carcinogenesis in BC (14, 17). Thus, DNA methylation has been proposed as potential therapeutic targets and biomarker for detection, prognosis, and prediction response to therapy in BC (13).

In the recent years, DNA methylation has been proposed as a biomarker for immunotherapy. The methylation status of *FOXP1* identified non-small cell lung cancer patients that benefit from anti-PD-1 therapy (18). In another study, 269 CpG signatures were identified as related to objective response rates to anti-PD-1/PD-L1 blockage in 18 different cancers (19). Other studies also found differently methylated profiles between responders and non-responders to ICI (20, 21). In BC, different methylation patterns were observed between BCG responders and failures, with *GPR158* being the best predictor of response to BCG (22). Recently, hypomethylation status of PD-L1 predicted objective response rate to ICI in metastatic BC, with *PD-L1* hypermethylation being associated with worst prognosis (23).

Our main goal is to assess the value of DNA methylation-based biomarkers in identifying BC patients that may benefit from ICI. In this study, we present a descriptive analysis based on the EPIC array exploring the differential DNA methylation signatures associated with response to immunotherapy. We also investigated the effects of ICI on the methylation patterns by comparing DNA methylation profile of treatment-naïve and paired treated tumors. We found different methylation profiles between responders and non-responders and that ICI influences tumors' DNA methylation profile.

## Material and Methods

### *Clinical Samples*

A total of 36 patients corresponding to 36 TURBT formalin-fixed paraffin-embedded (FFPE) samples and paired 18 cystectomies were included in this study a sample set. All patients were diagnosed with MIBC and treated with neoadjuvant ICI schemes (at least two cycles) followed by cystectomy. Information about the sample set can be found on Table 1. Informed consent was obtained from all patients included and the studies were approved by the ethics committee for clinical research of University Hospital "12 de Octubre" in Madrid, Spain. One sample from the TURBT non-responder

cohort was excluded from analysis due to software-related issues encountered during data processing.

*DNA extraction*

DNA from FFPE tissues was extracted using the QIAamp DNA FFPE Tissue Kit (Qiagen, Hilden, Germany), according to the manufacturer's instructions and using the QIAcube Connect (Qiagen). DNA concentration was measured using the Qubit 4 Fluorometer (Thermo Fisher Scientific) and the Qubit™ 1X dsDNA High Sensitivity assay kit (Thermo Fisher Scientific). DNA was stored at -20ºC until further use.

*EPIC methylation array*

Firstly, DNA integrity was evaluated using Agilent's TapeStation 4200 (Agilent Technologies, Santa Clara, California, USA). Samples undergone a quality control (QC) using the Illumina FFPE QC kit (Illumina, San Diego, California, USA) according to the manufacturer recommendations. Then, 500 ng of the extracted DNA was bisulfite-converted with the EZ DNA Methylation Kit (Zymo Research, Irvine, California, USA) according to the manufacturer's instructions, followed by a restoration step with the Illumina Infinium HD FFPE Restoration kit (Illumina, San Diego, California, USA). The bisulfite-converted DNA was then hybridized using the Infinium Methylation EPIC array (EPIC; Illumina, San Diego, California, USA), analyzing about 850,000 CpG sites in the human genome. The Bead Chip was imaged on the HiScan System and intensity values (IDAT files) were extracted.

*Bioinformatic and statistical analyzes*

DNA methylation array data were processed in the R 4.2.2 (24) using the RnBeads package version 2.14.0 (25). Briefly, quality control, a greedycut algorithm to filter out probes and/or samples and filtering for single nucleotide polymorphisms and sex chromosomes were performed. The SWAN was used as the normalization method and CpG positions were mapped according to the human hg19 reference genome. Both exploratory and differential analyses were included. For every CpG site, a β value was calculated. This β value represents the ratio of fluorescent signals from the methylated (M) probe in relation to the total of both the methylated (M) and unmethylated (UM) probes ($\beta = M/(M + UM)$). The β values go from 0 (indicating no methylation) to 1 (indicating 100% methylation of both alleles).

Analysis of responders *vs.* non-responders was performed by comparing TURBT samples. Principal component analysis (PCA), scatter plots and volcano plots for CpG sites, promoters and CpG islands were performed in R environment using the RnBeads

package representing the 1000 best ranking sites. In order to obtain the relevant differently methylated (DM), sites, promoters and CpG islands were ranked according to the combined Rank and filtered by *p*-value <0.05 (computed using the limma method). From those, sites, promoters and CpG islands displaying mean.quot.log2 (log2 of fold change) above 0 were considered hypermethylated, whereas below 0 were classified as hypomethylated. Hierarchical clustering was performed using the β values from each sample with the DM sites, promoters and CpG islands using Pearson correlation and average linkage using the Multi-Experiment Viewer (MeV 4.9.0). Differences in β value between cystectomy non-responders and partial responders were evaluated in MeV 4.9.0 using the *t* test for each CpG site. Enrichr analysis for DM promoters was carried out using Enrich webtool (https://maayanlab.cloud/Enrichr/) and results were represented using horizontal bar plots displaying the -log10 of the *p*-value. Pie charts, heatmaps and horizontal bar plots were represented using SRplot (https://www.bioinformatics.com.cn/en).

## Results

*Study characteristics*

The schematic representation of the experimental setting used in this study is summarized in Figure 1. Samples from 36 BC patients collected in a clinical trial setting were included in the discovery set (Table 1; Figure 1). Specifically, MIBC patients received immunotherapy with different ICI from several different clinical trials in a neoadjuvant setting and then were subjected to cystectomy. Both TURBT samples (collected before the starting of immunotherapy - treatment naïve) and cystectomy samples (collected after immunotherapy treatment) were included. Pathological response was evaluated in cystectomy samples by expert pathologists in a blinded approach.

About 64% (n=23) of patients were classified as non-responders across all clinical trials, whereas 36% (n=13) responded to immunotherapy by presenting both partial and complete responses (identified by the lack of tumor signs in cystectomy specimens). Furthermore, paired tumor samples were collected from cystectomy from 4 partial responders and 14 non-responders. Further clinical and pathological cannot be disclosed at this time as the results of the different clinical trials were not yet published.

**Table 1.** Parameters describing sample type and response to immunotherapy in the sample set.

| **Parameters** | | **Sample set (n=36)** |
|---|---|---|
| Sample type | TURBT | 36 |

| | | | |
|---|---|---|---|
| | Cystectomy | | 18 |
| Response to immunotherapy | Non-responders | | 23 |
| | Responders | | 13 |
| | | Partial | 4 |
| | | Complete | 9 |

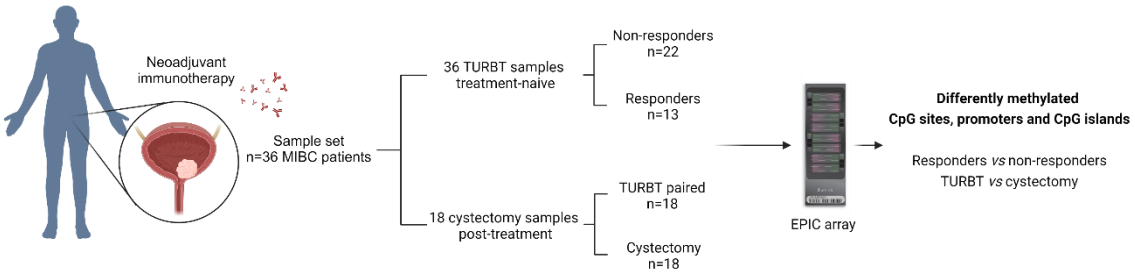


**Figure 1.** Schematic representation of the experimental setting used in this study. Thirty-six patients diagnosed with muscle-invasive bladder cancer (MIBC) were include in the sample set. These patients were included in clinical trials and proposed for neoadjuvant immunotherapy with immune checkpoint inhibitors followed by cystectomy, where the response to the treatment was evaluated. TURBT samples were collected before treatment start. 36 TURBT treatment-naïve samples, in which 22 non-responders and 13 responders to immunotherapy were included. Additionally, 18 cystectomy samples, including non-responders tumors and partial responders were compared with the paired 18 TURBT samples. The EPIC array was used to find differently methylated CpG sites, promoters and CpG islands in responders versus non-responders and TURBT versus cystectomy samples.

*Methylation patterns across non-responders* versus *responders to immunotherapy*

The methylation profile was assessed in TURBT samples of non-responders and responders (including both partial and complete responders to immunotherapy). No clear hierarchical clustering was observed in PCA analysis both at CpG sites and regional levels (promoters and CpG islands), indicating heterogenous patterns of methylation among the samples (Supplementary Figure S1a, b and c). Nevertheless, differential analysis revealed DM CpG sites, promoters and CpG islands (Figure 2). Specifically, 22,758 DM CpG sites were found between responders and non-responders, with a slightly higher percentage of CpG sites hypermethylated in responders to immunotherapy (12,163 out of 22,758 DM CpG sites) (Figure 2a). From these, 4,502 CpG sites were significantly different between ICI non-responders and complete responders (Supplementary Figure S1d). Although not striking, the differences between responders and non-responders were also apparent in the scatter (Figure 2b) and volcano plot analysis (Figure 2c). About 58% of the DM CpG sites were distributed in regions with low CpG density (open sea), whereas the remaining were located within CpG sites enriched regions, including CpG islands, shores and shelfs (Figure 2d). Regarding gene region distribution, 55.79% of the CpG sites were located in the gene

body, whereas the remaining were located 200-1500 bases upstream of the TSS, 0-200 bases of the TSS, 5' UTR, 3' UTR and 1st exon (Figure 2e). About 6.75% of the CpG sites were located at transcription factor-binding sites (TFBS) (Figure 2f). Differences in the methylation patterns at a regional level were also found (Figure g-l). Most of the promoters and CpG islands were hypermethylated in responders: 172 out of 285 DM promoters and 253 out of 387 DM CpG islands (Figure 2g and j).

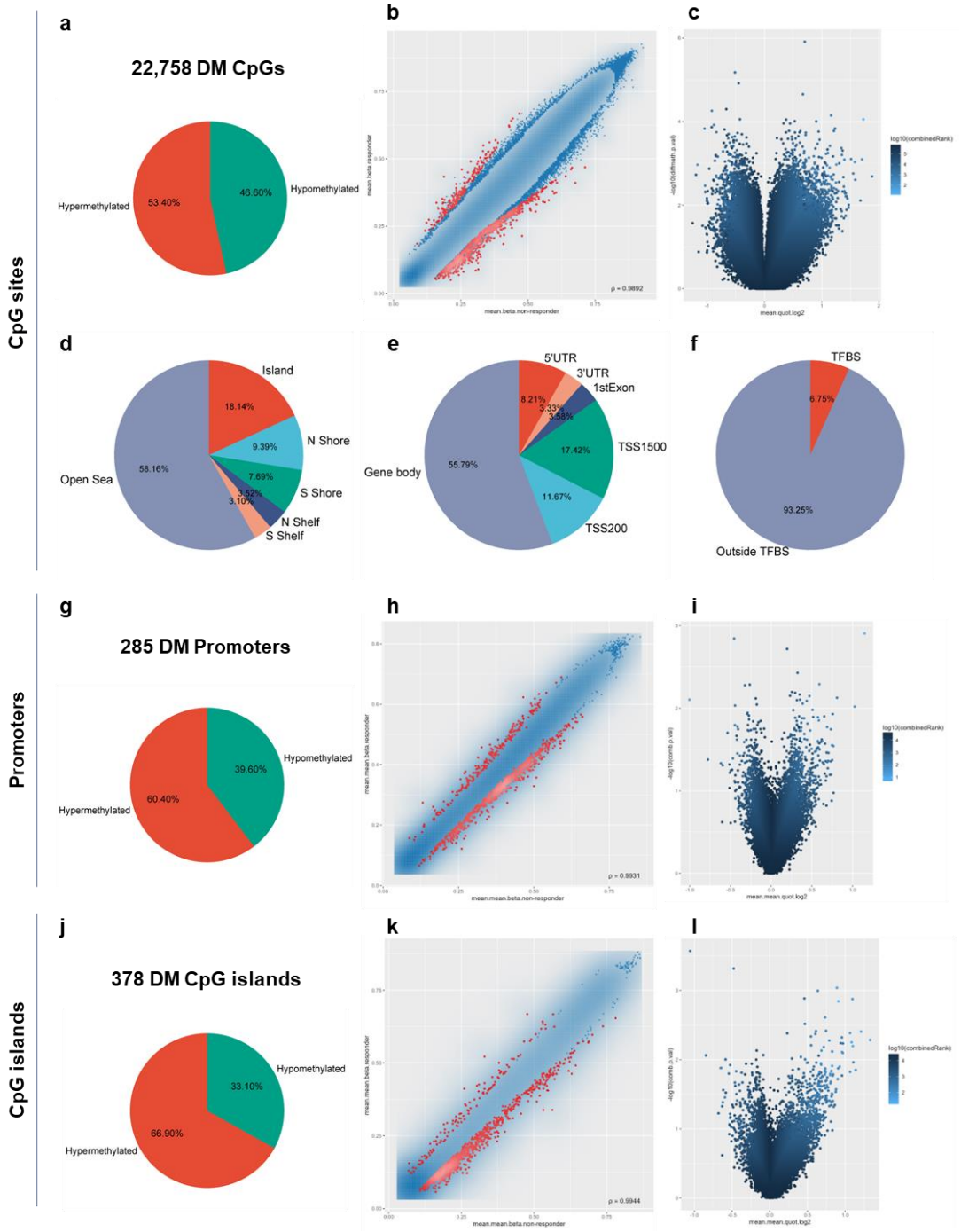


**Figure 2.** Differential methylation patterns between responders and non-responders to immune checkpoint inhibitors in TURBT samples. Pie chart describing the methylation status of the differently methylated (DM) (a) CpG sites, (g) promoters and (j) CpG islands. Scatterplots of the mean beta values of (b) CpG sites, (h) promoters and (k) CpG islands. Red dots represent the

1000 best ranking sites. Volcano plots of the pairwise comparison between responders and non-responders of (c) CpG sites, (i) promoters and (l) CpG islands. In the volcano plots, dots are colored according to the combined rank. (d) CpG context, (e) gene location and (f) transcription factor-binding sites (TFBS) of the 10,000 best ranking CpG sites. DM – Differently methylated.

Supervised hierarchical clustering analysis revealed that responders and non-responders to immunotherapy at both site and regional levels display different DNA methylation signatures (Figure 3a, b and c). In particular, DM CpG sites and islands seem to allow for the clustering of almost all responders and non-responders, revealing that methylation patterns of both groups are significantly different (Figure 3a and c).

Enrichment analysis of the genes of the 10,000 most DM CpG sites revealed that several immune and signaling pathways were DM in responders (Figure 3d and e; Supplementary Table S1). Notably, pathways involving cell junction assembly, epithelial mesenchymal transition and glutamate signaling emerged as well as the presence of hypermethylated genes linked to transmembrane receptor protein tyrosine kinase, indicating potential alterations in signal transduction cascades and cellular responses. Furthermore, enrichment of hypermethylated CpG sites were found in pathways related to positive regulation of signal transduction, enzyme-linked receptor proteins, Wnt signaling and KRAS signaling UP (Figure 3d; Supplementary Table S1). Several immune-related pathways were also found to be hypermethylated, namely those associated with natural killer cell cytokine production, T cell differentiation and chemotaxis positive regulation along with interleukin-1 production negative regulation (Figure 3d; Supplementary Table S1).

On the other hand, hypomethylated CpG sites are implicated in pathways regulating fundamental aspects of cellular architecture and signaling dynamics (Figure 3e; Supplementary Table S1). Pathways associated with actin filament organization, integrin-mediated signaling, and positive regulation of focal adhesion show potential alterations in cellular structural integrity and adhesive properties within the tumor microenvironment of responders (Figure 3e; Supplementary Table S1). In parallel, enrichment in pathways related to MHC Class II antigen processing and presentation namely, immunoglobulin-mediated immune responses, and phagocytosis were also found (Figure 3e; Supplementary Table S1). Collectively these findings portray the complex landscape of DM CpGs associated with pathways that may be implicated in ICI response.

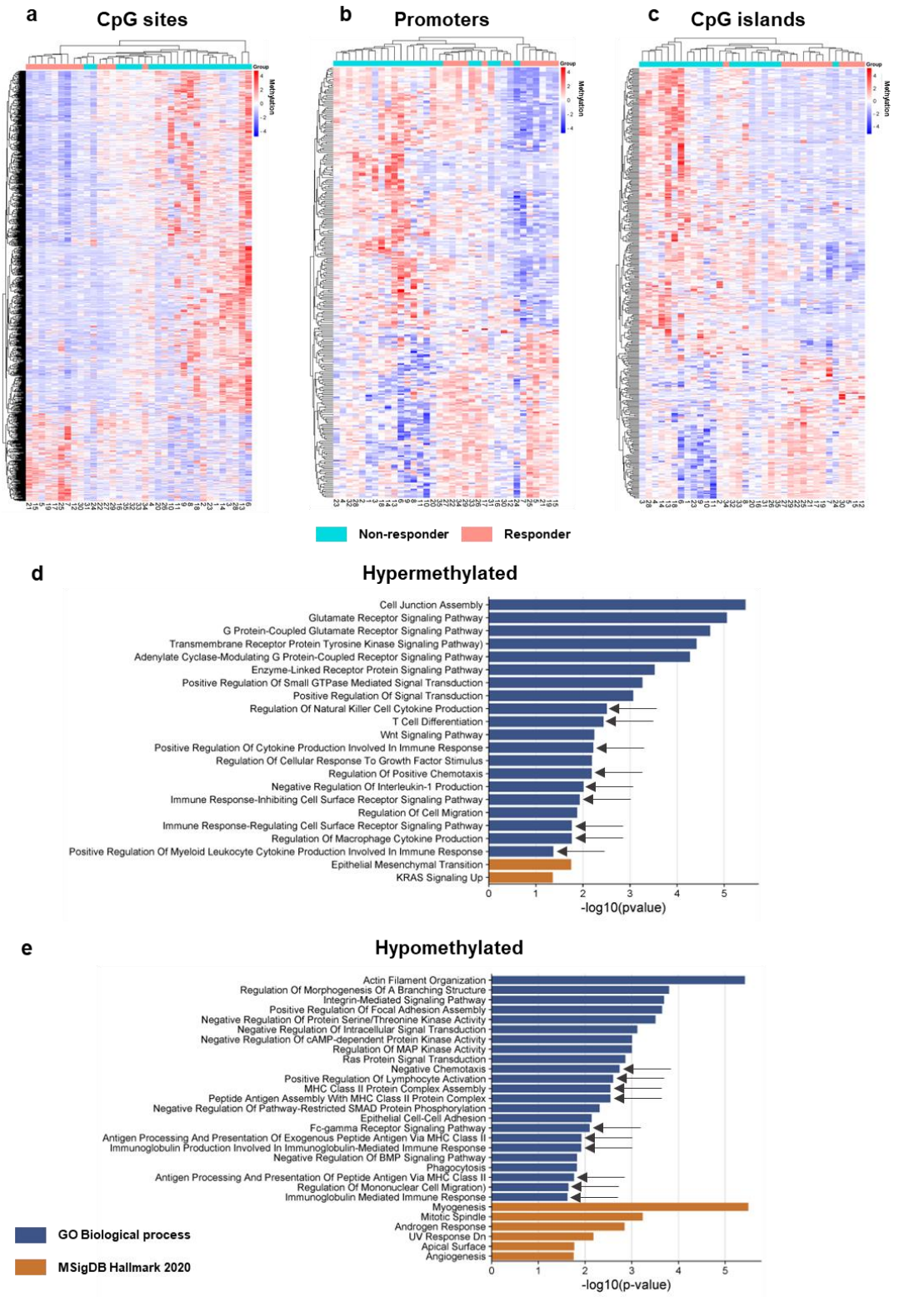


**Figure 3.** Comparative methylation profiling between non-responders and responders to immunotherapy. Supervised hierarchical clustering heatmap of the (a) 1,000 CpG sites, (b) 285 promoters and (c) 378 CpG islands most differently methylated between responders and non-responders to immunotherapy. Enrichr analysis of the (d) hypermethylated and (e) hypomethylated using Gene Ontology (GO) dataset biological processes and MSigDB Hallmark 2020 representing some of the most cancer and immune relevant gene signatures based on the 10,000 most differently methylated CpGs sites of responders compared to non-responders. Grey arrows denote the most relevant immune-related pathways.

*Methylation profiling in paired TURBT and cystectomy tumor samples*

Next, we investigated the DNA methylation profiles in TURBT (treatment-naïve) and cystectomy (after treatment with ICI) samples to understand if immunotherapy influenced the DNA methylation profile of bladder tumors. For that, 18 paired TURBT and cystectomy samples were analyzed. PCA analysis showed a tendency for TURBT and cystectomy samples cluster separately, either considering CpG sites, islands, or promoters (Supplementary Figure S2a, b and c). Globally, 173,393 CpG sites were found to be DM, being 28,123 CpG sites hypomethylated, while 145,270 CpG sites were hypermethylated (Figure 4a). The different methylation signature can also be observed in the scatter and volcano plots (Figure 4b and c). Most of the DM CpG sites were found in open sea, whereas about 25% were found in islands, shores and shelfs (Figure 4d). Furthermore, about 61% of the DM CpGs were in gene body, followed by 200-1500 bases upstream of the TSS and by 5' UTR region (Figure 5e) and about 6% were located in TFBS (Figure 4f). Promoters and CpG islands were also found to be DM (Figure 4h, I, k and l). Specifically, 671 promoters were hypomethylated whereas 7,401 were found hypermethylated, and 943 CpG islands were hypomethylated and 1,505 hypermethylated (Figure g and j).

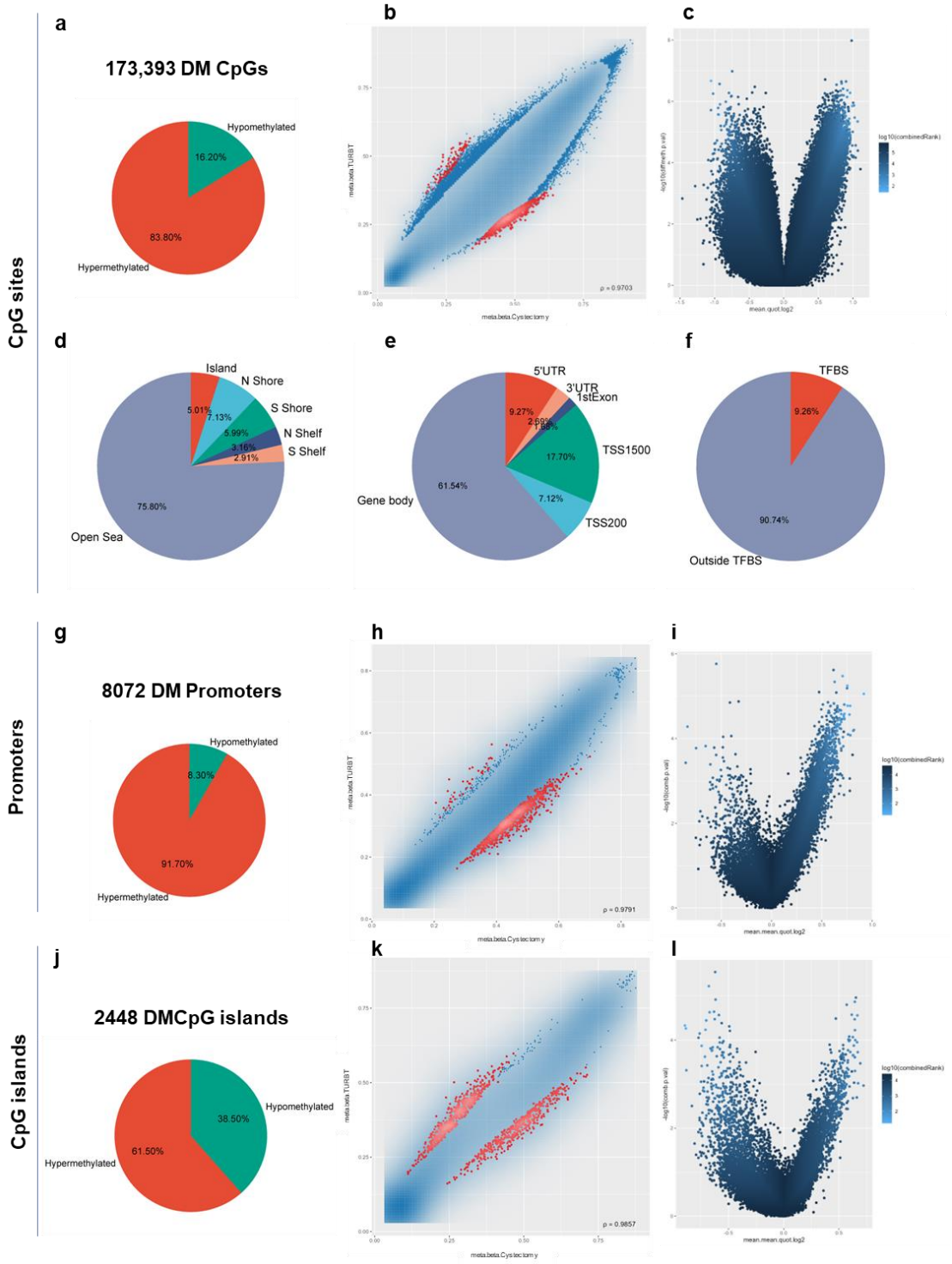


**Figure 4.** Differential methylation patterns between paired TURBT and cystectomy samples. Pie chart describing methylation status of the differently methylated (DM) (a) CpG sites, (g) promoters and (j) CpG islands. Scatterplots of the mean beta values for (e) CpG sites, (h) promoters and (k) CpG islands comparing TURBT and cystectomy samples. Volcano plots of (f) CpG sites, (i) promoters and (l) CpG islands for TURBT versus cystectomy comparison. The transparency represents points' density in scatter plots and the red dots denotes the 1,000 best ranking sites, promoters or islands. (d) CpG context, (e) gene location and (f) transcription factor-binding sites (TFBS) of the 10,000 best ranking CpG sites. DM – Differently methylated.

Similar to PCA analysis, supervised hierarchical clustering analysis demonstrated that cystectomy and TURBT samples cluster separately, taking into account CpG sites, promoters and islands. These findings indicate that the depicted distinctive methylation profiles, influenced either directly by ICI therapy or through the remodeling of the TME induced by ICI treatment, may give rise to diverse cell populations. (Figure 5a, b and c).

Enrichment of hypermethylated CpG sites was observed in pathways associated with cell-cell adhesion, adherens junction organization, and extracellular structure organization, indicating potential alterations in cellular architecture and intercellular interactions within the post-immunotherapy tumor microenvironment (Figure 5d; Supplementary Table S2). Furthermore, the enrichment of pathways associated with negative regulation of SMAD protein signal transduction, enzyme-linked receptor protein signaling, and regulation of kinase activity suggests potential modulations in intracellular signaling cascades and cellular response pathways. Also, pathways related to immune modulation, such as positive regulation of B cell receptor signaling, Fc-gamma receptor signaling, and regulation of positive chemotaxis were altered (Figure 5d; Supplementary Table S2).

Moreover, Enrichr analysis of hypomethylated genes associated with DM CpG sites uncovered pathways related to transcriptional regulation such as RNA polymerase II-mediated transcription and DNA-templated transcriptional control (Figure 5e; Supplementary Table S2). Additionally, pathways regulating signal transduction, including small GTPase mediated signaling and Ras protein signal transduction, hinted at potential alterations in intracellular signaling dynamics post-immunotherapy. Interestingly, pathways linked to cellular responses, such as phagocytosis, epithelial cell migration regulation, and macrophage activation were enriched, as well as pathways related to myeloid cell differentiation and regulation of cell proliferation were found (Figure 5e; Supplementary Table S2). Ultimately, these results highlight that immunotherapy treatment in bladder tumors determines DNA methylation signatures in BC.

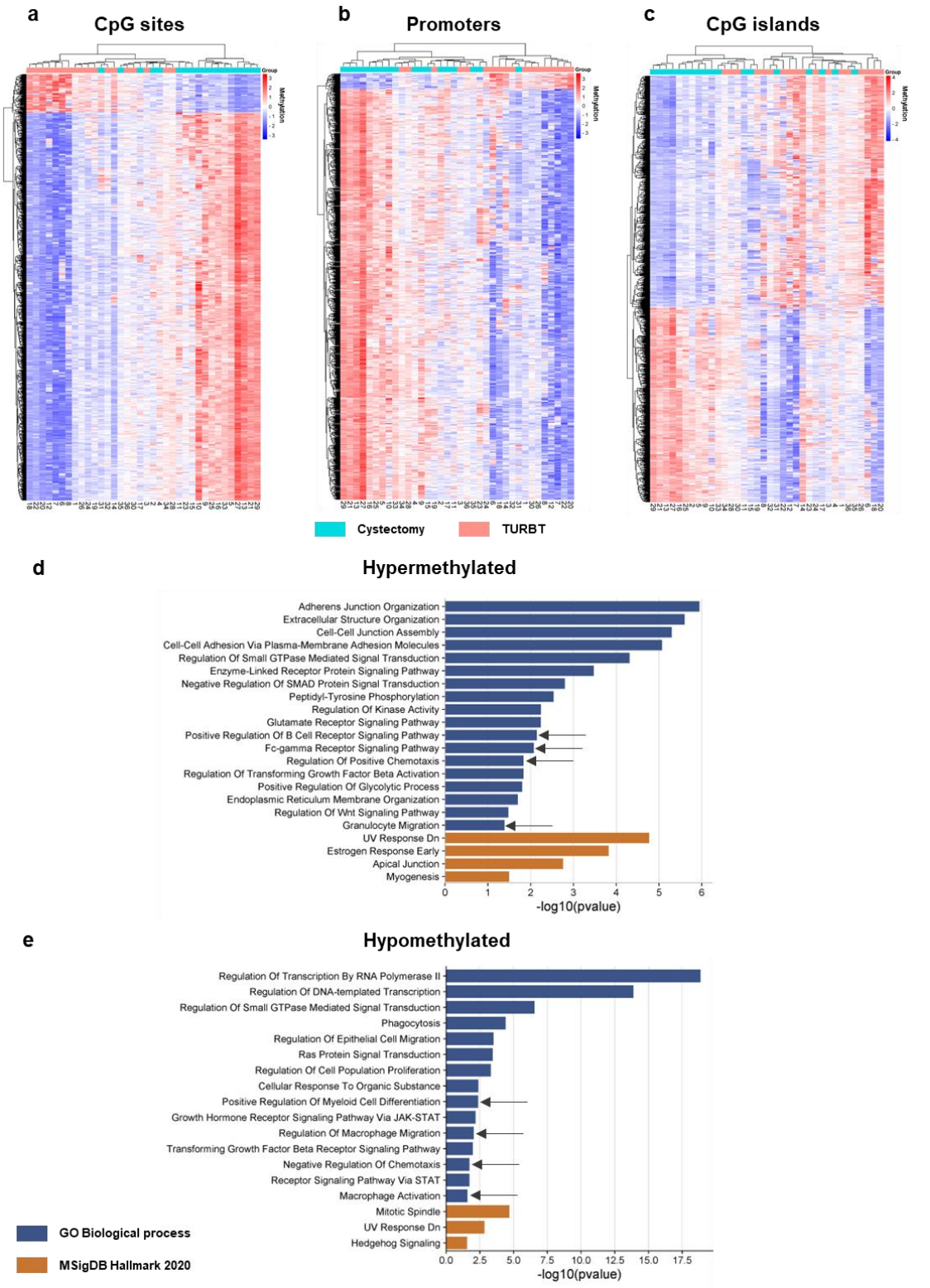


**Figure 5.** Comparative methylation profiling between paired TURBT and cystectomy samples. Supervised hierarchical clustering heatmap of the (a) 1,000 CpG sites, (b) 1,000 promoters and (c) 1,000 CpG islands most differently methylated between TURBT and cystectomy. Enrichr analysis of the (d) hypermethylated and (e) hypomethylated using Gene Ontology (GO) dataset biological processes and MSigDB Hallmark 2020 representing some of the most cancer and immune relevant gene signatures based on the 10,000 most differently methylated CpGs sites of cystectomy samples compared to TURBT samples. Grey arrows denote the most relevant immune-related pathways.

*Comparative methylation analysis of previously identified differentially methylated CpG sites in cystectomy samples*

Next, we analyzed the methylation status of the 22,758 CpG sites, previously identified in TURBT samples as DM between responders and non-responders, in cystectomy samples from non-responders and partial responders to immunotherapy. From these, the methylation status of 3,309 CpG sites were significantly different between cystectomy samples from non-responders and partial responders (Figure 6). Supervised hierarchical clustering of these samples showed that non-responders and partial responders have distinct methylation patterns by clustering separately (Figure 6a). The same was observed at a region level, respectively for 14 promoters and 27 CpG islands (Supplementary Figure S3a and d). Since a low number of promoters and CpG islands were found, we proceed the analyzes with CpG sites.

In the enrichment analysis of CpG sites-associated genes, hypermethylation was found in pathways associated with estrogen response early, myogenesis, apical junction, and glycolysis (Figure 6b; Supplementary Table S3). Additionally, hypomethylation delineated pathways associated with UV response downregulation, interferon alpha and gamma responses, mitotic spindle regulation, G2-M checkpoint control, and TGF-beta signaling (Figure 6b; Supplementary Table S3). The CpG sites were fairly distributed among regions with low and high CpG density, with 22% being in CpG islands, followed by shores and shelfs (Figure 6c). Nevertheless, 55% were in the gene body, followed by 16% located 200-1500 bases upstream of the TSS and 0-200 bases of the TSS (Figure 6d). About 6% of the CpG sites were found in TFBS, whereas the remaining were located outside of TFBS (Figure 6e).

Then, we assessed the methylation status of these 3,309 CpG sites comparing TURBT and cystectomy paired samples from non-responders and partial responders to ICI. We found that methylation patterns of these CpG sites did not change between TURBT and cystectomy samples in non-responders (Figure 6f). On the other hand, clear distinct methylation status can be observed between TURBT and cystectomy samples from partial responders by clustering independently from one another (Figure 6g). The same tendency can be observed in promoters and CpG islands (Supplementary Figure S3b, c, e and f), suggesting that the methylation status of these CpG sites, islands and promoters is important to define response to immunotherapy.

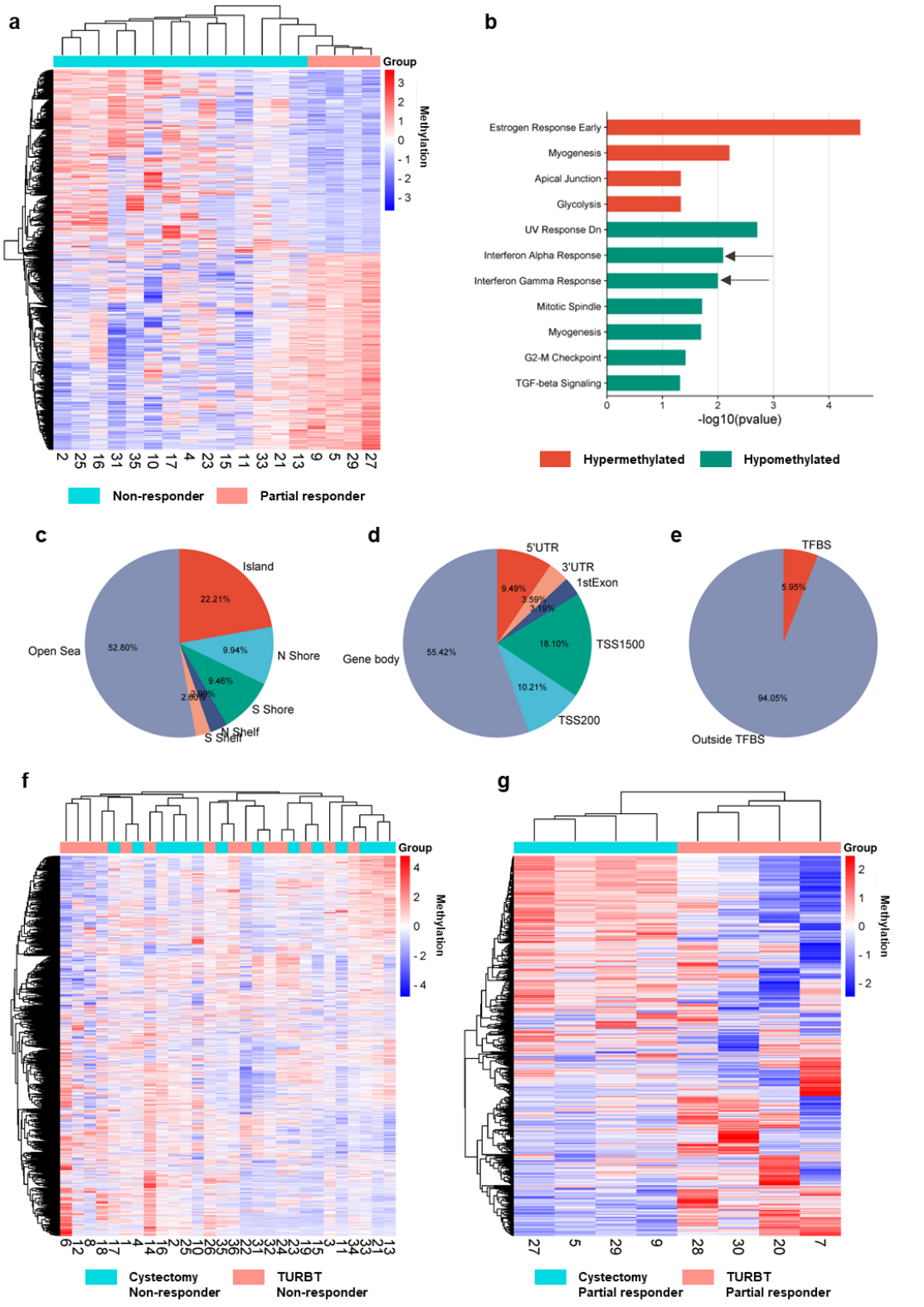


**Figure 6.** Comparison of the methylation patterns of previously identified differentially methylated CpG sites in cystectomy samples of non-responders and partial responders to immunotherapy. (a) Supervised hierarchical clustering heatmap of the 3,309 significantly different CpG sites between cystectomy samples from non-responders and partial responders. (b) Enrichr analysis of the hypermethylated and hypomethylated using MSigDB Hallmark 2020 dataset representing some of the most cancer and immune relevant gene signatures based on the 3,309 differently methylated CpGs sites. (c) CpG context, (d) gene location and (e) transcription factor-binding sites (TFBS) of the 3,309 CpG sites. (f) Supervised hierarchical clustering heatmap of the 3,309

significantly different CpG sites between TURBT and cystectomy samples from non-responders. (g) Supervised hierarchical clustering heatmap of the 3,309 significantly different CpG sites between TURBT and cystectomy samples from partial responders. Grey arrows denote the most relevant immune-related pathways.

## Discussion

In the recent years, ICI therapy has revolutionized BC treatment by improving overall survival of MIBC patients (26). Despite this, a considerable proportion of patients do not present any clinical benefits from ICI (8). Thus, a significant challenge lies on the identification of biomarkers that accurately predict which patients will respond favorably to ICI. The current recommended biomarker for ICI therapy relies on tumor PD-L1/PD-1 expression, which hold well known relevant limitations (8). In this regard, new predictors were proposed including an IFN-γ signature, which failed in selecting MIBC patients that would benefit from neoadjuvant immunotherapy *vs.* chemotherapy (27). DNA methylation plays a pivotal role in BC development and can impact the immune response, influencing the efficacy of immunotherapy (13). Thus, deeper understanding of bladder tumors' epigenetic landscape may provide new biomarkers that accurately predict patient response to immunotherapy. Herein, we focused on exploring DNA methylation profile of bladder tumors treated with ICI not only to investigate the epigenetic mechanisms behind ICI resistance, but also to find DNA methylated-based biomarkers may better identify BC patients that would benefit from immunotherapy.

We started by analyzing DNA methylation differences between responders and non-responders in TURBT samples. The lack of a distinct separation in PCA across responders and non-responders reflected the high heterogeneity between samples from the same group. This heterogeneity was expected given the inclusion of samples from 5 different clinical trials, with different treatments and patient selection criteria. Nevertheless, this can be seen as one of the advantages of this study since this heterogeneity reflets the day-to-day variability found in a hospital treating BC patients. Additionally, by analyzing treatment naïve TURBT samples with a direct pathological assessment of the response when the tumor is collected in the cystectomy, we are able to reduce biases associated with previous treatments, enabling a direct association between DNA methylation and immunotherapy response. Nonetheless, our study was performed as a bulk analysis of the DNA methylation profile, which constitutes an important limitation of this work. Indeed, the differently methylated CpG sites, promoters or CpG islands were obtained from the tumor bulk, and not from specific cell populations, either tumor, immune or stromal cells. The potential association between DNA methylation and different cell types could be achieved by single-cell approaches, projecting differently methylated genes onto UMAP or t-SNE plots. Additionally, RNA-

sequencing deconvolution analysis may aid in subpopulations discrimination contributing in a larger-scale for the differences observed.

While global clustering analysis did not yield a distinct separation between responders and non-responders, differential analysis did reveal significant differences. The majority of CpG sites, promoters and CpG islands were hypermethylated in responders, implying a potential link between increased methylation levels and response to ICI. In the same line, more than half of the DM CpG sites were located in open sea regions. It is known that open sea regions are low density CpG regions important for the maintenance of the genome integrity, suggesting that these can be determinant in ICI response (28). In addition, significantly different CpG sites were also present on the gene body region. Gene body methylation impacts alternative splicing, influencing the sequence of the mature mRNA (14). These results indicate that genomic regions not always well explored and often overlooked can be pivotal to define response to immunotherapy. Nevertheless, about 40% of the CpG sites were found in CpG high-density regions such as islands, shores and shelfs. CpG islands stand out as the most extensively studied gene region when delving into the impact of DNA methylation on gene expression (15). Classically, most studies finding DNA methylation biomarkers of cancer detection and definition of response to therapies focus on promoters and CpG islands (29). Interestingly, we also found differently methylated promoters and CpG islands between responders and non-responders. To further sustain these findings, we aim to assess the direct impact of DNA methylation patters in the gene expression profiles of these samples. Only then, we will be able to determine whether our focus on finding a DNA methylation biomarker or signature will be on a site or region (promoter and CpG island) level, and we may correlate the differential methylation with differential gene expression. Another aspect to consider is the tumor microenvironment remodeling caused by ICI, namely by changes in tumors' immune repertoire (30), that may also alter DNA methylation profile obtained from tumor bulk. As mentioned before, deconvolution analysis using RNA-sequencing is imperative to assess the contribution of the different immune cells' populations to the DNA methylation changes.

Our next aim was to unveil which pathways were altered in responders to ICI using the genes associated with the differently methylated CpG sites. Responders exhibited hypomethylation in pathways linked to MHC Class II and antigen presentation, while pathways associated with cytokine production regulation and T cell differentiation, and immune response signaling were found to be hypermethylated. Interestingly it was shown before that the machinery associated to antigen presentation plays a pivotal role in responses to ICI (31) and that HLA class I are differently methylated in responders to anti-PD-1/anti-PD-L1 immunotherapy (19). Additionally, other pathways, not directly

associated with the immune system, can indirectly modulate the effectiveness of the antitumoral response although. For instance, pathways associated with actin filament organization and cell adhesion may influence immune cell migration to the tumor and cell motility (32). Similarly, cAMP-dependent protein kinase activity was associated with T cells activation and proliferation (33). On the other hand, SMAD phosphorylation was shown to affect TGF-β signaling (34), which positively correlated with the levels of immune cells infiltrating the tumor (35). These results suggest a critical influence of DNA methylation on the immune response within the tumor microenvironment, implying its potential role in modulating responsiveness to ICI treatment. However, as previously mentioned, to comprehensively understand the underlying mechanisms, the effect of differentially methylated CpG sites in genes' transcription and expression needs to be addressed. This will provide deeper insights into the precise role of DNA methylation in the development of resistance mechanisms in BC.

In the next step, we evaluated the influence of immunotherapy on the DNA methylation profiling by comparing TURBT and cystectomy paired samples. A clear difference was found between the methylation profiles of pre- and post-treatment, indicating a significant impact of ICI on DNA methylation patterns. As expected, several pathways associated with transcriptional regulation, extracellular structure organization and cellular architecture are altered, indicating that ICI is indeed leading to tumor remodeling. Interestingly, our investigation revealed that the majority of CpG sites, including those at the promoters and CpG islands, exhibited hypermethylation. Given the observed remodeling of the tumors' DNA methylation landscape occurs with immunotherapy, our results align with the notion that combining DNMT inhibitors with ICI could potentially improve ICI efficacy rates in treating BC. Indeed, this concept is currently under evaluation in several clinical trials focusing on treating advanced BC in combination with anti-PD-1/PD-L1 (13).

Finally, we studied the methylation status of the CpG sites identified as DM on responders in cystectomy samples from partial and non-responders. Intriguingly, the CpG sites' methylation patterns of TURBT and cystectomy samples in non-responders were not altered by immunotherapy. Conversely, samples pre- and post-treatment in partial responders showed different methylation profiles at the CpG sites of interest. This result support the significant role of these CpG sites in determining responsiveness to ICI, as ICI seems to only induce significant changes in CpG methylation profile among partial responders. Notably, two gene signatures appearing as hypomethylated in partial responders are associated with interferon alpha and gamma responses. Both interferons contribute to the upregulation of MHC molecules, enhancing antigen presentation (36), a mechanisms previously found as enriched in responders to ICI in our data. Moreover,

given the limited success of the IFN-γ signature proposed for selecting BC patients for neoadjuvant immunotherapy (27), exploring a DNA methylation signature of these genes might offer a more informative as a biomarker for better selection of urothelial cancer patients.

The quest of reliable biomarkers that accurately predict which patients will respond to immunotherapy poses a major challenge in cancer treatment. Our study uncovers the potential of DNA methylation as a successful tool for identifying responders to ICI and emphasizes the important role of epigenetic mechanisms in shaping BC resistance to immunotherapy. As this study is primarily descriptive, the next step involves delving into the transcriptomic profile of these samples to gain further insights into the interplay between DNA methylation and gene expression in determining response to ICI. Building on these findings, our future aim is to define a DNA methylation signature or panel tailored for the precise selection of BC patients poised to benefit from ICI, with plans to validate this in additional sets of tissue samples and paired liquid biopsies.

**References**

1. Sung H, Ferlay J, Siegel RL, Laversanne M, Soerjomataram I, Jemal A, et al. Global Cancer Statistics 2020: GLOBOCAN Estimates of Incidence and Mortality Worldwide for 36 Cancers in 185 Countries. CA Cancer J Clin. 2021;71(3):209-49.

2. Cumberbatch MGK, Jubber I, Black PC, Esperto F, Figueroa JD, Kamat AM, et al. Epidemiology of Bladder Cancer: A Systematic Review and Contemporary Update of Risk Factors in 2018. Eur Urol. 2018;74(6):784-95.

3. Bilim V, Kuroki H, Shirono Y, Murata M, Hiruma K, Tomita Y. Advanced Bladder Cancer: Changing the Treatment Landscape. J Pers Med. 2022;12(10).

4. Powles T, Bellmunt J, Comperat E, De Santis M, Huddart R, Loriot Y, et al. Bladder cancer: ESMO Clinical Practice Guideline for diagnosis, treatment and follow-up☆. Annals of Oncology. 2022;33(3):244-58.

5. Siefker-Radtke A, Curti B. Immunotherapy in metastatic urothelial carcinoma: focus on immune checkpoint inhibition. Nat Rev Urol. 2018;15(2):112-24.

6. Hussain SA, Birtle A, Crabb S, Huddart R, Small D, Summerhayes M, et al. From Clinical Trials to Real-life Clinical Practice: The Role of Immunotherapy with PD-1/PD-L1 Inhibitors in Advanced Urothelial Carcinoma. Eur Urol Oncol. 2018;1(6):486-500.

7. Powles T, Walker J, Andrew Williams J, Bellmunt J. The evolving role of PD-L1 testing in patients with metastatic urothelial carcinoma. Cancer Treat Rev. 2020;82:101925.

8. Duffy MJ, Crown J. Biomarkers for predicting response to immunotherapy with immune checkpoint inhibitors in cancer patients. Clinical chemistry. 2019;65(10):1228-38.
9. Shen X, Zhao B. Efficacy of PD-1 or PD-L1 inhibitors and PD-L1 expression status in cancer: meta-analysis. Bmj. 2018;362:k3529.
10. Karachaliou N, Gonzalez-Cao M, Crespo G, Drozdowskyj A, Aldeguer E, Gimenez-Capitan A, et al. Interferon gamma, an important marker of response to immune checkpoint blockade in non-small cell lung cancer and melanoma patients. Ther Adv Med Oncol. 2018;10:1758834017749748.
11. Strickler JH, Hanks BA, Khasraw M. Tumor Mutational Burden as a Predictor of Immunotherapy Response: Is More Always Better? Clin Cancer Res. 2021;27(5):1236-41.
12. Presti D, Dall'Olio FG, Besse B, Ribeiro JM, Di Meglio A, Soldato D. Tumor infiltrating lymphocytes (TILs) as a predictive biomarker of response to checkpoint blockers in solid tumors: A systematic review. Crit Rev Oncol Hematol. 2022;177:103773.
13. Nunes SP, Henrique R, Jerónimo C, Paramio JM. DNA Methylation as a Therapeutic Target for Bladder Cancer. Cells. 2020;9(8).
14. Baylin SB, Jones PA. Epigenetic Determinants of Cancer. Cold Spring Harb Perspect Biol. 2016;8(9).
15. Ferreira HJ, Esteller M. CpG Islands in Cancer: Heads, Tails, and Sides. Methods Mol Biol. 2018;1766:49-80.
16. Rodriguez J, Frigola J, Vendrell E, Risques RA, Fraga MF, Morales C, et al. Chromosomal instability correlates with genome-wide DNA demethylation in human primary colorectal cancers. Cancer Res. 2006;66(17):8462-9468.
17. Saif I, Kasmi Y, Allali K, Ennaji MM. Prediction of DNA methylation in the promoter of gene suppressor tumor. Gene. 2018;651:166-73.
18. Duruisseaux M, Martínez-Cardús A, Calleja-Cervantes ME, Moran S, Castro de Moura M, Davalos V, et al. Epigenetic prediction of response to anti-PD-1 treatment in non-small-cell lung cancer: a multicentre, retrospective analysis. Lancet Respir Med. 2018;6(10):771-81.
19. Xue G, Cui ZJ, Zhou XH, Zhu YX, Chen Y, Liang FJ, et al. DNA Methylation Biomarkers Predict Objective Responses to PD-1/PD-L1 Inhibition Blockade. Front Genet. 2019;10:724.
20. Filipski K, Scherer M, Zeiner KN, Bucher A, Kleemann J, Jurmeister P, et al. DNA methylation-based prediction of response to immune checkpoint inhibition in metastatic melanoma. J Immunother Cancer. 2021;9(7).

21. Cho JW, Hong MH, Ha SJ, Kim YJ, Cho BC, Lee I, et al. Genome-wide identification of differentially methylated promoters and enhancers associated with response to anti-PD-1 therapy in non-small cell lung cancer. Exp Mol Med. 2020;52(9):1550-63.
22. Ilijazi D, Pulverer W, Ertl IE, Lemberger U, Kimura S, Abufaraj M, et al. Discovery of Molecular DNA Methylation-Based Biomarkers through Genome-Wide Analysis of Response Patterns to BCG for Bladder Cancer. Cells. 2020;9(8).
23. Klümper N, Wüst L, Saal J, Ralser DJ, Zarbl R, Jarczyk J, et al. PD-L1 (CD274) promoter hypomethylation predicts immunotherapy response in metastatic urothelial carcinoma. Oncoimmunology. 2023;12(1):2267744.
24. Team RC. R: A language and environment for statistical computing. R Foundation for Statistical Computing 2022.
25. Müller F, Scherer M, Assenov Y, Lutsik P, Walter J, Lengauer T, et al. RnBeads 2.0: comprehensive analysis of DNA methylation data. Genome Biol. 2019;20(1):55.
26. Rhea LP, Mendez-Marti S, Kim D, Aragon-Ching JB. Role of immunotherapy in bladder cancer. Cancer Treat Res Commun. 2021;26:100296.
27. Grande E, Guerrero F, Puente J, Galante I, Duran I, Dominguez M, et al. DUTRENEO Trial: A randomized phase II trial of DUrvalumab and TREmelimumab versus chemotherapy as a NEOadjuvant approach to muscle-invasive urothelial bladder cancer (MIBC) patients (pts) prospectively selected by an interferon (INF)-gamma immune signature. American Society of Clinical Oncology; 2020.
28. Esteller M. Epigenetics in cancer. N Engl J Med. 2008;358(11):1148-59.
29. Yamashita K, Hosoda K, Nishizawa N, Katoh H, Watanabe M. Epigenetic biomarkers of promoter DNA methylation in the new era of cancer treatment. Cancer science. 2018;109(12):3695-706.
30. O'Donnell JS, Teng MWL, Smyth MJ. Cancer immunoediting and resistance to T cell-based immunotherapy. Nat Rev Clin Oncol. 2019;16(3):151-67.
31. Chowell D, Morris LGT, Grigg CM, Weber JK, Samstein RM, Makarov V, et al. Patient HLA class I genotype influences cancer response to checkpoint blockade immunotherapy. Science. 2018;359(6375):582-7.
32. Harjunpää H, Llort Asens M, Guenther C, Fagerholm SC. Cell Adhesion Molecules and Their Roles and Regulation in the Immune and Tumor Microenvironment. Front Immunol. 2019;10:1078.
33. Arumugham VB, Baldari CT. cAMP: a multifaceted modulator of immune synapse assembly and T cell activation. J Leukoc Biol. 2017;101(6):1301-16.
34. Shi Y, Massagué J. Mechanisms of TGF-beta signaling from cell membrane to the nucleus. Cell. 2003;113(6):685-700.

35. Liu Z, Qi T, Li X, Yao Y, Othmane B, Chen J, et al. A Novel TGF-β Risk Score Predicts the Clinical Outcomes and Tumour Microenvironment Phenotypes in Bladder Cancer. Front Immunol. 2021;12:791924.
36. Massa C, Wang Y, Marr N, Seliger B. Interferons and Resistance Mechanisms in Tumors and Pathogen-Driven Diseases-Focus on the Major Histocompatibility Complex (MHC) Antigen Processing Pathway. Int J Mol Sci. 2023;24(7).

## Supplementary Information

## Supplementary Figures

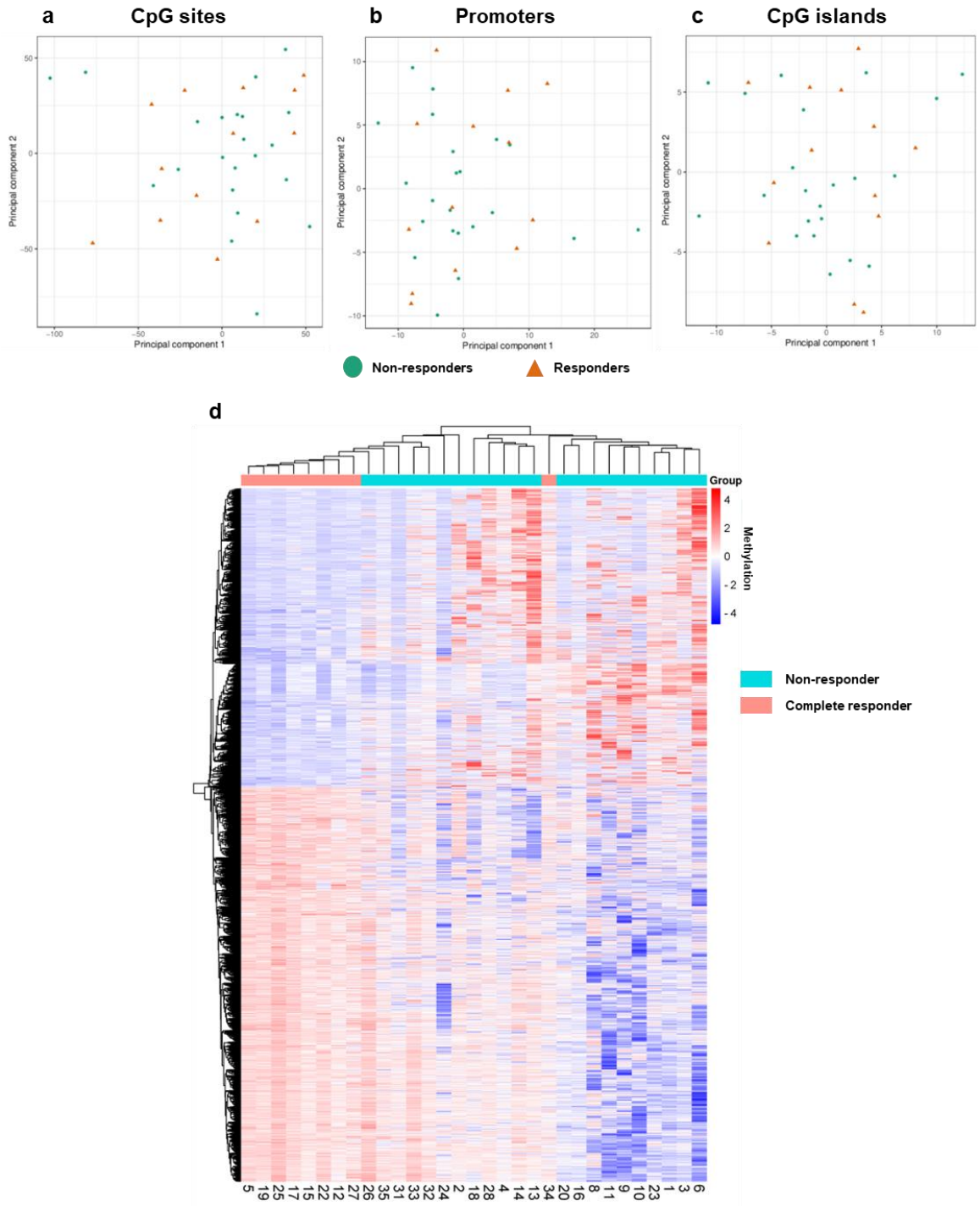


**Figure S1.** Principal component analysis of paired samples of (a) CpG sites, (B) promoters and (c) CpG islands. Non-responders represented as green circles and responders as orange triangles. (d) Supervised hierarchical clustering heatmap of the 4,502 significantly different CpG sites between non-responders and complete responders in TURBT.

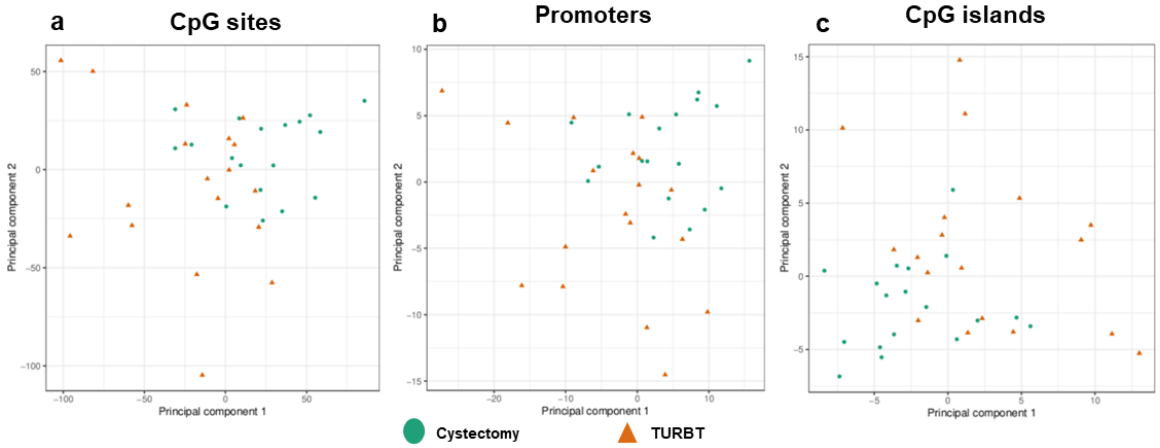


**Figure S2.** Principal component analysis of paired TURBT and cystectomy samples of (a) CpG sites, (b) promoters and (c) CpG islands. Cystectomy represented as green circles and TURBT as orange triangles.

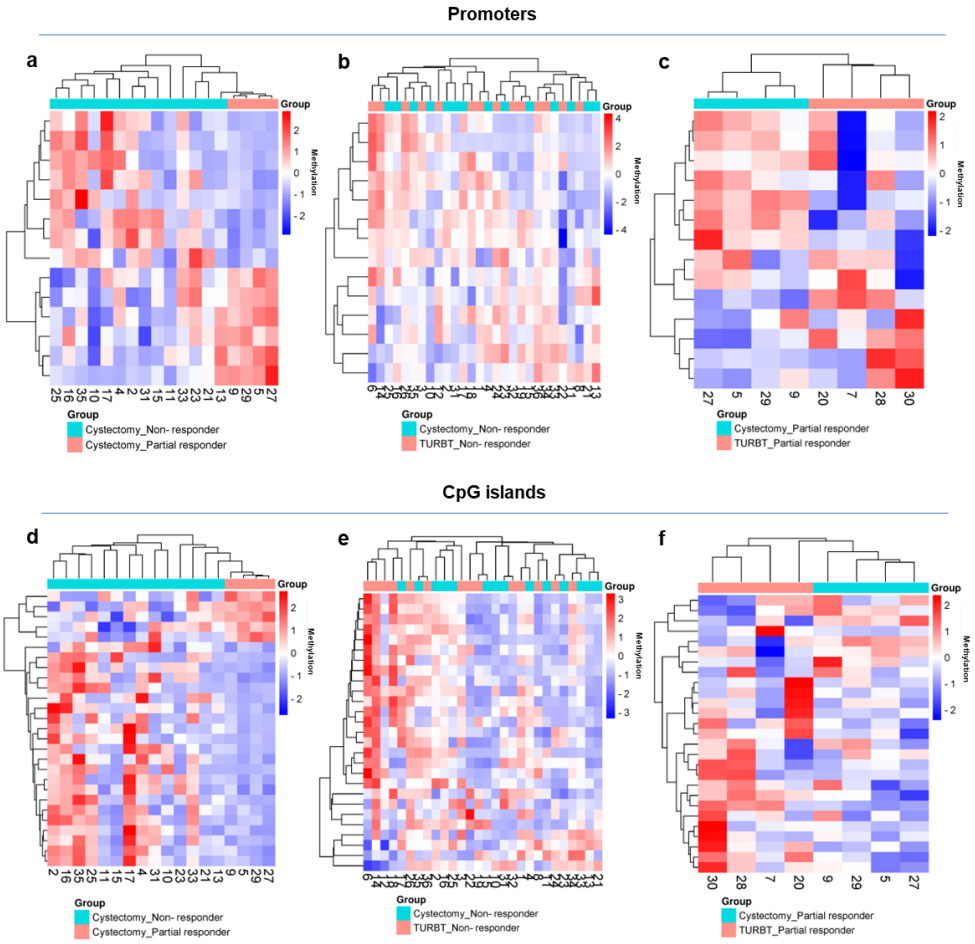


**Figure S3.** Supervised hierarchical clustering heatmap of the (a) 14 promoters and (b) 27 CpG islands significantly different CpG sites between cystectomy samples from non-responders and partial responders. Supervised hierarchical clustering heatmap of the (b) 14 promoters and (e) 27 CpG islands significantly different CpG sites between TURBT and cystectomy samples from non-responders. Supervised hierarchical clustering heatmap of the (b) 14 promoters and (e) 27 CpG islands significantly different CpG sites between TURBT and cystectomy samples from partial responders.

## Supplementary Tables

**Table S1.** Genes associated with the CpG sites differently methylated (hyper- and hypomethylated) in responders compared to non-responders from the Enrichr analysis using Gene Ontology (GO) dataset biological processes and MSigDB Hallmark 2020 representing some of the most cancer and immune relevant gene signatures based on the 10,000 most differently methylated CpGs sites.

| Term | Genes |
|---|---|
| ***Hypermethylated*** | |
| **Cell Junction Assembly** | NLGN1;PLXND1;CTNND2;NRXN1;PTEN;CDH8;CDH7;CDH4;ARVCF;SPOCK2;DNER; GJA4;NRCAM;KIRREL3;DBNL;DSCAM;BDNF;PCDHB11;PCDHB10;DNM3;SDK1;TRPV4; CDH11;CDH13;PCDHB5;TLN2;PCDHB9;SHANK2;SDK2 |
| **Glutamate Receptor Signaling Pathway** | GRIA2;GRID2;HOMER1;GRIK4;GRIN2C;GRM1;GRIN2D;GRM3;TRPM1;GRM2;GRIN2A;GRM5;GRM7;GRM6;PTK2B |
| **G Protein-Coupled Glutamate Receptor Signaling Pathway** | GRM3;TRPM1;GRM2;GRM5;GRM7;HOMER1;GRM6;GRM1 |
| **Transmembrane Receptor Protein Tyrosine Kinase Signaling Pathway** | PTPRT;RET;TRIM71;PLAT;IDE;FGF1;FGF2;FGF4;IGF1R;FGF5;FGF7;FGF8;UBASH3B; KDR;GRB10;EPHB1;ROS1;ANKS1B;EPHA6;NRG1;NGF;GFRA2;FGR;ZAP70;CD8B; COL4A2;CD8A;DOK5;LCK;DOK6;KIT;RAPGEF1;NGEF;DDR2;LTK;SHC3;PDGFB;PAK1; EFS;NTF3;MAPK1;PTK2B;FYN;NTRK1;KL;NTRK2;SRMS;BDNF;NTRK3;TIE1;IGF1;SULF1; NFATC4;SULF2;NELL1;AXL;FGF19;CLNK;GRB2;FRK |
| **Adenylate Cyclase-Modulating G Protein-Coupled Receptor Signaling Pathway** | VIPR1;VIPR2;PTGER1;FPR1;ADCY4;CACNA1D;ADRA1D;ADCY2;FPR2; ADRA1B;RIMS2;AKAP12;ADGRE2;GALR3;GRK5;ADGRE5;GNAT3;CNR1; FFAR3;PRKACB;TCP11;LHCGR;PSAPL1;GLP2R;SCTR;HTR1B;GPR4;TSHR; ADGRD1;MTNR1A;ADCY9;ADRB3;ADGRB3;ADM2;MC5R;GNAS;ADGRL1;ADGRL2;PF4 |
| **Enzyme-Linked Receptor Protein Signaling Pathway** | PTPRT;RET;LTK;SHC3;PTPRF;EFS;NTF3;KDR;FYN;ROS1;NTRK1;NTRK2;SRMS;BDNF;NTRK3;TIE1;NGF; GFRA2;FGR;ZAP70;CD8B;CD8A;DOK5;LCK;AXL;DOK6;RAPGEF1;CLNK;FRK;DDR2 |
| **Positive Regulation Of Small GTPase Mediated Signal Transduction** | NTRK1;RELN;RASGRF1;STK19;IGF1;NGF;RASGRP1;TGM2 |

| | |
|---|---|
| **Positive Regulation Of Signal Transduction** | PTEN;RBPJ;FGF1;RIMS2;RIMS1;HHEX;NETO1;RSPO2;GRB10;TNFSF11;NKX31;PTGIS; VWF;PRKCB;CD226;SHANK1;MACF1;CD63;NLGN1;TNXB;CTBP2;LAMA2;DHH;LAMA1;NRXN1; KLK5;NOD2;PRKCZ;GRIN2A;RELN;MGAT5;PTK2B;WNT1;JAG2;TGFB2;HOMER1;BDNF;NOS3;PDE6G;WNT7A;IGF1; GRIN2C;SULF1;GRIN2D;SULF2;SMOC2;NELL1;PTPRC;AXL;DLG4;CNTN1;LGR6 |
| **Regulation Of Natural Killer Cell Cytokine Production** | CD226;HLA-F;HLA-G;HLA-E |
| **T Cell Differentiation** | JAG2;USP44;CHD7;SOX13;RHOH;ZFP36L1;ZAP70;PTPRC;CD8A;LCK;LEP;KIT;CD28 |
| **Wnt Signaling Pathway** | TCF7L1;WNT2B;WNT5B;NXN;WNT3A;WNT5A;PTEN;WNT9B;FZD9;WNT7A;WNT16;SFRP2; FRZB;TMEM67;CCDC88C;PLCG2;STRN;WNT1 |
| **Positive Regulation Of Cytokine Production Involved In Immune Response** | WNT5A;KIT;PLCG2;FFAR3;CD226;NOD2;HLA-A;HLA-F;HLA-G;HLA-E |
| **Regulation Of Cellular Response To Growth Factor Stimulus** | TFAP2B;NELL1;DOK5;SULF1;FSTL1;FSTL4;FSTL3 |
| **Regulation Of Positive Chemotaxis** | NTRK3;CNTN1;KDR;CDH13 |
| **Positive Regulation Of Chemotaxis** | SEMA5A;NELL1;SMOC2;DSCAM;NTRK3;PDGFB;KDR;CNTN1;CDH13;MEGF8;FGF2;IL6R |
| **Negative Regulation Of Interleukin-1 Production** | CX3CR1;GHSR;NLRP12;NLRP7;GSTP1;NLRP3;FFAR1;IGF1;MEFV |
| **Immune Response-Inhibiting Cell Surface Receptor Signaling Pathway** | PSG4;KIR2DL1;LILRB2;HLA-G |
| **Regulation Of Cell Migration** | RET;SEMA5A;PTPRT;MCTP1;PLXND1;PTEN;PTPRK;FGF1;FGF2;SYNE2;FGF4;IGF1R;FGF5;ING2;FGF7; FGF8;KDR;EMILIN2;PHACTR1;WNT5B;SEMA6D;F2R;MAGI2;RNF41;FGR;SFRP2;SMO;SPATA13;KIT;CDH11;NUMB; |

| | |
|---|---|
| | MYADM;CDH13;SGK1;CAMK2B;MACF1;TNXB;PDGFB;STC1;TWIST1;NKD1;PAK1;RELN;MGAT5;NTF3;PDPN;NKX2-1;MGAT3;PTK2B;FYN;SRGAP3;SRGAP1;PLXNA4;TCAF1;NTRK3;IGF1;SULF1;TBX5;ALOX15B;IGSF10;CXCL12;SST;KIF26A;FGF19;BRMS1L;CNTN1;SPRY2;EPPK1;LGR6;RECK;FERMT3 |
| **Immune Response-Regulating Cell Surface Receptor Signaling Pathway** | FGR;KIT;FPR2;LILRB2;HLA-G |
| **Regulation Of Macrophage Cytokine Production** | TGFB2;TGFB3;WNT5A;PLCG2;HLA-G |
| **Positive Regulation Of Myeloid Leukocyte Cytokine Production Involved In Immune Response** | WNT5A;KIT;PLCG2;TICAM1;HLA-G |
| **Epithelial Mesenchymal Transition** | COPA;LAMA2;LAMA1;NTM;COL12A1;LAMA3;THBS2;FSTL1;FGF2;FBLN2;FSTL3;LOXL2;COMP;ANPEP;SPOCK1;QSOX1;SLIT3;PDLIM4;TGM2;PRRX1;BDNF;MMP1;WNT5A;VCAN;BMP1;CXCL12;FAP;COL4A2;COL5A1;COL4A1;COL6A2;ADAM12;CDH11;PMP22;COL6A3;VIM |
| **KRAS Signaling Up** | SPON1;PLVAP;ABCB1;USP12;PLAT;IKZF1;AKAP12;RBM4;RELN;ANKH;PRKG2;EVI5;CMKLR1;ST6GAL1;RABGAP1L;CDADC1;PEG3;PRRX1;CCL20;GFPT2;ATG10;CIDEA;WNT7A;NGF;PSMB8;PCP4;CCSER2;IRF8;SPRY2;STRN;DOCK2;TRIB2;CFB;SDCCAG8 |
| ***Hypomethylated*** | |
| **Regulation Of Morphogenesis Of A Branching Structure** | LRRK2;SIX2;FGFR2;RTN4 |
| **Negative Regulation Of cAMP-dependent Protein Kinase Activity** | PKIB;PRKAR1B;PRKAR2B;PKIG |

| | |
|---|---|
| **Positive Regulation Of Focal Adhesion Assembly** | NELL1;PTPRJ;TSC1;PPM1F;FERMT2;LIMS1;MAP4K4 |
| **Negative Regulation Of Pathway-Restricted SMAD Protein Phosphorylation** | SNX25;PPARG;SMAD6;SMAD7 |
| **MHC Class II Protein Complex Assembly** | HLA-DRB5;HLA-DQA1;HLA-DQB2;HLA-DRB1;HLA-DPA1 |
| **Peptide Antigen Assembly With MHC Class II Protein Complex** | HLA-DRB5;HLA-DQA1;HLA-DQB2;HLA-DRB1;HLA-DPA1 |
| **Actin Filament Organization** | WIPF1;FLII;NEDD9;CAPG;PPP1R9A;CNN3;SCIN;GAS2L2;ACTN1;MYO7B;SHROOM3;EMP2;MYO7A; SERPINB8;ENAH;MYO1D;MYO1E;MYO1B;MYO1C;TRPV4;ELMO1;CORO6;FAT1;CDC42EP2;TCAP; EVL;ALDOA;BCAR1 |
| **Epithelial Cell-Cell Adhesion** | ITGB5;KIFC3;SERPINB8;VCL |
| **Negative Chemotaxis** | SEMA7A;SEMA6A;SEMA3D;LRTM1;PDGFA;LGR6;NTN1;ROBO1 |
| **Integrin-Mediated Signaling Pathway** | SEMA7A;ITGB5;DST;PLEK;NEDD9;FBLN1;ITGAL;PTK2;NELL1;ITGA8;ADAM9;MYH9;ITGBL1;DOCK1;BCAR1;FERMT2;ITGA9 |
| **Negative Regulation Of Protein Serine/Threonine Kinase Activity** | LYN;LRP5;DAB2IP;PTPRJ;NR2F2;IPO7;SORL1;PKIB;HHEX;LATS2;PRKAR1B;PRKAR2B;PKIA;PPARG;PKIG;SH2B3 |
| **Positive Regulation Of Lymphocyte Activation** | HLA-DRB5;TICAM2;TYROBP;FCHO1;TLR9;NOD2;HLA-DQA1;HLA-DQB2;HLA-DRB1;HLA-DPA1 |
| **Fc-gamma Receptor Signaling Pathway** | LYN;PAK1;PRKCE;CD247;PTK2;VAV2 |

| | |
|---|---|
| **Immunoglobulin Production Involved In Immunoglobulin-Mediated Immune Response** | HLA-DRB5;HLA-DQA1;HLA-DQB2;HLA-DRB1;HLA-DPA1 |
| **Regulation Of MAP Kinase Activity** | LYN;MEF2C;KSR1;LRRK2;DAB2IP;PDGFA;TGFA;PTPRJ;NOD2;SORL1;EGFR;ROBO1;NEK10;ADAM9; S100A12;PPARG;CDK12;SH2B3;ELANE |
| **Antigen Processing And Presentation Of Exogenous Peptide Antigen Via MHC Class II** | HLA-DRB5;HLA-DQA1;HLA-DQB2;HLA-DRB1;HLA-DPA1;DNM2 |
| **Ras Protein Signal Transduction** | BRAP;RTKN;KSR1;PLEKHG7;RASGRF1;IGF1;CELSR1;PLD1;ARHGAP5;NTN1;RAPGEFL1;RASSF1; RIT1;DOK4;GRAP2;ARHGDIB;GNA12;ELMO1;EPS8L2;RGL1;CTNNAL1;RAPGEF3 |
| **Negative Regulation Of Intracellular Signal Transduction** | DGKG;PPM1N;RTKN2;PDE3B;PLEK;ITPR1;PTPRJ;LIMD1;TANK;HDAC9;UACA;IGF1R;PKHD1;SPRED2; NUAK1;DEPTOR;DRD2;SH2B3;LYN;EPM2A;DUSP2;PDE4D;DAB2IP;TSC1;ESR1;P2RX7;MYO1C; PPARG;TRIM59;GPD1L;SHANK2;BCL2L1 |
| **Regulation Of Mononuclear Cell Migration** | LYN;STK10;CXCL17;MAPK1;PTK2 |
| **Antigen Processing And Presentation Of Peptide Antigen Via MHC Class II** | HLA-DRB5;HLA-DQA1;HLA-DQB2;HLA-DRB1;HLA-DPA1;DNM2 |
| **Negative Regulation Of BMP Signaling Pathway** | DLX1;BMPER;CAPN5;CRIM1;PPARG;SMAD6;SORL1;SMAD7 |
| **Immunoglobulin Mediated Immune Response** | HLA-DRB5;IL21R;HLA-DQA1;HLA-DQB2;HLA-DRB1;HLA-DPA1 |
| **Phagocytosis** | TICAM2;TYROBP;BIN2;ANXA3;ELMO1;MYH9;NR1H3;PIP5K1C;MERTK;DOCK1;ELANE |

| | |
|---|---|
| **Myogenesis** | CHRNA1;APP;VIPR1;ITGB5;FLII;AK1;CACNA1H;CNN3;CKMT2;SH3BGR;PDLIM7;SH2B1;KCNH2; CHRNB1;MEF2C;PTGIS;ACTN2;ACSL1;DAPK2;IFRD1;IGF1;NAV2;SORBS3;COL1A1;RIT1;ADCY9;MYO1C;SCD; PKIA;ADAM12;TCAP;PLXNB2;MYH9;KIFC3;LPIN1 |
| **Mitotic Spindle** | NOTCH2;DOCK4;TUBGCP2;PXN;NEDD9;BRCA2;ARHGAP5;ABR;FGD6;SYNPO;SPTBN1;FARP1;DST; TBCD;RANBP9;KIF23;SORBS2;TSC1;ACTN4;MYO1E;PALLD;TAOK2;CDC42EP2; FSCN1;CDK1;MYH9;ARHGEF7;VCL;BCAR1 |
| **Androgen Response** | TNFAIP8;UBE2I;TSC22D1;ACTN1;IQGAP2;MERTK;NDRG1;CDC14B;INPP4B;AZGP1; MAF;ZMIZ1;SCD;MAP7;GPD1L;BMPR1B;SGK1 |
| **UV Response Dn** | NOTCH2;RBPMS;MIOS;SFMBT1;MGMT;PRKCE;ANXA4;PIK3R3;PTPRM;IGF1R;SMAD7; VAV2;COL1A1;INPP4B;RXRA;ZMIZ1;PRKAR2B;ADORA2B;PMP22;PPARG |
| **Apical Surface** | PKHD1;LYN;APP;AFAP1L2;ATP8B1;CROCC;LYPD3;ATP6V0A4 |
| **Angiogenesis** | LRPAP1;APP;PDGFA;OLR1;MSX1;PTK2;VAV2 |

**Table S2.** Genes associated with the CpG sites differently methylated (hyper- and hypomethylated) in cystectomy compared to TURBT samples from the Enrichr analysis using Gene Ontology (GO) dataset biological processes and MSigDB Hallmark 2020 representing some of the most cancer and immune relevant gene signatures based on the 10,000 most differently methylated CpGs sites.

| Term | Genes |
|---|---|
| ***Hypermethylated*** | |
| **Adherens Junction Organization** | TBCD;CDH8;MTSS1;TJP1;CDH4;CDH2;CDH1;CDH10;CDH11;CDH12;CDH13;DCHS1; CDH26;PIP5K1C;CDH15;CDH17;CDH18;JAM3 |
| **Extracellular Structure Organization** | HPSE2;COL13A1;COL11A1;DMP1;FURIN;ADAMTS12;ADAMTS10;COL19A1;THSD4;ADAMTS16; ADAMTS2;ADAMTS3;MMP26;ADAMTS17;ADAMTS9;ADAMTS6;COL24A1;MMP1;COL22A1;COL23A1; TEX14;MMP10;ADAMTS20;SMOC2;MMP13;COL4A2;SPINT1;COL5A1;COL4A1;MANSC4;PXDN; COL9A1;MATN1;COL8A1;COL9A3;COL9A2;RECK |
| **Cell-Cell Junction Assembly** | CTNND2;CDH8;CDH4;PARD6B;CDH2;CDH1;GJA4;EPB41L3;CDH26;PIP5K1C;JAM3;JUP;TBCD; PRKCA;TJP1;CDH10;CDH11;CDH12;PKP2;CDH13;CD9;PKP4;DCHS1;CDH15;PKP3;CDH17;CDH18 |
| **Cell-Cell Adhesion Via Plasma-Membrane Adhesion Molecules** | CD84;TENM2;ITGAM;TENM3;TENM4;ITGB2;PTPRM;CDH8;PTPRF;CDH4;CDH2;CDH1;HMCN2;NPTN; KIRREL3;GRID2;CXADR;DSCAM;UNC5D;TGFBR2;CLDN4;MAG;CLDN14;CLDN8;CDH10;CDH11;CDH12; PECAM1;CDH13;CDH15;CDH17;DSCAML1;CDH18;CRB1;GATA5;UMOD;CDH26;LRRC4C;LRRC4B;MPZL2; CADM3;CADM1;CADM2;CRTAM;CEACAM19;PTPRD;LRFN5;DCHS1;CNTN4;SDK2 |
| **Regulation Of Small GTPase Mediated Signal Transduction** | SRC;ARHGEF28;RASGRF2;FAM13A;ITSN1;ARHGAP15;KALRN;ARHGAP12;PREX2;ARHGAP22; FGD3;GNA13;AKAP13;FGD5;RELN;CHN2;SLIT2;CGNL1;TGM2;VAV3;STARD13;ARHGEF12;PLEKHG6; ARHGAP26;ARHGAP25;RHOD;CD2AP;ARHGAP23;VAV2;TIAM1;ARHGAP32;OBSCN;DNMBP;SPATA13;ARHGEF3;DOCK2 |
| **Enzyme-Linked Receptor Protein Signaling Pathway** | ALK;FLT1;LRP1;FLT3;FLT4;NEDD9;PTN;PTPRF;PDZD3;ERBB3;ERBB4;ERBB2;FYN;NTRK2; MUSK;NTRK3;LIFR;PTK6;NGF;MERTK;MTSS1;PTPRD;CNKSR1;HCK;ZAP70;DOK5;LCK;DOK6;CLNK;ROR1;LCP2; TEK;FGFR4;FGFR2;EPHA2 |
| **Negative Regulation Of SMAD Protein Signal Transduction** | LRP1;SLC2A10;VEPH1;PPARG;PBLD |
| **Peptidyl-Tyrosine Phosphorylation** | ALK;FLT1;FLT3;SRC;FLT4;PTK6;PRLR;TTBK1;HCK;ZAP70;RELN;LCK;ERBB4;ERBB2;FYN;TEK;EPHB2;FGFR4;EPHA3;FGFR2 |
| **Regulation Of Kinase Activity** | VAC14;NTRK2;FLT1;MUSK;FLT3;FLT4;NTRK3;LDB2;MERTK;TTN;SOD1;RBL2;CSRP3; CCNY;ERBB3;ERBB4;ERBB2;CCNYL1;ROR1;TEK;FGFR4;FGFR2;EPHA2 |

| | |
|---|---|
| **Glutamate Receptor Signaling Pathway** | TRPM1;GRIN2A;GRM5;GRID2;GRIN3B;GRM4;GRM7;KCNB1;GNAQ;GRIK4;GRIK1;GRIA4 |
| **Positive Regulation Of B Cell Receptor Signaling Pathway** | PRKCH;PRKCB;NFAM1;FOXP1 |
| **Fc-gamma Receptor Signaling Pathway** | VAV3;HCK;SRC;LCK;PRKCE;FYN;CD247;PLA2G6;VAV2 |
| **Regulation Of Positive Chemotaxis** | F7;NTRK3;CNTN1;CDH13 |
| **Regulation Of Transforming Growth Factor Beta Activation** | TNXB;ITGB6;LRRC32;LTBP1 |
| **Positive Regulation Of Glycolytic Process** | P2RX7;RPTOR;PRKAA1;ARNT;ZBTB20;IGF1;SLC4A4 |
| **Endoplasmic Reticulum Membrane Organization** | VAPB;ATL1;ATL2;RTN4;TRDN |
| **Regulation Of Wnt Signaling Pathway** | KANK1;LRP1;NXN;CTNND2;CMAHP;TSKU;SNX3;STK11;GRB10;RSPO1;BTRC;ATP6V1C2; RNF43;WWOX;TCF7L1;CTNNBIP1;SULF1;SULF2;TIAM1;CCNY;DAAM2;GNAQ;CCNYL1;FGFR2;VGLL4 |
| **Granulocyte Migration** | ITGB2;GP2;UMOD;JAM3 |
| **UV Response Dn** | NOTCH2;NRP1;YTHDC1;INSIG1;CELF2;COL11A1;FHL2;ICA1;CACNA1A;PTPRM;PRDM2;SRI;LTBP1; KALRN;SLC7A1;SYNE1;ATXN1;SIPA1L1;RXRA;ZMIZ1;AKT3;ERBB2;FYN;CDON;SMAD3;PRKCE;ANXA4;MAGI2; PRKCA;SYNJ2;ATP2B1;CDC42BPA;PEX14;RUNX1;VAV2;TGFBR2;TJP1;INPP4B;PLCB4;KCNMA1;AMPH;PPARG;ADGRL2 |
| **Estrogen Response Early** | B4GALT1;WWC1;FHL2;AQP3;TSKU;RAPGEFL1;RPS6KA2;MYB;RRP12;SYBU;TGM2;MREG; KRT8;KAZN;GFRA1;NAV2;CBFA2T3;RHOD;SULT2B1;TIAM1;ELF3;ESRP2;SCNN1A;PGR;NBL1;SLC22A5;SLC24A3; PEX11A;TMPRSS3;ABHD2;RHOBTB3;THSD4;SYNGR1;ABLIM1;ALDH3B1;SH3BP5;SFN;FLNB;SLC19A2; FARP1;KDM4B;SLC37A1;OPN3;SIAH2;SNX24;DHRS3;TTC39A;REEP1;KRT19;KRT18;SYT12;TJP3 |

| | |
|---|---|
| **Apical Junction** | B4GALT1;ITGB4;SRC;INSIG1;LAMA3;ATP1A3;PARD6G;DMP1;GNAI1;CDH8;SGCE;LIMA1;CDH4;PDZD3;<br>CDH1;AKT3;ADAM23;TSPAN4;RSU1;SLIT2;PCDH1;TMEM8B;JAM3;MPZL2;CADM3;CDSN;JUP;<br>VWF;LAMB3;CADM2;ITGA2;TSC1;BAIAP2;VAV2;TJP1;CLDN4;VCAN;NFASC;BMP1;PPP2R2C;<br>CLDN14;CLDN8;CDH11;COL9A1;CNTN1;PECAM1;CDH15;FBN1 |
| **Myogenesis** | RYR1;CAMK2B;MYOM1;VIPR1;CDKN1A;ITGB4;AEBP1;MYOM2;CACNA1H;MYLK;CSRP3;ABLIM1;ERBB3;<br>TNNI1;NCAM1;ANKRD2;CD36;NOS1;MEF2D;MYBPC3;WWTR1;MEF2C;DTNA;ACSL1;DAPK2;AGL;<br>PGAM2;IGF1;NAV2;MAPK12;REEP1;COL4A2;SCD;TNNT2;TNNT3;ADAM12;CASQ2;CDH13;KIFC3;MYH4;PFKM;PVALB |
| ***Hypomethylated*** | |
| **Regulation Of Transcription By RNA Polymerase II** | CD81;FOXI2;PRDM2;ETS1;IKZF4;SOX1;ZMIZ1;TP63;NKX26;KDM2B;RFX1;PIAS1;ISL2;MAML3;<br>GCM2;ZNF791;DLX5;FOXG1;DLX6;PRDM14;HOXB13;ZNF709;ATXN1;GALR1;HIVEP1;ZSCAN12;ALX4;ALX1;<br>OTX1;NKX61;NKX24;TFAP2A;STAT5B;ZBTB17;ZFHX3;BCL11B;TFAP2E;EVX1;SMARCA2;HOPX;PHOX2B;NR2F6;NR4A2;<br>HOXD3;SIM1;SIM2;ZNF652;ZNF497;ONECUT2;TCF21;NR2E1;LYL1;SHH;SIX6;ZIC1;LRRFIP1;TEAD1;NKX32;FOXD3;<br>KLF12;ANXA4;DNMT3A;EN1;KLF16;ETV6;NCOR2;DMRTA2;RIPPLY3;TAL1;PAX9;ARHGEF2;MDFI;KANK2;<br>ASCL4;LRP5;BARX1;MSX1;MEF2D;IRX1;TCF7L1;USP22;STAT3;ZIC5;ARID3C;POU4F1;TBX4;MEIS2;KLF2;<br>TBX18;GATAD2A;SKI;ASXL1;PER1;KLF7;TBX15;MEIS1;NFIA;AGRN |
| **Regulation Of DNA-templated Transcription** | ONECUT2;FOXI2;TCF21;PRDM2;ETS1;IKZF4;LYL1;SHH;SIX6;SOX1;ZMIZ1;ZIC1;LRRFIP1;<br>TEAD1;TP63;NKX32;FOXD3;KLF12;NKX26;KDM2B;ANXA4;DNMT3A;EN1;RFX1;KLF16;PIAS1;ETV6;NCOR2;DMRTA2;<br>TAL1;PAX9;GCM2;ZNF791;ASCL4;DLX5;FOXG1;DLX6;LRP5;PRDM14;HOXB13;BARX1;CAMKK2;ZNF709;<br>ATXN1;HIVEP1;ZSCAN12;ALX4;ZNF503;ALX1;MSX1;OTX1;NKX61;NKX24;TFAP2A;IRX1;STAT5B;ZFHX3;TCF7L1;TFAP2E;<br>INSR;USP22;STAT3;EVX1;FOXN3;ZIC5;ARID3C;SMARCA2;POU4F1;TBX4;HOPX;PHOX2B;KLF2;TBX18;<br>GDF7;GATAD2A;NR4A2;PER1;KLF7;TBX15;NFIA;HOXD3;SIM1;SIM2;ZNF652;ZNF497 |
| **Regulation Of Small GTPase Mediated Signal Transduction** | ARHGEF17;RASGRF1;MYO9B;ARHGAP25;AKAP13;FGD4;ARHGAP30;DNMBP;PLCE1;TNFRSF25;SRGAP3;ARHGEF2;SLIT2 |
| **Phagocytosis** | GSN;CD93;ALOX15;MYH9;PIP5K1C;DOCK1;AIF1;ARHGAP25 |
| **Regulation Of Epithelial Cell Migration** | DOCK5;MACF1;PRKCE;CTSH;DOCK1;ARSB |
| **Ras Protein Signal Transduction** | RASGRF1;GNA12;PLCE1;EPS8L1;TNFRSF25;EPS8L2;MYO9B;RAPGEF6;AIF1;RAPGEFL1 |

| | |
|---|---|
| **Regulation Of Cell Population Proliferation** | KANK2;CD81;LRP5;AIF1;ETS1;SHH;CYP1B1;CTSH;ZNF503;TFAP2A;STAT5B;ZBTB17;NKX2-6;TSC22D1;TFAP2E;INSR;STAT3;GAB2;AVPR1A;PPP2R5C;SMARCA2;MEIS2;PIAS1;SKI;MEIS1;ALDH1A2;ARHGEF2;SHANK2 |
| **Cellular Response To Organic Substance** | STAT5B;STAT3;CYP1B1;AVPR1A;SLIT2;POU4F1 |
| **Positive Regulation Of Myeloid Cell Differentiation** | STAT5B;TAL1;STAT3;ETS1 |
| **Growth Hormone Receptor Signaling Pathway Via JAK-STAT** | STAT5B;STAT3 |
| **Regulation Of Macrophage Migration** | CD81;MTUS1 |
| **Transforming Growth Factor Beta Receptor Signaling Pathway** | TGFBR3;SKI;ITGB5;ZMIZ1;STAT3 |
| **Negative Regulation Of Chemotaxis** | SEMA4A;SEMA6A;SLIT2 |
| **Receptor Signaling Pathway Via STAT** | STAT5B;STAT3;PIAS1 |
| **Macrophage Activation** | CD93;AIF1;TMEM106A |
| **Mitotic Spindle** | GSN;MYO9B;SHROOM1;AKAP13;FGD4;ARHGAP10;CYTH2;CAPZB;CEP250;MYH9;ARHGEF2;RAPGEF6;WASF2;SPTBN1 |
| **UV Response Dn** | TGFBR3;ATXN1;ZMIZ1;BDNF;PRKCE;ANXA4;ICA1;PRDM2;FYN |
| **Hedgehog Signaling** | SHH;MYH9;NKX6-1 |

**Table S3.** Genes associated with the CpG sites differently methylated (hyper- and hypomethylated) in cystectomy samples comparing non-responders and partial responders from the Enrichr analysis using Gene Ontology (GO) dataset biological processes and MSigDB Hallmark 2020 representing some of the most cancer and immune relevant gene signatures based on the 3,309 differently methylated CpGs sites.

| Term | Genes |
|---|---|
| ***Hypermethylated*** | |
| **Estrogen Response Early** | NXT1;ABHD2;SLC1A1;RHOBTB3;PRSS23;PAPSS2;THSD4;AKAP1;IGF1R;SYNGR1;DEPTOR; LRIG1;HES1;TFAP2C;WFS1;ITPK1;KCNK15;RHOD;MED13L;ADCY9;CXCL12;TFF3;BCL2;RAB17;FRK |
| **Myogenesis** | KCNH2;CHRNA1;CHRNB1;NOTCH1;AK1;PDE4DIP;COX6A2;MYOM2;CACNA1H;MYLPF; ADCY9;BIN1;PKIA;TCAP;CDH13;NOS1;LPIN1;SH3BGR;EPHB3 |
| **Apical Junction** | KCNH2;CDSN;VWF;SDC3;LAMA3;NEXN;PTK2;CLDN6;CDH4;PTPRC;TAOK2;EXOC4;ADAM9;EVL;TGFBI;ITGA9 |
| **Glycolysis** | PYGB;CYB5A;SDC3;B3GAT1;SPAG4;XYLT2;AK4;CACNA1H;GCLC;CAPN5;TFF3;TGFBI;LCT;PFKP;GNE;LHPP |
| ***Hypomethylated*** | |
| **UV Response Dn** | DUSP1;ANXA4;MAGI2;NEK7;PRDM2;CDC42BPA;LTBP1;VAV2;ATXN1;ZMIZ1;ADORA2B;NFIB;MYC;SLC22A18;KIT;MAP2K5 |
| **Interferon Alpha Response** | LGALS3BP;CASP8;LPAR6;DHX58;IRF2;TAP1;TRIM26;NCOA7;B2M;PSMB8;PSMB9 |
| **Interferon Gamma Response** | LGALS3BP;PTPN1;AUTS2;MVP;TAP1;HLA-A;HLA-G;PSMB8;PSMB9;CASP8;LATS2;DHX58;IRF2;ST8SIA4;IRF8;TRIM26;B2M;VAMP5 |
| **Mitotic Spindle** | FARP1;NUMA1;TUBGCP2;TBCD;CSNK1D;SSH2;CDC42BPA;MYO1E;CENPF;PPP4R2;PALLD; ABL1;NCK2;FLNB;FBXO5;SYNPO;BCAR1 |
| **Myogenesis** | RB1;WWTR1;CHRNB1;VIPR1;TAGLN;PTGIS;ITGB5;GPX3;SOD3;MYOM2;SMTN;MYO1C;COL4A2;FXYD1;ADAM12;PLXNB2;CKB |
| **G2-M Checkpoint** | TLE3;POLQ;SMARCC1;NUMA1;CUL1;RPA2;PRPF4B;FOXN3;PURA;CENPF;MYC;ABL1;FBXO5;TOP1;TNPO2;CDKN3 |
| **TGF-beta Signaling** | ACVR1;SKI;SMAD1;WWTR1;CDH1;HIPK2 |

# *CHAPTER V*

# MAJOR FINDINGS AND CHALLENGES

### *Review paper 1*

**Targeting DNA methylation is a promising strategy for BC management.**

- DNMTi have antitumoral effects on BC cells by inhibiting cell proliferation, inducing apoptosis, and modulating key pathways such as IFN-γ and Wnt signaling.
- Synergistic effects were observed combining DNMTi with chemotherapeutic agents and HDAC inhibitors.
- DNMTi demonstrated promise in overcoming chemoresistance and enhancing therapy effectiveness.
- Clinical responses were seen in specific patients subsets, yet the overall efficacy in BC treatment is still undergoing evaluation.

**Outstanding challenges**

- Urgent need for biomarkers to predict treatment response to DNMTi in BC.
- Enhance DNMTi bioavailability while minimizing side effects.
- Explore the long-term impact of DNMTi on BC patient outcomes.
- Understand the mechanisms behind poor responses to DNMTi.
- Identifying optimal combination therapies for effective BC management.

### *Review paper 2*

**Epigenetic alterations shape immune responses, offering potential targets for therapeutic intervention to enhance the efficacy of immunotherapy in cancer.**

- Epigenetic alterations significantly contribute to the formation and maintenance of an immunosuppressive TME, affecting different immune cell populations.
- Specific epigenetic modulators, such as HDACs and EZH2, play crucial roles in modifying immune cell behavior in the TME.
- Immune checkpoint inhibitors have transformed cancer treatment. However, a subset of patients fails to present clinical benefits due to primary or acquired resistance.
- Epigenetic alterations impact the immune response and the efficacy of immunotherapy.

- Demethylating agents and histone modifiers have demonstrated the ability to modulate the expression of immune-related genes, thereby enhancing response to immunotherapy.

**Outstanding challenges**

- Understanding the mechanisms that underly resistance to immunotherapy.
- Identify predictive biomarkers and overcome primary/acquired resistance to immunotherapy.
- Decipher the roles of specific epigenetic modifications in different immune cell populations and cancer types.
- Select patients who stand to benefit the most from epigenetic-based therapies and comprehend how these therapies interact with TME.
- Explore the combination of epigenetic drugs and immunotherapy in the context of BC.

### *Research paper 1*

**CM-1758 dual impact on BC by having antitumoral effects while reshaping the TME hints at its potential as a novel therapeutic modality in combination with immunotherapy.**

- CM-1758 demonstrated significant cytotoxic and cytostatic effects in BC cell lines at low micromolar concentrations.
- Increased PD-L1 expression via histone acetylation at the PD-L1 promoter by showcased a potential mechanism for CM-1758 modulating immune response.
- CM-1758 alone exhibited anti-tumoral effects in a mouse model of advanced BC, with slight enhancement when combined with anti-PD-L1 therapy.
- CM-1758 treatment altered the TME, increasing CD8+ T cell infiltration and inducting pro-inflammatory cytokines.

**Outstanding challenges**

- Determine the most effective combination strategies with CM-1758, especially in the context of ICI.
- Understand the transient nature of PD-L1 induction by CM-1758 and its optimal timing for synergistic effects with anti-PD-L1 therapy.

- Unravel the complex interplay of epigenetic alterations and their specific impact on different immune cell populations in the TME.
- Define the optimal duration and dosage of CM-1758 treatment, especially in combination regimens for maximal efficacy and minimal adverse effects.

### *Research paper 2*

**CM-272 and/or anti-PD-L1 pre-treated mice demonstrated a higher tumor elimination upon rechallenge, highlighting an enhanced immune response against diverse BC cell lines post-treatment.**

- In the rechallenge, mice injected with the same cell line as in the 1$^{st}$ challenge showed no tumor growth in either the control or treated groups, suggesting the development of immunity against these cells.
- Over half of the mice successfully eliminated 3K20 tumors in the 2$^{nd}$ challenge, with a preference for elimination among previously treated mice (CM-272, anti-PD-L1, or their combination).
- First challenge tumors from mice that eliminated the 2$^{nd}$ tumor displayed a higher infiltration of immune cells.
- Mice treated with CM-272 and anti-PD-L1 demonstrated enhanced immune responses, marked by increased tumor infiltration of key immune cells such as CD8+ T cells and M1-like macrophages in 2$^{nd}$ challenge tumors.
- CM-272 treatment induced changes in the gene expression profile of BC cells, particularly enriching immune-related pathways.

**Outstanding challenges**

- Comprehend the exact impact of individual treatments (CM-272 or anti-PD-L1) *versus* their combination in the observed immune response.
- Unravel the molecular mechanisms underlying the observed immune response post-treatment, particularly delineating the role of neoantigens and immune memory.
- Determine the durability of the immune response generated by CM-272 and anti-PD-L1 treatment over extended periods to determine the effectiveness against BC reappearance.

- Evaluating the efficacy of the treatments by rechallenge the mice with tumor cells from other cancer types.

### *Research paper 3*

**Differential DNA methylation patterns between responders and non-responders to immunotherapy in bladder tumors indicate the potential for using DNA methylation as a predictive biomarker for ICI response.**

- Distinct DNA methylation patterns were found between non-responders and responders to ICI in bladder tumor samples, underscoring the potential of using DNA methylation as a predictive biomarker for immunotherapy.
- Differently methylated CpG sites in responders were notably enriched in pathways related to antigen processing and presentation.
- Significant alterations in DNA methylation post-immunotherapy were observed, indicating that immunotherapy modulates epigenetic landscape of bladder tumors.
- The clear differential methylation patterns observed in samples from partial responders post-ICI, in comparison with non-responders, suggests that the methylation status of specific CpG sites plays an important role in response to immunotherapy in BC.

**Outstanding challenges**

- Heterogeneity in methylation profiles among patients hinders the development of a standardized and universally applicable methylation-based biomarker for predicting immunotherapy response.
- Find a panel of DNA methylation-based biomarkers fast and reliable, possible to be evaluated with techniques available in a hospital laboratory setting.
- Validation and standardization of DNA methylation-based biomarkers in different patient cohorts and clinical settings.
- Integrate genomic and transcriptomic data to comprehensively understand the interplay of molecular mechanisms influencing immunotherapy response.

*CHAPTER VI*

# GENERAL DISCUSSION AND CONCLUSIONS

BC stands as one of the most frequent cancers worldwide, remaining a major global health concern (1). The spectrum of BC extends from NMIBC to the more aggressive form of the disease, either MIBC or metastatic BC, presenting distinct clinical challenges (2). While NMIBC generally holds a favorable prognosis, the recurrence and progression rates remain high. Treatment options for those diagnosed with MIBC are limited, offering reduced clinical benefit. Current approaches include radical cystectomy combined with chemotherapy and, more recently, ICI for patients ineligible for chemotherapy. Nevertheless, between 17-26% of advanced BC patients do not respond to immunotherapy and PD-L1 expression fails as a reliable biomarker to correctly identify BC patients that will benefit from ICI (3). Thus, there is an urgent need for novel and more effective treatment options. Aberrant epigenetic mechanisms including histone acetylation, histone methylation and DNA methylation are key players contributing to the development of BC, affecting not only the tumor cells but also the immune compartment of the TME (**Review paper 1; Review paper 2**). Understanding this interplay between immune cells and epigenetic mechanisms in the tumor context can unveil intricate molecular pathways crucial for BC. Unraveling these mechanisms not only can lead to the development of new therapeutic targets but also to potential biomarkers tailored to the diverse molecular profiles observed in BC patients. This may pave the way for more personalized and effective strategies in managing BC, addressing the complexity and heterogeneity inherent to bladder tumors.

Therefore, this Thesis explored the interplay between epigenetic mechanisms and the immune landscape of BC with the main goal of finding novel epigenetic therapeutic targets and predictive biomarkers to improve response to ICI in BC. Specifically, we aimed to address the following questions:

1. How does the combination of novel epidrugs with ICI enhance the effectiveness of immunotherapy in BC treatment?
2. What is the impact of epidrugs on the TME in bladder tumors?
3. Could the combination of epidrugs and ICI lead to sustained and enhanced antitumor responses?
4. Can DNA methylation be used a reliable biomarker for predicting response to ICI in BC?

Since these are emerging topics on the cancer research field, the works presented in this Thesis constitute further steppingstones on the importance of epigenetics as therapeutic targets and biomarkers for BC.

**Combining epidrugs and immunotherapy in bladder cancer: impact on the tumor microenvironment**

The search for novel treatment strategies for BC, particularly the use of epidrugs either alone or in combination with immunotherapy has been the focus of some studies in the past years. Indeed, several HDACi and DNMTi, already approved for hematologic malignancies, have shown promising outcomes in BC, with ongoing trials corroborating improved overall survival. Nonetheless, the current HDACi and DNMTi have demonstrated to have limited bioavailability, half-life, and relevant dose-dependent toxicity, impeding their clinical approval for the treatment of solid cancers (**Review paper 1; Review paper 2**). Therefore, the search for new epidrugs that overcome these issues is of major relevance to improve BC patients' management. The first two works presented in this Thesis focused on novel epidrugs CM-1758, targeting histone acetylation, and CM-272, inhibiting histone and DNA methylation. The "CMs" are a novel class of reversible small molecules targeting epigenetic enzymes (4, 5). CM-1758 is a selective pan-HDAC inhibitor, whereas CM-272 is a dual inhibitor for G9a and DNMT1, with both molecules binding to the active site of the different enzymes (4, 5). Several studies have already shown the antitumoral effects of CM-272 in different cancer types (5-9), whereas CM-1758 still under investigation, with **Research paper 1** and another study from San José-Enériz et al currently under revision being the first exploring the antitumoral effects of CM-1758 in BC and acute myeloid leukemia, respectively. Different epigenetic mechanisms cooperate in cancer development and cells malignant transformation. Thus, simultaneous targeting of several epigenetic mechanisms constitutes a promising approach potentiate antitumoral effects of epidrugs, which is the goal with CM-272 by targeting methylation of both histones and DNA. Interestingly, we found that CM-1758 affects not only histone acetylation, but also DNA methylation in an indirect manner (**Research paper 1**). This can help potentiate the effects of epidrugs, reducing doses, time of treatment and, consequently, reduce side effects. Further research and development on this field is required to fully find the potential of epidrugs targeting different epigenetic enzymes in cancer treatment.

Our study showed that CM-1758 displayed potent anti-cancer effects in both *in vitro* and *in vivo* models of advanced BC. Given the crucial role of epigenetic mechanisms in BC development, particularly in immune regulation and TME modulation, we also studied CM-1758's effects on PD-L1 expression—a commonly targeted ICI in BC (**Review paper 2**). Treatment with CM-1758 increased PD-L1 expression in various BC cell lines, associated with higher levels of histone acetylation at the PD-L1 promoter (**Research paper 1**). Although CM-1758 combination with anti-PD-L1 *in vivo* exhibited

significant anti-tumor effects, surpassing anti-PD-L1 alone, it was similar to CM-1758 alone (**Research paper 1**). The same was observed when CM-272, which was shown to increase PD-L1 expression before (9), was combined with anti-PD-L1 in our experimental setting using the DKO mouse model (**Research paper 2**). As well, we did not find an increase in PD-L1 levels of tumor cells in the single treatment arms with CM-1758 and CM-272 at the end point of the *in vivo* experiment (**Research paper 1; Research paper 2**). As earlier mentioned, we hypothesized that the increase on PD-L1 expression can be transient and perhaps we are not treating with the anti-PD-L1 at the times where PD-L1 expression is higher. Additional studies analyzing the tumor PD-L1 expression in several timepoints during the experiment will provide us clues to when to better treat with the anti-PD-L1, potentiating the synergy between the epidrugs and ICI in our *in vivo* model. Nevertheless, these results can be particularly pertinent for BC patients with low PD-L1 expression or reduced immune cell infiltration, hinting at CM-1758 and CM-272 potential as an alternative or supplementary approach to ICI.

The changes in the TME landscape following CM-1758 or CM-272 treatments underscores the complex interplay between immune cells and their epigenetic regulatory mechanisms. Notably, CM-1758 alone or in combination with ICI led to a higher infiltration of CD8+ T cells and M1-like macrophages. Furthermore, it mitigates the immune-suppressive effects associated with tumor necrosis, potentially enhancing the anti-tumor immune response (**Research paper 1**). Similarly, tumors from mice previously treated with CM-272 in combination with anti-PD-L1 presented an increased infiltration of CD8+ T cells and phagocytic cells presence, suggesting a pivotal role in enhancing the immune response during rechallenge (**Research paper 2**). Both studies underscore the significance of epigenetic modulation in shaping the immune landscape within BC tumors. CM-1758 and CM-272 demonstrate their potential in remodeling the TME, influencing immune cell infiltration, cytokine profiles, and tumor-associated stromal cells. Additionally, the enhanced immune response after the rechallenge with different BC cells shows the potential of combining epidrugs and ICI in sustaining immune responses against BC.

The exploration of transcriptomic profiles in CM-272 and CM-1758 treated BC showed the potential immunomodulatory effects, which was translated *in vivo* with the TME remodeling observed (**Research paper 1; Research paper 2**). Moreover, the hypothesis that CM-272 augments a prolonged immune response by increasing the expression of neoantigens offers promising prospects. Neoantigens serve as targets for the immune system and can potentially trigger immune memory cells, essential for an effective and targeted immune response against cancer cells. Drawing parallels with previous studies on HDAC inhibitors and immune memory generation, the potential of

CM-272 in diversifying the repertoire of immune memory cells to eliminate various BC cells upon rechallenge presents an intriguing avenue for further investigation in the realm of BC treatment.

The studies presented in this Thesis highlight the promise of CM-1758 and CM-272 as potent inhibitors with antitumoral effects in BC, not only directly impacting tumor growth but also activating the immune system. By modulating epigenetic mechanisms, CM-1758 and CM-272 present appealing avenues for immune system modulation to eliminate tumors and enhance BC patients' management. This underlines the necessity for continued research into novel epidrugs, seeking enhanced efficacy, minimized off-target effects, and suitability for clinical trials either as monotherapy or in combination therapies for BC management.

**DNA methylation: key to predict immunotherapy response in bladder cancer?**

The landscape of BC treatment has been significantly improved by including ICI as an option for MIBC and metastatic patients, yet predicting response remains a challenge. The use of PD-L1 expression as a sole biomarker to predict response to immunotherapy falls short in correctly identifying those patients, prompting the study of alternative predictive biomarkers. DNA methylation, known to play a crucial role in BC development and immune response modulation, was shown to be able to predict response to ICI not only in BC, but also in melanoma and lung cancers. Thus, our study focused on addressing the DNA methylation profile in bladder tumors subjected to ICI, aiming to uncover potential biomarkers that accurately predict response and unravel new epigenetic mechanisms related to resistance to ICI (**Research paper 3**).

Differential methylation patterns were found in both site and region levels indicating that indeed DNA methylation can distinguish between responders and non-responders to ICI (**Research paper 3**). The next step consists in understanding which type of biomarker is more successful as predictive for ICI, either a DNA-methylation signature or compiling a panel of DM genes, having specific CpG sites or regions (promoters or CpG islands) into account. Another important factor to consider is whether the same predictive biomarker works for several types of ICI or just specific therapies, *i.e.,* anti-PD-L1 or anti-PD-1.

Our study also unveiled that pathways associated with differentially methylated CpG sites in responders display alterations in antigen presentation, cytokine production, and immune response signaling pathways, underscoring the profound influence of DNA methylation on the TME immune response dynamics. Notably, the differential methylation patterns observed post-treatment in partial responders, but not non-

responders underscore the importance of these CpG sites in defining responsiveness to ICI (**Research paper 3**). In the near future, we intend to evaluate the correlation of these differential methylation patterns with gene expression and provide insights into their functional significance, while associating specific methylation patterns with cells from the TME. These findings will offer further insights on the mechanisms associated with response to ICI in BC. However, further studies integrating transcriptomic profiles and validation across diverse sample sets, including liquid biopsies, are crucial to translate these findings into clinical applications.

In conclusion, this Thesis explored the interplay between epigenetics and the immune landscape in BC, aiming at identifying therapeutic targets and predictive biomarkers for improving immunotherapy responses. These studies tackled critical questions regarding novel epidrugs' efficacy in combination with immunotherapy, their impact on the TME, and the potential of DNA methylation as a reliable predictor for immunotherapy response in BC. Specifically, we found that combining novel epidrugs and immunotherapy has potential as a therapeutic strategy for BC, modulating the immune landscape of bladder tumors and that DNA methylation might be valuable as a biomarker to predict ICI response in BC. The exploration of epigenetic mechanisms and their impact on immunotherapy in BC signifies a step forward in addressing the complexity and heterogeneity of this disease. These insights lay the groundwork for tailored therapeutic interventions and more accurate predictive tools, aiming to improve BC patient’s management and outcomes.

**References**


1. Sung H, Ferlay J, Siegel RL, Laversanne M, Soerjomataram I, Jemal A, et al. Global Cancer Statistics 2020: GLOBOCAN Estimates of Incidence and Mortality Worldwide for 36 Cancers in 185 Countries. CA Cancer J Clin. 2021;71(3):209-49.
2. Dyrskjøt L, Hansel DE, Efstathiou JA, Knowles MA, Galsky MD, Teoh J, et al. Bladder cancer. Nat Rev Dis Primers. 2023;9(1):58.
3. Hussain SA, Birtle A, Crabb S, Huddart R, Small D, Summerhayes M, et al. From Clinical Trials to Real-life Clinical Practice: The Role of Immunotherapy with PD-1/PD-L1 Inhibitors in Advanced Urothelial Carcinoma. Eur Urol Oncol. 2018;1(6):486-500.
4. Rabal O, San José-Enériz E, Agirre X, Sánchez-Arias JA, de Miguel I, Ordoñez R, et al. Design and Synthesis of Novel Epigenetic Inhibitors Targeting Histone Deacetylases, DNA Methyltransferase 1, and Lysine Methyltransferase G9a with In Vivo Efficacy in Multiple Myeloma. J Med Chem. 2021;64(6):3392-426.
5. San José-Enériz E, Agirre X, Rabal O, Vilas-Zornoza A, Sanchez-Arias JA, Miranda E, et al. Discovery of first-in-class reversible dual small molecule inhibitors against G9a and DNMTs in hematological malignancies. Nat Commun. 2017;8:15424.
6. Bárcena-Varela M, Caruso S, Llerena S, Álvarez-Sola G, Uriarte I, Latasa MU, et al. Dual Targeting of Histone Methyltransferase G9a and DNA-Methyltransferase 1 for the Treatment of Experimental Hepatocellular Carcinoma. Hepatology. 2019;69(2):587-603.
7. Liu R, Yang J, Du Y, Yu X, Liao Y, Wang B, et al. A "One Arrow Three Eagle" Strategy to Improve CM-272 Primed Bladder Cancer Immunotherapy. Adv Mater. 2023:e2310522.
8. Moreira-Silva F, Outeiro-Pinho G, Lobo J, Guimarães R, Gaspar VM, Mano JF, et al. G9a inhibition by CM-272: Developing a novel anti-tumoral strategy for castration-resistant prostate cancer using 2D and 3D in vitro models. Biomed Pharmacother. 2022;150:113031.
9. Segovia C, San José-Enériz E, Munera-Maravilla E, Martínez-Fernández M, Garate L, Miranda E, et al. Inhibition of a G9a/DNMT network triggers immune-mediated bladder cancer regression. Nat Med. 2019;25(7):1073-81.

*APPENDIX*

# Original PDF files of the published papers included in the Thesis

cells

MDPI

*Review*

# DNA Methylation as a Therapeutic Target for Bladder Cancer

**Sandra P. Nunes [1,2,3], Rui Henrique [1,4,5], Carmen Jerónimo [1,5,*] and Jesús M. Paramio [2,3,6,*]**

1 Cancer Biology & Epigenetics Group-Research Center, Portuguese Oncology Institute of Porto (CI-IPOP), 4200-072 Porto, Portugal; sandra22nunes@gmail.com (S.P.N.); rmhenrique@icbas.up.pt (R.H.)
2 Molecular Oncology Unit, Centro de Investigaciones Energéticas, Medioambientales y Tecnológicas (CIEMAT), 28040 Madrid, Spain
3 Biomedical Research Institute I+12, University Hospital "12 de Octubre", 28041 Madrid, Spain
4 Department of Pathology, Portuguese Oncology Institute of Porto, 4200-072 Porto, Portugal
5 Department of Pathology and Molecular Immunology, Institute of Biomedical Sciences Abel Salazar—University of Porto (ICBAS-UP), 4050-313 Porto, Portugal
6 Centro de Investigación Biomédica en Red de Cáncer (CIBERONC), 28029 Madrid, Spain
* Correspondence: carmenjeronimo@ipoporto.min-saude.pt (C.J.); jesusm.paramio@ciemat.es (J.M.P.); Tel.: +351-2250-84000 (C.J.); +34-9149-62517 (J.M.P.); Fax: +351-2250-84047 (C.J.); +34-9134-66484 (J.M.P.)

Received: 10 July 2020; Accepted: 5 August 2020; Published: 7 August 2020

**Abstract:** Bladder cancer (BC) is the tenth most frequent cancer worldwide and is associated with high mortality when diagnosed in its most aggressive form, which is not reverted by the current treatment options. Thus, the development of new therapeutic strategies, either alternative or complementary to the current ones, is of major importance. The disruption of normal epigenetic mechanisms, namely, DNA methylation, is a known early event in cancer development. Consequently, DNA methyltransferase (DNMT) inhibitors constitute a promising therapeutic target for the treatment of BC. Although these inhibitors, mainly nucleoside analogues such as 5-azacytidine (5-aza) and decitabine (DAC), cause re-expression of tumor suppressor genes, inhibition of tumor cell growth, and increased apoptosis in BC experimental models and clinical trials, they also show important drawbacks that prevent their use as a valuable option for the treatment of BC. However, their combination with chemotherapy and/or immune-checkpoint inhibitors could aid in their implementation in the clinical practice. Here, we provide a comprehensive review of the studies exploring the effects of DNA methylation inhibition using DNMTs inhibitors in BC, from in vitro and in vivo studies to clinical trials.

**Keywords:** bladder cancer; DNA methylation; DNA methyltransferases; nucleoside analogues; therapy

## 1. Introduction

Bladder cancer (BC) is estimated to be the tenth most frequent cancer worldwide, being more common in men, in which it is the sixth most frequent cancer and the ninth cause of death due to cancer [1]. At diagnosis, approximately 75% of patients display a non-muscle-invasive BC (NMIBC), whereas 25% are diagnosed with muscle-invasive BC (MIBC) [2]. These differences have important implications regarding the treatment and clinical outcome [3]. NMIBC comprises Ta, T1, and carcinoma in situ (CIS), which do not reach the bladder muscle layer and show relatively good outcomes [4], being treated by transurethral resection (TUR) [3]. Depending on different clinicopathological features, such as number of implants, size, and patient's age, NMBICs are classified as high or low risk. High risk tumor management includes a regimen of local instillation, mainly of Bacillus Calmette Guérin (BCG),

after TUR to prevent recurrences and progression. BCG instillations promote local acute inflammation responses and represent the first approved immunotherapy for human cancers [5]. Recurrence is extremely frequent in NMIBC (up to 70%), and, in a proportion of cases, tumors progress to MIBC (stage T2 or higher) [4,6]. This represents a clinical problem demanding systematic follow-up of patients, frequently requiring cystoscopy, with a serious impact on the patient's quality of life and generating important costs to health systems [7]. The management of MIBC often requires radical cystectomy and, depending on the clinicopathological characteristics of the neoplasm, platin-based chemotherapy schemes in neoadjuvant or adjuvant settings can be administered [3]. MIBC recurrence and progression are also frequent, with survival at metastatic stage below 5% [6]. In addition to this poor outcome, a percentage of MIBC patients cannot be treated using standard protocols due to comorbidities or other health problems, regularly related to old age at diagnosis. Currently, patients that are considered to be unfit for such protocols have few therapeutic options. The development of immune checkpoint blockade (ICI) with antibodies inhibiting programmed death 1 (PD-1), programmed death-ligand 1 (PD-L1), or cytotoxic T-lymphocyte antigen 4 (CTLA-4) allowed for a substantial improvement in patient survival with good and sustained responses [8]. However, the percentage of patients showing clinical response is still rather limited [9]. Hence, a full understanding of the biological mechanisms underlying the development of BC would not only provide novel biomarkers for early detection but also as candidate therapeutic targets, improving patient survival. To gain better knowledge of BC molecular features, different international initiatives and multiple groups generated large amounts of data including different genomic analyses [10,11]. Such studies revealed the existence of different molecular subtypes and suggested the possibility for designing appropriate subtype-specific therapeutic approaches [12].

One of the most prevalent characteristics of BC is the presence of alterations in the cancer cell epigenetic machinery. The genetic and epigenetic landscapes allow for a cell to acquire an identity associated with a specific tissue, establishing proper organismal physiology [13], and their disruption represents the basis of multiple disorders [13]. Epigenetics comprises the study of heritable alterations that modify gene expression patterns without changing their DNA sequence [13–15]. DNA methylation, histone variants, chromatin remodeling, and histone post-translation modifications are the main epigenetic mechanisms with an impact on gene expression (Figure 1) [16]. Although often considered to be independent, different mechanisms cooperate closely in regulating the epigenome [17]. Because the deregulation of such epigenetic mechanisms is implicated in cancer development, in-depth characterization of the cancer epigenome boosted the understanding of tumor initiation and progression [14].

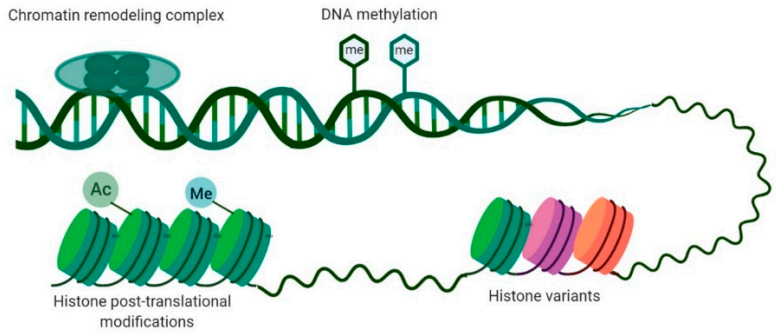


**Figure 1.** Main epigenetic mechanisms involved in gene expression regulation. DNA methylation consists of the addition of a methyl group in cytosine present in a cytosine–phosphate–guanine (CpG) dinucleotide. Histone post-translational modifications comprise alterations in histone tails such as methylation, acetylation, phosphorylation, and ubiquitination. Histone variants differ in few amino acids from canonical histones and regulate chromatin remodeling and histone post-translational modifications. Chromatin-remodeling complexes regulate the nucleosome structure by removing, relocating, and shifting histones.

Early in their development and progression, several epigenetic mechanisms are disrupted in BC [18]. For example, mutations in *EP300* and *CREBBP*, two chromatin-remodeling genes, led to the inactivation of the complex's histone-acetyltransferase domain, resulting in changes in chromatin conformation. Furthermore, a gene expression signature allied with the loss of histone acetyltransferase activity was associated with more aggressive bladder tumors [19]. Interestingly, 89% of MIBC lesions display mutations in the histone-modifying genes [20]. Specifically, a high mutation rate was found in *KMT2D* (also known as *MLL2*) gene and in *KDM6A* (also referred as *UTX*), which encode a histone H3 lysine 4 methyltransferase and a histone lysine demethylase, respectively [21–23]. The most explored epigenetic mechanism is DNA methylation [18,24]. By comparing methylation patterns, Wolff et al. found global hypomethylation in NMIBC, whereas hypermethylation patters were more commonly found in invasive tumors, supporting the concept that DNA methylation has an important role in BC development and aggressiveness, constituting a putative target for anti-cancer therapy [24,25].

The main goal of this review is to summarize the impact of aberrant DNA methylation in BC, focusing on therapeutic strategies that target this epigenetic alteration, based on the information provided by preclinical studies, both in vitro and in vivo, and clinical trials.

## 2. DNA Methylation

DNA methylation is the covalent addition of a methyl group at the 5-position carbon of cytosine in a cytosine–phosphatidyl–guanine (CpG) dinucleotide [17]. Methylation occurs mainly at CpG islands—CpG-rich regions (at least 50% of cytosines and guanines) in the genome with a size larger than 200 bp [26,27]. Moreover, methylation can also be found in repetitive sequences such as retrotransposon elements and centromeres, in the X chromosome (leading to its inactivation) and genomic imprinting [28]. Approximately 29,000 CpG islands can be found in the human genome, most commonly in the promoter regions, close to the transcription starting site (TSS) or first exons [27]. Remarkably, 75% of cytosines in CpG dinucleotides dispersed throughout the genome are methylated, whereas cytosines of CpG islands located within gene promoters remain mostly hypomethylated [27,29]. Promoter DNA methylation is classically associated with transcription repression by inducing binding of transcriptional repressors or hampering binding of transcriptional factors [15,17]. In fact, a family of methyl-CpG-binding proteins (MBPs) intervenes in gene silencing by binding to methylated CpGs and recruiting histone modifier enzymes to establish histone post-translation modifications, which further sustain transcriptional repression [30]. DNA methylation can also be found in CpG island shores, 2-kb areas upstream of a CpG island, displaying lower CpG dinucleotide density. CpG island shore methylation is also associated with transcriptional repression [31]. On the other hand, methylation in the gene body was shown to stimulate transcription elongation and to have an impact on splicing, with exons disclosing higher methylation levels than introns [28,32]. Furthermore, tissue-specific methylation seems to be more frequent in intragenic CpG islands [33]. CpG islands in enhancers also influence gene regulation, i.e., hypermethylation is associated with loss of enhancer marks resulting in gene silencing [34].

DNMTs catalyze the covalent bond between the methyl group donated by *S*-adenosyl methionine (SAM) and the unmethylated CpG dinucleotide at the fifth position of the cytosine by positioning the target base into the catalytic pocket of the enzyme using a base-flipping mechanism [35–37]. Five DNA methyltransferases (DNMTs) are encoded by the human genome, including DNMT1, DNMT2, DNMT3a, DNMT3b, and DNMT3L [37–39]. Specifically, DNMT3a and DNMT3b catalyze de novo DNA methylation, whereas DNMT1 preferentially maintains methylation patterns already existing by copying methylation patterns in the course of replication during embryonic development [37–39]. DNMT2 and DNMT3L do not display DNMT catalytic activity, serving as post-transcriptional gene regulation and cofactors of other DNMTs, respectively. By contrast, ten-eleven translocation (TET) enzymes mediate active DNA demethylation through 5-hydroxymethylcytosine (5hmC) [40,41], followed by deamination by activation-induced cytidine deaminase (AID), apolipoprotein B mRNA editing enzyme catalytic subunit 1 (APOBEC1) proteins, and base or nucleotide excision repair [17,42,43].

Overall, the cancer epigenome is characterized by global hypomethylation, which contributes to the overexpression of proto-oncogenes, an increased mutation rate, and the loss of imprinting [44]. Indeed, a decrease from 80% to 40–60% in the methylation levels from normal to cancer cells was observed [44,45]. More specifically, genomic repetitive regions become unmethylated, stimulating early cancer events through chromosomal instability that result in increased mutation rates, chromosomal rearrangements, and centromere instability (Figure 2) [46,47]. Simultaneously, the promoter hypermethylation of tumor suppressor genes (TSG) is also a frequent event in cancer cells [48], thus contributing to processes such as invasion, metastasis, and angiogenesis [44]. Typically, 5–10% of CpG islands at gene promoters are methylated in cancer (Figure 2) [44].

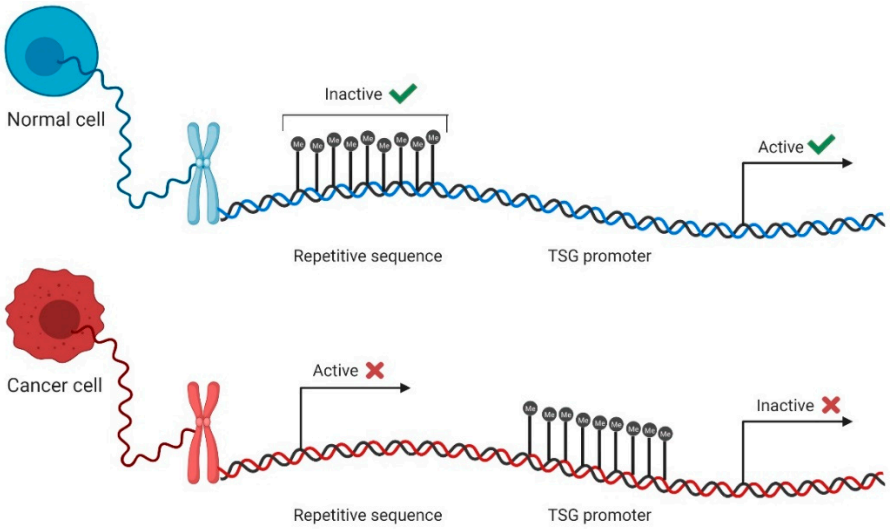


**Figure 2.** DNA methylation in normal and cancer cells. In normal cells, most repetitive sequences are methylated, whereas the promoters of tumor suppressor genes (TSG) stay unmethylated, remaining active and leading to gene expression (green check mark). Contrarily, in cancer cells, repetitive sequences become unmethylated and active, contributing to genomic instability, and TSG promoters become methylated, inactivating these genes and promoting cell aggressiveness and escape (red cross mark).

DNA methylation is a known contributor to BC development [49]. Hence, aberrant DNA methylation was proposed as a promising biomarker for BC detection, prognosis, and therapeutic target [50,51]. For example, a panel comprising *HOXA9*, *PCDH17*, *POU4F2*, and *ONECUT2* methylation detected BC with 90.5% sensitivity and 73.2% specificity in urine samples from Chinese patients presenting hematuria, leading the authors to estimate that about 60% of cystoscopies could be avoided [52]. Furthermore, a methylation panel composed of *GDF15*, *TMEFF2*, and *VIM* discriminated BC patients from healthy controls and prostate or renal cancer patients with a sensitivity of 94% and specificity of 90% in urine sediment samples [53], whereas the UroMark assay based on 150 CpG loci detected BC in voided urine samples with 98% sensitivity and 97% specificity [54]. On the other hand, in an analysis of formalin-fixed paraffin-embedded primary BC tissue samples, methylation of *SFRP5* was associated with recurrence and *CACNA1G* was associated with BC progression [55]. Moreover, DNMTs were shown to be overexpressed in BC, representing an attractive target for anti-cancer therapies [56].

## 3. DNMT Inhibitors

As previously stated, DNA methylation is a reversible alteration that contributes to BC development and progression, and DNMTs are overexpressed in this tumor type [49,56]. Thus, DNMTs constitute attractive targets for cancer treatment, and several "epidrugs" are already approved for the treatment of specific conditions [57]. Indeed, 5-azacytidine (or azacytidine (5-aza, Vidaza®))

and 5-aza-2′-deoxycytidine (or decitabine (DAC, Dacogen®)) are two DNMT inhibitors approved by the European Medicines Agency (EMA) and Food and Drug Administration (FDA) for the treatment of acute myeloid leukemia (AML), myelodysplastic syndrome, and chronic myelomonocytic leukemia (CMML) [30,57,58]. DNMT inhibitors can be classified, depending on their mechanism of action, as nucleoside and non-nucleoside analogues [24].

### 3.1. Nucleoside Analogues

Nucleoside analogues (or cytidine analogues) are a group of compounds that integrate into DNA instead of cytosine, resulting in the formation of a covalent bond with a DNMT in the carbon-6 position of the cytosine during the synthesis (S) phase of the cell cycle [57,59] (Figure 3; Figure S1, Supplementary Materials). 5-Aza and DAC are the nucleoside analogues most commonly used as therapeutic agents in cancer [60], with DAC having 90% more demethylating power than 5-aza [61]. Although their mode of action remains controversial, several mechanisms were proposed [59,62–64]. After the cellular uptake, mediated by nucleoside transporters, nucleoside analogues are activated through conversion to 5-aza-2′-deoxycytidine-5′-triphosphate, a substrate for the DNA replication machinery, to be incorporated in DNA, replacing cytosine [59]. At that point, DNMTs recognize azacytosine–guanine dinucleotides and catalyze the methylation reaction by forming a covalent bond with the cytosine ring [65,66]. Since azacytosine has a nitrogen substituting the carbon at position 5, the covalent bond cannot be broken, resulting in DNMT inactivation [59]. In addition to DNMT degradation, the complex formed between DNA and DNMT prompts DNA damage by causing double-strand breaks, leading to loss of methylation marks [59,67]. DAC and 5-aza seem to cause different effects in cancer cells. Although they both lead to a depletion of DNMT1 and a decrease in DNA methylation levels in non-small-cell lung cancer cells, 5-aza induces DNA damage, apoptosis, and cell arrest at phase sub-gap 1 (G1), whereas DAC increases the number of cells arrested in gap 2 (G2)/mitosis (M). As a consequence, their effects on gene expression are also different, with 5-aza decreasing the expression of genes related to cell cycle and metabolic processes, while DAC upregulates genes related to cell differentiation [63]. Furthermore, response rates to DAC treatment in AML patients with p53 mutations were higher in comparison with patients with wild-type p53, showing that mutations in p53 may play a role in epigenetically mediated cell death after DAC treatment [62,68]. Remarkably, phosphorylation of DNMT1 by protein kinase δ leads to its faster degradation after treatment with 5-aza or DAC, constituting another possible mechanism via which hypomethylation is achieved [64]. However, 5-aza and DAC are characterized by poor bioavailability, since they are easily degraded by hydrolysis in aqueous acidic or basic environments and have a limited half-life [59,69]. Indeed, both compounds can be deaminated by cytidine deaminase and converted into 5-azauridine, which results in their inactivation [70]. Furthermore, DAC is only incorporated into DNA, whereas 5-aza is incorporated into both DNA and RNA [70] and, since none of the compounds target specific DNMT isoforms, DAC and 5-aza cause significant side effects [70]. Thus, several alternative nucleoside analogues were developed to overcome these limitations.

Zebularine is a cytidine analogue that lacks the amino group at position 4 of the pyrimidine ring. It displays high stability as it inhibits both DNMTs and cytidine deaminase, and it is stable in acidic and neutral pH, enabling oral administration [71]. Moreover, zebularine has low cytotoxicity, which might translate into longer treatments with low doses to maintain a demethylated state [71], as well as an apparent specificity for cancer cells and not fibroblasts [72,73]. Zebularine leads to S-phase delay and cell death in mesothelioma cells [72], causes formation of replication-dependent double-strand DNA breaks [74], and enhances colon cancer cell immunogenicity [75]. Nevertheless, high concentrations of zebularine are needed to achieve demethylation levels similar to those of DAC since it forms a reversible complex with DNMTs, with slow dissociation kinetics [76], hindering the transition to clinical practice [57,71]. 5′-Fluoro-2′-deoxycytidine (FdCyd) is a fluoropyrimidine nucleoside analogue with a mechanism of action similar to 5-aza and DAC [24]. However, it is more stable and induces less toxicity compared to 5-aza and DAC [77]. As these nucleoside analogues are rapidly metabolized, combining

them with tetrahydrouridine (THU), a cytidine deaminase inhibitor, was proposed to overcome such limitation [78–81]. Indeed, co-administration of FdCyd and THU induced plasma concentrations of FdCyd in patients similar to those established as needed for inhibiting DNA methylation in vitro [80].

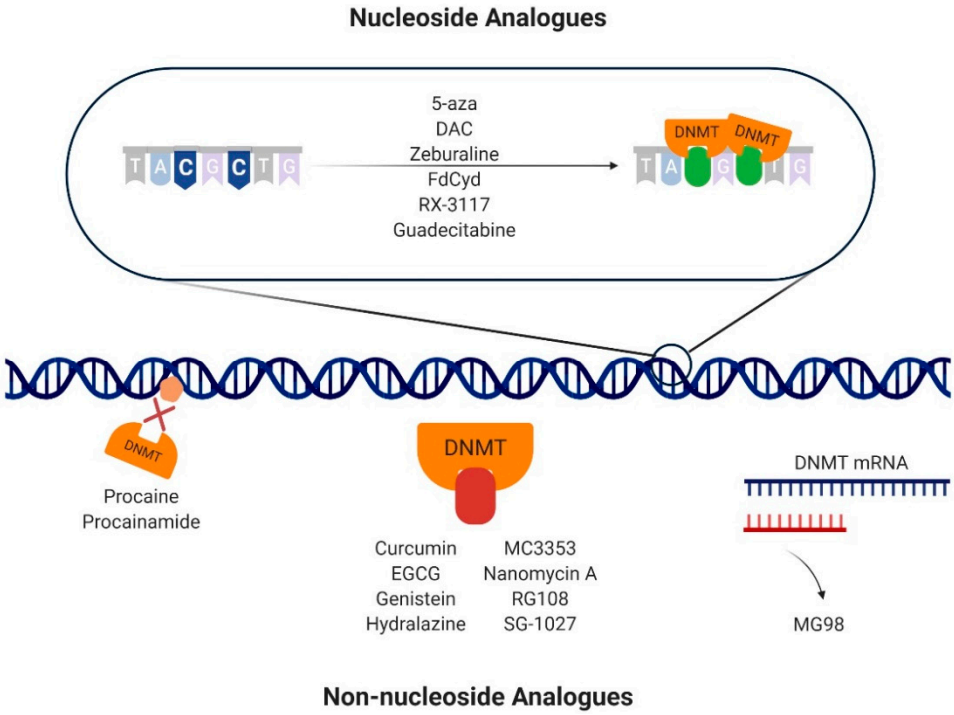


**Figure 3.** Mechanisms of action of DNA methyltransferase (DNMT) inhibitors. The nucleoside analogues 5-azacitydine (5-aza), decitabine (DAC), zebularine, 5′-fluoro-2′-deoxycytidine (FdCyd), RX-3117, and guadecitabine are integrated into DNA instead of cytosine. When DNMTs bind, a covalent bond is formed between the DNMT and the cytosine analogue. The non-nucleoside analogues have different mechanism of action to achieve inhibition of DNA methylation. Specifically, procaine and procainamide bind directly to the DNA, impeding DNMT binding. Curcumin, epigallocatechin-3-gallate (EGCG), genistein, hydralazine, MC3353, nanomycin A, RG108, and SG-1027 bind directly to the catalytic pockets of DNMTs, hampering their action. MG98 is an oligodeoxynucleotide that binds to the DNMT1 messenger RNA (mRNA) by base pair complementarity, impeding its translation.

SGI-110 or guadecitabine is a second-generation hypomethylating agent containing DAC coupled with a deoxyguanosine—a CpG dinucleotide analogue [70]. It is not a substrate for cytidine deaminase, a fact that increases the compound's exposure time without being inactivated [82]. Guadecitabine was tested in several clinical trials. Specifically, a combination of guadecitabine and irinotecan was shown to be safe and to possess clinical activity in metastatic colorectal cancer patients in a phase I dose escalation study [83]. Likewise, guadecitabine was clinically active in intermediate- and high-risk myelodysplastic syndromes, namely, in patients who did not respond to the currently approved demethylating agents [84]. More recently, an oral formulation of 5-aza, CC-486, was developed and tested in several clinical trials [85–88]. Some advantages of the oral route include a more convenient and easier administration to monitor, a high exposure time to the drug, and the elimination of local reactions [88]. Although a combination treatment with CC-486 and pembrolizumab was not effective in improving progression-free survival (PFS) in non-small-cell lung cancer patients [86], CC-486 as a single treatment showed clinical activity in nasopharyngeal cancer in a phase I clinical trial [87]. Furthermore, extending doses of CC-486 in low-risk myelodysplastic syndromes patients might provide an effective long-term treatment [88]. RX-3117 (fluorocyclopentenylcytosine) is a novel cytidine analogue with a modified ribose molecule [89]. To be incorporated into DNA or RNA, the RX-3117 molecule is firstly activated through transformation into a triphosphate form by uridine–cytidine kinase 2 [90]. Although

RX-3117 is not a substrate for cytidine deaminase [89], other enzymes such as NT5C3 may have a role in breaking an intermediate monophosphate form, resulting in RX-3117 inactivation [90]. RX-3117's anti-tumor effects were evaluated in nine different xenograft mouse models and showed promise for the treatment of tumors that are sensitive and resistant to gemcitabine [91].

### 3.2. Non-Nucleoside Analogues

Although nucleoside analogues are potent inhibitors of DNA methylation, they lack specificity, resulting in important side effects. To overcome this, non-nucleoside molecules were developed in the last few years. Non-nucleoside analogues comprise all DNMT inhibitors whose mechanism is independent of DNA incorporation [92], including DNA binders, oligonucleotides, natural compounds, SAM competitors, and repurposed drugs, i.e., drugs that were designed for a specific target and treatment but were found to have a novel therapeutic effect [92,93] (Figure 3; Figure S1, Supplementary Materials).

Procaine and procainamide, derivatives of 4-aminobenzoic acid, are FDA-approved drugs as anesthetic and anti-arrhythmic, respectively [94,95]. Both drugs were shown to cause global DNA hypomethylation in MCF7 cells inducing cell growth inhibition [94]. Additionally, procaine reduces the activity of DNMT1 and DNMT3a without influencing their expressions [96]. By directly binding to DNA, procaine and procainamide hamper DNMTs binding, leading to decreased global DNA methylation levels, although to a lesser extent when compared to DAC [94,96]. The antibiotic nanaomycin A also induces global hypomethylation and reactivates TSGs such as Ras association domain family 1 isoform A (RASSF1A) [97]. Remarkably, nanaomycin A showed specificity for DNMT3b inhibition by interacting with key amino-acid residues of this enzyme [98]. Hydralazine is an arterial vasodilator approved for the treatment of severe hypertension and heart failure [99]. It causes re-expression of TSGs by reversing promoter hypermethylation, both in cancer cell lines and in primary tumors [100]. Hydralazine inhibits DNA methylation, although weakly, by interacting with the DNMT active site [99]. Furthermore, hydralazine treatment caused a decrease in cell growth and invasiveness, increased apoptosis, cell-cycle arrest, and lowered DNMT messenger RNA (mRNA) and protein levels [101]. On the other hand, the combined treatment with hydralazine and valproic acid also demonstrated anti-metastatic effects, both in vitro and in vivo [102], and it showed potential clinical benefit in patients with disease progression under chemotherapy [103] including advanced cervical cancer patients [104].

Oligodeoxynucleotides that bind a target mRNA by base pair complementarity also show promise as DNMTs inhibitors [105]. In particular, MG98 is a second-generation 20-nucleotide antisense oligonucleotide that binds specifically to DNMT1 mRNA, causing a decrease in DNMT levels [105]. In an initial phase I clinical trial, MG98 was not well tolerated in high doses, and its anticancer effects were not observed in patients with solid tumors [106]. The lack of clinical activity was also observed in patients with high-risk myelodysplasia and acute myeloid leukemia [107]. However, in another clinical trial in patients with advanced solid tumors using escalating doses, MG98 was well tolerated and showed early clinical benefit [108], similarly to a combination of MG98 and interferon (IFN) $\alpha$-2$\beta$ in the treatment of advanced renal cell carcinoma [109]. RG108 is a synthetic molecule considered to be a SAM competitor that targets the binding pockets of DNMTs, establishing covalent bonds and leading to inhibition of their enzymatic activity [110]. Treatment with RG108 caused inhibition of DNMTs and cell growth, and it increased apoptosis in endometrial and prostate cancer cell lines [111,112]. SGI-1027 is a quinolone-based molecule which directly binds to the cofactor-binding site of DNMT3a and to both the cofactor- and the substrate-binding sites of DNMT1 [113]. Treatment of RKO cells with SGI-1027 resulted in demethylation and re-expression of TSGs including p16, mutL homolog 1(MLH1), and metalloproteinase inhibitor 3 (TIMP3), with no significant toxicity [114]. Another quinolone-based molecule, MC3353, caused cell arrest and decreased cell viability in a panel of different cancer cell lines. Furthermore, E-cadherin mRNA and protein levels increased while a reduction of matrix metalloproteinase levels was observed in PC-3 and HCT116 cells, hampering their epithelial-to-mesenchymal transition [115].

Several natural compounds were shown to have DNMT inhibitory activity [24]. The natural polyphenol epigallocatechin-3-gallate (EGCG), found in green tea, was shown to inhibit DNMT activity by interacting with the enzyme catalytic pocket, reactivating the expression of several TSGs by reversing the hypermethylation status [116,117]. EGCG also decreased cell viability, migration and invasion of breast cancer cells, and *SCUBE2* methylation by decreasing DNMT expression and activity [118]. Genistein is an isoflavone present in soybeans which displays anti-cancer activity [24]. In prostate tissue cancer samples, differences in methylation patterns and expressed genes were found comparing patients with genistein supplementation prior to prostatectomy and those receiving placebo [119]. After genistein treatment, DNA methylation levels decreased in several promoters of TSGs such as *ATM*, *APC*, *PTEN*, and *SERPINB5*, with a concomitant increase in the mRNA levels of those genes. Genistein interacts with the catalytic domain of DNMT1, competing with hemi-methylated DNA for the catalytic pocket [120]. Furthermore, in colon cancer cells, genistein demethylated *WIF1* and decreased invasiveness and migration of cancer cells by reducing expression of matrix metalloproteinases 2 and 9 [121]. Curcumin, a polyphenol compound with anti-inflammatory properties, also influences methylation status. In colorectal cancer cells, exposure to curcumin led to demethylation of specific CpG loci without inducing global methylation changes [122].

## 4. DNA Methylation as a Therapeutic Target in BC

### *4.1. Preclinical Studies*

A summary of the preclinical studies testing DNMT inhibitors in BC is depicted in Table 1. The effects of 5-aza were evaluated in cell lines in vitro and in a tumor xenograph model. 5-Aza was shown to inhibit cell proliferation and arrest cells at G0/G1, whereas volume and weight of tumor xenografts in mice were reduced. Interestingly, DNMT3a and DNMT3b expressions were also reduced after 5-aza treatment, causing the re-expression of hepaCAM, a TSG [56]. DAC treatment also led to an increase in hepaCAM expression in T24 and BIU87 cells, associated with arrest at G0/G1 phase [123]. In a canine model of invasive urothelial carcinoma, 5-aza disclosed anti-tumor effects, with 22.2% of the dogs demonstrating partial response and 50% depicting stable disease [124].

Non-toxic concentrations of DAC were used to treat four BC cell lines in order to evaluate the impact of hypomethylation in the BC cell transcriptome. Notch receptor 1 (NOTCH1) expression increased after treatment with DAC, in parallel with 50% demethylation of the promoter and enhancer regions. Interestingly, DAC-treated cells displayed morphological changes, i.e., cell enlargement compared to the controls. To explore these effects, the active intracellular domain of NOTCH1, ICN1, was overexpressed in cell lines and a decrease in cell proliferation was observed. Moreover, there was an increase of interleukin (IL)-6, probably due to a rise in ICN1 expression and double-stranded RNA levels [125]. ICN1 overexpression also led to a decrease in basal stem-like cells, as assessed by the decreased cytokeratin 5 (CK5) levels, contributing to a more differentiated cell state [125], which may prevent BC progression [126]. DAC was also shown to inhibit cell proliferation, migration, and invasiveness, inducing apoptosis in T24 cells while increasing the expression of the TSG Maspin [127]. Another gene that appears to be regulated by methylation in BC is *BTG2*. After treating EJ cells with DAC, BTG anti-proliferation factor 2 (BTG2) expression increased mainly due to DNMT1 inhibition, and cell growth decreased. Furthermore, H3K9me2 levels decreased, whereas H3K4me3 increased, leading to an open chromatin state in the promoter and intronic region of *BTG2* [128]. Apoptotic peptidase activating factor 1 (APAF-1) and death associated protein kinase 1 (DAPK-1) expressions also increased after DAC treatment in both RT4 and T24 cells, whereas zebularine caused an increased expression of those genes in cell line T24, which is p53 mutated [129]. Remarkably, Cheng et al. showed that treatment of T24 cells with zebularine for 48 h was not enough to maintain a long-term hypomethylated state and sustained p16 expression, as the percentage of methylation at day 0 was 97% and decreased to 75% at day 3. Inversely, a continuous treatment for 40 days, renewing dosage every three days, repressed cell growth and sustained p16 expression, while DNMT1 recovery was

null. However, sequential treatment with DAC and zebularine was the most effective in increasing and retaining p16 expression, maintaining promoter hypomethylation, and hampering re-methylation patterns observed before treatment [130]. Therefore, to increase treatment efficacy with this type of drug, a prolonged treatment seems to be pivotal.

The epigenetic regulation of Wnt inhibitory factor 1 (Wif-1), an antagonist of the Wnt pathway, important for carcinogenesis, was explored in four BC cell lines. DAC treatment led to increased Wif-1 mRNA levels with a simultaneous decrease in promoter methylation levels. Furthermore, Wif-1 expression was primarily regulated by DNA methylation and not genetic alterations [131]. DAC treatment in T24 cells induced the expression of several genes related to the IFN pathway, which could theoretically lead to inhibition of tumor cell growth [132]. Interestingly, Velicescu et al. showed that de novo methylation does not occur in non-dividing BC cells. Treating T24 cells with DAC allows for cell arrest at G0/G1 and determines how much time is necessary for re-methylation to occur. Indeed, no re-methylation was found in CpG islands, whereas various degrees of methylation reappeared in CpG poor regions. Furthermore, DNMT1 and 3b3 protein levels were not detected, whereas DNMT3a mRNA levels were maintained after day 10 of the experiment. This result demonstrates that DNMT3a might catalyze a de novo methylation in CpG poor regions outside the S phase of the cell cycle [133]. In another study, the carcinogen *N*-butyl-*N*-(4-hydroxybutyl)nitrosamine) (BBN) was used to induce bladder tumors in mice. These tumors showed downregulation of several genes including GSTM1, which seems to be regulated, in part, by DNA methylation, since treatment with DAC in 5637 cells increased GSTM1 expression [134]. Kawakami et al. reported for the first time that *MSH3* epigenetic regulation by means of DNA methylation might contribute to gene silencing, being implicated in BC carcinogenesis [135].

Recently, a study comprising a wide range of different cancer cell lines, containing BC, showed that DNMT inhibitors, including DAC and 5-aza, increase methylation levels throughout the cancer epigenome. Specifically, in BC cell lines, DAC treatment increased methylation levels of 616 common CpGs and decreased methylation levels of 590 different CpGs, demonstrating that the DNMT inhibitor mechanism of action is complex and requires further exploration [136].

After treatment with S110, global methylation levels decreased, concomitantly with increased p16 expression [137]. The effects of S110 in vivo were also assessed in a tumor xenograft mouse model using EJ6 cells. Tumor-free animals tolerated S110 better than DAC, with less weight loss and mortality. S110 failed to cause reduction in tumor sizes, yet their growth rate was lower and p16 expression was induced [138]. The development of DAC and 5-aza variants could potentially increase their half-life, improving bioavailability and therapeutic efficacy.

Procainamide and hydralazine inhibitory effects on DNA methylation were studied in T24 cells. Both compounds decreased the methylation levels of TSGs *p16* and *RARβ*, which associated with their re-expression, both at the transcript and at the protein levels. Interestingly, hydralazine treatment maintained p16 reactivation for longer than DAC [100]. A novel strategy to inhibit DNMT1, using an essential enzyme for cancer cell viability [139] highly expressed in BC [140], was proposed using DNAzymes. A DNAzyme is a stable DNA molecule with catalytic activity that targets specific RNA molecules leading to their destruction [141,142]. The DNAzyme DT433, constructed and selected to target DNMT1, displayed effects that were similar to those of 5-aza. Additionally, DT433 led to an increase in p16 expression and inhibition of cell proliferation [142]. Novel strategies applying repurposed drugs or DNAzymes to achieve DNMT inhibition constitute interesting alternatives to the demethylating drugs already approved. On the one hand, DNAzymes showed that increasing specificity toward the target may be achieved, whereas repurposed drugs, with negligible toxicity and known safety profiles, may be administered for longer periods and be considered as the next step for DNA methylation inhibition as anti-cancer therapy.

**Table 1.** Summary of pre-clinical studies targeting DNMTs in bladder cancer (BC).

| Drug | Model | Concentration | Treatment Scheme | Effects | Year | Reference |
|---|---|---|---|---|---|---|
| DAC | T24 | 1 μM | 1 day | ↑ Gene expression related to IFN pathway | 2002 | [132] |
| DAC | T24 | 3 μM | 1 day | No remethylation in CpG islands in the absence of cell division | 2002 | [133] |
| Hydralazine and procainamide | T24 | 10 μM | 5 days | ↓ *p16* and *RARβ* methylation levels<br>↑ p16 and RARβ expression | 2003 | [100] |
| DAC | TCC and UMUC | 5 μM | n.a. | ↑ MSH3 mRNA levels | 2004 | [135] |
| Zebularine | T24 | 100 μM | Every 3 days for 40 days | ↓ Global methylation levels<br>↑ p16 expression | 2004 | [130] |
| DAC | J82C, T24C, TCC, and UMUC | 5 μM | 3 days | ↑ Wif-1 mRNA expression levels | 2006 | [131] |
| DAC<br>Zebularine | RT4 and T24 | 2 μM<br>100 μM | 2 days<br>Every 3 days for 7 days | ↑ Cells doubling time<br>↑ APAF-1 and DAPK-1 expression | 2006 | [129] |
| S110 | T24 | 0.1–10 μM | Every 3 days for 6 days | ↓ Global methylation levels<br>↑ p16 expression | 2007 | [137] |
| DAC | BIU87 | 0.1–5 μM | 3 days | Re-expression of RASSF1A | 2009 | [143] |
| DAC | BOY | 1 μM | 4 days | ↑ COL1A2 expression | 2009 | [144] |
| DAC | BOY, T24, and UMUC | 10 μM | 7 days | ↑ FHL1 mRNA expression levels | 2010 | [145] |
| S110 | Mouse tumor xenograft | 10 mg/kg | Daily injection for 6 days | ↓ Tumor growth rate<br>↑ p16 expression | 2010 | [138] |
| 5-Aza | Dogs with naturally occurring invasive urothelial carcinoma | 0.1–0.3 mg/kg | Two doses schedules:<br>Everyday days 1 to 5 or<br>days 1 to 5 and 15 to 19<br>Each cycle 28 days | 22.2% Tumor partial response<br>50% Stable disease<br>22.2% Progressive disease | 2012 | [124] |
| DAC | BIU87 and T24 | 0.1–10 μM | 3 days | Cell arrest at G0/G1<br>↑ hepaCAM expression | 2013 | [123] |
| DAC | T24 | 0.25–2 μM | 2 days [1] | ↑ Maspin expression levels<br>↓ Cell proliferation, migration and invasion | 2013 | [127] |
| DAC | 5637 | 1–3 μM | 6 days | ↑ GSTM1 expression | 2014 | [134] |

**Table 1.** *Cont.*

| Drug | Model | Concentration | Treatment Scheme | Effects | Year | Reference |
|---|---|---|---|---|---|---|
| DAC | EJ | 1 μM | Every day for 3 days | ↓ Cell tumorigenesis and invasiveness<br>Cell arrest at G2/M<br>↑ BTG2 expression | 2014 | [128] |
| DNAzyme | T24 | n.a. | n.a. | ↓ Cell proliferation<br>↑ p16 expression | 2015 | [142] |
| 5-Aza | BIU87, EJ, and T24<br>Mouse tumor xenograft | 0.5–7 μM<br>n.a. | 1–4 days<br>Every 3 days for 18 days | ↓ Cell proliferation<br>↓ Tumor volume and weight | 2016 | [56] |
| DAC | T24 and J82 | 0.3 μM | 1 day | ↓ *RSPH9* methylation levels | 2016 | [146] |
| DAC | BLCAb001 (B01), BLCAb002 (B02), HT1376, and T24 | 0.1–1 μM | Every 2 days for 5 days | ↑ NOTCH1 expression<br>↓ CK5 positive cells<br>↑ IL-6 release | 2017 | [125] |
| DAC | T24 | 1 μM | 1 day | ↓ Methylation of 590 CpGs<br>↑ Methylation of 616 CpGs | 2019 | [136] |

[1] For migration and invasiveness assays. Abbreviations: 5-aza—5-azacytidine; APAF-1—apoptotic peptidase activating factor 1; BTG2-BTG anti-proliferation factor 2; CK5—Cytokeratin 5; CpG—Cytosine–phosphatidyl–guanine; COL1A2—collagen type I alpha 2 chain; DAC—decitabine; DAPK-1—death associated protein kinase 1; FHL1—four and a half LIM domains 1; GSTM1—glutathione S-transferase mu 1; IFN—Interferon; IL-6—Interleukin 6; MSH3—mutS homolog 3; n.a.—not available; NOTCH1—Notch receptor 1; RARβ—retinoic acid receptor beta; RASSF1A—Ras association domain family 1 isoform A; ↑—increase, ↓—decrease.

### 4.2. Combination Studies

The anti-tumor effects of 5-aza, trichostatin A (TSA), and FK228 (the latter is a class I histone deacetylase (HDAC) inhibitor) were evaluated individually and in combination in a set of BC cell lines, as well as xenograft and orthotopic mouse models. The combination 5-aza and FK228 was shown to be toxic for 90% of the BC cells, inducing apoptosis and decreasing the G2/M cell population. The same combination in in vivo models led to a decrease in tumor size, mainly due to the effect of FK228 alone [147]. Combination treatments using 5-aza and TSA also reduced the cell number and a shift in the expression of proteins that regulate the cell cycle in canine BC cell lines [148]. More recently, combination of DAC and entinostat, another HDAC1 inhibitor, was tested in bladder cell lines, including two cisplatin-sensitive (J82 and RT112) and one cisplatin-resistant (J82CisR) cell lines, as well as one urothelial cell line isolate from normal tissue (HBLAK). The combination treatment did not revert cisplatin resistance of J82CisR, although treatment with both drugs promoted cell growth arrest. Additionally, increased apoptosis was observed, related to caspases 3 and 7, prompting cell arrest at G2/M transition. Forkhead box O1 (FoxO1) expression increased after the combination treatment, as well as BIM and p21, along with a decrease in survivin expression [149].

Several strategies using epigenetic drugs were devised to overcome chemoresistance and increase therapy success. Ramachandran et al. showed that pre-treatment with 5-aza followed by cisplatin or docetaxel exposure increased cytotoxicity in BC cells. Moreover, in UMUC3 cells that developed resistance to cisplatin or docetaxel in vitro, pre-treatment with 5-aza resulted in 44% and 55% of cytotoxicity in cisplatin- and docetaxel-resistant cells, respectively, in opposition to 2% with no pre-treatment [150]. Pre-treatment with DAC also enhanced cytotoxicity of cisplatin and doxorubicin in BC cells. Furthermore, RASSF1A expression was observed concomitantly with activation of the Hippo pathway [151]. Interestingly, UMUC14, RT4, 96-1, and 97-1 cell lines displayed low sensitivity to cisplatin, being associated with high *HOXA9* methylation levels. This was also verified in MIBC patients in which high *HOXA9* methylation levels were associated with resistance to chemotherapy. In line with other studies, DAC led to a 4–5-fold decrease in half maximal inhibitory concentration ($IC_{50}$) for cisplatin, vinblastine, doxorubicin, and etoposide in BC cells [152]. Wu et al. demonstrated for the first time that DAC treatment reduced the cancer stem-cell population in mice. Specifically, in a BNN-induced mouse model of BC, DAC alone or in combination with cisplatin or gemcitabine led to a decline in the keratin 14 (KRT14)+ cell population, which originates from the bladder urothelium [153]. Consistently, the percentage of SRY-box transcription factor 2 (SOX2)+ cell population assumed to be responsible for the spread of the tumor [154] was also lower. Curiously, the percentage of such cells increased in mice treated with chemotherapy only [155]. These results were replicated in patient sample-derived xenografts, demonstrating that a combination treatment of DAC with chemotherapeutic agents might constitute a valuable option for BC therapy [155]. Another study showed that a quadruple combination therapy comprising gemcitabine, cisplatin, DAC, and TSA increased apoptosis via cyclin D1 (CCND1) downregulation, DNA fragmentation, and caspase 3 expression in T24 cells. On the other hand, a cell proliferation reduction and lower BCL2L1 mRNA levels were observed after treatment [156].

A novel dual inhibitor, CM-272, targeting G9a, a histone methyltransferase that catalyzes H3K9me2, and DNMTs demonstrated activity against a wide range of cancer cells [157]. Specifically, treatment of hematologic malignancies cell lines with concentrations in the nanomolar range led to a global decrease in H3K9me2 and 5-methylcytosine levels, a reduction in cell proliferation, induction of cell-cycle arrest and apoptosis, and a decrease in TSG promoter methylation. Interestingly, CM-272 also induced an IFN-$\gamma$ type I response and immunogenic cell death. In an in vivo mouse model, CM-272 was safe to administer, with an increased overall survival of the treated mice [157]. Furthermore, CM-272 was also active against hepatocellular carcinoma cell lines [158]. Recently, the effects of CM-272 were evaluated in in vitro and in vivo models of BC. CM-272 in combination with cisplatin led to inhibition of cell proliferation, which was also verified in a BC xenograft mouse model, leading to a decreased tumor growth, whereas apoptosis and autophagy were increased [159]. These effects were

also observed in a quadruple-knockout transgenic mouse model of advanced BC. Remarkably, BC cells treated with CM-272 showed upregulation of genes linked to the immune response, including IFN-α and γ, and tumor necrosis factor (TNF)-α, probably through induction of an endogenous retrovirus response [159]. Taking into account these results, the combination of CM-272 with anti-PD-L1 in the quadruple-knockout mouse model was explored. A sustained response to the combination treatment was observed, with the number of animals developing tumors or metastases being lower in the combination group when compared with the group treated with anti-PD-L1 monotherapy [159]. Remarkably, CM-272 treatment led to an immune reactivation of tumor cells, turning "cold" tumors into "hot" ones [159]. A brief overview of the main studies exploring the combination therapies in BC experimental models can be found in Table 2.

**Table 2.** Summary of combination studies targeting DNMTs in BC.

| Drug | Model | Concentration | Treatment Scheme | Effects | Year | Reference |
|---|---|---|---|---|---|---|
| 5-Aza and FK228 | 253J, T24, TCCSUP, UMUC3, and WH | 5-aza 1–25 μM<br>FK228 0.25-5 ng/mL | 3 days | ↑ Apoptosis<br>↓ G2/M cell population | 2007 | [147] |
| DAC and cisplatin | 253J, RT112, T24, and TCCSUP | DAC 0.1–8 μM<br>Cisplatin 0.25–2 μg/mL | 3 days | ↑ Cell arrest at G2/M<br>↓ Proliferative ability<br>↑ Apoptosis<br>↑ Susceptibility to cisplatin | 2008 | [160] |
| 5-Aza, cisplatin, and docetaxel | T24, TCCSUP, and UMUC3 | 5-Aza 0.6 μM<br>Cisplatin 1 μM<br>Docetaxel 5 nM | 5-Aza for 72 h followed by cisplatin or docetaxel for 72 h | ↑ Cell toxicity with combined treatment | 2011 | [150] |
| 5-Aza and TSA | K9TCC, K9TCC-PU-Nk, and K9TCC-PU-Sh | 5-Aza 1–50 μM<br>TSA 0.5 μM | 2 days | ↑ p16 expression<br>↓ Cell number<br>↓ Cyclin D1, p21, pRb, survivin, and PARP expression | 2013 | [148] |
| DAC, TSA, cisplatin, and gemcitabine | T24 | Gemcitabine 2.5 μM<br>Cisplatin 1.25 μM<br>DAC 10 μM<br>TSA 300 nM | Gemcitabine and cisplatin for 48 h followed by DAC for 48 h and TSA for 6 h | ↑ Apoptosis<br>↓ Cell proliferation<br>↑ DNA fragmentation<br>↑ CASP-3 mRNA levels<br>↑ GSK3β mRNA levels<br>↑ Canonical Wnt pathway<br>↓ BCL2L1 mRNA levels | 2014 | [156] |
| DAC, cisplatin, doxorubicin, etoposide, and vinblastine | 96-1, 97-1, RT4, and SW1710 | DAC 100 nM<br>Cisplatin 0.3–3000 μM<br>Etoposide, vinblastine, and doxorubicin 0.1–1000 μM | DAC for 120 h followed by chemotherapeutic drugs for 48 h | ↓ $IC_{50}$ of chemotherapeutic drugs with combined treatment | 2016 | [152] |
| DAC, cisplatin, and doxorubicin | HT1376 and T24 | DAC 1 and 5 μM<br>Cisplatin and doxorubicin 1–10 μg/mL | DAC for 72 h followed by cisplatin or doxorubicin for 72 h | ↑ Cell toxicity<br>↑ RASSF1A expression<br>Hippo pathway activation | 2018 | [151] |
| DAC, cisplatin, and gemcitabine | 5637 and SCaBER | DAC 100 nM<br>Cisplatin 100–150 ng/mL<br>Gemcitabine 2–150 ng/mL | Daily for 72 h | ↑ Apoptosis<br>↓ Ratio of CD44v6+ and ALDH+ cells<br>↑ SOCS3 expression | 2019 | [155] |
| | BNN-induced mouse model | Cisplatin 2.5 mg/kg<br>Gemcitabine 120 mg/kg<br>DAC 0.05–0.2 mg/kg | Cisplatin weekly for 3 weeks<br>Gemcitabine weekly for 3 weeks<br>DAC once daily for 5 consecutive days and 3 times per week | ↓ Number of invasive tumors<br>↓ Cancer cells proliferation<br>↑ Apoptosis<br>↓ KRT14+ expressing cells<br>↓ SOX2+ expression cells<br>↓ STAT3 phosphorylation | | |
| | Patient sample-derived xenografts | | | | | |

**Table 2.** *Cont.*

| Drug | Model | Concentration | Treatment Scheme | Effects | Year | Reference |
|---|---|---|---|---|---|---|
| DAC and cisplatin | CR-T24 and T24 | DAC 2 μM<br>Cisplatin 1 μg/mL | DAC for 48 h followed by cisplatin for 24 h | ↓ Colonies formation<br>↑ Tap73 expression<br>↑ Cisplatin response | 2019 | [161] |
| CM-272 and pembrolizumab | Quadruple-knockout transgenic mouse model of metastatic BC. Cre-dependent inactivation of *Pten*, *Trp53*, and *Rb1* specifically in urothelial cells (AdK5Cre) of Rbl1-deficient mice | CM-272 5 mg $kg^{-1}$<br>Anti-PD-L1 200 μg per injection | Treatment of mice started at the time of tumor detection. CM-272 intraperitoneally 5 days per week. Anti-PD-L1 once a week for a total of 3 injections. | Extensive immune infiltrations comprising CD3+, CD8+, and NK cells<br>Low number of animals showing tumor or metastasis evidence.<br>Prolonged anti-tumor effect without any treatment | 2019 | [159] |
| DAC and entinostat | J82, J82CisR, HBLAK, and RT112 | DAC 0.1 and 1 μM<br>Entinostat $IC_{50}$ according to cell line | DAC for 48 h followed by entinostat for 48 h | Growth inhibition<br>↑ Apoptosis<br>↑ Cell arrest in G2/M transition<br>↑ FoxO1 expression<br>↑ BIM and p21 expression<br>↓ Survivin expression | 2020 | [149] |

Abbreviations: 5-aza—5-azacytidine; CASP-3—caspase 3; DAC—decitabine; FoxO1—forkhead box O1; GSK3β—glycogen synthase kinase 3 beta; KRT14—keratin 14; PARP—poly(ADP-ribose) polymerase; RASSF1A—Ras association domain family 1 isoform A; SOCS3—suppressor of cytokine signaling 3; SOX2—SRY-box transcription factor 2; STAT3—signal transducer and activator of transcription 3; Tap73—tumor protein P73; TSA—trichostatin A. ↑—increase, ↓—decrease.

### 4.3. Clinical Studies

A non-randomized multicenter phase II study evaluated the effects of FdCyd in THU [80,162]. The safety, maximum tolerated dose (MTD), pharmacokinetics, and pharmacodynamics of this combination were determined in a previous phase I clinical trial (FyCyd 100 mg/m$^2$/day and THU 350 mg/m$^2$/day) [81]. Patients with metastatic or unresectable breast cancer ($n$ = 29), head and neck cancer ($n$ = 21), non-small-cell lung cancer ($n$ = 25), and urothelial cell carcinoma ($n$ = 18) which endured progression after at least one line of standard therapy were included in this study. The combination was well tolerated, and urothelial carcinoma patients showed some clinical responses, with an objective response rate (ORR) of 5.6%, a progression-free survival (PFS) of 3.6 months, and a four-month PFS probability of 42%. Furthermore, increased p16 expression was observed in cytokeratin-positive circulating tumor cells (CTCs) of some patients, although it did not associate with clinical response (Table 3) [162].

The pharmacokinetics, toxicity, and clinical relevance of combining 5-aza and sodium phenylbutyrate, a first-generation HDAC inhibitor, was assessed in 34 patients with refractory solid tumors with no curative options, including two BC patients. Twenty-seven patients were eligible to proceed with treatment in three different regiments. The treatment was well tolerated with the most common toxicity effects including neutropenia, anemia, nausea, vomiting, transaminase elevation, and edema. The results of the study were mostly disappointing, with only one leiomyosarcoma patient displaying stable disease for 4.5 months and the rest disclosing disease progression. Although inhibition of DNMT activity was observed in two patients, this drug combination failed to show clinical benefit (Table 3) [163].

In a phase Ib clinical trial, the effects of CC-486 to potentiate carboplatin or paclitaxel protein-bound particles (ABI-007) in 169 patients with relapsed or refractory solid tumors including BC were evaluated. Two arms were defined: arm A comprising treatment with CC-486 and carboplatin and arm B including combination treatment of CC-486 and ABI-007 [164]. Preliminary results showed that CC-486 (200 and 300 mg) was well tolerated, with treatment-emergent adverse events (TEAEs) including anemia and neutropenia in about 50% of the patients in arm A and nausea/vomiting and peripheral neuropathy in patients of arm B. Five patients in arm A showed stable disease whereas three patients displayed partial response, with both combinations disclosing clinical value. Interestingly, peripheral blood mononuclear cells (PBMCs) were found to be hypomethylated. A recommended phase II dose (RP2D) study will comprise an expansion of cohorts and the combinations of 300 mg of CC-486 with carboplatin and 200 mg of CC-486 with ABI-007 [165].

Other clinical trials are at this date assessing the clinical benefit of combining immune checkpoint inhibitors with epigenetic drugs. In a recently completed study, the combination of pembrolizumab, epacadostat [indoleamine 2,3-dioxygenase 1 (IDO1)-selective inhibitor], and 5-aza was assessed in a phase I and II trial enrolling 70 patients, including urothelial cancer patients [166]. Furthermore, in a currently recruiting phase II clinical trial, the biological and clinical efficacy of atezolizumab (which targets PD-L1) in combination with guadecitabine will be evaluated in 53 patients with checkpoint inhibitor-refractory or -resistant urothelial carcinoma (Table 3) [167].

**Table 3.** Clinical trials in BC using DNMT inhibitors.

| Drug | Phase (ID) | Status | Enrollment | Schedule | Results | Period | Reference |
|---|---|---|---|---|---|---|---|
| 5-Aza and sodium phenylbutyrate | I (NCT00005639) | Completed | Patients with diagnosis of a refractory solid tumor malignancy with no curative options including BC ($n$ = 34) | Regimen A: Low-dose of 5-aza with intermittent phenylbutyrate 400 mg/m$^2$/day over 24 h on days 6 and 13. Regiment B: 5-aza 75 mg/m$^2$/day for 7 days, followed by two different doses of phenylbutyrate starting on day 8 and continuing for 7 days. Each cycle lasts 35 days for A and B. Regiment C: 2 different daily doses of 5-AC for 21 days and phenylbutyrate 400 mg/m$^2$/day over 24 h once per week. Each cycle lasts 42 days. | Three doses were well tolerated. Common toxicities included bone marrow suppression-related neutropenia and anemia. One patient showed stable disease; the remaining did not show any clinical response. | 2000–2005 | [163] |
| DAC | I (NCT00030615) | Completed | Advanced metastatic solid tumor patients after other standard therapies fail including BC ($n$ = 24) | DAC intravenous (IV) over 30 min on days 1–5 weekly for 4 weeks. Course repeated every 6 weeks in the absence of disease progression or unacceptable toxicity. | Not available | 2001–2008 | [168] |
| FdCyd and THU | II (NCT00978250) | Completed | Metastatic or unresectable solid tumors including urothelial transitional cell carcinoma ($n$ = 18), whose disease progressed after at least one line of standard therapy. | FdCyd (100 mg/m$^2$/day) by 3 h intravenous infusion and THU (350 mg/m$^2$/day) 20% as a bolus, with the remaining co-administered with FdCyd over 3-h infusion on days 1–5 and 8–12 of each 28-day cycle. | Co-administration with THU was shown to increase the area under the curve of FdCyd more than 4-fold. Combination was well tolerated. ORR of 5.6%, PFS of 3.6 months, and 42% of 4-month PFS probability for urothelial cancer patients. | 2009–2019 | [162,169] |

**Table 3.** *Cont.*

| Drug | Phase (ID) | Status | Enrollment | Schedule | Results | Period | Reference |
|---|---|---|---|---|---|---|---|
| CC-486, carboplatin, and paclitaxel protein-bound particles (ABI-007) | I (NCT01478685) | Completed | Patients with relapsed or refractory solid tumors including urinary bladder neoplasms ($n$ = 169) | Arm A: CC-486 (doses between 100–300 mg) was administered orally daily either 14 or 21 days. Carboplatin was given by intravenous (IV) infusion once every 21 days<br>Arm B: CC-486 (doses between 100–300 mg) was administered orally daily for either 14 or 21 days<br>ABI-007 was administered by intravenous (IV) infusion on two of every three weeks<br>Arm C: CC-486 (doses between 100–300 mg) was administered orally daily for either 14 or 21 days. | CC-486 dosed 14/21 days was tolerated as a priming agent with carboplatin and ABI-007. Both combinations show evidence of clinical activity. | 2011–2015 | [164,165] |
| RX-3317 | I (NCT02030067) | Completed | Patients with advanced or metastatic solid tumors including advanced BC ($n$ = 124) | A cycle was 4 weeks, with up to 8 cycles. RX-3117 dosing was given 3 times each week for 3 weeks followed by 1 week off treatment. All subjects were followed for at least 30 days after the last dose of RX-3117. | Not available | 2013–2019 | [170] |
| CC-486 | I (NCT02223052) | Completed | Subjects with hematologic or solid tumor malignancies including BC patients ($n$ = 89) | Arm 1: Two 150-mg tablets of CC-486 on day 1 and 1 × 300 mg CC-486 on day 2 Arm 2: 1 × 300 mg tablet of CC-486 on day 1 and 2 × 150 mg CC-486 on day 2. | Not available | 2014–2018 | [171] |

**Table 3.** *Cont.*

| Drug | Phase (ID) | Status | Enrollment | Schedule | Results | Period | Reference |
|---|---|---|---|---|---|---|---|
| SGI-110, gemcitabine, and cisplatin | Ib/IIa (2015-004062-29) | Recruiting | Urothelial BC patients with stages T2-4aN0M0 ($n$ = 20) | Arm 1: SGI-110 days 1–5 at the determined dose, gemcitabine 1000 mg/m$^2$ days 8 + 15, cisplatin 70 mg/m$^2$ day 8. 3–4 cycles of 21 days each. Arm 2: Gemcitabine 1000 mg/m$^2$ days 8 + 15, cisplatin 70 mg/m$^2$ day 8 3–4 cycles of 21 days each for both arms. 3–4 cycles of 21 days each. | Not available | 2015–present | [172] |
| 75 approved agents | II (NCT02788201) | Completed | Patients with a diagnosis of metastatic, progressive urothelial carcinoma of the bladder, urethra, ureter, or renal pelvis ($n$ = 8) | COXEN algorithm was used to determine the best therapy from among 75 FDA-approved agents (single agent or combination). Patients had regular visits for blood, urine, and tumor scans. | Not available | 2017–2019 | [173] |
| Azacitidine, pembrolizumab, and epacadostat | I (NCT02959437) | Completed | Subjects with advanced or metastatic solid tumors including BC patients ($n$ = 70) | Five doses of azacitidine were administered by subcutaneous injection or intravenously (IV) over days 1 to 7 in cycles 1 through 6. Pembrolizumab was administered in a 30-min IV infusion every 3 weeks on day 1 of each 21-day cycle. Epacadostat tablets were administered orally twice daily. | Not available | 2017–2020 | [166] |
| Atezolizumab and guadecitabine | II (NCT03179943) | Suspended | Recurrent/advanced urothelial carcinoma (stage IV) patients who previously progressed on checkpoint inhibitor therapy with anti-PD-1 or PD-L1 therapy ($n$ = 53) | Atezolizumab is administered intravenously on day 1 and day 22 of a 6-week cycle for a period of 8 cycles. Guadecitabine is administered subcutaneously on days 1 through 5 of the 6-week cycle for a period of 4 cycles. | Not available | 2017–estimated end 2022 | [167] |

Abbreviations: 5-aza—5-azacytidine; DAC—decitabine.

## 5. Conclusions

DNA methylation machinery is a promising target for BC treatment. Among the anti-tumor effects caused by DNMT inhibitors, the most frequently reported are reactivation of TSGs and inhibition of tumor cell growth (Figure 4). However, DNMT inhibitors still present several drawbacks that preclude their use for BC treatment, including the reversal of the inhibitory effects after drug withdrawal, short half-life, and significant toxicity. To overcome these, combination therapies comprising DNMT inhibitors, chemotherapeutic agents, and, more recently, immune checkpoint inhibitors might constitute a valid option for BC patients, as demonstrated by the currently ongoing clinical trials. Furthermore, the discovery of novel biomarkers to select patients more likely to respond to those therapies and the evaluation of the long-term effect of this class of compounds are required for the transition into clinical practice.

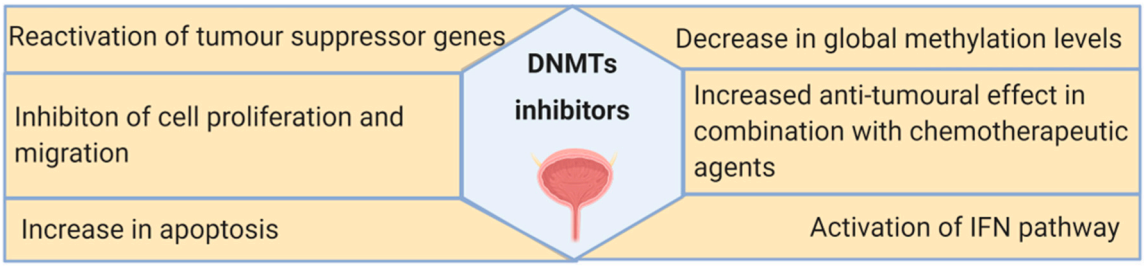


**Figure 4.** Summary of the main effects of DNMT inhibitors observed in bladder cancer in vitro and in vivo models, as well as in clinical trials.

In conclusion, modulation of the epigenetic landscape of BC tumors constitutes an encouraging alternative to the currently available therapeutic strategies for BC patients, requiring further exploitation in a clinical trial setting, aiming at a future implementation in clinical practice.

**Supplementary Materials:** The following are available online at http://www.mdpi.com/2073-4409/9/8/1850/s1: Figure S1. Chemical structure of nucleoside and non-nucleosides DNMT inhibitors.

**Author Contributions:** Reviewed the literature and drafted the manuscript, S.P.N.; supervised the work and revised the manuscript, R.H., C.J., and J.M.P. All figures are original and were created with BioRender.com. All authors read and agreed to the submitted version of the manuscript.

**Funding:** This study was co-funded by European Regional Development Fund (FEDER) grants from Science and Innovation (SAF2015-66015-R and PID2019-110758RB-I00 to J.M.P.) and the Instituto de Salud Carlos III (RETIC no. RD12/0036/0009 to J.M.P., CIBERONC no. CB16/12/00228 to J.M.P.). S.P.N. is supported by an FCT Fundação para a Ciência e Tecnologia grant (SFRH/BD/144241/2019).

**Conflicts of Interest:** The authors declare no conflict of interest.

## References

1. Bray, F.; Ferlay, J.; Soerjomataram, I.; Siegel, R.L.; Torre, L.A.; Jemal, A. Global cancer statistics 2018: GLOBOCAN estimates of incidence and mortality worldwide for 36 cancers in 185 countries. *CA Cancer J. Clin.* **2018**, *68*, 394–424. [CrossRef]
2. Kamat, A.M.; Hahn, N.M.; Efstathiou, J.A.; Lerner, S.P.; Malmström, P.U.; Choi, W.; Guo, C.C.; Lotan, Y.; Kassouf, W. Bladder cancer. *Lancet* **2016**, *388*, 2796–2810. [CrossRef]
3. Bellmunt, J.; Orsola, A.; Leow, J.J.; Wiegel, T.; De Santis, M.; Horwich, A. Bladder cancer: ESMO Practice Guidelines for diagnosis, treatment and follow-up. *Ann. Oncol.* **2014**, *25* (Suppl. S3), iii40–iii48. [CrossRef] [PubMed]
4. Amin, M.B.; Edge, S.; Greene, F.; Byrd, D.R.; Brookland, R.K.; Washington, M.K.; Gershenwald, J.E.; Compton, C.C.; Hess, K.R.; Sullivan, D.C.; et al. *AJCC Cancer Staging Manual*, 8th ed.; Springer International Publishing: New York, NY, USA; American Joint Commission on Cancer: Chicago, IL, USA, 2017.
5. Redelman-Sidi, G.; Glickman, M.S.; Bochner, B.H. The mechanism of action of BCG therapy for bladder cancer—A current perspective. *Nat. Rev. Urol.* **2014**, *11*, 153–162. [CrossRef] [PubMed]

6. Cancer Stat Facts: Bladder Cancer. Available online: https://seer.cancer.gov/statfacts/html/urinb.html (accessed on 1 April 2020).
7. Mariotto, A.B.; Yabroff, K.R.; Shao, Y.; Feuer, E.J.; Brown, M.L. Projections of the cost of cancer care in the United States: 2010–2020. *J. Natl. Cancer Inst.* **2011**, *103*, 117–128. [CrossRef] [PubMed]
8. Lobo, J.; Jerónimo, C.; Henrique, R. Targeting the immune system and epigenetic landscape of urological tumors. *Int. J. Mol. Sci.* **2020**, *21*, 829. [CrossRef]
9. Hussain, S.A.; Birtle, A.; Crabb, S.; Huddart, R.; Small, D.; Summerhayes, M.; Jones, R.; Protheroe, A. From clinical trials to real-life clinical practice: The role of immunotherapy with PD-1/PD-L1 inhibitors in advanced urothelial carcinoma. *Eur. Urol. Oncol.* **2018**, *1*, 486–500. [CrossRef]
10. Tan, T.Z.; Rouanne, M.; Tan, K.T.; Huang, R.Y.; Thiery, J.P. Molecular subtypes of urothelial bladder cancer: Results from a meta-cohort analysis of 2411 tumors. *Eur. Urol.* **2019**, *75*, 423–432. [CrossRef]
11. Choi, W.; Ochoa, A.; McConkey, D.J.; Aine, M.; Höglund, M.; Kim, W.Y.; Real, F.X.; Kiltie, A.E.; Milsom, I.; Dyrskjøt, L.; et al. Genetic alterations in the molecular subtypes of bladder cancer: Illustration in the cancer genome atlas dataset. *Eur. Urol.* **2017**, *72*, 354–365. [CrossRef]
12. Robertson, A.G.; Kim, J.; Al-Ahmadie, H.; Bellmunt, J.; Guo, G.; Cherniack, A.D.; Hinoue, T.; Laird, P.W.; Hoadley, K.A.; Akbani, R.; et al. Comprehensive molecular characterization of muscle-invasive bladder cancer. *Cell* **2017**, *171*, 540–556.e25. [CrossRef]
13. Kelly, A.D.; Issa, J.J. The promise of epigenetic therapy: Reprogramming the cancer epigenome. *Curr. Opin. Genet. Dev.* **2017**, *42*, 68–77. [CrossRef] [PubMed]
14. Baylin, S.B.; Jones, P.A. A decade of exploring the cancer epigenome—Biological and translational implications. *Nat. Rev. Cancer* **2011**, *11*, 726–734. [CrossRef] [PubMed]
15. Bennett, R.L.; Licht, J.D. Targeting epigenetics in cancer. *Annu. Rev. Pharmacol. Toxicol.* **2018**, *58*, 187–207. [CrossRef] [PubMed]
16. Voyias, P.; Patel, A.; Arasaradnam, R. Epigenetic biomarkers of disease. In *Medical Epigenetics*; Elsevier: Amsterdam, The Netherlands, 2016; pp. 159–176.
17. Inbar-Feigenberg, M.; Choufani, S.; Butcher, D.T.; Roifman, M.; Weksberg, R. Basic concepts of epigenetics. *Fertil. Steril.* **2013**, *99*, 607–615. [CrossRef] [PubMed]
18. Porten, S.P. Epigenetic alterations in bladder cancer. *Curr. Urol. Rep.* **2018**, *19*, 102. [CrossRef]
19. Duex, J.E.; Swain, K.E.; Dancik, G.M.; Paucek, R.D.; Owens, C.; Churchill, M.E.A.; Theodorescu, D. Functional impact of chromatin remodeling gene mutations and predictive signature for therapeutic response in bladder cancer. *Mol. Cancer Res.* **2018**, *16*, 69–77. [CrossRef]
20. Cancer Genome Atlas Research Network. Comprehensive molecular characterization of urothelial bladder carcinoma. *Nature* **2014**, *507*, 315–322. [CrossRef]
21. Hurst, C.D.; Alder, O.; Platt, F.M.; Droop, A.; Stead, L.F.; Burns, J.E.; Burghel, G.J.; Jain, S.; Klimczak, L.J.; Lindsay, H.; et al. Genomic subtypes of non-invasive bladder cancer with distinct metabolic profile and female gender bias in KDM6A mutation frequency. *Cancer Cell* **2017**, *32*, 701–715.e7. [CrossRef]
22. Ler, L.D.; Ghosh, S.; Chai, X.; Thike, A.A.; Heng, H.L.; Siew, E.Y.; Dey, S.; Koh, L.K.; Lim, J.Q.; Lim, W.K.; et al. Loss of tumor suppressor KDM6A amplifies PRC2-regulated transcriptional repression in bladder cancer and can be targeted through inhibition of EZH2. *Sci. Transl. Med.* **2017**, *9*, eaai8312. [CrossRef]
23. Ding, B.; Yan, L.; Zhang, Y.; Wang, Z.; Zhang, Y.; Xia, D.; Ye, Z.; Xu, H. Analysis of the role of mutations in the KMT2D histone lysine methyltransferase in bladder cancer. *FEBS Open Bio.* **2019**, *9*, 693–706. [CrossRef]
24. Marques-Magalhães, Â.; Graça, I.; Henrique, R.; Jerónimo, C. Targeting DNA Methyltranferases in Urological Tumors. *Front. Pharmacol.* **2018**, *9*, 366. [CrossRef] [PubMed]
25. Wolff, E.M.; Chihara, Y.; Pan, F.; Weisenberger, D.J.; Siegmund, K.D.; Sugano, K.; Kawashima, K.; Laird, P.W.; Jones, P.A.; Liang, G. Unique DNA methylation patterns distinguish noninvasive and invasive urothelial cancers and establish an epigenetic field defect in premalignant tissue. *Cancer Res.* **2010**, *70*, 8169–8178. [CrossRef] [PubMed]
26. Wu, H.; Caffo, B.; Jaffee, H.A.; Irizarry, R.A.; Feinberg, A.P. Redefining CpG islands using hidden Markov models. *Biostatistics* **2010**, *11*, 499–514. [CrossRef] [PubMed]
27. Ferreira, H.J.; Esteller, M. CpG Islands in Cancer: Heads, Tails, and Sides. *Methods Mol. Biol.* **2018**, *1766*, 49–80. [CrossRef]
28. Rodríguez-Paredes, M.; Esteller, M. Cancer epigenetics reaches mainstream oncology. *Nat. Med.* **2011**, *17*, 330–339. [CrossRef]

29. Kanwal, R.; Gupta, S. Epigenetic modifications in cancer. *Clin. Genet.* **2012**, *81*, 303–311. [CrossRef]
30. Pasculli, B.; Barbano, R.; Parrella, P. Epigenetics of breast cancer: Biology and clinical implication in the era of precision medicine. *Semin. Cancer Biol.* **2018**, *51*, 22–35. [CrossRef]
31. Lao, V.V.; Grady, W.M. Epigenetics and colorectal cancer. *Nat. Rev. Gastroenterol. Hepatol.* **2011**, *8*, 686–700. [CrossRef]
32. Maunakea, A.K.; Chepelev, I.; Cui, K.; Zhao, K. Intragenic DNA methylation modulates alternative splicing by recruiting MeCP2 to promote exon recognition. *Cell Res.* **2013**, *23*, 1256–1269. [CrossRef]
33. Maunakea, A.K.; Nagarajan, R.P.; Bilenky, M.; Ballinger, T.J.; D'Souza, C.; Fouse, S.D.; Johnson, B.E.; Hong, C.; Nielsen, C.; Zhao, Y.; et al. Conserved role of intragenic DNA methylation in regulating alternative promoters. *Nature* **2010**, *466*, 253–257. [CrossRef]
34. Bae, M.G.; Kim, J.Y.; Choi, J.K. Frequent hypermethylation of orphan CpG islands with enhancer activity in cancer. *BMC Med. Genom.* **2016**, *9* (Suppl. S1), 38. [CrossRef] [PubMed]
35. Baubec, T.; Colombo, D.F.; Wirbelauer, C.; Schmidt, J.; Burger, L.; Krebs, A.R.; Akalin, A.; Schübeler, D. Genomic profiling of DNA methyltransferases reveals a role for DNMT3B in genic methylation. *Nature* **2015**, *520*, 243–247. [CrossRef] [PubMed]
36. Timinskas, A.; Butkus, V.; Janulaitis, A. Sequence motifs characteristic for DNA [cytosine-N4] and DNA [adenine-N6] methyltransferases. Classification of all DNA methyltransferases. *Gene* **1995**, *157*, 3–11. [CrossRef]
37. Lyko, F. The DNA methyltransferase family: A versatile toolkit for epigenetic regulation. *Nat. Rev. Genet.* **2018**, *19*, 81–92. [CrossRef]
38. Gruenbaum, Y.; Cedar, H.; Razin, A. Substrate and sequence specificity of a eukaryotic DNA methylase. *Nature* **1982**, *295*, 620–622. [CrossRef] [PubMed]
39. Bestor, T.H.; Ingram, V.M. Two DNA methyltransferases from murine erythroleukemia cells: Purification, sequence specificity, and mode of interaction with DNA. *Proc. Natl. Acad. Sci. USA* **1983**, *80*, 5559–5563. [CrossRef] [PubMed]
40. Tahiliani, M.; Koh, K.P.; Shen, Y.; Pastor, W.A.; Bandukwala, H.; Brudno, Y.; Agarwal, S.; Iyer, L.M.; Liu, D.R.; Aravind, L.; et al. Conversion of 5-methylcytosine to 5-hydroxymethylcytosine in mammalian DNA by MLL partner TET1. *Science* **2009**, *324*, 930–935. [CrossRef]
41. Kohli, R.M.; Zhang, Y. TET enzymes, TDG and the dynamics of DNA demethylation. *Nature* **2013**, *502*, 472–479. [CrossRef]
42. Cedar, H.; Bergman, Y. Programming of DNA methylation patterns. *Annu. Rev. Biochem.* **2012**, *81*, 97–117. [CrossRef]
43. Bhutani, N.; Burns, D.M.; Blau, H.M. DNA demethylation dynamics. *Cell* **2011**, *146*, 866–872. [CrossRef]
44. Baylin, S.B.; Jones, P.A. Epigenetic determinants of cancer. *Cold Spring Harb. Perspect. Biol.* **2016**, *8*, a019505. [CrossRef] [PubMed]
45. Hansen, K.D.; Timp, W.; Bravo, H.C.; Sabunciyan, S.; Langmead, B.; McDonald, O.G.; Wen, B.; Wu, H.; Liu, Y.; Diep, D.; et al. Increased methylation variation in epigenetic domains across cancer types. *Nat. Genet.* **2011**, *43*, 768–775. [CrossRef] [PubMed]
46. Ross, J.P.; Rand, K.N.; Molloy, P.L. Hypomethylation of repeated DNA sequences in cancer. *Epigenomics* **2010**, *2*, 245–269. [CrossRef]
47. Rodriguez, J.; Frigola, J.; Vendrell, E.; Risques, R.A.; Fraga, M.F.; Morales, C.; Moreno, V.; Esteller, M.; Capellà, G.; Ribas, M.; et al. Chromosomal instability correlates with genome-wide DNA demethylation in human primary colorectal cancers. *Cancer Res.* **2006**, *66*, 8462–9468. [CrossRef] [PubMed]
48. Saif, I.; Kasmi, Y.; Allali, K.; Ennaji, M.M. Prediction of DNA methylation in the promoter of gene suppressor tumor. *Gene* **2018**, *651*, 166–173. [CrossRef]
49. Kandimalla, R.; van Tilborg, A.A.; Zwarthoff, E.C. DNA methylation-based biomarkers in bladder cancer. *Nat. Rev. Urol.* **2013**, *10*, 327–335. [CrossRef]
50. Larsen, L.K.; Lind, G.E.; Guldberg, P.; Dahl, C. DNA-methylation-based detection of urological cancer in urine: Overview of biomarkers and considerations on biomarker design, source of DNA, and detection technologies. *Int. J. Mol. Sci.* **2019**, *20*, 2657. [CrossRef]
51. Padrão, N.A.; Monteiro-Reis, S.; Torres-Ferreira, J.; Antunes, L.; Leça, L.; Montezuma, D.; Ramalho-Carvalho, J.; Dias, P.C.; Monteiro, P.; Oliveira, J.; et al. MicroRNA promoter methylation: A new tool for accurate detection of urothelial carcinoma. *Br. J. Cancer* **2017**, *116*, 634–639. [CrossRef]

52. Wu, Y.; Jiang, G.; Zhang, N.; Liu, S.; Lin, X.; Perschon, C.; Zheng, S.L.; Ding, Q.; Wang, X.; Na, R.; et al. HOXA9, PCDH17, POU4F2, and ONECUT2 as a urinary biomarker combination for the detection of bladder cancer in Chinese patients with hematuria. *Eur. Urol. Focus* **2020**, *6*, 284–291. [CrossRef]
53. Costa, V.L.; Henrique, R.; Danielsen, S.A.; Duarte-Pereira, S.; Eknaes, M.; Skotheim, R.I.; Rodrigues, A.; Magalhães, J.S.; Oliveira, J.; Lothe, R.A.; et al. Three epigenetic biomarkers, GDF15, TMEFF2, and VIM, accurately predict bladder cancer from DNA-based analyses of urine samples. *Clin. Cancer Res.* **2010**, *16*, 5842–5851. [CrossRef]
54. Feber, A.; Dhami, P.; Dong, L.; de Winter, P.; Tan, W.S.; Martínez-Fernández, M.; Paul, D.S.; Hynes-Allen, A.; Rezaee, S.; Gurung, P.; et al. UroMark-a urinary biomarker assay for the detection of bladder cancer. *Clin. Epigenet.* **2017**, *9*, 8. [CrossRef] [PubMed]
55. García-Baquero, R.; Puerta, P.; Beltran, M.; Alvarez-Mújica, M.; Alvarez-Ossorio, J.L.; Sánchez-Carbayo, M. Methylation of tumor suppressor genes in a novel panel predicts clinical outcome in paraffin-embedded bladder tumors. *Tumour Biol* **2014**, *35*, 5777–5786. [CrossRef] [PubMed]
56. Wang, X.; Chen, E.; Yang, X.; Wang, Y.; Quan, Z.; Wu, X.; Luo, C. 5-azacytidine inhibits the proliferation of bladder cancer cells via reversal of the aberrant hypermethylation of the hepaCAM gene. *Oncol. Rep.* **2016**, *35*, 1375–1384. [CrossRef] [PubMed]
57. Erdmann, A.; Halby, L.; Fahy, J.; Arimondo, P.B. Targeting DNA methylation with small molecules: What's next? *J. Med. Chem.* **2015**, *58*, 2569–2583. [CrossRef]
58. Bohl, S.R.; Bullinger, L.; Rücker, F.G. Epigenetic therapy: Azacytidine and decitabine in acute myeloid leukemia. *Expert Rev. Hematol.* **2018**, *11*, 361–371. [CrossRef]
59. Stresemann, C.; Lyko, F. Modes of action of the DNA methyltransferase inhibitors azacytidine and decitabine. *Int. J. Cancer* **2008**, *123*, 8–13. [CrossRef]
60. Egger, G.; Liang, G.; Aparicio, A.; Jones, P.A. Epigenetics in human disease and prospects for epigenetic therapy. *Nature* **2004**, *429*, 457–463. [CrossRef]
61. Jones, P.A.; Taylor, S.M. Cellular differentiation, cytidine analogues and DNA methylation. *Cell* **1980**, *20*, 85–93. [CrossRef]
62. Levine, A.J. The p53 protein plays a central role in the mechanism of action of epigentic drugs that alter the methylation of cytosine residues in DNA. *Oncotarget* **2017**, *8*, 7228–7230. [CrossRef]
63. Nguyen, A.N.; Hollenbach, P.W.; Richard, N.; Luna-Moran, A.; Brady, H.; Heise, C.; MacBeth, K.J. Azacitidine and decitabine have different mechanisms of action in non-small cell lung cancer cell lines. *Lung Cancer (Auckl.)* **2010**, *1*, 119–140. [CrossRef]
64. Datta, J.; Ghoshal, K.; Motiwala, T.; Jacob, S.T. Novel insights into the molecular mechanism of action of DNA Hypomethylating agents: Role of protein kinase C δ in decitabine-induced degradation of DNA methyltransferase 1. *Genes Cancer* **2012**, *3*, 71–81. [CrossRef] [PubMed]
65. Santi, D.V.; Norment, A.; Garrett, C.E. Covalent bond formation between a DNA-cytosine methyltransferase and DNA containing 5-azacytosine. *Proc. Natl. Acad. Sci. USA* **1984**, *81*, 6993–6997. [CrossRef] [PubMed]
66. Chen, L.; MacMillan, A.M.; Chang, W.; Ezaz-Nikpay, K.; Lane, W.S.; Verdine, G.L. Direct identification of the active-site nucleophile in a DNA (cytosine-5)-methyltransferase. *Biochemistry* **1991**, *30*, 11018–11025. [CrossRef] [PubMed]
67. Mortusewicz, O.; Schermelleh, L.; Walter, J.; Cardoso, M.C.; Leonhardt, H. Recruitment of DNA methyltransferase I to DNA repair sites. *Proc. Natl. Acad. Sci. USA* **2005**, *102*, 8905–8909. [CrossRef]
68. Welch, J.S.; Petti, A.A.; Miller, C.A.; Fronick, C.C.; O'Laughlin, M.; Fulton, R.S.; Wilson, R.K.; Baty, J.D.; Duncavage, E.J.; Tandon, B.; et al. TP53 and decitabine in acute myeloid leukemia and myelodysplastic syndromes. *N. Engl. J. Med.* **2016**, *375*, 2023–2036. [CrossRef]
69. Gros, C.; Fahy, J.; Halby, L.; Dufau, I.; Erdmann, A.; Gregoire, J.M.; Ausseil, F.; Vispé, S.; Arimondo, P.B. DNA methylation inhibitors in cancer: Recent and future approaches. *Biochimie* **2012**, *94*, 2280–2296. [CrossRef]
70. Ganesan, A.; Arimondo, P.B.; Rots, M.G.; Jeronimo, C.; Berdasco, M. The timeline of epigenetic drug discovery: From reality to dreams. *Clin. Epigenet.* **2019**, *11*, 174. [CrossRef]
71. Yoo, C.B.; Cheng, J.C.; Jones, P.A. Zebularine: A new drug for epigenetic therapy. *Biochem. Soc. Trans.* **2004**, *32*, 910–912. [CrossRef]
72. Takemura, Y.; Satoh, M.; Hatanaka, K.; Kubota, S. Zebularine exerts its antiproliferative activity through S phase delay and cell death in human malignant mesothelioma cells. *Biosci. Biotechnol. Biochem.* **2018**, *82*, 1159–1164. [CrossRef]

73. Cheng, J.C.; Yoo, C.B.; Weisenberger, D.J.; Chuang, J.; Wozniak, C.; Liang, G.; Marquez, V.E.; Greer, S.; Orntoft, T.F.; Thykjaer, T.; et al. Preferential response of cancer cells to zebularine. *Cancer Cell* **2004**, *6*, 151–158. [CrossRef]
74. Orta, M.L.; Pastor, N.; Burgos-Morón, E.; Domínguez, I.; Calderón-Montaño, J.M.; Huertas Castaño, C.; López-Lázaro, M.; Helleday, T.; Mateos, S. Zebularine induces replication-dependent double-strand breaks which are preferentially repaired by homologous recombination. *DNA Repair (Amst.)* **2017**, *57*, 116–124. [CrossRef] [PubMed]
75. Liu, H.; Xue, Z.T.; Sjögren, H.O.; Salford, L.G.; Widegren, B. Low dose Zebularine treatment enhances immunogenicity of tumor cells. *Cancer Lett.* **2007**, *257*, 107–115. [CrossRef] [PubMed]
76. Champion, C.; Guianvarc'h, D.; Sénamaud-Beaufort, C.; Jurkowska, R.Z.; Jeltsch, A.; Ponger, L.; Arimondo, P.B.; Guieysse-Peugeot, A.L. Mechanistic insights on the inhibition of c5 DNA methyltransferases by zebularine. *PLoS ONE* **2010**, *5*, e12388. [CrossRef] [PubMed]
77. Gowher, H.; Jeltsch, A. Mechanism of inhibition of DNA methyltransferases by cytidine analogues in cancer therapy. *Cancer Biol. Ther.* **2004**, *3*, 1062–1068. [CrossRef] [PubMed]
78. Beumer, J.H.; Eiseman, J.L.; Parise, R.A.; Joseph, E.; Holleran, J.L.; Covey, J.M.; Egorin, M.J. Pharmacokinetics, metabolism, and oral bioavailability of the DNA methyltransferase inhibitor 5-fluoro-2′-deoxycytidine in mice. *Clin. Cancer Res.* **2006**, *12*, 7483–7491. [CrossRef]
79. Neil, G.L.; Moxley, T.E.; Kuentzel, S.L.; Manak, R.C.; Hanka, L.J. Enhancement by tetrahydrouridine (NSC-112907) of the oral activity of 5-azacytidine (NSC-102816) in L1210 leukemic mice. *Cancer Chemother. Rep.* **1975**, *59*, 459–465.
80. Beumer, J.H.; Parise, R.A.; Newman, E.M.; Doroshow, J.H.; Synold, T.W.; Lenz, H.J.; Egorin, M.J. Concentrations of the DNA methyltransferase inhibitor 5-fluoro-2′-deoxycytidine (FdCyd) and its cytotoxic metabolites in plasma of patients treated with FdCyd and tetrahydrouridine (THU). *Cancer Chemother. Pharmacol.* **2008**, *62*, 363–368. [CrossRef]
81. Newman, E.M.; Morgan, R.J.; Kummar, S.; Beumer, J.H.; Blanchard, M.S.; Ruel, C.; El-Khoueiry, A.B.; Carroll, M.I.; Hou, J.M.; Li, C.; et al. A phase I, pharmacokinetic, and pharmacodynamic evaluation of the DNA methyltransferase inhibitor 5-fluoro-2′-deoxycytidine, administered with tetrahydrouridine. *Cancer Chemother. Pharmacol.* **2015**, *75*, 537–546. [CrossRef]
82. Kantarjian, H.M.; Roboz, G.J.; Kropf, P.L.; Yee, K.W.L.; O'Connell, C.L.; Tibes, R.; Walsh, K.J.; Podoltsev, N.A.; Griffiths, E.A.; Jabbour, E.; et al. Guadecitabine (SGI-110) in treatment-naive patients with acute myeloid leukaemia: Phase 2 results from a multicentre, randomised, phase 1/2 trial. *Lancet Oncol.* **2017**, *18*, 1317–1326. [CrossRef]
83. Lee, V.; Wang, J.; Zahurak, M.; Gootjes, E.; Verheul, H.M.; Parkinson, R.; Kerner, Z.; Sharma, A.; Rosner, G.; De Jesus-Acosta, A.; et al. A phase I trial of a guadecitabine (SGI-110) and irinotecan in metastatic colorectal cancer patients previously exposed to irinotecan. *Clin. Cancer Res.* **2018**, *24*, 6160–6167. [CrossRef]
84. Garcia-Manero, G.; Roboz, G.; Walsh, K.; Kantarjian, H.; Ritchie, E.; Kropf, P.; O'Connell, C.; Tibes, R.; Lunin, S.; Rosenblat, T.; et al. Guadecitabine (SGI-110) in patients with intermediate or high-risk myelodysplastic syndromes: Phase 2 results from a multicentre, open-label, randomised, phase 1/2 trial. *Lancet Haematol.* **2019**, *6*, e317–e327. [CrossRef]
85. Laille, E.; Savona, M.R.; Scott, B.L.; Boyd, T.E.; Dong, Q.; Skikne, B. Pharmacokinetics of different formulations of oral azacitidine (CC-486) and the effect of food and modified gastric pH on pharmacokinetics in subjects with hematologic malignancies. *J. Clin. Pharmacol.* **2014**, *54*, 630–639. [CrossRef] [PubMed]
86. Levy, B.P.; Giaccone, G.; Besse, B.; Felip, E.; Garassino, M.C.; Domine Gomez, M.; Garrido, P.; Piperdi, B.; Ponce-Aix, S.; Menezes, D.; et al. Randomised phase 2 study of pembrolizumab plus CC-486 versus pembrolizumab plus placebo in patients with previously treated advanced non-small cell lung cancer. *Eur. J. Cancer* **2019**, *108*, 120–128. [CrossRef] [PubMed]
87. Von Hoff, D.D.; Rasco, D.W.; Heath, E.I.; Munster, P.N.; Schellens, J.H.M.; Isambert, N.; Le Tourneau, C.; O'Neil, B.; Mathijssen, R.H.J.; Lopez-Martin, J.A.; et al. Phase I study of CC-486 alone and in combination with carboplatin or nab-paclitaxel in patients with relapsed or refractory solid tumors. *Clin. Cancer Res.* **2018**, *24*, 4072–4080. [CrossRef] [PubMed]
88. Garcia-Manero, G.; Gore, S.D.; Kambhampati, S.; Scott, B.; Tefferi, A.; Cogle, C.R.; Edenfield, W.J.; Hetzer, J.; Kumar, K.; Laille, E.; et al. Efficacy and safety of extended dosing schedules of CC-486 (oral azacitidine) in patients with lower-risk myelodysplastic syndromes. *Leukemia* **2016**, *30*, 889–896. [CrossRef]

89. Peters, G.J.; Smid, K.; Vecchi, L.; Kathmann, I.; Sarkisjan, D.; Honeywell, R.J.; Losekoot, N.; Ohne, O.; Orbach, A.; Blaugrund, E.; et al. Metabolism, mechanism of action and sensitivity profile of fluorocyclopentenylcytosine (RX-3117; TV-1360). *Investig. New Drugs* **2013**, *31*, 1444–1457. [CrossRef]
90. Balboni, B.; El Hassouni, B.; Honeywell, R.J.; Sarkisjan, D.; Giovannetti, E.; Poore, J.; Heaton, C.; Peterson, C.; Benaim, E.; Lee, Y.B.; et al. RX-3117 (fluorocyclopentenyl cytosine): A novel specific antimetabolite for selective cancer treatment. *Expert Opin. Investig. Drugs* **2019**, *28*, 311–322. [CrossRef]
91. Yang, M.Y.; Lee, Y.B.; Ahn, C.H.; Kaye, J.; Fine, T.; Kashi, R.; Ohne, O.; Smid, K.; Peters, G.J.; Kim, D.J. A novel cytidine analog, RX-3117, shows potent efficacy in xenograft models, even in tumors that are resistant to gemcitabine. *Anticancer Res.* **2014**, *34*, 6951–6959.
92. Castillo-Aguilera, O.; Depreux, P.; Halby, L.; Arimondo, P.B.; Goossens, L. DNA Methylation Targeting: The DNMT/HMT Crosstalk Challenge. *Biomolecules* **2017**, *7*, 3. [CrossRef]
93. Pushpakom, S.; Iorio, F.; Eyers, P.A.; Escott, K.J.; Hopper, S.; Wells, A.; Doig, A.; Guilliams, T.; Latimer, J.; McNamee, C.; et al. Drug repurposing: Progress, challenges and recommendations. *Nat. Rev. Drug Discov.* **2019**, *18*, 41–58. [CrossRef]
94. Villar-Garea, A.; Fraga, M.F.; Espada, J.; Esteller, M. Procaine is a DNA-demethylating agent with growth-inhibitory effects in human cancer cells. *Cancer Res.* **2003**, *63*, 4984–4989. [PubMed]
95. Moreira-Silva, F.; Camilo, V.; Gaspar, V.; Mano, J.F.; Henrique, R.; Jerónimo, C. Repurposing old drugs into new epigenetic inhibitors: Promising candidates for cancer treatment? *Pharmaceutics* **2020**, *12*, 410. [CrossRef] [PubMed]
96. Li, Y.C.; Wang, Y.; Li, D.D.; Zhang, Y.; Zhao, T.C.; Li, C.F. Procaine is a specific DNA methylation inhibitor with anti-tumor effect for human gastric cancer. *J. Cell Biochem.* **2018**, *119*, 2440–2449. [CrossRef]
97. Kuck, D.; Caulfield, T.; Lyko, F.; Medina-Franco, J.L. Nanaomycin A selectively inhibits DNMT3B and reactivates silenced tumor suppressor genes in human cancer cells. *Mol. Cancer Ther.* **2010**, *9*, 3015–3023. [CrossRef] [PubMed]
98. Caulfield, T.; Medina-Franco, J.L. Molecular dynamics simulations of human DNA methyltransferase 3B with selective inhibitor nanaomycin A. *J. Struct. Biol.* **2011**, *176*, 185–191. [CrossRef]
99. Dueñas-Gonzalez, A.; Coronel, J.; Cetina, L.; González-Fierro, A.; Chavez-Blanco, A.; Taja-Chayeb, L. Hydralazine-valproate: A repositioned drug combination for the epigenetic therapy of cancer. *Expert Opin. Drug Metab. Toxicol.* **2014**, *10*, 1433–1444. [CrossRef]
100. Segura-Pacheco, B.; Trejo-Becerril, C.; Perez-Cardenas, E.; Taja-Chayeb, L.; Mariscal, I.; Chavez, A.; Acuña, C.; Salazar, A.M.; Lizano, M.; Dueñas-Gonzalez, A. Reactivation of tumor suppressor genes by the cardiovascular drugs hydralazine and procainamide and their potential use in cancer therapy. *Clin. Cancer Res.* **2003**, *9*, 1596–1603.
101. Graça, I.; Sousa, E.J.; Costa-Pinheiro, P.; Vieira, F.Q.; Torres-Ferreira, J.; Martins, M.G.; Henrique, R.; Jerónimo, C. Anti-neoplastic properties of hydralazine in prostate cancer. *Oncotarget* **2014**, *5*, 5950–5964. [CrossRef]
102. Pérez-Cárdenas, E.; Taja-Chayeb, L.; Trejo-Becerril, C.; Chanona-Vilchis, J.; Chávez-Blanco, A.; Domínguez-Gómez, G.; Langley, E.; García-Carrancá, A.; Dueñas-González, A. Antimetastatic effect of epigenetic drugs, hydralazine and valproic acid, in Ras-transformed NIH 3T3 cells. *Onco Targets Ther.* **2018**, *11*, 8823–8833. [CrossRef]
103. Candelaria, M.; Gallardo-Rincón, D.; Arce, C.; Cetina, L.; Aguilar-Ponce, J.L.; Arrieta, O.; González-Fierro, A.; Chávez-Blanco, A.; de la Cruz-Hernández, E.; Camargo, M.F.; et al. A phase II study of epigenetic therapy with hydralazine and magnesium valproate to overcome chemotherapy resistance in refractory solid tumors. *Ann. Oncol.* **2007**, *18*, 1529–1538. [CrossRef]
104. Coronel, J.; Cetina, L.; Pacheco, I.; Trejo-Becerril, C.; González-Fierro, A.; de la Cruz-Hernandez, E.; Perez-Cardenas, E.; Taja-Chayeb, L.; Arias-Bofill, D.; Candelaria, M.; et al. A double-blind, placebo-controlled, randomized phase III trial of chemotherapy plus epigenetic therapy with hydralazine valproate for advanced cervical cancer. Preliminary results. *Med. Oncol.* **2011**, *28* (Suppl. S1), S540–S546. [CrossRef]
105. Amato, R.J. Inhibition of DNA methylation by antisense oligonucleotide MG98 as cancer therapy. *Clin. Genitourin. Cancer* **2007**, *5*, 422–426. [CrossRef] [PubMed]

106. Davis, A.J.; Gelmon, K.A.; Siu, L.L.; Moore, M.J.; Britten, C.D.; Mistry, N.; Klamut, H.; D'Aloisio, S.; MacLean, M.; Wainman, N.; et al. Phase I and pharmacologic study of the human DNA methyltransferase antisense oligodeoxynucleotide MG98 given as a 21-day continuous infusion every 4 weeks. *Investig. New Drugs* **2003**, *21*, 85–97. [CrossRef] [PubMed]
107. Klisovic, R.B.; Stock, W.; Cataland, S.; Klisovic, M.I.; Liu, S.; Blum, W.; Green, M.; Odenike, O.; Godley, L.; Burgt, J.V.; et al. A phase I biological study of MG98, an oligodeoxynucleotide antisense to DNA methyltransferase 1, in patients with high-risk myelodysplasia and acute myeloid leukemia. *Clin. Cancer Res.* **2008**, *14*, 2444–2449. [CrossRef] [PubMed]
108. Plummer, R.; Vidal, L.; Griffin, M.; Lesley, M.; de Bono, J.; Coulthard, S.; Sludden, J.; Siu, L.L.; Chen, E.X.; Oza, A.M.; et al. Phase I study of MG98, an oligonucleotide antisense inhibitor of human DNA methyltransferase 1, given as a 7-day infusion in patients with advanced solid tumors. *Clin. Cancer Res.* **2009**, *15*, 3177–3183. [CrossRef]
109. Amato, R.J.; Stephenson, J.; Hotte, S.; Nemunaitis, J.; Bélanger, K.; Reid, G.; Martell, R.E. MG98, a second-generation DNMT1 inhibitor, in the treatment of advanced renal cell carcinoma. *Cancer Investig.* **2012**, *30*, 415–421. [CrossRef]
110. Rondelet, G.; Fleury, L.; Faux, C.; Masson, V.; Dubois, J.; Arimondo, P.B.; Willems, L.; Wouters, J. Inhibition studies of DNA methyltransferases by maleimide derivatives of RG108 as non-nucleoside inhibitors. *Future Med. Chem.* **2017**, *9*, 1465–1481. [CrossRef]
111. Yang, L.; Hou, J.; Cui, X.H.; Suo, L.N.; Lv, Y.W. RG108 induces the apoptosis of endometrial cancer Ishikawa cell lines by inhibiting the expression of DNMT3B and demethylation of HMLH1. *Eur Rev. Med. Pharmacol. Sci.* **2017**, *21*, 5056–5064. [CrossRef]
112. Graça, I.; Sousa, E.J.; Baptista, T.; Almeida, M.; Ramalho-Carvalho, J.; Palmeira, C.; Henrique, R.; Jerónimo, C. Anti-tumoral effect of the non-nucleoside DNMT inhibitor RG108 in human prostate cancer cells. *Curr. Pharm. Des.* **2014**, *20*, 1803–1811. [CrossRef]
113. Yoo, J.; Choi, S.; Medina-Franco, J.L. Molecular modeling studies of the novel inhibitors of DNA methyltransferases SGI-1027 and CBC12: Implications for the mechanism of inhibition of DNMTs. *PLoS ONE* **2013**, *8*, e62152. [CrossRef]
114. Datta, J.; Ghoshal, K.; Denny, W.A.; Gamage, S.A.; Brooke, D.G.; Phiasivongsa, P.; Redkar, S.; Jacob, S.T. A new class of quinoline-based DNA hypomethylating agents reactivates tumor suppressor genes by blocking DNA methyltransferase 1 activity and inducing its degradation. *Cancer Res.* **2009**, *69*, 4277–4285. [CrossRef] [PubMed]
115. Zwergel, C.; Schnekenburger, M.; Sarno, F.; Battistelli, C.; Manara, M.C.; Stazi, G.; Mazzone, R.; Fioravanti, R.; Gros, C.; Ausseil, F.; et al. Identification of a novel quinoline-based DNA demethylating compound highly potent in cancer cells. *Clin. Epigenet.* **2019**, *11*, 68. [CrossRef] [PubMed]
116. Fang, M.Z.; Wang, Y.; Ai, N.; Hou, Z.; Sun, Y.; Lu, H.; Welsh, W.; Yang, C.S. Tea polyphenol (−)-epigallocatechin-3-gallate inhibits DNA methyltransferase and reactivates methylation-silenced genes in cancer cell lines. *Cancer Res.* **2003**, *63*, 7563–7570. [PubMed]
117. Nandakumar, V.; Vaid, M.; Katiyar, S.K. (−)-Epigallocatechin-3-gallate reactivates silenced tumor suppressor genes, Cip1/p21 and p16INK4a, by reducing DNA methylation and increasing histones acetylation in human skin cancer cells. *Carcinogenesis* **2011**, *32*, 537–544. [CrossRef]
118. Sheng, J.; Shi, W.; Guo, H.; Long, W.; Wang, Y.; Qi, J.; Liu, J.; Xu, Y. The inhibitory effect of (−)-epigallocatechin-3-gallate on breast cancer progression via reducing SCUBE2 methylation and DNMT activity. *Molecules* **2019**, *24*, 2899. [CrossRef]
119. Bilir, B.; Sharma, N.V.; Lee, J.; Hammarstrom, B.; Svindland, A.; Kucuk, O.; Moreno, C.S. Effects of genistein supplementation on genome-wide DNA methylation and gene expression in patients with localized prostate cancer. *Int. J. Oncol.* **2017**, *51*, 223–234. [CrossRef]
120. Xie, Q.; Bai, Q.; Zou, L.Y.; Zhang, Q.Y.; Zhou, Y.; Chang, H.; Yi, L.; Zhu, J.D.; Mi, M.T. Genistein inhibits DNA methylation and increases expression of tumor suppressor genes in human breast cancer cells. *Genes Chromosomes Cancer* **2014**, *53*, 422–431. [CrossRef]
121. Zhu, J.; Ren, J.; Tang, L. Genistein inhibits invasion and migration of colon cancer cells by recovering WIF1 expression. *Mol. Med. Rep.* **2018**, *17*, 7265–7273. [CrossRef]
122. Link, A.; Balaguer, F.; Shen, Y.; Lozano, J.J.; Leung, H.C.; Boland, C.R.; Goel, A. Curcumin modulates DNA methylation in colorectal cancer cells. *PLoS ONE* **2013**, *8*, e57709. [CrossRef]

123. Tao, J.; Liu, Q.; Wu, X.; Xu, X.; Zhang, Y.; Wang, Q.; Luo, C. Identification of hypermethylation in hepatocyte cell adhesion molecule gene promoter region in bladder carcinoma. *Int. J. Med. Sci.* **2013**, *10*, 1860–1867. [CrossRef]
124. Hahn, N.M.; Bonney, P.L.; Dhawan, D.; Jones, D.R.; Balch, C.; Guo, Z.; Hartman-Frey, C.; Fang, F.; Parker, H.G.; Kwon, E.M.; et al. Subcutaneous 5-azacitidine treatment of naturally occurring canine urothelial carcinoma: A novel epigenetic approach to human urothelial carcinoma drug development. *J. Urol.* **2012**, *187*, 302–309. [CrossRef] [PubMed]
125. Ramakrishnan, S.; Hu, Q.; Krishnan, N.; Wang, D.; Smit, E.; Granger, V.; Rak, M.; Attwood, K.; Johnson, C.; Morrison, C.; et al. Decitabine, a DNA-demethylating agent, promotes differentiation via NOTCH1 signaling and alters immune-related pathways in muscle-invasive bladder cancer. *Cell Death Dis.* **2017**, *8*, 3217. [CrossRef] [PubMed]
126. Maraver, A.; Fernandez-Marcos, P.J.; Cash, T.P.; Mendez-Pertuz, M.; Dueñas, M.; Maietta, P.; Martinelli, P.; Muñoz-Martin, M.; Martínez-Fernández, M.; Cañamero, M.; et al. NOTCH pathway inactivation promotes bladder cancer progression. *J. Clin. Investig.* **2015**, *125*, 824–830. [CrossRef] [PubMed]
127. Zhang, H.; Qi, F.; Cao, Y.; Zu, X.; Chen, M.; Li, Z.; Qi, L. 5-Aza-2′-deoxycytidine enhances maspin expression and inhibits proliferation, migration, and invasion of the bladder cancer T24 cell line. *Cancer Biother. Radiopharm.* **2013**, *28*, 343–350. [CrossRef]
128. Devanand, P.; Kim, S.I.; Choi, Y.W.; Sheen, S.S.; Yim, H.; Ryu, M.S.; Kim, S.J.; Kim, W.J.; Lim, I.K. Inhibition of bladder cancer invasion by Sp1-mediated BTG2 expression via inhibition of DNA methyltransferase 1. *FEBS J.* **2014**, *281*, 5581–5601. [CrossRef]
129. Christoph, F.; Kempkensteffen, C.; Weikert, S.; Köllermann, J.; Krause, H.; Miller, K.; Schostak, M.; Schrader, M. Methylation of tumour suppressor genes APAF-1 and DAPK-1 and in vitro effects of demethylating agents in bladder and kidney cancer. *Br. J. Cancer* **2006**, *95*, 1701–1707. [CrossRef]
130. Cheng, J.C.; Weisenberger, D.J.; Gonzales, F.A.; Liang, G.; Xu, G.L.; Hu, Y.G.; Marquez, V.E.; Jones, P.A. Continuous zebularine treatment effectively sustains demethylation in human bladder cancer cells. *Mol. Cell Biol.* **2004**, *24*, 1270–1278. [CrossRef]
131. Urakami, S.; Shiina, H.; Enokida, H.; Kawakami, T.; Tokizane, T.; Ogishima, T.; Tanaka, Y.; Li, L.C.; Ribeiro-Filho, L.A.; Terashima, M.; et al. Epigenetic inactivation of Wnt inhibitory factor-1 plays an important role in bladder cancer through aberrant canonical Wnt/beta-catenin signaling pathway. *Clin. Cancer Res.* **2006**, *12*, 383–391. [CrossRef]
132. Liang, G.; Gonzales, F.A.; Jones, P.A.; Orntoft, T.F.; Thykjaer, T. Analysis of gene induction in human fibroblasts and bladder cancer cells exposed to the methylation inhibitor 5-aza-2′-deoxycytidine. *Cancer Res.* **2002**, *62*, 961–966.
133. Velicescu, M.; Weisenberger, D.J.; Gonzales, F.A.; Tsai, Y.C.; Nguyen, C.T.; Jones, P.A. Cell division is required for de novo methylation of CpG islands in bladder cancer cells. *Cancer Res.* **2002**, *62*, 2378–2384.
134. Chuang, J.J.; Dai, Y.C.; Lin, Y.L.; Chen, Y.Y.; Lin, W.H.; Chan, H.L.; Liu, Y.W. Downregulation of glutathione S-transferase M1 protein in N-butyl-N-(4-hydroxybutyl)nitrosamine-induced mouse bladder carcinogenesis. *Toxicol. Appl. Pharmacol.* **2014**, *279*, 322–330. [CrossRef] [PubMed]
135. Kawakami, T.; Shiina, H.; Igawa, M.; Deguchi, M.; Nakajima, K.; Ogishima, T.; Tokizane, T.; Urakami, S.; Enokida, H.; Miura, K.; et al. Inactivation of the hMSH3 mismatch repair gene in bladder cancer. *Biochem. Biophys. Res. Commun.* **2004**, *325*, 934–942. [CrossRef] [PubMed]
136. Giri, A.K.; Aittokallio, T. DNMT Inhibitors increase methylation in the cancer genome. *Front. Pharmacol.* **2019**, *10*, 385. [CrossRef] [PubMed]
137. Yoo, C.B.; Jeong, S.; Egger, G.; Liang, G.; Phiasivongsa, P.; Tang, C.; Redkar, S.; Jones, P.A. Delivery of 5-aza-2′-deoxycytidine to cells using oligodeoxynucleotides. *Cancer Res.* **2007**, *67*, 6400–6408. [CrossRef]
138. Chuang, J.C.; Warner, S.L.; Vollmer, D.; Vankayalapati, H.; Redkar, S.; Bearss, D.J.; Qiu, X.; Yoo, C.B.; Jones, P.A. S110, a 5-Aza-2′-deoxycytidine–containing dinucleotide, is an effective DNA methylation inhibitor in vivo and can reduce tumor growth. *Mol. Cancer Ther.* **2010**, *9*, 1443–1450. [CrossRef]
139. Chen, T.; Hevi, S.; Gay, F.; Tsujimoto, N.; He, T.; Zhang, B.; Ueda, Y.; Li, E. Complete inactivation of DNMT1 leads to mitotic catastrophe in human cancer cells. *Nat. Genet.* **2007**, *39*, 391–396. [CrossRef]
140. Wu, C.T.; Wu, C.F.; Lu, C.H.; Lin, C.C.; Chen, W.C.; Lin, P.Y.; Chen, M.F. Expression and function role of DNA methyltransferase 1 in human bladder cancer. *Cancer* **2011**, *117*, 5221–5233. [CrossRef]

141. Santoro, S.W.; Joyce, G.F. A general purpose RNA-cleaving DNA enzyme. *Proc. Natl. Acad. Sci. USA* **1997**, *94*, 4262–4266. [CrossRef]
142. Wang, X.; Zhang, L.; Ding, N.; Yang, X.; Zhang, J.; He, J.; Li, Z.; Sun, L.Q. Identification and characterization of DNAzymes targeting DNA methyltransferase I for suppressing bladder cancer proliferation. *Biochem Biophys. Res. Commun.* **2015**, *461*, 329–333. [CrossRef]
143. Liu, X.; Dai, X.; Wu, B. Study of 5-Aza-CdR on transcription regulation of RASSF1A gene in the BIU87 cell line. *Urol. Int.* **2009**, *82*, 108–112. [CrossRef]
144. Mori, K.; Enokida, H.; Kagara, I.; Kawakami, K.; Chiyomaru, T.; Tatarano, S.; Kawahara, K.; Nishiyama, K.; Seki, N.; Nakagawa, M. CpG hypermethylation of collagen type I alpha 2 contributes to proliferation and migration activity of human bladder cancer. *Int. J. Oncol.* **2009**, *34*, 1593–1602. [CrossRef] [PubMed]
145. Matsumoto, M.; Kawakami, K.; Enokida, H.; Toki, K.; Matsuda, R.; Chiyomaru, T.; Nishiyama, K.; Kawahara, K.; Seki, N.; Nakagawa, M. CpG hypermethylation of human four-and-a-half LIM domains 1 contributes to migration and invasion activity of human bladder cancer. *Int. J. Mol. Med.* **2010**, *26*, 241–247. [CrossRef] [PubMed]
146. Yoon, H.Y.; Kim, Y.J.; Kim, J.S.; Kim, Y.W.; Kang, H.W.; Kim, W.T.; Yun, S.J.; Ryu, K.H.; Lee, S.C.; Kim, W.J. RSPH9 methylation pattern as a prognostic indicator in patients with non-muscle invasive bladder cancer. *Oncol. Rep.* **2016**, *35*, 1195–1203. [CrossRef] [PubMed]
147. Karam, J.A.; Fan, J.; Stanfield, J.; Richer, E.; Benaim, E.A.; Frenkel, E.; Antich, P.; Sagalowsky, A.I.; Mason, R.P.; Hsieh, J.T. The use of histone deacetylase inhibitor FK228 and DNA hypomethylation agent 5-azacytidine in human bladder cancer therapy. *Int. J. Cancer* **2007**, *120*, 1795–1802. [CrossRef]
148. Dhawan, D.; Ramos-Vara, J.A.; Hahn, N.M.; Waddell, J.; Olbricht, G.R.; Zheng, R.; Stewart, J.C.; Knapp, D.W. DNMT1: An emerging target in the treatment of invasive urinary bladder cancer. *Urol. Oncol.* **2013**, *31*, 1761–1769. [CrossRef]
149. Wang, C.; Hamacher, A.; Petzsch, P.; Köhrer, K.; Niegisch, G.; Hoffmann, M.J.; Schulz, W.A.; Kassack, M.U. Combination of decitabine and entinostat synergistically inhibits urothelial bladder cancer cells via activation of FoxO1. *Cancers (Basel)* **2020**, *12*, 337. [CrossRef]
150. Ramachandran, K.; Gordian, E.; Singal, R. 5-azacytidine reverses drug resistance in bladder cancer cells. *Anticancer Res.* **2011**, *31*, 3757–3766.
151. Khandelwal, M.; Anand, V.; Appunni, S.; Seth, A.; Singh, P.; Mathur, S.; Sharma, A. Decitabine augments cytotoxicity of cisplatin and doxorubicin to bladder cancer cells by activating hippo pathway through RASSF1A. *Mol. Cell Biochem.* **2018**, *446*, 105–114. [CrossRef]
152. Xylinas, E.; Hassler, M.R.; Zhuang, D.; Krzywinski, M.; Erdem, Z.; Robinson, B.D.; Elemento, O.; Clozel, T.; Shariat, S.F. An epigenomic approach to improving response to neoadjuvant cisplatin chemotherapy in bladder cancer. *Biomolecules* **2016**, *6*, 37. [CrossRef]
153. Papafotiou, G.; Paraskevopoulou, V.; Vasilaki, E.; Kanaki, Z.; Paschalidis, N.; Klinakis, A. KRT14 marks a subpopulation of bladder basal cells with pivotal role in regeneration and tumorigenesis. *Nat. Commun.* **2016**, *7*, 11914. [CrossRef]
154. Zhu, F.; Qian, W.; Zhang, H.; Liang, Y.; Wu, M.; Zhang, Y.; Zhang, X.; Gao, Q.; Li, Y. SOX2 Is a marker for stem-like tumor cells in bladder cancer. *Stem Cell Rep.* **2017**, *9*, 429–437. [CrossRef] [PubMed]
155. Wu, M.; Sheng, L.; Cheng, M.; Zhang, H.; Jiang, Y.; Lin, S.; Liang, Y.; Zhu, F.; Liu, Z.; Zhang, Y.; et al. Low doses of decitabine improve the chemotherapy efficacy against basal-like bladder cancer by targeting cancer stem cells. *Oncogene* **2019**, *38*, 5425–5439. [CrossRef] [PubMed]
156. Varol, N.; Konac, E.; Onen, I.H.; Gurocak, S.; Alp, E.; Yilmaz, A.; Menevse, S.; Sozen, S. The epigenetically regulated effects of Wnt antagonists on the expression of genes in the apoptosis pathway in human bladder cancer cell line (T24). *DNA Cell Biol.* **2014**, *33*, 408–417. [CrossRef] [PubMed]
157. San José-Enériz, E.; Agirre, X.; Rabal, O.; Vilas-Zornoza, A.; Sanchez-Arias, J.A.; Miranda, E.; Ugarte, A.; Roa, S.; Paiva, B.; Estella-Hermoso de Mendoza, A.; et al. Discovery of first-in-class reversible dual small molecule inhibitors against G9a and DNMTs in hematological malignancies. *Nat. Commun.* **2017**, *8*, 15424. [CrossRef]
158. Bárcena-Varela, M.; Caruso, S.; Llerena, S.; Álvarez-Sola, G.; Uriarte, I.; Latasa, M.U.; Urtasun, R.; Rebouissou, S.; Alvarez, L.; Jimenez, M.; et al. Dual targeting of histone methyltransferase G9a and DNA-methyltransferase 1 for the treatment of experimental hepatocellular carcinoma. *Hepatology* **2019**, *69*, 587–603. [CrossRef]

159. Segovia, C.; San José-Enériz, E.; Munera-Maravilla, E.; Martínez-Fernández, M.; Garate, L.; Miranda, E.; Vilas-Zornoza, A.; Lodewijk, I.; Rubio, C.; Segrelles, C.; et al. Inhibition of a G9a/DNMT network triggers immune-mediated bladder cancer regression. *Nat. Med.* **2019**, *25*, 1073–1081. [CrossRef]
160. Shang, D.; Liu, Y.; Matsui, Y.; Ito, N.; Nishiyama, H.; Kamoto, T.; Ogawa, O. Demethylating agent 5-aza-2′-deoxycytidine enhances susceptibility of bladder transitional cell carcinoma to Cisplatin. *Urology* **2008**, *71*, 1220–1225. [CrossRef]
161. Bunch, B.; Krishnan, N.; Greenspan, R.D.; Ramakrishnan, S.; Attwood, K.; Yan, L.; Qi, Q.; Wang, D.; Morrison, C.; Omilian, A.; et al. TAp73 expression and P1 promoter methylation, a potential marker for chemoresponsiveness to cisplatin therapy and survival in muscle-invasive bladder cancer (MIBC). *Cell Cycle* **2019**, *18*, 2055–2066. [CrossRef]
162. Coyne, G.O.; Wang, L.; Zlott, J.; Juwara, L.; Covey, J.M.; Beumer, J.H.; Cristea, M.C.; Newman, E.M.; Koehler, S.; Nieva, J.J.; et al. Intravenous 5-fluoro-2′-deoxycytidine administered with tetrahydrouridine increases the proportion of p16-expressing circulating tumor cells in patients with advanced solid tumors. *Cancer Chemother. Pharmacol.* **2020**, *85*, 979–993. [CrossRef]
163. Lin, J.; Gilbert, J.; Rudek, M.A.; Zwiebel, J.A.; Gore, S.; Jiemjit, A.; Zhao, M.; Baker, S.D.; Ambinder, R.F.; Herman, J.G.; et al. A phase I dose-finding study of 5-azacytidine in combination with sodium phenylbutyrate in patients with refractory solid tumors. *Clin. Cancer Res.* **2009**, *15*, 6241–6249. [CrossRef]
164. A Phase 1 Study of CC-486 as a Single Agent and in Combination with Carboplatin or ABI-007 in Subjects with Relapsed or Refractory Solid Tumors. Available online: https://clinicaltrials.gov/ct2/show/results/NCT01478685 (accessed on 28 April 2020).
165. LoRusso, P.; Rasco, D.; Bendell, J.; Sachdev, J.; Ramanathan, R.; Weiss, G.; Munster, P.; Edenfield, W.J.; Liu, K.; Blackwood-Chirchir, A.; et al. Abstract A120: A phase Ib study of CC-486 (oral azacitidine) as a priming agent for carboplatin or NAB-paclitaxel in subjects with relapsed and refractory solid tumors. *Mol. Cancer Ther.* **2013**, *12*, A120. [CrossRef]
166. Azacitidine Combined with Pembrolizumab and Epacadostat in Subjects with Advanced Solid Tumors (ECHO-206). Available online: https://clinicaltrials.gov/ct2/show/results/NCT02959437 (accessed on 28 April 2020).
167. Atezolizumab + Guadecitabine in Patients with Checkpoint Inhibitor Refractory or Resistant Urothelial Carcinoma. Available online: https://clinicaltrials.gov/ct2/show/results/NCT03179943 (accessed on 28 April 2020).
168. Decitabine in Treating Patients with Advanced Solid Tumors. Available online: https://clinicaltrials.gov/ct2/show/study/NCT00030615 (accessed on 28 April 2020).
169. A Multi-Histology Phase II Study of 5-Fluoro-2′-Deoxycytidine with Tetrahydrouridine (FdCyd + THU). Available online: https://clinicaltrials.gov/ct2/show/results/NCT00978250 (accessed on 28 April 2020).
170. Dose-Finding and Safety Study for Oral Single-Agent to Treat Advanced Malignancies. Available online: https://clinicaltrials.gov/ct2/show/results/NCT02030067 (accessed on 28 April 2020).
171. Bioequivalence & Food Effect Study in Patients with Solid Tumor or Hematologic Malignancies. Available online: https://clinicaltrials.gov/ct2/show/study/NCT02223052 (accessed on 28 April 2020).
172. Crabb, S.; Danson, S.J.; Catto, J.W.F.; McDowell, C.; Lowder, J.N.; Caddy, J.; Dunkley, D.; Rajaram, J.; Ellis, D.; Hill, S.; et al. SPIRE—Combining SGI-110 with cisplatin and gemcitabine chemotherapy for solid malignancies including bladder cancer: Study protocol for a phase Ib/randomised IIa open label clinical trial. *Trials* **2018**, *19*, 216. [CrossRef] [PubMed]
173. Genomic Based Assignment of Therapy in Advanced Urothelial Carcinoma. Available online: https://clinicaltrials.gov/ct2/show/study/NCT02788201 (accessed on 28 April 2020).

© 2020 by the authors. Licensee MDPI, Basel, Switzerland. This article is an open access article distributed under the terms and conditions of the Creative Commons Attribution (CC BY) license (http://creativecommons.org/licenses/by/4.0/).

Lodewijk *et al. Clin Epigenet* (2021) 13:63
https://doi.org/10.1186/s13148-021-01046-0

Clinical Epigenetics

REVIEW

Open Access

# Tackling tumor microenvironment through epigenetic tools to improve cancer immunotherapy

Iris Lodewijk[1,2†], Sandra P. Nunes[1,2,3†], Rui Henrique[3,4,5], Carmen Jerónimo[3,5], Marta Dueñas[1,2,6] and Jesús M. Paramio[1,2,6*]

## Abstract

**Background:** Epigenetic alterations are known contributors to cancer development and aggressiveness. Additional to alterations in cancer cells, aberrant epigenetic marks are present in cells of the tumor microenvironment, including lymphocytes and tumor-associated macrophages, which are often overlooked but known to be a contributing factor to a favorable environment for tumor growth. Therefore, the main aim of this review is to give an overview of the epigenetic alterations affecting immune cells in the tumor microenvironment to provoke an immunosuppressive function and contribute to cancer development. Moreover, immunotherapy is briefly discussed in the context of epigenetics, describing both its combination with epigenetic drugs and the need for epigenetic biomarkers to predict response to immune checkpoint blockage.

**Main body:** Combining both topics, epigenetic machinery plays a central role in generating an immunosuppressive environment for cancer growth, which creates a barrier for immunotherapy to be successful. Furthermore, epigenetic-directed compounds may not only affect cancer cells but also immune cells in the tumor microenvironment, which could be beneficial for the clinical response to immunotherapy.

**Conclusion:** Thus, modulating epigenetics in combination with immunotherapy might be a promising therapeutic option to improve the success of this therapy. Further studies are necessary to (1) understand in depth the impact of the epigenetic machinery in the tumor microenvironment; (2) how the epigenetic machinery can be modulated according to tumor type to increase response to immunotherapy and (3) find reliable biomarkers for a better selection of patients eligible to immunotherapy.

**Keywords:** Epigenetics, Immunotherapy, Tumor microenvironment, Therapy, Bladder cancer

## Background

The epigenome is defined by heritable alterations in gene expression, either activation or suppression, without altering the DNA nucleotide sequence. The mechanisms responsible for these changes can be broadly divided into altered gene accessibility for the transcriptional machinery, disrupted chromatin organization or modulation of gene expression at the post-transcriptional level through altered mRNA translation mainly by non-coding RNAs, including miRNAs. Fundamental mechanisms for epigenetic regulation include DNA methylation, histone modifications, chromatin remodeling and non-coding RNA interference [1]. Nevertheless, these modifications of the RNA sequence and their associated regulatory factors represent functionally relevant changes to the transcriptome without altering the RNA ribonucleotide sequence,

*Correspondence: jesusm.paramio@ciemat.es
†Iris Lodewijk and Sandra P. Nunes have contributed equally to this work
[1] Molecular Oncology Unit, Centro de Investigaciones Energéticas, Medioambientales Y Tecnológicas (CIEMAT), 28040 Madrid, Spain
Full list of author information is available at the end of the article

© The Author(s) 2021. **Open Access** This article is licensed under a Creative Commons Attribution 4.0 International License, which permits use, sharing, adaptation, distribution and reproduction in any medium or format, as long as you give appropriate credit to the original author(s) and the source, provide a link to the Creative Commons licence, and indicate if changes were made. The images or other third party material in this article are included in the article's Creative Commons licence, unless indicated otherwise in a credit line to the material. If material is not included in the article's Creative Commons licence and your intended use is not permitted by statutory regulation or exceeds the permitted use, you will need to obtain permission directly from the copyright holder. To view a copy of this licence, visit http://creativecommons.org/licenses/by/4.0/. The Creative Commons Public Domain Dedication waiver (http://creativecommons.org/publicdomain/zero/1.0/) applies to the data made available in this article, unless otherwise stated in a credit line to the data.

recently encompassed by the term 'epitranscriptomics' [2]. Since epitranscriptomics is recognized as a different area of study that goes beyond the scope of this review, we will only focus on DNA methylation, histone modifications and chromatin remodeling as epigenetic regulatory mechanisms. Those mechanisms are briefly discussed below.

Epigenome functions are essential for normal gene expression, and their modifications affect primary cellular processes like proliferation, differentiation, and apoptosis. Even though its effect on human carcinogenesis is not entirely acknowledged, epigenetic dysfunction is a rising hallmark of malignancy. As epigenetic modifications are essential in the regulation of normal gene expression, epigenetic deregulation results in aberrant gene expression patterns which have been found to favor tumorigenesis, among others [1].

Whereas the role of epigenetic modifications in cancer research has been mainly focused on cancer cells, rising evidence indicates their contribution to the development of a favorable tumor microenvironment (TME), including their effect on surrounding cell phenotypes like fibroblasts, immune cells, endothelial and inflammatory cells, blood and lymphatic vascular networks, and the extracellular matrix (Table 1) [3]. Nevertheless, due to the extreme complexity of the variety of cells and their potential epigenetic modifications affecting tumorigenesis, this review will be focused on the epigenetic regulation of different immune cell types in the TME and their involvement in the generation of a cancer-prone TME.

We further discuss the inhibition of epigenetic modulators as therapeutic option to modify the immunosuppressive TME, and we provide an overview on immunotherapy and the potential of epigenetic biomarkers of response to this therapy. Finally, the application and success of immunotherapy as well as the inhibition of epigenetic processes involved in immune activation will be briefly discussed in the context of bladder cancer (BC).

## Epigenetic regulatory mechanisms

### DNA methylation

DNA methylation represents a process by which methyl groups are transferred onto the 5′ position of a cytosine molecule without altering the DNA sequence. Methylation commonly occurs on the cytosine of CpG sites, meaning that the cytosine molecule precedes a guanine. DNA regions with a higher density of these CpG sites (so-called CpG islands) have been found throughout the genome, mostly coinciding with gene regulatory regions. This way, methylation of CpG islands plays an important role in the regulation of normal gene expression (Fig. 1) [62, 63].

DNA methyltransferases (DNMTs) are the enzymes responsible for the control of DNA methylation patterns through maintenance DNA methylation and de novo DNA methylation. In general, DNMT1 is the enzyme responsible for maintenance of inherited DNA methylation, whereas DNMT3a and DNMT3b provide de novo DNA methylation. Nevertheless, DNMT3a and DNMT3b methyltransferases have been described to perform maintenance methylation as well, and DNMT1 has also been found to carry out de novo DNA methylation [63].

Alterations in DNA methylation status have been described in various diseases, including cancer. For example, gene silencing of tumor suppressor genes (TSGs) is the result of the hypermethylation of CpG islands in the promoter regions of those genes. TSGs are mainly involved in biological pathways like cell cycle control, DNA repair and apoptosis, and its silencing has been frequently found in tumorigenesis [64].

### Histone modifications

Chromatin structure changes as a result of dynamic processes involving post-translational modifications (PTMs) at the histone N-terminal tails. Various PTMs can be distinguished, including histone acetylation, methylation and phosphorylation as well as less known ubiquitylation, deamination and sumoylation, which affect chromatin packaging and availability to the gene transcription machinery (Fig. 1) [65]. Currently known histone PTMs have been extensively reviewed. Here, we briefly mention the three most common histone PTM activities.

Histone acetylation consists of the reversible addition of acetyl groups to the histone tail by histone acetyltransferases (HATs), which weakens the DNA-histone bonds and allows binding of transcription factors. Contrarily, histone deacetylases (HDACs) remove those acetyl groups, allowing for compact wrapping of the DNA around histones, disabling the access of other enzymes. Regarding histone methylation, the transfer of methyl groups is a reversible process regulated by histone methyltransferases and demethylases. The attachment of a methyl group to the histone tail may differentially affect gene expression depending on the specific residue modified. Likewise, the interaction between the DNA and histone tails is regulated by histone (de)phosphorylation processes [66].

### Chromatin remodeling

Changes in nucleosome position have also been found responsible for rearrangement of chromatin structure, a process known as chromatin remodeling. Nucleosomes, consisting of a histone core (H2A, H2B, H3 and H4) wrapped by an approximately 150-bp DNA sequence, can

**Table 1** Cell populations contributing to the development of a favorable tumor microenvironment

| TME components | Reported in various tumor types, including: | Characteristics controlled by epigenetic regulation | Contribution to favorable TME | References |
|---|---|---|---|---|
| Pro-tumor DCs | Bladder, Breast, Colon, Colorectal, Esophageal, Gastric, Glioma, Intestinal, Liver, Lung, Lymphomas, Osteosarcoma, Ovarian, Pancreas, Prostate | Enhanced production of pro-tumorigenic cytokine IL-6<br>Augmented secretion of immunosuppressive Galectin-1 | Tumor-infiltrating DCs show an immune-tolerant phenotype favoring tumor growth | [4–21] |
| Immunosuppressive MDSCs | Bladder, Breast, Colorectal, Head and Neck, Liver, Lung, Pancreas, Prostate, Renal | Expression of immunosuppressive factors S100A8, S100A9 and Arg1 | MDSCs promote immune suppression favoring tumor growth and metastasis | [16, 22–31] |
| TAMs | Bladder, Breast, Colon, Cervical, Gastric, Glioma, Lung, Lymphoma, Melanoma, Neuroblastoma, Ovarian, Pancreas, Prostate | Increased expression of Arg1<br>Activation of ALOX15<br>Enhanced expression of PPARγ<br>Decreased NFkB signaling and suppression of IL-1β expression | Immunosuppressive subsets of TAMs promote tumor growth | [16, 32–42] |
| TILs | Bladder, Brain, Breast, Colorectal, Gastric, Genitourinary, Glioblastoma, Glioma, Head and Neck, Liver, Lung, Melanoma, Meningioma, Ovarian, Pancreatic, Prostate, Renal | *Impaired TILs CD8 + infiltration*<br>Downregulation of CXCL9 and CXCL10 chemokine expression<br>Elevated levels of PD-1<br>*Exhausted CD8 + T cells*<br>Enhanced expression of CTLA4, PDCD1 and LAG3 | Impaired CD8 + T cell functions as well as T-cell exhaustion seem to play a major role in the generation of an immunosuppressive TME | [43–46] |
| Mature Tregs | Bladder, Breast, Colorectal, Glioblastoma, Lung, Lymphoma, Melanoma, Ovarian, Pancreas | Downregulation of genes involved in effector T-cell activation | Mature Tregs provide a tumor-supportive microenvironment | [16, 47–50] |
| NK cells | Breast, Colorectal, Gastric, Melanoma, Multiple myeloma, Pancreas, Renal | Decreased expression of activating NKG2D NK-cell receptor | Impaired NK-cell mediated anti-tumor immune response | [51–54] |
| Fibroblasts | | | Fibroblasts in the TME differentiate into cancer-associated fibroblasts (CAFs), representing one of the main components in the tumor stroma. The majority of the studies show pro-tumoral functions for CAFs, which include immune suppression, extracellular remodeling and angiogenesis | [55–57] |
| Endothelial cells | | | Angiogenesis refers to the de novo formation of blood vessels, a process essential for tumor growth. This blood vasculature consists of tumor endothelial cells (TECs), which line the insides of the blood vessels. Different characteristics between TECs and normal endothelium have been described | [58, 59] |
| Blood and lymphatic vascular networks | | | Blood and lymphatic vascular networks play a key role in supporting tumor growth and progression. They support oxygen supply and adequate nourishment to the tumor and provide a gateway for metastasizing tumor cells | [60] |

**Table 1** (continued)

| TME components | Reported in various tumor types, including: | Characteristics controlled by epigenetic regulation | Contribution to favorable TME | References |
|---|---|---|---|---|
| Extracellular matrix | | | The tumor extracellular matrix (ECM) differs greatly from the ECM in normal tissue, not only in amount of deposition but also in organization and composition. The tumor ECM is generally stiffer, a characteristic that has been associated with an increase in nuclear localization of transcription factors able to drive epithelial-mesenchymal-transition and, consequently, tumor metastasis | [61] |

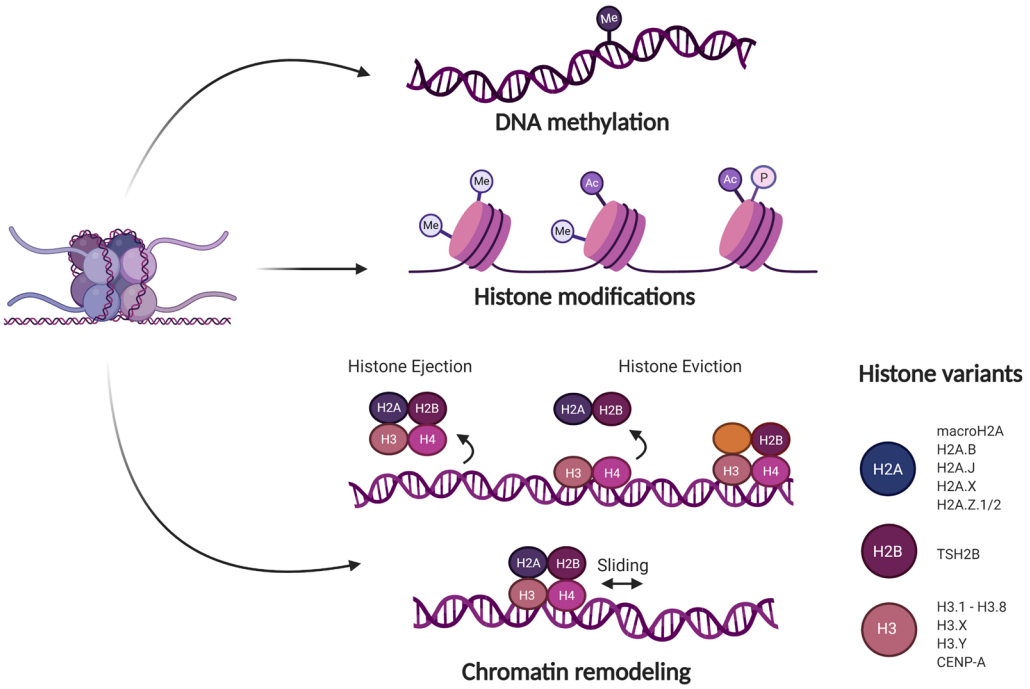


**Fig. 1** DNA methylation, histone modifications and chromatin remodeling as regulatory mechanisms of epigenetic gene regulation. DNA methylation represents a process by which methyl groups are transferred onto the 5′ position of a cytosine molecule, commonly in the context of CpG sites, without altering the DNA sequence. Histone modifications include post-translational modifications at the histone N-terminal tails, such as acetylation, methylation and phosphorylation, causing chromatin structure alterations. Changes in nucleosome position are also responsible for rearrangement of chromatin structure, a process known as chromatin remodeling. Nucleosomes can be affected in several ways, including nucleosome sliding, nucleosome ejection and histone eviction. Histone variants add further complexity to epigenetic regulation of the genome. Various histone variants are characterized for H2A, H2B and H3. All these mechanisms are highly interrelated and play an important role in the regulation of gene accessibility to the transcriptional machinery

be affected in several ways, including nucleosome sliding, nucleosome ejection and histone eviction. Nucleosome sliding represents the movement of the histone octamer across the DNA sequence, whereas nucleosome ejection implies the complete segregation of the histone core from the DNA. Histone eviction includes the disintegration of the core histone octamer trough removal or replacement of H2A–H2B dimers (Fig. 1) [67].

Since nucleosome sliding and ejection as well as removal of the H2A–H2B dimers result in DNA exposition and nucleosome destabilization, these processes play an important role in the regulation of gene accessibility to the transcriptional machinery.

### Histone variants

Histone variants add further complexity to epigenetic regulation of the genome. They represent a unique protein sequence compared to core histones and can be identified by a combination of variant-specific proteins and chromatin remodeling complexes which control their localization within the genome. Various histone variants are characterized for H2A (such as macroH2A, H2A.B, H2A.J, H2A.X and H2A.Z.1/2), H2B (including TSH2B) and H3 (like H3.1 till H3.8, H3.X, H3.Y and CENP-A), whereas no variants have been described for H4. Additionally, histone variants are subjected to post-translational modifications which elaborates the epigenetic control of gene expression (Fig. 1) [68, 69].

## Epigenetic regulation of immune cell function in TME

A favorable TME is characterized by immune tolerance. Cancer cells employ a variety of epigenetic regulated-immune escape mechanisms, including downregulation of tumor-associated antigens (TAAs), loss of antigen processing and presentation machinery (APM) as well as expression of a tumor-promoting balance in co-stimulatory and co-inhibitory molecules (also known as immune checkpoint receptors). Whereas these processes have been extensively studied and reviewed, epigenetic alterations affecting immune cell function in the TME represent a growing area of investigation. The epigenetic-induced immunosuppressive function of dendritic cells (DCs), myeloid-derived suppressor cells (MDSCs),

tumor-associated macrophages (TAMs), tumor-infiltrating lymphocytes (TILs), regulatory T cells (Tregs) and natural killer cells (NK cells) in the TME will be discussed below.

### Dendritic cells

DCs represent important antigen-presenting cells (APCs) that mediate antigen-specific anti-tumor immune responses mainly through the activation of T cells. Whereas these cells are normally able to capture TAAs expressed on cancer cells through accurate MHC expression and cross-present them to cytotoxic T cells (CTLs) by the expression of co-stimulatory molecules, resulting in tumor elimination, tumor-infiltrating DCs show an immune-tolerant phenotype favoring tumor growth [18]. Next to low MHC expression and repression of various co-stimulatory molecules in tumor-infiltrating DCs, epigenetic alterations affecting DC polarization and activity are suggested to impair an effective anti-tumor immune response.

For example, dynamic changes in the levels of chromatin regulator 'special AT-rich sequence binding 1 (SATB1)' are essential for the generation of inflammatory DCs and their anti-tumorigenic activity. SATB1 recruits chromatin remodeling complexes to anchored DNA regions, consisting of a characteristic 'ATC-sequence context' (well-mixed A's, T's and C's but not G's on a single strand), thereby controlling gene transcription over long-distance DNA sequences through the regulation of nucleosomal positioning and histone modification [70]. Additionally, the recruitment of HATs and HDACs directly to gene promoter regions has been reported [71]. A continuous increased expression of SATB1 has been described to convert inflammatory anti-tumor DCs into pro-tumor DCs by enhanced secretion of pro-tumorigenic cytokine IL-6 and immunosuppressive factor Galectin-1, activating immune-evasive pathways in these cells [7]. Accordingly, SATB1 has been found to be overexpressed in a wide range of tumors, including breast, lung, pancreas, colorectal, liver, bladder, prostate and ovarian cancer, and has been associated with tumor progression and poor prognosis [19]. Additionally, next to its role in the direct activation of *IL-6* transcription, Kruppel-like factor 4 (KLF4) modulates IL-6 production at the post-translational level through histone acetylation. Decreased expression of KLF4 has been described in many tumors, including esophageal, lung, gastric, intestinal, colon and prostate cancer, leading to altered production of cytokine IL-6 in DCs (Fig. 2, Table 1) [20, 21].

Taken together, increasing our knowledge on tumor-induced epigenetic modifications affecting DC polarization and activity might help modifying the TME to become more "receptive" to the development of an effective anti-tumor response.

### Myeloid-derived suppressor cells

MDSCs represent immature myeloid cells and are mainly characterized by their immunosuppressive function providing tumor immune evasion [27]. These cells are known to have a major impact on cancer progression as the TME has been found to support this cell population, promoting MDSC persistence, proliferation and function. Indeed, the presence of MDSCs has been associated with poor prognosis and reduced patients' survival in many cancer types, including head and neck, breast, lung, kidney and prostate [26, 27]. Several studies have suggested the role of epigenetic mechanisms in MDSC accumulation and functions.

For example, an elevated expression of signal transducer and activator of transcription 3 (STAT3) has been defined in several tumor types including lung, pancreas and renal cancer [28–31]. Overexpression of STAT3 can be the result of promoter silencing of DNMT3a and DNMT3b through hypermethylation, followed by promoter hypomethylation of the *STAT3* gene. Besides, Villagra et al. proposed HDAC11 as a transcriptional repressor of IL-10 (a STAT3-activating cytokine) through interaction with the IL-10 promoter at the chromatin level and indicated that elevated levels of STAT3 in APCs might be associated with the absence of HDAC11 [72]. More recently, HDAC11 has been described as an essential regulator of IL-10 levels in myeloid cells and its role in the MDSC expansion was demonstrated [73]. Moreover, Cheng et al. showed that HDAC6 has a regulatory function in STAT3 activation in the MDSC population. Surprisingly, HDAC6 seems to act as a transcriptional activator of *IL-10* expression [74]. Next to their possible individual implications, HDAC6 and HDAC11 have been reported to interact and be recruited together toward the *IL-10* promoter site where they control *IL-10* transcription and subsequent STAT3 expression [74]. Increased STAT3 expression leads to augmented expression of immunosuppressive factors S100A8 and Arginase 1 (Arg1) in MDSCs. Additionally, the induction of these proteins, together with the STAT3-mediated induction of S100A9 expression, has been shown to provide expansion, accumulation and recruitment of immunosuppressive MDSCs in TME (Fig. 2, Table 1) [29, 75].

As abovementioned, this MDSC population represents immature myeloid cells which fail to differentiate into macrophages and DCs. Several studies already described the accumulation of immature myeloid cells as a result of retinoblastoma gene (*Rb*) transcriptional silencing [76, 77]. Concordantly, Young et al. proposed that HDAC2 might be the epigenetic regulator provoking Rb

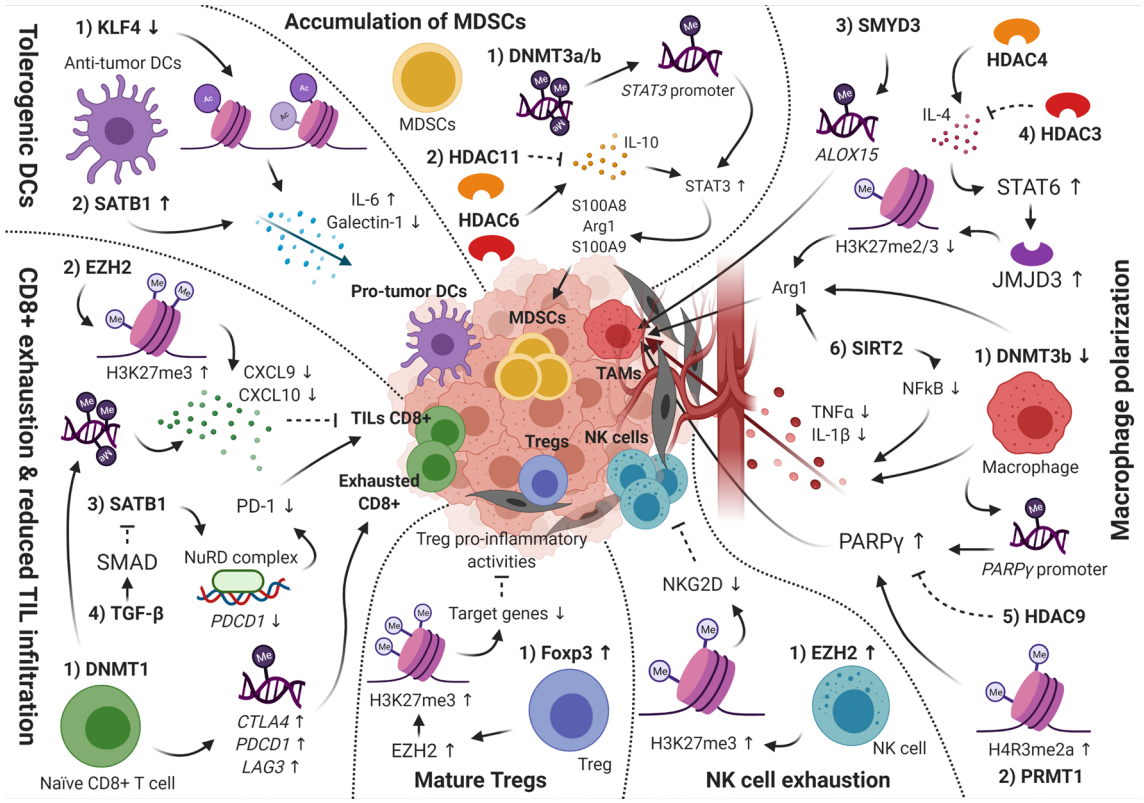


**Fig. 2** Epigenetic regulation of immune cells in the tumor microenvironment. Decreased KLF4 and increased SATB1 expression affect IL-6 (upregulation) and Galectin (downregulation) expression, remodeling anti-tumor DCs into pro-tumor DCs. MDSCs expansion, accumulation and recruitment are favored by STAT3-induced expression of immunosuppressive factors S100A8, Arg1 and S100A9. In this cell population, STAT3 expression is controlled by DNMTT3a/b, HDAC6 and HDAC11. Macrophages can convert into TAMs under the influence of multiple epigenetic factors, including DNMT3b, PRMT1, HDAC3/4, HDAC9 and SIRT2, favoring acquisition of the M2 phenotype through various pathways, such as increased PPARγ and Arg1 expression as well as downregulation of inflammatory factors TNF-α and IL-1β. SMYD3 activates M2 marker ALOX15. Impaired NK-cell anti-tumor cytotoxicity can be the result of increased EZH2 expression, which downregulates activating NK-cell receptor NKG2D through enhanced H3K27me3 levels. The same way, EZH2 also regulates inhibition of regulatory T-cell pro-inflammatory activities. Naïve CD8 + T-cells differentiate into TILs or exhausted CD8 + cells dependent on epigenetic profile. Whereas specific DNA methylation patterns of *CTLA4*, *PDCD1* and *LAG3* are identified in exhausted CD8 + T-cells, DNMT1 and EZH2 inhibit CD8 + TILs infiltration through downregulation of CXCL9 and CXCL10 chemokines. TGF-β and SATB1 affect TILs infiltration by controlling PD-1 expression. DCs, dendritic cells; MDSCs, myeloid-derived suppressor cells; TAMs, tumor-associated macrophages; NK, natural killer; Tregs, regulatory T-cells; TILs, tumor-infiltrating lymphocytes

transcriptional silencing in this cell population through its direct interaction with the *Rb1* gene promoter [78].

Taken together, the MDSC population represents a major barrier for immunotherapy. Accordingly, further research is needed to increase our knowledge on MDSCs in the TME and be able to improve the ability to revert their immunosuppressive function.

### Tumor-associated macrophages

TAMs represent the main component of the immune infiltrates in TME of solid tumors and have frequently been associated with worse prognosis [79]. By continuously sensing their surrounding environment, this cell population has refined regulatory epigenetic mechanisms to manage their polarization state. Depending on their polarization into classically activated (M1) or alternatively activated (M2) macrophages, they inhibit or promote tumor growth, respectively. Epigenetic modifications have been widely shown to be involved in macrophage differentiation, activation and survival [80].

Yang et al. indicated a significant role for DNMT3b in macrophage polarization. They showed that DNMT3b knockdown induces elevated expression of M2 macrophage markers, such as Arg1, as well as increased Arg1 function. In concordance with these results, Arg1 activity has been reported to define immunosuppressive subsets of TAMs. Additionally, DNMT3 knockdown resulted in significantly decreased expression of inflammatory genes,

such as *TNF-α* and *IL-1β*, emphasizing the importance of DNMT3b in the regulation of both macrophage differentiation and inflammation [81, 82]. Moreover, DNMT3b has been reported to methylate the peroxisome proliferator-activated receptor γ (PPARγ) promoter region.

Protein arginine methyltransferase 1 (PRMT1) has been reported as a positive regulator of PPARγ-dependent M2 polarization through methylation of the arginine located at residue 3 on the tail of histone 4 (H4R3me2a). Furthermore, Ishii et al. demonstrated that expression of M2 macrophage markers seems to be epigenetically controlled by convertible changes in H3K4 and H3K27 methylation [83]. Accordingly, H3K4 methyltransferase SET and MYND Domain 3 (SMYD3) has been shown to play a role in M2 differentiation. Kittan et al. [84] showed that the increased expression of SMYD3 is associated with the methylation and activation of the M2 marker arachidonate 15-lipoxygenase (ALOX15). The only histone demethylase recognized as a crucial regulator of M2 polarization is Jumonji domain-containing protein D3 (JMJD3), a H3K27 demethylase. IL-4-induced STAT6 activation leads to STAT6-mediated increased expression of JMJD3, provoking H3K27me2/3 demethylation and subsequent transcriptional activation of several M2 marker genes, including *Arg1* [83, 85]. IL-4 increased expression has been found in various tumor types, including breast, lung, pancreatic, colon, bladder and ovarian carcinomas [42].

Whereas the role of HATs in macrophage polarization remains unclear, the function of HDACs as epigenetic modifiers in the regulation of M2 differentiation and phenotypic control has been explored by various studies. Mullican et al. indicated that HDAC3 activity leads to suppressed IL-4 activity through deacetylation of histone tails at regulatory sequences. Together with the finding that HDAC3 knockdown resulted in decreased inflammatory gene expression, HDAC3 has been proposed to negatively regulate M2 polarization [86, 87]. HDAC9 has also been described as a negative regulator of M2 phenotype as HDAC9 deficiency results in PPARγ promoter acetylation and increased PPARγ expression levels, promoting M2 polarization and downregulating M1 phenotype inflammatory genes [88]. Contrarily, HDAC4 positively regulates the M2 phenotype through IL-4-activated HDAC4-induced STAT6 signaling and Arg1 expression [89]. Another HDAC, SIRT2, positively controls M2 polarization through its function in the expression of M2 macrophage markers, such as Arg1, and downregulation of M1 polarization by NFkB acetylation, provoking decreased NFkB signaling and suppression of IL-1β expression (Fig. 2, Table 1) [90].

Accordingly, targeting these epigenetic enzymes responsible for polarization of TAMs into M2 macrophages would prevent their tumor-supporting function. Nevertheless, it should be considered that these regulators disclose secondary functions and that histone-modifying enzymes also affect proteins other than histones.

#### Tumor-infiltrating lymphocytes

TILs represent the major component of the adaptive immune system in the TME and can be classified into two main categories: 1) CD4-expressing T cells (CD4 + T cells), which can differentiate into the T helper1 (Th1) or T helper2 (Th2) phenotype, and 2) CD8-expressing T cells (CD8 + T cells), which are able to eliminate tumor cells after differentiation into cytotoxic effector T lymphocytes.

Whereas the important role of CD8 + CTLs in anti-tumor immune response has been known for many years, the potential importance of CD4 + Th cells in the generation and maintenance of anti-tumor activity has only recently been reported [91]. Even though further research is needed to find out whether and, if so, how epigenetic mechanisms affect CD4 + cells in an immunosuppressive TME, DNA demethylation has been reported to play an important role in differentiation of CD4 + T cells toward Th1/Th2 lymphocytes [92].

Additionally, epigenetic modulation has been found to control rapid activation and differentiation of naïve CD8 + into CTLs upon antigen stimulation. For example, Peng et al. associated DNMT1-mediated DNA methylation and enhancer of zeste homolog 2 (EZH2)-mediated H3K27 trimethylation with impaired T-cell infiltration in the TME through downregulation of CXCL9 and CXCL10 chemokine expression [93]. Furthermore, Yang et al. reported that whole-genome methylation profiling showed a distinct methylome pattern for tumor-reactive CD8 + T cells compared to the naïve subtype. Moreover, specific DNA methylation patterns have been discovered in exhausted CD8 + T cells. *PDCD1* and *CTLA4* expression in exhausted CD8 + T cells has been found to be epigenetically controlled by DNA demethylation, and the *LAG3* gene has been found methylated in naïve cells but demethylated during the activation of naïve CD8 + T cells [94]. Ghoneim et al. [95] found that high programmed death 1 (PD-1)-expressing tumor-infiltrating CD8 + T cells in prostate cancer display exhaustion-associated DNA methylation patterns. Stephen et al. further showed that chromatin organizer Satb1 recruits the nucleosome remodeling deacetylase complex to regulatory regions of the *Pdcd1* gene, reducing PD-1 expression levels upon T-cell activation. Nevertheless, Satb1 is known to be downregulated by Smad proteins under the influence of TGF-β, an immunosuppressive cytokine found to play a relevant role in cancer, resulting in elevated PD-1 levels.

Accordingly, Satb1 prevents premature T-cell exhaustion by controlling PD-1 expression, a pathway that is altered in cancer, causing reduced anti-tumor activity [96, 97]. Another mechanism underlying tumor-specific T-cell dysfunction in tumor progression is represented by chromatin state dynamics. Philip et al. reported that naïve T cells differentiate into a dysfunctional but reprogrammable chromatin state upon tumor antigen recognition in premalignant lesions, which converts into a fixed non-reprogrammable dysfunctional state during tumor progression. The presence of surface markers CD101 and CD38 has been associated with reduced reprogrammability of high PD-1-expressing tumor-infiltrating CD8 + T cells, a finding with important clinical relevance as these markers can be used to discriminate reprogrammable from non-reprogrammable PD-1 high T cells within the heterogeneous TIL populations [98]. This mechanism might explain why certain patients do not respond to therapies based on immune-checkpoint blockade as well as it provides new insights in possible strategies to revert non-reprogrammable PD-1 high T cells into tumor-reactive CD8 + T cells (Fig. 2, Table 1).

Taken together, impaired CD8 + T cell functions seem to play a major role in the generation of an immunosuppressive TME. Importantly, the prevention of T-cell exhaustion might represent a potential strategy to reverse a TIL-mediated immunosuppressive TME.

#### Regulatory T cells

Tregs represent a functionally different T cell population which is essential for the maintenance of homeostasis and immune tolerance. Accordingly, mature Tregs provide a tumor-supportive microenvironment [47]. Various studies have reported a key role for Foxp3 in the development of these cells as well as their function, and epigenetic regulation of Tregs through Foxp3 has been emphasized by recent studies [99, 100].

Moreover, epigenetic modifications controlling Treg development and function have been found to play an important role in the establishment of an immunosuppressive TME. Ohkura et al. reported that Treg maturation involves the generation of genome-wide CpG DNA hypomethylation pattern, needed for Treg-specific gene expression and immunosuppressive activity [101]. Besides, Foxp3 seems to exert an EZH2-mediated repressive role upon CD28-mediated Treg activation as target genes show elevated H2K27me3 levels. As CD28 not only provides a key role in the stimulation of Tregs, but also in effector T-cell (CD4+/CD8+) activation, this suppressive role of Foxp3 might be essential to preserve the Treg-specific gene expression profile upon T cell stimulation through downregulation of genes involved in the effector T-cell activation [102]. Indeed, Wang et al. showed that inhibition of EZH2 resulted in Treg-mediated pro-inflammatory activities in the TME, supporting the generation of an effector T-cell-mediated anti-tumor immune response (Fig. 2, Table 1) [103].

Taken together, targeting the maturation of functional Tregs might be a potential strategy to convert an immunosuppressive TME into a microenvironment able to provide anti-tumor activity.

#### Natural killer cells

The NK cell population forms part of the innate immune system and is able to control tumor growth by their ability to recognize and eliminate tumor cells. Epigenetic modification has been reported to play an key role in the NK cell maturation, differentiation and activation [104]. Regulation of the effector function of this cell population mainly depends on the balance between inhibiting and activating receptors present on NK cell surface, the activation status of which seems to be epigenetically modulated, as well. Accordingly, rising evidence indicates the involvement of epigenetic processes in impairing NK-cell mediated anti-tumor immune response.

An impaired NK-cell-mediated anti-tumor immune response is highly associated with NK-cell exhaustion because of diminished expression of activating receptors and increased expression of inhibitory receptors, among others. Specific activating NK-cell receptors include NKG2D, NKp30, NKp44, NKp46 and DNAM-1/CD226, whereas inhibitory receptors are represented by PD-1, TIM-3, TIGIT and CD94-NKG2A. Fernandez-Sanchez et al. reported the involvement of DNA methylation and histone acetylation in the regulation of NKG2D levels, with *NKG2D* gene demethylation and H3K9 acetylation providing *NKG2D* expression [105]. Nevertheless, whether reduced expression of this receptor is due to *NKG2D* hypermethylation remains unknown. Additionally, Ogbomo et al. proposed that the regulation of NKp30 and NKp46 expression levels is controlled by histone acetylation [106]. Using an HDAC inhibitor (HDACi), they showed that the suppression of NK-cell activity is caused by decreased expression of NKp30 and NKp46, but is independent of activating NKG2D, NKp44 and DNAM-1 expression levels as well as inhibitory *NKG2A* expression. Finally, Yin et al. revealed that enhanced levels of the activating NKG2D receptor are associated with elevated NK cell expansion and cytotoxicity against the tumor. Inhibition of EZH2 activity has been associated with decreased H3K27me3 levels, providing increased expression of the NKG2D receptor (Fig. 2, Table 1) [107, 108].

Although epigenetic modifications affecting NK cell development and function are widely examined, further studies are needed to increase our knowledge on the

epigenetic regulation of NK cells and the potential of epigenetic enzymes/markers as therapeutic targets.

## Inhibition of epigenetic modulators as therapeutic option to modify the immunosuppressive TME

A favorable TME, created by tumor cells affecting different immune cell populations, forms a major barrier for cancer therapy. Nevertheless, the study into epigenetic mechanisms underlying the generation of this immunosuppressive TME currently represents subject of utmost interest. As previously stated, a variety of epigenetic modifications affects the phenotypes of diverse immune cell populations in the TME to become immunosuppressive. Accordingly, modifying the TME to become more "receptive" to the development of an effective anti-tumor response could be achieved by molecular re-wiring using pharmacologic modulators of epigenetic enzymes. In this regard, when considering the use of compounds targeting the epigenetic machinery, it is worth considering that these compounds not only affect tumor cells, but also TME cells. Accordingly, a proper selection of inhibitors could become a two-edge sword to tackle tumors.

For example, SATB1 represents an attractive therapeutic target as it modifies different immune cell populations under tumor's influence, including DCs and CTLs. The statins fluvastatin and simvastatin have been found to suppress SATB1 expression, probably acting at the post-translational level [109, 110]. Additionally, in vivo silencing of *Satb1* expression in tumor-associated DCs was found to diminish immunosuppression in the TME, boost T-cell mediated anti-tumor activity and delay tumor progression [7]. In the context of immunotherapy, Satb1 has been described as a possible TAA that can be recognized by CD8 + T cells. Accordingly, Wang et al. proposed that Satb1-derived epitope might be used as immune target for cancer vaccine generation [111].

Furthermore, the importance of HDAC activation and IL-6 signaling in controlling the immunosuppressive function of MDSCs as well as its recruitment to the TME has been reported by Nair et al. [26]. Various studies demonstrated the potential of entinostat, a class I HDACi, as therapeutic compound to modulate the immunosuppressive TME through inhibition of MDSC activity. Besides, the application of entinostat not only resulted in decreased MDSC function, but also augmented the effect of checkpoint inhibitor treatment [112–115]. Kim et al. reported that entinostat reduces the MDSC population and the combination of entinostat with PD-1 and cytotoxic T-lymphocyte-associated protein 4 (CTLA-4) antibodies resulted in an elimination of approximately 80% of the tumor, whereas the use of immune checkpoint inhibitors against PD-1 and CTLA-4 alone did not provide an anti-tumor immune response [113]. The potential role of HDACi in priming the TME for enhanced response to immunotherapy has been further emphasized by Briere et al., who obtained similar results using a class I/IV HDACi (mocetinostat) in combination with anti-programmed death-ligand 1 (PD-L1) antibody [114]. Additionally, Orillion et al. observed reduced macrophage population in the TME after entinostat treatment [112]. Other potential therapeutic targets to suppress MDSCs function would be HDAC2, HDAC6 and HDAC11. Nevertheless, further studies are needed to investigate the therapeutic potential of their corresponding inhibitors [78, 115, 116].

Regarding the polarization of TAMs into M2 macrophages, targeting the enzymes responsible for the acquisition of M2 phenotype would attenuate their tumor-promoting function. Accordingly, Tikhanovich et al. reported the therapeutic potential of AMI-1, a PRMT1 inhibitor, inhibiting M2 processes [117]. Additionally, GSK-J4 might diminish the immunosuppressive, tumor-supporting function of M2 macrophages through KDM6B (a lysine-specific demethylase that demethylates H3K27me2 or H3K27me3) inhibition. Nevertheless, in concordance with the essential role of KDM6B in both M1 and M2 polarization, GSK-J4 has also been found to inhibit the expression of TNF and other M1 inflammatory cytokines [118, 119]. Noteworthy is the effect of histone-modifying enzymes on proteins other than histones and the importance of non-histone protein modifications in macrophage-polarizing process. Moreover, macrophage polarization is a complex dynamic process in which most epigenetic enzymes are neither involved exclusively in the polarization toward M1 or M2 phenotype nor do they all have opposing roles in M1 versus M2 phenotype acquisition [120]. Accordingly, the discovery of therapeutic epigenetic targets in this cell population is very challenging.

Another attractive therapeutic target is EZH2, responsible for the immunosuppressive phenotype of several immune cell populations in the TME, including TILs, Tregs and NK cells. This epigenetic regulator has already been extensively studied for its potential as therapeutic target to convert the immunosuppressive TME into an immune-promoting microenvironment. Various studies described an enhanced effector-T cell infiltration and cytotoxic activation in the TME upon EZH2 inhibition as well as functional alterations of the Treg population resulting in Treg-mediated pro-inflammatory activities [93, 103, 121, 122]. Additionally, targeting EZH2 has been reported as an attractive strategy to combine with immunotherapy, as it might overcome resistance to immune checkpoint therapies, including CTLA-4, PD-1 and PD-L1 [93, 121–123]. Among the EZH2-inhibiting compounds, small molecule inhibitors of EZH2,

GSK-126, PF-06821497, MAK683, CPI-0209, CPI-1205 and DS-3201 have entered into clinical trials, although none of these has been approved for cancer treatment, yet [122]. Tazemetostat, a selective inhibitor of EZH2, has been approved by the Food and Drug Administration (FDA) in 2020.

Another relevant aspect is the profound interaction between the different immune cell populations in immune response regulation. Therefore, it is important to take into account that epigenetic reprogramming of a certain immunosuppressive immune cell population might positively co-opt other immune cell populations to provoke an effective anti-tumor immune response. One example is the Treg-mediated pro-inflammatory function upon EZH2 inhibition causing increased effector-T cell infiltration and activity. Furthermore, MDSCs play a central role in the immunosuppressive, tumor-promoting TME and have been found to interact with many of the other immune cell populations. Accordingly, epigenetic targeting of this cell type might be sufficient to modify the TME to become more "receptive" to the development of an effective anti-tumor response.

## Immunotherapy—an overview

The immune system plays a critical role in cancer development and progression by both eliminating cancer cells and determining tumor immunogenicity [124]. Thus, cancer immunoediting helps to understand how tumors escape the immune system by dividing the process in three distinct phases: "elimination," "equilibrium" and "escape." At first, when cancer cells are present, the immune system can recognize these and eliminate them. However, when not all cancer cells are eradicated in this process and an equilibrium is reached, the adaptive immune system impedes tumor's growth associated with a dormancy state and high genomic instability. T cells, IL-12 and interferon (IFN)-γ are needed to maintain tumor dormancy [125, 126]. Subsequently, cancer cells escape from the immune system by expressing suppressive effects and losing target antigen expression. At this stage, tumor immune escape occurs, since the adaptive immune system fails to recognize cancer cells, which became resistant to immune effector mechanisms and induced an immunosuppressive state [127].

Immune responses are regulated by an interplay of costimulatory and inhibitory signals that balance the immune response and self-tolerance [128]. Immune checkpoint inhibitors are essential as negative signals to stop immune response and impede autoimmunity [129]. PD-1 is expressed in T lymphocytes and prevents the activation of these cells by binding to its ligands PD-L1 and PD-L2 [130]. Additionally, cytotoxic T lymphocyte-associated antigen 4 (CTLA-4) leads to suppression of T-cells activation by competing with the costimulatory signal CD28 for binding to B7-1 and B7-2, attenuating the activation signals of CD28 [131, 132]. Interestingly, PD-L1 is overexpressed in cancer cells, facilitating cancer cells to escape immune surveillance by T cells [133].

Checkpoint inhibitor immunotherapies consist of monoclonal antibodies that target CTLA-4 or the programmed cell death protein 1 pathway (PD-L1, PD-1) [133]. When the antibodies bind to PD-L1/PD-1 or CTLA-4, the inhibitory effect is canceled and an immunological response against cancer cells starts by activation of tumor-reactive T cells [134]. Of note, several clinical trials have demonstrated increased efficacy of combining anti PD-L1/PD1 and anti-CTLA4, although with increased risk of adverse reactions. The use of immune checkpoint inhibitors as cancer therapy was firstly approved for treatment of metastatic melanoma. Since then, several antibodies have been approved for treatment of non-small cell lung cancer, head and neck squamous cell carcinoma, hepatocellular carcinoma and BC [134].

A significant subset of cancer patients does not respond or respond poorly to immune checkpoint blockage treatments [135]. This can be a consequence of primary resistance that occurs prior to treatment, associated with a reduction of antigen expression and changes in metabolic pathways or through acquired resistance during the course of the treatment [136]. The one and foremost biomarker used for prediction of response to PD-L1/PD-1 blockade is PD-L1 expression [137]. It seems to be a biomarker of aggressive disease and it might also be considered a prognostic biomarker. However, the evaluation of PD-L1 as a single biomarker across clinical trials was shown to be heterogeneous [138]. Several reasons can be appointed for the presence of this heterogeneity: (1) clinical trials used different PD-L1 immunohistochemistry scoring assays [137]; (2) the scoring compartment differs for each specific therapy, namely pembrolizumab and nivolumab use PD-L1 tumor cell expression, whereas atezolizumab uses PD-L1 immune cell expression; (3) intratumoral heterogeneity; and (4) the sample available may not represent the full intratumoral heterogeneity [139]. All these data indicate that PD-L1 expression as a single biomarker is probably not adequate to accurately predict immunotherapy response and more reliable biomarkers could help to better predict and improve patient selection for these therapies [139].

Other approaches have been used to try to predict immunotherapy response including tumor mutational burden, tumor mismatch-repair deficiency, grade of TILs [140–142], among others, depending on tumor type. For example, the TCGA-based molecular subtypes in BC have been associated with response to immune

checkpoint blockage. Specifically, the neuronal subtype seems to display a better response to immunotherapy [143]. However, the criteria to define BC subtypes have to be uniformed before it may be considered a possible biomarker for immunotherapy [144]. Moreover, tumor mutational burden has been proposed to predict response to immunotherapy [145]. With a high rate of mutations, novel antigens emerge regularly so it could potentiate the use of immunotherapy. Nonetheless, some patients with low mutational burden endure response to immunotherapy, which demonstrates that criteria to define the tumor mutational burden have to be clarified [145]. Interestingly, pembrolizumab was approved for patients with microsatellite instability and mismatch repair-deficient malignancies showing progression after failure of other approved treatments [142]. Finally, immune expression profiling has the potential to correctly identify "hot" or "cold" tumors by assessing levels of chemokines, cytokines and cell surface proteins reflecting the inflammatory status [146]. Also, it can take into account the several cell types present in the TME, which can be useful in defining immunotherapy response [147]. Examples include IFN-γ, CXCL9 and CXLC10 whose expression correlates with response to immunotherapy [146, 148].

Epigenetic mechanisms are known to regulate several aspects related to immune regulation and actions [149]. 5-Azacytidine (5-aza), a demethylating agent, was shown to upregulate innate and adaptative immune-related genes, specifically to immune invasion, such as PD-L1 at both transcript and protein levels without altering CD80 and CD86. Furthermore, genes related to antigen presentation including HLA class I, *B2M*, *CD58*, *TAP1*, *PMSB9* and *PSMB8* were upregulated after 5-aza treatment [150]. Treatment of leukemia cells with decitabine (DAC) translated into upregulation of PD-L1, PD-L2, PD-1 and CTLA-4 in these cells [151]. This topic is thoroughly discussed in a recently published review [152]. A DNA methylation-based profile—EPIMMUNE signature—of stage IV non-small cell lung cancer patients treated with anti-PD-1 therapies associated with improved progression-free and overall survival. EPIMMUNE-negative tumors disclosed a TME enriched in TAMs, cancer-associated fibroblasts and neutrophils. Moreover, unmethylated *FOXP1* associated with better progression-free and overall survival [153]. Promoter methylation of *RAD51B* seems to associate with PD-L1 expression in lung cancer patients, with high levels of *RAD51B* methylation associating with lower risk of disease progression. Remarkably, combining *RAD51B* methylation and PD-L1 improved sensitivity to predict response to anti-PD-1 blockade and associated with a lower risk of death [154].

Although several studies showed that modulating epigenetic marks can improve therapeutic response to immune checkpoint inhibitors, the search for biomarkers is ongoing and needs further exploitation (Additional file 1: Table 1).

## Epidrugs in cancer

Epigenetic mechanisms including DNA methylation and histone post-translational modifications represent an alluring target for cancer therapy since they are reversible alterations important for tumor cells' development [155, 156]. Therefore, a class of compounds that came to be known as "epidrugs" were developed targeting these alterations (Table 2) [157]. Currently, DNMT and HDAC inhibitors are the most used epidrugs for cancer treatment in both clinic and clinical trials, namely in combination with chemo- and immunotherapy (Table 2).

DNMT inhibitors are classified into two main groups: nucleoside and non-nucleoside analogues (Table 2) [158]. 5-aza was the first compound developed and approved for clinical usage for DNMT inhibition. Indeed, 5-aza and decitabine (5-aza-2′-deoxycytidine) are already approved for treatment of hematological malignancies including acute myeloid leukemia (AML), myelodysplastic syndrome and chronic myelomonocytic leukemia (CMML) by European Medicines Agency (EMA) and FDA (Table 3) [157, 159, 160]. Nucleoside analogues include analogues of cytosine that are integrated in DNA and lead to the formation of a covalent bond with the DNMT, which results in its degradation and DNA methylation inhibition [157, 161]. Both are nucleoside analogues characterized by replacing cytosine during DNA replication, which translates in the formation of a covalent bond when DNMTs exert their function, resulting in DNMTs' inhibition and further degradation [161–163]. Despite both showing to have anti-tumoral effects, namely by inducing apoptosis, cell and re-expression of tumor suppressor genes [164, 165], 5-aza and DAC display low bioavailability and a limited half-life, which hinders their wide implementation in clinical practice [161, 166]. More stable compounds with the same effect and mechanism of action have been described in the past years including zebularine, 5′-fluoro-2′-deoxycytidine (FdCyd), guadecitabine and RX-3117. For example, FdCyd, a fluoropyrimidine analogue, is less toxic and more stable when compared to 5-aza and DAC (77). Furthermore, FdCyd showed to stop cell arrest at G2/M in HCT116 cells though the DNA damage response pathway [167]. RX-3117 (fluorocyclopentenylcytosine) is a recent cytidine analogue with a modified ribose molecule being activated specifically by uridine-cytidine kinase 2 (UCK2), leading to DNA damage and lower DNA methylation levels though DNMT1 inhibition [168]. Another

**Table 2** Epidrugs approved and in clinical trial for cancer treatment, with respective effects and drug category

| Drug | Approved | Clinical trial | Effects |
|---|---|---|---|
| Azacitidine Vidaza® | High-risk myelodysplastic syndromes<br>Chronic Myelomonocytic Leukemia<br>Acute Myeloid Leukemia | Pancreatic, colorectal, prostate, esophageal, breast, non-small cell lung cancer, thyroid, ovarian, nasopharyngeal and bladder cancer, hematological malignancies sarcoma, melanoma, germ cell tumors and renal cell carcinomas | Nucleoside DNMT inhibitor |
| Decitabine Dacogen® | High-risk myelodysplastic syndromes<br>Chronic Myelomonocytic Leukemia<br>Acute Myeloid Leukemia | Ovary, head and neck, colorectal, breast, esophageal, non-small cell lung, prostate, thyroid cancers, B cell lymphoma, glioma and medulloblastoma | Nucleoside DNMT inhibitor |
| 5′-Fluoro-2′-deoxycytidine (FdCyd) | – | Head and neck, lung, urinary bladder, breast cancer and acute myeloid leukemia | Nucleoside DNMT inhibitor |
| Guadecitabine | – | Kidney, lung, ovarian, prostate, colorectal, gallbladder, pancreatic, urothelial cancer, extrahepatic bile duct adenocarcinoma, biliary type, testicular germ cell tumors, chondrosarcoma, melanoma, acute myeloid leukemia and myelodysplastic syndrome | Nucleoside DNMT inhibitor |
| RX-3117 (fluorocyclopentenylcytosine) | – | Pancreatic and bladder cancer | Nucleoside DNMT inhibitor |
| Genistein | – | Breast, prostate, colorectal, lung, pancreatic, bladder, kidney, endometrial cancer and melanoma | Isoflavone non-nucleoside DNMT inhibitor |
| Curcumin | – | Prostate, colorectal, breast, lung, head and neck and cervical cancer | Natural phenol non-nucleoside DNMT inhibitor |
| Hydralazine | – | Ovarian, cervical, lung and breast cancer | Repurposed drug non-nucleoside DNMT inhibitor |
| Belinostat Beleodaq® | Peripheral T-cell Lymphoma | Lung, breast, ovary, hematological malignancies, bladder, liver cancer and chondrosarcoma | Hydroxamic acid pan-HDAC inhibitor |
| Givinostat | – | Chronic Myeloproliferative Neoplasms Polycythemia Vera | Hydroxamic acid pan-HDAC inhibitor |
| Panobinostat Farydak® | Multiple Myeloma | Breast, lung, pancreatic, prostate, colorectal, head and neck, esophageal, neuroendocrine, renal, thyroid, brain cancer, hematologic neoplasms and melanoma | Hydroxamic acid pan-HDAC inhibitor |
| Trichostatin A | – | Hematological malignancies | Hydroxamic acid pan-HDAC inhibitor |
| Vorinostat Zolinza® | Cutaneous T cell Lymphoma | Breast, ovarian, pancreatic, lung, colorectal, gastric, liver, prostate, renal, bladder brain cancer, melanoma and hematological malignancies | Hydroxamic acid pan-HDAC inhibitor |
| Entinostat | – | Breast, colorectal, ovarian, neuroendocrine, lung, prostate, renal, pancreatic, endometrial cancer, hematological malignancies and cholangiocarcinoma | Benzamide class I HDAC inhibitor |
| Romidepsin Istodax® | Cutaneous T-cell lymphoma | Lung, breast, pancreatic, colorectal, thyroid, bladder, ovarian cancer, glioma and hematological malignancies | Benzamide class I HDAC inhibitor |

**Table 2** (continued)

| Drug | Approved | Clinical trial | Effects |
|---|---|---|---|
| Valproic acid | – | Cervical, brain, lung. breast, pancreatic, prostate, bladder, thyroid, head and neck cancer and hematological malignancies | Short-chain and aromatic fatty acids pan-HDAC inhibitor |
| Abexinostat | – | Breast cancer, renal cell carcinoma, sarcoma, melanoma and hematologic malignancies | Hydroxamic acid pan-HDAC inhibitor |
| Tazemetostat Tazverik® | Advanced epithelioid sarcoma Follicular lymphoma | Prostate, ovarian, endometrial, head and neck cancer, melanoma, hematological malignancies, urothelial carcinoma and malignant mesothelioma | EZH2 inhibitor |
| Domatinostat | – | Melanoma and Merkel cell carcinoma | Benzamide class I HDAC inhibitor |

compound that shows great stability, including being possible to administer orally, is zebularine [169], which showed to have an specific effect on cancer cells and not fibroblasts [170, 171]. However, since it showed great toxicity in primates, it was not continued for clinical trials (Table 3) [172, 173]. Guadecitabine is a CpG dinucleotide analogue hypomethylating agent [174] with proven antitumoral activity, such as in combination with cisplatin in platinum-refractory germ cell tumors [175].

Another heterogeneous group of compounds with DNMT inhibition activity is the non-nucleoside analogs, which inhibit DNMTs independently from DNA incorporation (Table 2) [176]. These include natural compounds, DNA binders, SAM competitors and repurposed drugs [176, 177]. Regarding natural compounds, molecules such as genistein, the natural polyphenol epigallocatechin-3-gallate (EGCG) and curcumin that displays anti-inflammatory and anti-oxidant properties showed to inhibit DNA methylation, translating in anti-tumoral activity [158, 178–180]. 3-Halo-3-nitroflavanones, a novel class of DNMT inhibitors described recently, showed anti-tumoral activity associated with higher stability and low cytotoxicity than the most used DNMT inhibitors [181]. Interestingly, a compound from this family MLo1302 caused a decrease in cell viability, namely in cisplatin-resistant cell lines, pluripotency markers and an activation of apoptosis and cell cycle arrest in germ cell tumors cell lines [182]. RG108 is a SAM competitor that binds to the catalytic pockets of DNMTs, forming covalent bonds and inhibiting the enzyme action [183]. Treatment with RG108 caused radiosensitivity of esophageal cancer cells, enhancing apoptosis and G2/M phase arrest by radiation [184]. SGI-1027, a quinolone-based molecule which binds to both DNMT3a and DNMT1 [185], combined with AH057 (JAK inhibitor) increased cervical cancer cells apoptotic cell death and cell-cycle arrest [186]. Furthermore, MG98 is a second-generation 20-nucleotide antisense oligonucleotide that binds specifically to DNMT1 mRNA, decreasing DNMT1 levels [187].

Selected repurposed drugs, designed for a specific treatment that were found to have other therapeutic targets, also showed effect against DNMTs [176, 177]. For example, procaine and procainamide, approved as anesthetic and anti-arrhythmic drugs, respectively, bind to the catalytic center of DNMTs, which translated in a decrease in DNA methylation levels [188, 189]. The arterial vasodilator hydralazine also leads to the loss of promoter hypermethylation of TSGs in cancer cell lines and primary tumors [190, 191]. In this line, the antibiotic nanaomycin A also causes the same effects, being selective for DNMT3b [192].

HDAC inhibitors can be classified according to chemical group as hydroxamic acids, short-chain and aromatic fatty acids, benzamides and cyclic peptides (Table 2). The hydroxamic acids and cycle peptides constitute the most potent inhibitors, with $IC_{50}$ in the low micro- or nanomolar range, while short-chain fatty acids require doses in the millimolar range [193].

Hydroxamic acids include belinostat (approved for peripheral T-cell lymphoma), givinostat, panobinostat, trichostatin A and vorinostat, all pan-HDAC inhibitors. Vorinostat or suberanilohydroxamic acid (SAHA) was the first HDAC inhibitor to be approved for the treatment of advanced cutaneous T-cell lymphoma, and it shows several anti-tumor effects in several hematological and solid tumors in vitro and in vivo (Table 3) [194]. It inhibits class I and II HDACs by binding to the catalytic domain of the enzymes [195]. Similar to vorinostat, trichostatin A (TSA), also a class I and II inhibitor, acts as a non-competitive inhibitor of HDAC by mimicking the lysin substrate as a chelating agent to the zinc atom in the

**Table 3** Major clinical trials comprising epidrugs and immunotherapy for cancer treatment

| Clinical trial | Phase | State | Cancer | Combination | Dates |
|---|---|---|---|---|---|
| NCT01928576 | II | Recruiting | Non-small cell lung cancer | Nivolumab<br>Entinostat<br>Azacitidine | 2013-estimated end 2022 |
| NCT02260440 | II | Completed | Metastatic colorectal cancer | Pembrolizumab<br>Azacitidine | 2015–2017 |
| NCT02546986 | II | Active, not recruiting | Non-small cell lung carcinoma | CC-486<br>Pembrolizumab | 2015-estimated end 2021 |
| NCT02453620 | I | Active, not recruiting | Breast Cancer | Ipilimumab<br>Nivolumab<br>Entinostat | 2015-estimated end 2021 |
| NCT02961101 | I/II | Recruiting | Non-Hodgkin lymphoma, Hodgkin lymphoma, gastrointestinal cancers, hepatocellular carcinoma, breast cancer, ovarian cancer, lung cancer, renal-cell cancer, pancreatic cancer and bile duct cancer | Anti-PD-1 antibody<br>Decitabine<br>Chemotherapy | 2016–2020 |
| NCT02890069 | I | Recruiting | Colorectal cancer<br>Non-small cell lung adenocarcinoma<br>Triple-negative breast cancer<br>Renal cell carcinoma | PDR001 (Anti-PD-1 antibody)<br>Everolimus<br>Panobinostat | 2016-estimated end 2021 |
| NCT02619253 | I/Ib | Active, not recruiting | Renal cell carcinoma<br>Urinary bladder neoplasms | Pembrolizumab<br>Vorinostat | 2016-estimated end 2022 |
| NCT02512172 | I | Active, not recruiting | Colorectal cancer | CC-486 (Oral 5-Aza)<br>Romidepsin<br>MK–3475 (Anti-PD-1 antibody) | 2016-estimated end 2022 |
| NCT02811497 | II | Active, not recruiting | Microsatellite stable colorectal carcinoma<br>Platinum-resistant epithelial ovarian cancer type II<br>Estrogen receptor-positive and HER2-negative breast cancer | Durvalumab<br>Azacitidine | 2016-estimated end 2022 |
| NCT02957968 | II | Recruiting | Breast cancer | Decitabine<br>Pembrolizumab<br>Doxorubicin<br>Cyclophosphamide<br>Paclitaxel<br>Carboplatin | 2016-estimated end 2023 |
| NCT02638090 | I/II | Recruiting | Lung cancer | Vorinostat<br>Pembrolizumab | 2016-estimated end 2023 |
| NCT02959437 | I/II | Completed | Advanced or metastatic solid tumors | Azacitidine<br>Pembrolizumab<br>Epacadostat<br>INCB057643 (BET inhibitor)<br>INCB059872<br>(LSD1 inhibitor) | 2017–2020 |
| NCT03308396 | Ib/II | Active, not recruiting | Advanced kidney cancer<br>Kidney cancer<br>Clear cell renal cell carcinoma | Durvalumab<br>Guadecitabine | 2017-estimated end 2021 |
| NCT03206047 | I/II | Active, not recruiting | Platinum-resistant fallopian tube carcinoma<br>Platinum-resistant ovarian carcinoma<br>Platinum-resistant primary peritoneal carcinoma<br>Recurrent fallopian tube carcinoma<br>Recurrent ovarian carcinoma<br>Recurrent primary peritoneal carcinoma | Atezolizumab<br>Guadecitabine | 2017-estimated end 2021 |
| NCT03264404 | II | Recruiting | Pancreas cancer | Pembrolizumab<br>Azacitidine | 2017-estimated end 2021 |
| NCT03179943 | II | Active, not recruiting | Urothelial carcinoma | Atezolizumab<br>Guadecitabine | 2017-estimated end 2022 |
| NCT03019003 | I/II | Recruiting | Head and neck cancer | Durvalumab<br>Oral Decitabine | 2017-estimated end 2024 |

**Table 3** (continued)

| Clinical trial | Phase | State | Cancer | Combination | Dates |
|---|---|---|---|---|---|
| NCT02816021 | II | Recruiting | Melanoma and other malignant neoplasms of skin<br>Metastatic melanoma | Pembrolizumab<br>Azacitidine | 2017-estimated end 2026 |
| NCT03590054 | I | Recruiting | Melanoma<br>Metastatic head and neck squamous cell carcinoma<br>Urothelial carcinoma<br>Non-small cell lung carcinoma | Pembrolizumab<br>Abexinostat | 2018-estimated end 2022 |
| NCT03426891 | I | Recruiting | Glioblastoma<br>Brain tumor | Pembrolizumab<br>Vorinostat<br>Temozolomide | 2018-estimated end 2022 |
| NCT03233724 | I/II | Recruiting | Non-small cell lung Cancer<br>Esophageal carcinoma<br>Malignant pleural mesotheliomas | Pembrolizumab<br>Decitabine<br>Tetrahydrouridine (THU) | 2018-estimated end 2026 |
| NCT03854474 | I/II | Recruiting | Locally and metastatic urothelial carcinoma | Pembrolizumab<br>Tazemetostat | 2019-estimated end 2021 |
| NCT03812796 | II | Recruiting | Gastrointestinal cancer | Domatinostat<br>Avelumab | 2019-estimated end 2021 |
| NCT03765229 | II | Recruiting | Melanoma | Pembrolizumab<br>Entinostat | 2019-estimated end 2023 |
| NCT03978624 | II | Recruiting | Bladder cancer | Pembrolizumab<br>Entinostat | 2020-estimated end 2022 |
| NCT04357873 | II | Recruiting | Squamous cell lung cancer<br>Vulvar cancer<br>Penile cancer<br>Cervix cancer<br>Head and neck squamous cell carcinoma<br>Anal cancer | Pembrolizumab<br>Vorinostat | 2020-estimated end 2024 |
| NCT04624113 | I/II | Not yet recruiting | Head and neck squamous cell carcinoma | Pembrolizumab<br>Tazemetostat | 2021-estimated end 2024 |
| NCT04190056 | II | Not yet recruiting | Breast cancer | Pembrolizumab<br>Tamoxifen<br>Vorinostat | 2021-estimated end 2029 |

active site [195]. Interestingly, it showed to reverse chemoresistance in lung cancer cell lines with high expression of IGFBP2, with IGFBP2 being a biomarker of chemoresistance poor outcome in lung cancer patients [196]. Panobinostat is approved for patients with recurrent multiple myeloma who have received at least two prior treatment regiments (Table 3) [193]. Indeed, the progression-free survival of patients treated with panobinostat was 10.6 months in comparison with 5.8 months in the control arm [197]. Belinostat also inhibits HDACs by binding to the zinc finger in the enzymes' active catalytic site and, recently, showed to be active in testicular germ cell tumor cell lines resistant to cisplatin, with $IC_{50}$ in the low nanomolar range for all cell lines [198].

Entinostat belongs to the benzamide group of HDAC inhibitors and inhibits class I HDACs [193]. Remarkably, entinostat boosted the effects of PD-1 inhibition in in vivo models of lung and renal cancers by impairing the immunosuppressive function of polymorphonuclear and monocytic-myeloid derived suppressor cell populations [112]. Another inhibitor of class I HDACs is romidepsin (FK228) belonging to the cyclic peptide family [193]. Romidepsin has been approved by the FDA for the treatment of advanced cutaneous T-cell lymphoma and peripheral T-cell lymphoma (Table 3) [199]. The triple combination of romidepsin, gemcitabine and cisplatin acted synergically and induced death by creating reactive oxygen species in triple-negative breast cancer cell lines [200].

The short-chain and aromatic fatty acids sodium butyrate and valproic acid also were shown to be pan-HDACs inhibitors [193]. Sodium butyrate is a short-chain fatty acid produced by fermentation by anaerobic bacterial fermentation that inhibits growth, induces apoptosis, migration and EMT of colorectal cancer cells [201]. Valproic acid, used for the treatment of epilepsy and bipolar disorder, in combination with cisplatin and cetuximab, showed antiproliferative and pro-apoptotic effects in 3D-self-assembled spheroid models of ad and neck squamous cell carcinoma cells [202].

## Bladder cancer

BC is estimated to be the tenth most frequent cancer worldwide and the ninth cause of death by cancer [203]. About 70% of the patients are diagnosed as a non-muscle invasive BC (NMIBC), while 30% are diagnosed with muscle invasive BC (MIBC) [204]. NMIBC is mostly comprised of urothelial papillary neoplasms with varying propensity for recurrence and progression, which may be predicted based on grading [205]. According to the 2016 WHO classification, the spectrum of papillary neoplasms includes urothelial papilloma, papillary urothelial neoplasm of low malignant potential, low-grade and high-grade papillary urothelial carcinoma, in ascending order of biological and clinical aggressiveness [206]. On the other hand, urothelial carcinoma in situ (CIS) represents a high-grade form of non-papillary NMIBC, with substantial risk of progression to invasive disease [206]. Although NMIBC mostly contributes to the overall BC 5-year survival rate of 77.1%, 80% of high-grade papillary carcinomas and CIS recur and 20–50% progress to MIBC [207]. In addition to grade, evaluation of disease stage [by means of clinical examination, cystoscopy, radiographic evaluation and/or pathological examination using tissue collected by transurethral resection of the bladder tumor (TURBT)] is mandatory to define the best therapeutic strategy [208, 209]. For NMIBC, treatment mostly consists of TURBT eventually complemented with mitomycin or Bacillus Calmette-Guérin (BCG) instillation, whereas radical cystectomy with lymphadenectomy remains the gold standard for MIBC, complemented with neo-adjuvant or adjuvant cisplatin-based chemotherapy, which is also the main option for metastatic BC [209]. Recently, immunotherapies targeting PD-1/PD-L1 immune checkpoint were approved for BC patients that are refractory or ineligible to cisplatin-based chemotherapy [210]. Although chemotherapy and immunotherapy have improved the outcome of locally advanced and metastatic disease, 5-year survival remains poor (36% and 5%, respectively) [207].

BCG, which is a weakened strain of *Mycobacterium bovis*, was the first form of immunotherapy approved for cancer treatment and, specifically, for BC. Currently, it is administrated by intravesical instillation after TURBT in NMIBC patients with high risk of recurrence [211]. Although the mechanism is not fully known, BCG leads to localized innate and adaptative immune responses, including CD4 and CD8 lymphocytes, NK cells, macrophages, granulocytes and DCs [212]. About 55–75% of the high-risk patients suffering from papillary tumors to CIS respond to this therapy. However, 25 to 45% of these eventually relapse and progress to invasive disease. Hypermethylation of *CDKN2B* and of *MUS81a* and *MSH6* involved in DNA repair and *THBS1*, important for cell adhesion, have been associated with response to BCG therapy [210, 213]. Likewise, low methylation levels of *PMF1* have been associated with disease recurrence, poor outcome and lack of response to BCG in BC patients (Fig. 3) [214].

The immune landscape of BC is composed by different immune populations, including CD8 + T lymphocytes and Th1 CD4 + T lymphocytes. Interestingly, tumor-infiltrating CD4 + lymphocytes were found to be hypomethylated in four lineage loci compared to CD4 + lymphocytes in lymph nodes and blood. Patients with complete response to neoadjuvant chemotherapy (NACT) showed hypomethylation in CD4 + T cells, namely in IFN- γ. Furthermore, shifts in methylation patterns of Th1 CD4 + T cells after NACT show a relocation of cells from blood to the tumor (Fig. 3) [215]. Tissue-resident memory T cells showed low PRF1 DNA methylation levels concomitantly with increased perforin expression [216]. The analysis of DNA methylation in neutrophils and lymphocytes predicted the outcome of BC patients, *i.e.*, high levels of DNA methylation-derived neutrophil-to-lymphocyte ratio associated with poor outcome [217].

Demethylating agents lead to reactivation of TSGs, inhibition of cancer cells' proliferation and migration, increased apoptosis and activation of IFN pathway in BC [218]. Ramakrishnan et al. showed that low concentrations of DAC lead to the activation of NOTCH1, which may prevent epithelial-mesenchymal transition of tumor cells, thus impairing cancer cell dissemination [219, 220]. Moreover, increased IL-6 levels were observed in DAC-treated cells, and reduction of cytokeratin 5 expression associated with cell differentiation and impaired BC progression [221]. Another epigenetic inhibitor for G9a, CM-272, in combination with cisplatin caused an increase in expression of genes associated with immune response, such as TNF-α, IFN-α and IFN-γ, which correlated with an endogenous retrovirus response. Furthermore, an extensive infiltration of CD8 + T cells and NK cells was observed in tumors and metastases in an in vivo immunocompetent model of MIBC. This was also observed with CM-272 in combination with an anti-PD-L1 antibody, with immune infiltration by CD3 +, CD8 + and NK cells, and the absence of CD4 + and CD163 + cells [222].

## Conclusions

Epigenetic alterations in cells of the TME play a major role in creating an immunosuppressive environment ideal for tumor development, which translates in a lack of effectiveness of immune checkpoint blockage therapies. The inhibition of epigenetic modulators might be an interesting therapeutic option to modify the

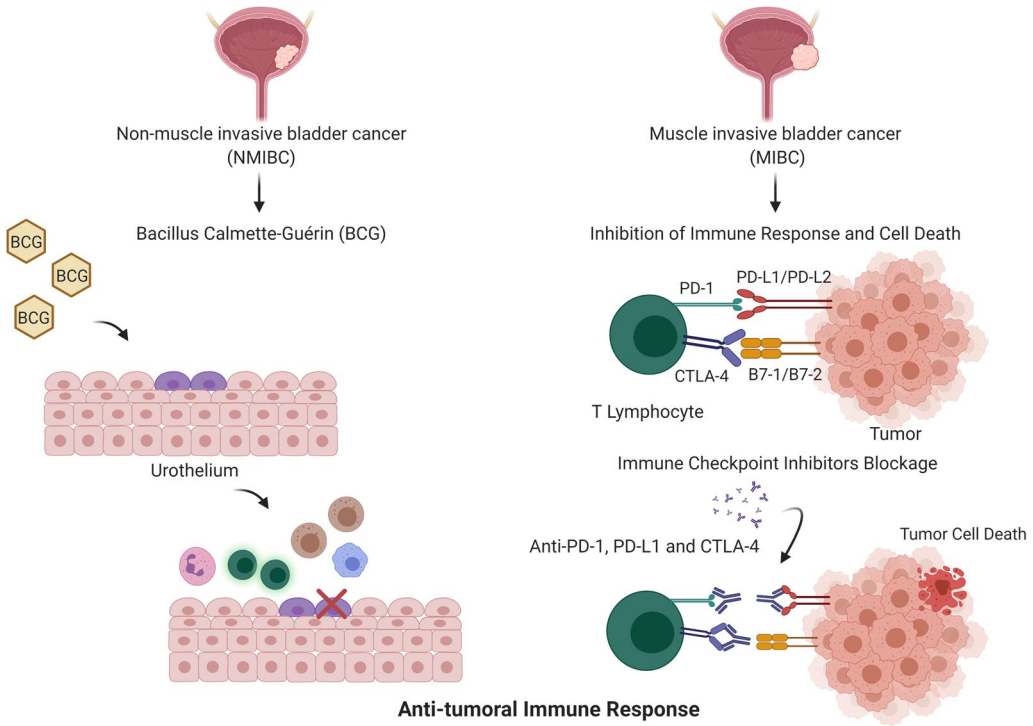


**Fig. 3** Modalities of immunotherapy in bladder cancer. BCG is a weakened strain of *Mycobacterium bovis* and was the first of immunotherapy approved for BC. NMIBC patients with high risk of recurrence are subjected to BCG therapy. The administration of BCG leads to a stimulation of both adaptative and innate immune response by recruiting lymphocytes, macrophages, NK cells and neutrophils, leading to the elimination of the remaining tumor cells. On the other hand, BC patients with MIBC are candidates for immune checkpoint blockage. Tumor cells express repression signals that lead to the inhibition of the immune response, namely by expressing PD-L1/PD-L2 and B7-1/B7-2, that will bind to PD-1 and CTLA-4 present in T lymphocytes, respectively. Nevertheless, with the administration of antibodies against PD-1, PD-L1 or CTL4-A, this process is reverted, leading to the activation of T cells and the start of an immune response against tumor cells, leading ultimately to their death

immunosuppressive TME, and their potential in combination with immunotherapy has already been discussed. Additionally, refining patient selection for immunotherapy by exploring new biomarkers with higher sensitivity and specificity might improve the success rate of this therapy. Combining these findings, exploring aberrant epigenetic marks in both cancer cells and in cells of the TME might provide potential biomarkers for this purpose.

Thus, further studies are needed to increase our knowledge on the epigenetic mechanisms underlying the acquisition of immunosuppressive immune cell phenotypes and how these affect immunotherapy response. Additionally, a promising strategy to generate an immune-promoting TME might be the combination of epigenetic modulator targeting and immunotherapy.

**Abbreviations**

5-aza: 5-Azacytidine; FdCyd: 5′-fluoro-2′-deoxycytidine; ALOX15: Arachidonate 15-lipoxygenase; AML: Acute myeloid leukemia; APCs: Antigen-presenting cells; APM: Antigen processing and presentation machinery; Arg1: Arginase 1; BC: Bladder cancer; BCG: Bacillus Calmette-Guérin; CAFs: Cancer-associated fibroblasts; CIS: Carcinoma in situ; CMML: Chronic myelomonocytic leukemia; CTLs: Cytotoxic T cells; CTLA-4: Cytotoxic T-lymphocyte-associated protein 4; DAC: Decitabine; DCs: Dendritic cells; DNMTs: DNA methyltransferases; ECM: Extracellular matrix; EGCG: Epigallocatechin-3-gallate; EMA: European Medicines Agency; EZH2: Enhancer of zeste homolog 2; FDA: Food and Drug Administration; HATs: Histone acetyltransferases; HDACs: Histone deacetylases; IFN: Interferon; JMJD3: Jumonji domain-containing protein D3; KLF4: Kruppel-like factor 4; MDSCs: Myeloid-derived suppressor cells; MIBC: Muscle invasive BC; NACT: Neoadjuvant chemotherapy; NK: Natural killer; NMIBC: Non-muscle invasive BC; PD-1: Programmed death 1; PD-L1: Programmed death-ligand 1; PPARγ: Peroxisome proliferator-activated receptor γ; PRMT1: Protein arginine methyltransferase 1; PTMs: Post-translational modifications; Rb: Retinoblastoma gene; SATB1: Special AT-rich sequence binding 1; SAHA: Suberanilohydroxamic acid; SMYD3: SET and MYND Domain 3; STAT3: Signal transducer and activator of transcription 3; TAAs: Tumor-associated antigens; TAMs: Tumor-associated macrophages; TECs: Tumor endothelial cells; Th: T helper; TILs: Tumor-infiltrating lymphocytes; TME: Tumor microenvironment; Tregs: Regulatory T cells; TSA: Trichostatin A; TSGs: Tumor suppressor genes; TURBT: Transurethral resection of the bladder; UCK2: Uridine-cytidine kinase 2.

## Supplementary Information

The online version contains supplementary material available at https://doi.org/10.1186/s13148-021-01046-0.

**Additional file 1: Table 1.** Main studies comprising epigenetic drugs and biomarkers associated with immunotherapy.

**Authors' contributions**
IL, SPN and JMP conceptualized the study; IL and SPN wrote the manuscript; RH, CJ, MD and JMP reviewed and edited the manuscript; RH, CJ, MD and JMP supervised the study; CJ, MD and JMP acquired the funding. All authors have read and agreed to the published version of the manuscript. All figures are original and were created with BioRender.com.

**Funding**
This study was cofunded by European Regional Development Fund (FEDER) Grants from Science and Innovation (SAF2015-66015-R, and PID2019-110758RB-I00 to JMP), Instituto de Salud Carlos III (CIBERONC no. CB16/12/00228 to JMP; PI20/00813 and DTS20/00043 to MD) and Programa Operacional Competitividade e Internacionalização (POCI), in the component FEDER, and by national funds (OE) through FCT/MCTES, in the scope of the project HyTherCaP- PO-CI-01-0145-FEDER-29030 to CJ). IL is supported by a predoctoral fellowship from AECC (Spanish Ass. against Cancer), Predoctoral AECC 2019 grant number PRDMA19024LODE. SPN is supported by an FCT-Fundação para a Ciência e Tecnologia Grant (SFRH/BD/ 144241/2019).

**Availability of data and materials**
Not applicable.

## Declarations

**Ethics approval and consent to participate**
Not applicable.

**Consent for publication**
Not applicable.

**Competing interests**
The authors declare that they have no competing interests.

**Author details**
[1] Molecular Oncology Unit, Centro de Investigaciones Energéticas, Medioambientales Y Tecnológicas (CIEMAT), 28040 Madrid, Spain. [2] Biomedical Research Institute I+12, University Hospital "12 de Octubre", 28041 Madrid, Spain. [3] Cancer Biology and Epigenetics Group – Research Center, Portuguese Oncology Institute of Porto (CI-IPOP), 4200-072 Porto, Portugal. [4] Department of Pathology, Portuguese Oncology Institute of Porto, 4200-072 Porto, Portugal. [5] Department of Pathology and Molecular Immunology, Institute of Biomedical Sciences Abel Salazar – University of Porto (ICBAS-UP), 4050-313 Porto, Portugal. [6] Centro de Investigación Biomédica en Red de Cáncer (CIBERONC), 28029 Madrid, Spain.

Received: 13 January 2021 Accepted: 1 March 2021
Published online: 24 March 2021

**References**

1. Baylin SB, Jones PA. Epigenetic determinants of cancer. Cold Spring Harb Perspect Biol. 2016;8:a019505.
2. Song H, Liu D, Dong S, Zeng L, Wu Z, Zhao P, et al. Epitranscriptomics and epiproteomics in cancer drug resistance: therapeutic implications. Signal Transduct Target Ther. 2020;5:193.
3. Rinaldi G, Rossi M, Fendt SM. Metabolic interactions in cancer: cellular metabolism at the interface between the microenvironment, the cancer cell phenotype and the epigenetic landscape. Wiley Interdiscip Rev Syst Biol Med. 2018;10:e1397.
4. Mao L, Yang C, Wang J, Li W, Wen R, Chen J, et al. SATB1 is overexpressed in metastatic prostate cancer and promotes prostate cancer cell growth and invasion. J Transl Med. 2013;11:111.
5. Guo L, Zheng J, Yu T, Liu Y, Duo L. Elevated expression of SATB1 is involved in pancreatic tumorigenesis and is associated with poor patient survival. Mol Med Rep. 2017;16:8842–8.
6. Nodin B, Hedner C, Uhlén M, Jirström K. Expression of the global regulator SATB1 is an independent factor of poor prognosis in high grade epithelial ovarian cancer. J Ovarian Res. 2012;5:24.
7. Tesone AJ, Rutkowski MR, Brencicova E, Svoronos N, Perales-Puchalt A, Stephen TL, et al. Satb1 overexpression drives tumor-promoting activities in cancer-associated dendritic cells. Cell Rep. 2016;14:1774–86.
8. Zhang H, Qu S, Li S, Wang Y, Li Y, Wang Y, et al. Silencing SATB1 inhibits proliferation of human osteosarcoma U2OS cells. Mol Cell Biochem. 2013;378:39–45.
9. Selinger CI, Cooper WA, Al-Sohaily S, Mladenova DN, Pangon L, Kennedy CW, et al. Loss of special at-rich binding protein 1 expression is a marker of poor survival in lung cancer. J Thorac Oncol. 2011;6:1179–89.
10. Tu W, Luo M, Wang Z, Yan W, Xia Y, Deng H, et al. Upregulation of SATB1 promotes tumor growth and metastasis in liver cancer. Liver Int Liver Int. 2012;32:1064–78.
11. Chu SH, Ma YB, Feng DF, Zhang H, Zhu ZA, Li ZQ, et al. Upregulation of SATB1 is associated with the development and progression of glioma. J Transl Med. 2012;10:149.
12. Yuan CL, Li L, Zhou X, Liz H, Han L. Expression of SATB1 and HER2 in gastric cancer and its clinical significance. Eur Rev Med Pharmacol Sci. 2016;20:2256–64.
13. Nodin B, Johannesson H, Wangefjord S, O'Connor DP, Lindquist KE, Uhlén M, et al. Molecular correlates and prognostic significance of SATB1 expression in colorectal cancer. Diagn Pathol. 2012;7:1–9.
14. Fromberg A, Rabe M, Aigner A. Multiple effects of the special AT-rich binding protein 1 (SATB1) in colon carcinoma. Int J Cancer. 2014;135:2537–46.
15. Palucka K, Coussens LM, O'Shaughnessy J. Dendritic cells, inflammation, and breast cancer. Cancer J. (United States). 2013; 511–6.
16. Crispen PL, Kusmartsev S. Mechanisms of immune evasion in bladder cancer. Cancer Immunol Immunother. 2020;69:3–14.
17. Han B, Luan L, Xu Z, Wu B. Expression and biological roles of SATB1 in human bladder cancer. Tumor Biol. 2013;34:2943–9.
18. Tran Janco JM, Lamichhane P, Karyampudi L, Knutson KL. Tumor-infiltrating dendritic cells in cancer pathogenesis. J Immunol. 2015;194:2985–91.
19. Glatzel-Plucí Nska N, Piotrowska A, Dzięgiel P, Podhorska-Okołów M. The role of SATB1 in tumour progression and metastasis. Int J Mol Sci. 2019;20:4156.
20. Ding B, Liu P, Liu W, Sun P, Wang CL. Emerging roles of krüppel-like factor 4 in cancer and cancer stem cells. Asian Pac J Cancer Prev. 2015;16:3629–33.
21. Rosenzweig JM, Glenn JD, Calabresi PA, Whartenby KA. KLF4 modulates expression of IL-6 in dendritic cells via both promoter activation and epigenetic modification. J Biol Chem. 2013;288:23868–74.
22. Gabrilovich DI, Nagaraj S. Myeloid-derived suppressor cells as regulators of the immune system. Nat Rev Immunol. 2009;9:162–74.
23. Sanaei M, Salimzadeh L, Bagheri N. Crosstalk between myeloid-derived suppressor cells and the immune system in prostate cancer. J Leukoc Biol. 2020;107:43–56.
24. Medina-Echeverz J, Eggert T, Han M, Greten TF. Hepatic myeloid-derived suppressor cells in cancer. Cancer Immunol Immunother. 2015;64:931–40.
25. Ma J, Xu H, Wang S. Immunosuppressive role of myeloid-derived suppressor cells and therapeutic targeting in lung cancer. J Immunol Res. 2018;6319649.
26. Sasidharan Nair V, Saleh R, Toor SM, Taha RZ, Ahmed AA, Kurer MA, et al. Transcriptomic profiling disclosed the role of DNA methylation and histone modifications in tumor-infiltrating myeloid-derived suppressor cell subsets in colorectal cancer. Clin Epigenet. 2020;12:13.
27. Gabrilovich DI, Bronte V, Chen SH, Colombo MP, Ochoa A, Ostrand-Rosenberg S, et al. The terminology issue for myeloid-derived suppressor cells [1]. Cancer Res. 2007;67:425.
28. Wu L, Du H, Li Y, Qu P, Yan C. Signal transducer and activator of transcription 3 (Stat3C) promotes myeloid-derived suppressor cell expansion and immune suppression during lung tumorigenesis. Am J Pathol. 2011;179:2131–41.
29. Trikha P, Carson WE. Signaling pathways involved in MDSC regulation. Biochim Biophys Acta Rev Cancer. 2014;1846:55–65.
30. Mace TA, Bloomston M, Lesinski GB. Pancreatic cancer-associated stellate cells: a viable target for reducing immunosuppression in the tumor microenvironment. Oncoimmunology. 2013;2:e24891.

31. Xin H, Zhang C, Herrmann A, Du Y, Figlin R, Yu H. Sunitinib inhibition of Stat3 induces renal cell carcinoma tumor cell apoptosis and reduces immunosuppressive cells. Cancer Res. 2009;69:2506–13.
32. Lissbrant IF, Stattin P, Wikstrom P, Damber JE, Egevad L, Bergh A. Tumor associated macrophages in human prostate cancer: relation to clinicopathological variables and survival. Int J Oncol. 2000;17:445–51.
33. Mielgo A, Schmid MC. Impact of tumour associated macrophages in pancreatic cancer. BMB Rep. 2013;46:131–8.
34. Yin M, Shen J, Yu S, Fei J, Zhu X, Zhao J, et al. Tumor-associated macrophages (Tams): a critical activator in ovarian cancer metastasis. OncoTargets Ther. 2019;12:8687–99.
35. Malfitano AM, Pisanti S, Napolitano F, Di Somma S, Martinelli R, Portella G. Tumor-associated macrophage status in cancer treatment. Cancers (Basel). 2020;12:1987.
36. Sumitomo R, Hirai T, Fujita M, Murakami H, Otake Y, Huang C. M2 tumor-associated macrophages promote tumor progression in non-small-cell lung cancer. Exp Ther Med. 2019;18:4490–8.
37. Vidyarthi A, Agnihotri T, Khan N, Singh S, Tewari MK, Radotra BD, et al. Predominance of M2 macrophages in gliomas leads to the suppression of local and systemic immunity. Cancer Immunol Immunother. 2019;68:1995–2004.
38. Gambardella V, Castillo J, Tarazona N, Gimeno-Valiente F, Martínez-Ciarpaglini C, Cabeza-Segura M, et al. The role of tumor-associated macrophages in gastric cancer development and their potential as a therapeutic target. Cancer Treat Rev. 2020;86:102015.
39. Liu Y, Li L, Li Y, Zhao X. Research Progress on Tumor-Associated Macrophages and Inflammation in Cervical Cancer. Biomed Res Int. 2020;6842963.
40. Zhong X, Chen B, Yang Z. The role of tumor-associated macrophages in colorectal carcinoma progression. Cell Physiol Biochem. 2018;45:356–65.
41. Choi J, Gyamfi J, Jang H, Koo JS. The role of tumor-associated macrophage in breast cancer biology. Histol Histopathol. 2018;33:133–45.
42. Setrerrahmane S, Xu H. Tumor-related interleukins: old validated targets for new anti-cancer drug development. Mol Cancer. 2017;16:1–17.
43. Hendry S, Salgado R, Gevaert T, Russell PA, John T, Thapa B, et al. Assessing tumor-infiltrating lymphocytes in solid tumors: a practical review for pathologists and proposal for a standardized method from the international immuno-oncology biomarkers working group: part 2: TILs in melanoma, gastrointestinal tract carcinomas, non-small cell lung carcinoma and mesothelioma, endometrial and ovarian carcinomas, squamous cell carcinoma of the head and neck, genitourinary carcinomas, and primary brain tumors. Adv Anat Pathol. 2017;24:311–35.
44. Hendry S, Salgado R, Gevaert T, Russell PA, John T, Thapa B, et al. Assessing tumor-infiltrating lymphocytes in solid tumors: a practical review for pathologists and proposal for a standardized method from the international immunooncology biomarkers working group: part 1: assessing the host immune response, TILs in invasive breast carcinoma and ductal carcinoma in situ, metastatic tumor deposits and areas for further research. Adv Anat Pathol. 2017;24:235–51.
45. Woroniecka K, Chongsathidkiet P, Rhodin K, Kemeny H, Dechant C, Harrison Farber S, et al. T-cell exhaustion signatures vary with tumor type and are severe in glioblastoma. Clin Cancer Res. 2018;24:4175–86.
46. Baitsch L, Baumgaertner P, Devêvre E, Raghav SK, Legat A, Barba L, et al. Exhaustion of tumor-specific CD8+ T cells in metastases from melanoma patients. J Clin Invest. 2011;121:2350–60.
47. Li C, Jiang P, Wei S, Xu X, Wang J. Regulatory T cells in tumor microenvironment: new mechanisms, potential therapeutic strategies and future prospects. Mol Cancer. 2020;19:116.
48. Halim L, Romano M, McGregor R, Correa I, Pavlidis P, Grageda N, et al. An atlas of human regulatory T helper-like cells reveals features of Th2-like tregs that support a tumorigenic environment. Cell Rep. 2017;20:757–70.
49. Tao H, Mimura Y, Aoe K, Kobayashi S, Yamamoto H, Matsuda E, et al. Prognostic potential of FOXP3 expression in non-small cell lung cancer cells combined with tumor-infiltrating regulatory T cells. Lung Cancer. 2012;75:95–101.
50. Sayour EJ, McLendon P, McLendon R, De Leon G, Reynolds R, Kresak J, et al. Increased proportion of FoxP3+ regulatory T cells in tumor infiltrating lymphocytes is associated with tumor recurrence and reduced survival in patients with glioblastoma. Cancer Immunol Immunother. 2015;64:419–27.
51. Judge SJ, Murphy WJ, Canter RJ. Characterizing the dysfunctional NK Cell: assessing the clinical relevance of exhaustion, anergy, and senescence. Front Cell Infect Microbiol. 2020;10:49.
52. Peng YP, Zhu Y, Zhang JJ, Xu ZK, Qian ZY, Dai CC, et al. Comprehensive analysis of the percentage of surface receptors and cytotoxic granules positive natural killer cells in patients with pancreatic cancer, gastric cancer, and colorectal cancer. J Transl Med. 2013;11:262.
53. Bi J, Tian Z. NK cell exhaustion. Front Immunol. 2017;8:760.
54. Mamessier E, Sylvain A, Thibult ML, Houvenaeghel G, Jacquemier J, Castellano R, et al. Human breast cancer cells enhance self tolerance by promoting evasion from NK cell antitumor immunity. J Clin Invest. 2011;121:3609–22.
55. Kalluri R. The biology and function of fibroblasts in cancer. Nat Rev Cancer. 2016;16:582–98.
56. Tao L, Huang G, Song H, Chen Y, Chen L. Cancer associated fibroblasts: An essential role in the tumor microenvironment (review). Oncol Lett. 2017;14:2611–20.
57. Ziani L, Chouaib S, Thiery J. Alteration of the antitumor immune response by cancer-associated fibroblasts. Front Immunol. 2018;9:1.
58. Hashizume H, Baluk P, Morikawa S, McLean JW, Thurston G, Roberge S, et al. Openings between defective endothelial cells explain tumor vessel leakiness. Am J Pathol. 2000;156:1363–80.
59. Hida K, Hida Y, Amin DN, Flint AF, Panigrahy D, Morton CC, et al. Tumor-associated endothelial cells with cytogenetic abnormalities. Cancer Res. 2004;64:8249–55.
60. Farnsworth RH, Lackmann M, Achen MG, Stacker SA. Vascular remodeling in cancer. Oncogene. 2014;33:3496–505.
61. Henke E, Nandigama R, Ergün S. Extracellular matrix in the tumor microenvironment and its impact on cancer therapy. Front Mol Biosci. 2020;6:160.
62. Lyko F. The DNA methyltransferase family: a versatile toolkit for epigenetic regulation. Nat Rev Genet. 2018;19:81–92.
63. Chen Z, Chen Z, Chen Z, Zhang Y, Zhang Y, Zhang Y, et al. Role of mammalian DNA methyltransferases in development. Annu Rev Biochem. 2020;89:135–58.
64. Esteller M. Epigenetic gene silencing in cancer: the DNA hypermethylome. Hum Mol Genet. 2007;16:50–9.
65. Rothbart SB, Strahl BD. Interpreting the language of histone and DNA modifications. Biochim Biophys Acta Gene Regul Mech. 2014;1839:627–43.
66. Zhao Z, Shilatifard A. Epigenetic modifications of histones in cancer. Genome Biol. 2019;20:1–16.
67. Cairns BR. Chromatin remodeling: insights and intrigue from single-molecule studies. Nat Struct Mol Biol. 2007;14:989–96.
68. Martire S, Banaszynski LA. The roles of histone variants in fine-tuning chromatin organization and function. Nat Rev Mol Cell Biol. 2020;21:522–41.
69. Kurumizaka H, Kujirai T, Takizawa Y. Contributions of histone variants in nucleosome structure and function. J Mol Biol. 2020;166678.
70. Yasui D, Miyano M, Cai S, Varga-Weisz P, Kohwi-Shigematsu T. SATB1 targets chromatin remodelling to regulate genes over long distances. Nature. 2002;419:641–5.
71. Pavan Kumar P, Purbey PK, Sinha CK, Notani D, Limaye A, Jayani RS, et al. Phosphorylation of SATB1, a global gene regulator, acts as a molecular switch regulating its transcriptional activity in vivo. Mol Cell. 2006;22:231–43.
72. Villagra A, Cheng F, Wang HW, Suarez I, Glozak M, Maurin M, et al. The histone deacetylase HDAC11 regulates the expression of interleukin 10 and immune tolerance. Nat Immunol. 2009;10:92–100.
73. Sahakian E, Powers JJ, Chen J, Deng SL, Cheng F, Distler A, et al. Histone deacetylase 11: a novel epigenetic regulator of myeloid derived suppressor cell expansion and function. Mol Immunol. 2015;63:579–85.
74. Cheng F, Lienlaf M, Perez-Villarroel P, Wang HW, Lee C, Woan K, et al. Divergent roles of histone deacetylase 6 (HDAC6) and histone deacetylase 11 (HDAC11) on the transcriptional regulation of IL10 in antigen presenting cells. Mol Immunol. 2014;60:44–53.
75. Sido JM, Yang X, Nagarkatti PS, Nagarkatti M. Δ 9 -Tetrahydrocannabinol-mediated epigenetic modifications elicit myeloid-derived suppressor cell activation via STAT3/S100A8. J Leukoc Biol. 2015;97:677–88.

76. Viatour P, Somervaille TC, Venkatasubrahmanyam S, Kogan S, McLaughlin ME, Weissman IL, et al. Hematopoietic stem cell quiescence is maintained by compound contributions of the retinoblastoma gene family. Cell Stem Cell. 2008;3:416–28.
77. Walkley CR, Shea JM, Sims NA, Purton LE, Orkin SH. Rb regulates interactions between hematopoietic stem cells and their bone marrow microenvironment. Cell. 2007;129:1081–95.
78. Youn JI, Kumar V, Collazo M, Nefedova Y, Condamine T, Cheng P, et al. Epigenetic silencing of retinoblastoma gene regulates pathologic differentiation of myeloid cells in cancer. Nat Immunol. 2013;14:211–20.
79. Ojalvo LS, Whittaker CA, Condeelis JS, Pollard JW. Gene expression analysis of macrophages that facilitate tumor invasion supports a role for Wnt-signaling in mediating their activity in primary mammary tumors. J Immunol. 2010;184:702–12.
80. Rubio C, Munera-Maravilla E, Lodewijk I, Suarez-Cabrera C, Karaivanova V, Ruiz-Palomares R, et al. Macrophage polarization as a novel weapon in conditioning tumor microenvironment for bladder cancer: can we turn demons into gods? Clin Transl Oncol. 2019;21:391–403.
81. Yang X, Wang X, Liu D, Yu L, Xue B, Shi H. Epigenetic regulation of macrophage polarization by DNA methyltransferase 3b. Mol Endocrinol. 2014;28:565–74.
82. Arlauckas SP, Garren SB, Garris CS, Kohler RH, Oh J, Pittet MJ, et al. Arg1 expression defines immunosuppressive subsets of tumor-associated macrophages. Theranostics. 2018;8:5842–54.
83. Ishii M, Wen H, Corsa CAS, Liu T, Coelho AL, Allen RM, et al. Epigenetic regulation of the alternatively activated macrophage phenotype. Blood. 2009;114:3244–54.
84. Kittan NA, Allen RM, Dhaliwal A, Cavassani KA, Schaller M, Gallagher KA, et al. Cytokine induced phenotypic and epigenetic signatures are key to establishing specific macrophage phenotypes. Zissel G, editor. PLoS ONE. 2013;8:e78045.
85. Satoh T, Takeuchi O, Vandenbon A, Yasuda K, Tanaka Y, Kumagai Y, et al. The Jmjd3-Irf4 axis regulates M2 macrophage polarization and host responses against helminth infection. Nat Immunol. 2010;11:936–44.
86. Chen X, Barozzi I, Termanini A, Prosperini E, Recchiuti A, Dalli J, et al. Requirement for the histone deacetylase Hdac3 for the inflammatory gene expression program in macrophages. Proc Natl Acad Sci U S A. 2012;109:E2865–74.
87. Mullican SE, Gaddis CA, Alenghat T, Nair MG, Giacomin PR, Everett LJ, et al. Histone deacetylase 3 is an epigenomic brake in macrophage alternative activation. Genes Dev Genes Dev. 2011;25:2480–8.
88. Cao Q, Rong S, Repa JJ, Clair RS, Parks JS, Mishra N. Histone deacetylase 9 represses cholesterol efflux and alternatively activated macrophages in atherosclerosis development. Arterioscler Thromb Vasc Biol. 2014;34:1871–9.
89. Yang Q, Wei J, Zhong L, Shi M, Zhou P, Zuo S, et al. Cross talk between histone deacetylase 4 and STAT6 in the transcriptional regulation of arginase 1 during mouse dendritic cell differentiation. Mol Cell Biol. 2015;35:63–75.
90. Lo Sasso G, Joe Menzies K, Mottis A, Piersigilli A, Perino A, Yamamoto H, et al. SIRT2 deficiency modulates macrophage polarization and susceptibility to experimental colitis. PLoS ONE. 2014;9:e103573.
91. Tay RE, Richardson EK, Toh HC. Revisiting the role of CD4+ T cells in cancer immunotherapy—new insights into old paradigms. Cancer Gene Ther. 2020;28:5–17.
92. Janson PCJ, Marits P, Thörn M, Ohlsson R, Winqvist O. CpG methylation of the IFNG gene as a mechanism to induce immunosupression in tumor-infiltrating lymphocytes. J Immunol. 2008;181:2878–86.
93. Peng D, Kryczek I, Nagarsheth N, Zhao L, Wei S, Wang W, et al. Epigenetic silencing of TH1-type chemokines shapes tumour immunity and immunotherapy. Nature. 2015;527:249–53.
94. Yang R, Cheng S, Luo N, Gao R, Yu K, Kang B, et al. Distinct epigenetic features of tumor-reactive CD8+ T cells in colorectal cancer patients revealed by genome-wide DNA methylation analysis. Genome Biol. 2019;21:2.
95. Ghoneim HE, Fan Y, Moustaki A, Abdelsamed HA, Dash P, Dogra P, et al. De Novo epigenetic programs inhibit PD-1 blockade-mediated T cell rejuvenation. Cell. 2017;170:142–57.
96. Massagué J. TGFβ in Cancer. Cell. 2008; 215–30.
97. Stephen TL, Payne KK, Chaurio RA, Allegrezza MJ, Zhu H, Perez-Sanz J, et al. SATB1 expression governs epigenetic repression of PD-1 in tumor-reactive T cells. Immunity. 2017;46:51–64.
98. Philip M, Fairchild L, Sun L, Horste EL, Camara S, Shakiba M, et al. Chromatin states define tumour-specific T cell dysfunction and reprogramming. Nature. 2017;545:452–6.
99. Waight JD, Takai S, Marelli B, Qin G, Hance KW, Zhang D, et al. Cutting edge: epigenetic regulation of Foxp3 defines a stable population of CD4 + regulatory T cells in tumors from mice and humans. J Immunol. 2015;194:878–82.
100. Ohkura N, Kitagawa Y, Sakaguchi S. Development and maintenance of regulatory T cells. Immunity. 2013;38:414–23.
101. Ohkura N, Hamaguchi M, Morikawa H, Sugimura K, Tanaka A, Ito Y, et al. T Cell receptor stimulation-induced epigenetic changes and Foxp3 expression are independent and complementary events required for treg cell development. Immunity. 2012;37:785–99.
102. DuPage M, Chopra G, Quiros J, Rosenthal WL, Morar MM, Holohan D, et al. The chromatin-modifying enzyme Ezh2 is critical for the maintenance of regulatory T cell identity after activation. Immunity. 2015;42:227–38.
103. Wang D, Quiros J, Mahuron K, Pai CC, Ranzani V, Young A, et al. Targeting EZH2 reprograms intratumoral regulatory T cells to enhance cancer immunity. Cell Rep. 2018;23:3262–74.
104. Schenk A, Bloch W, Zimmer P. Natural killer cells—an epigenetic perspective of development and regulation. Int J Mol Sci. 2016;17:326.
105. Fernández-Sánchez A, Raneros AB, Palao RC, Sanz AB, Ortiz A, Ortega F, et al. DNA demethylation and histone H3K9 acetylation determine the active transcription of the NKG2D gene in human CD8+ T and NK cells. Epigenetics. 2013;8:66–78.
106. Ogbomo H, Michaelis M, Kreuter J, Doerr HW, Cinatl J. Histone deacetylase inhibitors suppress natural killer cell cytolytic activity. FEBS Lett. 2007;581:1317–22.
107. Yin J, Leavenworth JW, Li Y, Luo Q, Xie H, Liu X, et al. Ezh2 regulates differentiation and function of natural killer cells through histone methyltransferase activity. Proc Natl Acad Sci U S A. 2015;112:15988–93.
108. Sauvageau M, Sauvageau G. Polycomb group proteins: multi-faceted regulators of somatic stem cells and cancer. Cell Stem Cell. 2010;7:299–313.
109. Gao XY, Xue XH, Ma YN, Zhang SQ. Effect of baicalein on the expression of SATB1 in human breast cancer cells. Exp Ther Med. 2015;9:1665–9.
110. Lakshminarayana Reddy CN, Vyjayanti VN, Notani D, Galande S, Kotamraju S. Down-regulation of the global regulator SATB1 by statins in COLO205 colon cancer cells. Mol Med Rep. 2010;3:857–61.
111. Wang M, Yin B, Matsueda S, Deng L, Li Y, Zhao W, et al. Identification of special AT-rich sequence binding protein 1 as a novel tumor antigen recognized by CD8+ T cells: implication for cancer immunotherapy. PLoS ONE. 2013;8:e56730.
112. Orillion A, Hashimoto A, Damayanti N, Shen L, Adelaiye-Ogala R, Arisa S, et al. Entinostat neutralizes myeloid-derived suppressor cells and enhances the antitumor effect of PD-1 inhibition in murine models of lung and renal cell carcinoma. Clin Cancer Res. 2017;23:5187–201.
113. Kim K, Skora AD, Li Z, Liu Q, Tam AJ, Blosser RL, et al. Eradication of metastatic mouse cancers resistant to immune checkpoint blockade by suppression of myeloid-derived cells. Proc Natl Acad Sci U S A. 2014;111:11774–9.
114. Briere D, Sudhakar N, Woods DM, Hallin J, Engstrom LD, Aranda R, et al. The class I/IV HDAC inhibitor mocetinostat increases tumor antigen presentation, decreases immune suppressive cell types and augments checkpoint inhibitor therapy. Cancer Immunol Immunother. 2018;67:381–92.
115. Hashimoto A, Fukumoto T, Zhang R, Gabrilovich D. Selective targeting of different populations of myeloid-derived suppressor cells by histone deacetylase inhibitors. Cancer Immunol Immunother. 2020;69:1929–36.
116. Liu SS, Wu F, Jin YM, Chang WQ, Xu TM. HDAC11: a rising star in epigenetics. Biomed Pharmacother. 2020;131:110607.
117. Tikhanovich I, Zhao J, Olson J, Adams A, Taylor R, Bridges B, et al. Protein arginine methyltransferase 1 modulates innate immune responses through regulation of peroxisome proliferator-activated

receptor γ-dependent macrophage differentiation. J Biol Chem. 2017;292:6882–94.
118. Yildirim-Buharalioğlu G, Bond M, Sala-Newby GB, Hindmarch CCT, Newby AC. Regulation of epigenetic modifiers, including KDM6B, by interferon-γ and interleukin-4 in human macrophages. Front Immunol. 2017;8:1.
119. Kruidenier L, Chung CW, Cheng Z, Liddle J, Che K, Joberty G, et al. A selective jumonji H3K27 demethylase inhibitor modulates the proinflammatory macrophage response. Nature. 2012;488:404–8.
120. de Groot AE, Pienta KJ. Epigenetic control of macrophage polarization: Implications for targeting tumor-associated macrophages. Oncotarget. 2018;9:20908–27.
121. Goswami S, Apostolou I, Zhang J, Skepner J, Anandhan S, Zhang X, et al. Modulation of EZH2 expression in T cells improves efficacy of anti-CTLA-4 therapy. J Clin Invest. 2018;128:3813–8.
122. Qiu J, Sharma S, Rollins RA, Paul TA. The complex role of EZH2 in the tumor microenvironment: opportunities and challenges for immunotherapy combinations. Future Med Chem. 2020;12:1415–30.
123. Zingg D, Arenas-Ramirez N, Sahin D, Rosalia RA, Antunes AT, Haeusel J, et al. The histone methyltransferase Ezh2 controls mechanisms of adaptive resistance to tumor immunotherapy. Cell Rep. 2017;20:854–67.
124. Schreiber RD, Old LJ, Smyth MJ. Cancer immunoediting: Integrating immunity's roles in cancer suppression and promotion. Science. 2011;331:1565–70.
125. Aqbi HF, Wallace M, Sappal S, Payne KK, Manjili MH. IFN-γ orchestrates tumor elimination, tumor dormancy, tumor escape, and progression. J Leukoc Biol. 2018;103:1219–23.
126. Jahanban-Esfahlan R, Seidi K, Manjili MH, Jahanban-Esfahlan A, Javaheri T, Zare P. Tumor cell dormancy: threat or opportunity in the fight against cancer. Cancers (Basel). 2019;11:1207.
127. O'Donnell JS, Teng MWL, Smyth MJ. Cancer immunoediting and resistance to T cell-based immunotherapy. Nat Rev Clin Oncol. 2019;16:151–67.
128. Chen L, Flies DB. Molecular mechanisms of T cell co-stimulation and co-inhibition. Nat Rev Immunol. 2013;13:227–42.
129. Pardoll DM. The blockade of immune checkpoints in cancer immunotherapy. Nat Rev Cancer. 2012;12:252–64.
130. Okazaki T, Honjo T. PD-1 and PD-1 ligands: from discovery to clinical application. Int Immunol. 2007;19:813–24.
131. Wei SC, Levine JH, Cogdill AP, Zhao Y, Anang NAAS, Andrews MC, et al. Distinct cellular mechanisms underlie anti-CTLA-4 and anti-PD-1 checkpoint blockade. Cell. 2017;170:1120–33.
132. Van Der Merwe PA, Bodian DL, Daenke S, Linsley P, Davis SJ. CD80 (B7–1) binds both CD28 and CTLA-4 with a low affinity and very fast kinetics. J Exp Med. 1997;185:393–403.
133. Ohaegbulam KC, Assal A, Lazar-Molnar E, Yao Y, Zang X. Human cancer immunotherapy with antibodies to the PD-1 and PD-L1 pathway. Trends Mol Med. 2015;21:24–33.
134. Lee HT, Lee SH, Heo YS. Molecular interactions of antibody drugs targeting PD-1, PD-L1, and CTLA-4 in immuno-oncology. Molecules. 2019;24:1190.
135. Borcoman E, Nandikolla A, Long G, Goel S, Le Tourneau C. Patterns of Response and Progression to Immunotherapy. Am Soc Clin Oncol Educ B. 2018;38:169–78.
136. Rieth J, Subramanian S. Mechanisms of intrinsic tumor resistance to immunotherapy. Int J Mol Sci. 2018;19:1340.
137. Patel SP, Kurzrock R. PD-L1 expression as a predictive biomarker in cancer immunotherapy. Mol. Cancer Ther. 2015;847–56.
138. Haragan A, Field JK, Davies MPA, Escriu C, Gruver A, Gosney JR. Heterogeneity of PD-L1 expression in non-small cell lung cancer: Implications for specimen sampling in predicting treatment response. Lung Cancer. 2019;134:79–84.
139. Aggen DH, Drake CG. Biomarkers for immunotherapy in bladder cancer: a moving target. J Immunother Cancer. 2017;5:94.
140. Lee N, Zakka LR, Mihm MC, Schatton T. Tumour-infiltrating lymphocytes in melanoma prognosis and cancer immunotherapy. Pathology. 2016;48:177–87.
141. Fumet JD, Truntzer C, Yarchoan M, Ghiringhelli F. Tumour mutational burden as a biomarker for immunotherapy: current data and emerging concepts. Eur J Cancer. 2020; 40–50.
142. Zhao P, Li L, Jiang X, Li Q. Mismatch repair deficiency/microsatellite instability-high as a predictor for anti-PD-1/PD-L1 immunotherapy efficacy. J Hematol Oncol. 2019;12:54.
143. Kim J, Kwiatkowski D, McConkey DJ, Meeks JJ, Freeman SS, Bellmunt J, et al. The cancer genome atlas expression subtypes stratify response to checkpoint inhibition in advanced urothelial cancer and identify a subset of patients with high survival probability. Eur Urol. 2019;75:961–4.
144. Kamoun A, de Reyniès A, Allory Y, Sjödahl G, Robertson AG, Seiler R, et al. A consensus molecular classification of muscle-invasive bladder cancer[Formula presented]. Eur Urol. 2020;77:420–33.
145. Goodman AM, Kato S, Bazhenova L, Patel SP, Frampton GM, Miller V, et al. Tumor mutational burden as an independent predictor of response to immunotherapy in diverse cancers. Mol Cancer Ther. 2017;16:2598–608.
146. Qin Y, Bollin K, De MacEdo MP, Carapeto F, Kim KB, Roszik J, et al. Immune profiling of uveal melanoma identifies a potential signature associated with response to immunotherapy. J Immunother Cancer. 2020;8.
147. Wargo JA, Reddy SM, Reuben A, Sharma P. Monitoring immune responses in the tumor microenvironment. Curr Opin Immunol 2016; p. 23–31.
148. House IG, Savas P, Lai J, Chen AXY, Oliver AJ, Teo ZL, et al. Macrophage-derived CXCL9 and CXCL10 are required for antitumor immune responses following immune checkpoint blockade. Clin Cancer Res. 2020;26:487–504.
149. Ali MA, Matboli M, Tarek M, Reda M, Kamal KM, Nouh M, et al. Epigenetic regulation of immune checkpoints: Another target for cancer immunotherapy?. Immunotherapy. 2017; 99–108.
150. Wrangle J, Wang W, Koch A, Easwaran H, Mohammad HP, Vendetti F, et al. Alterations of immune response of non-small cell lung cancer with Azacytidine. Oncotarget. 2013;4:2067–79.
151. Yang H, Bueso-Ramos C, Dinardo C, Estecio MR, Davanlou M, Geng QR, et al. Expression of PD-L1, PD-L2, PD-1 and CTLA4 in myelodysplastic syndromes is enhanced by treatment with hypomethylating agents. Leukemia. 2014;28:1280–8.
152. Chen X, Pan X, Zhang W, Guo H, Cheng S, He Q, et al. Epigenetic strategies synergize with PD-L1/PD-1 targeted cancer immunotherapies to enhance antitumor responses. Acta Pharm Sin B. 2020;10:723–33.
153. Duruisseaux M, Martínez-Cardús A, Calleja-Cervantes ME, Moran S, Castro de Moura M, Davalos V, et al. Epigenetic prediction of response to anti-PD-1 treatment in non-small-cell lung cancer: a multicentre, retrospective analysis. Lancet Respir Med. 2018;6:771–81.
154. Guerreiro IM, Barros-Silva D, Lopes P, Cantante M, Cunha AL, Lobo J, et al. RAD51Bme levels as a potential predictive biomarker for PD-1 blockade response in non-small cell lung cancer. J Clin Med. 2020;9:1000.
155. Kandimalla R, van Tilborg AA, Zwarthoff EC. DNA methylation-based biomarkers in bladder cancer. Nat Rev Urol. 2013;10:327–35.
156. Wang X, Chen E, Yang X, Wang Y, Quan Z, Wu X, et al. 5-azacytidine inhibits the proliferation of bladder cancer cells via reversal of the aberrant hypermethylation of the hepaCAM gene. Oncol Rep. 2016;35:1375–84.
157. Erdmann A, Halby L, Fahy J, Arimondo PB. Targeting DNA methylation with small molecules: what's next? J Med Chem. 2015;58:2569–83.
158. Marques-Magalhães Â, Graça I, Henrique R, Jerónimo C. Targeting DNA methyltranferases in urological tumors. Front Pharmacol. 2018;9:366.
159. Pasculli B, Barbano R, Parrella P. Epigenetics of breast cancer: Biology and clinical implication in the era of precision medicine. Semin Cancer Biol. 2018;51:22–35.
160. Bohl SR, Bullinger L, Rücker FG. Epigenetic therapy: azacytidine and decitabine in acute myeloid leukemia. Expert Rev Hematol. 2018;11:361–71.
161. Stresemann C, Lyko F. Modes of action of the DNA methyltransferase inhibitors azacytidine and decitabine. Int J Cancer. 2008;123:8–13.
162. Santi DV, Norment A, Garrett CE. Covalent bond formation between a DNA-cytosine methyltransferase and DNA containing 5-azacytosine. Proc Natl Acad Sci U S A. 1984;81:6993–7.
163. Chen L, MacMillan AM, Chang W, Ezaz-Nikpay K, Lane WS, Verdine GL. Direct identification of the active-site nucleophile in a DNA (cytosine-5)-methyltransferase. Biochemistry. 1991;30:11018–25.

164. Liu X, Dai X, Wu B. Study of 5-Aza-CdR on transcription regulation of RASSF1A gene in the BIU87 cell line. Urol Int. 2009;82:108–12.
165. Nguyen AN, Hollenbach PW, Richard N, Luna-Moran A, Brady H, Heise C, et al. Azacitidine and decitabine have different mechanisms of action in non-small cell lung cancer cell lines. Lung Cancer. 2010;1:119–40.
166. Gros C, Fahy J, Halby L, Dufau I, Erdmann A, Gregoire JM, et al. DNA methylation inhibitors in cancer: recent and future approaches. Biochimie. 2012;94:2280–96.
167. Zhao Q, Fan J, Hong W, Li L, Wu M. Inhibition of cancer cell proliferation by 5-fluoro-2'-deoxycytidine, a DNA methylation inhibitor, through activation of DNA damage response pathway. Springerplus. 2012;1:65.
168. Balboni B, El Hassouni B, Honeywell RJ, Sarkisjan D, Giovannetti E, Poore J, et al. RX-3117 (fluorocyclopentenyl cytosine): a novel specific antimetabolite for selective cancer treatment. Expert Opin Investig Drugs. 2019;28:311–22.
169. Yoo CB, Cheng JC, Jones PA. Zebularine: a new drug for epigenetic therapy. Biochem Soc Trans. 2004;32:910–2.
170. Takemura Y, Satoh M, Hatanaka K, Kubota S. Zebularine exerts its antiproliferative activity through S phase delay and cell death in human malignant mesothelioma cells. Biosci Biotechnol Biochem. 2018;82:1159–64.
171. Cheng JC, Yoo CB, Weisenberger DJ, Chuang J, Wozniak C, Liang G, et al. Preferential response of cancer cells to zebularine. Cancer Cell. 2004;6:151–8.
172. Raynal NJM, Issa JPJ. DNA methyltransferase inhibitors. Drug Discov Cancer Epigenet. 2015; 169–90.
173. Johnson WD, Harder JB, Naylor J, McCormick DL, Detrisac CJ, Glaze ER, et al. A pharmacokinetic/pharmacodynamic approach to evaluating the safety of zebularine in non-human primates. Cancer Res. 2006;66.
174. Ganesan A, Arimondo PB, Rots MG, Jeronimo C, Berdasco M. The timeline of epigenetic drug discovery: from reality to dreams. Clin Epigenet. 2019;11:174.
175. Albany C, Fazal Z, Singh R, Bikorimana E, Adra N, Hanna NH, et al. A phase 1 study of combined guadecitabine and cisplatin in platinum refractory germ cell cancer. Cancer Med. 2021;10:156–63.
176. Castillo-Aguilera O, Depreux P, Halby L, Arimondo PB, Goossens L. DNA methylation targeting: the DNMT/HMT crosstalk challenge. Biomolecules. 2017;7.
177. Pushpakom S, Iorio F, Eyers PA, Escott KJ, Hopper S, Wells A, et al. Drug repurposing: progress, challenges and recommendations. Nat Rev Drug Discov. 2019;18:41–58.
178. Fang MZ, Wang Y, Ai N, Hou Z, Sun Y, Lu H, et al. Tea polyphenol (-)-epigallocatechin-3-gallate inhibits DNA methyltransferase and reactivates methylation-silenced genes in cancer cell lines. Cancer Res. 2003;63:7563–70.
179. Nandakumar V, Vaid M, Katiyar SK. (-)-Epigallocatechin-3-gallate reactivates silenced tumor suppressor genes, Cip1/p21 and p16INK4a, by reducing DNA methylation and increasing histones acetylation in human skin cancer cells. Carcinogenesis. 2011;32:537–44.
180. Link A, Balaguer F, Shen Y, Lozano JJ, Leung HC, Boland CR, et al. Curcumin modulates DNA methylation in colorectal cancer cells. PLoS ONE. 2013;8:e57709.
181. Pechalrieu D, Dauzonne D, Arimondo PB, Lopez M. Synthesis of novel 3-halo-3-nitroflavanones and their activities as DNA methyltransferase inhibitors in cancer cells. Eur J Med Chem. 2020;186.
182. Lobo J, Cardoso AR, Miranda-Gonçalves V, Looijenga LHJ, Lopez M, Arimondo PB, et al. Targeting germ cell tumors with the newly synthesized flavanone-derived compound mlo1302 efficiently reduces tumor cell viability and induces apoptosis and cell cycle arrest. Pharmaceutics. 2021;13:1–18.
183. Rondelet G, Fleury L, Faux C, Masson V, Dubois J, Arimondo PB, et al. Inhibition studies of DNA methyltransferases by maleimide derivatives of RG108 as non-nucleoside inhibitors. Futur Med Chem. 2017;9:1465–81.
184. Ou Y, Zhang Q, Tang Y, Lu Z, Lu X, Zhou X, et al. DNA methylation enzyme inhibitor RG108 suppresses the radioresistance of esophageal cancer. Oncol Rep. 2018;39:993–1002.
185. Yoo J, Choi S, Medina-Franco JL. Molecular modeling studies of the novel inhibitors of DNA methyltransferases SGI-1027 and CBC12: implications for the mechanism of inhibition of DNMTs. PLoS ONE. 2013;8:e62152.
186. She S, Zhao Y, Kang B, Chen C, Chen X, Zhang X, et al. Combined inhibition of JAK1/2 and DNMT1 by newly identified small-molecule compounds synergistically suppresses the survival and proliferation of cervical cancer cells. Cell Death Dis. 2020;11.
187. Amato RJ. Inhibition of DNA methylation by antisense oligonucleotide MG98 as cancer therapy. Clin Genitourin Cancer. 2007;5:422–6.
188. Villar-Garea A, Fraga MF, Espada J, Esteller M. Procaine is a DNA-demethylating agent with growth-inhibitory effects in human cancer cells. Cancer Res. 2003;63:4984–9.
189. Li YC, Wang Y, Li DD, Zhang Y, Zhao TC, Li CF. Procaine is a specific DNA methylation inhibitor with anti-tumor effect for human gastric cancer. J Cell Biochem. 2018;119:2440–9.
190. Dueñas-Gonzalez A, Coronel J, Cetina L, González-Fierro A, Chavez-Blanco A, Taja-Chayeb L. Hydralazine-valproate: a repositioned drug combination for the epigenetic therapy of cancer. Expert Opin Drug Metab Toxicol. 2014;10:1433–44.
191. Segura-Pacheco B, Trejo-Becerril C, Perez-Cardenas E, Taja-Chayeb L, Mariscal I, Chavez A, et al. Reactivation of tumor suppressor genes by the cardiovascular drugs hydralazine and procainamide and their potential use in cancer therapy. Clin Cancer Res. 2003;9:1596–603.
192. Kuck D, Caulfield T, Lyko F, Medina-Franco JL. Nanaomycin A selectively inhibits DNMT3B and reactivates silenced tumor suppressor genes in human cancer cells. Mol Cancer Ther. 2010;9:3015–23.
193. Giannopoulou AF, Velentzas AD, Konstantakou EG, Avgeris M, Katarachia SA, Papandreou NC, et al. Revisiting histone deacetylases in human tumorigenesis: The paradigm of urothelial bladder cancer. Int J Mol Sci. 2019;20:1291.
194. Siegel D, Hussein M, Belani C, Robert F, Galanis E, Richon VM, et al. Vorinostat in solid and hematologic malignancies. J Hematol Oncol. 2009;2.
195. Finnin MS, Donigian JR, Cohen A, Richon VM, Rifkind RA, Marks PA, et al. Structures of a histone deacetylase homologue bound to the TSA and SAHA inhibitors. Nature. 1999;401:188–93.
196. Tang D, Yao R, Zhao D, Zhou L, Wu Y, Yang Y, et al. Trichostatin A reverses the chemoresistance of lung cancer with high IGFBP2 expression through enhancing autophagy. Sci Rep. 2018;8.
197. Yee AJ, Raje NS. Panobinostat and multiple myeloma in 2018. Oncologist. 2018;23:516–7.
198. Lobo J, Guimarães-Teixeira C, Barros-Silva D, Miranda-Gonçalves V, Camilo V, Guimarães R, et al. Efficacy of HDAC inhibitors belinostat and panobinostat against cisplatin-sensitive and cisplatin-resistant testicular germ cell tumors. Cancers (Basel). 2020;12:2903.
199. Vandermolen KM, McCulloch W, Pearce CJ, Oberlies NH. Romidepsin (Istodax, NSC 630176, FR901228, FK228, depsipeptide): a natural product recently approved for cutaneous T-cell lymphoma. J Antibiot (Tokyo). 2011; 525–531.
200. Pattarawat P, Wallace S, Pfisterer B, Odoi A, Wang HCR. Formulation of a triple combination gemcitabine plus romidepsin + cisplatin regimen to efficaciously and safely control triple-negative breast cancer tumor development. Cancer Chemother Pharmacol. 2020;85:141–52.
201. Wang W, Fang D, Zhang H, Xue J, Wangchuk D, Du J, et al. Sodium butyrate selectively kills cancer cells and inhibits migration in colorectal cancer by targeting thioredoxin-1. Onco Targets Ther. 2020;13:4691–704.
202. Iannelli F, Zotti AI, Roca MS, Grumetti L, Lombardi R, Moccia T, et al. Valproic Acid synergizes with cisplatin and cetuximab in vitro and in vivo in head and neck cancer by targeting the mechanisms of resistance. Front Cell Dev Biol. 2020;8.
203. Bray F, Ferlay J, Soerjomataram I, Siegel RL, Torre LA, Jemal A. Global cancer statistics 2018: GLOBOCAN estimates of incidence and mortality worldwide for 36 cancers in 185 countries. CA Cancer J Clin. 2018;68:394–424.
204. Kamat AM, Hahn NM, Efstathiou JA, Lerner SP, Malmström PU, Choi W, et al. Bladder cancer. Lancet. 2016;388:2796–810.
205. Chen Z, Ding W, Xu K, Tan J, Sun C, Gou Y, et al. The 1973 WHO Classification is more suitable than the 2004 WHO Classification for predicting prognosis in non-muscle-invasive bladder cancer. PLoS ONE. 2012;7:e47199.
206. Humphrey PA, Moch H, Cubilla AL, Ulbright TM, Reuter VE. The 2016 WHO classification of tumours of the urinary system and male

genital organs—part B: prostate and bladder tumours. Eur Urol. 2016;70:106–19.
207. Woldu SL, Şanli Ö, Lotan Y. Tackling non-muscle invasive bladder cancer in the clinic. Expert Rev Anticancer Ther. 2017;17:467–80.
208. Amin MB, Edge S, Greene F, Byrd DR, Brookland RK, Washington MK, et al. AJCC Cancer Staging Manual. Eighth edn. Springer. 2017.
209. Bellmunt J, Orsola A, Leow JJ, Wiegel T, De Santis M, Horwich A. Bladder cancer: ESMO practice guidelines for diagnosis, treatment and follow-up. Ann Oncol. 2014;25(Suppl 3):40–8.
210. Lobo J, Jerónimo C, Henrique R. Targeting the immune system and epigenetic landscape of urological tumors. Int J Mol Sci. 2020;21:829.
211. Herr HW, Morales A. History of bacillus Calmette-Guerin and bladder cancer: an immunotherapy success story. J Urol. 2008;179:53–6.
212. Zhang C, Berndt-Paetz M, Neuhaus J. Identification of key biomarkers in bladder cancer: evidence from a bioinformatics analysis. Diagnostics. 2020;10.
213. Agundez M, Grau L, Palou J, Algaba F, Villavicencio H, Sanchez-Carbayo M. Evaluation of the methylation status of tumour suppressor genes for predicting bacillus Calmette-Guérin response in patients with T1G3 high-risk bladder tumours. Eur Urol. 2011;60:131–40.
214. Alvarez-Múgica M, Fernández-Gómez JM, Cebrian V, Fresno F, Escaf S, Sánchez-Carbayo M. Polyamine-modulated factor-1 methylation predicts bacillus Calmette-Guérin response in patients with high-grade non-muscle-invasive bladder carcinoma. Eur Urol. 2013;63:364–70.
215. Ahlén Bergman E, Hartana CA, Johansson M, Linton LB, Berglund S, Hyllienmark M, et al. Increased CD4 + T cell lineage commitment determined by CpG methylation correlates with better prognosis in urinary bladder cancer patients. Clin Epigenet. 2018;10.
216. Hartana CA, Ahlén Bergman E, Broomé A, Berglund S, Johansson M, Alamdari F, et al. Tissue-resident memory T cells are epigenetically cytotoxic with signs of exhaustion in human urinary bladder cancer. Clin Exp Immunol. 2018;194:39–53.
217. Koestler DC, Usset J, Christensen BC, Marsit CJ, Karagas MR, Kelsey KT, et al. DNA methylation-derived neutrophil-tolymphocyte ratio: An epigenetic tool to explore cancer inflammation and outcomes. Cancer Epidemiol Biomark. 2017;26:328–38.
218. Nunes SP, Henrique R, Jerónimo C, Paramio JM. DNA Methylation as a Therapeutic Target for Bladder Cancer. Cells. 2020;9:1850.
219. Maraver A, Fernandez-Marcos PJ, Cash TP, Mendez-Pertuz M, Dueñas M, Maietta P, et al. NOTCH pathway inactivation promotes bladder cancer progression. J Clin Invest. 2015;125:824–30.
220. Rampias T, Vgenopoulou P, Avgeris M, Polyzos A, Stravodimos K, Valavanis C, et al. A new tumor suppressor role for the Notch pathway in bladder cancer. Nat Med. 2014;20:1199–205.
221. Ramakrishnan S, Hu Q, Krishnan N, Wang D, Smit E, Granger V, et al. Decitabine, a DNA-demethylating agent, promotes differentiation via NOTCH1 signaling and alters immune-related pathways in muscle-invasive bladder cancer. Cell Death Dis. 2017;8.
222. Segovia C, San José-Enériz E, Munera-Maravilla E, Martínez-Fernández M, Garate L, Miranda E, et al. Inhibition of a G9a/DNMT network triggers immune-mediated bladder cancer regression. Nat Med. 2019;25:1073–81.

## Publisher's Note

Springer Nature remains neutral with regard to jurisdictional claims in published maps and institutional affiliations.

**Ready to submit your research? Choose BMC and benefit from:**

- fast, convenient online submission
- thorough peer review by experienced researchers in your field
- rapid publication on acceptance
- support for research data, including large and complex data types
- gold Open Access which fosters wider collaboration and increased citations
- maximum visibility for your research: over 100M website views per year

**At BMC, research is always in progress.**

**Learn more** biomedcentral.com/submissions

BMC

CDDpress

www.nature.com/cddiscovery

ARTICLE OPEN

# Modulation of tumor microenvironment by targeting histone acetylation in bladder cancer

Sandra P. Nunes[1,2,3,4], Lucia Morales[2,3,5], Carolina Rubio[2,3,5], Ester Munera-Maravilla[2,3,5], Iris Lodewijk[2,3,5], Cristian Suárez-Cabrera[2,3,5], Victor G. Martínez[2,3,5], Mercedes Pérez-Escavy[2,3], Miriam Pérez-Crespo[2,3,5], Miguel Alonso Sánchez[2,3], Esther Montesinos[2,3], Edurne San José-Enériz[5,6], Xabier Agirre[5,6], Felipe Prósper[5,6,7], Antonio Pineda-Lucena[8], Rui Henrique[1,9,10], Marta Dueñas[2,3,5], Margareta P. Correia[1,10], Carmen Jerónimo[1,10] and Jesús M. Paramio[2,3,5]✉

© The Author(s) 2024

Alterations in the epigenetic machinery in both tumor and immune cells contribute to bladder cancer (BC) development, constituting a promising target as an alternative therapeutic option. Here, we have explored the effects of a novel histone deacetylase (HDAC) inhibitor CM-1758, alone or in combination with immune checkpoint inhibitors (ICI) in BC. We determined the antitumor effects of CM-1758 in various BC cell lines together with the induction of broad transcriptional changes, with focus on the epigenetic regulation of PD-L1. Using an immunocompetent syngeneic mouse model of metastatic BC, we studied the effects of CM-1758 alone or in combination with anti-PD-L1 not only on tumor cells, but also in the tumor microenvironment. In vitro, we found that CM-1758 has cytotoxic and cytostatic effects either by inducing apoptosis or cell cycle arrest in BC cells at low micromolar levels. PD-L1 is epigenetically regulated by histone acetylation marks and is induced after treatment with CM-1758. We also observed that treatment with CM-1758 led to an important delay in tumor growth and a higher CD8 + T cell tumor infiltration. Moreover, anti-PD-L1 alone or in combination with CM-1758 reprogramed macrophage differentiation towards a M1-like polarization state and increased of pro-inflammatory cytokines systemically, yielding potential further antitumor effects. Our results suggest the possibility of combining HDAC inhibitors with immunotherapies for the management of advanced metastatic BC.

*Cell Death Discovery* (2024)10:1 ; https://doi.org/10.1038/s41420-023-01786-3

## INTRODUCTION

Bladder cancer (BC) is the tenth most common cancer diagnosed worldwide, listing as the sixth most incident cancer in men [1]. About 75% of the patients are diagnosed with nonmuscle-invasive BC (NMIBC), whereas the remaining 25% display muscle-invasive BC (MIBC) [2]. Although NMIBC patients are associated with a good outcome, up to 70% of patients recur, with a significant percentage progressing to MIBC [3]. The treatment of MIBC comprises radical cystectomy and platin-based chemotherapy in a neoadjuvant or adjuvant setting [4]. Nevertheless, MIBC patients considered to be unfit for chemotherapy or surgery, presenting comorbidities or metastatic disease have few therapeutic options available. The implementation of immune checkpoint inhibitors (ICI), such as anti-programmed death-ligand 1 (PD-L1), as an option for patients positive for PD-L1 expression led to an increase of overall survival [5]. However, the percentage of patients with significant clinical response ranges between 17 and 26%, which is quite limited [6]. Thus, understanding the mechanisms behind BC development can unravel new therapeutic targets and strategies, with the main goal of improving patients' survival.

Epigenetic landscape reprograming is one of the main mechanisms contributing to BC progression and is considered an emergent hallmark of cancer [7]. Histone acetylation is of the most prominent mechanisms involved in gene expression regulation favoring tumorigenesis [8]. Accordingly, histone acetylation is involved in transcriptional activation, through the addition of acetyl groups in lysine residues of histone tails by histone acetyltransferases (HATs). Histone deacetylases (HDACs), by removing acetylation marks, lead to transcriptional repression by turning DNA into a closed-chromatin state [9].

Since epigenetic marks represent an enticing target for cancer therapeutics, a group of drugs has been developed throughout the years targeting several epigenetic enzymes, called epigenetic modulating drugs or epidrugs [10]. The most well-known HDAC inhibitors (HDACi) comprise hydroxamic acids, including belinostat, vorinostat and panobinostat, all pan-HDACi FDA-approved for

[1]Cancer Biology and Epigenetics Group, Research Center of IPO Porto (CI-IPOP)/CI-IPOP@RISE (Health Research Network), Portuguese Oncology Institute of Porto (IPO-Porto)/Porto Comprehensive Cancer Center Raquel Seruca (Porto.CCC), Porto, Portugal. [2]Molecular Oncology Unit, Centro de Investigaciones Energéticas, Medioambientales y Tecnológicas (CIEMAT), Madrid, Spain. [3]Biomedical Research Institute I+12, University Hospital "12 de Octubre", Madrid, Spain. [4]Doctoral Program in Biomedical Sciences, ICBAS - School of Medicine and Biomedical Sciences, University of Porto, Porto, Portugal. [5]Centro de Investigación Biomédica en Red de Cáncer (CIBERONC), Madrid, Spain. [6]Hemato-Oncology Program, Center for Applied Medical Research (CIMA), Universidad de Navarra, IDISNA, Pamplona, Spain. [7]Departmento de Hematología, Clínica Universidad de Navarra, and CCUN, Universidad de Navarra, Pamplona, Spain. [8]Small-Molecule Discovery Platform, Molecular Therapeutics Program, Center for Applied Medical Research (CIMA), Universidad de Navarra, Pamplona, Spain. [9]Department of Pathology, Portuguese Oncology Institute of Porto, Porto, Portugal. [10]Department of Pathology and Molecular Immunology, ICBAS - School of Medicine & Biomedical Sciences, University of Porto, Porto, Portugal. ✉email: jesusm.paramio@ciemat.es

Received: 28 June 2023 Revised: 12 December 2023 Accepted: 19 December 2023
Published online: 04 January 2024

several haematological cancers [11]. HDACi also display antitumoral effects in BC cells [12, 13].

Most studies comprising epidrugs focus on the effects on cancer cells, yet the tumor microenvironment cells can also be affected since they are also epigenetically regulated. HDACi have been previously shown to modulate tumor microenvironment and improve response to ICI in BC and other cancer types [14–16]. Specifically, the combination of entinostat, a selective HDAC1/3 inhibitor, and anti-PD-1 therapy led to complete responses in an immunocompetent mouse model of BC [16]. Having into account the pre-clinical evidence, several clinical trials are being carried out to evaluate the efficacy of the combination of epidrugs and ICI in various solid tumors including BC [17]. Nevertheless, HDACi were shown to have low bioavailability, limited half-life and dose-limiting toxicity, hampering their use in clinical practice for cancer treatment [18]. Thus, the search for new epidrugs with more specific epigenetic targets at low therapeutic doses would fast-track their usage in clinical practice.

Here, we describe the antitumor efficacy of CM-1758, a novel HDAC inhibitor, in BC in vitro and in vivo models. First, the cytotoxic/cytostatic effects of CM-1758 were evaluated in several BC cell lines. Then, the effects on immune-related pathways were also studied, namely by assessing PD-L1 expression and its epigenetic regulation. Since CM-1758 up-regulated PD-L1, we postulated that combining CM-1758 and PD-L1 blockage could be a promising strategy for BC treatment. For that, an immunocompetent syngeneic mouse model of aggressive BC was used to assess CM-1758 effects in vivo alone or in combination with anti-PD-L1. The effects of CM-1758 were evaluated not only in tumor cells, but also in the tumor microenvironment comprising immune and non-immune cells and cytokine profile. CM-1758 displayed significant antitumor effects in vitro and in vivo concomitantly with tumor microenvironment remodeling.

## RESULTS

### CM-1758 displayed cytotoxic/cytostatic effects in bladder cancer cells

The effects of the CM-1758 inhibitor were evaluated in a wide array of BC cell lines. CM-1758 demonstrated effects on the low micromolar range, with $IC_{50}$ ranging between 0.33 and 4.8 μM (Fig. 1a; Supplementary Table S4). Remarkably, CM-1758 also affected the cell cycle, with a decrease in the percentage of S-phase cells observed for 253 J, 5637, J82 and TCCSUP cell lines after treatment (Fig. 1b). J82 cells also displayed higher percentage of G2/M phase in the treated cells, which was more evident for RT112 cells (Fig. 1b). The mouse 4K5 cell line disclosed cell arrest at the S-phase (Fig. 1b). Interestingly, 253 J and RT112 cells displayed a reduced percentage of G0/G1 phase upon treatment (Fig. 1b).

A decrease in the percentage of live cells in 253 J, RT112, TCCSUP and 4K5 treated cells was observed, in parallel with an increase in the percentage of cells in late apoptosis (Fig. 1c and d), with a more pronounced effect in 253 J and RT112 cell lines (Fig. 1c and d). 253 J, RT112, TCCSUP and 4K5 cells showed a higher percentage of early apoptosis, while only 253 J displayed higher levels of necrotic cells, with no apparent differences for the other cell lines (Fig. 1c and d). Altogether, these data demonstrate that CM-1758 has both cytotoxic and cytostatic effects in BC cell lines, either by inducing cell cycle arrest and/or apoptosis at low $IC_{50}$ micromolar concentration.

### CM-1758 induced changes in the transcriptomic profile of bladder cancer cells

Hereafter, we evaluated the transcriptomic profile of BC cells by RNA-seq after treatment with the $IC_{50}$ doses of CM-1758. Treatment with CM-1758 drove marked changes in the transcriptomic profile of BC cells (Fig. 2a). Remarkably, there was limited overlap in the genes upregulated (Fig. 2b1) or downregulated (Fig. 2b2) considering all cell lines, although all cell lines showed homogeneous clustering in PCA analysis when comparing control vs. treated (Supplementary Fig. S5a–e). GSEA (Supplementary Fig. S6a–d) and GSVA analysis (Fig. 2c) revealed that the treatment decreased the expression of multiple genes involved in cell proliferation, such as E2F and MYC targets and epithelial-mesenchymal transition. Moreover, in some cell lines there was an effect on various immunological pathways such as IL-2/STAT5, IFN-α, IFN-γ and TNF- α signaling via NF- κB (Fig. 2c). However, these effects on immunological pathways were cell line dependent. Having into account the genes upregulated by CM-1758, further analyzes of the transcription factors and histone using the Enrichr webtool revealed a prominent role of IRF1 and IRF8 as well as acetylation of various histone H2B residues, more noticeable in TCCSUP cells (Fig. 2d). Also, analyzes of transcriptional regulatory networks (regulons) showed that some key elements in BC such as *FOXM1* were downregulated, while others, such as *STAT3*, were predominantly upregulated (Fig. 2e, Supplementary Fig. 6e). We also observed that many regulons modulating chromatin remodeling were also affected by treatment, including epigenetic machinery related not only to acetylation, but also histone and DNA methylation including lysine demethylases (KDMs) and DNA methyltransferases (DNMTs) (Fig. 2f). Overall, CM-1758 led to profound changes in the transcriptomic profile of BC cells, affecting pathways related to tumor cell aggressiveness and epigenetic machinery.

### CM-1758 treatment regulated PD-L1 expression by induction of histone acetylation

Next, we studied the effects of CM-1758 on histone acetylation in BC cell lines. We observed increased H3, H3K9 and H3K27 acetylation levels by western blot (Fig. 3a and Supplementary Fig. S7a) in all the analyzed cell lines after treatment with CM-1758. Of note, the expression of HDACs was altered in BC cells either by transcript or protein levels (Supplementary Fig. S7b and c). Since DNA methylation and histone modifications are two epigenetic mechanisms intertwined in the regulation of gene expression, we also explored the global levels of 5-methylcytosine in J82 and 4K5 BC cells. Immunofluorescence analyzes demonstrated that total 5-methylcytosine levels were decreased in J82 and 4K5 BC cells after CM-1758 treatment (Fig. 3b and c), which was paralleled by decreased DNMTs' levels (Supplementary Fig. S7c and d). The lower levels of DNA methylation could be a direct consequence of the higher levels of acetylation observed after treatment with CM-1758. These results show that CM-1758 treatment affects histone acetylation, but also other epigenetic mechanisms, such as DNA methylation indirectly.

Some epidrugs were shown by others to have synergistic effects with immunotherapies, since drug treatments can induce immune checkpoints' expression, conferring higher sensitivity to ICI [15, 16]. Furthermore, transcriptomic data showed that CM-1758 has effects on immune pathways in cancer cells. Thus, we investigated whether the global changes in acetylation and DNA methylation levels induced by CM-1758 treatment could have an impact on PD-L1 expression in BC cell lines, as previously reported for other solid tumors [19, 20]. Remarkably, we observed that PD-L1 levels increase in cells after CM-1758 treatment at both mRNA (Fig. 3d) and membrane protein (Fig. 3e and f) levels. Afterwards, we hypothesized whether this increased expression was attributable to epigenetic regulation of PD-L1. CUT&RUN experiments showed that H3K9ac and H3K27ac marks were increased at the PD-L1 promoter in 4 different regions, from 100 to 1200 bp upstream of initiation transcription site, after CM-1758 treatment (Fig. 3g and h). On the other hand, DNA methylation levels in these regions, assessed by qMSP, were not affected by treatment showing low levels of DNA methylation on the analyzed CGs (Supplementary Fig. S8a and b). These results indicated that CM-1758 increased PD-L1 levels through its effect on HDACs and, consequently, PD-L1 promoter acetylation marks.

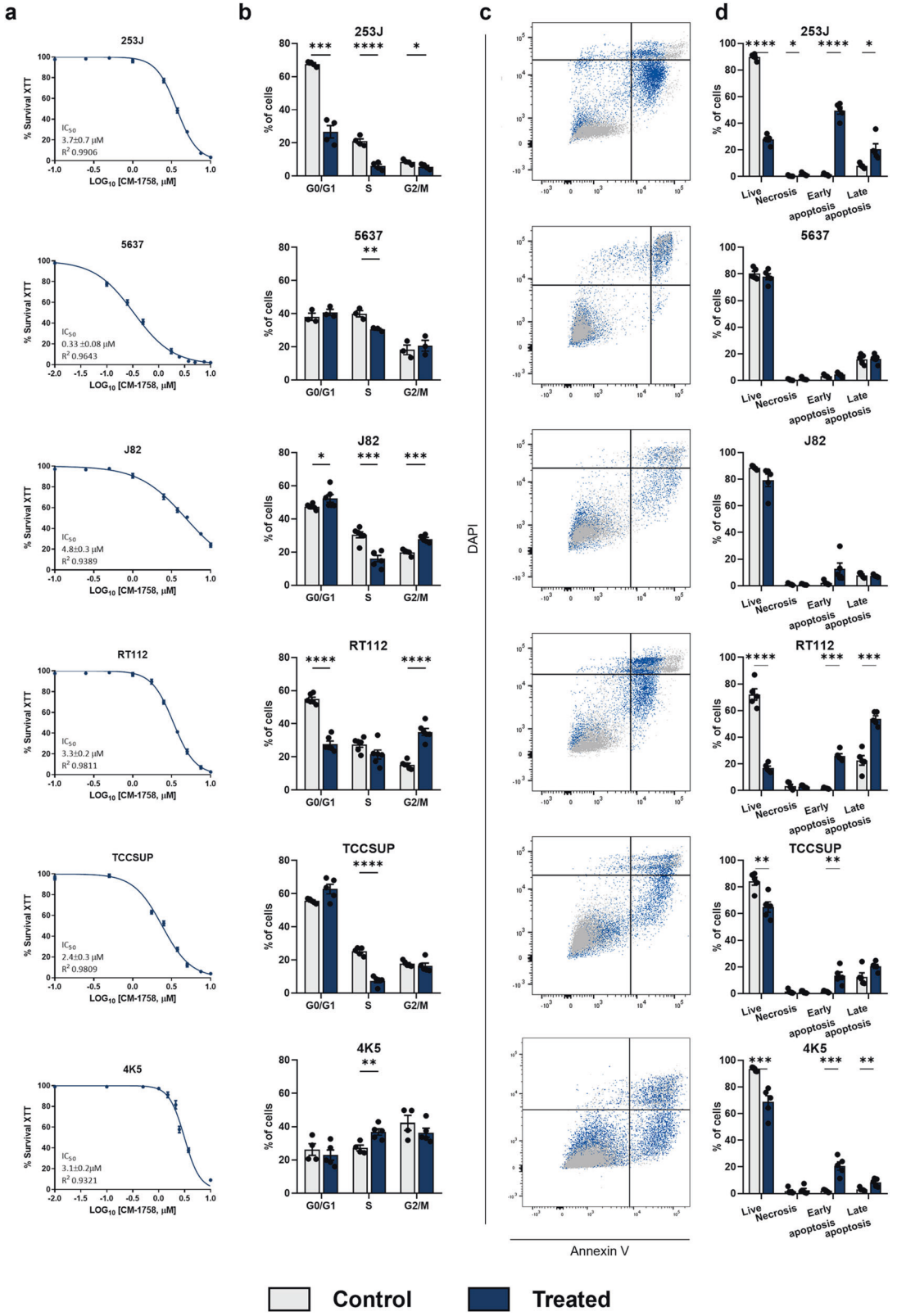


**Fig. 1 Cytotoxic and cytostatic effects of CM-1758 in bladder cancer cell lines. a** Survival curves with the $IC_{50}$ value for the BC cell lines 253 J, 5637, J82, RT112, TCCSUP and 4K5 (percentage of survival with calculated with XTT vs $log_{10}$ of CM-1758 concentrations) with respective standard deviation and $R^2$. **b** Cell cycle profiles containing G0/G1, S and G2/M phases for 253 J, 5637, J82, RT112, TCCSUP and 4K5 after treatment with CM-1758. **c** Representative gating of live (DAPI negative, annexin V negative), necrotic (DAPI positive, annexin V negative), early apoptotic (DAPI negative, annexin V positive) and late apoptotic cells (DAPI positive, annexin V positive) cells. **d** Percentage of live, necrotic, early and late apoptotic cells for all cell lines after treatment with CM-1758. Non-treated cells are represented in grey and CM-1758 treated cells are shown in blue. Treatment with CM-1758 was given for 48 h with $IC_{50}$ dose calculated for each cell line for cell cycle and annexin V analyzes. Data shown are the mean of ≥3 experiments ± SEM. *P*-values are represented as ns – not significant, *<0.05, **<0.01, ***<0.001 and ****<0.0001.

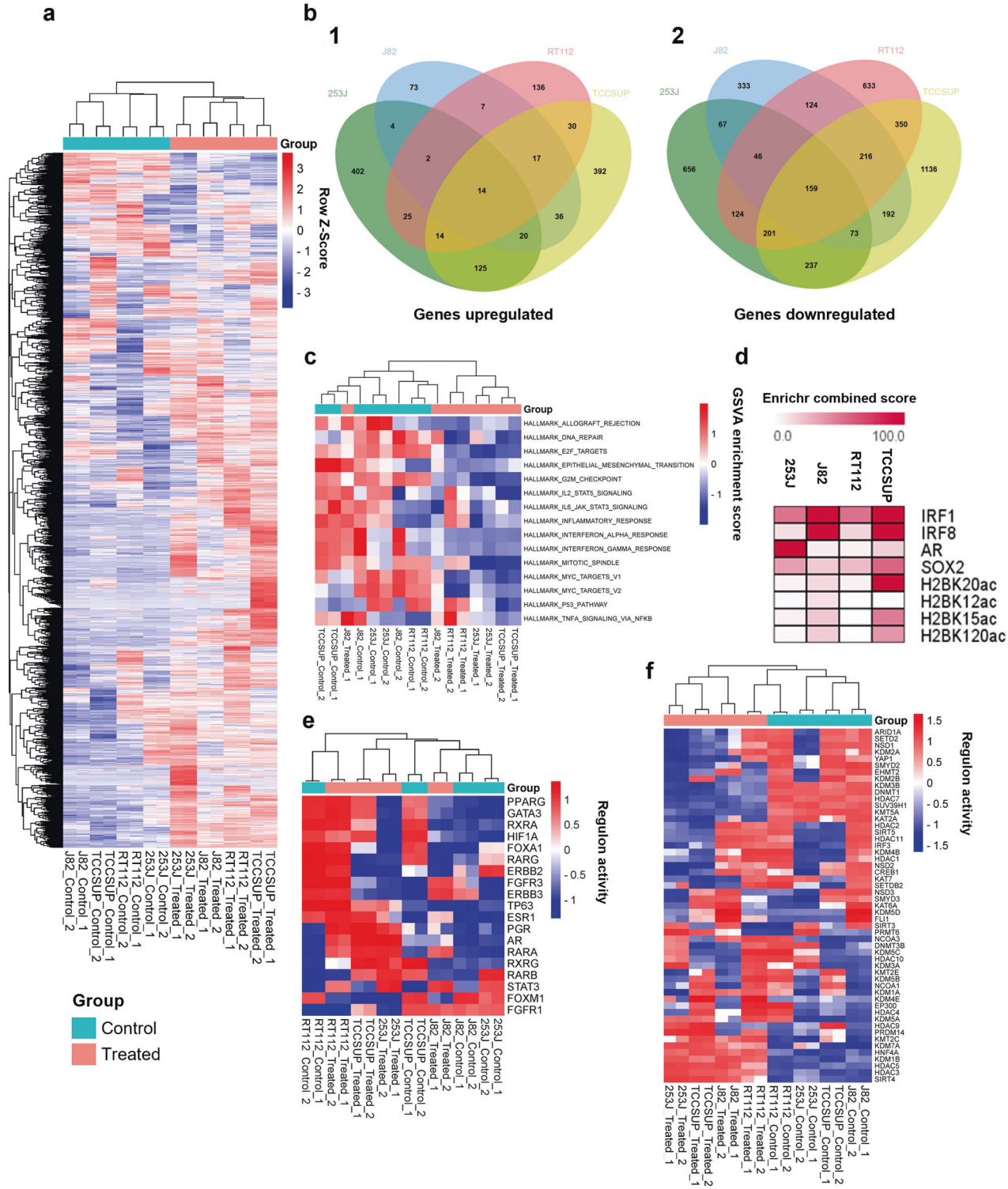


**Fig. 2 CM-1758 effects on the transcriptomic profile of 253 J, J82, RT112 and TCCSUP cells. a** Heatmap of the dysregulated genes between untreated control vs. treated cells with $IC_{50}$ dose of CM-1758. Genes and groups (control and treated) are hierarchically clustered. **b** Venn diagrams of genes (1) up and (2) downregulated in treated cells *vs.* control cells. **c** Heatmap of GSVA analysis showing the main signaling pathways from hallmarks in cancer enriched in control and treated cells. Control and treated groups are hierarchically clustered. **d** Enrichr analysis of the upregulated genes in all cell lines when compared to the respective untreated control cells. **e** Regulon activity profiles for potential regulators associated with BC. Control and treated groups are hierarchically clustered. **f** Regulon activity profiles for potential regulators associated with chromatin remodeling. Control and treated groups are hierarchically clustered. Control denotes untreated cells, whereas treated refers to CM-1758 treated cells. Treatment with CM-1758 was given for 48 h with $IC_{50}$ dose calculated for each cell line. Two independent experiments were included for each cell line and condition.

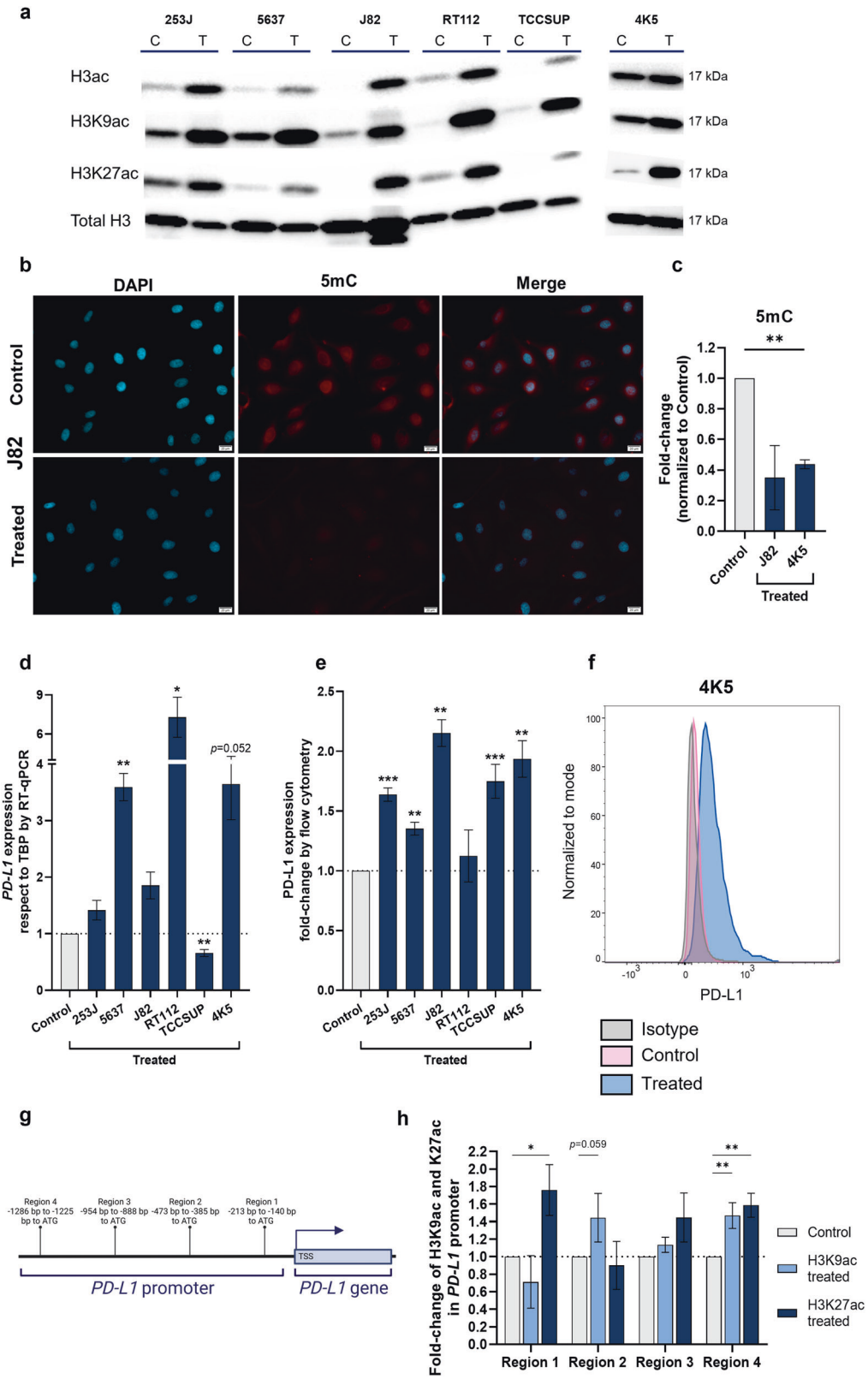


**CM-1758 and anti-PD-L1 as a therapeutic strategy in a bladder cancer immunocompetent mouse model**

The data obtained concerning increased PD-L1 expression together with gene expression changes as a consequence of CM-1758 treatment in vitro prompted us to study in vivo the effects of CM-1758 combined with anti-PD-L1 using a double knock-out (*Pten*$^{F/F}$, *Trp53*$^{F/F}$; DKO) immunocompetent BC mouse model. For that, GFP-expressing 4K5 cells (derived from a BC tumor developed in a DKO mouse injected with adenoviruses expressing Cre-recombinase under the control of keratin 5

**Fig. 3 Histone acetylation and DNA methylation levels after treatment with CM-1758. PD-L1 epigenetic regulation by promoter acetylation. a** Western blot analysis of total acetylation of H3 (H3ac), acetylation of lysine 9 of histone 3 (H3K9ac) and acetylation of lysine 27 of histone 3 (H3K27ac) respect to total histone 3 (H3) levels for all cell lines after treatment with CM-1758. C – Control, T - Treated. **b** Representative immunofluorescence for 5-methylcytosine of J82 cells after treatment with CM-1758 (in red). Cell nuclei were identified by DAPI staining (in blue). Scale bar 20 µm. **c** Quantification of 5-methylcytosine levels by immunofluorescence after treatment with CM-1758 represented by fold-change respective to the untreated control cells in J82 and 4K5 cells. **d** Relative expression by RT-qPCR of *PD-L1* respect to TBP for all BC lines after treatment with CM-1758. **e** PD-L1 expression evaluated by flow cytometry represented by fold-change respective to non-treated control cells and (**f**) Single parameter histogram of mean intensity fluorescence (MFI) of PD-L1 levels with CM-1758 treatment in 4K5 cells (**g**) Schematic representation of the *PD-L1* promoter regions evaluated by CUT&RUN (**h**) Presence of H3K9 and H3K27 acetylation in four different regions [region 1 -213 to -140 bp, region 2 -473 to -385 bp, region 3 -954 to -888 bp and region 4 -1286 to -1225 bp before the transcription start site (TSS)] of *PD-L1* promoter after treatment with CM-1758 evaluated by CUT&RUN. Values are represented as fold-change relative to the untreated control cells. Cells were treated with CM-1758 for 48 h with the $IC_{50}$ dose calculated for each cell line. Data shown are the mean of ≥3 experiments ± SEM. *P*-values are represented as ns – not significant, *<0.05, **<0.01 and ***<0.001.

promoter) were subcutaneously injected in the flank of syngeneic mice and treated with CM-1758 and/or PD-L1 blockade (Fig. 4a). Even with only two weeks of treatment period, an anti-tumoral effect of CM-1758 was observed, which was slightly increased by the combination with anti-PD-L1 (Table 1, Fig. 4b, c and d1, 2, 3 and 4; Supplementary Fig. S9a, b, c, and d). Both Ki67 and BrdU immunohistochemistry analyses demonstrated a significant decrease in tumor cell proliferation levels in CM-1758 treatment group (Fig. 4e and f1, 2, 3 and 4; Supplementary Figs. S9e and S9f1, 2, 3 and 4). Furthermore, more prominent immune infiltrates were found in the tumors treated with the combination, confirmed by the immunostaining analysis for CD8 + T cells (Supplementary Fig. 9g). The assessment of necrotic areas revealed that CM-1758, either alone or in combination with anti-PD-L1, resulted in a higher percentage of necrotic regions within the examined tumors (Fig. 4g). Interestingly, the combination-treated tumors displayed a clear tendency revealing a higher infiltration of CD8 + T cells in necrotic areas compared to control, anti-PD-L1, and CM-1758-treated tumors (Figs. 4h and i1, 2, 3 and 4). However, it did not reach statistical significance, and there was no observed correlation between these variables (Fig. 4h; Supplementary Fig. 9h, i, j, and k).

### CM-1758 treatment increased CD8+ cytotoxic T cells presence in the tumor microenvironment and promoted pro-inflammatory cytokine release

Treatment with CM-1758, alone or in combination with anti-PD-L1, led to changes in tumor lymphoid repertoire. We did not find any differences in CD3 + T cells percentage respect to the CD45+ leucocytes population (Fig. 5a). However, when we looked for the type of lymphocytes present in the tumor, we did observe a reduction in CD4 + T cells, alongside with an increase in CD8 + T cells in tumors treated with CM-1758 or upon combination treatment (Fig. 5b and c), whereas no significant differences were observed for the B cell percentage (Fig. 5d). Thus, CM-1758 led to increased CD8+ cytotoxic T cells presence independently of immunotherapy, whereas CD4 + T cells detection was decreased (Fig. 5e).

The non-immune compartment of the tumor microenvironment also underwent changes upon ICI and CM-1758 treatments (Fig. 5f, g and h). The percentage of blood and lymphatic endothelial cells in the tumor significantly decreased after treatment with CM-1758+anti-PD-L1 in comparison with the control and anti-PD-L1 groups (Fig. 5f and g). On the other hand, the percentage of lymphatic endothelial cells was increased in the CM-1758 treated group in comparison with control, anti-PD-L1 and combination groups (Fig. 5g). The percentage of fibroblasts was increased in both anti-PD-L1 and CM-1758 groups (Fig. 5h). Almost all fibroblasts found in the tumor microenvironment were positive for α-SMA, a cancer-associated fibroblasts (CAFs) marker (Supplementary Fig. S10a; mean percentage of cells positive for α-SMA higher than 97%).

Next, we explored whether the treatment with CM-1758 might led to the release of pro-inflammatory cytokines systemically. Thus, multiple cytokines were measured in plasma upon different treatments using a cytometric bead-based assay (mean concentrations of each cytokine per treatment group are displayed in Supplementary Table S5). Anti-PD-L1 treatment led to an increase in IFN-γ, which was further boosted by the combination with CM-1758 (Fig. 5i). Moreover, increased TNF-α and IL-12 levels were observed in both anti-PD-L1 and CM-1758 treatment groups. The combination treatment increased CCL5 levels mainly by action of the anti-PD-L1 therapy and with no changes in CCL5 levels on the CM-1758 group, suggesting that CCL5 is regulated by ICI (Fig. 5i). The same seems to happen with CXCL10, which levels were significantly increased in the anti-PD-L1 treatment group, with the same tendency observed for the combination (Fig. 5i). These results highlight the importance of epigenetic mechanisms and ICI in cytokines' expression regulation, which remains a poorly explored topic in BC.

### Anti-PD-L1 alone or in combination with CM-1758 reprogramed macrophages towards a M1-like polarization

We also investigated whether anti-PD-L1 and/or CM-1758 treatments could induce myeloid compartment remodeling. Although no differences were apparent in the percentage of myeloid cell present in the tumor (Fig. 6a), a lower percentage of phagocytic myeloid cells, identified by their positivity for GFP arising from the phagocytosis of GFP-expressing tumor cells, was found for anti-PD-L1 treated groups alone or in combination with CM-1758 (Fig. 6b). Furthermore, a significant decrease in the percentage of tumor cells was found for the treatment groups, including CM-1758 alone or in combination as compared with non-treated control mice (Fig. 6c).

Anti-PD-L1 treatment alone or in combination with CM-1758 led to significantly lower detectable PD-L1 levels in myeloid cells, both in all myeloid cells and phagocytic myeloid cells (Fig. 6d–f). No significant changes were found in tumor cells' PD-L1 levels, showing that the anti-PD-L1 treatment mainly affected the myeloid cell population (Fig. 6g). Additionally, no changes at PD-L1 transcriptional levels were observed in the tumor bulk, indicating that the decreased cell surface PD-L1 detection might be due to anti-PD-L1 antibody still bound to the cells or to PD-L1 loss at the cell membrane by internalization processes (Supplementary Fig. S10b). On the other hand, CM-1758 alone seemed to slightly increase PD-L1 levels in tumor cells as observed in the in vitro conditions, although without statistical significance (Fig. 6g).

Compared with untreated samples, single treatment with anti-PD-L1 or CM-1758 led to a partial decrease in total macrophages (Fig. 6h). Interestingly, anti-PD-L1 (alone or in combination) treatment increased the presence of M1-like macrophages, while decreasing M2-like macrophages (Fig. 6i–l). Contrarily, CM-1758 alone did not seem to have a major impact in macrophages polarization (Fig. 6i–l). These findings suggest that the shift of macrophages toward an M1-like pro-inflammatory polarization is dependent on ICI treatment, with no observed syngeneic effect in combination with CM-1758.

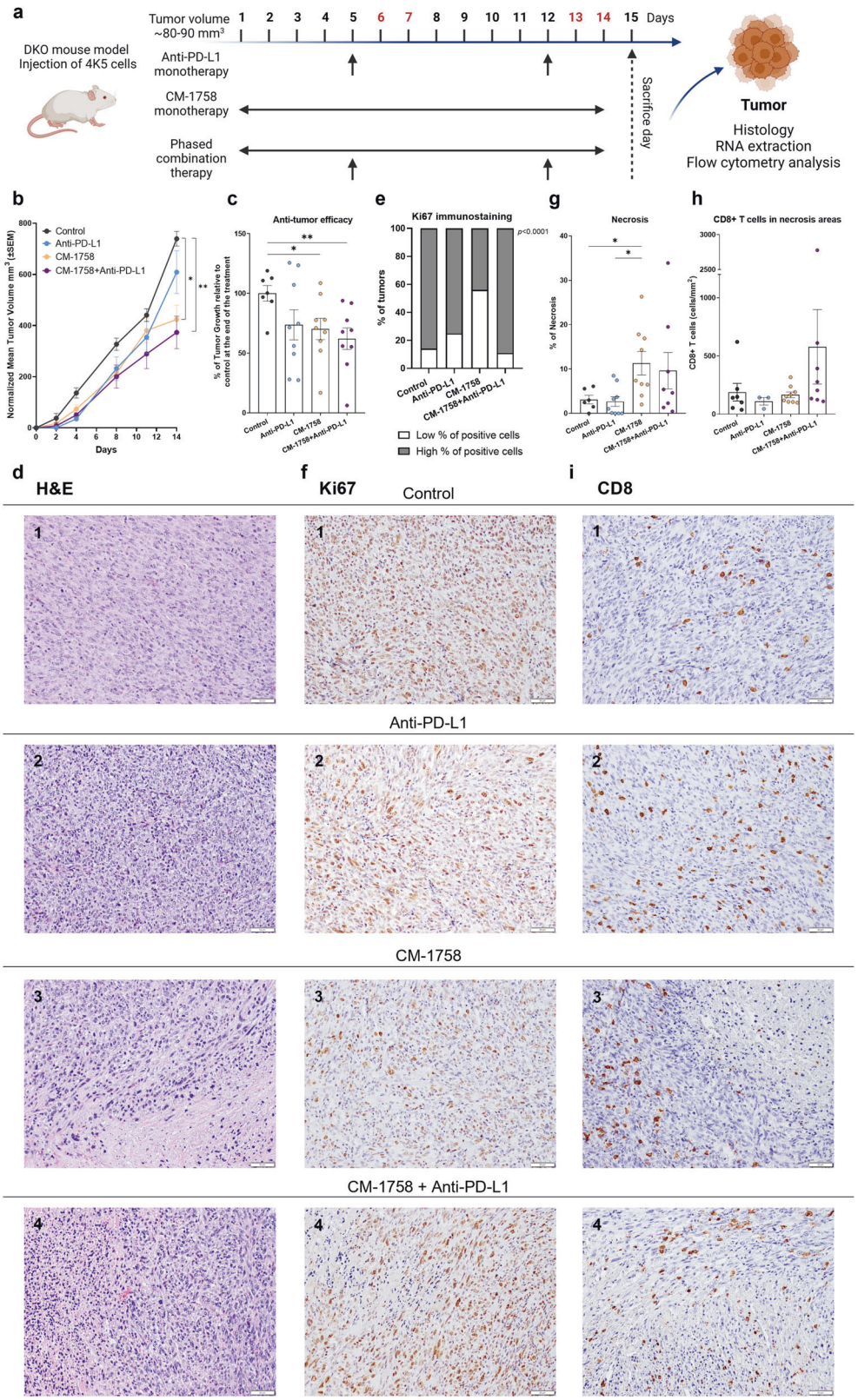


## DISCUSSION

BC represents a major public health concern due to its high incidence and prevalence, with current treatment options falling short to avoid disease recurrence and progression [1]. Although implementation of immunotherapy in advanced BC improved patients' overall survival, a significant percentage of BC patients does not respond or become unresponsive within the course of ICI treatment [21]. Thus, new treatment strategies, such as epidrugs, alone or in combination with immunotherapy, are currently being explored [17]. Several HDACi are FDA-approved for treatment of hematologic malignancies, and are under clinical trials for BC patients, with a confirmed improvement of overall survival [22].

**Fig. 4 In vivo effects of CM-1758 alone and in combination with immune checkpoint inhibitors. a** Schematic representation of the protocols used for treatment with CM-1758 and anti-PD-L1 alone or in combination. CM-1758 was applied for two weeks, five days a week with two rest days represented in red. Anti-PD-L1 was injected once a week for two weeks. Mice in all groups were sacrificed at day 15. Tumors were collected for histology, flow cytometry analysis and RNA extraction. Created with BioRender.com (**b**) Normalized tumor growth curves for the first day of treatment in control, anti-PD-L1, CM-1758 and CM-1758+anti-PD-L1 groups. **c** Anti-tumor efficacy of anti-PD-L1, CM-1758 and CM-1758+anti-PD-L1. **d** Representative H&E staining of the tumors from each group (1) control, (2) anti-PD-L1, (3) CM-1758 and (4) CM-1758+anti-PD-L1); **e** Graphical representation of percentage of Ki67 expression for each group. Cut-off was defined as <80% as low and >80% as high percentage of positive cells. **f** Representative immunohistochemistry staining of Ki67 for (1) control, (2) anti-PD-L1, (3) CM-1758, and (4) CM-1758+anti-PD-L1 tumors. **g** Percentage of necrosis present in tumors from each treatment group at the end of treatment of control, anti-PD-L1, CM-1758 or combination. **h** Number of CD8 + T cells (cells/mm$^2$) infiltrating in necrosis areas in control, anti-PD-L1, CM-1758 and CM-1758+anti-PD-L1 groups. Only tumors displaying necrosis areas were evaluated. **i** Representative immunohistochemistry staining of CD8 for (1) control, (2) anti-PD-L1, (3) CM-1758, and (4) CM-1758+anti-PD-L1 tumors. Graphs show individual values as the mean ± SEM for ≥8 mice included in each group. Scale bar 50 µM. *P*-values are represented as ns – not significant, *<0.05, **<0.01 and ***<0.001.

**Table 1.** Antitumor efficacy of anti-PD-L1, CM-1758 and CM-1758+anti-PD-L1 in comparison with the control group.

| Treatment group | Mean % T/C (± SD) | *p* value | | |
|---|---|---|---|---|
| | | vs. Control | vs. Anti-PD-L1 | vs. CM-1758 |
| Anti-PD-L1 | 74 ± 38 | 0.112 | - | - |
| CM-1758 | 70 ± 27 | 0.023 | 0.822 | - |
| CM-1758+Anti-PD-L1 | 62 ± 27 | 0.006 | 0.463 | 0.532 |

Percentage calculated as [T (tumor) / C (control)] x 100 of growth inhibition by anti-PD-L1, CM-1758 or the combination. Values represented as mean ± SD and *p*-values < 0.05 were considered statistically significant.

Furthermore, several in vivo and in vitro studies showed the synergistic effect of commercial HDACi and immunotherapy [14, 15]. Herein, we present encouraging data showing the anti-cancer effects of CM-1758, a novel inhibitor of HDACs, both in in vitro and in vivo models of advanced BC.

CM-1758 effects leading to cell cytotoxicity and cytostasis by either apoptosis or cell cycle arrest is in line with previous reports on HDACi such as vorinostat (SAHA) or entinostat [12, 13, 23–26]. Additionally, CM-1758 had inhibitory effects on HDACs and further transcriptomic analyzes revealed that not only the epigenetic machinery associated with acetylation was altered, but also the machinery responsible for the regulation of methylation of both histones and DNA. It is known that histone acetylation and DNA methylation are epigenetic mechanisms closely related in regulating gene expression, *i.e.*, elevated histone acetylation can trigger DNA demethylation, promoting gene expression [27].

PD-L1 blocking antibodies are among the most frequently used ICI in BC [28] and, importantly, PD-L1 expression was shown to be regulated by epigenetic mechanisms [29, 30]. In line with previous studies using HDACi, we found increased PD-L1 expression levels upon CM-1758 treatment in several BC cell lines, consequence of higher acetylation levels in the PD-L1 promoter [30]. Histone acetylation increases gene expression since it neutralizes lysine residues positive charge, decreasing the interaction of histone proteins with DNA, making it more accessible for transcription factors [9, 31]. Conversely, although PD-L1 expression has been reported to be regulated by DNA methylation [29], no apparent effect was seen in PD-L1 promoter DNA methylation levels with CM-1758 treatment.

Since CM-1758 led to increased PD-L1 expression, the in vivo effects of a combinatory therapy of CM-1758 with anti-PD-L1 antibody were investigated. A subcutaneous syngeneic mouse model was used to evaluate the efficacy of CM-1758, with the main advantage of having a fully immunocompetent system and enabling easy following of tumor growth. Treatment with CM-1758 alone has significant anti-tumor effects, with better results than anti-PD-L1 blockade alone and a slightly synergistic effect when combined with ICI. Because a significant proportion of BC patients do not respond to ICI due to low PD-L1 expression levels or reduced immune cell infiltration (immune deserted and excluded tumors), our results suggest that CM-1758 may be a promising alternative approach to ICI.

It is acknowledged that epigenetics plays a major expression regulatory role not only in tumor cells, but also in tumor microenvironment cells including immune and nonimmune compartment [17]. In our hands, both CM-1758 and anti-PD-L1 induced changes in both immune and non-immune cells. Importantly, CM-1758 incremented CD8+ cytotoxic T cells infiltration, which is a rather favorable prognostic factor in BC [32]. Also, we found an increase in CD8 + T cell infiltration within the necrotic regions of tumors following the combined administration of CM-1758 and anti-PD-L1. Necrotic areas often exhibit immune suppression, either through the recruitment of M2 macrophages or due to the absence of active T cells [33], characteristics commonly associated with high-risk pathological features in upper tract urothelial carcinoma [34]. Our findings indicate that the combination treatment effectively counteracts the immune-suppressive effects associated with tumor necrosis, signifying a potential synergistic effect between CM-1758 and anti-PD-L1. In contrast, the decrease of CD4 + T cells after treatment may be associated with a reduction in regulatory T cells ($T_{reg}$), as previously observed after in vivo entinostat treatment in a different BC model [16]. CM-1758 showed the ability to regulate the lymphoid repertoire, further supporting that epigenetic factors modulate BC tumors' immune infiltrate features, specifically of T cells [35]. Henceforth, epidrugs to target tumor immune cells constitutes a strategy that should be exploited in conjunction with other immunotherapies in BC.

Myeloid cells are also key players for the effectiveness of immunotherapy [36]. A lower percentage of phagocytic myeloid cells was observed in the anti-PD-L1 treated groups, alone or in combination with CM-1758. Additionally, in our experimental conditions, phagocytic myeloid cells seemed to be the main population affected by anti-PD-L1 antibody treatment. This might be consequence of antibody-dependent cell-mediated cytotoxicity (ADCC) against the phagocytic myeloid cells. Indeed, avelumab was previously shown to mediate ADCC in tumor cells, which is in line with our findings [37]. Importantly, anti-PD-L1 alone or in combination with CM-1758 impacted macrophage status, shifting from an M2 anti-inflammatory to an M1 pro-inflammatory profile and sustaining a "hot tumor" paradigm, as already reported by other studies for ICI [15, 38]. Although epigenetic regulation has been previously implicated in macrophage polarization [15], in our hands CM-1758 did not alter macrophage differentiation. Moreover, despite observing a trend within the CM-1758 group, we did not find a significant change in the PD-L1 expression in tumor cells in vivo, which could be attributed to the fact that PD-L1 expression increase may be transient. Understanding when the PD-L1 levels detected are the highest by induction of CM-1758 could provide insights into

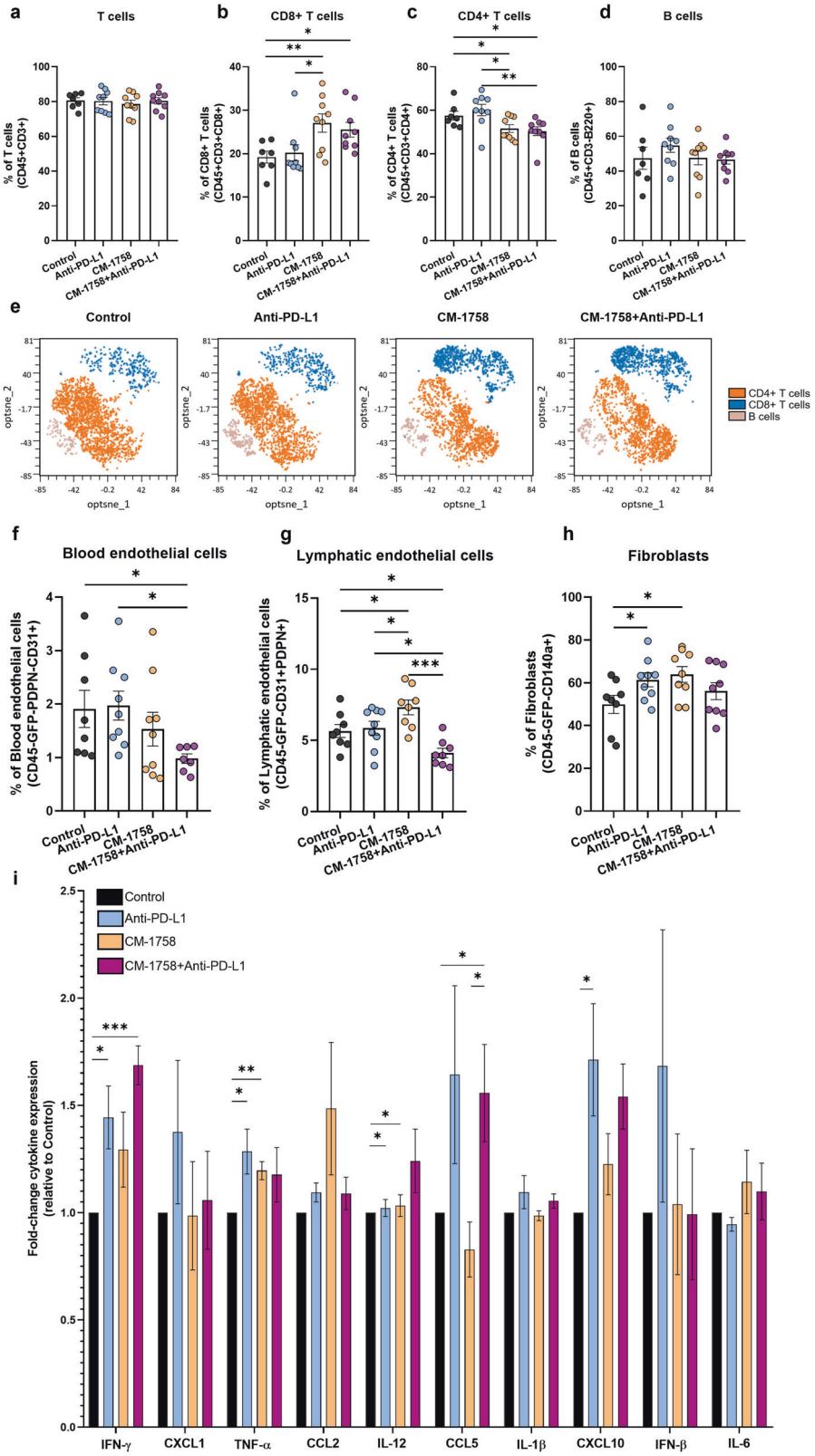


**Fig. 5 Effects of CM-1758 and immune checkpoint inhibitors in tumor lymphoid cells, the non-immune compartment and cytokine profile.** Percentage of (a) T cells gated in CD45+ cells, (**b**) CD8 + T cells gated in CD3+ cells, (**c**) CD4 + T cells gated in CD3+ cells and (**d**) B cells gated in CD45+ cells present in the tumors. (**e**) Representative opt-tSNE analysis of CD8 + T, CD4 + T and B cells repertoire according to treatment groups. Percentage of (**f**) blood endothelial cells gated in CD45-GFP- cells, (**g**) lymphatic endothelial cells gated in CD45-GFP- cells (**h**) fibroblasts gated in CD45-GFP- cells present in the tumor microenvironment. (**i**) Fold-change of cytokine profile (IFN-γ, CXCL1, TNF-α, CCL2, IL-12, CCL5, IL-1β, CXCL10, IFN-β and IL-6) analyzed in plasma of control, anti-PD-L1, CM-1758 and CM-1758+anti-PD-L1 treated mice. Graphs show individual values as the mean ± SEM for ≥8 mice included in each group. *P* values are represented as ns – not significant, *<0.05, **<0.01 and ***<0.001.

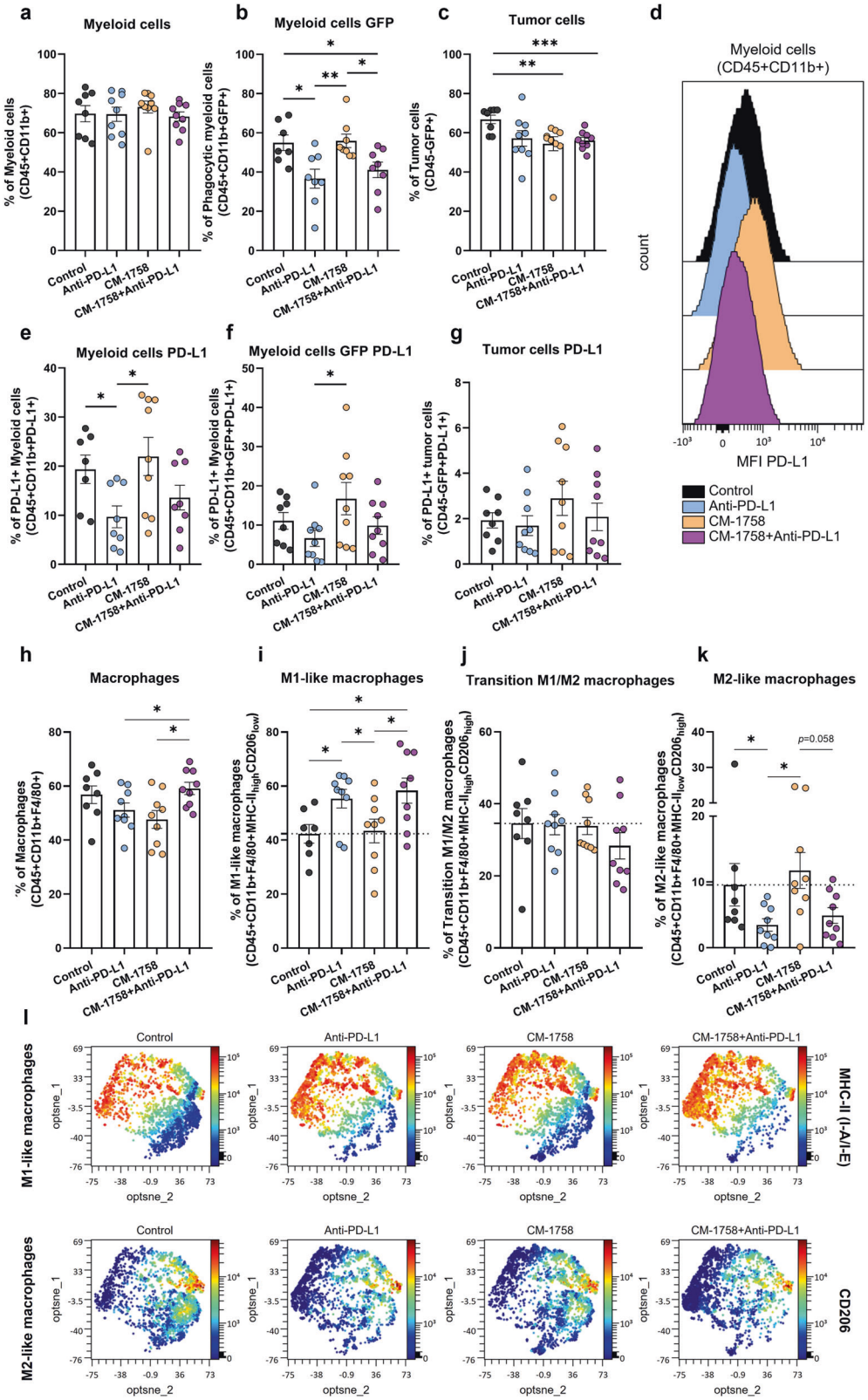


**Fig. 6 Myeloid repertoire changes after treatment with CM-1758 and PD-L1 blockade therapy.** Percentage of (**a**) myeloid cells gated in CD45+ cells, (**b**) phagocytic myeloid cells gated in CD45+ cells and (**c**) tumor cells gated in live cells. (**d**) Single parameter histograms of mean intensity fluorescence (MFI) of PD-L1 expression in the four treatment groups. Percentage of PD-L1 positive of (**e**) myeloid cells gated in CD45 + CD11b+ cells, (**f**) phagocytic myeloid cells gated in CD45 + CD11b+GFP+ cells, and (**g**) tumor cells gated in GFP+ cells. Percentage of (**h**) macrophages gated in CD45 + CD11b+ cells, (**i**) M1-like macrophages gated in CD45 + CD11b + F4/80+ cells, **j** transition M1/M2 macrophages gated in CD45 + CD1b + F4/80+ cells and (**k**) M2-like macrophages gated in CD45 + CD11b + F4/80+ cells. **l** Opt-tSNE analyzes of tumor-present M1-like and M2-like macrophages for MHC-II (I-A/I-E) and CD206 markers. Graphs show individual values as the mean ± SEM for ≥8 mice included in each group. *P*-values are represented as ns – not significant, *<0.05, **<0.01 and ***<0.001.

alternative treatment regimens that may potentiate the synergy between CM-1758 and ICI. The non-immune compartment has a crucial role in tumor maintenance, either through angiogenesis, by providing nutrients and oxygen, or by supporting tumor cell growth [39]. CM-1758 altered the non-immune cell compartment by reducing the percentage of blood endothelial cells, which may decrease the tumor access to nutrients and diminishing metastasis development via blood vessels. Nonetheless, the percentage of lymphatic endothelial cells was increased in the CM-1758 treated group. The role of lymphatic endothelial cells remains under discussion since it increases the amount of tumor antigens in circulation, augmenting the probability of immune system activation [40], although it has been also implicated in tumor cell dissemination. Further studies are needed to explore the role and the impact of epigenetic regulation in lymphatic endothelial cells. Interestingly, we found that virtually all fibroblasts were positive for α-SMA, being classified as myofibroblast-like CAFs (myCAFs) [41]. MyCAFs play a crucial role in the tumor microenvironment by contributing to the deposition and organization of extracellular matrix components, including collagen and fibronectin, which provide structural support to the growing tumor mass in mouse subcutaneous tumor models [42]. In this line, the increase in the percentage of myCAFs in the treatment groups could be associated with a remodeling in the tumor's extracellular matrix by treatments' actions. However, comprehensive studies focusing on the effects of HDACi on CAFs in the context of BC in mouse orthotopic models are required to be better elucidate the contribution of these cells within the BC tumor microenvironment.

The cytokine profile was evaluated in plasma, indicating a systemic immune activation status of mice upon therapy by increasing pro-inflammatory cytokines in circulation. IFN-γ and TNF-α are mainly produced by CD4 + T helper type 1 (Th1) cells, CD8+ cytotoxic T cells and NK cells, stimulating M1 macrophages' antitumor effects and promoting the cytotoxic activity of CD8 + T cells and NK cells [43, 44]. Thus, the increase in cytokines levels is in accordance with increased CD8 + T cells and M1-macrophages depicted by the tumor microenvironment analysis. In our study, both CCL5 and CXCL10 levels seemed to be regulated by ICI. CCL5 is often seen as a "double-edge sword" in cancer, since it has been associated both with promoting antitumor immunity, as well as being implicated in tumor growth and migration [45]. In BC cell lines, conditioned media from TAMs increased invasiveness concomitantly with augmented CCL5 levels [46], although in BC patients high CCL5 expression in tumors associated with better prognosis [47]. In contrast, CXCL10 was shown to increase infiltration of CD8 + T cells, increasing migration and activation of immune cells in the tumor microenvironment [48, 49]. No relevant alterations in cytokines' levels were exclusive to the combination treatment, suggesting that cytokines were independently regulated by ICI and/or CM-1758. Additional studies are required to unravel the exact role of cytokine epigenetic regulatory mechanisms in response to ICI and epidrugs in MIBC.

To conclude, our study describes a novel epigenetic inhibitor targeting HDACs, disclosing antitumor properties in BC both in vitro and in vivo models. Although CM-1758 was shown to have only a slight synergistic effect when combined with ICI, this epidrug may constitute an alternative to current ICI treatment schemes prescribed for BC patients. Besides having a direct impact in tumor growth, CM-1758 also leads to immune system activation. Undoubtedly, epigenetic mechanisms have an important role in regulating the tumor microenvironment and constitute an attractive target to modulate the immune system, with the final goal of tumor elimination and improving BC patients' quality of life. Further investment in novel epidrugs, with extended bioavailability, reduced off-target effects and amenable to be tested in clinical trials as monotherapy, or in combination with chemotherapy and/or ICI, is mandatory to allow for the development of new and more effective strategies for BC management.

## MATERIAL AND METHODS

### Cell culture

American type culture collection (ATCC) human BC cell lines 253 J, 5637, J82, RT112 and TCCSUP, including several tumor stages and BC subtypes [50] acquired in 2008, were selected for the purpose of this study. Cells lines were authenticated by short tandem repeat analysis (Unidad de Genómica, CIMA Lab Diagnostics) and routinely checked for the presence of mycoplasma using Venor®GeM One Step (Minerva Biolabs, Berlin, Germany). Additionally, a previously established mouse bladder tumor cell line 4K5 (*Pten* $^{-/-}$; *Trp53* $^{-/-}$; Adeno-Krt5-Cre) expressing GFP was also included in the study. 253 J, J82, RT112 and 4K5 cells were maintained in DMEM GlutaMAX™ medium (Thermo Fisher Scientific, Waltham, Massachusetts, USA), whereas TCCSUP cells were grown in EMEM medium (Lonza, Basel, Switzerland) and 5637 cells were maintained in RPMI 1640 medium (Thermo Fisher Scientific), all supplemented with 10% fetal bovine serum (FBS) and 1% of Antibiotic Antimycotic solution (Thermo Fisher Scientific), at 5% CO2 and 37°C in a humidifying chamber.

### Cell treatment with CM-1758 and $IC_{50}$ calculation

CM-1758 (HDACs inhibitor) was stored in DMSO (Sigma Aldrich, Burlington, Massachusetts, USA) at the concentration of 100 mM at -20°C. The chemical structure was described previously [Compound 13e [18]]. The half-maximal inhibitory concentration ($IC_{50}$) of CM-1758 was calculated for all cell lines. Cells were plated in 96-well plates at different densities according to cell line and, after 24 h, cells were treated with concentrations of CM-1758 ranging from 0.01 to 10 µM in complete medium, and left in culture for 48 h. Two controls were added per plate, including one with complete medium and another containing 0.01% of DMSO. Cell Proliferation Kit II XTT (Roche, Basel, Switzerland) was then used according to the manufacturer's instructions. Absorbance was measured at 490 nm using a Genios Pro microplate reader (Tecan, Männedorf, Switzerland). At least four experimental replicates were used for $IC_{50}$ calculation.

### Cell cycle analysis

All cell lines were seeded in 6-well plates and treated with CM-1758 for 48 h with the $IC_{50}$ concentration calculated for each cell line, or with DMSO control. After that, cells were trypsinized (Trypsin-EDTA Solution, Sigma-Aldrich), collected and counted. Cells from control and treated conditions were collected for cell cycle analysis. Next, cells were washed with PBS and fixed with ethanol 70% for 1.5 h at 4°C. Cells were treated with RNAse and incubated at 37°C for 20 min with shaking. Finally, propidium iodide (Sigma Aldrich) at 50 µL/mL was added and incubated for 15 min in the dark. Cell cycle was analyzed in a LSR Fortessa cell analyzer (Becton Dickinson (BD) Biosciences, Franklin Lakes, New Jersey USA). Results were analyzed using FlowJo™ v10.8.1 (BD Biosciences). Five experimental replicates were used for data analysis.

### PD-L1 expression and Apoptosis assay by flow cytometry

Cells were seeded in 6-well plates and treated with CM-1758 at $IC_{50}$ concentration for 48 h, or DMSO as a control, for evaluation of PD-L1 expression and apoptosis. Cells were trypsinized, collected and washed with PBS. Then, cells were incubated with 1 µL of human or mouse FcR blocking reagent (Miltenyi Biotec, Bergisch Gladbach, Germany) for 10 min at room temperature (RT). Samples were stained with human anti-PD-L1 (clone MIH3; Biolegend, San Diego, California, USA) or mouse anti-PD-L1 antibody (clone MIH5; BD Biosciences) for 30 min at 4°C in the dark. After washing, cells were incubated with a mix of Annexin Binding Buffer 1x (BD Biosciences), DAPI (Roche) and 2 µL of PE Annexin V (Ref 556421, BD Biosciences) for mouse, and FITC Annexin V (Ref 556419, BD Biosciences) for human cell lines, for 15 min in the dark at RT. Cells were acquired in a BD LSR Fortessa cell analyzer, and data analysis was performed using FlowJo™ v10.8.1 (BD Biosciences). For apoptosis, live cells were identified as AnnexinV-DAPI-, early apoptotic as AnnexinV+DAPI-, late apoptotic as AnnexinV+DAPI+ and necrotic by Annexin-DAPI + . PD-L1 expression was analyzed only in live cells (DAPI-). Single stained and fluorescence minus one (FMO) controls were included.

### RNA extraction and RNA-sequencing sample preparation

Total RNA was extracted using the miRNAeasy Mini kit (Qiagen, Hilden, Germany), according to the manufacturer's instructions. RNA concentration was measured on a Qubit 4 Fluorometer (Thermo Fisher Scientific), using a Qubit RNA broad range assay kit (Thermo Fisher Scientific) and stored at -80°C. RNA integrity number (RIN) was measured using the Qubit RNA IQ

assay kit (Thermo Fisher Scientific) and samples with values higher than 8 were considered for RNA sequencing (RNAseq) analysis. One µg of total RNA was sent for RNAseq analysis by Macrogen RNA-seq services (Seoul, South Korea) using the Truseq stranded total RNA Library with Ribo-Zero Gold (Illumina, San Diego, California, USA) and the NovaSeq 6000 (Illumina) of two independent biological replicates for each condition (control and treated with CM-1758) of 253 J, J82, RT112 and TCCSUP.

### Real-time quantitative PCR (RT-qPCR)

One µg of RNA was used to synthetize cDNA using the High Capacity cDNA Reverse Transcription kit (Applied Biosystems™, Waltham, Massachusetts, USA) according to the manufacturer's recommendations. Four µL of diluted 20x cDNA, 5 µL of GoTaq PCR Master Mix (Promega, Madison, Wisconsin, USA) and primers (Supplementary Table S1) at 0.5 µM were used per well. The RT-qPCR reactions were run in a QuantStudio™ 6 Flex Real-Time PCR (Thermo Fisher Scientific), along with the melting curves. *TBP* for mouse and human was used as housekeeping gene to normalize the results, and the relative expression for each transcript was calculated using the $2^{-\Delta\Delta Ct}$, as previously described [51]. Primers sequences can be found in Supplementary Table S1.

### CUT&RUN

Cleavage under targets & release using nuclease (CUT&RUN) was performed using the CUT&RUN assay kit (Cell Signaling Technology, Danvers, Massachusetts, USA), according to the manufacturer's instructions. Briefly, 100 000 of J82 cells treated with the $IC_{50}$ dose of CM-1758, or DMSO 0.01% as control, were collected, washed and incubated with 10 µL of concavalin A beads. Then, bead-bound cells were incubated with the primary antibodies for H3K9ac (dilution 1:50, #9649, Cell Signaling Technology), H3K27ac (dilution 1:100, #8173, Cell Signaling Technology), H3K4me3 for positive control (dilution 1:50, #9751, Cell Signaling Technology), or Rabbit IgG Isotype Control (dilution 1:50, #66362, Cell Signaling Technology), overnight at 4°C with rotation. After a wash, the cell-bead mixture was incubated with pAG-MNase at 4°C for 1 h. Next, after washing with wash buffer, calcium chloride was added, and samples were incubated at 4°C. After 30 min, stop buffer was added and DNA was purified using the QIAquick PCR Purification kit (Qiagen). For input samples preparation, cells were incubated with DNA extraction buffer (plus proteinase K and RNAse A) for 1 h at 55°C. Then, for cell lysis, cells were sonicated, and DNA was purified. Two µL of purified DNA, 5 µL of GoTaq PCR Master Mix (Promega) and 2 µM primers for four different regions of PD-L1 promoter were used for the qPCR analysis (Supplementary Table S1) in a QuantStudio™ 6 Flex Real-Time PCR (Thermo Fisher Scientific). Intronic regions were not considered for qPCR analysis. Relative fold-change was calculated with $2^{-\Delta\Delta Ct}$ using *RPL30* as a reference gene.

### Immunofluorescence

J82 and 4K5 cells treated with the respective $IC_{50}$ doses of CM-1758 or DMSO 0.01% as a control for 48 h were fixed in 4% paraformaldehyde for 15 min at 4°C. Then, cells were washed with PBS and permeabilized with 0.1% Triton X-100 in PBS for 10 min at RT. After another wash with PBS, fixed cells were blocked with 10% horse serum for 1 h at RT, followed by the incubation with a primary antibody against 5-methylcytosine with the 10% horse serum overnight at 4°C (Supplementary Table S2). Next, after a wash with PBS, cells were incubated with the respective secondary antibody conjugated with fluorochromes in 10% horse serum at RT for 1 h (Supplementary Table S2). Finally, a mounting medium (Mowiol, Thermo Fisher Scientific) with DAPI at 1 µL/mL, for staining nuclei, was used for mounting the slides. Images were acquired with an Olympus IX51 microscope.

### Protein and histone extraction

Total protein and histones were extracted from cells treated with the $IC_{50}$ dose of CM-1758, or DMSO-treated cells. Cells were scrapped, collected and total protein was extracted from cell pellets by adding 1:1 of lysis buffer (Hepes 40 mM, Triton X-100 2%, NaCl 200 mM, MgCl2 40 mM, EGTA 20 mM, β- glycerophosphate 80 mM and distilled water) and a mix of proteinase and phosphatase inhibitors, and phenylmethylsulfonyl fluoride (PMSF) at a final dilution of 200x, followed by a centrifugation at 16 100 g for 10 min at 4°C. The supernatant was collected and stored at -80°C until further use.

For histone extraction, 500 µL of hypotonic buffer (Tris-HCL pH=8.0 10 mM, KCl 1 mM, $MgCl_2$ 1.5 mM, dithiothreitol 1 mM and distilled water), proteinase and phosphatase inhibitors, and PMSF, were added to each cell pellet and incubated for 30 min at 4°C with rotation. Then, after a 10 min centrifugation at 4°C at 10 400 g, the supernatant was discarded and 400 µL of $H_2SO_4$ at 0.2 M was added to the nucleus pellet and incubated overnight at 4°C with rotation. The samples were centrifugated at 4°C for 10 min at 10 400 g and the supernatant was transferred to another tube. Next, 132 µL of trichloroacetic acid was added and incubated for 30 min on ice. After another centrifugation, the supernatant was disregarded, and the histone pellet was washed with cold acetone. Lastly, after drying, the histone pellet was eluted in water and stored at -80°C until further use. Histones and total protein samples were quantified by Qubit™ Protein Assay Kit (ThermoFisher Scientific), according to the manufacturer's recommendations, using a Qubit 4 Fluorometer (ThermoFisher Scientific).

### Western blot

Twenty µg or 3 µg of total protein or histones, respectively, were separated in Mini-protean TGX Stain-Free gels 4-15% (Bio-Rad, Hercules, California, USA) by sodium dodecyl sulfate-polyacrylamide gel electrophoresis (SDS-PAGE). Then, were transferred by using a Trans-Blot Turbo transfer system (Bio-Rad) into an immunoblot nitrocellulose membrane in a transfer buffer containing ethanol, distilled water, and Trans-Blot® TurboTM 5x Tranfer Buffer (Bio-Rad). After that, membranes were blocked with 5% milk in tris-buffer saline (TBS)/0.1% Tween (TBS-T) for 1 h at RT. Then, membranes were incubated with primary antibodies overnight at 4°C (Supplementary Table S2). Next, membranes were washed with TBS-T and incubated with a secondary antibody coupled with horseradish peroxidase (Supplementary Table S2) for 1 h at RT. Blots were visualized by chemiluminescence (Clarity WB ECL substrate, Bio-Rad) using a ChemiDoc XRS+ (Bio-Rad). Western blots were quantified using band densitometry analysis with ImageJ software (version 1.6.1., National Institute of Health). All antibodies and dilutions used are described in Supplementary Table S2.

### Animal care and maintenance

All the animal experiments were conducted according to the European and Spanish regulations in the field: European convention ETS 123, regarding the use and protection of vertebrate mammals used in experimentation and other scientific purposes, and Directive 2010/63/UE, Spanish Law 6/2013 and Real Decreto (R.D.) 53/2013 regarding the protection and use of animals in scientific research. Procedures involving genetically modified organisms were conducted according to the proper European and Spanish Regulations: Directive 2009/41/CE, Spanish Law 9/2003, and R.D. 178/2004. The protocols were approved by "Consejería de Medio Ambiente y Ordenación del Territorio y Sostenibilidad" (protocol number PROEX 150.8/21) and all procedures were approved by CIEMAT Animal Experimentation Ethics Committee according to external and internal biosafety and bio-ethics guidelines.

Mice were housed at the CIEMAT laboratory Animal Facility (registration number ES280790000183) and routinely screened for pathogens, following the Spanish Society for the Laboratory Animal Science (SECAL) and the Federation of European Laboratory Animal Science Associations (FELASA, Tamworth, UK) recommendations. Mice were provided with food (TEKLAD Global Diet 2918) and acidified and filtered (0.2 µm) water *ad libitum*. Mice were maintained in cages type IIL, in a maximum of 5 mice per cage. Room lighting was controlled with light/dark cycles for 12/12 h, with temperature and humidity being regulated at 21 ± 2°C and 55 ± 10%, respectively.

### Syngeneic graft mouse model

Immunocompetent double knock-out mice (DKO; $Pten^{F/F}$, $Trp53^{F/F}$) were developed by our group through a conventional crossing of mice from different collaborators (Netherlands Cancer Institute, Mass. Institute of Technology, Stanford University), resulting in a mixed FVB/129 S background. A syngeneic graft mouse model was generated by injecting subcutaneously cells (4K5 cell line) previously established from an aggressive mouse bladder tumor ($Pten^{-/-}$; $Trp53^{-/-}$), generated with adenoviruses expressing Cre recombinase under the control of the regulatory elements of keratin 5 (Adeno-Krt5-Cre) [52]. Three million 4K5 cells were resuspended in 100 µL of DMEM and injected subcutaneously in the right flank of 3–4-month-old male and female DKO mice. Tumor growth was monitored 3 times per week using a digital caliper and tumor volume was calculated using the formula $4\pi/3$ x (length/2) x $(width/2)^2$ [2]. After tumors reached volumes between 80-90 $mm^3$, mice were randomly assigned to four groups: control ($n = 8$), anti-PD-L1 ($n = 9$), CM-1758 ($n = 9$) and CM-1758+anti-PD-L1 ($n = 9$). CM-1758 (10 mg/kg; 5 times a week) and anti-PD-L1 (avelumab; 200 µg/mouse; once a week) were injected

intraperitoneally. In the combination group, a phased dosing schedule was administered. Tumor sizes were normalized by subtracting the volume calculated on the treatment initiation day. After two weeks of treatment, mice were sacrificed and tumors and whole blood were collected at the time of euthanasia. For RNA extraction, tumors were embedded in RNAlater™ Stabilization solution (Thermo Fisher Scientific) at 4 °C for 24 h, and then stored at -80°C until further use. For flow cytometry, tumor tissue was embedded in DMEM and kept at 4 °C overnight to be processed and analyzed in the following day. Regarding histological analysis, tumors were fixed in 3.7-4% buffered formalin overnight at the time of the harvesting. Then, samples were embedded in paraffin and sections of 3-5 µm were stained for hematoxylin and eosin. Blood was collected in Microvette® CB 300 blood collection system with lithium heparin (Kent Scientific, Torrington, Connecticut, USA). Tubes were centrifuged at 1000 g for 10 min at 4 °C, plasma was collected and stored at -80°C until further use.

### Cell population analysis by flow cytometry

For cell population analysis, tumors were minced in small pieces and incubated with an enzymatic cocktail containing collagenase P (200 µg/mL; Roche), dispase II (800 µg/mL; Roche) and DNase I (100 µg/mL; Roche) in DMEM at 37°C, with vortex and mixing every 20 min 3-4 times. Disaggregated tissue was filtered using a 40 µm cell strainer and centrifuged at 16 100 g for 7 min. Cells were resuspended in FACS buffer (0.05% sodium azide, 0.5% bovine serum albumin and PBS) and stained with the viability dye Zombie Aqua (Biolegend), for 20 min in the dark at RT. After washing, cells were incubated with mouse FcR blocking reagent (Milteny Biotec) for 10 min in the dark at RT. Then, the antibodies described in Supplementary Table S3 were added and incubated for 30 min at 4°C. After washing, cells were fixed with 150 µL of BD Cytofix/Cytoperm™ (BD Biosciences) and acquired in the next day in a BD LSR Fortessa flow cytometer. FlowJo™ 10.8.1 software (BD Biosciences) and OMIQ (Dotmatics, Boston, Massachusetts, USA) were used for data analysis.

### Cytokine analysis

Cytokine levels were analyzed using the LEGENDplex™ mouse anti-virus response panel (Biolegend) according to the manufacturer's recommendations and using a filter 96-well plate. Briefly, 25 µL of plasma was added to each well along with assay buffer and beads. The mixture was incubated for 2 h with shaking, and next wells were washed and incubated with the detection antibodies for 1 h with shaking at RT. Subsequently, SA-PE was added and incubated for 30 min at RT with shaking. Finally, samples were analyzed in CytoFLEX and CytExpert (Beckman Coulter, USA). Data was presented as fold-change in anti-PD-L1, CM-1758 and CM-1758+anti-PD-L1 groups relative to the mean value of each cytokine for control mice.

### Immunohistochemistry

Sections of formalin-fixed paraffin-embedded (FFPE) tumors were deparaffinized and incubated with hydrogen peroxide (0.3%) in methanol for 10 min. Then, antigen retrieval was performed using sodium citrate buffer (citric acid monohydrate 1.8 mM, trisodium citrate dihydrate 8.2 mM, pH=6.0) and a pressure cooker (Dako Agilent Tecnologies, Santa Clara, California, USA). Subsequently, tumor sections were blocked with 10% horse serum for 1 h at RT and incubated with the primary antibody overnight at 4°C (Supplementary Table S2). In the next day, slides were incubated with the appropriate secondary antibody for 1 h at RT. Next, the slides were incubated with the biotin-avidin-peroxidase system Vectastain Elite ABC HRP kit (Vector Labs, Newark, California, USA) for 30 min at RT, and staining was revealed with a DAB substrate kit (Vector Labs). Slides were counterstained with hematoxylin and mounted with DPX mounting media. All slides were scanned in a Pannoramic MIDI II (3DHISTECH, Budapest, Hungary) at ×20 magnification.

### Bioinformatic analyzes

For flow cytometry analysis, single and live cells were selected using the gating strategy demonstrated in Supplementary Figs. S1–4. Optimization of t-Distributed Stochastic Neighbor Embedding (opt-tSNE) was performed using OMIQ (Dotmatics) for lymphocyte and macrophage populations. Subsampling with 3000 events for each sample and 3000 interactions were used for opt-tSNE.

Regarding RNA-sequencing data, differential analyzes were performed using the DESeq2 software package (version 1.38.2) in R software [53, 54]. Normalized gene expression data were transformed into log2 scale, and the value range was adjusted for each gene. Hierarchical clustering was performed using Multi-Experiment Viewer (Mev 4.9.0). Supervised hierarchical clustering was applied using Pearson correlation and average linkage. Heatmaps were represented using SRplot (http://www.bioinformatics.com.cn/srplot). Gene set enrichment analysis (GSEA) was performed using GSEA version 4.3.2 and Molecular Signature Database (MSigDB) [55]. The h.all.v7.5.symbols.gmt (Hallmarks) gene set database was used as the gene set collection analysis. GSEA was performed using 1000 permutations and the maximum and minimum sizes for gene sets were 500 and 15, respectively. Data was represented by enrichment bubble plots, using SRplot. Venn diagrams were plotted using jvenn (https://xcmsonline.scripps.edu/lib/jvenn/example.html). Genes with a log2(foldchange) >2 for upregulated genes and <-2 downregulated genes and a $p$ value adjust <0.01 were selected for venn diagram and Enrichr analysis (https://maayanlab.cloud/Enrichr/). Gene set variation analysis (GSVA) was performed using GSVA package in R software (v1.42.0) and a hallmark gene set. Data was represented by a heatmap using SRplot. We reconstructed transcriptional regulatory networks (regulons) using the R package RTN78. We investigated 1612 transcription factors (TFs) compiled from [56]. Potential associations between a regulator and all possible target genes were inferred from the expression matrix by Mutual Information and Spearman's correlation, and permutation analysis was used to remove associations with a BH-adjusted $p$ value > 0.05. Unstable associations were eliminated by bootstrap analysis (1000 resamplings, consensus bootstrap > 95%) and the weakest association in triangles of two regulators and common target genes were removed by data processing inequality (DPI) filtering (tolerance = 0.01). Regulon activity scores for all samples were calculated by two-tailed gene set enrichment analysis [56–58]. Principal component analysis (PCA) was performed using the "prcomp" command in R and the normalized matrix obtained from DeSEq2. The PCA was plotted using the PCA 3D Visualiser tool (https://prismtc.co.uk/resources/free-tools/pca-3d-visualiser).

QuPath software was used for the analysis of the necrosis areas and BrdU immunohistochemistry [59]. Briefly, the protocol for nucleus detection was optimized according to staining-intrinsic characteristics. Both BrdU and CD8 showed a clear staining and the positive cell detection tool was used to detect the positive cells using a threshold manually refined for each tumor. BrDU-positive cells are displayed as a percentage of positive cells, whereas CD8 + T cells are presented as cells per $mm^2$ (cells/$mm^2$). The necrosis areas were defined manually by a trained pathologist and the area value was determined using the annotation tool. The percentage of necrosis was calculated for each tumor by dividing the value of the necrosis area by the total value of tumor area and multiplying by 100.

### Statistical analysis

The in vitro studies were conducted in a minimum of 3 independent experiments. $IC_{50}$ analyzes were performed using GraphPad Prim 8.0 software (GraphPad Software, USA). Graphics are represented by mean ± SEM. Normal distribution was evaluated using the Shapiro-Wilk test ($p > 0.05$). Data showing normal distribution were analyzed using parametric two-tailed t-test with Levene's test for equality of variances ($p < 0.05$, variances considered not equal; $p > 0.05$, variances considered equal). Nonparametric Mann-Whitney U test was used to compare data not having a normal distribution. Immunohistochemistry results were analyzed by Fisher's exact test. Two-tailed $p$ values calculation were performed using a computer-assisted program (SPSS Version 28.0, USA). Graphics were assembled with GraphPad 8 Prism (GraphPad Software, USA). $P$ values were considered statistically significant when inferior to 0.05. Significance is depicted as follows: *$p < 0.05$, **$p < 0.01$, ***$p < 0.001$, ****$p < 0.0001$ and ns > 0.05 (nonsignificant).

## DATA AVAILABILITY

The datasets discussed in this publication have been deposited in NCBI's Gene Expression Omnibus and are accessible through GEO Series accession number GSE245122.

## REFERENCES

1. Sung H, Ferlay J, Siegel RL, Laversanne M, Soerjomataram I, Jemal A, et al. Global Cancer Statistics 2020: GLOBOCAN Estimates of Incidence and Mortality Worldwide for 36 Cancers in 185 Countries. CA Cancer J Clin. 2021;71:209–49.

2. Cumberbatch MGK, Jubber I, Black PC, Esperto F, Figueroa JD, Kamat AM, et al. Epidemiology of Bladder Cancer: A Systematic Review and Contemporary Update of Risk Factors in 2018. Eur Urol. 2018;74:784–95.
3. Amin MB, Edge SB, Greene FL, Byrd DR, Brookland RK, Washington MK, et al. AJCC Cancer Staging Manual. Springer International Publishing, (2018).
4. Powles T, Bellmunt J, Comperat E, De Santis M, Huddart R, Loriot Y, et al. Bladder cancer: ESMO Clinical Practice Guideline for diagnosis, treatment and follow-up. Ann Oncol. 2022;33:244–58.
5. Rhea LP, Mendez-Marti S, Kim D, Aragon-Ching JB. Role of immunotherapy in bladder cancer. Cancer Treat Res Commun. 2021;26:100296.
6. Hussain SA, Birtle A, Crabb S, Huddart R, Small D, Summerhayes M, et al. From Clinical Trials to Real-life Clinical Practice: The Role of Immunotherapy with PD-1/PD-L1 Inhibitors in Advanced Urothelial Carcinoma. Eur Urol Oncol. 2018;1:486–500.
7. Hanahan D. Hallmarks of Cancer: New Dimensions. Cancer Discov. 2022;12:31–46.
8. Baylin SB, Jones PA. Epigenetic Determinants of Cancer. Cold Spring Harb Perspect Biol. 2016;8:a019505.
9. Audia JE, Campbell RM. Histone Modifications and Cancer. Cold Spring Harb Perspect Biol. 2016;8:a019521.
10. Miranda Furtado CL, Dos Santos Luciano MC, Silva Santos RD, Furtado GP, Moraes MO, Pessoa C. Epidrugs: targeting epigenetic marks in cancer treatment. Epigenetics. 2019;14:1164–76.
11. Ramaiah MJ, Tangutur AD, Manyam RR. Epigenetic modulation and understanding of HDAC inhibitors in cancer therapy. Life Sci. 2021;277:119504.
12. Rubio C, Avendaño-Ortiz J, Ruiz-Palomares R, Karaivanova V, Alberquilla O, Sánchez-Domínguez R, et al. Toward Tumor Fight and Tumor Microenvironment Remodeling: PBA Induces Cell Cycle Arrest and Reduces Tumor Hybrid Cells' Pluripotency in Bladder Cancer. Cancers (Basel). 2022;14:287.
13. Wang SC, Wang ST, Liu HT, Wang XY, Wu SC, Chen LC, et al. Trichostatin A induces bladder cancer cell death via intrinsic apoptosis at the early phase and Sp1-survivin downregulation at the late phase of treatment. Oncol Rep. 2017;38:1587–96.
14. Burke B, Eden C, Perez C, Belshoff A, Hart S, Plaza-Rojas L, et al. Inhibition of Histone Deacetylase (HDAC) Enhances Checkpoint Blockade Efficacy by Rendering Bladder Cancer Cells Visible for T Cell-Mediated Destruction. Front Oncol. 2020;10:699.
15. Li X, Su X, Liu R, Pan Y, Fang J, Cao L, et al. HDAC inhibition potentiates anti-tumor activity of macrophages and enhances anti-PD-L1-mediated tumor suppression. Oncogene. 2021;40:1836–50.
16. Truong AS, Zhou M, Krishnan B, Utsumi T, Manocha U, Stewart KG, et al. Entinostat induces antitumor immune responses through immune editing of tumor neoantigens. J Clin Invest. 2021;131:e138560.
17. Lodewijk I, Nunes SP, Henrique R, Jerónimo C, Dueñas M, Paramio JM. Tackling tumor microenvironment through epigenetic tools to improve cancer immunotherapy. Clin Epigene. 2021;13:63.
18. Rabal O, San José-Enériz E, Agirre X, Sánchez-Arias JA, de Miguel I, Ordoñez R, et al. Design and Synthesis of Novel Epigenetic Inhibitors Targeting Histone Deacetylases, DNA Methyltransferase 1, and Lysine Methyltransferase G9a with In Vivo Efficacy in Multiple Myeloma. J Med Chem. 2021;64:3392–426.
19. Huang KC, Chiang SF, Chen WT, Chen TW, Hu CH, Yang PC, et al. Decitabine Augments Chemotherapy-Induced PD-L1 Upregulation for PD-L1 Blockade in Colorectal Cancer. Cancers (Basel). 2020;12:462.
20. Woods DM, Sodré AL, Villagra A, Sarnaik A, Sotomayor EM, Weber J. HDAC Inhibition Upregulates PD-1 Ligands in Melanoma and Augments Immunotherapy with PD-1 Blockade. Cancer Immunol Res. 2015;3:1375–85.
21. Zang J, Ye K, Fei Y, Zhang R, Chen H, Zhuang G. Immunotherapy in the Treatment of Urothelial Bladder Cancer: Insights From Single-Cell Analysis. Front Oncol. 2021;11:696716.
22. Singh M, Kumar V, Sehrawat N, Yadav M, Chaudhary M, Upadhyay SK, et al. Current paradigms in epigenetic anticancer therapeutics and future challenges. Semin Cancer Biol. 2022;83:422–40.
23. Hoffmann MJ, Meneceur S, Hommel K, Schulz WA, Niegisch G. Downregulation of Cell Cycle and Checkpoint Genes by Class I HDAC Inhibitors Limits Synergism with G2/M Checkpoint Inhibitor MK-1775 in Bladder Cancer Cells. Genes (Basel). 2021;12:260.
24. Wang C, Hamacher A, Petzsch P, Köhrer K, Niegisch G, Hoffmann MJ, et al. Combination of Decitabine and Entinostat Synergistically Inhibits Urothelial Bladder Cancer Cells via Activation of FoxO1. Cancers (Basel). 2020;12:337.
25. Li QQ, Hao JJ, Zhang Z, Hsu I, Liu Y, Tao Z, et al. Histone deacetylase inhibitor-induced cell death in bladder cancer is associated with chromatin modification and modifying protein expression: A proteomic approach. Int J Oncol. 2016;48:2591–607.
26. Kaletsch A, Pinkerneil M, Hoffmann MJ, Jaguva Vasudevan AA, Wang C, Hansen FK, et al. Effects of novel HDAC inhibitors on urothelial carcinoma cells. Clin Epigenetics. 2018;10:100.
27. Moore LD, Le T, Fan G. DNA methylation and its basic function. Neuropsychopharmacology. 2013;38:23–38.
28. Witjes JA, Bruins HM, Cathomas R, Compérat EM, Cowan NC, Gakis G, et al. European Association of Urology Guidelines on Muscle-invasive and Metastatic Bladder Cancer: Summary of the 2020 Guidelines. Eur Urol. 2021;79:82–104.
29. Segovia C, San José-Enériz E, Munera-Maravilla E, Martínez-Fernández M, Garate L, Miranda E, et al. Inhibition of a G9a/DNMT network triggers immune-mediated bladder cancer regression. Nat Med. 2019;25:1073–81.
30. Shen Y, Liu L, Wang M, Xu B, Lyu R, Shi YG, et al. TET2 Inhibits PD-L1 Gene Expression in Breast Cancer Cells through Histone Deacetylation. Cancers (Basel). 2021;13:2207.
31. Bannister AJ, Kouzarides T. Regulation of chromatin by histone modifications. Cell Res. 2011;21:381–95.
32. Chen X, Xu R, He D, Zhang Y, Chen H, Zhu Y, et al. CD8(+) T effector and immune checkpoint signatures predict prognosis and responsiveness to immunotherapy in bladder cancer. Oncogene. 2021;40:6223–34.
33. Sprooten J, De Wijngaert P, Vanmeerbeerk I, Martin S, Vangheluwe P, Schlenner S, et al. Necroptosis in Immuno-Oncology and Cancer Immunotherapy. Cells. 2020;9:1823.
34. Seitz C, Gupta A, Shariat SF, Matsumoto K, Kassouf W, Walton TJ, et al. Association of tumor necrosis with pathological features and clinical outcome in 754 patients undergoing radical nephroureterectomy for upper tract urothelial carcinoma: an international validation study. J Urol. 2010;184:1895–1900.
35. Chow A, Perica K, Klebanoff CA, Wolchok JD. Clinical implications of T cell exhaustion for cancer immunotherapy. Nat Rev Clin Oncol. 2022;19:775–90.
36. Niu Y, Chen J, Qiao Y. Epigenetic Modifications in Tumor-Associated Macrophages: A New Perspective for an Old Foe. Front Immunol. 2022;13:836223.
37. Boyerinas B, Jochems C, Fantini M, Heery CR, Gulley JL, Tsang KY, et al. Antibody-Dependent Cellular Cytotoxicity Activity of a Novel Anti-PD-L1 Antibody Avelumab (MSB0010718C) on Human Tumor Cells. Cancer Immunol Res. 2015;3:1148–57.
38. Gubin MM, Esaulova E, Ward JP, Malkova ON, Runci D, Wong P, et al. High-Dimensional Analysis Delineates Myeloid and Lymphoid Compartment Remodeling during Successful Immune-Checkpoint Cancer Therapy. Cell. 2018;175:1014–1030.e1019.
39. Martinez VG, Munera-Maravilla E, Bernardini A, Rubio C, Suarez-Cabrera C, Segovia C, et al. Epigenetics of Bladder Cancer: Where Biomarkers and Therapeutic Targets Meet. Front Genet. 2019;10:1125.
40. He M, He Q, Cai X, Chen Z, Lao S, Deng H, et al. Role of lymphatic endothelial cells in the tumor microenvironment-a narrative review of recent advances. Transl Lung Cancer Res. 2021;10:2252–77.
41. Yang D, Liu J, Qian H, Zhuang Q. Cancer-associated fibroblasts: from basic science to anticancer therapy. Exp Mol Med. 2023;55:1322–32.
42. Martins-Lima C, Chianese U, Benedetti R, Altucci L, Jerónimo C, Correia MP. Tumor microenvironment and epithelial-mesenchymal transition in bladder cancer: Cytokines in the game? Front Mol Biosci. 2022;9:1070383.
43. Ivashkiv LB. IFNγ: signalling, epigenetics and roles in immunity, metabolism, disease and cancer immunotherapy. Nat Rev Immunol. 2018;18:545–58.
44. Quaranta V, Schmid MC. Macrophage-Mediated Subversion of Anti-Tumour Immunity. Cells. 2019;8:747.
45. Aldinucci D, Borghese C, Casagrande N. The CCL5/CCR5 Axis in Cancer Progression. Cancers (Basel). 2020;12:1765.
46. Huang CP, Liu LX, Shyr CR. Tumor-associated Macrophages Facilitate Bladder Cancer Progression by Increasing Cell Growth, Migration, Invasion and Cytokine Expression. Anticancer Res. 2020;40:2715–24.
47. Li Y, Chen X, Li D, Yang Z, Bai Y, Hu S, et al. Identification of prognostic and therapeutic value of CC chemokines in Urothelial bladder cancer: evidence from comprehensive bioinformatic analysis. BMC Urol. 2021;21:173.
48. Fridman WH, Pagès F, Sautès-Fridman C, Galon J. The immune contexture in human tumours: impact on clinical outcome. Nat Rev Cancer. 2012;12:298–306.
49. Tham SM, Ng KH, Pook SH, Esuvaranathan K, Mahendran R. Tumor and microenvironment modification during progression of murine orthotopic bladder cancer. Clin Dev Immunol. 2011;2011:865684.
50. Earl J, Rico D, Carrillo-de-Santa-Pau E, Rodríguez-Santiago B, Méndez-Pertuz M, Auer H, et al. The UBC-40 Urothelial Bladder Cancer cell line index: a genomic resource for functional studies. BMC Genom. 2015;16:403.
51. Livak KJ, Schmittgen TD. Analysis of relative gene expression data using real-time quantitative PCR and the 2(-Delta Delta C(T)) Method. Methods. 2001;25:402–8.
52. Ramírez A, Bravo A, Jorcano JL, Vidal M. Sequences 5′ of the bovine keratin 5 gene direct tissue- and cell-type-specific expression of a lacZ gene in the adult and during development. Differentiation. 1994;58:53–64.
53. Team RC. R: A language and environment for statistical computing. R Foundation for Statistical Computing (2022).
54. Love MI, Huber W, Anders S. Moderated estimation of fold change and dispersion for RNA-seq data with DESeq2. Genome Biol. 2014;15:550.

55. Subramanian A, Tamayo P, Mootha VK, Mukherjee S, Ebert BL, Gillette MA, et al. Gene set enrichment analysis: a knowledge-based approach for interpreting genome-wide expression profiles. Proc Natl Acad Sci USA. 2005;102:15545–50.
56. Lambert SA, Jolma A, Campitelli LF, Das PK, Yin Y, Albu M, et al. The Human Transcription Factors. Cell. 2018;172:650–65.
57. Robertson AG, Kim J, Al-Ahmadie H, Bellmunt J, Guo G, Cherniack AD, et al. Comprehensive Molecular Characterization of Muscle-Invasive Bladder. Cancer Cell. 2017;171:540–556.e525.
58. Lindskrog SV, Prip F, Lamy P, Taber A, Groeneveld CS, Birkenkamp-Demtröder K, et al. An integrated multi-omics analysis identifies prognostic molecular subtypes of non-muscle-invasive bladder cancer. Nat Commun. 2021;12:2301.
59. Bankhead P, Loughrey MB, Fernández JA, Dombrowski Y, McArt DG, Dunne PD, et al. QuPath: Open source software for digital pathology image analysis. Sci Rep. 2017;7:16878.

## ACKNOWLEDGEMENTS

We thank the Histology Laboratory from CIEMAT, namely Pilar Hernandez Lorenzo, for the histological processing of tumor samples and the Laboratory of Cytometry and Cellular Separation, specifically Rebeca Sánchez-Domínguez and Omaira Alberquilla for their help with the flow cytometry protocols and analyzes. We acknowledge Filipa Quintela Vieira and Regina Augusta Silva for the help in using the Pannoramic MIDI II. This study was cofounded by grants from the European Regional Development Fund for Science and Innovation (SAF2015-66015-R and PID2019-110758RB-I00 to JMP), Instituto de Salud Carlos III (CIBERONC no. CB16/12/00228) to JMP and Project "FINANCED BY NEXTGENERATION EU FUNDS, WHICH FINANCE THE ACTIONS OF THE RECOVERY AND RESILIENCE MECHANISM (MRR)". Funding entity: CARLOS III HEALTH INSTITUTE (ISCIII). ISCIII project code: AC22/00015 - Title: "Circulating tumor microenvironment components as predictors of response to immunotherapy in urothelial cancer" - PI: Marta Dueñas Porto. Project also funded by the Scientific Foundation of the Spanish Association Against Cancer (FCAECC) with project ID TRNSC213883DUEN, Transcan-3 JTC2022 and Fundación Eugenio Rodríguez Pascual (FERP-2022-79 to CR). SPN is supported by an FCT-Fundação para a Ciência e Tecnologia Grant (SFRH/BD/ 144241/2019). IL is supported by a predoctoral fellowship from AECC (Spanish Ass. against Cancer), Predoctoral AECC 2019 grant number PRDMA19024LODE. LM position is funded by Fundación Científica Asociación Española Contra el Cáncer (AECC), Postdoctoral AECC 2019 grant number POSTD19036MORA. MPC is funded by FCT—Fundação para a Ciência e Tecnologia (CEECINST/00091/2018). This research was funded by grants from the Instituto de Salud Carlos III (ISCIII) and co-financed by FEDER: CIBERONC CB16/12/00489 Gobierno de Navarra: Departament of Health (44/2021) (also co-financed by FEDER) and Department of Economic Development AGATA (0011-1411-2020-000011 and 0011-1411-2020-000010), NanoRC (0011-1411-2022-000068 and 0011-1411-2022-000068) and MEET-AML (0011-2750-2019-000001), MEET-AML is cofunded by ERA-NET program. AECC Innova (INNOV211822SANJ). The study was also supported by Cancer Research UK [C355/A26819] and FC AECC and AIRC under the Accelerator Award Programme.

## AUTHOR CONTRIBUTIONS

Conceptualization – SPN, LM, MD, MPC and JMP; Data curation – SPN, CR and JMP; Formal analysis – SPN, EM-M, CR, RH and JMP; Funding acquisition – JMP; Investigation – SPN, LM, CR, EM-M, IL, CS-C, VGM, MP-E, MP-C and MAS; Methodology - SPN, LM, CR, EM-M, CS-C, EM, VGM and JMP; Project Administration – SPN and JMP; Resources – ESJ-E, XA, FP and AP-L, Software – SPN, CR and JMP; Supervision – MPC, RH, CJ, MD and JMP; Validation - SPN, LM, CR, EM-M, IL, CS-C, VGM, MP-E, MD, MPC and JMP; Visualization – SPN, CR and JMP; Writing – original draft – SPN and JMP; Writing – review & editing – SPN, LM, MPC, CR, CS-C, MD, RH, CJ and JMP. All authors reviewed the manuscript.

## COMPETING INTERESTS

The authors declare no competing interests.

## ADDITIONAL INFORMATION

**Supplementary information** The online version contains supplementary material available at https://doi.org/10.1038/s41420-023-01786-3.

**Correspondence** and requests for materials should be addressed to Jesús M. Paramio.

**Reprints and permission information** is available at http://www.nature.com/reprints

**Publisher's note** Springer Nature remains neutral with regard to jurisdictional claims in published maps and institutional affiliations.

**Open Access** This article is licensed under a Creative Commons Attribution 4.0 International License, which permits use, sharing, adaptation, distribution and reproduction in any medium or format, as long as you give appropriate credit to the original author(s) and the source, provide a link to the Creative Commons license, and indicate if changes were made. The images or other third party material in this article are included in the article's Creative Commons license, unless indicated otherwise in a credit line to the material. If material is not included in the article's Creative Commons license and your intended use is not permitted by statutory regulation or exceeds the permitted use, you will need to obtain permission directly from the copyright holder. To view a copy of this license, visit http://creativecommons.org/licenses/by/4.0/.

© The Author(s) 2024